Distribution Agreement

In presenting this thesis or dissertation as a partial fulfillment of the requirements for an advanced degree from Emory University, I hereby grant to Emory University and its agents the non-exclusive license to archive, make accessible, and display my thesis or dissertation in whole or in part in all forms of media, now or hereafter known, including display on the world wide web. I understand that I may select some access restrictions as part of the online submission of this thesis or dissertation. I retain all ownership rights to the copyright of the thesis or dissertation. I also retain the right to use in future works (such as articles or books) all or part of this thesis or dissertation.

Signature:

_____ _____

Alyse N. Steves Date

Ubiquitous Halogenated Flame Retardant Toxicants Impair Spermatogenesis in a Human Stem Cell Model

By

Alyse N. Steves
Doctor of Philosophy

Graduate Division of Biological and Biomedical Sciences
Genetics and Molecular Biology

_____	_____
Anthony W.S. Chan, DVM, Ph.D. Advisor	David J. Katz, Ph.D. Committee Member
_____	_____
Charles A. Easley IV, Ph.D. Advisor	Michele Marcus, Ph.D. Committee Member
_____	_____
Alicia K. Smith, Ph.D. Committee Member	W. Michael Caudle, Ph.D. Committee Member

Accepted:

_____
Lisa A. Tedesco, Ph.D.
Dean of the James T. Laney School of Graduate Studies

_____
Date

Ubiquitous Halogenated Flame Retardant Toxicants Impair Spermatogenesis in a Human Stem Cell Model

By

Alyse N. Steves
B.S., Kennesaw State University, 2014

Advisor: Anthony W.S. Chan, DVM, Ph.D
Advisor: Charles A Easley IV, Ph.D.

An abstract of
A dissertation submitted to the Faculty of the
James T. Laney School of Graduate Studies of Emory University
in partial fulfillment of the requirements for the degree of
Doctor of Philosophy
in Genetics and Molecular Biology
2018

Abstract

Ubiquitous Halogenated Flame Retardant Toxicants Impair Spermatogenesis in a Human Stem Cell Model

By

Alyse N. Steves

Sperm counts have rapidly declined in the Western male over the past four decades. This rapid decline remains largely unexplained. Exposure to environmental toxicants provides one potential explanation for this decline. Flame retardants are highly prevalent and persistent in the environment, but many have not been assessed for their effects on human spermatogenesis. Using a human stem cell-based model of spermatogenesis, we evaluated four major flame retardants, TDCPP, TDBPP, HBCDD, and TBBPA, under acute conditions simulating occupational-level exposures. Here we show that TDCPP, TDBPP, HBCDD, and TBBPA are human male reproductive toxicants *in vitro*. While not specifically impacting the survival of haploid spermatids, these toxicants affect spermatogonia and primary spermatocytes through mitochondrial membrane potential perturbation and ROS generation, ultimately causing apoptosis. These results are in stark contrast to persistent per- and polyfluoroalkyl substance exposure, where sub-cellular processes such as spermatogenic cell marker expression are perturbed upon exposure to PFOS, PFOA, and PFNA, but cell viability is ultimately unaffected. Additionally, tentative results looking at persistent exposure to halogenated flame retardants in distinctively different genetic backgrounds suggest different mechanisms of action for acute versus persistent conditions and also highlights how genetics may play a vital role in mediating the reproductive toxicity of these compounds. Taken together, these results show that halogenated flame retardants affect human spermatogenesis *in vitro* and potentially implicate this highly prevalent class of toxicants in the decline of Western males' sperm counts.

Ubiquitous Halogenated Flame Retardant Toxicants Impair Spermatogenesis in a Human Stem Cell Model

By

Alyse N. Steves
B.S., Kennesaw State University, 2014

Advisor: Anthony W.S. Chan, DVM, Ph.D.
Advisor: Charles A. Easley IV, Ph.D.

A dissertation submitted to the Faculty of the
James T. Laney School of Graduate Studies of Emory University
in partial fulfillment of the requirements for the degree of
Doctor of Philosophy
in Genetics and Molecular Biology
2018

Acknowledgments

I would like to thank Drs. Anthony Chan and Chas Easley for the wonderful mentorship over the past four years. I would not be able to complete this chapter in my scientific career without your unwavering support and guidance. I would also like to thank my committee members: Drs. Mike Caudle, Alicia Smith, Michele Marcus, and David Katz. Your advice and feedback over the years have been integral to the completion of my degree. I would also like to thank our collaborators from Dr. Gary Miller's lab, particularly Josh Bradner, who trained me on the ArrayScan. Without the time and dedication from any of you, I could not have done this. I also have to express my thanks to Emory University, Laney Graduate School, and the Genetics and Molecular Biology program. Emory University and its programs have opened doors for me, and I cannot express my gratitude enough. Additionally, I have to thank Drs. Martin L. Hudson and Lisa G. Adams from Kennesaw State University. Without your constant encouragement during my undergraduate career, I never would have believed this was possible.

I also have to thank my lab mates, particularly Danielle Clarkson-Townsend, Kristen Fowler, Brittany Gill, Adam Turry, Katherine Watkins, and Krista Symosko. Getting through the day was often a team effort, and I sincerely appreciate all of the support I have received from you. I wish you all the best of luck as you progress through your own careers.

This work was supported by the National Science Foundation [DGE-1444932] to Alyse Steves, the National Institutes of Health [1K22 ES025418-01] to Chas Easley, Emory University's Atlanta Clinical & Translational Science Institute and University Research Committee (ACTSI/URC) award to Chas Easley, and the National Institutes of Health [P30 ES019776-01-A1] to Gary Miller. Without this funding, none of this work would be possible.

Finally, I have to thank my friends and family. Without my parents, sister, and supportive partner, I would not have had the foundation to complete this extremely arduous endeavor.

Table of Contents

List of Abbreviations

1,2,3,7,8-pentabromodibenzofuran (1PeBDF)

1,2-dibromo-3-chloropropane (DBCP)

2,2-bis(bromomethyl)-1,3-propanediol (BMP)

2,3,4,7,8-pentabromodibenzofuran (4PeBDF)

2,3,7,8-tetrabromodibenzofuran (TBDF)

2,3,7,8-tetrabromodibenzo-p-dioxin (TBDD)

2,3-dibromopropyl-2,4,6-tribromophenyl ether (DPTE)

2-bromoallyl 2,4,6-tribromophenyl ether (BATE)

2-bromopropane (2-BP)

2-ethylhexyl-2,3,4,5 tetrabromobenzoate (TBB)

3,3'-T2 TH sulfotransferase (SULT)

adult Leydig cell (ALC)

allyl 2,4,6-tribromophenyl ether (ATE)

androgen receptor (AR)

bis(1,3-dichloro-2-propyl) phosphate (BDCIPP)

bis(2-ethylhexyl)-2,3,4,5-tetrabromophthalate (TBPH)

bovine serum albumin (BSA)

di(ethylhexyl)phthalate (DEHP)

dimethyl sulfoxide (DMSO)

estradiol (E2)

flame retardant (FR)

hexabromocyclododecane (HBCDD)

HILI (piwi like RNA-mediated gene silencing 2)

human albumin (hALB)

human basic fibroblast growth factor (hbFGF)

human embryonic stem cell (hESC)

human glial-derived neurotrophic factor (hGDNF)

human pluripotent stem cell (hPSC)

human transthyretin (hTTR)

hydrogen peroxide (H_2O_2)

local exhaust ventilation (LEV)

non-human primate (nhp)

p,p'-dichlorodiphenyldichloroethylene (DDE)

p,p'-dichlorodiphenyltrichloroethane (DDT)

per- and polyfluoroalkyl substance (PFAS)

perfluorinated compound (PFC)

perfluorohexane sulfonic acid (PFHxS)

perfluorononanoic acid (PFNA)

perfluorooctanesulfonic acid (PFOS)

perfluorooctanoic acid (PFOA)

polybrominated biphenyl ether (PBDE)

polychlorinated biphenyl ether (PCB)

promyelocytic leukemia zinc finger (PLZF)

protamine 1 (P1)

protamine 2 (P2)

puberty (PT)

reactive oxygen species (ROS)

sex hormone binding globulin (SHBG)

spermatogonial stem cell (SSC)

tetrabromobisphenol A (TBBPA)

tetradecabromo-1,4-diphenoxybenzene (TeDB-DiPhOBz)

thryroxine (T4)

thyroid hormone (TH)

thyroid receptor β (TRβ)

triiodothyronine (T3)

tris(1,3-dichloro-2-propyl)phosphate (TDCPP)

tris(2,3-dibromopropyl)phosphate (TDBPP)

tumor necrosis factor alpha (TNFα)

type 3 deiodinase (DIO3)

List of Figures

Chapter 1: Introduction

1.1 Chemical exposure has been linked to declining male fertility

Over 80,000 chemicals approved for market use are registered with the U.S. EPA (Wilding BC, 2013). Of these chemicals, the Centers for Disease Control's (CDC's) National Biomonitoring Program assesses the average exposure of Americans to 308 chemicals (Wilding BC, 2013, Prevention, 2017)—alarmingly few in comparison to the number approved. The average person has no less than twenty four of these surveyed chemicals detectable in their circulatory system at any given time (Wilding BC, 2013), though the number of chemicals accumulating in the human body is likely considerably higher. With an estimated 2,000 new chemicals entering the market each year (Wilding BC, 2013), researchers are grossly behind in the detection of chemicals entering and bioaccumulating in the human body, let alone our understanding of how these chemicals may impact human health. Because these chemicals are not extensively screened on humans before their release into the market, more often than naught, their toxic effects are not known.

Male reproductive function is highly sensitive to certain chemical toxicants (Boekelheide et al., 2004, Cannon et al., 1978, Whorton et al., 1977, Whorton et al., 1979, Campion et al., 2012). Exposure of the male reproductive system to toxicants can result in adverse outcomes ranging from impaired androgen production to adverse changes in semen parameters and infertility (Whorton et al., 1977, Whorton et al., 1979, Campion et al., 2012, Cannon et al., 1978, Boekelheide et al., 2004). Environmental pollutants such as insecticides have been linked to increases in human infertility in acutely exposed populations (Harley et al., 2010, Campion et al., 2012, Biava et al.,

1978, Lipshultz et al., 1980, Marshall et al., 1978, Whorton et al., 1977, Whorton et al., 1979, Cannon et al., 1978). Specifically, the nematocide 1,2-dibromo-3-chloropropane (DBCP) has been shown to cause male infertility in agricultural workers (Biava et al., 1978, Lipshultz et al., 1980, Marshall et al., 1978, Whorton et al., 1977, Whorton et al., 1979). Different chemical classes have also been shown to be male reproductive toxicants in animal models (Chauvigne et al., 2009, Stroheker et al., 2006). However, the number of toxicants that have been shown to adversely impact human spermatogenesis is small, and conclusions regarding the effects of these compounds have been drawn primarily from a few cross-sectional studies involving occupationally exposed populations that were exposed to these substances at very high concentrations (Hofmann et al., 2006, Potashnik et al., 1979, Whorton et al., 1979, Johnson et al., 2013, Meeker and Stapleton, 2010, Stapleton et al., 2008, Cannon et al., 1978, Boekelheide et al., 2004, Whorton et al., 1977, Campion et al., 2012).

1.2 Halogenated flame retardants have been linked to human disease phenotypes

Of particular concern to male reproduction is toxic assault by halogenated flame retardants. Halogenated flame retardants are found in everyday appliances, including in televisions and computers, and in furniture such as seat cushions, couches, and baby products, where they can make up as much as 30% of the product (Segev et al., 2009). Flame retardants are typically blended with polymers and are not covalently linked to their products and thus leach out of the product (Dishaw et al., 2014, Segev et al., 2009). Flame retardants can enter the environment in large-scale contaminating events through the waste of

facilities that produce flame retardants, through the waste of manufacturing facilities that incorporate flame retardants into their products, and through the breakdown of foam products or from leaching from products disposed of in landfills (Segev et al., 2009). Flame retardants will enter home and office environments through absorption into dust particles from common household items, exposing individuals to continuous, daily contact to these compounds (Segev et al., 2009). Halogenated flame retardants have been measured in dust samples from indoor environments, in water, soil, and sediment from outdoor environments, and in human sewage, indicating that their presence in the environment is ubiquitous (Watanabe and Sakai, 2003, Stapleton et al., 2005, Segev et al., 2009). Halogenated flame retardants have also been detected in the tissues of wildlife, particularly in aquatic life, and in human tissues such as blood serum and breast milk of individuals in the general population, indicating that they can be found in multiple tissue types across multiple species (Muller et al., 2016, Segev et al., 2009). Furthermore, acute and chronic effects of some halogenated flame retardants have been linked to adverse outcomes in the immune system, in the endocrine system, and in the nervous system, and they have been found to cause cancer and to cause defects during embryogenesis, suggesting the potential for multiple mechanisms of toxicity and numerous vulnerable cell/tissue types (Segev et al., 2009, Johnson et al., 2013, Meeker and Stapleton, 2010). Despite these observations and the prolific distribution of halogenated flame retardants in the environment, only limited information is available on some halogenated flame retardants regarding their effects on male fertility (Johnson et al., 2013, Meeker and Stapleton, 2010, Stapleton et al., 2008).

Historically, halogenated flame retardants have existed as polychlorinated biphenyl ethers (PCBs) and polybrominated biphenyl ethers (PBDEs). These compounds are known to leach out of their products into the environment, and because of their lipophilic nature, they readily bioaccumulate in human and animal tissues, as well as persisting in the environment (de Wit, 2002, Covaci et al., 2011). PCBs and PBDEs have been implicated in male reproductive issues, including reduced sperm motility, abnormal sperm morphology, endocrine-disrupting activity, changes in reproductive organs, and are hypothesized to impact male fecundity, among other concerns (Mumford et al., 2015, Czerska et al., 2013, Abdelouahab et al., 2011, Meeker and Hauser, 2010). Additionally, animal studies have shown that exposure to some flame retardants results in adverse reproductive outcomes such as reduced sperm counts and reduced fertility (Kuriyama and Chahoud, 2004, Kuriyama et al., 2005, Chauvigne et al., 2009, Stroheker et al., 2006, Aly, 2013, Prados et al., 2015, Andrade et al., 2006, Aniagu et al., 2008, Zatecka et al., 2014, Liu et al., 2016a, Li et al., 2014a, Salamone and Katz, 1981). In studies that have directly assessed relationships between newer, replacement halogenated flame retardants in the environment and human male infertility, some flame retardants have been associated with changes in male hormones, though no effects on sperm quantity or quality were reported, and genetic and epigenetic data has never been gathered in a human cohort (Johnson et al., 2013, Meeker and Stapleton, 2010, Stapleton et al., 2008). As such, no direct relationship between replacement flame retardants and male infertility has ever been shown, suggesting that they may be safer

alternatives to their predecessors. As awareness of the health impacts of PCBs and PBDEs grows, their production is being phased out, and replacement flame retardants have taken their place on the market. However, of notable concern is that their replacement compounds may, in fact, be no safer and merely perpetuate the health effects associated with this class of chemical, though not enough studies have been conducted to report these findings. The focus of this research is on the impacts of tris(1,3-dichloro-2-propyl)phosphate (TDCPP), which is present in 70% of baby products, tris(2,3-dibromopropyl)phosphate (TDBPP), which is an understudied, banned flame retardant that is still detected in the house dust of 80% of homes tested, hexabromocyclododecane (HBCDD), which is the second most prevalent novel halogenated flame retardant, and tetrabromobisphenol A (TBBPA), which comprises 25% of global flame retardant demand (Stapleton et al., 2011, Dishaw et al., 2014, Dodson et al., 2012, Schecter et al., 2012, Wang et al., 2015b). However, this review will cover all known reproductive dysfunction caused by halogenated flame retardant exposure. Similar to TDCPP, TDBPP, HBCDD, and TBBPA, the compounds described below are lipophilic, halogenated compounds with at least one ring structure.

1.3 Halogenated flame retardants and male infertility

Animal studies have shown that exposure to some flame retardants results in adverse reproductive outcomes such as reduced sperm counts and reduced fertility (Kuriyama and Chahoud, 2004, Kuriyama et al., 2005, Chauvigne et al., 2009, Stroheker et al., 2006, Aly, 2013, Prados et al., 2015, Andrade et al., 2006, Aniagu et al., 2008, Zatecka et al., 2014, Liu et al., 2016a, Li et al., 2014a, Salamone and Katz, 1981). In studies that have directly assessed relationships between flame retardants in

the environment and human male infertility, TDCPP, HBCDD, 2-ethylhexyl-2,3,4,5 tetrabromobenzoate (TBB), and bis(2-ethylhexyl)-2,3,4,5-tetrabromophthalate (TBPH) have been associated with changes in male hormones, though no effects on sperm quantity or quality were reported, and genetic and epigenetic data has never been gathered in a human cohort (Johnson et al., 2013, Meeker and Stapleton, 2010, Stapleton et al., 2008). In addition, no study to date has assessed the concentrations of flame retardants in the biological fluids of infertile men. As such, no direct relationship between flame retardants and male infertility has ever been shown, leaving a significant knowledge gap. This is of significant importance, as the flame retardants TBPH and TBB, which are entering the market as replacement flame retardants, are brominated analogues of di(ethylhexyl)phthalate (DEHP), which is listed under California's Proposition 65 as a reproductive and developmental toxicant (Erkekoglu and Kocer-Gumusel, 2014). Exposure to phthalates has been demonstrated to cause reproductive toxicity in both human and animal models, including disrupting sperm DNA integrity, inducing spermatozoa apoptosis, and affecting histone modifications, imprinting, and DNA methylation in sperm (Bloom et al., 2015, Aitken and Baker, 2013, Chauvigne et al., 2009, Stroheker et al., 2006, Prados et al., 2015, Andrade et al., 2006, Liu et al., 2016a, Li et al., 2014a). Also of significance, the flame retardant TBBPA is one of the most widely used flame retardants on the market. TBBPA exposure in rats resulted in sperm DNA damage and altered epigenetic marks on sperm chromatin through improper protamine distribution (Osimitz et al., 2016). Additional studies have

suggested that TBBPA targets the mitochondria and can affect histone modifications (Otsuka et al., 2014, Nakagawa et al., 2007). These results raise the concern that TBBPA could cause infertility that is not detectable through sperm counts or assessing other semen parameters. Taken together, these studies highlight a lack of understanding regarding if these flame retardants can impact human male infertility, a significant knowledge gap regarding their subcellular targets and mechanisms of action, and the significant need for an accurate, high-throughput model of human spermatogenesis to assess the reproductive toxicity of flame retardants.

1.4 Tris(1,3-dichloro-2-propyl)phosphate (TDCPP)

Tris(1,3-dichloro-2-propyl)phosphate (TDCPP) is used in plastic foams that are found in the automotive industry and some furniture, resins, and latexes (van der Veen and de Boer, 2012, Betts, 2013, United Nations Environment Programme, 2004). TDCPP is not bonded to its products and readily enters the environment (van der Veen and de Boer, 2012). TDCPP has been detected in the dust of 96% of homes tested (Meeker and Stapleton, 2010, Betts, 2013). In foam samples and baby products tested, TDCPP is the most prominent flame retardant detected (Stapleton et al., 2011, Betts, 2013). Globally, TDCPP has been detected in human adipose tissue, breast milk, blood, and urine (Betts, 2013, van der Veen and de Boer, 2012, Carignan et al., 2013). The half-life of TDCPP in humans is not currently known, and daily exposure for the general population has not been assessed (Carignan et al., 2013). The effects of TDCPP on male reproduction has been investigated in rats and rabbits with no effects seen, though TDCPP has been shown to cause testicular tumors in rat models (van der Veen and de Boer, 2012, United Nations Environment Programme, 2004). TDCPP has been shown

to increase oxidative stress (Dishaw et al., 2014), and it has been shown that exposure to TDCPP decreases cell growth and increases apoptosis (Ta et al., 2014). Studies have shown that TDCPP induces delays in re-methylation of the zygotic zebrafish genome (McGee et al., 2012). TDCPP has also been shown to inhibit DNA synthesis and expression of specific genes (Dishaw et al., 2014, Ta et al., 2014, Farhat et al., 2014). Based on this information, it is possible that TDCPP will specifically affect DNA methylation in spermatogenesis. There are currently no studies investigating the role TDCPP may play in human male spermatogenesis, though it has been implicated as a potential endocrine disruptor in males (Meeker and Stapleton, 2010). At this time, only one study has ever examined TDCPP's effects on occupationally exposed workers, with no significant findings reported (United Nations Environment Programme, 2004). One study reported TDCPP in the semen of the majority human males tested, though no reproductive outcomes were measured (Hudec et al., 1981). The limited studies on the impact of TDCPP on human health have thus far added little to our understanding of how TDCPP may adversely impact human health in general (United Nations Environment Programme, 2004).

1.5 Tris(2,3-dibromopropyl)phosphate (TDBPP)

In the late 1970s, tris(2,3-dibromopropyl)phosphate (TDBPP) was found to leach out of children's pajamas and was detected in children's urine samples at alarmingly high levels (Blum et al., 1978). At the same time, TDBPP had been shown to cause sterility in animals (Gold et al., 1978). Additionally, TDBPP is highly clastogenic and has been shown to cause DNA damage in the rat testis

and sperm (van Beerendonk et al., 1994, Soderlund et al., 1992, Salamone and Katz, 1981). While TDBPP is banned, it still holds relevance, as TDBPP still contaminates the Velsicol Superfund site, and TDBPP has been found to persist in the environment despite its discontinued use (Peverly et al., 2014, Hu et al., 2014). Shockingly, TDBPP can still be found in 75% of house dust samples tested (Dodson et al., 2012). Human data for TDBPP is limited, and it was never confirmed as a human male reproductive toxicant. However, examining this flame retardant provides needed information as we continue to live with TDBPP in our environment.

1.6 Hexabromocyclododecane (HBCDD)

Like its predecessors, hexabromocyclododecane (HBCDD) is highly lipophilic, accumulates in tissues, is difficult to breakdown, and is known to persist in the environment (Covaci et al., 2006). HBCDD is used primarily in rigid foam insulation in the construction industry, as well as in textiles, high-impact polystyrene, and electrical equipment (Covaci et al., 2006, Agency, 2014). HBCDD can enter the environment during production or from leaching out of its product, as HBCDD is not bonded to its product (Schecter et al., 2012, Covaci et al., 2006, Agency, 2014). HBCDD has been detected as far as the Arctic, where there is no known source for HBCDD, suggesting it is highly persistent in the environment and capable of long-range transport (Agency, 2014). HBCDD has been detected in the house dust of 97% of homes tested, where it can enter the human body though inhalation or contact, and it has been detected in food, where it is ingested (Schecter et al., 2012, Johnson et al., 2013). Globally, HBCDD has been detected in adipose tissue, blood, breast milk, and has been shown to cross the placenta (Fromme et al., 2016b, Bjermo et al., 2017, Fromme et al., 2016a,

Rawn et al., 2014b, Darnerud et al., 2011, Rawn et al., 2014a). HBCDD's estimated half-life in human adipose tissue is an estimated 64 days, with an estimated daily intake of 142ng/day, making it likely that HBCDD is never fully cleared from the human body (Geyer HJ, 2004). Two groups have estimated or assessed the exposure of occupation workers to HBCDD (Yi et al., 2016b, Thomsen et al., 2007). HBCDD is estimated by the EPA to be a moderate hazard to human reproductive health, including adverse effects on gamete production (Agency, 2014). However, this designation was based on reduced primordial follicles in female mice (Agency, 2014). HBCDD has been shown to induce cell death and inhibit the Ca^{2+} ATPase in human neuroblastoma cells (Al-Mousa and Michelangeli, 2014). HBCDD has also been shown to increase cytochrome P450 monooxygenase enzymes (Aniagu et al., 2008). As such, it is likely that HBCDD affects mitochondrial function and causes ROS generation, DNA damage, and cell death in spermatogenic lineages. To date, HBCDD has been identified as a possible endocrine disruptor in the human male in the general population, but semen parameters have not been assessed, and no investigation into the spermatogenesis and fertility of occupational exposed workers has been conducted (Johnson et al., 2013).

1.7 Tetrabromobisphenal A (TBBPA)

Tetrabromobisphenal A (TBBPA) is found primarily in epoxy resin printed circuit boards and other electronics, where it is covalently bonded to its product (E.C.B. European Commission Directrate-General Joint Research Center, 2006). However, as much as 30% of TBBPA produced is used as an additive flame

retardant that is added to high impact polystyrenes and resins, which can leach out into the environment (E.C.B. European Commission Directrate-General Joint Research Center, 2006). TBBPA is currently the most produced brominated flame retardant in the world and accounts for 25% of global flame retardant demand (E.C.B. European Commission Directrate-General Joint Research Center, 2006, Wang et al., 2015b, Jarosiewicz and Bukowska, 2017). Globally, TBBPA has been detected in human blood, breast milk, hair, and adipose tissue (E.C.B. European Commission Directrate-General Joint Research Center, 2006, KE, 2002, Jakobsson et al., 2002, Thomsen et al., 2001, Thomsen et al., 2002a, Thomsen et al., 2002b, Agency). TBBPA has also been detected in food and house dust (Abafe and Martincigh, 2016, E.C.B. European Commission Directrate-General Joint Research Center, 2006). The half-life of TBBPA in human plasma is 76 days (Geyer HJ, 2004). In the occupational exposure setting, it has been assessed that an occupational worker using local exhaust ventilation (LEV) may still be exposed to inhalable TBBPA particles at a concentration as high as 10,000 $\mu g/m^3$, making exposure remarkably high for this population (E.C.B. European Commission Directrate-General Joint Research Center, 2006). Without LEV, exposure could be as high as 200,000 $\mu g/m^3$ (E.C.B. European Commission Directrate-General Joint Research Center, 2006). Dermal exposure in an occupational setting has been estimated to be as high as 900$\mu g/cm^2$ (E.C.B. European Commission Directrate-General Joint Research Center, 2006). While roughly half a dozen studies examine TBBPA exposure in an occupational setting, only two studies have measured blood levels of TBBPA in these occupationally exposed populations, and health outcomes were not assessed in any of the studies (Zhou et al., 2014, Deng et al., 2014, Shaw et

al., 2013, Makinen et al., 2009, Jakobsson et al., 2002). There is evidence that TBBPA targets the testis, though no analysis of the effects of TBBPA on human spermatogenesis have been conducted in an occupationally exposed or normally exposed human population (Choi et al., 2011). However, in animal models, TBBPA has been shown to cause DNA damage, alter the epigenetic landscape, increase ROS generation, and cause changes in genes required for spermatogenesis, highlighting the importance of investigating this chemical in a human model, particularly for those exposed at high than average concentrations (Zatecka et al., 2014, Linhartova et al., 2015, Zatecka et al., 2013). TBBPA exposure in rats has also resulted in altered epigenetic marks on sperm chromatin through improper protamine distribution (Zatecka et al., 2014). Studies in rodents have shown that exposure to TBBPA results in a significantly decreased protamine 1 (P1)/protamine 2 (P2) ratio and increased total protamine/DNA ratio (Zatecka et al., 2014). In humans, all but 10-15% of a mature sperm's genome is packaged by histones, with the remaining DNA tightly wrapped around P1 and P2 (Balhorn, 2007). P1 and P2 are both required for proper sperm maturation and fertility in the mouse, with perturbations in in the P1/P2 ratio leading to increased DNA damage, incomplete chromatin condensation, and other defects in rodent sperm (Balhorn, 2007). Notably, higher P2 content has been associated with more rapid decondensation of the sperm genome, resulting in failed fertilization in mice and possibly explaining why humans who produce sperm with abnormal proportions or P1 and P2 are infertile (Balhorn, 2007). In addition, TBBPA has been shown to repress triiodothyronine

(T3)-induced H3K4me3 and H3K36me3 at thyroid hormone (TH) response genes (Otsuka et al., 2014). Additional studies have suggested that TBBPA targets the mitochondria by causing oxidative phosphorylation-related mitochondrial dysfunction and can affect histone modifications (Otsuka et al., 2014, Nakagawa et al., 2007). These results raise the concern that TBBPA could cause infertility that is not detectable through sperm counts or assessing other semen parameters, which are common methods used in epidemiological studies. For example, in the instance of improper protamine switching, decondensation of the sperm genome that occurs too early in fertilization will be missed in most, if not all, human epidemiological studies, particularly if these sperm have normal morphology and motility.

1.8 Halogenated flame retardant exposure and male sex hormone disruption

1.8.1 Human epidemiological studies

In utero, PBDEs have been detected in placental tissues, with PBDEs detected at higher concentrations in placental tissue associated with male embryos (Leonetti et al., 2016b, Leonetti et al., 2016a). BDE-209 concentrations were nearly twice as high in placental tissue associated with male embryos (Leonetti et al., 2016a). Placental PBDE concentrations for male fetuses have been negatively associated with T3 levels (Leonetti et al., 2016a). Type 3 deiodinase (DIO3) activity, which is critical for the regulation of T3 bioavailability, was also higher in placental tissue associated with male embryos than placental tissue associated with female embryos (Leonetti et al., 2016a). While it is unclear what impacts these changes in T3 and DIO3 had on the fetuses in the previous studies, high T3 and T4 concentrations early in development have been shown to be toxic to fetal tissues (de Escobar et al., 2004). Conversely, hypothyroidism

in pregnant women has been associated with poor neural development in developing fetuses that may contribute to learning disabilities later on (de Escobar et al., 2004)Prenatal exposure to the PBDEs BDE-153 and BDE-100 has been associated with an increase in LH in male children (Eskenazi et al., 2017). Similarly, *in utero* exposure to BDE-153 has also been associated with increases in FSH and testosterone (Eskenazi et al., 2017). *In utero* exposure to PCBs has similarly been associated with increases in FSH. (Eskenazi et al., 2017). Adult men whose prenatal exposures were unknown also showed a correlation between increasing concentrations of BDE-47 and BDE-100 and increasing concentrations of FSH (Makey et al., 2016). Also in adult men, increasing serum levels of pentaBDEs and octaBDEs, or BDEs with five and eight bromines in their structure, respectively, have been associated with increasing free T4, total T3, estradiol, sex hormone binding globulin (SHBG), TSH, and testosterone (Johnson et al., 2013). In this study, pentaBDEs and decaBDEs were inversely associated with FSH and testosterone, respectively (Johnson et al., 2013). HBCDD was associated with decreased SHBG and increased free androgen index (Johnson et al., 2013). The halogenated flame retardant TDCPP has been positively associated with prolactin, which has been associated with erectile dysfunction, and the thyroid hormone thyroxine (Betts, 2010a). In boys, PCB exposure has been associated with delayed puberty (Roy et al., 2009). The halogenated flame retardant TBBPA is an androgen receptor antagonist, and TBBPA has been shown to alter testosterone synthesis in MA-10 Leydig cells *in vitro* (Roelofs et al., 2015). Additionally, allyl 2,4,6-tribromophenyl ether (ATE), 2-bromoallyl 2,4,6-tribromophenyl ether (BATE), and 2,3-dibromopropyl-2,4,6-tribromophenyl ether (DPTE) all bind the ligand-binding domain of the human

AR and act as AR antagonists (Kharlyngdoh et al., 2015). An adverse hormonal environment during pregnancy has been associated with abnormal fetal brain growth (Miranda and Sousa, 2018). In particular, maternally supplied T3 and T4 are critical to the developing fetus's brain until the fetal thyroid gland is developed (Miranda and Sousa, 2018). Additionally, perturbations in androgen and estrogen levels during pregnancy have been associated with changes in sexually dimorphic brain areas such as the cortex, cerebellum, hippocampus, and other areas (Miranda and Sousa, 2018). In adult males, the thyroid gland has been shown to have critical functions in male fertility (Krajewska-Kulak and Sengupta, 2013). In males with hypothyroidism, significant decreases in mature germ cells are observed, and hypothyroidism was also associated with changes in sperm morphology and motility (Krajewska-Kulak and Sengupta, 2013). Similarly, hyperthyroidism has been associated with changes in male sex organ morphology and fertility, with decreases in sperm counts and motility (Krajewska-Kulak and Sengupta, 2013). In males with altered sex hormone levels, decreases in testosterone and/or increases in LH are present in 20 – 30% of all male infertility cases (Ring et al., 2016). Abnormalities in androgen receptor (AR) have also been associated with abnormalities in male sexual development and increased infertility (Ring et al., 2016). As such, perturbations in hormones have been shown to negatively impact male development in a wide variety of tissue types at different ages, further highlighting how endocrine disruption from halogenated flame retardants can be detrimental.

1.8.2 In vitro studies

The halogenated flame retardants TBB and TBPH have anti-androgenic activities at concentrations as low as 100 nM (Meerts et al., 2001). BDE-47 and PBDE-710

increase testosterone production in Rat adult Leydig cells (ALCs), with BDE-47 increasing testosterone production in a dose-wise manner (Zhao et al., 2011, Wang et al., 2011a).

1.8.3 In vivo animal studies

In the CF-1 strain of mice, subcutaneous injections of TBBPA increased estradiol (E2) concentrations in urine, indicating that TBBPA may inhibit enzymes required for E2 metabolism (Pollock et al., 2017). BDE-209 exposure significantly decreases testosterone production in Parkes strain male mice (Sarkar et al., 2016). In male zebrafish, testosterone decreased and E2 increased following fourteen days of exposure to TDCPP (Liu et al., 2012).

1.9 Halogenated flame retardant exposure and female sex hormone disruption

1.9.1 Human epidemiological studies

Unlike placental tissue associated with male embryos, 3,3'-T2 TH sulfotransferase (SULT) activity is higher in placental tissue associated with female embryos (Leonetti et al., 2016a). Additionally, female infants with placental concentrations of BDE-99 were positively associated with T3 concentrations (Leonetti et al., 2016a). Women with high concentrations of BDE-47, -99, and -100 are at higher risk of developing thyroid disease (OR = 1.5, 1.8, and 1.5, respectively), with risk increasing following menopause (Allen et al., 2016). Increased risk for hypothyroidism was associated with increased levels of BDE-47 and -100 in women aged 30-50 (Oulhote et al., 2016). In some studies examining the effects of PBDEs on thyroid function in pregnant women, PBDEs have been positively associated with levels of TSH, similar to results reported in men (Zota et al., 2011). However, conflicting studies indicate that

higher PBDEs may be associated with lower TSH (Betts, 2010b). Additionally, higher concentrations of PDBEs were detected in girls with premature thelarche, which is the beginning of breast development at the onset of puberty (PT) (Deodati et al., 2016). PBB exposure has been associated with earlier menarche and earlier thelarche in girls (Roy et al., 2009). Specifically, girls who were highly exposed to PBB *in utero* and through breastfeeding had an earlier appearance of pubic hair and reached menarche a full year earlier (Blanck et al., 2000).

1.9.2 In vitro studies

TDCPP has been shown to enhance thryroxine (T4) binding to human transthyretin (hTTR) transport protein, suggesting interactions with TDCPP that may lead to conformational changes that make the second binding site of hTTR accessible (Hill et al., 2018a). Conversely, the flame retardant tetradecabromo-1,4-diphenoxybenzene (TeDB-DiPhOBz) has been found to compete with T4 for binding with hTTR and albumin (hALB) (Hill et al., 2018b). Additionally, the halogenated flame retardants TBB and TBPH also have anti-thyroid hormonal activities (Klopcic et al., 2016). TDCPP is an antagonist to thyroid receptor β (TRβ) (Zhang et al., 2016b). TDCPP, HBCDD, and TBBPA all show both estrogenic and anti-estrogenic activity when co-treating with 17β-estradiol in the human breast adenocarcinoma cell line, MCF-7, indicating that these chemicals may alter estrogen homeostasis (Krivoshiev et al., 2016). TBBPA significantly induces estradiol secretion in human choriocarcinoma-derived placental JEG-3 cells *in vitro* (Honkisz and Wojtowicz, 2015). PBDE-47, -99, -100 and -209 have been shown to increase estradiol, testosterone, and progesterone secretion *in vitro* in co-cultures of theca and granulosa cells harvested from cycling pigs

(Karpeta and Gregoraszczuk, 2010, Gregoraszczuk et al., 2008). However, in the same model, p,p'-dichlorodiphenyltrichloroethane (DDT) and p,p'-dichlorodiphenyldichloroethylene (DDE) increase estradiol secretion while decreasing testosterone secretion (Gregoraszczuk et al., 2008).

1.9.3 Animal studies

In zebrafish exposed to TDCPP from two-hours post-fertilization until sexual maturity, exposure to TDCPP significantly increased estradiol and testosterone levels in females, but males exhibited no statistically significant changes in hormones (Wang et al., 2015a). These results were replicated in a study in which adult female zebrafish were exposed to TDCPP for two weeks, though male fish also experienced hormonal changes in this study (Liu et al., 2012)

1.10 Halogenated flame retardant exposure and spermatogenesis

1.10.1 Human epidemiological studies

Halogenated flame retardant exposure has been associated with changes in semen parameters. Men with high levels of BDE-209 in their serum had an increased odds ratio for subfertility (odds ratio = 7.22) (Den Hond et al., 2015). Studies have also associated TDCPP exposure with a decreased odds ratio for low sperm count (OR = 0.79) and inverse correlations with sperm concentration (Ingle et al., 2018, Akutsu et al., 2008). TDCPP exposure has also been associated with decreased sperm motility and changes in sperm morphology (Meeker et al., 2013).

1.10.2 In vitro studies

Assessment of TDCPP, TDBPP HBCDD, and TBBPA in an *in vitro* spermatogenesis model revealed TDCPP, TDBPP, HBCDD, and TBBPA all target

spermatogonia and primary spermatocytes by initiating apoptosis and impacting the cell cycle (Steves et al., 2018a). However, haploid spermatid production was not impacted in this model (Steves et al., 2018a).

1.10.3 Animal studies

In addition to changes in testicular histopathology, male CD-1 mice exposed to BDE-209 *in utero* showed a significant increase in sperm head abnormalities (Tseng et al., 2013). Exposure to TDCPP decreases spermiation in male zebrafish (Wang et al., 2015a). In the testes of zebrafish exposed to TDCCP, there is an increase in FSHR expression but a decrease in LHR expression (Liu et al., 2013). Male zebrafish exposed to a mixture of TBBPA and BDE-209 for 150 days experienced decreased sperm density and motility (Chen et al., 2018a). In adult male SD rats, exposure to BDE-47 for eight weeks resulted in apoptosis in early leptotene spermatocytes (Huang et al., 2015). In mice exposed to TBBPA, increased apoptosis in the testes and morphological changes of seminiferous tubules were reported, though this study did not report changes in sperm quality or fertility upon exposure to TBBPA (Zatecka et al., 2013). However, this study did report a change in gene expression for genes critical for spermatogenesis (Zatecka et al., 2013). In mice exposed to BDE-209, exposure caused increased sperm DNA damage and increased sperm chain breakage, with damage increasing in a dose-wise manner (Wang et al., 2011b). In mouse TM4 Sertoli cells, TBBPA exposure induces apoptosis via Ca^{2+}-dependent mitochondrial depolarization (Ogunbayo et al., 2008). In CD-1 male mice exposed to BDE-209, exposure reduced mitochondrial potential in epididymal sperm and induced the generation of reactive oxygen species (Tseng et al., 2006). However, this increase in ROS and mitochondrial

depolarization did not lead to decreased sperm counts, changes in motility or morphology, or testicular histopathology (Tseng et al., 2006). In zebrafish, exposure to BDE-71 enhanced gonadal development, though this was contrasted by decreases in gamete quality, fertilization success, hatching success, and larval survival rate (Han et al., 2013). Male offspring born to Wistar rats, which are an inbred Albino rat breed, which were exposed to BDE-47 during pregnancy from gestational day 8 to 21 had smaller testes, decreased sperm production, more morphologically abnormal sperm, increased sperm head size, and suppression of genes required for spermatogenesis (Khalil et al., 2017)

1.11 Halogenated flame retardant exposure and oogenesis

1.11.1 Human epidemiological studies

To date, no studies have reported the impacts of halogenated flame retardants on human oogenesis.

1.11.2 In vitro studies

No studies have reported the impacts of halogenated flame retardants on human oogenesis *in vitro*.

1.11.3 Animal studies

In zebrafish exposed to TDCPP for 120 to 150 days, female zebrafish produced fewer eggs compared to control (Zhu et al., 2015, Chen et al., 2018a). Similarly, zebrafish exposed to TDCPP from two-hours past fertilization also exhibited decreased egg production (Wang et al., 2015a). While these studies did reveal that TDCPP exposure may promote oocyte maturation in histological studies, decreased egg quality through decreased egg diameter and egg malformations were observed in the offspring

of TDCPP-exposed zebrafish, indicating intergenerational impacts (Wang et al., 2015a). In the ovaries of zebrafish, TDCPP exposure significantly upregulated FHSR and LHR expression (Liu et al., 2013).

1.12 Halogenated flame retardant exposure and birth outcomes

1.12.1 Human epidemiological studies

Studies have shown that halogenated flame retardants can cross the placenta and build up in fetal tissues, with PBDEs detected in cord blood samples and liver tissue of infants following birth (Schecter et al., 2007). In the placenta, PBDE congeners have been detected at concentrations as high as 140 ng/g (Leonetti et al., 2016b). Additionally, the halogenated flame retardant PBB persists in the body and can be transferred from mother to child *in utero* and through breastfeeding (Joseph et al., 2009). Children born to mothers who were exposed to PBB were more likely to have measurable serum levels of PBB years after the fact if they were breastfed (Joseph et al., 2009). In women who were exposed to PPB *in utero* and through breastfeeding, a dose-related increase in miscarriages has been reported (Small et al., 2011). Similarly, exposure to the PBDE congeners BDE-85, -153, and -183 increased the odds ratio for spontaneous abortion by as much as OR= 1.30 (Gao et al., 2016). Women exposed to high concentrations of PBDEs also had an increased odds ratio for pre-term birth, with odds ratios as high as OR = 3.8 (Peltier et al., 2015, Gao et al., 2016). Exposure to PBB did not impact time to pregnancy and was not associated with infertility in women exposed *in utero* (Small et al., 2011). However, in a study examining the relationship between flame retardant metabolites and pregnancy outcomes from IVF treatment, higher flame retardant exposure was associated with decreased successful fertilization,

implantation, clinical pregnancy, and live birth (Carignan et al., 2017). Similarly, zebrafish exposed to TDCPP for 150 days experienced decreased fertilization (Chen et al., 2018a). When assessing the impacts of paternal exposure to FRs with successful IVF cycles, exposure to FRs was associated with decreased fertilization, though successful implantation, clinical pregnancy, and live birth were not impacted in paternal-only exposures, suggesting gender differences regarding pregnancy outcomes (Carignan et al., 2018). Similarly, women who were occupationally exposed to BDE-28 experienced increased time to pregnancy (OR = 1.34) (Gao et al., 2016). Exposure to halogenated flame retardants *in utero* have been associated with decreased birth weight, though adverse outcomes in birth length, head circumference, and gestational duration were not reported; however; a study of occupationally exposed pregnant women reported increased gestational length and head circumference in women exposed to PBDEs (Harley et al., 2011, Chen Zee et al., 2013, Chen et al., 2018b). In a study examining the birth ratio of children born to parents exposed to PBBs and PCBs, parental exposure to PBBs and PCBs increased the odds of male birth, with an overall proportion of male offspring at 0.542 (national male proportion 0.514) (Terrell et al., 2009). Similarly, bis(1,3-dichloro-2-propyl) phosphate (BDCIPP) increases the risk of delivering daughters preterm, though this association was not true for sons (Hoffman et al., 2018). In individuals exposed to PBB, it has been reported that the father's exposure was associated with alterations in the sex ratio, with paternal exposure increasing the odds of a male birth (Terrell et al., 2009).

1.12.2 Animal studies

In zebrafish, exposure to a mixture containing TBBPA and BDE-209 resulted in a female-biased sex ratio to adults exposed for 150 days (Chen et al., 2018a). Swiss CD-1 mice exposed to 2,2-bis(bromomethyl)-1,3-propanediol (BMP) for 106 days experienced a reduced number of litters per pair, a reduced number of pups born alive per litter, and decreased pup weight compared to unexposed controls (Treinen et al., 1989). Interestingly, when exposed mice were crossed to unexposed control mice, it was discovered that the effect was seen only on female reproductive capacity (Treinen et al., 1989). These impacts carried to the F1 generation, with progeny displaying the same reproductive defects, even when mated to progeny of untreated control mice (Treinen et al., 1989). In zebrafish, exposure to BDE-71 increases the percentage of males born in the F1 generation (Han et al., 2013).

1.13 Halogenated flame retardant exposure and birth defects

1.13.1 Human epidemiological studies

Studies have associated PBDE exposure with decreased IQ (Lam et al., 2017). Similarly, children born to women with high PPB exposure were more likely to have lower Apgar scores (Terrell et al., 2015). Exposure to brominated flame retardants have been associated with lower scores on tests assessing mental and physical development from 12 – 48 and 72 months of age (Jurewicz et al., 2013, Herbstman et al., 2010). Similarly, brominated flame retardant and polychlorinated biphenyl exposure has been correlated with decreased fine manipulative abilities, worse attention, better coordination, better visual perception, and better behavior in five- to six-year-old children who were exposed to halogenated flame retardants *in utero* (Roze et al., 2009).

In children between 9 and 12 years of age, PBDE exposure has been associated with poor attention, poor executive function, and poorer working memory (Sagiv et al., 2015). While the case for an association between autism and halogenated flame retardant exposure has been made, more studies are needed (Lam et al., 2017, Gray and Billock, 2017, Kalkbrenner et al., 2014). Currently, PBDE exposure has been associated with both protective effects and an increased risk in autism in children exposed *in utero* (Lyall et al., 2017, Braun et al., 2014, Hertz-Picciotto et al., 2011). Interestingly, one study reported that PBDE exposure was protective in boys, though this was not the case for girls (Lyall et al., 2017). In infant boys exposed to PBDEs *in utero*, exposure to BDE-99, -100, and -154 was associated with cryptorchidism (Goodyer et al., 2017, Main et al., 2007). Similarly, high exposure to PBB *in utero* and following birth has been associated with genitourinary conditions, with men with high PBB exposure *in utero* reporting more genito-urinary problems (Small et al., 2009).

1.13.2 In vitro studies

There are no *in vitro* studies assessing flame retardant exposure and birth defects.

1.13.3 Animal studies

In zebrafish, the F1 progeny of fish exposed to a mixture of TBBPA and BDE-209 for 150 days exhibited decreased hatching and increased malformation (Chen et al., 2018a). In a study feeding a mixture of polybrominated diphenyl ethers and hexabromocyclododecane to female Sprague-Dawley rats prior to mating and during the first twenty days of gestation, no effects on litter size, fetal viability, or sex ratio was detected (Berger et al., 2014). However, this study reported that low-dose exposures to

a mixture of polybrominated diphenyl ethers and hexabromocyclododecane resulted in an increased number of offspring with anomalies of the digits (i.e. syndactyly) (Berger et al., 2014). Zebrafish embryos exposed to HBCDD developed cardiac arrhythmia and increased heart rate after only 72 hours of exposure, though survival rate was not affected (Wu et al., 2013). In *Xenopus tropicalis* embryos exposed to 1mg/L TBBPA, reduced body size was seen as early as 24 hours after exposure (Shi et al., 2010). These embryos also showed malformations in their eyes, including the absence of eyes, displayed skin hypopigmentation, and had pericardial edemas, among other defects (Shi et al., 2010). In zebrafish embryos exposed to HBCDD for 96 hours, exposure resulted in increased malformations and decreased survival rate (Deng et al., 2009). Offspring from pregnant C57BL/6N mice treated from day 10 to day 18 of gestation with 2,3,7,8-tetrabromodibenzofuran (TBDF) experienced higher mortality rates at concentrations above 500 µg/kg (Birnbaum et al., 1991). However, fetal weight increased upon exposure to 2,3,7,8-tetrabromodibenzo-p-dioxin (TBDD) and TBDF (Birnbaum et al., 1991). In this study, exposure to 2,3,7,8-tetrabromodibenzo-p-dioxin (TBDD), 2,3,7,8-tetrabromodibenzofuran (TBDF), 1,2,3,7,8-pentabromodibenzofuran (1PeBDF), and 2,3,4,7,8-pentabromodibenzofuran (4PeBDF) also resulted in cleft palate in offspring (Birnbaum et al., 1991).

1.14 Halogenated flame retardant exposure and potential intergenerational impacts

1.14.1 Human epidemiological studies

In human sperm, exposure to TDCPP resulted in hypomethylation at CpG5 of *MEG3-IG* and CpG3 of *H19* (Soubry et al., 2017). While these results suggest that

TDCPP exposure may lead to hypomethylation in human sperm, additional studies assessing more sites are required to make conclusions.

1.14.2 In vitro studies

No *in vitro* studies have assessed potential intergenerational impacts.

1.14.3 Animal studies

C57Bl/6J mice exposed to TBBPA from gestation up to seventy days of age showed a significantly decreased protamine 1: protamine 2 ratio and increased the total DNA: protamine ratio (Zatecka et al., 2014). Additionally, this study reported an increase in sperm DNA damage, highlighting the risk of TBBPA-induced DNA mutations that may be passed on to offspring (Zatecka et al., 2014). Male CD-1 mice exposed to BDE-209 *in utero* showed increased sperm head DNA denaturation and DNA fragmentation as a result of increase hydrogen peroxide (H_2O_2) production (Tseng et al., 2013). In a mammalian abnormal sperm head assay, TDBPP was found to be highly mutagenic, suggesting severe genetic damage to the germline (Salamone and Katz, 1981). In male mice exposed to BDE-47 *in utero*, BDE-47 exposure resulted in a four-fold decrease in the expression of all protamine and transition protein genes, suggesting that the switching of histones for protamines may have been impacted in these animals (Khalil et al., 2017). In early zebrafish embryogenesis, TDCPP exposure resulted in delays in re-methylation of the zygotic genome, which was linked to the developmental toxicity seen with TDCPP exposure (McGee et al., 2012). Similarly, TDCPP has been shown to cause hypomethylation in the embryonic zebrafish genome at positions outside of CpG

islands and within exon regions of genes, though *in vitro* analyses of DNMT activity in zebrafish embryonic nuclear extracts indicated that TDCPP does not impact DNMT activity (Volz et al., 2016). Additionally, in an analysis examining the relationship between maternal PBDE exposure and methylation of the promoter region of tumor necrosis factor alpha (TNFα) in fetal cord blood, PBDE exposure was associated with hypomethylation, with methylation status appearing to be dose-dependent (Dao et al., 2015).

1.15 Occupationally exposed workers are at highest risk for chemical exposure and reproductive toxicity

It has been shown that those most at risk for chemical exposure are the occupationally exposed, and occupationally exposed male workers may exhibit infertility phenotypes (El-Helaly et al., 2010, Foster et al., 2008, Harrison et al., 1997, Jurewicz et al., 2009, Kumar, 2004, Olsen, 1994, Sheiner et al., 2003). However, occupational exposure data is limited, and male fertility has not been assessed in occupationally exposed workers to halogenated flame retardants.

1.16 The future of reproductive toxicant research

Human pluripotent stem cells (hPSCs), including human embryonic stem cells (hESCs), provide investigators with the unprecedented ability to assess toxicants *in vitro* in almost any cell type, as these ES cells can be differentiated into almost every cell type in the adult organism (Easley et al., 2015). Our lab was the first to demonstrate that male human embryonic stem cells (hESCs) can be directly differentiated into spermatogonial stem cells/spermatogonia, primary and secondary spermatocytes, and post-meiotic spermatids; all major cell types observed in human spermatogenesis

(Easley et al., 2012) (Figure 1). Our lab was also the first to show that our *in vitro* model mimics clinical consequences seen in exposure cohorts for two known reproductive toxicants (Easley et al., 2015). These results suggest that our *in vitro* spermatogenic model is ideally suited for examining the effects of various toxicants on male gametogenesis. Our model also offers significant advantages over animal models. Current animal models possess challenges pertaining to the timing, differentiating cell types, and genetics and epigenetics that are distinctly different from humans. For example, rodent and non-human primate spermatogenesis involve multiple intermediate cell types that are not present in human spermatogenesis (Figure 2) (Fayomi and Orwig, 2018). Additionally, animal model studies typically focus on morphological/structural defects to assess exposure-related damage to male gametes (Li et al., 2014a). Because of the nature of these studies, sub-cellular effects of reproductive toxicants, such as gene expression, epigenetics, and protamine switching, are rarely studied and cannot be assessed in live cells, notwithstanding the distinct differences between rodent and human spermatogenesis (Ehmcke et al., 2006) (Figure 2). For the experiments described below, we will use this unique *in vitro* hESC model to bridge the significant gaps in knowledge concerning the impact of flame retardant exposure have on male infertility.

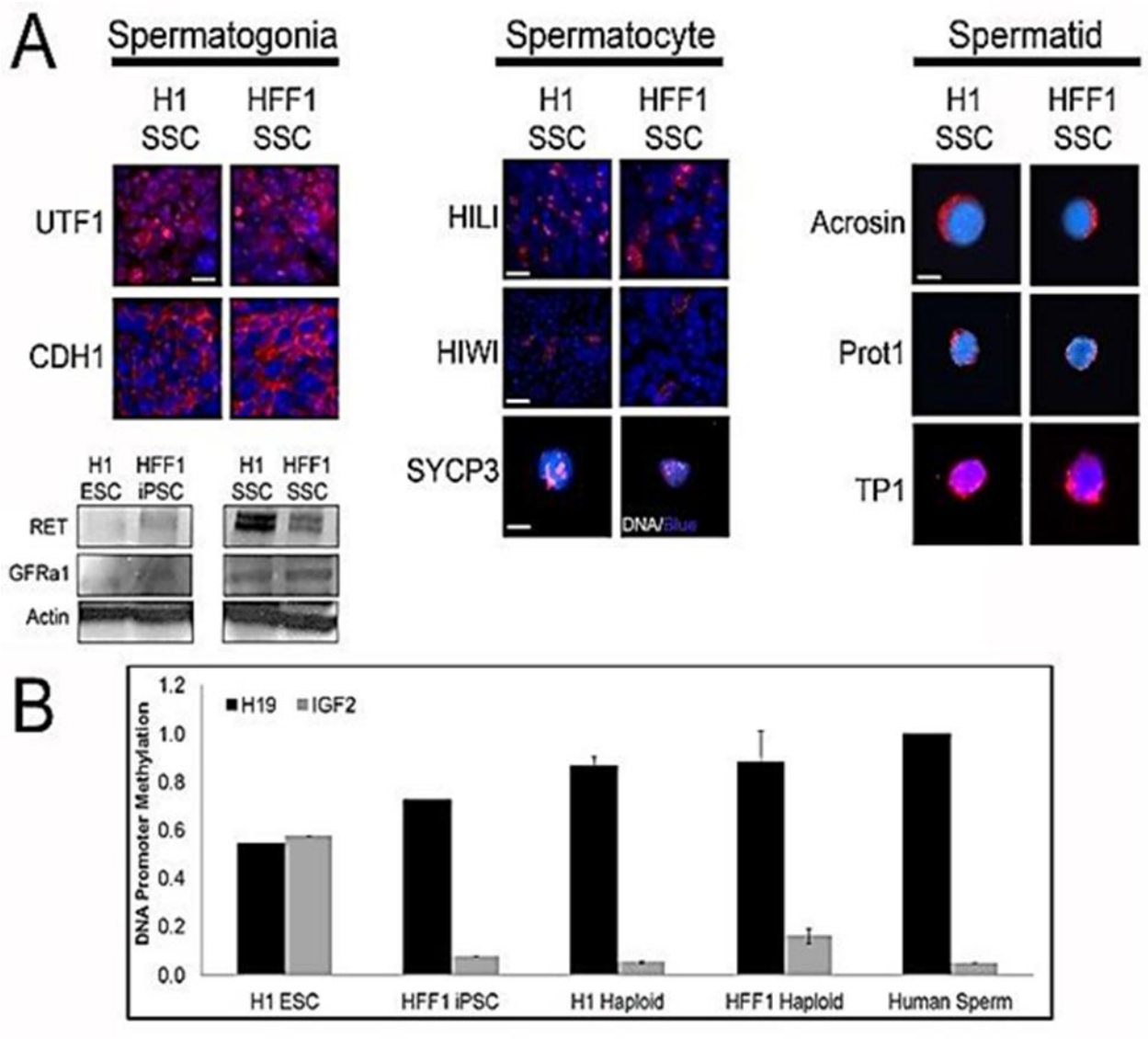
A
Spermatogonia
Spermatocyte
Spermatid
H1 SSC
HFF1 SSC
UTF1
CDH1
HILI
HIWI
SYCP3
DNA/Blue
Acrosin
Prot1
TP1
H1 ESC
HFF1 iPSC
H1 SSC
HFF1 SSC
RET
GFRa1
Actin
B
DNA Promoter Methylation
1.2
1.0
0.8
0.6
0.4
0.2
0.0
H19
IGF2
H1 ESC
HFF1 iPSC
H1 Haploid
HFF1 Haploid
Human Sperm

Figure 1. Differentiation of hESCs and hiPSCs in SSC culture yields cells that express markers for spermatogonia, spermatocytes, and spermatids. (A) Ten days post differentiation cultures of human ES (H1 SSC) and iPS (HFF1 SSC) cells express markers consistent with spermatogonia, pre-meiotic and post-meiotic spermatocytes, and spermatids. Scale, 50 μm. (B) Spermatids derived from human pluripotent stem cells show similar genomic methylation patterns to human sperm for two imprinted genes. Figure and legend taken from (Easley et al., 2012).

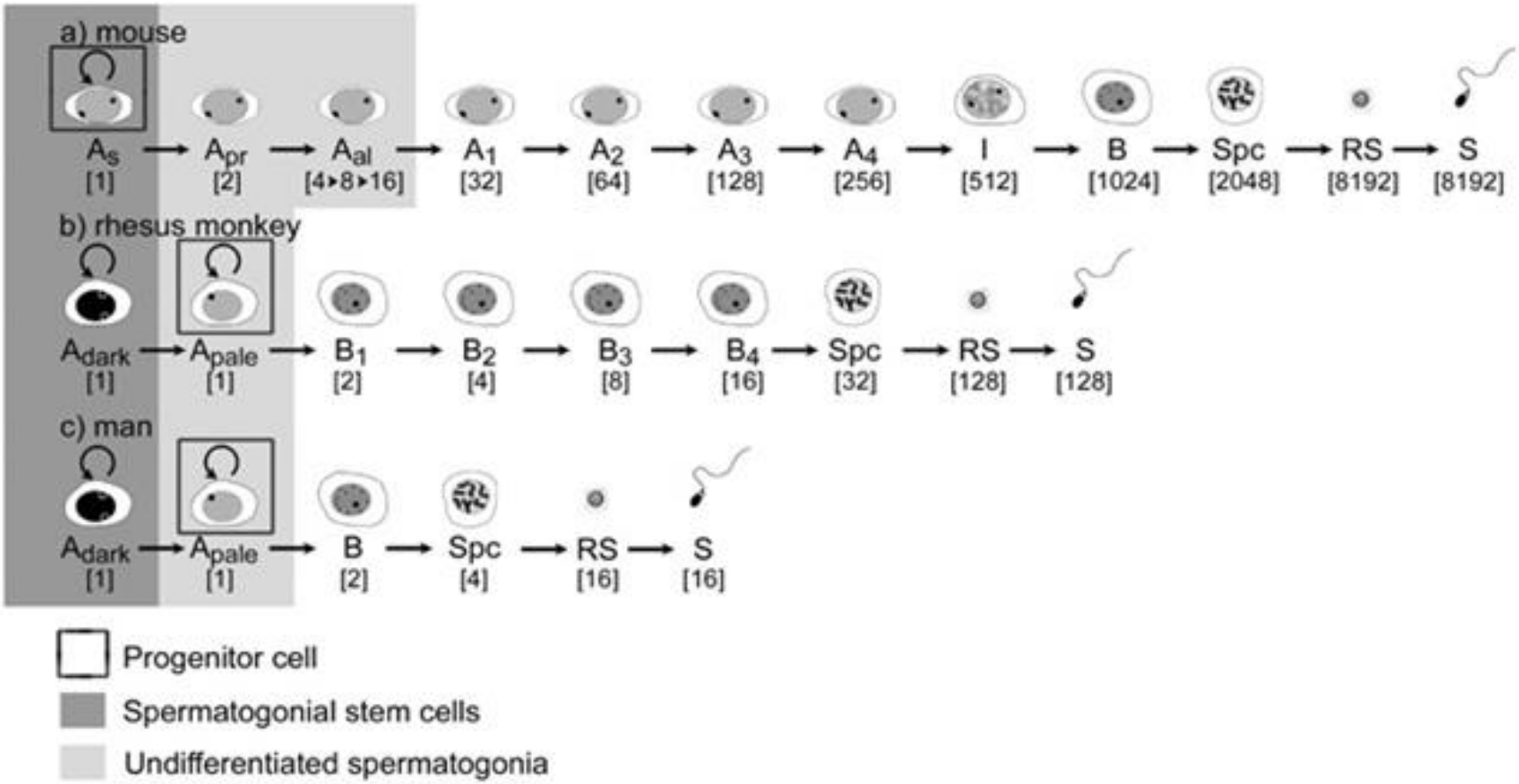
a) mouse
As [1]
Apr [2]
Aal [4▸8▸16]
A1 [32]
A2 [64]
A3 [128]
A4 [256]
I [512]
B [1024]
Spc [2048]
RS [8192]
S [8192]
b) rhesus monkey
Adark [1]
Apale [1]
B1 [2]
B2 [4]
B3 [8]
B4 [16]
Spc [32]
RS [128]
S [128]
c) man
Adark [1]
Apale [1]
B [2]
Spc [4]
RS [16]
S [16]
Progenitor cell
Spermatogonial stem cells
Undifferentiated spermatogonia

Figure 2. Diagram highlighting some of the major differences between human, rodent, and non-human primate (nhp) spermatogenesis. This graphical illustration shows some of the major differences between animal model and human spermatogenesis. This diagram was taken from (Ehmcke et al., 2006).

Chapter 2: Ubiquitous Halogenated Flame Retardant Toxicants Impair Spermatogenesis in a Human Stem Cell Model

This chapter has been modified from two published papers. The flame retardant results were published by *iScience* in May 2018 (Steves et al., 2018a). The PFAS results were published in *Systems Biology in Reproductive Medicine* in June 2018 (Steves et al., 2018b).

2.1 Author's Contribution and Acknowledgement of Reproduction

Alyse Steves, Dr. Anthony Chan, and Dr. Charles Easley conceived and coordinated the flame retardant study, designed the experiments, and wrote the paper. Danielle Clarkson-Townsend and Dr. Charles Easley conceived the PFAS study. Alyse Steves, Dr. Anthony Chan, and Dr. Charles Easley designed the experiments and wrote the paper for the PFAS study. Drs. Gary Miller and Mike Caudle assisted in experiment designs for Figures 3-8. Joshua Bradner collected the first replicate of PLZF area and intensity for TDCPP-exposed cells. Brittany Gill and Adam Turry wrote the first drafts for the sections on apoptosis, the cell cycle, mitochondrial potential, and ROS production and produced the initial images for those experiments. Alyse Steves performed and analyzed the experiments shown in Figures 3 -9. Danielle Clarkson-Townsend assisted in experimental design by determine the PFAS concentrations used. Brittany Gill assisted in performing the experiments for cell cycle and apoptosis for cells treated with PFASs. Adam Turry assisted in performing the experiments for Figures mitochondrial membrane potential and reactive oxygen production for cells treated with PFASs. Ian

Bachli performed the experiment on the control samples for Figure 8.18. All authors reviewed the results and approved the final versions of the manuscripts.

2.2 Abstract

Sperm counts have rapidly declined in the Western male over the past four decades. This rapid decline remains largely unexplained. Exposure to environmental toxicants provides one potential explanation for this decline. Flame retardants are highly prevalent and persistent in the environment, but many have not been assessed for their effects on human spermatogenesis. Using a human stem cell-based model of spermatogenesis, we evaluated four major flame retardants, TDCPP, TDBPP, HBCDD, and TBBPA, under acute conditions simulating occupational-level exposures. Here we show that TDCPP, TDBPP, HBCDD, and TBBPA are human male reproductive toxicants *in vitro*. While not specifically impacting the survival of haploid spermatids, these toxicants affect spermatogonia and primary spermatocytes through mitochondrial membrane potential perturbation and ROS generation, ultimately causing apoptosis. These results are in stark contrast to persistent PFAS exposure, where sub-cellular processes such as spermatogenic cell marker expression are perturbed upon exposure to PFOS, PFOA, and PFNA, but cell viability is ultimately unaffected. Taken together, these results show that halogenated flame retardants affect human spermatogenesis *in vitro* and potentially implicate this highly prevalent class of toxicants in the decline of Western males' sperm counts.

2.3 Introduction

Semen parameters, including sperm counts, in the Western male have declined rapidly since the 1970s, with no indication of leveling off (Levine, 2017). Between 1973 and 2011, sperm counts decreased by over 50%, with an average of a greater than 1% decline per year (Levine, 2017). It is uncertain if these declines are seen in other world regions due to sparse studies in developing nations (Deonandan and Jaleel, 2012). To date, nearly 15% of couples –roughly 50 to 80 million worldwide– are estimated to experience infertility (Khosrorad et al., 2015). Of these couples, male factor infertility accounts for 30% of cases and is a contributing factor in roughly another 30% (Quaas and Dokras, 2008). Should sperm counts continue to decline, cases of infertility may continue to rise. Chemical exposure has been linked to declines in male fertility and may be responsible for declining semen parameters in the Western world (Bloom et al., 2015). Polychlorinated biphenyls (PCBs) and polybrominated diphenyl ethers (PBDEs), which belong to a class of chemicals known as halogenated flame retardants (FRs), have been implicated in male reproductive issues, including reduced sperm motility, abnormal sperm morphology, endocrine-disrupting activity, changes in reproductive organs; and are hypothesized to impact male fecundity, among other concerns (Meeker and Hauser, 2010). While these chemicals have been phased out due to their adverse impacts on human health, replacement halogenated flame retardants have taken their place on the market. Though advertised as safer alternatives to their predecessors, limited data exists regarding their impacts on human health, including male fertility and spermatogenesis.

Tris(1,3-dichloro-2-propyl)phosphate (TDCPP), tris(2,3-dibromopropyl)phosphate (TDBPP), hexabromocyclododecane (HBCDD), and tetrabromobisphenal A (TBBPA) are replacement halogenated flame retardants that can be found as additives to products ranging from foams, resins, latexes, polystyrene, electrical equipment, and baby products (Covaci et al., 2006, Agency, 2014, van der Veen and de Boer, 2012, Betts, 2013, United Nations Environment Programme, 2004, Stapleton et al., 2011, E.C.B. European Commission Directrate-General Joint Research Center, 2006, Schecter et al., 2012). TDCPP, HBCDD, and TBBPA are the most widely used FRs globally, while TDBPP, a banned flame retardant, continues to persist in households worldwide and is a major contaminant of the Velsicol Superfund site in Michigan (Peverly et al., 2014, Hu et al., 2014, E.C.B. European Commission Directrate-General Joint Research Center, 2006, Wang et al., 2015b, Jarosiewicz and Bukowska, 2017). TBBPA accounts for approximately 25% of global FR demand (E.C.B. European Commission Directrate-General Joint Research Center, 2006). TDCPP, TDBPP, HBCDD, and TBBPA have been detected in the house dust of 96%, 75%, 97%, and 80% of homes sampled worldwide, respectively, highlighting their widespread distribution and potential impact on humans (Schecter et al., 2012, Johnson et al., 2013, Wang et al., 2015b, Meeker and Stapleton, 2010, Betts, 2013, Dodson et al., 2012). Due to the lipophilic nature of this class of chemicals, TDCPP, TDBPP, HBCDD, and TBBPA readily enter the human body through inhalation, dermal contact, or ingestion of contaminated food and have been detected in a range of human tissues including blood, adipose tissue, breast milk, urine, and semen (Schecter et al., 2012, Johnson et al., 2013, Fromme et al., 2016b, Bjermo et al., 2017, Fromme et al., 2016a, Rawn et al.,

2014b, Darnerud et al., 2011, Rawn et al., 2014a, Betts, 2013, van der Veen and de Boer, 2012, Carignan et al., 2013, E.C.B. European Commission Directrate-General Joint Research Center, 2006, KE, 2002, Jakobsson et al., 2002, Thomsen et al., 2001, Thomsen et al., 2002a, Thomsen et al., 2002b, Agency, Blum et al., 1978, Abafe and Martincigh, 2016). Despite the high prevalence of TDCPP, TDBPP, HBCDD and TBBPA, there is a significant lack of understanding regarding how these chemicals impact human health, particularly in individuals exposed to higher than average concentrations. Currently, no studies have examined the risk of occupational exposure to TDCPP or measured the concentrations of TDCPP and the bodily tissues of workers (Betts, 2013). Similarly, no studies have assessed if TDCPP can impact the fertility of occupational workers, though a study examining the mortality of workers exposed to brominated compounds, including TDBPP, reported a higher risk of mortality, with a strong association between brominated products and testicular cancer (Wong et al., 1984). The risk of occupational exposure is estimated to be upwards of 70% in workers responsible for the production and processing of HBCDD (Yi et al., 2016a). Similarly, industrial workers have shown HBCDD concentrations in their blood with some concentrations greater than 800 times the concentrations of HBCDD found in non-occupationally exposed populations (Thomsen et al., 2007, Li et al., 2014b). Similarly, in one study that assessed the concentration of TBBPA in the blood serum of occupationally exposed workers, TBBPA was found at concentrations as high as 3.4 pmol/g (Jakobsson et al., 2002). However, some studies of the general population's exposure have shown higher concentrations, reporting concentrations as high as 93 ng/g (0.171 µM) TBBPA in blood (Cariou et al., 2008). Additionally, other halogenated

FRs of similar prevalence have been reported at still higher concentrations, with the halogenated FR TDCPP detectable in human tissues at 10,490 ng/g (24.3 μM) (Liu et al., 2016b).

Despite the knowledge that HBCDD, TBBPA, and potentially TDCPP and TDBPP are entering and accumulating within the bodies of occupationally exposed workers and the history of their predecessors, PCBs and PBDEs, on human spermatogenesis, no studies on the impacts of TDCPP, TDBPP, HBCDD or TBBPA on human spermatogenesis have been reported. As predicted human endocrine disruptors, TDCPP, HBCDD, and TBBPA have been shown to correlate with changes in human male hormonal systems, and TDBPP has been shown to cause sterility in male animals (Johnson et al., 2013, Meeker and Stapleton, 2010, Stapleton et al., 2008, Gold et al., 1978). Toxicological studies have suggested that human male spermatogenesis may be susceptible to toxic assault by TDCPP, TDBPP, HBCDD, and TBBPA, though further research is required. The EPA predicts that HBCDD is a moderate hazard to human reproductive health, including adverse effects on gamete production (Agency, 2014). However, this designation is based on reduced primordial follicles in female mice (Agency, 2014). To date, the effects of HBCDD on human spermatogenesis have not been assessed. Additionally, there are currently no studies investigating the role TDCPP may play in human spermatogenesis. TDCPP was detectable in the semen of 28% of human males tested in a 1981 study, though neither semen parameters nor reproductive outcomes were measured (Hudec et al., 1981). There is evidence that TBBPA targets the testis, though no analysis of the effects of TBBPA on human spermatogenesis has been conducted for any population (Choi et al., 2011). However,

in animal models, TBBPA can cause changes in genes required for spermatogenesis, and TBBPA has been shown to decrease the number of mouse spermatogonia and impact the cell cycle of spermatogenic cells *in vitro* (Liang et al., 2017, Zatecka et al., 2014, Linhartova et al., 2015, Zatecka et al., 2013). Human data for TDBPP is limited, and to date, it has not been confirmed as a human male reproductive toxicant.

There is a significant lack of understanding regarding how these highly prevalent and ubiquitous FRs impact human spermatogenesis, and ultimately, male fertility. One potential explanation for the toxicity of halogenated flame retardants is the addition of the halogen compounds to the core background structure. In addition to assessing halogenated flame retardants, we assessed whether the per- and polyfluoroalkyl substances (PFASs), perfluorooctanesulfonic acid (PFOS), perfluorooctanoic acid (PFOA), and perfluorononanoic acid (PFNA), which are also lipophilic, halogenated compounds, can also cause male reproductive toxicity.

PFASs, previously called perfluorinated compounds (PFCs), are a group of synthetic chemicals that have been used in products ranging from water and oil repellents, lubricants, detergent products, coatings for furniture and food packages, waxes, firefighting foam (flame retardants), and other products since the 1940s (Lei et al., 2015, Louis et al., 2015, Arvaniti and Stasinakis, 2015, Hu et al., 2016). PFOS and PFOA are the two most widely produced and used PFASs in the United States, along with perfluorohexane sulfonic acid (PFHxS) and PFNA (Louis et al., 2015, Lei et al., 2015). Much like the halogenated FRs TDCPP, TDBPP, HBCDD, and TBBPA, PFASs enter the human body through ingestion, inhalation, and contact with commonly used consumer products, where they readily bioaccumulate within the body's tissues (Wu et

al., 2015, Louis et al., 2015). Similar to halogenated flame retardants, PFASs have been found in a wide range of matrices, including blood, urine, breast milk, and seminal plasma (Poothong et al., 2017, Worley et al., 2017, Jusko et al., 2016, Guruge et al., 2005). The American Red Cross and the CDC report that the average exposure of Americans to PFASs ranges from 0.9 ng/mL to over 100 ng/mL, with PFASs being detected in 100% of people tested in some studies (Olsen et al., 2011, Kato et al., 2011, Louis et al., 2015, Calafat et al., 2007). However, populations such as Ronneby, Sweden, where up to one-third of households were exposed to drinking water contaminated with PFASs, have been reported to have PFOS and PFOA concentrations in their blood serum at concentrations as high as 1,500 ng/mL (3.00 µM) and 92 ng/mL (0.22 µM), respectively (Li et al., 2017b). In the United States, widespread environmental contamination of PFOA from DuPont's Washington Works plant in West Virginia spurred epidemiological investigations of the exposure on the health of the surrounding community, where exposed workers had average serum concentrations of PFOA of 350 ng/mL (0.65 µM) (Steenland et al., 2009, Steenland and Woskie, 2012). Similarly, individuals who have been occupationally exposed to PFASs have been found to have PFOS and PFOA concentrations of up to 118,000 ng/mL (235.94 µM) and 32,000 ng/mL (77.28 µM), respectfully, values that are over 1,000 times higher than the highest concentrations reported by the American Red Cross and the CDC for the general population of Americans (Fu et al., 2016). These concentrations are nearly ten times higher than known concentrations in the human body for halogenated FRs.

The perfluoroalkyl acids PFOS and PFOA have been found in the seminal plasma of 100% and over 70% of men in a Sri Lankan population, respectively,

indicating that these chemicals may accumulate in the testis (Guruge et al., 2005). However, it is still uncertain whether these chemicals have detrimental impacts on human spermatogenesis and fertility. In studies analyzing the associations between PFOS, PFOA, and PFNA concentrations in the blood serum of adult men and semen parameters, most studies do not report declines in semen volume or sperm number, though one study reports a trend of lower sperm concentration and counts in response to PFOA exposure (Vested et al., 2013, Toft et al., 2012, Raymer et al., 2012, Kvist et al., 2012, Joensen et al., 2013, Louis et al., 2015, Governini et al., 2015, Specht et al., 2012). However, this association was found for men exposed to PFOA *in utero*, whereas all other studies involve participation of men from the general population. PFOS, PFOA, and PFNA exposure has been associated with changes in male hormones, sperm morphology, DNA fragmentation, and X:Y ratio and chromosomal abnormalities in adult men from the general population (Vested et al., 2013, Toft et al., 2012, Raymer et al., 2012, Kvist et al., 2012, Joensen et al., 2013, Louis et al., 2015, Governini et al., 2015). However, among studies, exact results have varied. These results are in stark contrast to studies in rodent models, which report significant declines in sperm counts upon exposure to PFASs (Liu et al., 2015, Fan et al., 2005, Kato et al., 2015). To date, no studies on occupationally exposed workers and semen parameters or pregnancy outcomes have been conducted, further contributing to the knowledge gap of whether PFASs impact male fertility, and thus, how halogenated compounds may impact fertility.

Our lab has developed a model of *in vitro* human spermatogenesis to close these knowledge gaps (Easley et al., 2012). In this model, male human embryonic stem cells

(hESCs) can be directly differentiated into spermatogonial stem cells/differentiating spermatogonia, pre-meiotic and post-meiotic spermatocytes, and post-meiotic spermatids (Easley et al., 2012). Using this model, we have successfully recapitulated the clinical phenotypes of known human male reproductive toxicants 1,2-dibromo-3-chloropropane (DBCP) and 2-bromopropane (2-BP) under acute, occupationally exposed conditions (Easley et al., 2015). The purpose of this study was to assess the reproductive toxicity of TDCPP, TDBPP, HBCDD, and TBBPA at occupationally-relevant concentrations to determine if these chemicals could affect spermatogenesis under short-term conditions. These results were compared to the results of our PFAS experiments, where we assessed whether PFOS, PFOA, PFNA, and a mixture of PFOS, PFOA, and PFNA directly affect the viability of spermatogenic cells in our human *in vitro* model under chronic conditions relevant to both the general and occupationally exposed populations. We assessed sub-cellular effects that could lead to impaired human spermatogenesis, including cell viability of spermatogenic lineages, mitochondrial membrane potential, reactive oxygen species (ROS) generation, haploid cell production, and cell cycle progression in a dose dependent manner. Here we show that our human *in vitro* model identifies TDCPP, TDBPP, HBCDD, and TBBPA as male reproductive toxicants by affecting viability of spermatogonia and primary spermatocytes through ROS generation and mitochondrial dysfunction within twenty-four hours of acute exposure. In stark contrast, we identify spermatogonia and primary spermatocytes as the main targets of PFOS, PFOA, and PFNA *in vitro,* but despite a ten-times longer exposure at similar concentrations, PFOS, PFOA, and PFNA exposures do not decrease cell viability, impact the cell cycle, or cause toxicity through

ROS production or mitochondrial dysfunction but do reduce the expression of spermatogonia and primary spermatocyte markers.

As such, we provide evidence for halogenated flame retardants to have a significant impact on male fertility *in vivo* for occupationally exposed workers and others and potentially implicate this highly prevalent class of toxicants in the decline of Western males' sperm counts. Interestingly, our studies indicate that increased halogenation or change in halogenation type similar to PFASs may decrease toxicity, but our studies also identify mechanistic differences between halogenated FRs, suggesting that core structure also plays a role in toxicity.

2.4 Methods

2.4.1 Cell culture of H1 ESCs

NIH-approved WA01 (H1, WiCell, Madison, WI), WA13 (H13, WiCell, Madison, WI), and WA23 (H23, WiCell, Madison, WI) male hESCs were cultured and maintained in mTeSR1 (STEMCELL Technologies, Vancouver, Canada) on Matrigel (Corning Life Sciences, Tewksbury, MA) as previously described (Easley et al., 2012). Briefly, cells were cultured in 10 cm plates and were re-fed with 10 mL mTeSR daily for five to seven days. Cells were split when cell density reached approximately 80% confluency. Matrigel coated plates were prepared a day before ESC passage by coating plates with 6-10 mLs of Matrigel per 10 cm plate and allowing plates to sit at room temperature for one hour. Matrigel was prepared by adding one aliquot of Matrigel thawed on ice to 25 mL DMEM:F12. Matrigel and DMEM:F12 solution was kept on ice until added to 10 cm plates. Plates were then moved to a 37˚C incubator overnight. ESCs were passaged by aspirating mTeSR medium and rinsing with 1X DPBS without calcium or magnesium. 1X DPS was aspirated, and 3-5 mL ReLeSR was added to each plate and allowed to sit for 30-40 seconds. ReLeSR was aspirated off plates, and plates were allowed to sit at room temperature 2.5 minutes. 10 mL mTeSR was added to each plate, and plates were scraped with a cell scraper. Cells were added to newly prepared plates with mTeSR with confluency at approximately 5%. Approximately 150 µL to 350 µL of cells should be added to each 10 cm plate per passage and spread back and forth evenly. H1 ESCs were used for acute flame retardant and persistent conditions PFAS experiments. H1, H13, and H23 ESCS were used for persistent condition flame retardant experiments.

Cell authentication was performed by WiCell but validated by the Easley lab. Markers for pluripotency (Oct4, Sox2, Nanog, SSEA4, TRA-1-60, and TRA-1-81) were examined by immunocytochemistry. Routine karyotyping to ensure proper chromosomal content and lack of translocation was performed every four to six months through WiCell's karyotyping core service.

2.4.2 Differentiation of ESCs

Direct differentiation into spermatogenic lineages was performed as described (Easley et al., 2012, Easley et al., 2015). Briefly, differentiating cells were maintained on 0.2% Gelatin in water and mitomycin C-inactivated mouse STOs in mouse spermatogonial stem cell (SSC) medium containing the following (all from MilliporeSigma, St. Louis, MO, unless noted): MEMalpha (Invitrogen, Waltham, MA), 0.2% Bovine Serum Albumin, 5 µg/ml insulin, 10 µg/ml transferrin, 60 µM putrescine, 2 mM L-glutamine (Invitrogen, Waltham, MA), 50 µM β-mercaptoethanol, 1 ng/ml hbFGF (human basic fibroblast growth factor, PeproTech, Rocky Hill, NJ), 20 ng/ml GDNF (glial-derived neurotrophic factor, PeproTech, Rocky Hill, NJ), 30 nM sodium selenite, 2.36 µM palmitic acid, 0.21 µM palmitoleic acid, 0.88 µM stearic acid, 1.02 µM oleic acid, 2.71 µM linoleic acid, 0.43 µM linolenic acid, 10 mM HEPES, and 0.5X penicillin/streptomycin (Invitrogen, Waltham, MA) for ten days. Prior to changing the medium to SCC medium with bFGF and GDNF, 1 mL of 0.2% Gelatin in water was added to each well of a six-well plate (0.5 mL for a twelve-well plate) and allowed to sit in a 37˚C incubator overnight. Approximately 400,000 STOs were added to each well the next day, and STOs were kept in a 37˚C incubator overnight. STOs were cultured in 1 mL Fibroblast medium.

After changing to SSC medium, media changes occurred every other day. The SSC medium was gassed every other day with a blood gas mixture for approximately thirty seconds. For acute flame retardant and chronic PFAS exposure experiments, cells were cultured in six-well plates containing 2 mL of SSC medium with a 1:1,000 dilution of bFGF and GDNF. For persistent flame retardant exposure experiments, cells were cultured in twelve-well dishes containing 1 mL SCC medium with a 1:1,000 dilution of bFGF and GDNF.

2.4.3 Chemical treatment of SSCs – Acute flame retardant exposure

On Day 9 of the SSC differentiation, cells were treated with 1 µM, 10 µM, 25 µM, 50 µM, 100 µM, and 200 µM of TDCPP (TCI Chemicals, Portland, OR), TDBPP (MPI Biomedical, Flemington, NJ), HBCDD (MilliporeSigma, St. Louis, MO) and TBPPA (Tokyo Chemical Industry Co., Ltd. (TCI), Portand, OR) dissolved in DMSO or 0.2% DMSO only for twenty-four hours. Chemicals were added to SSC medium with bFGF and GDNF, and differentiations were cultured under the previously described conditions. 100 mM chemical stocks were kept in brown, glass vials and stored at room temperature. Cells were collected on Day 10 using TrypLE™ Express (Thermofisher, Waltham, MA). Briefly, cells were rinsed with 1X DBPS without calcium or magnesium. 1 mL TrypLE™ Express was added to each well and allowed to sit at room temperature for five minutes. TrypLE™ was quenched with 2 mL 10% FBS DMEM, and cells were scraped with cell scrapers. Cells were analyzed according to the protocols described below.

2.4.4 Chemical treatment of SSCs – Persistent PFAS exposure

Differentiations occurred as described above, except that i*n vitro* differentiations were treated with PFOS at concentrations of 24 µM, 48 µM, or 126 µM; PFOA with concentrations of 11 µM, 25 µM, or 100 µM; PFNA at concentrations of 2.15 µM, 21.5 µM, or 43 µM, or 0.25% DMSO beginning on Day 1 of the differentiation to mimic persistent exposure condition. Cells were collected and analyzed as described above.

2.4.5 Chemical treatment of SSCs – Persistent flame retardant exposure

Differentiations occurred as described above, except that i*n vitro* differentiations were treated with TDCPP, TDBPP, HBCDD, or TBBPA at 10 nM, 100 nM, 500 nM, 1 µM, or 5 µM or 0.2% DMSO only beginning on Day 3 of the differentiation to mimic exposure after spermatogonial populations had been specified. Cells were collected and analyzed as described above on Day 12.

2.4.6 Cell viability and apoptosis

Cell viability for cells treated with TDCPP, TDBPP, HBCDD, TBBPA, PFOS, PFOA, or PFNA was assessed by measuring the percent of apoptotic cells in our cultures using the Muse® Annexin V and Dead Cell Assay Kit (MilliporeSigma, Billerica, MA) by staining with Annexin V and 7-AAD as per manufacturer's instructions to prepare samples for flow cytometry. Samples were run on the Muse® benchtop flow cytometer (MilliporeSigma, Billerica, MA). For each flow cytometry-based experiment, 5,000 events were analyzed for five replications (n = 5). Briefly, cells were collected via TrpyLE as described above. For the Muse® Annexin V and Dead Cell assays, 100 µL of

cells were added to a 1.5 mL tube, and 100 µL of Annexin V reagent were added to the cells. Cells were incubated for 20 minutes at room temperature prior to analysis.

Cell viability results for cells treated with TDCPP, TDBPP, HBCDD, or TBBPA were verified using the Promega ApoTox-Glo^{TM} Triplex Assay (Promega, Madison, WI) by staining with GF-AFC substrate and bis-AAF-R110 substrate as per manufacturer's instructions. Samples were assessed in triplicate (n = 3) using the Promega GloMax® Explorer (Promega, Madison, WI). Cells were cultured as described above in a 96-well plate with 200 µL SCC medium with bFGF and GDNF per well. Solutions containing GF-AFC Substrate and bis-AAF-R110 Substrate in Assay Buffer and Caspase-Glo® 3/7 Reagent were added to appropriate wells and allowed to incubate at 37˚C for thirty minutes. Fluorescence was measured on the Promega GloMax® Explorer at the following wavelengths:

400Ex/505Em (Viability)

485Ex/520Em (Cytotoxicity)

100 µL of Caspase-Glo® 3/7 Reagent was added to each well, and plate was allowed to shake on an orbital shaker for 30 seconds. Plate was then incubated at room temperature for 30 minutes, after which luminescence was measured with the Promega GloMax® Explorer.

2.4.7 Mitochondrial membrane potential

Mitochondrial membrane potential for cells treated with TDCPP, TDBPP, HBCDD, TBBPA, PFOS, PFOA, or PFNA was assessed by the Muse® MitoPotential Kit

(MilliporeSigma, Billerica, MA) by staining with a supplied cationic, lipophilic dye and 7-AAD as per manufacturer's instructions to prepare samples for flow cytometry. Samples were run on the Muse® benchtop flow cytometer (MilliporeSigma, Billerica, MA). For each flow cytometry-based experiment, 5,000 events were analyzed for three replications (n = 3). Time points collected at 0.5 hr., 1.5 hr., 3 hr., 6 hr., 9 hr., and 12 hr. following exposure to 100 µM HBCDD and TBBPA were also performed in triplicate (n = 3) as described. Briefly, cells were collected with TrypLE as described above. Cells were spun down and resuspended in 1 mL 1X Assay Buffer. 100 µL of cells were added to 1.5 mL tubes and incubated with 95 µL Muse™ MitoPotential working solution. Cells were incubated at 37˚C with tubes uncapped for 30 minutes. Following incubation, 5 µL Muse™ MitoPotential 7-AAD was added to each tube and allowed to sit at room temperature for five minutes. Cells were analyzed via flow cytometry.

2.4.8 Reactive oxygen species (ROS) generation

ROS generation for cells treated with TDCPP, TDBPP, HBCDD, TBBPA, PFOS, PFOA, or PFNA was assessed by the Muse® Oxidative Stress Kit (MilliporeSigma, Billerica, MA) by staining with dihydroethidium as per manufacturer's instructions to prepare samples for flow cytometry. Samples were run on the Muse® benchtop flow cytometer (MilliporeSigma, Billerica, MA). For each flow cytometry-based experiment, 5,000 events were analyzed for three replications (n = 3). ROS results were verified using the Promega GSH/GSSG-Glo^{TM} Assay (Promega, Madison, WI) as per manufacturer's instructions for cells treated with TDCPP, TDBPP, HBCDD, or TBBPA. Samples were assessed in triplicate (n = 3) using the Promega GloMax® Explorer (Promega, Madison,

WI). Time points collected at 0.5 hr., 1.5 hr., 3 hr., 6 hr., 9 hr., and 12 hr. following exposure to 100 µM HBCDD and TBBPA were performed in triplicate (n = 3) utilizing the Muse® Oxidative Stress Kit. Briefly, cells were collected with TrpyLE and spun down at 300 xg for five minutes. Medium was removed, and cells were resuspended in 1 mL 1X Assay Buffer. 10 µL of cells were added to a 1.5 mL tube, and 190 µL of Muse® Oxidative Stress working solution was added to the tube. Cells were left to incubate at 37˚C with the lids off for 30 minutes, after which cells were analyzed by flow cytometry.

For the Promega GSH/GSSG-Glo™ Assay, adherent cells grown in a 96-well plate as described above were treated with either 50 µL per well of Total Glutathione Lysis Reagent or Oxidized Glutathione Lysis Reagent. Plate was placed on a shaker and allowed to shake for five minutes at room temperature. 50 µL Luciferin Generation Reagent was added to all wells. Plate was mixed by gentle shaking back and forth and allowed to incubate at room temperature for 30 minutes. 100 µL Luciferin Detection Reagent was added to each well, and luminescence was measured.

2.4.9 l-Sulforaphane Rescue

l-Sulforaphane (Sigma-Aldrich, St. Louis, MO) rescue of ROS mediated cell death was performed by treating cells exposed to 100 µM HBCDD or TBBPA with 1 µM *l*-sulforaphane for twelve hours prior to chemical treatment. 1 µM *l*-sulforaphane was added to SCC medium with bFGF and GDNF, and cell culture occurred as previously described above. Cell viability was assessed as described above with the Muse®

Annexin V and Dead Cell Assay Kit (MilliporeSigma, Billerica, MA). Conditions were performed in triplicate (n = 3).

2.4.10 Haploid cell production and cell cycle progression

Haploid cell production and cell cycle progression were assessed for cells treated with TDCPP, TDBPP, HBCDD, TBBPA, PFOS, PFOA, or PFNA by generating cell cycle plots revealing haploid cell, G0/G1, S phase, and G2 peaks using the Muse® Cell Cycle Assay Kit (MilliporeSigma, Billerica, MA) by staining with propidium iodide as per manufacturer's instructions to prepare samples for flow cytometry. Samples were run on the Muse® benchtop flow cytometer (MilliporeSigma, Billerica, MA). For each flow cytometry-based experiment, 5,000 events were analyzed for five replications (n = 5). Haploid peaks were analyzed using guavaSoft™ 3.1.1 (MilliporeSigma, Billerica, MA). Briefly, cells were collected with TrypLE and spun down at 300 xg for 5 minutes. Cells were washed with 1X DPS without calcium or magnesium and spun down again at 300 xg for 5 minutes. Cells were resuspended in ice cold 70% ethanol and stored at -20˚C overnight. 300 µL cells were added to a 1.5 mL tube, and cells were then spun down again at 300 xg for 5 minutes. Cells were washed with 1X DPBS. Cells were spun at 300 xg for 5 minutes, and 200 µL Muse® Cell Cycle were added to each tube. Tubes were incubated for 30 minutes at room temperature, after which they were analyzed via flow cytometry.

2.4.11 Spermatogonial cell lineage markers

PLZF (promyelocytic leukemia zinc finger, R&D System, Minneapolis, MN) and HILI (piwi like RNA-mediated gene silencing 2, Abcam, Cambridge, MA) immunostaining was performed as previously described for cells treated with TDCPP, TDBPP, HBCDD, TBBPA, PFOS, PFOA, or PFNA (Easley et al., 2012). Briefly, cells were stained with 1.25 µg/mL PLZF or 2.25 µg/mL HILI following fixation with 4% paraformaldehyde and blocking with 4% bovine serum albumin (BSA) in 0.2% Triton X at 4˚C overnight. Following blocking, cells were stained with PLZF or HILI primary antibody at 4˚C overnight. Cells were then washed with 1X PBS in 0.2% Triton X for ten minutes in triplicate while shaking on an orbital shaker, protected from light. Cells were then stained with secondary at 4˚C overnight. Cells were then washed with 1X PBS in 0.2% Triton X for ten minutes in triplicate while shaking on an orbital shaker, protected from light. Cells were stained with a 1:1,000 dilution of Hoechst stain for 15 minutes at room temperature, protected from light. Solution containing Hoechst stain was then exchanged for 1x PBS and protected from light until imagining. High content imaging of differentiated hESCs was performed on the ThermoFisher Cellomics ArrayScan® VTI (ThermoFisher, Waltham, MA). Quantitative analyses for average PLZF+ and HILI+ total colony area and average total intensity of PLZF+ and HILI+ staining per colony were determined using HCS Studio™ 2.0 Cell Analysis Software included with the ArrayScan® suite. Five replications (n = 5) were performed per condition, with three replications (n = 3) performed for PLZF and HILI recovery assays assessing 100 µM HBCDD and TBBPA exposure. Each replication involved analysis of an entire well of a six-well dish. No less than 500 colonies were assessed for each replication/well.

Results were validated via qRT-PCR for PLZF and HILI mRNA transcripts using the Bio-Rad CFX Connect™ Real-Time PCR Detection System (Bio-Rad, Hercules, CA; see Figure S2 and S3). Two separate replications were performed in duplicate (n = 4) for qRT-PCR data. Significant changes in qRT-PCR data were determined using Bio-Rad CFX Manager™ Software (Bio-Rad, Hercules, CA).

2.4.12 Quantification and Statistical Analysis

A 1-way analysis of variance (1-way ANOVA) was used to test for differences in means in each treatment group versus the DMSO-only negative control, with the assumption that at least one treatment group would differ from the control (null hypothesis: there is no significant difference between treatment groups and a DMSO-only negative control). 1-way ANOVA results were validated via a Student's t-test, where * is $p<0.05$, ** is $p<0.01$, and *** is $p<0.001$, to determine which treatment group was statistically different from control. Significance for all experiments performed is considered $p \leq 0.05$. For PLZF and HILI immunostaining, n = 5 (>500 colonies/well) wells was analyzed for each condition, with n = 3 wells analyzed for recovery assays. n = 5 replications (wells) were performed for each condition for the Muse® Annexin V and Dead Cell assay and the Muse® Cell Cycle assay, with 5,000 events (cells) collected per replication. n = 3 replications were performed for each condition for the Muse® Oxidative Stress assay, the Muse® MitoPotential assay, and the Annexin V and Dead Cell assay following *l*-sulforaphane rescue, with 5,000 events collected per replication. n = 3 wells were analyzed for each condition using the Promega GSH/GSSG-Glo™ Assay and the

Promega ApoTox-Glo™ Triplex Assay. Two separate replications were performed in duplicate (n = 4) for qRT-PCR data. Significant changes in qRT-PCR data were determined using Bio-Rad CFX Manager™ Software. Statistical results are described in the “Results” section as well as figures and figure legends. Differences in the number of replications per assay arise largely from initial inexperience performing the assays. For example, due to the variation in colony sizes when plating down ESCs with the ReLeSR method, initial PLZF and HILI experiments were conducted n = 5 times. Continued experiments were repeated n = 3 times after concluding enough colonies are analyzed with each replication to provide sufficient data for statistical tests. Initial Annexin V and Cell Cycle assays were performed n = 5 times for the same reasons. MitoPotential, Oxidative stress, and fluorescent and luminescent assays were performed n = 3 times due to the reliable sensitivities of these assays after optimizing cell collection protocols performing the Annexin V and Cell Cycle assays.

2.5 Results

2.5.1 Acute TDCPP, TDBPP, HBCDD, and TBBPA exposure induce apoptosis in in vitro spermatogenic cells derived from H1 ESCs, but persistent PFAS exposure does not decrease cell viability

Multiple toxicants have been shown to increase apoptosis in human spermatogenic lineages, though the apoptotic effects of halogenated flame retardants on human spermatogenic lineages are largely unknown (Aly, 2013, Bloom et al., 2015, Aitken and Baker, 2013). Though no studies on TDCPP or HBCDD's effects on spermatogenic cells have been reported, TDCPP and HBCDD have been shown to induce apoptosis in cultured PC12 and SH-SY5Y human neuroblastoma cells, respectively (Ta et al., 2014, Al-Mousa and Michelangeli, 2014). While one group showed that TBBPA caused apoptosis in testicular tissue, this cell death was attributed to Sertoli cells while apoptosis in spermatogenic cell lineages was undetermined (Zatecka et al., 2013). A recent study showed that TBBPA decreased the number of mouse spermatogonia *in vitro*, suggesting an impact on spermatogenic cells (Liang et al., 2017). The apoptotic effects of TDBPP on spermatogenic lineages have thus far not been reported. To assess the effects of TDCPP, TDBPP, HBCDD, and TBBPA on the cell viability of *in vitro* spermatogenic cell lineages, male H1 ESCs were differentiated as described (Easley et al., 2012). This differentiation protocol produces a mixed population of spermatogonial stem cells/differentiating spermatogonia, primary spermatocytes, secondary spermatocytes, and haploid spermatids. After nine days of differentiation, mixed germ cell cultures were treated for twenty-four hours with concentrations of TDCPP, TDBPP, HBCDD, or TBBPA. Chemical concentrations of 1 µM, 10 µM, 25 µM,

50 µM, 100 µM, and 200 µM dissolved in dimethyl sulfoxide (DMSO) were chosen based on published, occupationally-relevant *in vivo* and *in vitro* data (Liang et al., 2017, Reistad et al., 2007, Crump et al., 2012, Liu et al., 2016b, Cariou et al., 2008, Jakobsson et al., 2002, Thomsen et al., 2007, Li et al., 2014b). While occupational exposure literature only reports concentrations as high as 25 µM, additional, higher concentrations were assessed due to the wide-ranging variability reported and to further elucidate mechanisms of toxicity. TDCPP, TDBPP, HBCDD and TBBPA treatment groups were analyzed in comparison to a 0.2% DMSO-only treated negative control, which represents the highest concentration of DMSO used in the halogenated flame retardant assessments, for cell viability/apoptosis by staining with propidium iodide and *7*-aminoactinomycin D (7-AAD) as per manufacturer's instructions by the Muse® Annexin V and Dead Cell Assay Kit (MilliporeSigma, Billerica, MA). Flow cytometry analyses reported the percentage of live, early apoptotic, late apoptotic/ dead, and dead cells in our *in vitro* cultures treated with TDCPP, TDBPP, HBCDD, or TBBPA (Figure 3.1).

Acute TDCPP, TDBPP, HBCDD, and TBPPA exposure all significantly reduced cell viability at higher concentrations in twenty-four hours. TDCPP significantly decreased the percentage of live cells only at 200 µM with an 12% decrease in cell viability (Figure 3.2). Similarly, TDBPP significantly reduced live cell populations starting at 50 µM, with viability decreases by as much as 12% at 200 µM (Figure 3.3). HBCDD and TBPPA both significantly reduced cell viability at higher concentrations, with HBCDD and TBBPA significantly reducing live cell populations at concentrations as low as 25 µM and 100 µM, with 200 µM significantly decreasing viability by 11% and 16%,

respectively (Figures 3.4 – 3.5). Cells treated with acute TDCPP, TDBPP, HBCDD, and TBBPA showed a significant increase in cells undergoing late apoptosis starting at 25 µM, 50 µM, 100 µM, and 200 µM, respectively (Figures 3.6 – 3.9). 200 µM TDCPP significantly increased the percentage of late apoptotic cells by 51%, while 200 µM TDBPP increased late apoptotic cells by 55% (Figures 3.6 – 3.7). 200 µM HBCDD and TBBPA increased late apoptotic cells by 59% and 68%, respectively (Figures 3.8 – 3.9).

Results from the Muse® Annexin V and Dead Cell Assay Kit were validated by staining acute TDCPP, TDBPP, HBCDD, and TBBPA treatment groups with GF-AFC substrate and bis-AAF-R110 substrate as per manufacturer's instructions by the Promega ApoTox-Glo^{TM} Triplex Assay (Promega, Madison, WI) to determine apoptotic luminescence and viability fluorescence (Figures 3.10 – 3.17).

TDCPP, TDBPP, HBCDD, and TBBPA all increase apoptotic luminescence and decrease viability fluorescence (Figures 3.10 – 3.17). Exposure to 100 µM and 200 µM TDCPP under acute, twenty-four hour conditions increases apoptotic luminescence in H1 ESCs differentiated into spermatogenic lineages (Figure 3.10). TDBPP increases apoptotic luminescence at as low as 25 µM, an HBCDD and TBBPA both increase apoptotic luminescence beginning at 10 µM and at 100 µM, respectively (Figures 3.11 - 3.13). TDCPP decreases viability fluorescence beginning at as low as 10 µM, and acute TDBPP exposure decreases viability fluorescence beginning at 25 µM (Figures 3.14 – 3.15). HBCDD and TBBPA both decrease viability fluorescence beginning at 100 µM (Figures 3.16 and 3.17). Taken together, these results show that TDCPP, TDBPP, HBCDD, and TBBPA are all capable of negatively impacting germ cell viability at

occupationally relevant concentrations during acute, twenty-four hour exposures in a mixed population of spermatogenic cells differentiated from H1 ESCs.

Unlike the halogenated flame retardants TDCPP, TDBPP, HBCDD, and TBBPA, there is significant evidence indicating that PFAS exposure negatively impacts male fertility in model systems, though human data is less conclusive. In rodents, PFOS exposure has been shown to upregulate p53 and BAX expression in the testis while downregulating BCL-2 expression, indicative of apoptosis (Liu et al., 2015, Qu et al., 2016). Similarly, PFNA exposure has been shown to induce apoptosis in germ cells in rat testis (Feng et al., 2009). In a study assessing apoptosis in semen samples of a human cohort, no associations between PFAS exposure, including PFOS, PFOA, and PFNA, and apoptosis in sperm were found (Specht et al., 2012). However, in a study assessing the effects of PFAS exposure on *Xenopus laevis* A6 kidney cell numbers, PFOS and PFOA decreased cell numbers, whereas PFNA had no effect on A6 cell numbers (Gorrochategui et al., 2016). To determine if PFAS exposure impacts the viability of *in vitro* spermatogenic cell lineages, male H1 ESCs were differentiated as described above (Easley et al., 2012). *In vitro* differentiations were treated with PFOS at concentrations of 24 µM, 48 µM, or 126 µM; PFOA with concentrations of 11 µM, 25 µM, or 100 µM; PFNA at concentrations of 2.15 µM, 21.5 µM, or 43 µM, or 0.25% DMSO beginning on day 1 of the differentiation. Persistent conditions were chosen for PFAS exposure due to a larger number of studies reporting physiologically relevant concentrations and a larger number of human studies reporting on observed human health impacts. Chemical concentrations are physiologically relevant to populations exposed to high concentrations of PFASs in their environment and those who are

occupationally exposed based on published data (Olsen et al., 2011, Kato et al., 2011, Louis et al., 2015, Calafat et al., 2007, Fu et al., 2016, Li et al., 2017b). PFOS, PFOA, and PFNA treatment groups were analyzed in comparison to a 0.25% DMSO-only treated negative control for cell viability/apoptosis. As a positive control, cells were treated with a 200 µM hydrogen peroxide (H_2O_2) for a period of six hours (Figures 3.18 – 3.20). Flow cytometry analyses reported the percentage of live, early apoptotic, late apoptotic/ dead, and dead cells in our *in vitro* cultures (Figure 3.21). The results of these analyses did not reveal any significant increases in apoptosis in cells treated with PFOS, PFOA, or PFNA at the concentrations used in this study (Figures 3.22 – 3.24). As such, our data supports the reports in human cohort studies that per- and polyfluoroalkyl substances do not induce cell death in germ cells. However, it is important to note that studies have shown that PFASs can cause cytotoxicity without utilizing an apoptotic mechanism (Buhrke et al., 2013). In cytotoxicity assays examining the effects of PFASs on the viability of the human hepatoma line HepG2, treatment with PFOA concentrations as low as 50 µM decreased cell viability (Buhrke et al., 2013), Similarly, this study calculated the IC_{50}s of PFOA and PFNA to be 47 µM and 23 µM, respectively, after analysis with a Neural Red assay (Buhrke et al., 2013). Notably, the EC_{50}s of PFOS, PFOA, and PFNA were calculated to be 107 µM, 594 µM, and 213 µM, respectively, using Alamar Blue in the human placental carcinoma cells JEG-3 (Gorrochategui et al., 2014). Though the sensitivity of various cell lines to PFAS exposure is highly variable, it is possible that our *in vitro* spermatogenic cells are not susceptible at the concentrations tested, as we do not observe any appreciable cell death in our cultures after prolonged exposure.

The results of these apoptosis studies highlight the toxicity of halogenated flame retardants such as TDCPP, TDBPP, HBCDD, and TBBPA. Though our *in vitro* spermatogenic cells were exposed to PFOS, PFOA, and PFNA at concentrations as high or higher than the FRs for a duration that was ten times longer, only the flame retardant toxicants had appreciable results. Notably, PFA exposure also began before spermatogenesis was initiated, further highlighting our cell's sensitivity to halogenated flame retardants, as this marks a window where it is possible to completely block the initiation of spermatogenesis. Future studies should assess relevant concentrations of TDCPP, TDBPP, HBCDD, and TBBPA to determine if these toxicants can block the initiation of spermatogenesis, as this may be relevant to *in utero* exposures.

Drastic differences in chemical toxicity may be related to the core structures of each chemical class. PFOS, PFOA, and PFNA are nearly insoluble, high weight polymers with attached fluorine molecules (Henry et al., 2018). PFOS and PFNA have seventeen highly electronegative fluorine molecules in their structure, and PFOA has fifteen fluorine molecules in its structure. Similarly, TDCPP, TDBPP, HBCDD, and TBBPA are highly lipophilic, halogenated compounds with comparable molecular weight to PFOS, PFOA, and PFNA. However, TDCPP, TDBPP, and HBCDD have six halogens (TDCPP, chlorine; TDBPP and HBCDD, bromine), and TBBPA has four bromine molecules in its structure. As such, despite having similar lipophilic properties, it is possible that the additional negative halogens in PFOS, PFOA, and PFNA reduce their toxicity by reducing their ability to cross the cell membrane.

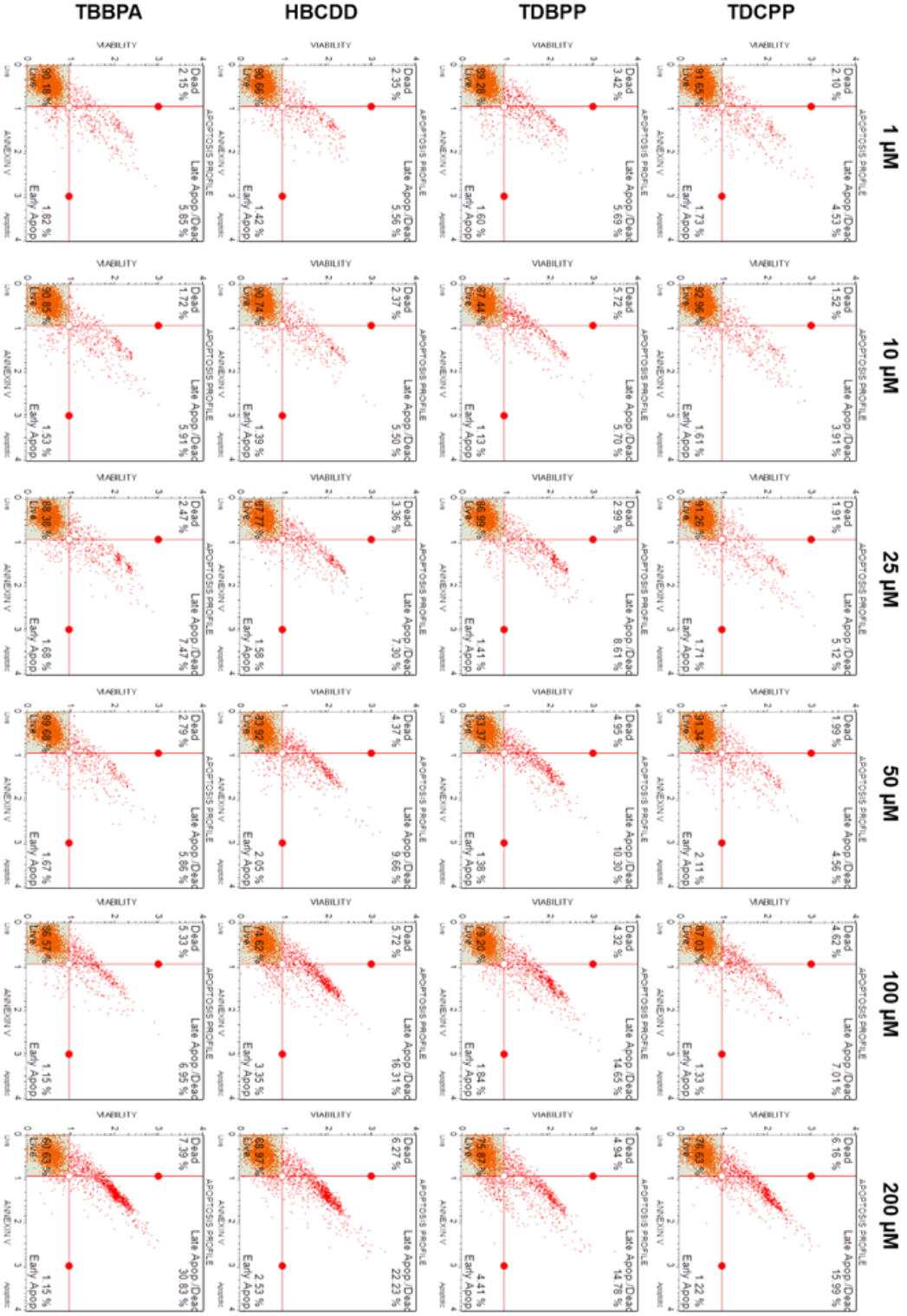
TDCPP
TDBPP
HBCDD
TBBPA
1 µM
10 µM
25 µM
50 µM
100 µM
200 µM
VIABILITY
APOPTOSIS PROFILE
ANNEXIN V
Live
Dead
Early Apop
Late Apop /Dead

Figure 3.1. Flow cytometry plots for acute TDCPP, TDBPP, HBCDD, and TBBPA treated spermatogenic cells derived from H1 ESCs for apoptotic data. Flow cytometry analyses for indicating percent viable cells, percent early apoptotic cells, percent late apoptotic cells, and percent dead/necrotic cells for all concentrations of TDCPP, TDBPP, HBCDD, and TBBPA assessed. Lower left quadrant represents viable cells, lower right quadrant represents early apoptotic cells, upper right quadrant is late apoptotic/dead cells, and the upper right quadrant is dead/necrotic cells.

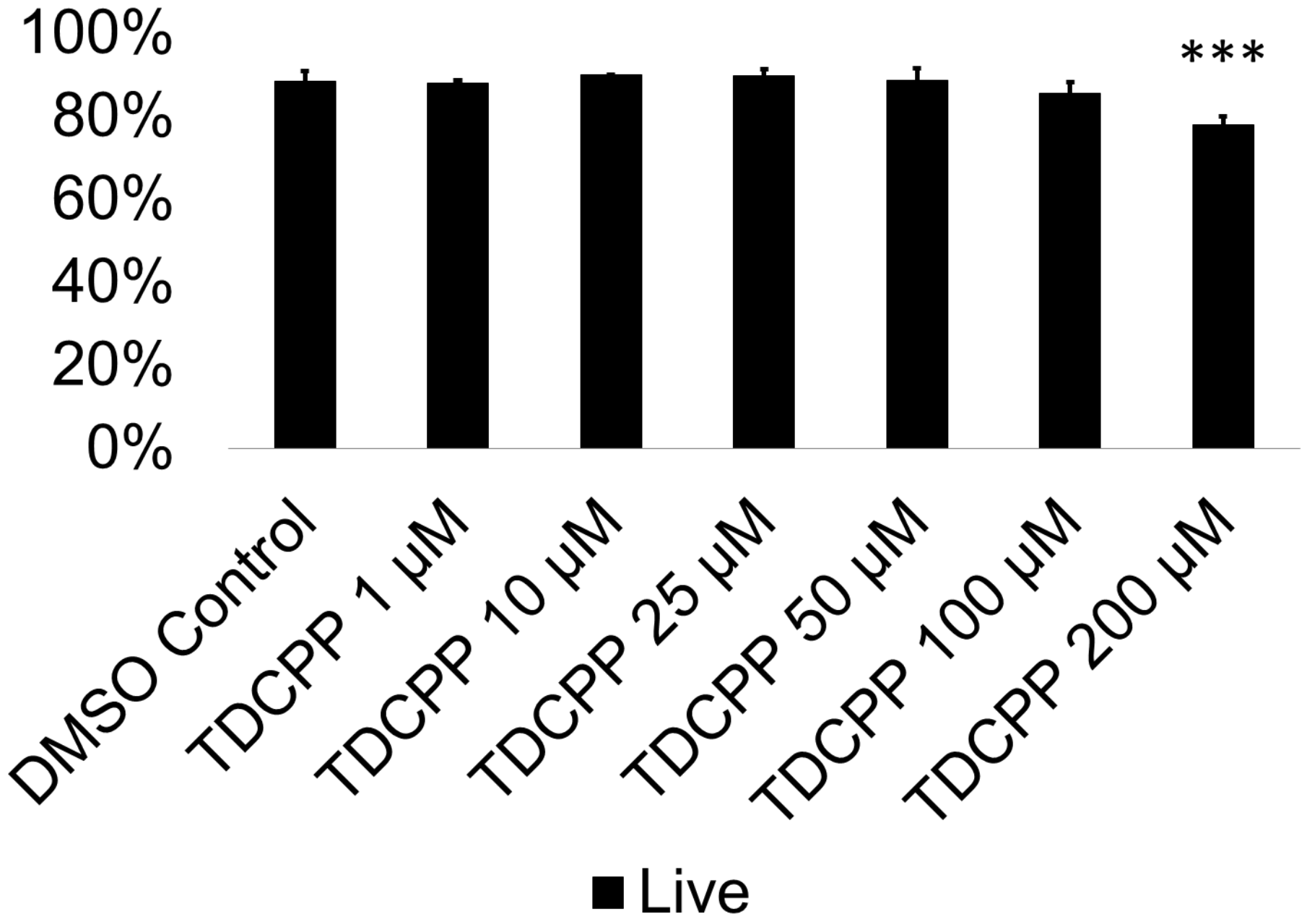
100%
80%
60%
40%
20%
0%
***
DMSO Control
TDCPP 1 µM
TDCPP 10 µM
TDCPP 25 µM
TDCPP 50 µM
TDCPP 100 µM
TDCPP 200 µM
Live

Figure 3.2. Acute TDCPP exposure decreases cell viability in spermatogenic cells derived from H1 ESCs. Graphical representation showing that acute, twenty-four hour exposure to 200 μM TDCPP decreased live cell percentages in H1 ESCs differentiated in *in vitro* spermatogenic conditions in comparison to a 0.2% DMSO-only control. 5,000 events were analyzed, with five replications performed for each condition (n = 5). Significant changes in cell viability were determined using a 1-way analysis of variance (1-way ANOVA) and validated via a Student's t-test, where * is $p<0.05$, ** is $p<0.01$, and *** is $p<0.001$. Data are represented as mean ± SEM.

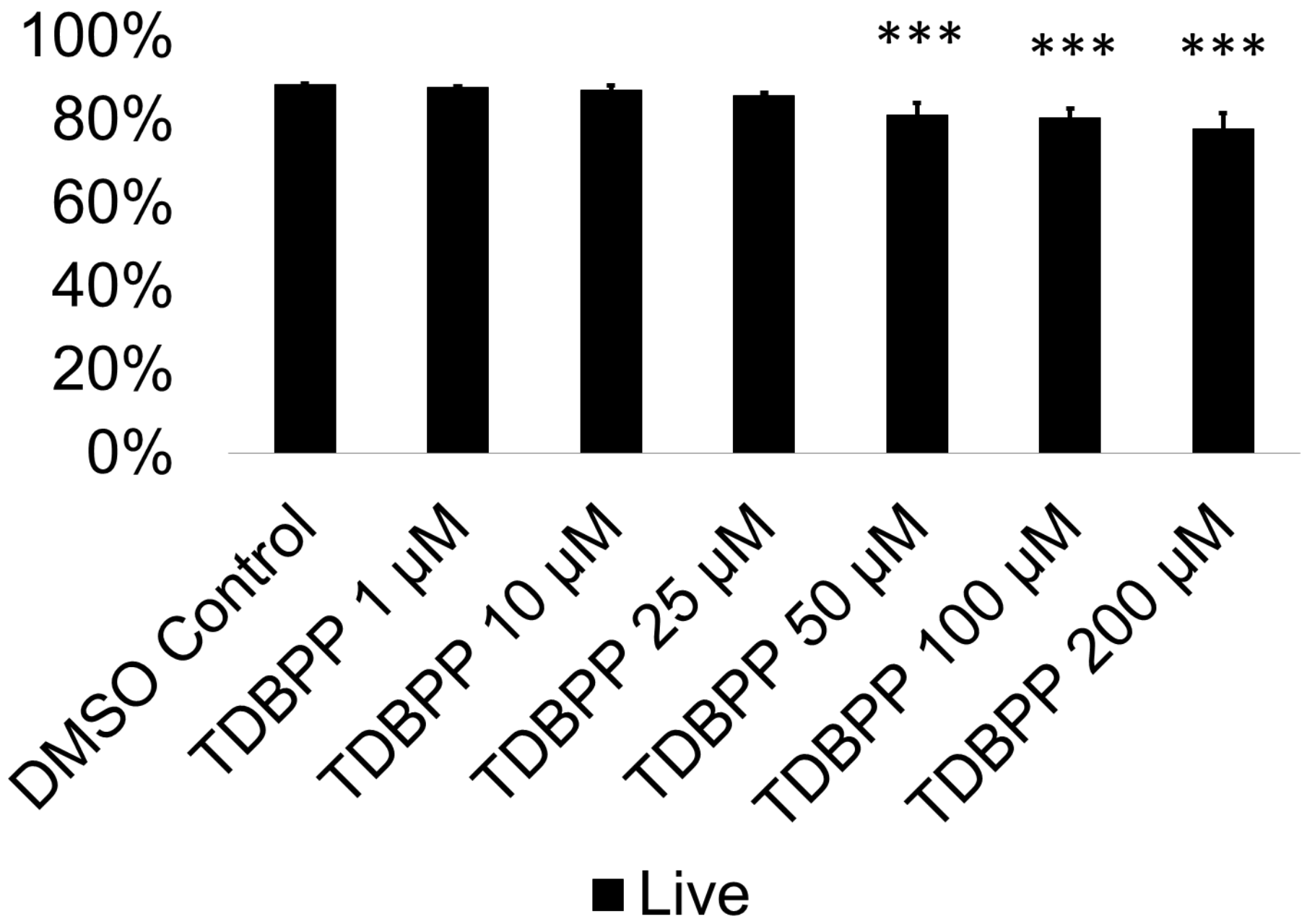
100%
80%
60%
40%
20%
0%
***
***
***
DMSO Control
TDBPP 1 µM
TDBPP 10 µM
TDBPP 25 µM
TDBPP 50 µM
TDBPP 100 µM
TDBPP 200 µM
Live

Figure 3.3. Acute TDBPP exposure decreases cell viability in spermatogenic cells derived from H1 ESCs. Graphical representation showing that acute, twenty-four hour exposure to 50 μM, 100 μM, and 200 μM TDBPP decreases live cell percentages in H1 ESCs differentiated in *in vitro* spermatogenic conditions in comparison to a 0.2% DMSO-only control. 5,000 events were analyzed, with five replications performed for each condition (n = 5). Significant changes in cell viability were determined using a 1-way analysis of variance (1-way ANOVA) and validated via a Student's t-test, where * is $p<0.05$, ** is $p<0.01$, and *** is $p<0.001$. Data are represented as mean ± SEM.

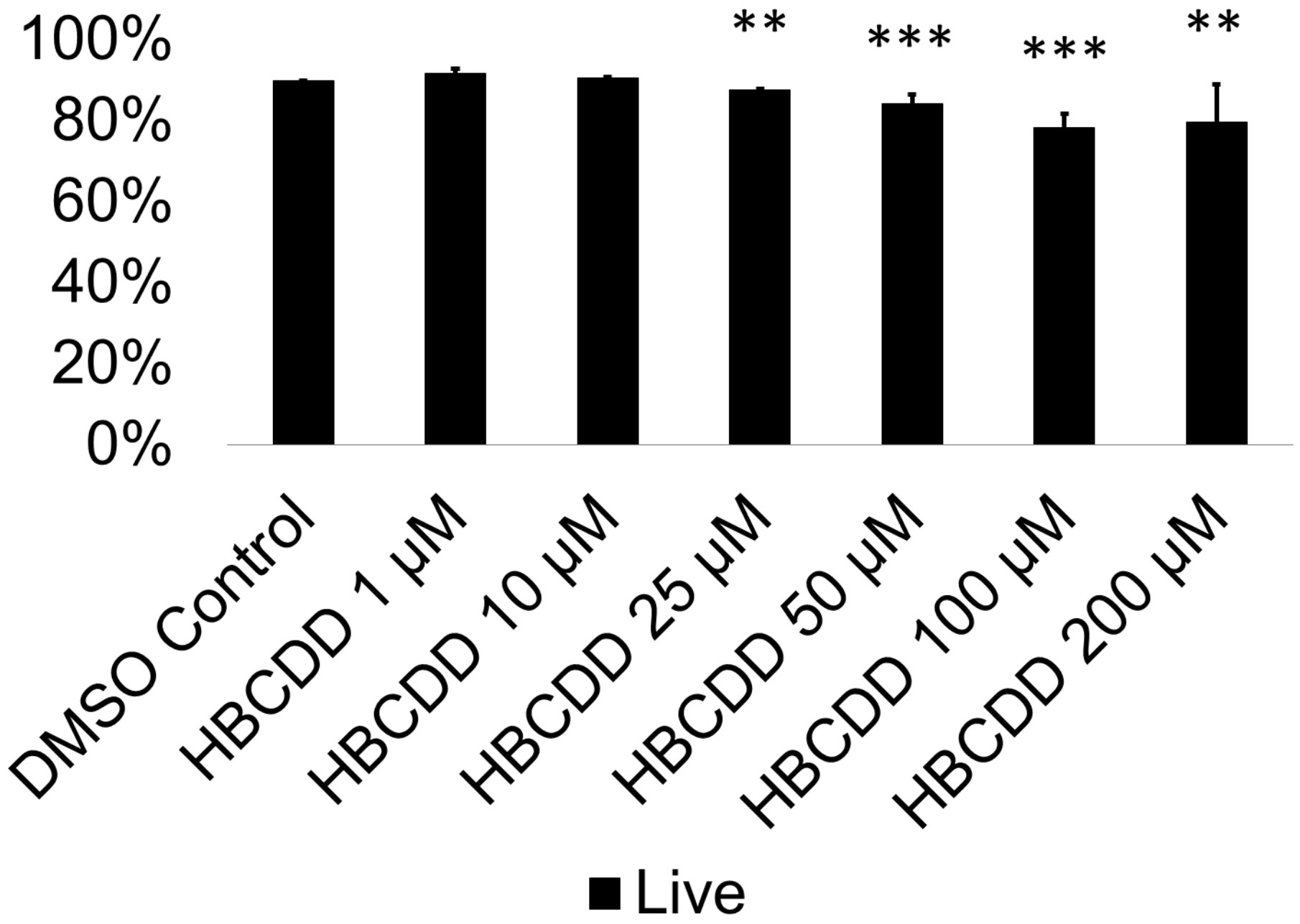
100%
80%
60%
40%
20%
0%
**
***
***
**
DMSO Control
HBCDD 1 µM
HBCDD 10 µM
HBCDD 25 µM
HBCDD 50 µM
HBCDD 100 µM
HBCDD 200 µM
Live

Figure 3.4. Acute HBCDD exposure decreases cell viability in spermatogenic cells derived from H1 ESCs. Graphical representation showing that acute, twenty-four hour exposure to 25 μM, 50 μM, 100 μM, and 200 μM HBCDD decreases live cell percentages in H1 ESCs differentiated in *in vitro* spermatogenic conditions in comparison to a 0.2% DMSO-only control. 5,000 events were analyzed, with five replications performed for each condition (n = 5). Significant changes in cell viability were determined using a 1-way analysis of variance (1-way ANOVA) and validated via a Student's t-test, where * is $p<0.05$, ** is $p<0.01$, and *** is $p<0.001$. Data are represented as mean ± SEM.

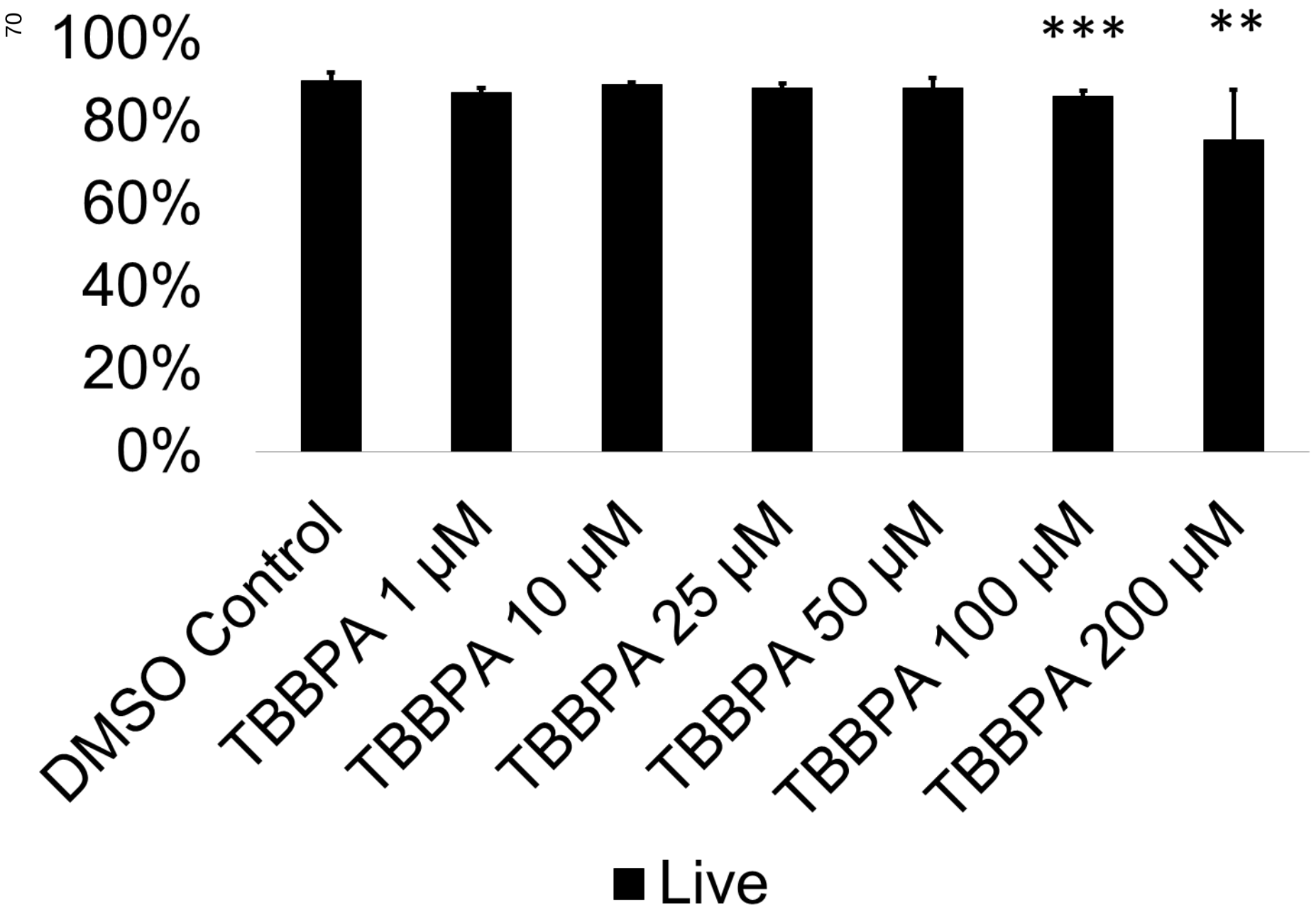
70
100%
80%
60%
40%
20%
0%
***
**
DMSO Control
TBBPA 1 µM
TBBPA 10 µM
TBBPA 25 µM
TBBPA 50 µM
TBBPA 100 µM
TBBPA 200 µM
Live

Figure 3.5. Acute TBBPA exposure decreases cell viability in spermatogenic cells derived from H1 ESCs. Graphical representation showing that acute, twenty-four hour exposure to 100 μM and 200 μM TBBPA decreases live cell percentages in H1 ESCs differentiated in *in vitro* spermatogenic conditions in comparison to a 0.2% DMSO-only control. 5,000 events were analyzed, with five replications performed for each condition (n = 5). Significant changes in cell viability were determined using a 1-way analysis of variance (1-way ANOVA) and validated via a Student's t-test, where * is $p<0.05$, ** is $p<0.01$, and *** is $p<0.001$. Data are represented as mean ± SEM.

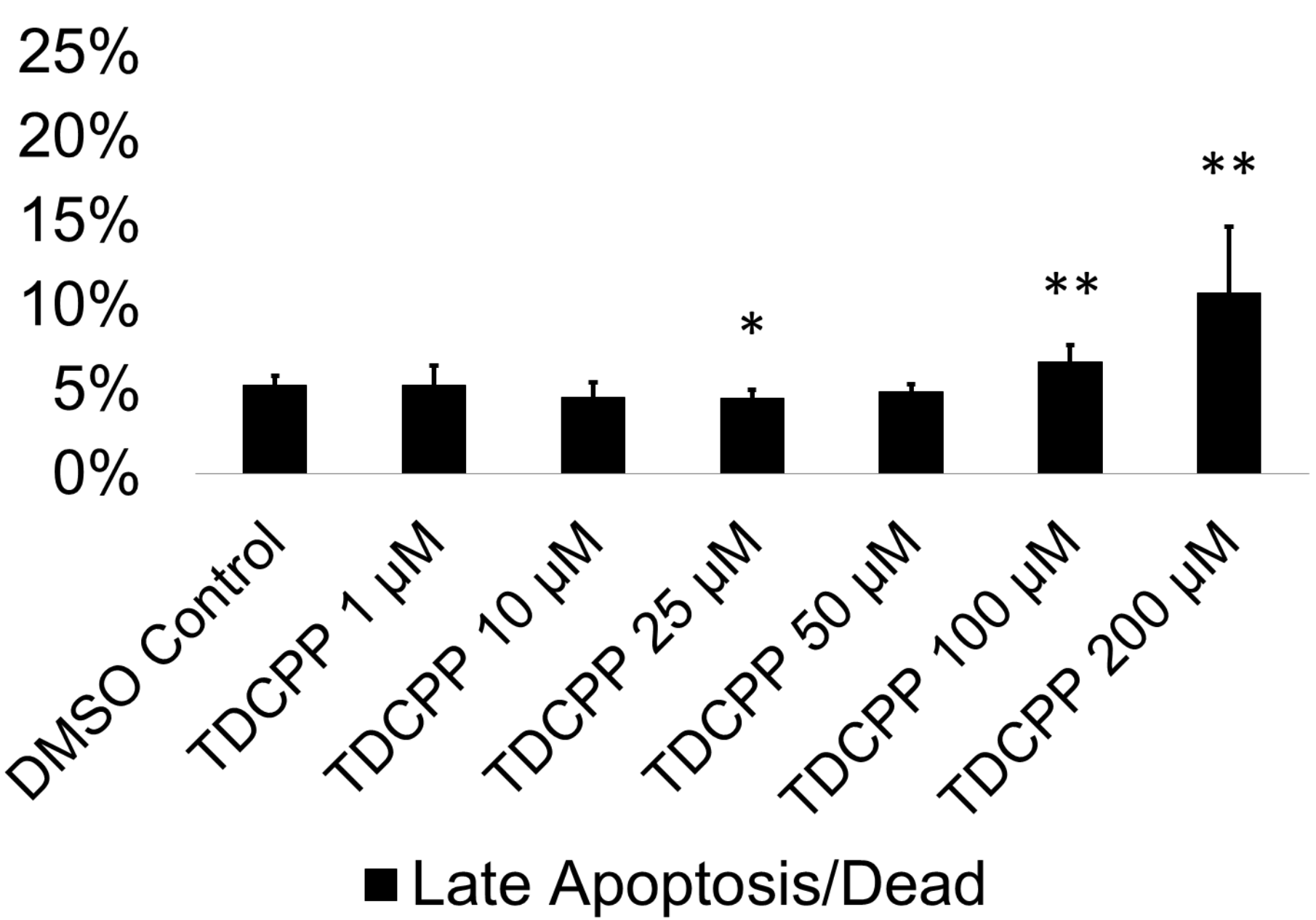
25%
20%
15%
10%
5%
0%
*
**
**
DMSO Control
TDCPP 1 µM
TDCPP 10 µM
TDCPP 25 µM
TDCPP 50 µM
TDCPP 100 µM
TDCPP 200 µM
Late Apoptosis/Dead

Figure 3.6. Acute TDCPP exposure induces apoptosis in spermatogenic cells derived from H1 ESCs. Graphical representation showing that acute, twenty-four hour exposure to 25 μM, 100 μM, and 200 μM TDCPP increases the percentage of germ cells undergoing late apoptosis/death in spermatogenic cells derived from H1 ESCs in comparison to a 0.2% DMSO-only control. 5,000 events were analyzed, with five replications performed for each condition (n = 5). Significant changes in cell viability were determined using a 1-way analysis of variance (1-way ANOVA) and validated via a Student's t-test, where * is $p<0.05$, ** is $p<0.01$, and *** is $p<0.001$. Data are represented as mean ± SEM.

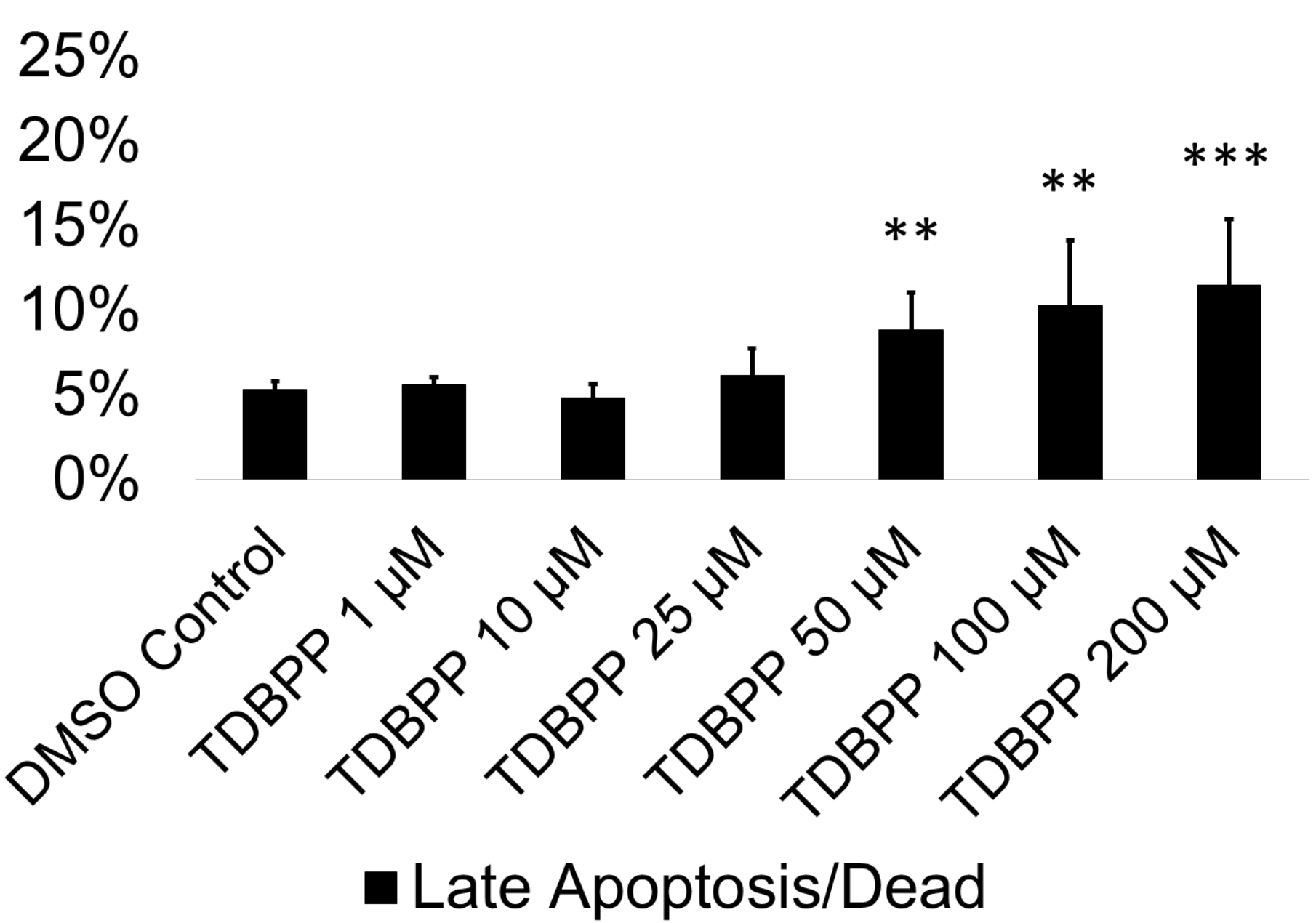
25%
20%
15%
10%
5%
0%
**
**
***
DMSO Control
TDBPP 1 µM
TDBPP 10 µM
TDBPP 25 µM
TDBPP 50 µM
TDBPP 100 µM
TDBPP 200 µM
Late Apoptosis/Dead

Figure 3.7. Acute TDBPP exposure induces apoptosis in spermatogenic cells derived from H1 ESCs. Graphical representation showing that acute, twenty-four hour exposure to 50 μM, 100 μM, and 200 μM TDBPP increases the percentage of germ cells undergoing late apoptosis/death in spermatogenic cells derived from H1 ESCs in comparison to a 0.2% DMSO-only control. 5,000 events were analyzed, with five replications performed for each condition (n = 5). Significant changes in cell viability were determined using a 1-way analysis of variance (1-way ANOVA) and validated via a Student's t-test, where * is $p<0.05$, ** is $p<0.01$, and *** is $p<0.001$. Data are represented as mean ± SEM.

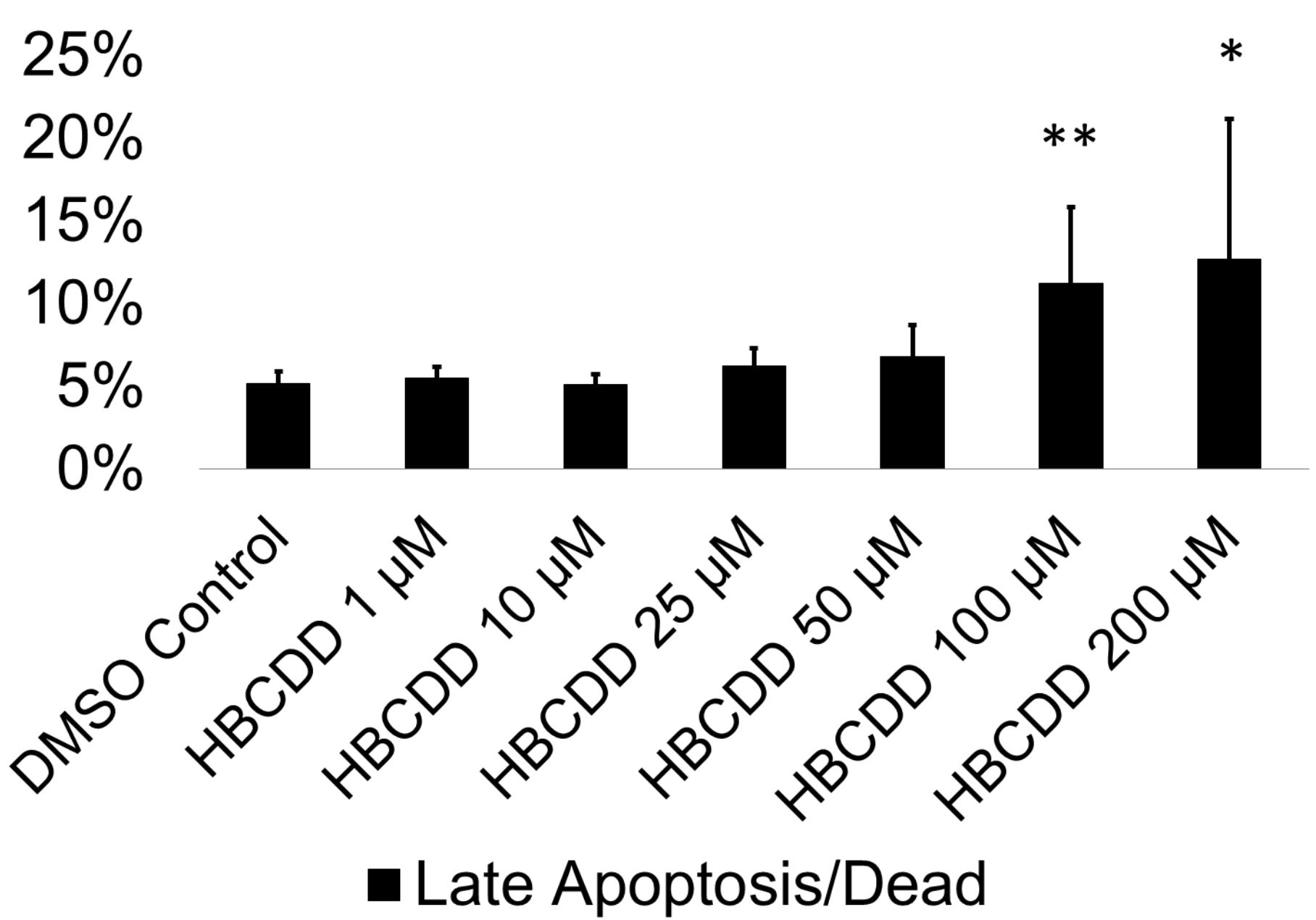
25%
20%
15%
10%
5%
0%
**
*
DMSO Control
HBCDD 1 µM
HBCDD 10 µM
HBCDD 25 µM
HBCDD 50 µM
HBCDD 100 µM
HBCDD 200 µM
Late Apoptosis/Dead

Figure 3.8. Acute HBCDD exposure induces apoptosis in spermatogenic cells derived from H1 ESCs. Graphical representation showing that acute, twenty-four hour exposure to 100 μM and 200 μM HBCDD increases the percentage of germ cells undergoing late apoptosis/death in spermatogenic cells derived from H1 ESCs in comparison to a 0.2% DMSO-only control. 5,000 events were analyzed, with five replications performed for each condition (n = 5). Significant changes in cell viability were determined using a 1-way analysis of variance (1-way ANOVA) and validated via a Student's t-test, where * is $p<0.05$, ** is $p<0.01$, and *** is $p<0.001$. Data are represented as mean ± SEM.

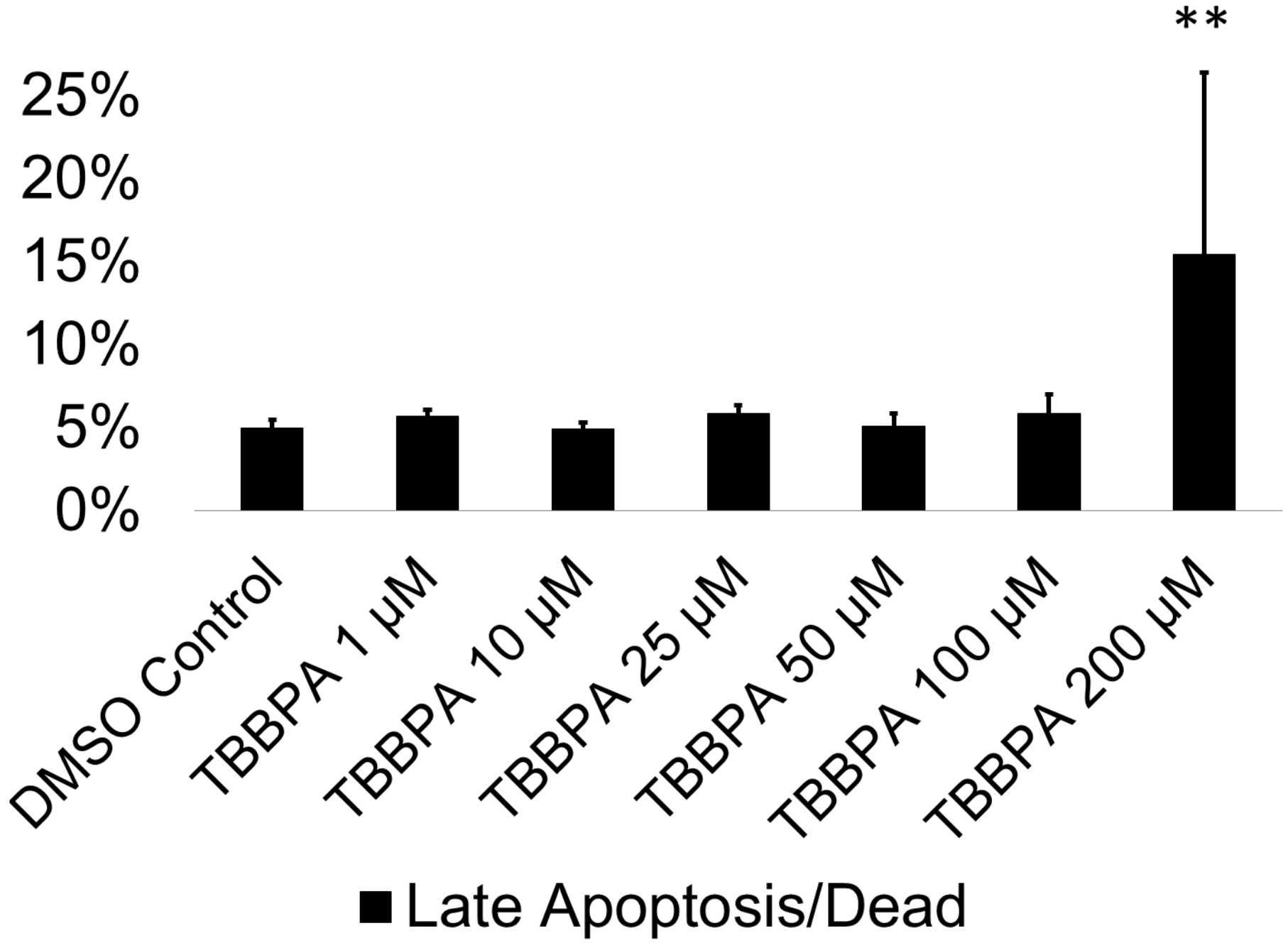
**
25%
20%
15%
10%
5%
0%
DMSO Control
TBBPA 1 µM
TBBPA 10 µM
TBBPA 25 µM
TBBPA 50 µM
TBBPA 100 µM
TBBPA 200 µM
Late Apoptosis/Dead

Figure 3.9. Acute TBBPA exposure induces apoptosis in spermatogenic cells derived from H1 ESCs. Graphical representation showing that acute, twenty-four hour exposure to 200 μM TBBPA increases the percentage of germ cells undergoing late apoptosis/death in spermatogenic cells derived from H1 ESCs in comparison to a 0.2% DMSO-only control. 5,000 events were analyzed, with five replications performed for each condition (n = 5). Significant changes in cell viability were determined using a 1-way analysis of variance (1-way ANOVA) and validated via a Student's t-test, where * is $p<0.05$, ** is $p<0.01$, and *** is $p<0.001$. Data are represented as mean ± SEM.

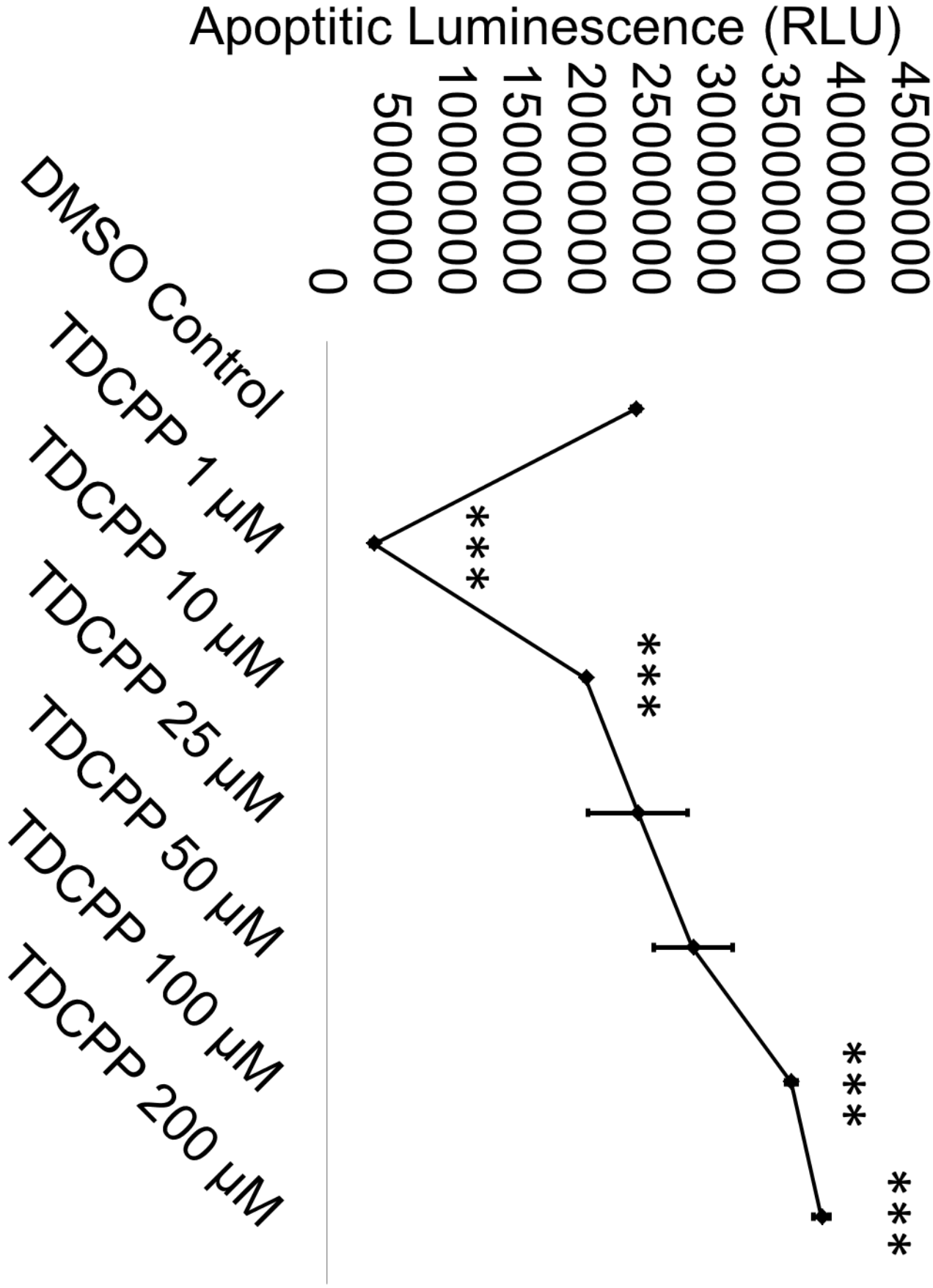
Apoptitic Luminescence (RLU)
0
5000000
10000000
15000000
20000000
25000000
30000000
35000000
40000000
45000000
DMSO Control
TDCPP 1 µM
TDCPP 10 µM
TDCPP 25 µM
TDCPP 50 µM
TDCPP 100 µM
TDCPP 200 µM
****
****
****
****

Figure 3.10. Acute TDCPP exposure increases apoptosis in spermatogenic cells derived from H1 ESCs. Graphical representation showing that exposure to 100 μM and 200 μM TDCPP under acute, twenty-four hour conditions increases apoptotic luminescence in H1 ESCs differentiated in *in vitro* spermatogenic conditions in comparison to a 0.2% DMSO-only control. Three replications were analyzed for each condition (n = 3). Significant changes in apoptotic luminescence were determined using a 1-way analysis of variance (1-way ANOVA) and validated via a Student's t-test, where * is $p<0.05$, ** is $p<0.01$, and *** is $p<0.001$. Data are represented as mean ± SEM.

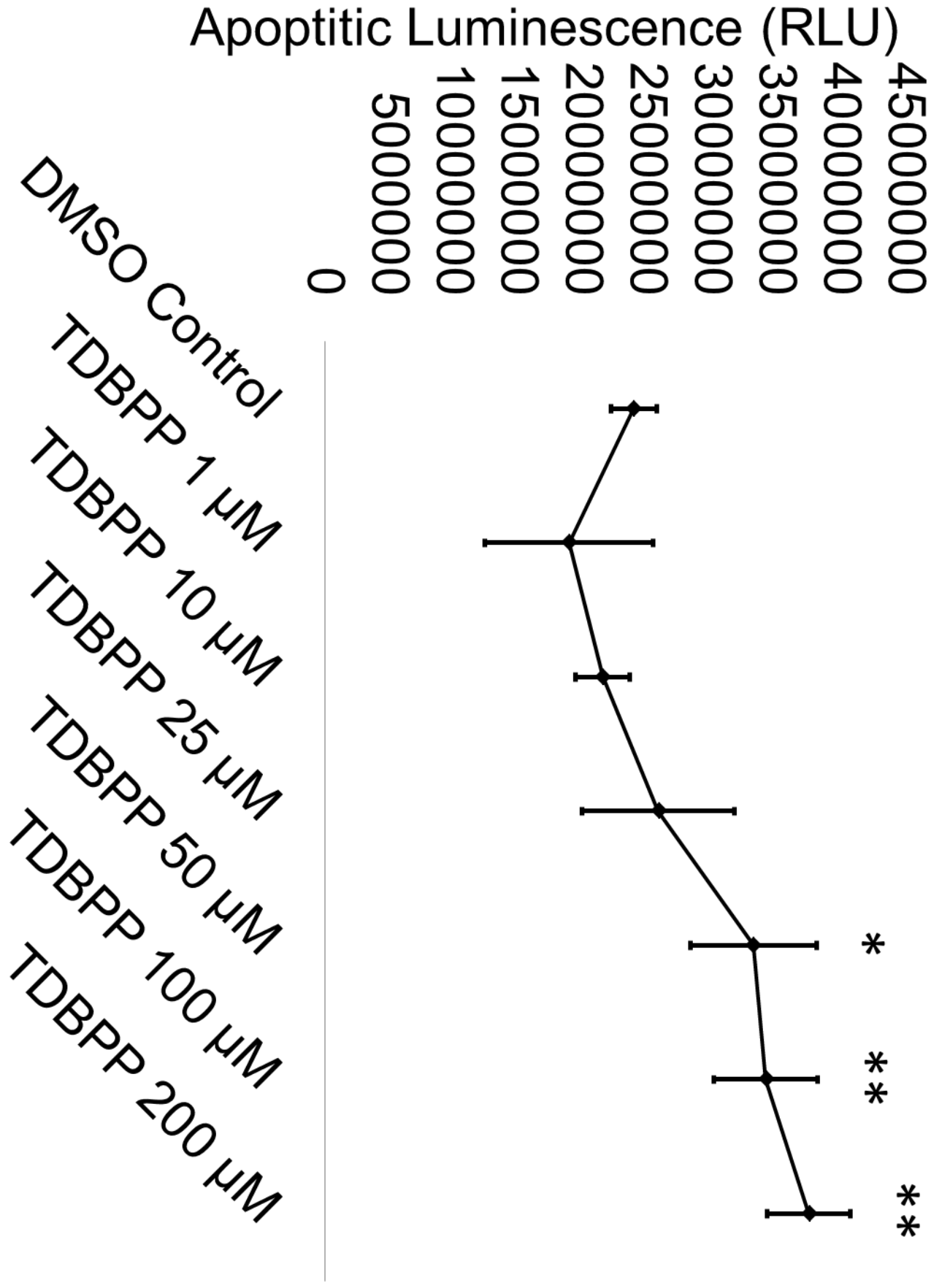
Apoptitic Luminescence (RLU)
0
5000000
10000000
15000000
20000000
25000000
30000000
35000000
40000000
45000000
DMSO Control
TDBPP 1 µM
TDBPP 10 µM
TDBPP 25 µM
TDBPP 50 µM
TDBPP 100 µM
TDBPP 200 µM
*
**
**

Figure 3.11. Acute TDBPP exposure increases apoptosis in spermatogenic cells derived from H1 ESCs. Graphical representation showing that exposure to 50 μM, 100 μM, and 200 μM TDBPP under acute, twenty-four hour conditions increases apoptotic luminescence in H1 ESCs differentiated in *in vitro* spermatogenic conditions in comparison to a 0.2% DMSO-only control. Three replications were analyzed for each condition (n = 3). Significant changes in apoptotic luminescence were determined using a 1-way analysis of variance (1-way ANOVA) and validated via a Student's t-test, where * is $p<0.05$, ** is $p<0.01$, and *** is $p<0.001$. Data are represented as mean ± SEM.

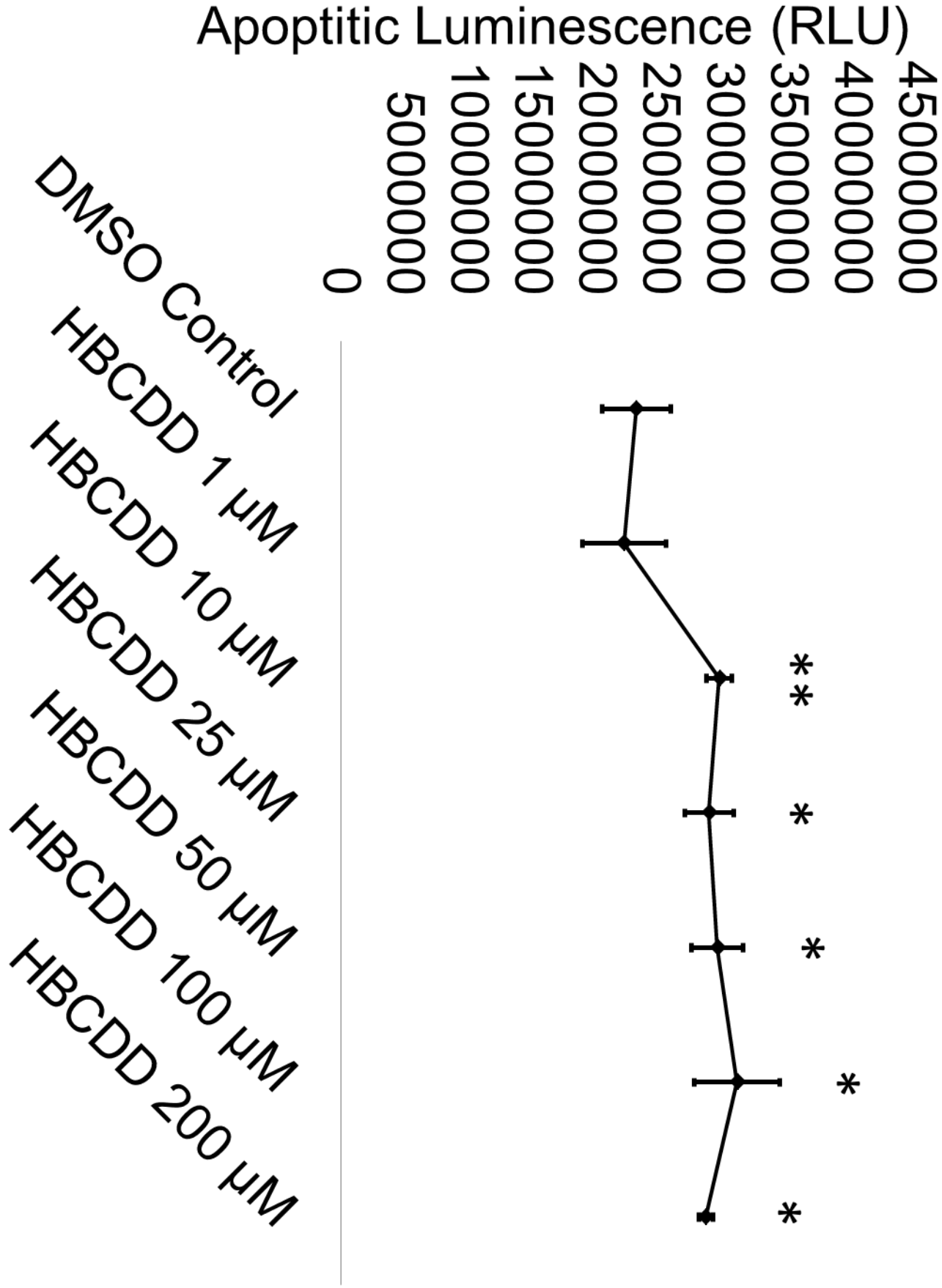
Apoptitic Luminescence (RLU)
0
5000000
10000000
15000000
20000000
25000000
30000000
35000000
40000000
45000000
DMSO Control
HBCDD 1 µM
HBCDD 10 µM
HBCDD 25 µM
HBCDD 50 µM
HBCDD 100 µM
HBCDD 200 µM
**
*
*
*
*

Figure 3.12. Acute HBCDD exposure increases apoptosis in spermatogenic cells derived from H1 ESCs. Graphical representation showing that exposure to 10 μM, 25 μM, 50 μM, 100 μM, and 200 μM TDBPP under acute, twenty-four hour conditions increases apoptotic luminescence in H1 ESCs differentiated in *in vitro* spermatogenic conditions in comparison to a 0.2% DMSO-only control. Three replications were analyzed for each condition (n = 3). Significant changes in apoptotic luminescence were determined using a 1-way analysis of variance (1-way ANOVA) and validated via a Student's t-test, where * is $p<0.05$, ** is $p<0.01$, and *** is $p<0.001$. Data are represented as mean ± SEM.

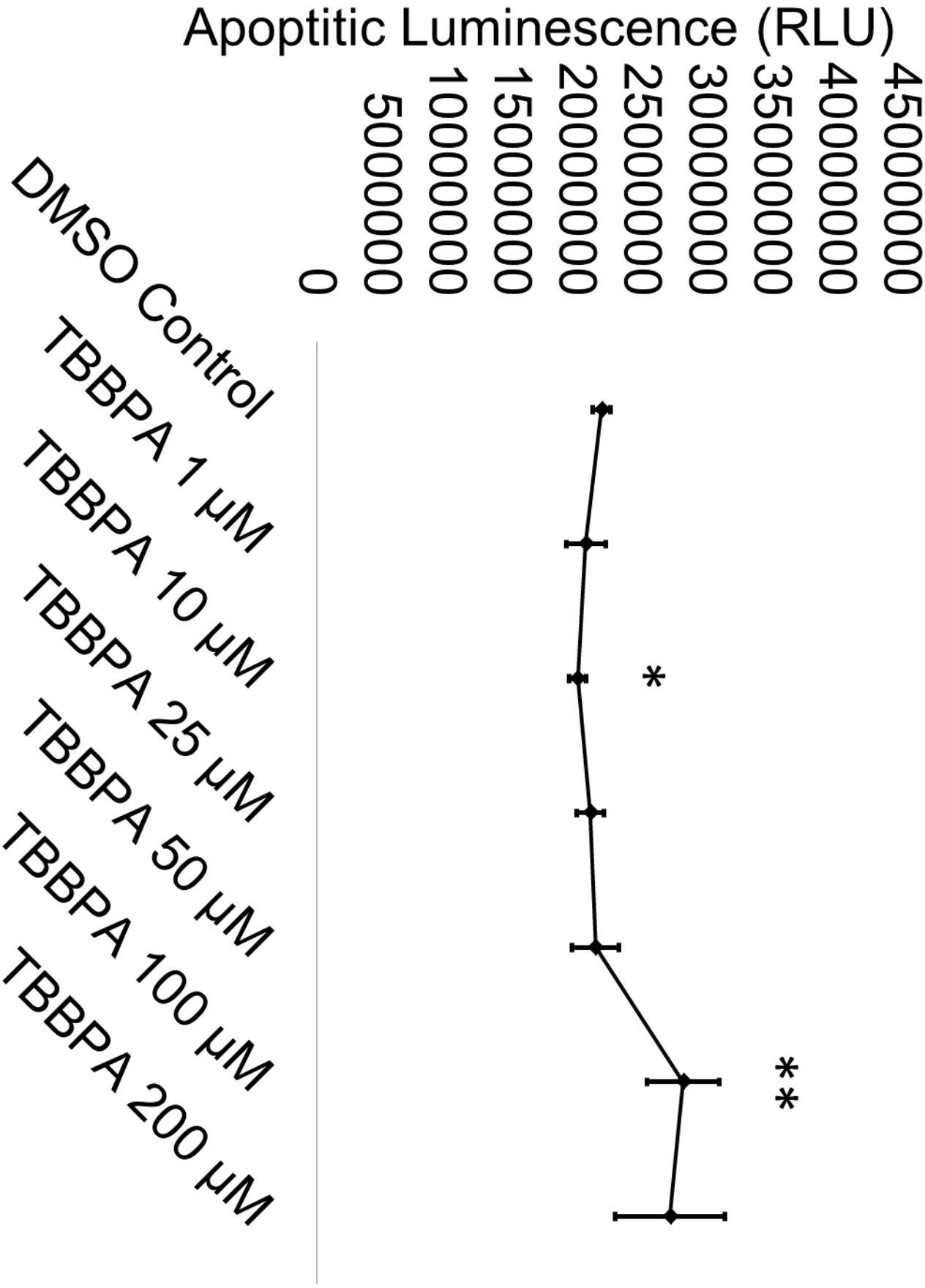
Apoptitic Luminescence (RLU)
0
5000000
10000000
15000000
20000000
25000000
30000000
35000000
40000000
45000000
DMSO Control
TBBPA 1 µM
TBBPA 10 µM
TBBPA 25 µM
TBBPA 50 µM
TBBPA 100 µM
TBBPA 200 µM
*
**

Figure 3.13. Acute TBBPA exposure increases apoptosis in spermatogenic cells derived from H1 ESCs. Graphical representation showing that exposure to 100 μM TBBPA under acute, twenty-four hour conditions increases apoptotic luminescence in H1 ESCs differentiated in *in vitro* spermatogenic conditions in comparison to a 0.2% DMSO-only control. Three replications were analyzed for each condition (n = 3). Significant changes in apoptotic luminescence were determined using a 1-way analysis of variance (1-way ANOVA) and validated via a Student's t-test, where * is $p<0.05$, ** is $p<0.01$, and *** is $p<0.001$. Data are represented as mean ± SEM.

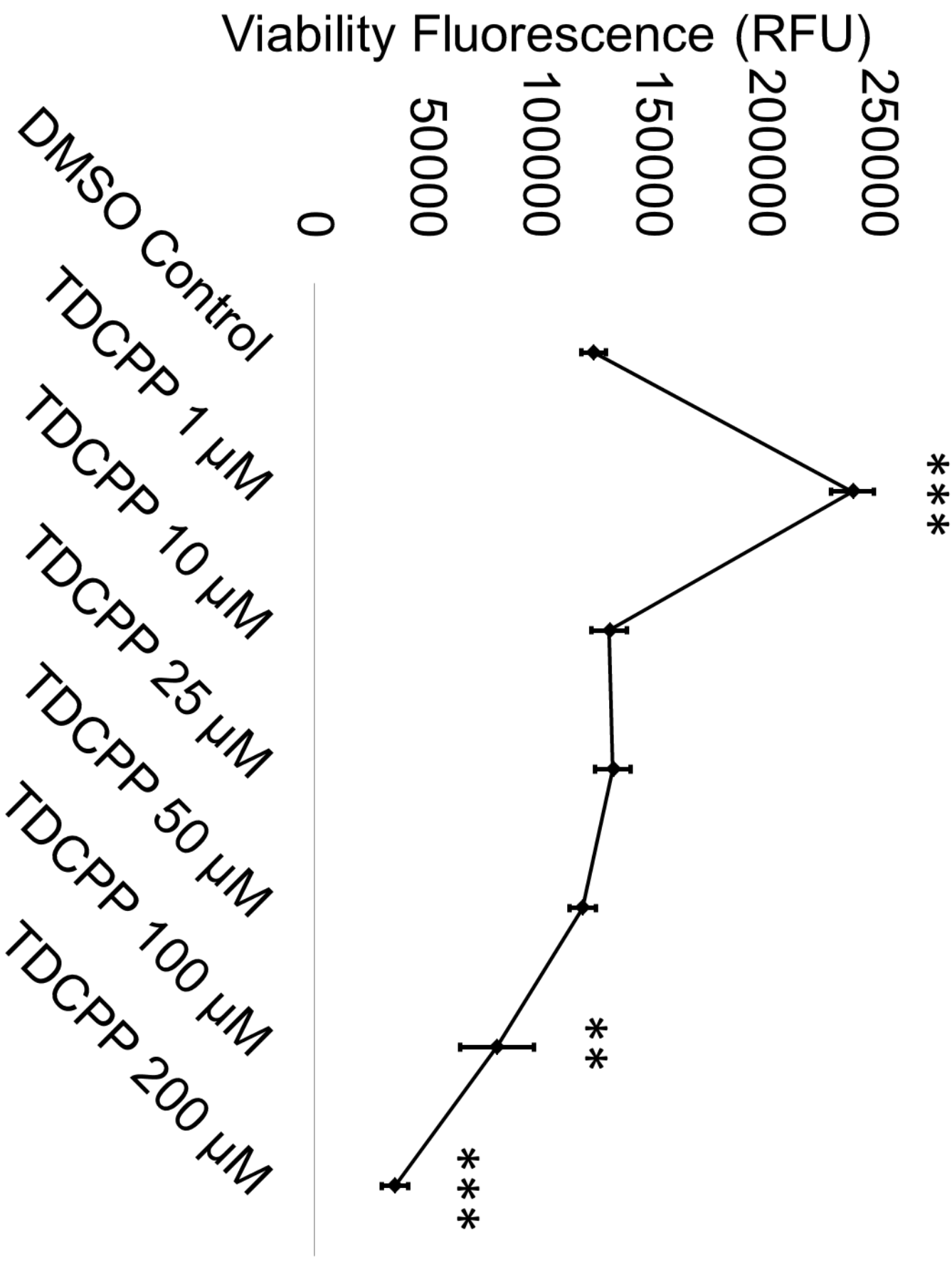
Viability Fluorescence (RFU)
0
50000
100000
150000
200000
250000
DMSO Control
TDCPP 1 µM
TDCPP 10 µM
TDCPP 25 µM
TDCPP 50 µM
TDCPP 100 µM
TDCPP 200 µM
****
**
****

Figure 3.14. Acute TDCPP exposure decreases cell viability in spermatogenic cells derived from H1 ESCs. Graphical representation showing that exposure to 100 μM and 200 μM TDCPP under acute, twenty-four hour conditions decreases viability fluorescence in H1 ESCs differentiated in *in vitro* spermatogenic conditions in comparison to a 0.2% DMSO-only control. Three replications were analyzed for each condition (n = 3). Significant changes in viability fluorescence were determined using a 1-way analysis of variance (1-way ANOVA) and validated via a Student's t-test, where * is $p<0.05$, ** is $p<0.01$, and *** is $p<0.001$. Data are represented as mean ± SEM.

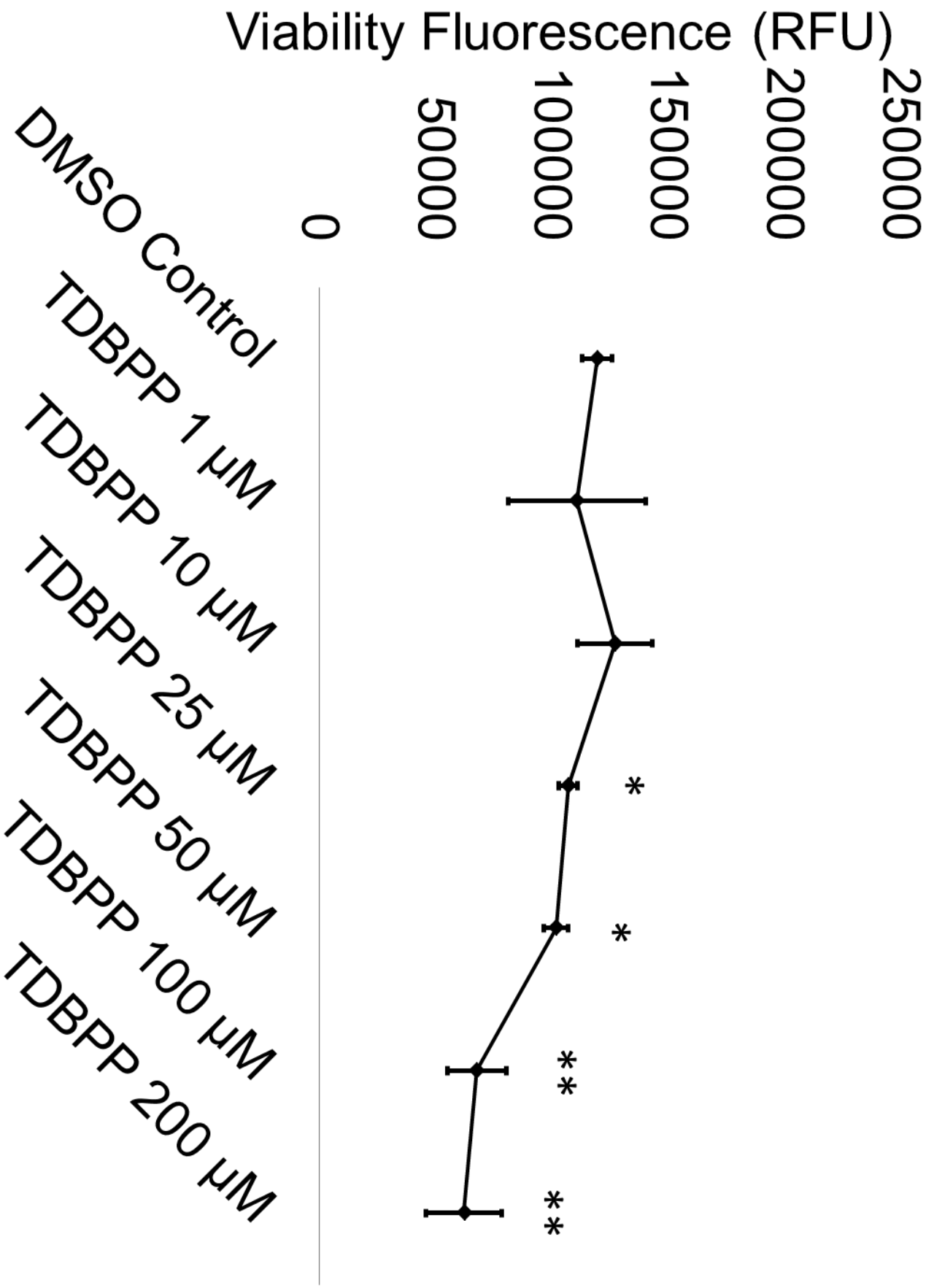
Viability Fluorescence (RFU)
0
50000
100000
150000
200000
250000
DMSO Control
TDBPP 1 µM
TDBPP 10 µM
TDBPP 25 µM
TDBPP 50 µM
TDBPP 100 µM
TDBPP 200 µM
*
*
**
**

Figure 3.15. Acute TDBPP exposure decreases cell viability in spermatogenic cells derived from H1 ESCs. Graphical representation showing that exposure to 25 μM, 50 μM, 100 μM, and 200 μM TDBPP under acute, twenty-four hour conditions decreases viability fluorescence in H1 ESCs differentiated in *in vitro* spermatogenic conditions in comparison to a 0.2% DMSO-only control. Three replications were analyzed for each condition (n = 3). Significant changes in viability fluorescence were determined using a 1-way analysis of variance (1-way ANOVA) and validated via a Student's t-test, where * is $p<0.05$, ** is $p<0.01$, and *** is $p<0.001$. Data are represented as mean ± SEM.

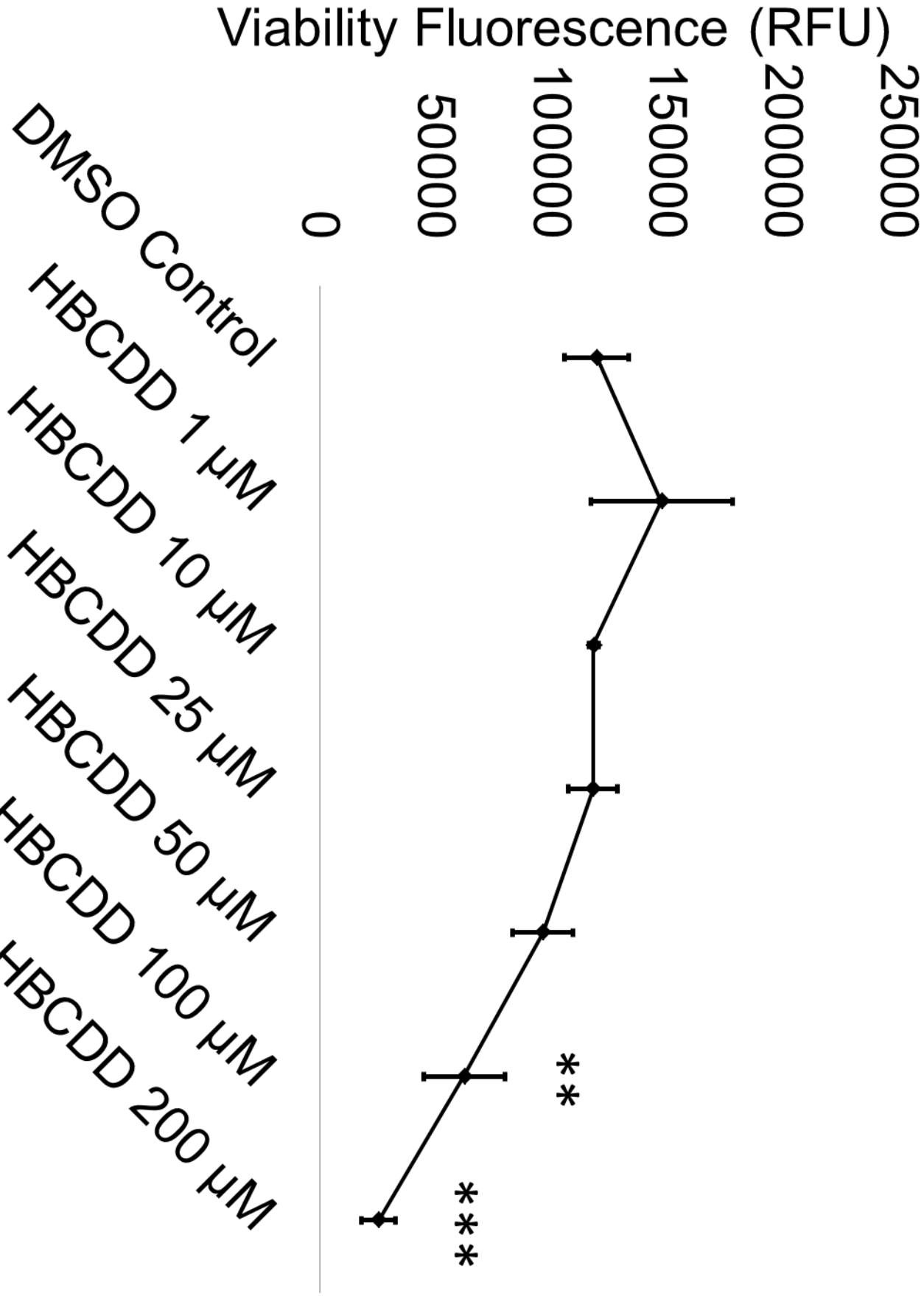
Viability Fluorescence (RFU)
0
50000
100000
150000
200000
250000
DMSO Control
HBCDD 1 µM
HBCDD 10 µM
HBCDD 25 µM
HBCDD 50 µM
HBCDD 100 µM
HBCDD 200 µM
**
***

Figure 3.16. Acute HBCDD exposure decreases cell viability in spermatogenic cells derived from H1 ESCs. Graphical representation showing that exposure to 100 μM and 200 μM HBCDD under acute, twenty-four hour conditions decreases viability fluorescence in H1 ESCs differentiated in *in vitro* spermatogenic conditions in comparison to a 0.2% DMSO-only control. Three replications were analyzed for each condition (n = 3). Significant changes in viability fluorescence were determined using a 1-way analysis of variance (1-way ANOVA) and validated via a Student's t-test, where * is $p<0.05$, ** is $p<0.01$, and *** is $p<0.001$. Data are represented as mean ± SEM.

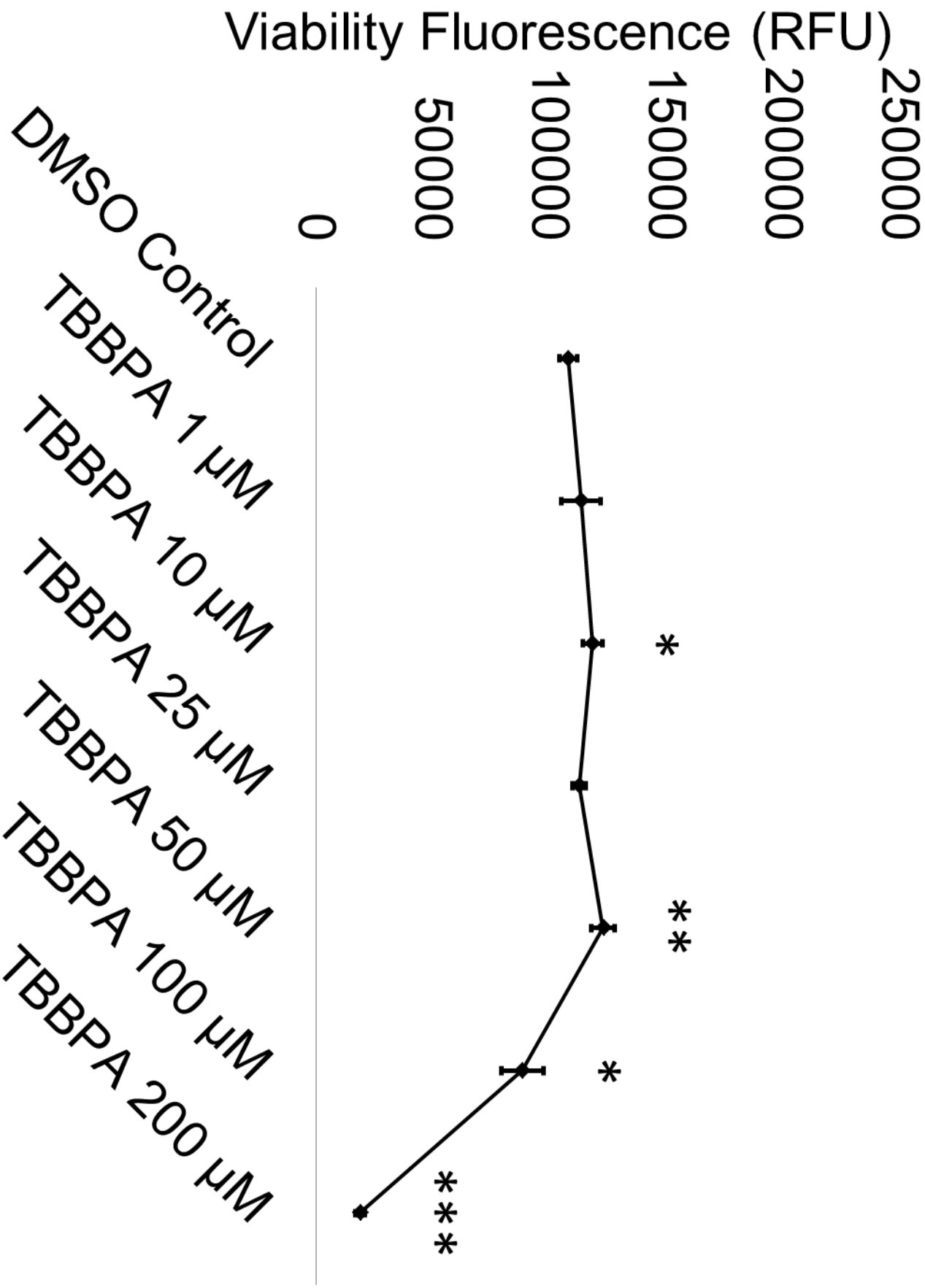
Viability Fluorescence (RFU)
0
50000
100000
150000
200000
250000
DMSO Control
TBBPA 1 µM
TBBPA 10 µM
TBBPA 25 µM
TBBPA 50 µM
TBBPA 100 µM
TBBPA 200 µM
*
**
*
****

Figure 3.17. Acute TBBPA exposure decreases cell viability in spermatogenic cells derived from H1 ESCs. Graphical representation showing that exposure to 10 μM, 50 μM, 100 μM, and 200 μM TBBPA under acute, twenty-four hour conditions decreases viability fluorescence in H1 ESCs differentiated in *in vitro* spermatogenic conditions in comparison to a 0.2% DMSO-only control. Three replications were analyzed for each condition (n = 3). Significant changes in viability fluorescence were determined using a 1-way analysis of variance (1-way ANOVA) and validated via a Student's t-test, where * is $p<0.05$, ** is $p<0.01$, and *** is $p<0.001$. Data are represented as mean ± SEM.

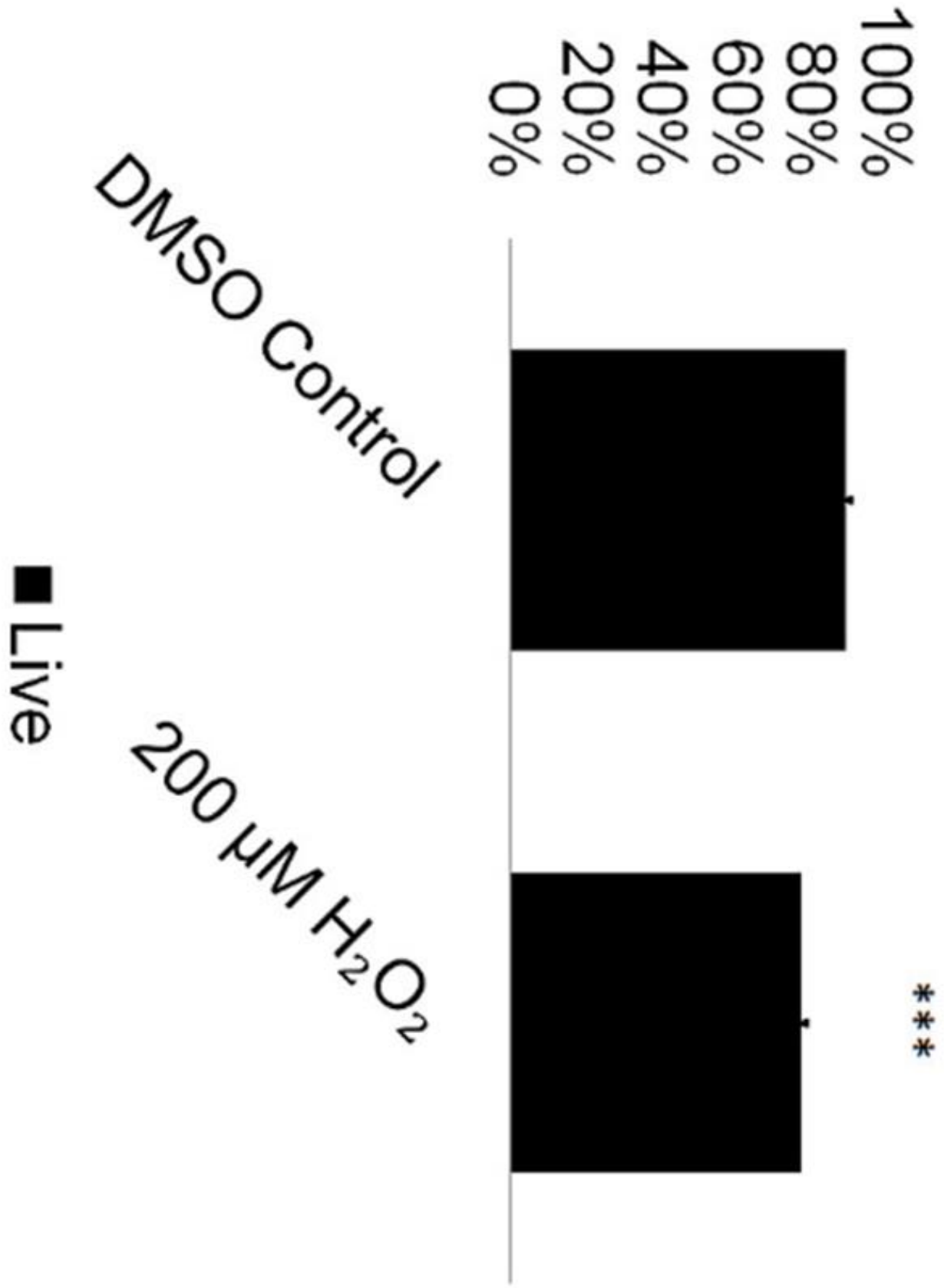
100%
80%
60%
40%
20%
0%
DMSO Control
200 μM H_2O_2
Live
***

Figure 3.18. A positive hydrogen peroxide control decreases live cell viability in spermatogenic cells derived from H1 ESCs. 200 µM hydrogen peroxide (H_2O_2) decreases live cell viability following a six-hour acute treatment in comparison to a 0.25% DMSO-only negative control. 5,000 events were analyzed, with three replications performed for each condition (n = 3). Significant changes in percentages of live cells were determined via a Student's t-test, where * is $p<0.05$, ** is $p<0.01$, and *** is $p<0.001$.

15%
10%
5%
0%
***
DMSO Control
200 μM H_2O_2
Early Apoptosis

Figure 3.19. A positive hydrogen peroxide control increases early apoptosis in spermatogenic cells derived from H1 ESCs. 200 µM hydrogen peroxide (H_2O_2) increases early apoptosis following a six-hour acute treatment in comparison to a 0.25% DMSO-only negative control. 5,000 events were analyzed, with three replications performed for each condition (n = 3). Significant changes in percentages of cells undergoing early apoptosis were determined via a Student's t-test, where * is $p<0.05$, ** is $p<0.01$, and *** is $p<0.001$.

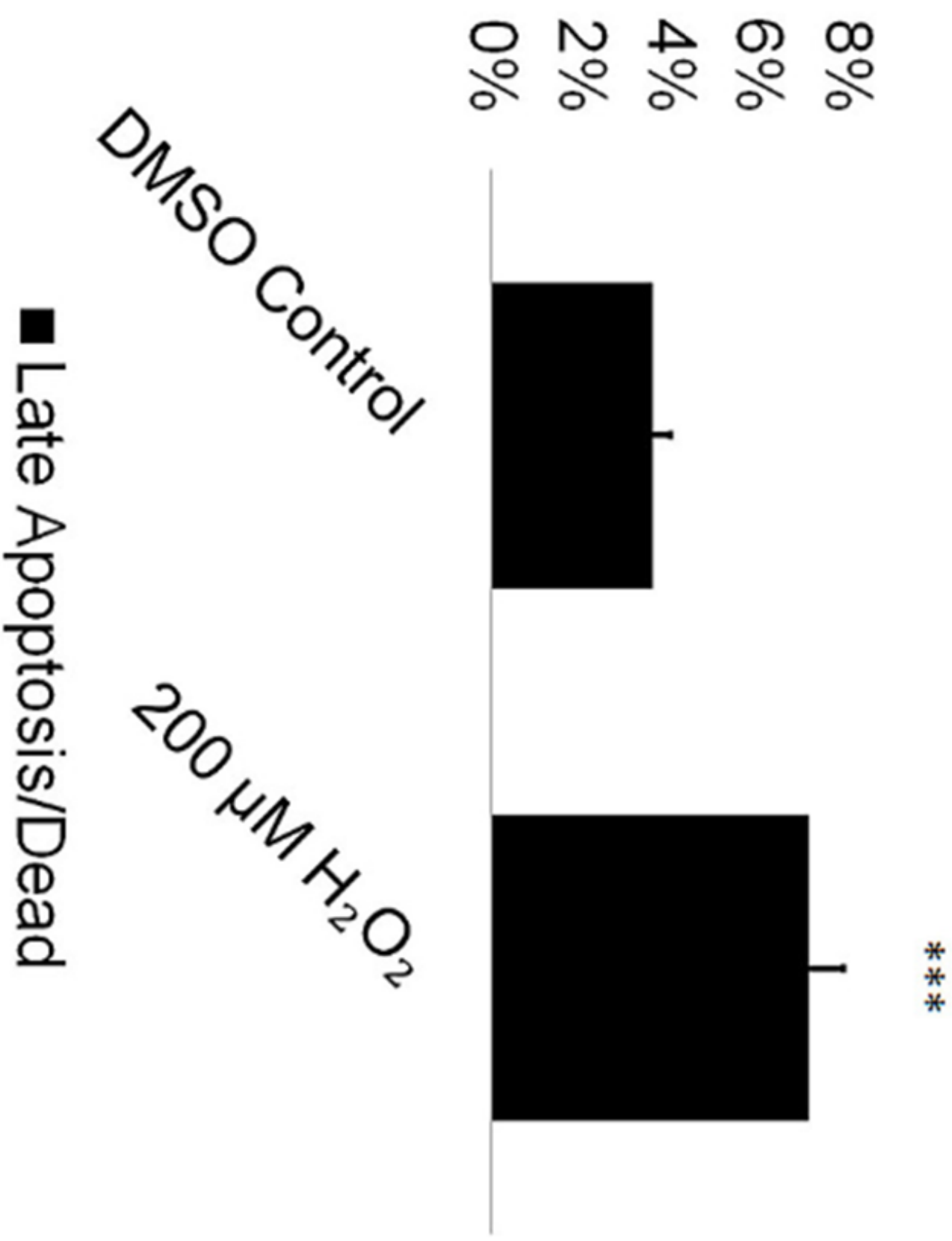
8%
6%
4%
2%
0%
DMSO Control
200 μM H_2O_2
***
Late Apoptosis/Dead

Figure 3.20. A positive hydrogen peroxide control increases late apoptosis and death in spermatogenic cells derived from H1 ESCs. 200 µM hydrogen peroxide (H_2O_2) increases early apoptosis and death following a six-hour acute treatment in comparison to a 0.25% DMSO-only negative control. 5,000 events were analyzed, with three replications performed for each condition (n = 3). Significant changes in percentages of cells undergoing late apoptosis were determined via a Student's t-test, where * is $p<0.05$, ** is $p<0.01$, and *** is $p<0.001$.

PFOS 24 µM

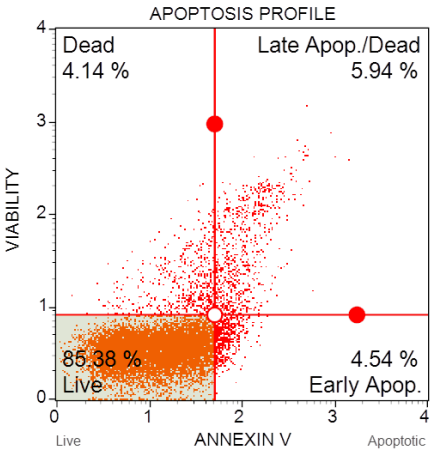

PFOS 48 µM

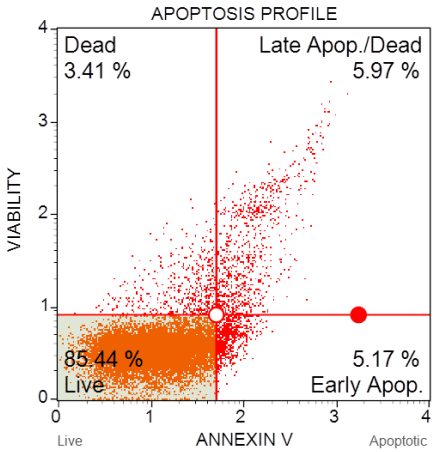

PFOS 126 µM

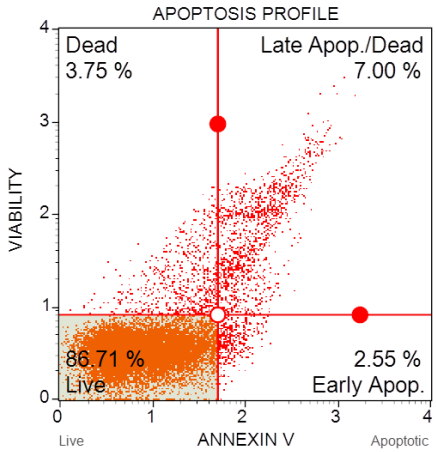

PFOA 11 µM

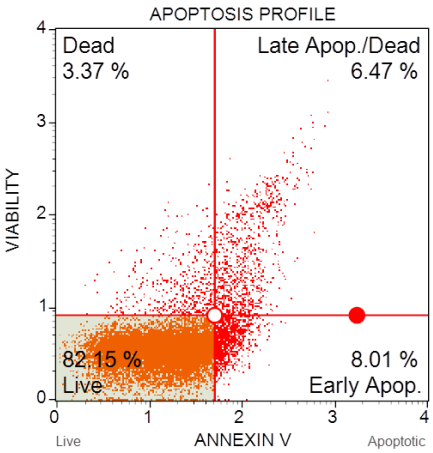

PFOA 25 µM

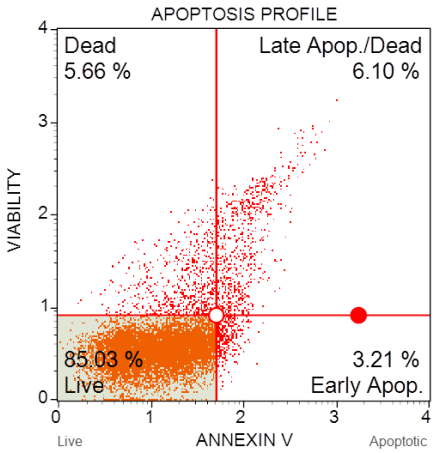

PFOA 100 µM

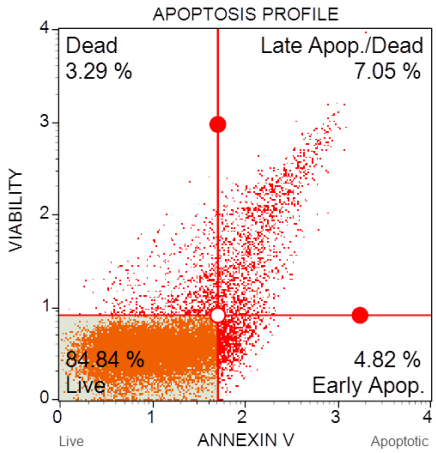

PFNA 2.15 µM

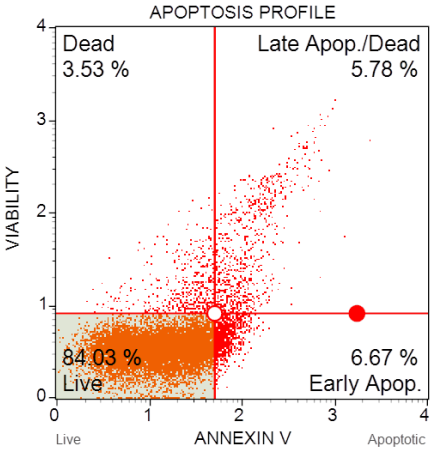

PFNA 21.5 µM

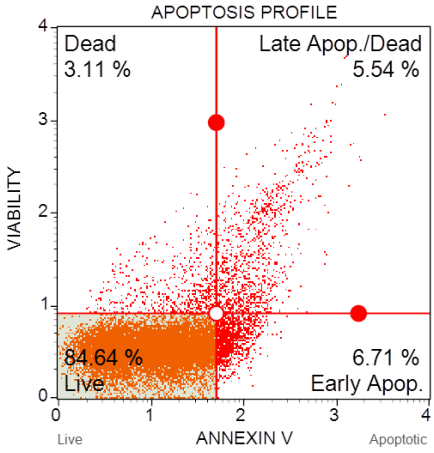

PFNA 43 µM

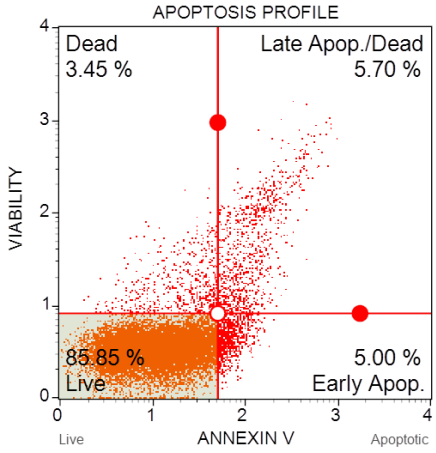

Figure 3.21. Flow cytometry plots for persistent PFOS, PFOA, and PFNA treated spermatogenic cells derived from H1 ESCs for apoptotic data. Flow cytometry analyses for indicating percent viable cells, percent early apoptotic cells, percent late apoptotic cells, and percent dead/necrotic cells for all concentrations of PFOS, PFOA, and PFNA assessed. Lower left quadrant represents viable cells, lower right quadrant represents early apoptotic cells, upper right quadrant is late apoptotic/dead cells, and the upper right quadrant is dead/necrotic cells.

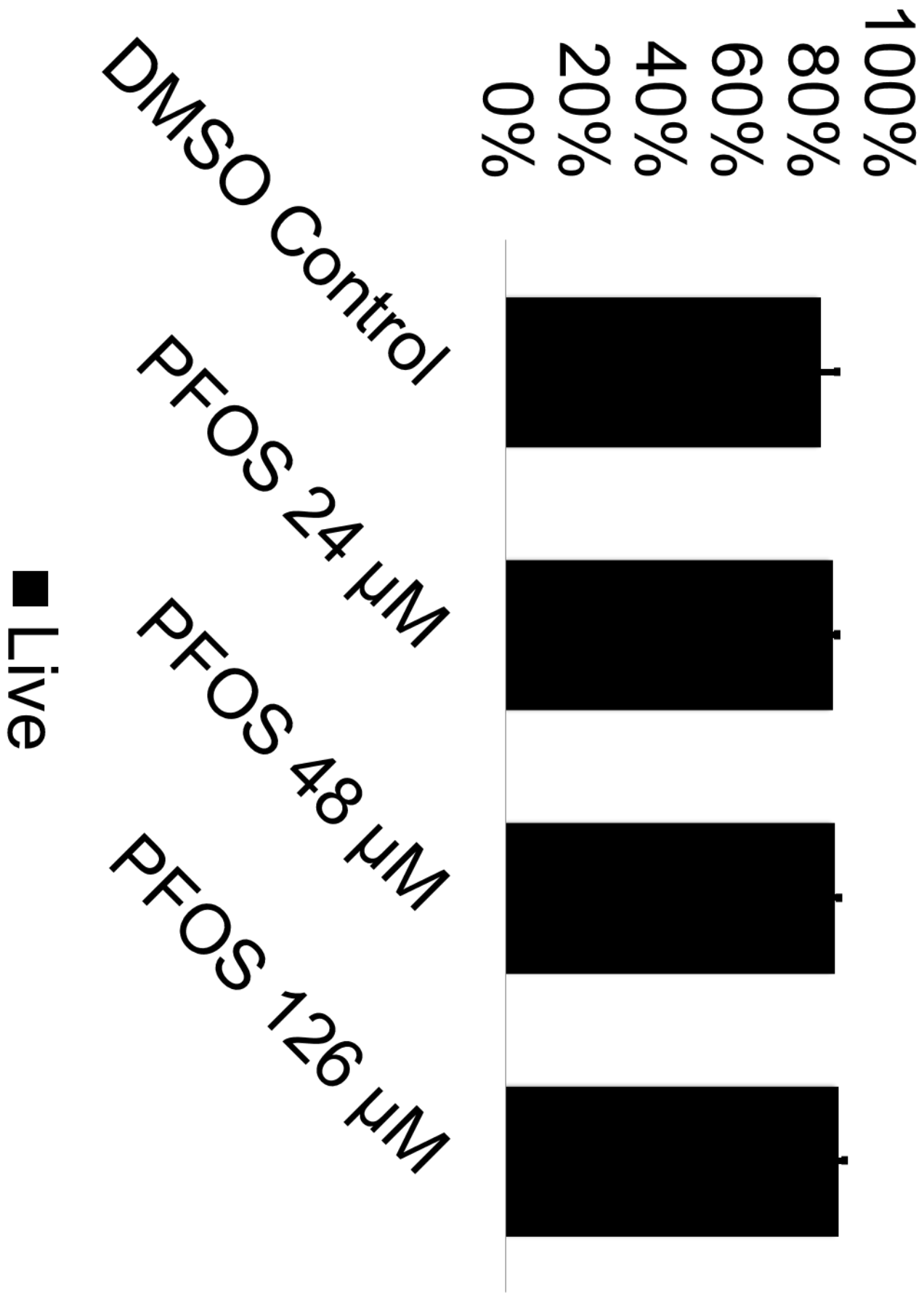
100%
80%
60%
40%
20%
0%
DMSO Control
PFOS 24 µM
PFOS 48 µM
PFOS 126 µM
Live

Figure 3.22. Persistent PFOS exposure does not impact cell viability in spermatogenic cells derived from H1 ESCs. Graphical representation showing that exposure to PFOS from Day 1 to Day 10 did not impact live cell percentages in H1 ESCs differentiated in *in vitro* spermatogenic conditions in comparison to a 0.25% DMSO-only control. 5,000 events were analyzed, with four replications performed for each condition (n = 4). Significant changes in cell viability were determined using a 1-way analysis of variance (1-way ANOVA) and validated via a Student's t-test, where * is $p<0.05$, ** is $p<0.01$, and *** is $p<0.001$. Data are represented as mean ± SEM.

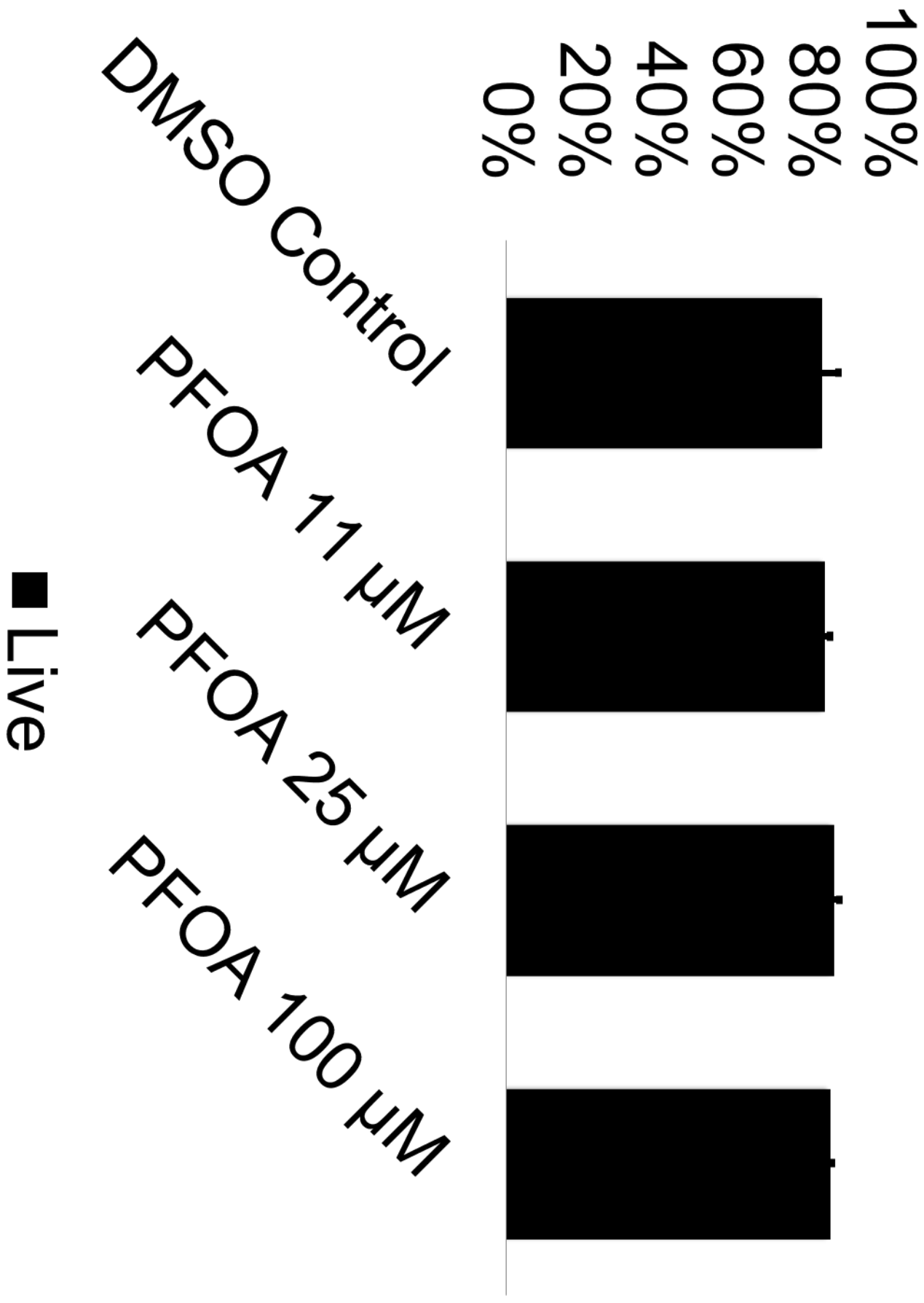
100%
80%
60%
40%
20%
0%
DMSO Control
PFOA 11 µM
PFOA 25 µM
PFOA 100 µM
Live

Figure 3.23. Persistent PFOA exposure does not impact cell viability in spermatogenic cells derived from H1 ESCs. Graphical representation showing that exposure to PFOA from Day 1 to Day 10 did not impact live cell percentages in H1 ESCs differentiated in *in vitro* spermatogenic conditions in comparison to a 0.25% DMSO-only control. 5,000 events were analyzed, with four replications performed for each condition (n = 4). Significant changes in cell viability were determined using a 1-way analysis of variance (1-way ANOVA) and validated via a Student's t-test, where * is $p<0.05$, ** is $p<0.01$, and *** is $p<0.001$. Data are represented as mean ± SEM.

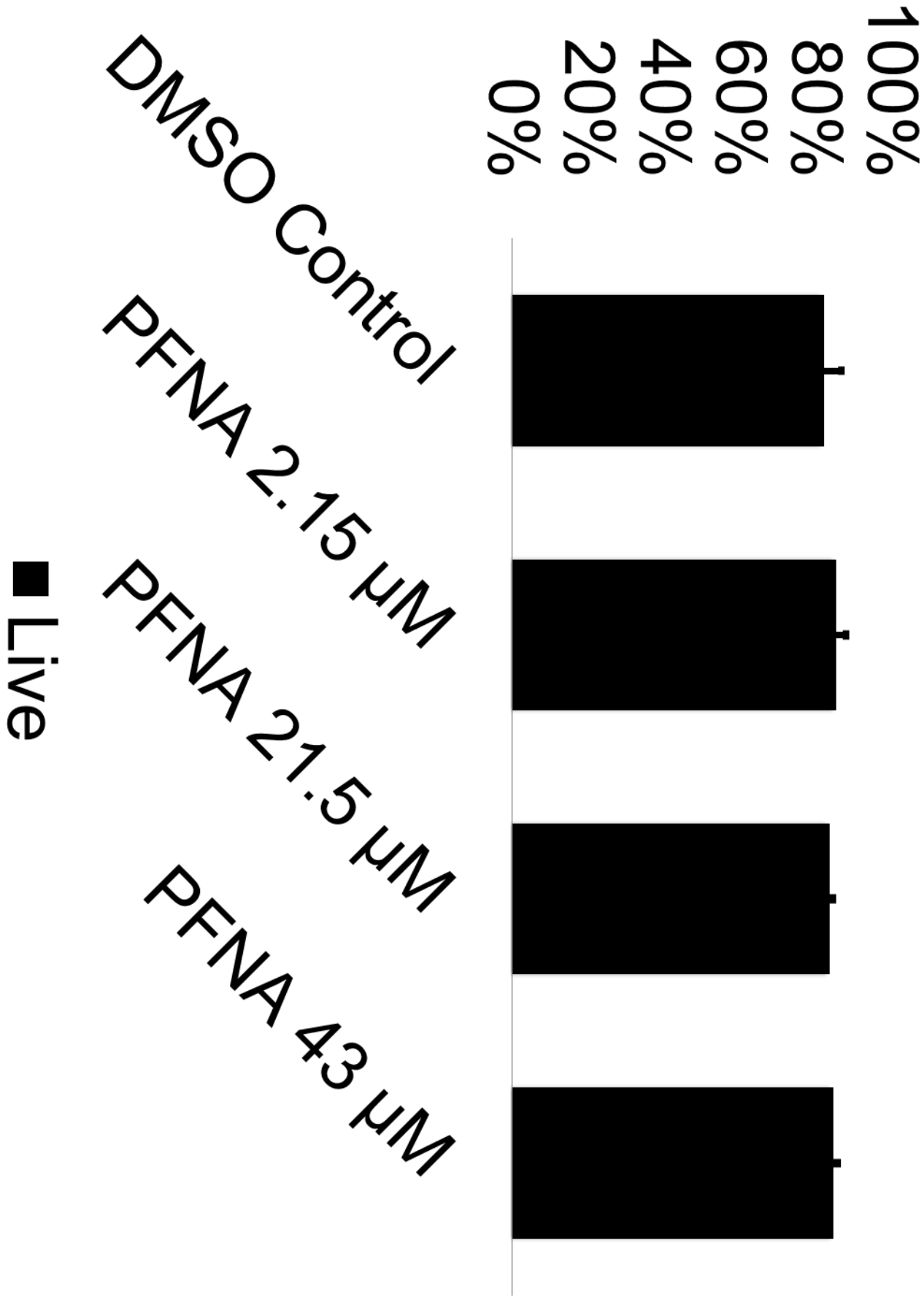
100%
80%
60%
40%
20%
0%
DMSO Control
PFNA 2.15 µM
PFNA 21.5 µM
PFNA 43 µM
Live

Figure 3.24. Persistent PFNA exposure does not impact cell viability in spermatogenic cells derived from H1 ESCs. Graphical representation showing that exposure to PFNA from Day 1 to Day 10 did not impact live cell percentages in H1 ESCs differentiated in *in vitro* spermatogenic conditions in comparison to a 0.25% DMSO-only control. 5,000 events were analyzed, with four replications performed for each condition (n = 4). Significant changes in cell viability were determined using a 1-way analysis of variance (1-way ANOVA) and validated via a Student's t-test, where * is $p<0.05$, ** is $p<0.01$, and *** is $p<0.001$. Data are represented as mean ± SEM.

2.5.2 Acute TDCPP, TDBPP, HBCDD, and TBBPA and persistent PFOS, PFOA, and PFNA exposure decreases the viability of spermatogonia derived from H1 ESCs

Spermatogonia are the foundation for male fertility, giving rise to primary and secondary spermatocytes, differentiating spermatids, and eventually, mature sperm capable of fertilizing an oocyte, all while maintaining their own pool through self-renewal (Phillips et al., 2010). As such, perturbations in this cell population could act to disturb the entire spermatogenesis process. To determine if spermatogonia are the cellular targets of our chemicals, we analyzed for expression of the consensus marker of stem and progenitor spermatogonia, promyelocytic leukemia zinc finger (PLZF). We have previously established PLZF as a reliable marker for spermatogonia in our *in vitro* model (Easley et al., 2012, Easley et al., 2015). Using high content imaging and quantification, we determined that TDCPP, TDBPP, HBCDD, and TBBPA all significantly reduce the total area of expression and total intensity of PLZF in our cell cultures differentiated form H1 ESCs (Figure 4.1). Area measurements of PLZF+ colonies show that all chemicals significantly reduce total PLZF+ area beginning at 1 µM (Figures 4.2 – 4.5). 100 µM TDCPP shows a 65% decrease in PLZF+ area, while 200 µM TDBBP, HBCDD, and TBBPA show a 42%, 56%, and 64% decrease in PLZF+ area compared to a 0.2% DMSO-only negative control, respectively (Figures 4.2 – 4.5). Notably, HBCDD treatment at 50 µM and 100 µM shows a return to PLZF+ area that is not significantly different from control (Figure 4.4). Expression levels of PLZF, represented by the total intensity of PLZF+ staining, show significant reductions for all chemicals beginning at 1 µM in comparison to a 0.2% DMSO-only negative control (Figures 4.6 – 4.9). 200 µM TDCPP, TDBPP, HBCDD, and TBBPA show a significant 70%, 60%, 85%, and 90%

decrease in total PLZF intensity compared to 0.2% DMSO-only control, respectively (Figures 4.6 – 4.9) qRT-PCR results from the amplification of *ZBTB16* (PLZF) transcripts in our *in vitro* model show a decreasing trend at 100 µM TDCPP, TDBPP, HBCDD, and TBBPA, with *ZBTB16* mRNA steady state levels at 20%, 30%, 30%, and 45% of DMSO-only control levels, respectively, which correlates with our staining data (Figure 4.10).

PLZF+ spermatogonia were not capable of recovery upon a twenty-four hour recovery period following the removal of 100 µM HBCDD and TBBPA (Figures 4.11 – 4.14). PLZF area and intensity continued to significantly decline following recovery of cells treated with 100 µM HBCDD by 36% and 41%, respectively (Figures 4.11 and 4.13). 100 µM TBBPA-treated cells show a significant 17% decline in PLZF area but an insignificant 5% increase in PLZF intensity following a twenty-four hour recovery period (Figures 4.12 – 4.14). The PLZF intensity of TBBPA-treated cells remains significantly less than DMSO-only treated cells (Figure 4.15). DMSO-only treated cells experience a 20% increase in PLZF area and intensity that is not significant during the same time period (Figures 4.16 and 4.17). However, PLZF+ area and intensity are not statistically different from DMSO negative control following a five day recovery from 100 µM HBCDD and 100 µM TBBPA exposure (Figures 4.18 – 4.21). Together, these data suggest that spermatogonia are sensitive to acute treatment with the flame retardants HBCDD and TBBPA at concentrations that are physiologically relevant. The differences in PLZF area and intensity recovery in HBCDD and TBBPA-treated cells suggests differences in mechanisms of toxicity. HBCDD-treated spermatogonia viability continues to decline precipitously following initial removal of the toxicant, though cells recover

following a longer recovery period. While the area of spermatogonia cells continues to decline immediately following TBBPA exposure, PLZF intensity shows evidence of attempted recovery after one day following removal of the toxicant, with PLZF area and intensity returning to control levels after five days. These data indicate that recovery from acute HBCDD and TBBPA exposure is possible following a prolonged recovery period, though it is unclear if this trend would persist following repeated exposures similar to daily occupational exposure.

Similar to TDCPP, TDBPP, HBCDD, and TBBPA, PFOS, PFOA, and PFNA impact spermatogonia and PLZF expression, despite having no apparent impact on cell viability (Figure 4.22). We determined that 24 µM and 126 µM PFOS significantly decreased the area of PLZF+ cells by 14% and 42%, respectively, in comparison to a 0.25% DMSO negative control (Figure 4.23). Interestingly, 48 µM PFOS shows a 9% decline in PLZF+ area although this result is not statistically significant (Figure 4.23). Additionally, 2.15 µM PFNA significantly decreased the area of PLZF+ cells by 15% (Figure 4.25). However, PFOA exposure had no impact on PLZF+ area (Figure 4.24). Expression levels of PLZF, represented by the total intensity of PLZF+ staining, significantly declined in cells exposed to 126 µM PFOS and 11 µM PFOA by 50% and 17%, respectively (Figures 4.26 – 4.27). Exposure to PFNA did not impact PLZF intensity in our *in vitro* cultures (Figure 4.28). The results from the Annexin V assay support the conclusion that PFAS exposure does not impact cell viability during human *in vitro* spermatogenesis. Therefore, it is unlikely that the decline in PLZF area and expression is the result of spermatogonia undergoing apoptosis in response to PFAS exposure. Decreases in PLZF intensity may be the result of the downregulation of PLZF

expression that could block the differentiation of spermatogonia to primary spermatocytes, or alternatively, the ability of spermatogonia to self-renew their own population. Under the conditions examined, certain PFASs do affect PLZF expression and could contribute to fertility issues with further, persistent exposure.

Despite differences in impacts on cell viability, both halogenated FRs and PFASs have impacts on spermatogonia. These impacts suggest that, despite their highly charged structures, PFASs can still enter the cell, which calls into question how bioaccumulation may play a role in their toxicity. It is unclear if PFASs impact spermatogonia by blocking their differentiation or by directly acting on PLZF expression, as exposure occurs before spermatogenesis is initiated. Similarly, there is a disconnect between TDCPP, TDBPP, HBCDD, and TBBPA's impacts on cell viability and PLZF expression. The data suggests that, as well as causing cell death, halogenated flame retardants may have direct impact on PLZF expression. All chemicals tested above have radically different structures. PFOS, PFOA, and PFNA consist of long chains of carbons with attached fluorine molecules. HBCDD and TBBPA are halogenated ring structures, and TDCPP and TDBPP are halogenated tris molecules. As such, it is unlikely that they have the same molecular targets, and the additional fact that they impacted the same target at different times during differentiation makes it unclear how all seven compounds can impact spermatogonia.

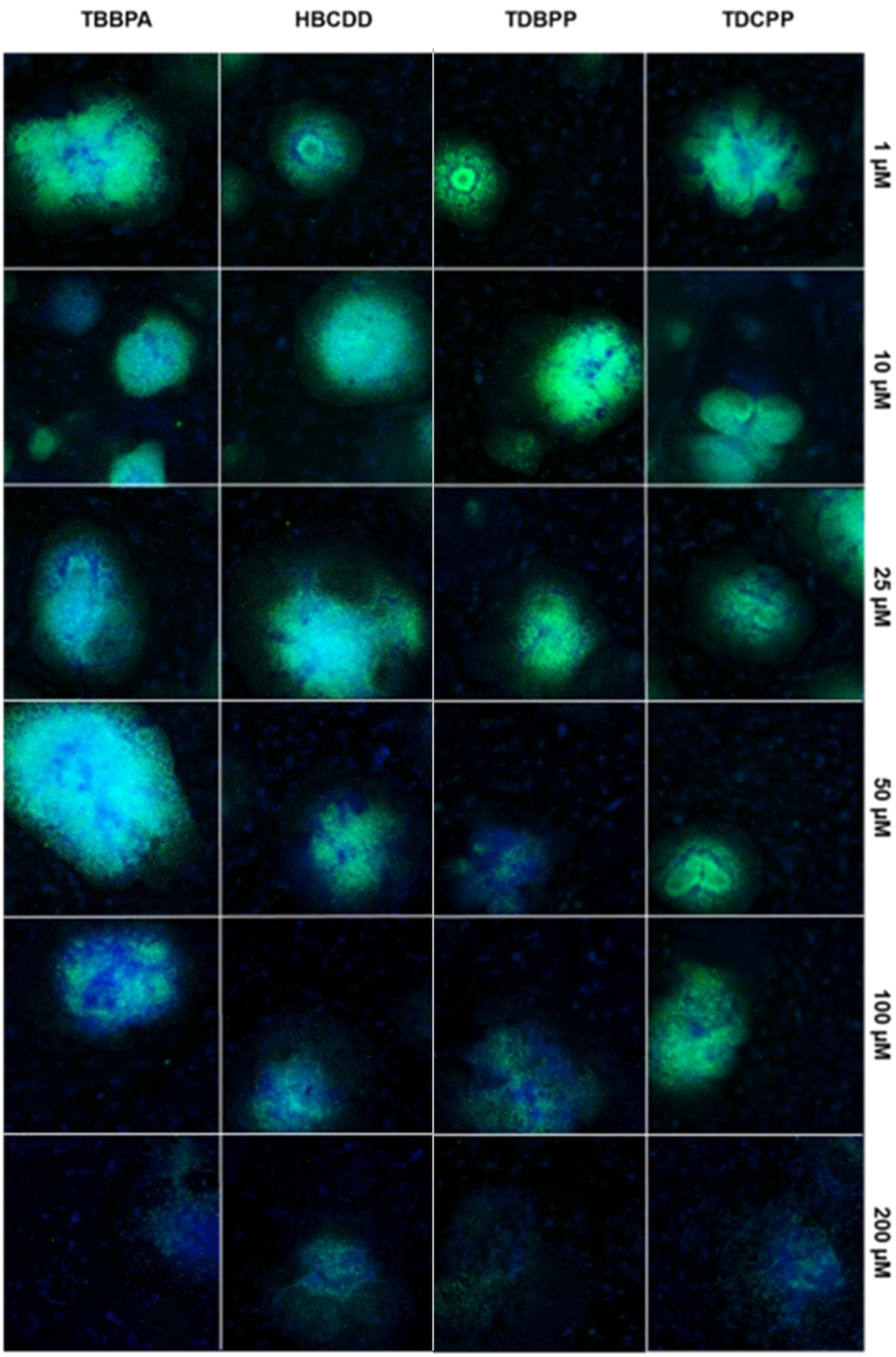
TBBPA
HBCDD
TDBPP
TDCPP
1 µM
10 µM
25 µM
50 µM
100 µM
200 µM

Figure 4.1. Acute TDCPP, TDBPP, HBCDD, and TBBPA exposure reduces PLZF+ area and intensity in spermatogonia in in vitro spermatogenic cultures derived from H1 ESCs. Representative 5X images obtained by the Cellomics ArrayScan VT1 of PLZF + (green) and DAPI (blue)-stained colonies treated with acute, twenty-four hour doses of 1 μM, 10 μM, 25 μM, 50 μM, 100 μM, and 200 μM TDCPP, TDBPP, HBCDD and TBBPA. Differentiations are derived from H1 ESCs. All images are taken under the same imaging conditions and parameters.

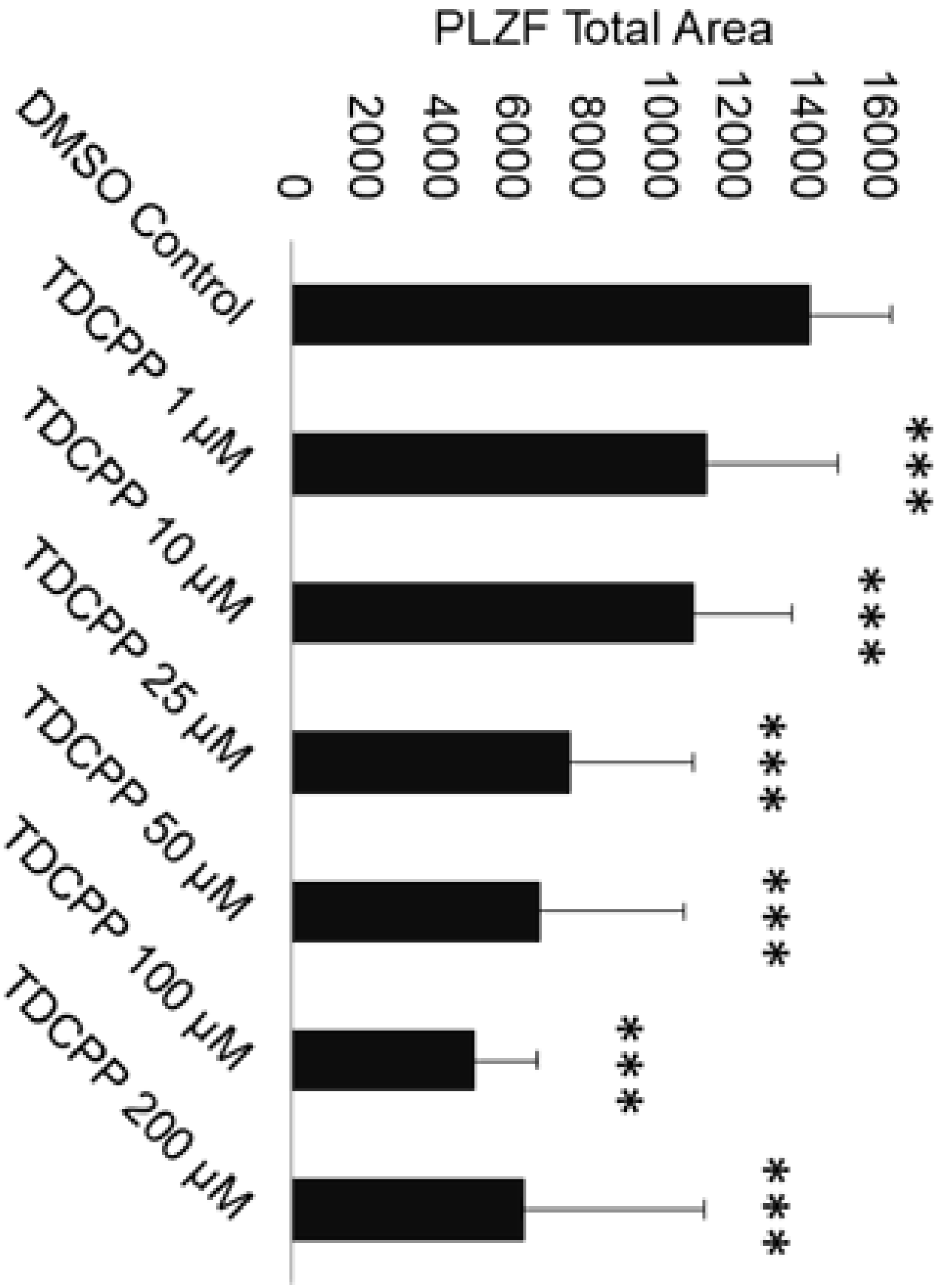
PLZF Total Area
0
2000
4000
6000
8000
10000
12000
14000
16000
DMSO Control
TDCPP 1 µM
TDCPP 10 µM
TDCPP 25 µM
TDCPP 50 µM
TDCPP 100 µM
TDCPP 200 µM
****
****
****
****
****
****

Figure 4.2. Acute TDCPP exposure reduces PLZF+ area in spermatogonia in in vitro spermatogenic cultures derived from H1 ESCs. Graphical representation showing that acute, twenty-four hour exposure to 1 μM, 10 μM, 25 μM, 50 μM, 100 μM, and 200 μM TDCPP reduces average total PLZF+ area in spermatogonia derived under *in vitro* spermatogenic conditions in comparison to a 0.2% DMSO-only control. Five replications were performed for each condition (n = 5). Significant changes in PLZF+ area were determined using a 1-way analysis of variance (1-way ANOVA) and validated via a Student's t-test, where * is $p<0.05$, ** is $p<0.01$, and *** is $p<0.001$. Data are represented as mean ± SEM.

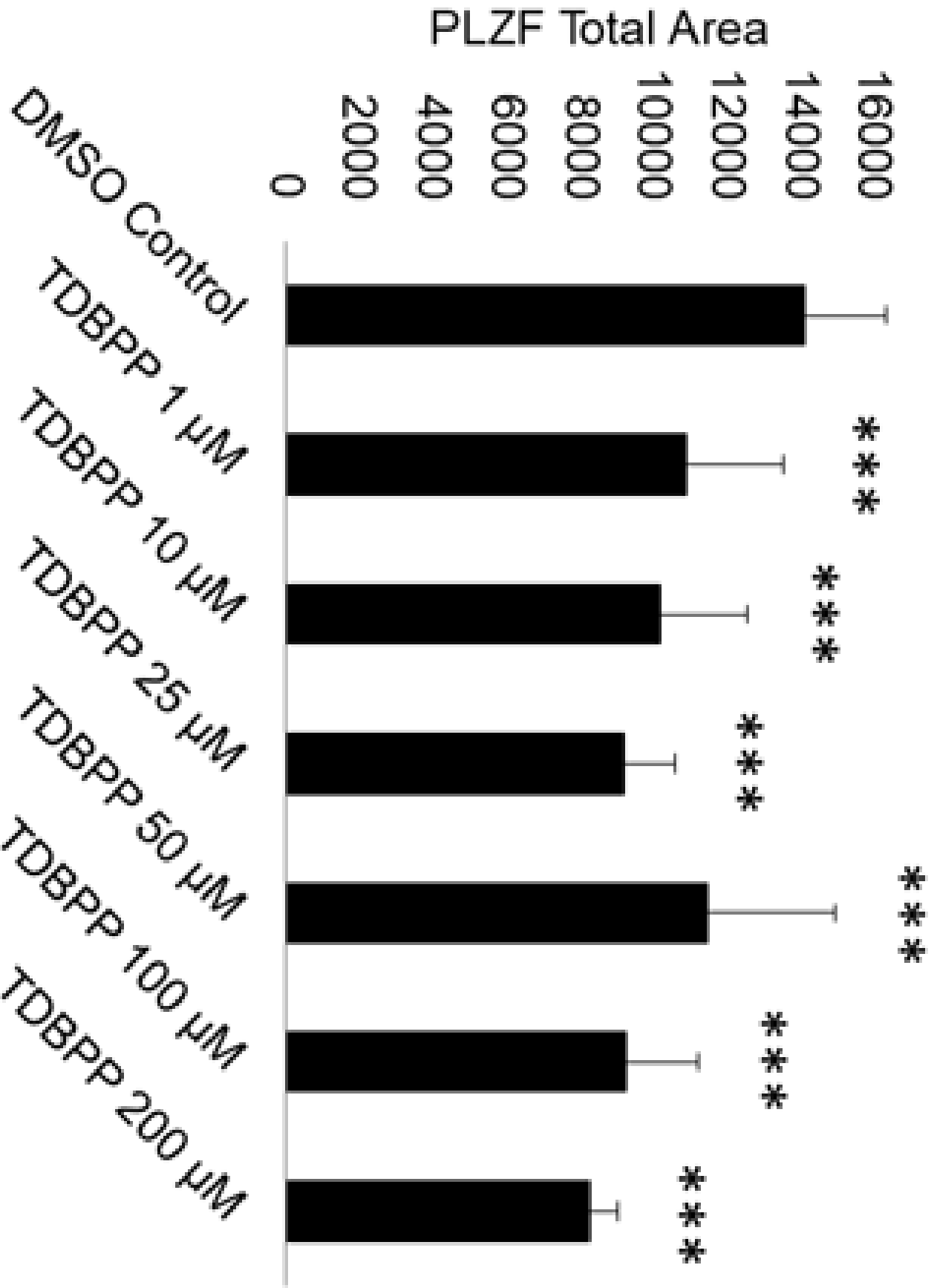
PLZF Total Area
0
2000
4000
6000
8000
10000
12000
14000
16000
DMSO Control
TDBPP 1 µM
TDBPP 10 µM
TDBPP 25 µM
TDBPP 50 µM
TDBPP 100 µM
TDBPP 200 µM
****
****
****
****
****
****
****

Figure 4.3. Acute TDBPP exposure reduces PLZF+ area in spermatogonia in in vitro spermatogenic cultures derived from H1 ESCs. Graphical representation showing that acute, twenty-four hour exposure to 1 μM, 10 μM, 25 μM, 50 μM, 100 μM, and 200 μM TDBPP reduces average total PLZF+ area in spermatogonia derived under *in vitro* spermatogenic conditions in comparison to a 0.2% DMSO-only control. Five replications were performed for each condition (n = 5). Significant changes in PLZF+ area were determined using a 1-way analysis of variance (1-way ANOVA) and validated via a Student's t-test, where * is $p<0.05$, ** is $p<0.01$, and *** is $p<0.001$. Data are represented as mean ± SEM.

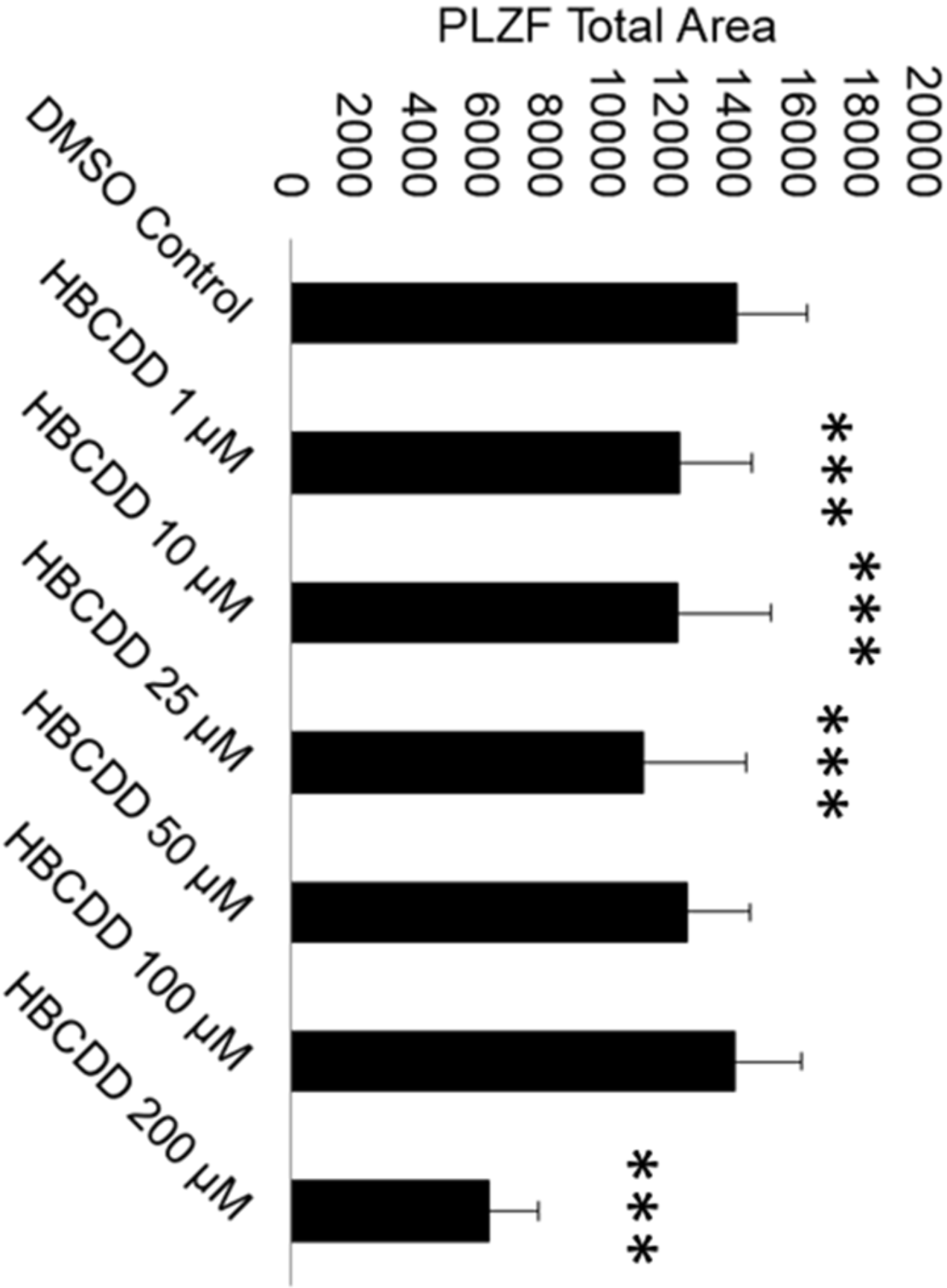
PLZF Total Area
0
2000
4000
6000
8000
10000
12000
14000
16000
18000
20000
DMSO Control
HBCDD 1 µM
HBCDD 10 µM
HBCDD 25 µM
HBCDD 50 µM
HBCDD 100 µM
HBCDD 200 µM
****
****
****
****
***

Figure 4.4. Acute HBCDD exposure reduces PLZF+ area in spermatogonia in in vitro spermatogenic cultures derived from H1 ESCs. Graphical representation showing that acute, twenty-four hour exposure to 1 μM, 10 μM, 25 μM, 50 μM, and 200 μM HBCDD reduces average total PLZF+ area in spermatogonia derived under *in vitro* spermatogenic conditions in comparison to a 0.2% DMSO-only control. Five replications were performed for each condition (n = 5). Significant changes in PLZF+ area were determined using a 1-way analysis of variance (1-way ANOVA) and validated via a Student's t-test, where * is $p<0.05$, ** is $p<0.01$, and *** is $p<0.001$. Data are represented as mean ± SEM.

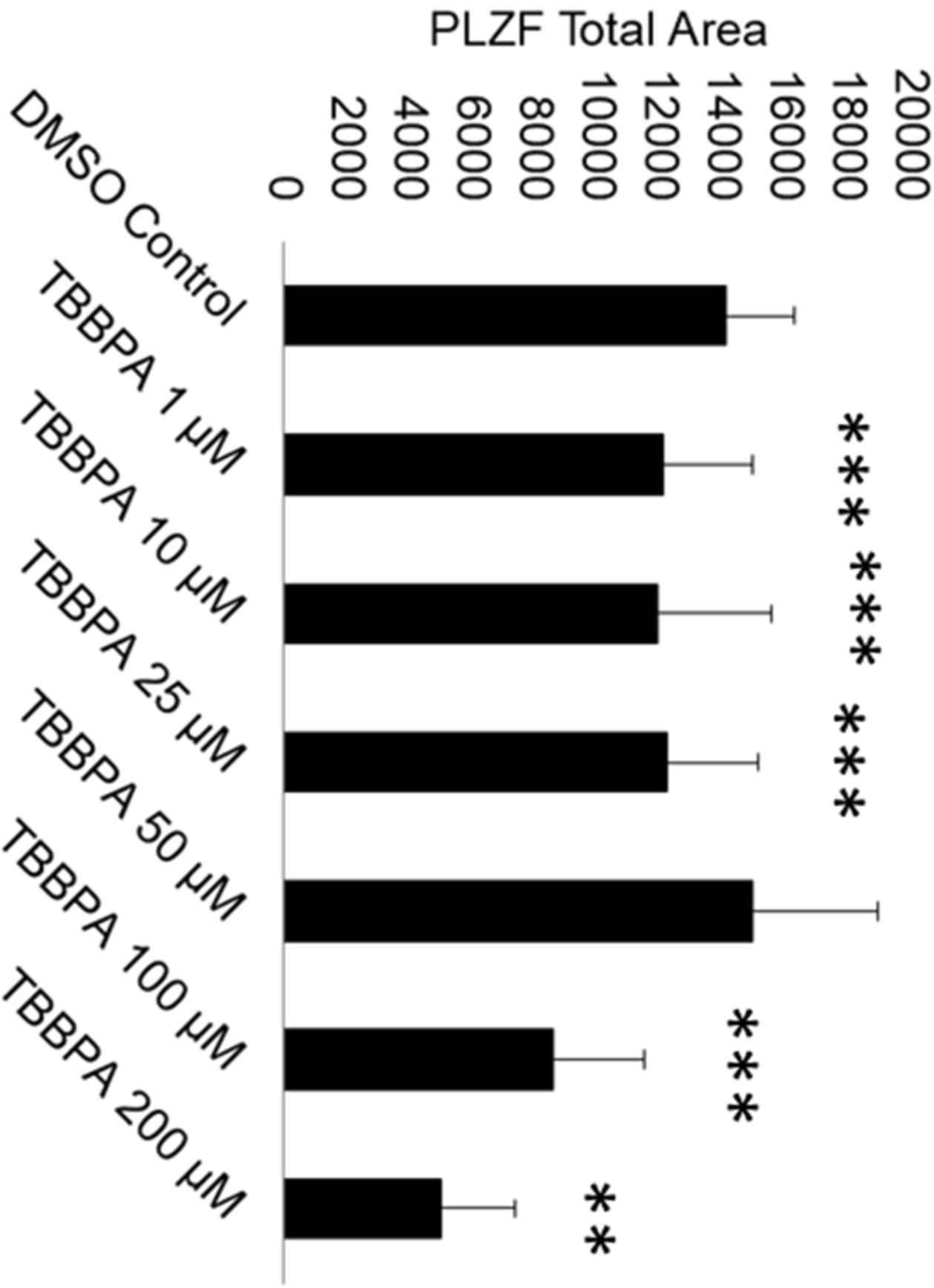
PLZF Total Area
0
2000
4000
6000
8000
10000
12000
14000
16000
18000
20000
DMSO Control
TBBPA 1 µM
TBBPA 10 µM
TBBPA 25 µM
TBBPA 50 µM
TBBPA 100 µM
TBBPA 200 µM
****
****
****
****
****
**

Figure 4.5. Acute TBBPA exposure reduces PLZF+ area in spermatogonia in in vitro spermatogenic cultures derived from H1 ESCs. Graphical representation showing that acute, twenty-four hour exposure to 1 μM, 10 μM, 25 μM, 100 μM, and 200 μM TBBPA reduces average total PLZF+ area in spermatogonia derived under *in vitro* spermatogenic conditions in comparison to a 0.2% DMSO-only control. Five replications were performed for each condition (n = 5). Significant changes in PLZF+ area were determined using a 1-way analysis of variance (1-way ANOVA) and validated via a Student's t-test, where * is $p<0.05$, ** is $p<0.01$, and *** is $p<0.001$. Data are represented as mean ± SEM.

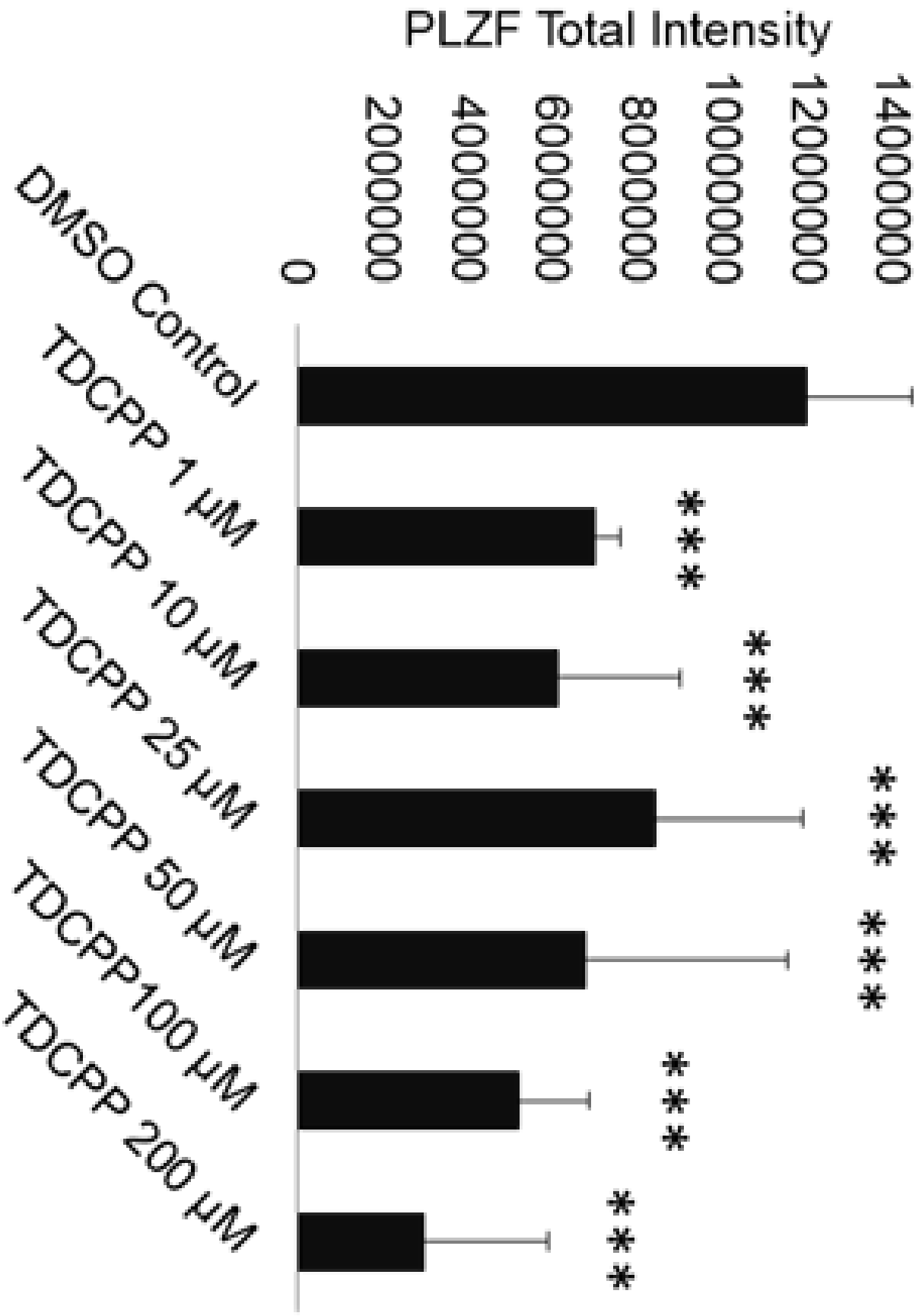
PLZF Total Intensity
0
20000000
40000000
60000000
80000000
100000000
120000000
140000000
DMSO Control
TDCPP 1 µM
TDCPP 10 µM
TDCPP 25 µM
TDCPP 50 µM
TDCPP100 µM
TDCPP 200 µM
****
****
****
****
****
****

Figure 4.6. Acute TDCPP exposure reduces PLZF+ intensity in spermatogonia in in vitro spermatogenic cultures derived from H1 ESCs. Graphical representation showing that acute, twenty-four hour exposure to 1 μM, 10 μM, 25 μM, 50 μM, 100 μM, and 200 μM TDBPP reduces average total PLZF+ intensity in spermatogonia derived under *in vitro* spermatogenic conditions in comparison to a 0.2% DMSO-only control. Five replications were performed for each condition (n = 5). Significant changes in PLZF+ intensity were determined using a 1-way analysis of variance (1-way ANOVA) and validated via a Student's t-test, where * is $p<0.05$, ** is $p<0.01$, and *** is $p<0.001$. Data are represented as mean ± SEM.

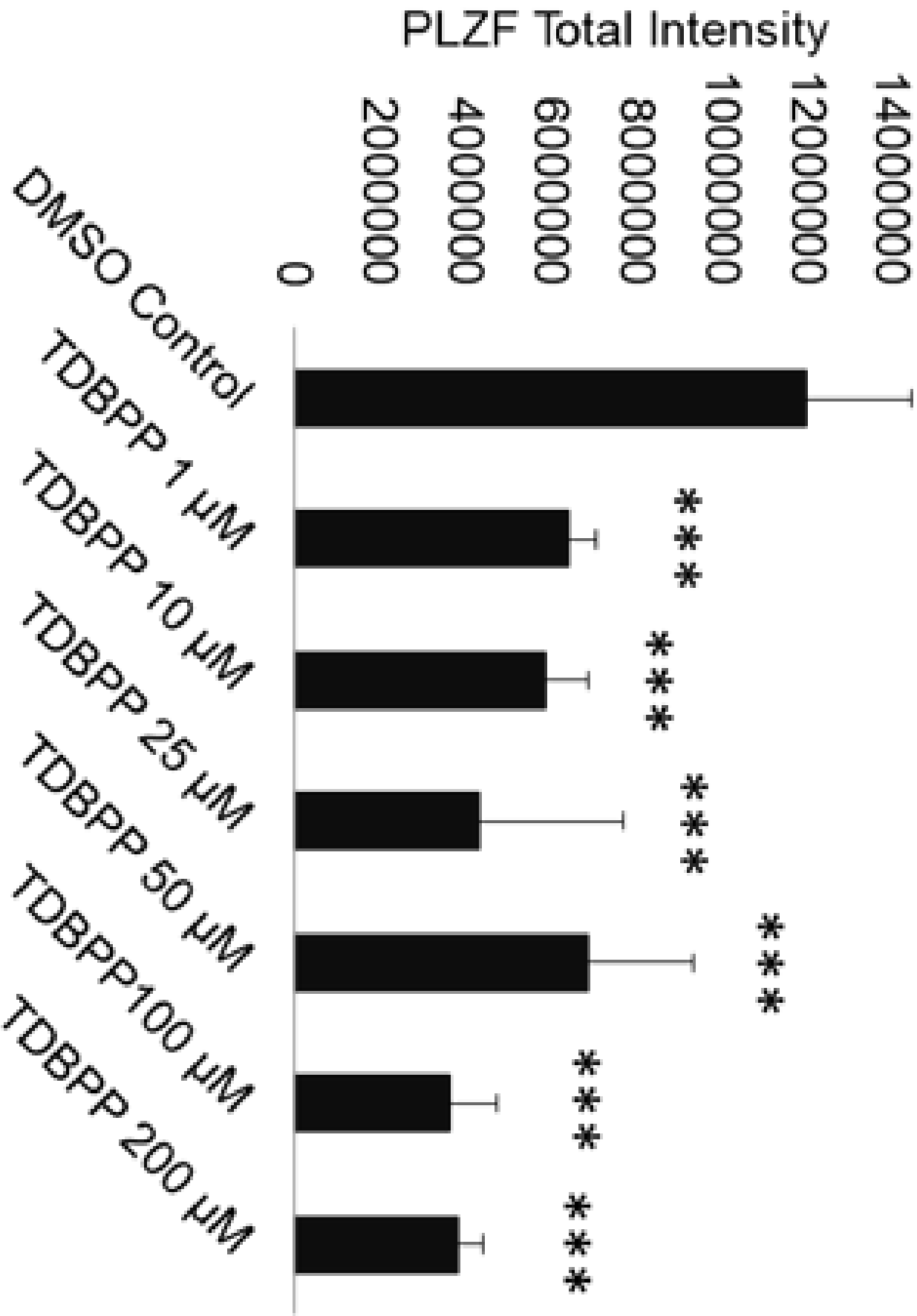
PLZF Total Intensity
0
20000000
40000000
60000000
80000000
100000000
120000000
140000000
DMSO Control
TDBPP 1 µM
TDBPP 10 µM
TDBPP 25 µM
TDBPP 50 µM
TDBPP100 µM
TDBPP 200 µM
****
****
****
****
****
****

Figure 4.7. Acute TDBPP exposure reduces PLZF+ intensity in spermatogonia in in vitro spermatogenic cultures derived from H1 ESCs. Graphical representation showing that acute, twenty-four hour exposure to 1 μM, 10 μM, 25 μM, 50 μM, 100 μM, and 200 μM TDBPP reduces average total PLZF+ intensity in spermatogonia derived under *in vitro* spermatogenic conditions in comparison to a 0.2% DMSO-only control. Five replications were performed for each condition (n = 5). Significant changes in PLZF+ intensity were determined using a 1-way analysis of variance (1-way ANOVA) and validated via a Student's t-test, where * is $p<0.05$, ** is $p<0.01$, and *** is $p<0.001$. Data are represented as mean ± SEM.

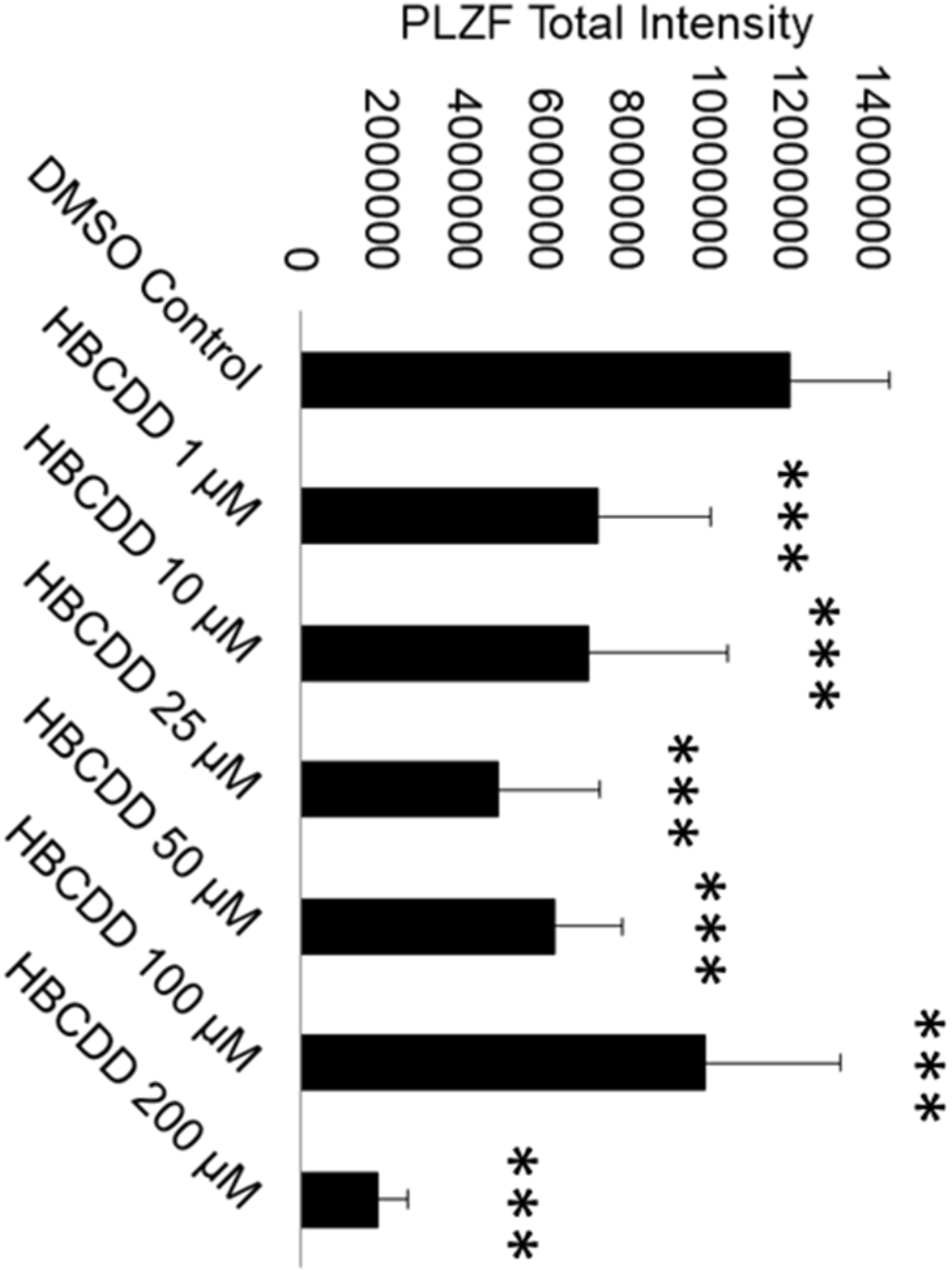
PLZF Total Intensity
0
2000000
4000000
6000000
8000000
10000000
12000000
14000000
DMSO Control
HBCDD 1 μM
HBCDD 10 μM
HBCDD 25 μM
HBCDD 50 μM
HBCDD 100 μM
HBCDD 200 μM
****
****
****
****
****
****

Figure 4.8. Acute HBCDD exposure reduces PLZF+ intensity in spermatogonia in in vitro spermatogenic cultures derived from H1 ESCs. Graphical representation showing that acute, twenty-four hour exposure to 1 μM, 10 μM, 25 μM, 50 μM, 100 μM, and 200 μM HBCDD reduces average total PLZF+ intensity in spermatogonia derived under *in vitro* spermatogenic conditions in comparison to a 0.2% DMSO-only control. Five replications were performed for each condition (n = 5). Significant changes in PLZF+ intensity were determined using a 1-way analysis of variance (1-way ANOVA) and validated via a Student's t-test, where * is $p<0.05$, ** is $p<0.01$, and *** is $p<0.001$. Data are represented as mean ± SEM.

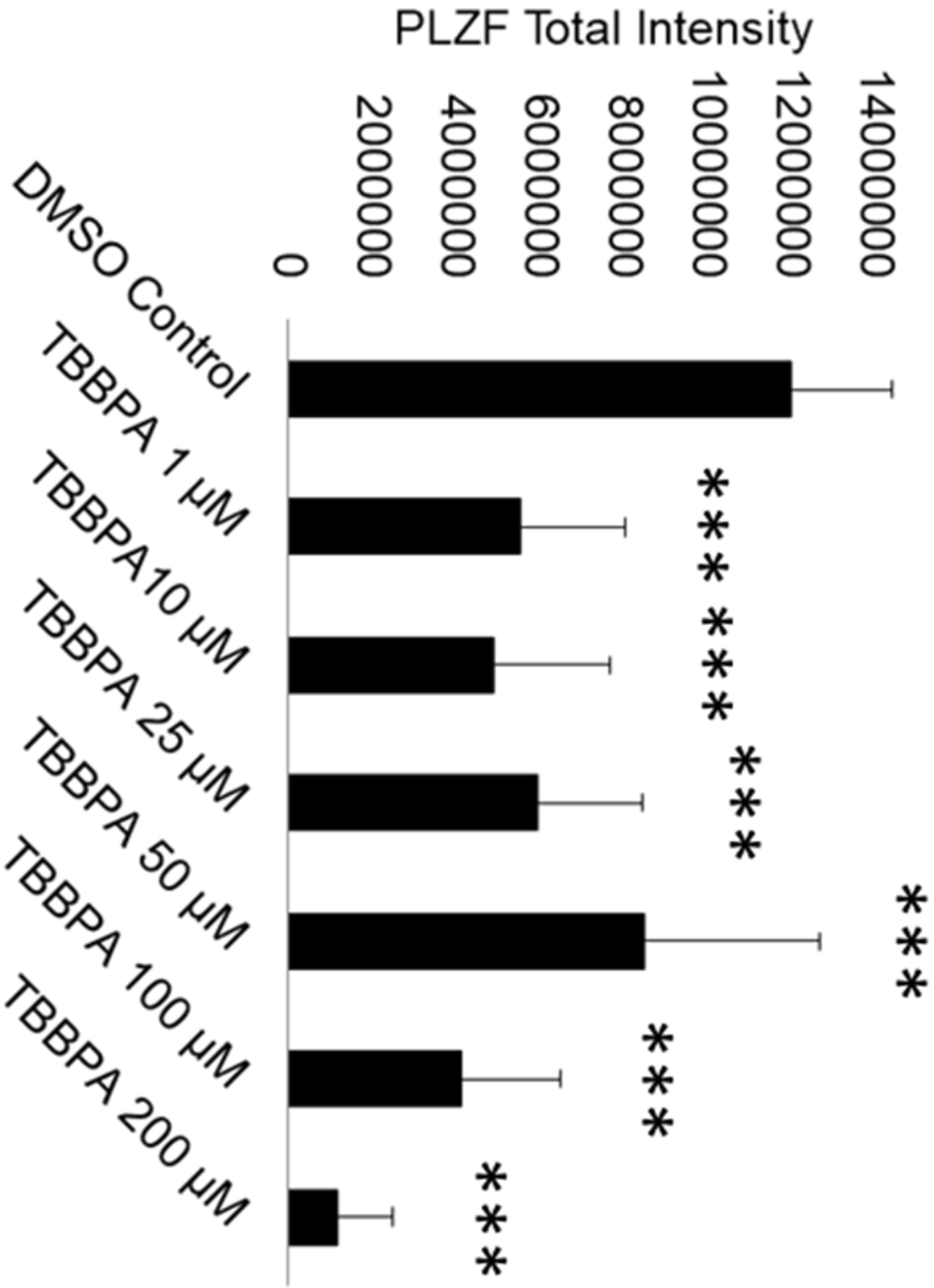
PLZF Total Intensity
0
2000000
4000000
6000000
8000000
10000000
12000000
14000000
DMSO Control
TBBPA 1 µM
TBBPA10 µM
TBBPA 25 µM
TBBPA 50 µM
TBBPA 100 µM
TBBPA 200 µM
****
****
****
****
****
****

Figure 4.9. Acute TBBPA exposure reduces PLZF+ intensity in spermatogonia in in vitro spermatogenic cultures derived from H1 ESCs. Graphical representation showing that acute, twenty-four hour exposure to 1 μM, 10 μM, 25 μM, 50 μM, 100 μM, and 200 μM TBBPA reduces average total PLZF+ intensity in spermatogonia derived under *in vitro* spermatogenic conditions in comparison to a 0.2% DMSO-only control. Five replications were performed for each condition (n = 5). Significant changes in PLZF+ intensity were determined using a 1-way analysis of variance (1-way ANOVA) and validated via a Student's t-test, where * is $p<0.05$, ** is $p<0.01$, and *** is $p<0.001$. Data are represented as mean ± SEM.

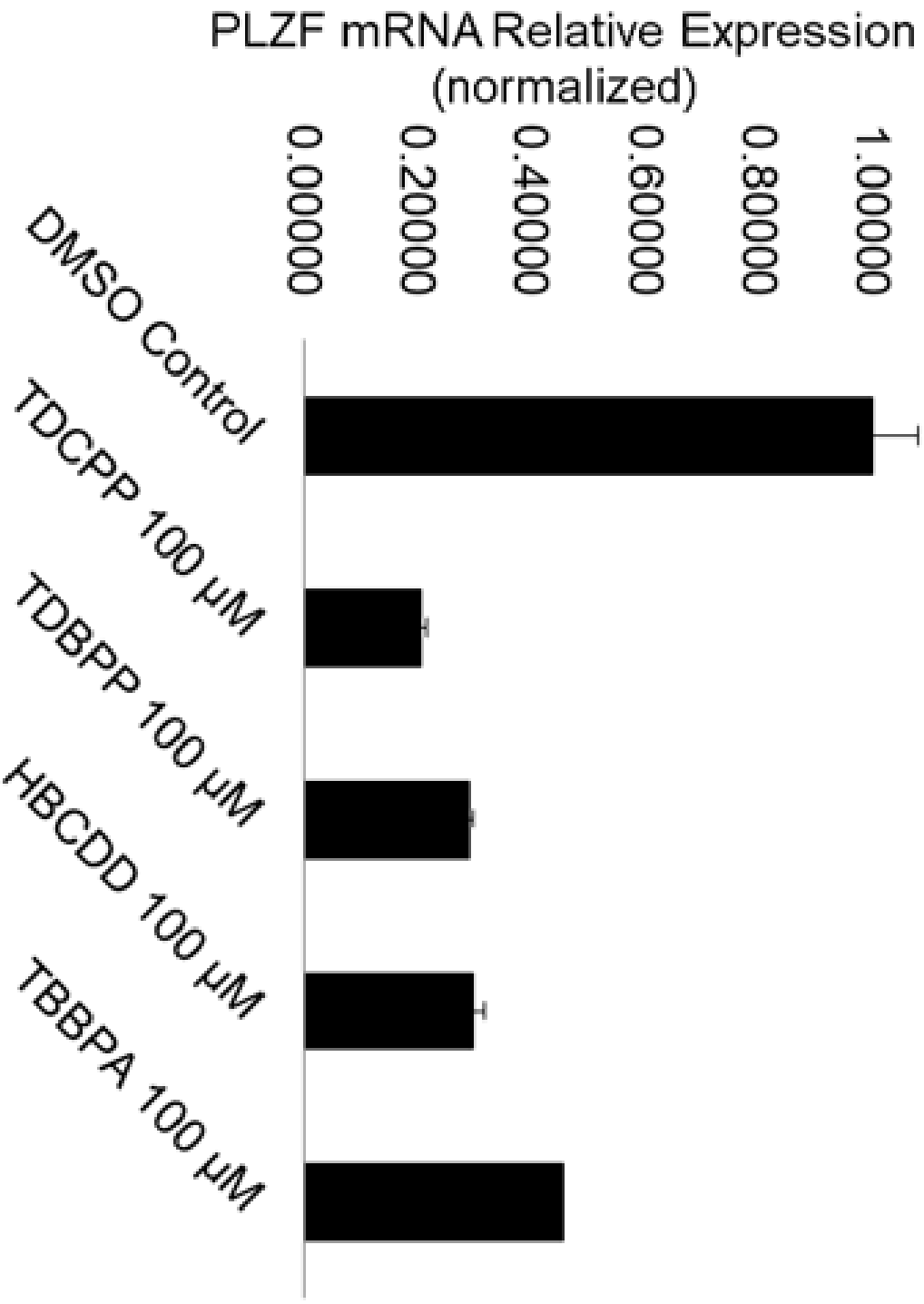
PLZF mRNA Relative Expression
(normalized)
0.00000
0.20000
0.40000
0.60000
0.80000
1.00000
DMSO Control
TDCPP 100 µM
TDBPP 100 µM
HBCDD 100 µM
TBBPA 100 µM

Figure 4.10. Acute TDCPP, TDBPP, HBCDD, and TBBPA exposure does not significantly impact ZBTB16 (PLZF) mRNA expression in spermatogonia in in vitro spermatogenic cultures derived from H1 ESCs. Graphical representation showing that acute, twenty-four hour exposure to 100 μM TDCPP, TDBPP, HBCDD, and TBBPA does not significantly impact average *ZBTB16* (PLZF) mRNA expression in spermatogonia derived under *in vitro* spermatogenic conditions. Transcript levels were normalized to 0.2% DMSO-only control. Two separate replications were performed in duplicate (n=4) for each condition. Significant changes in mRNA steady state levels were determined using Bio-Rad CFX Manager™ Software (Bio-Rad, Hercules, CA).

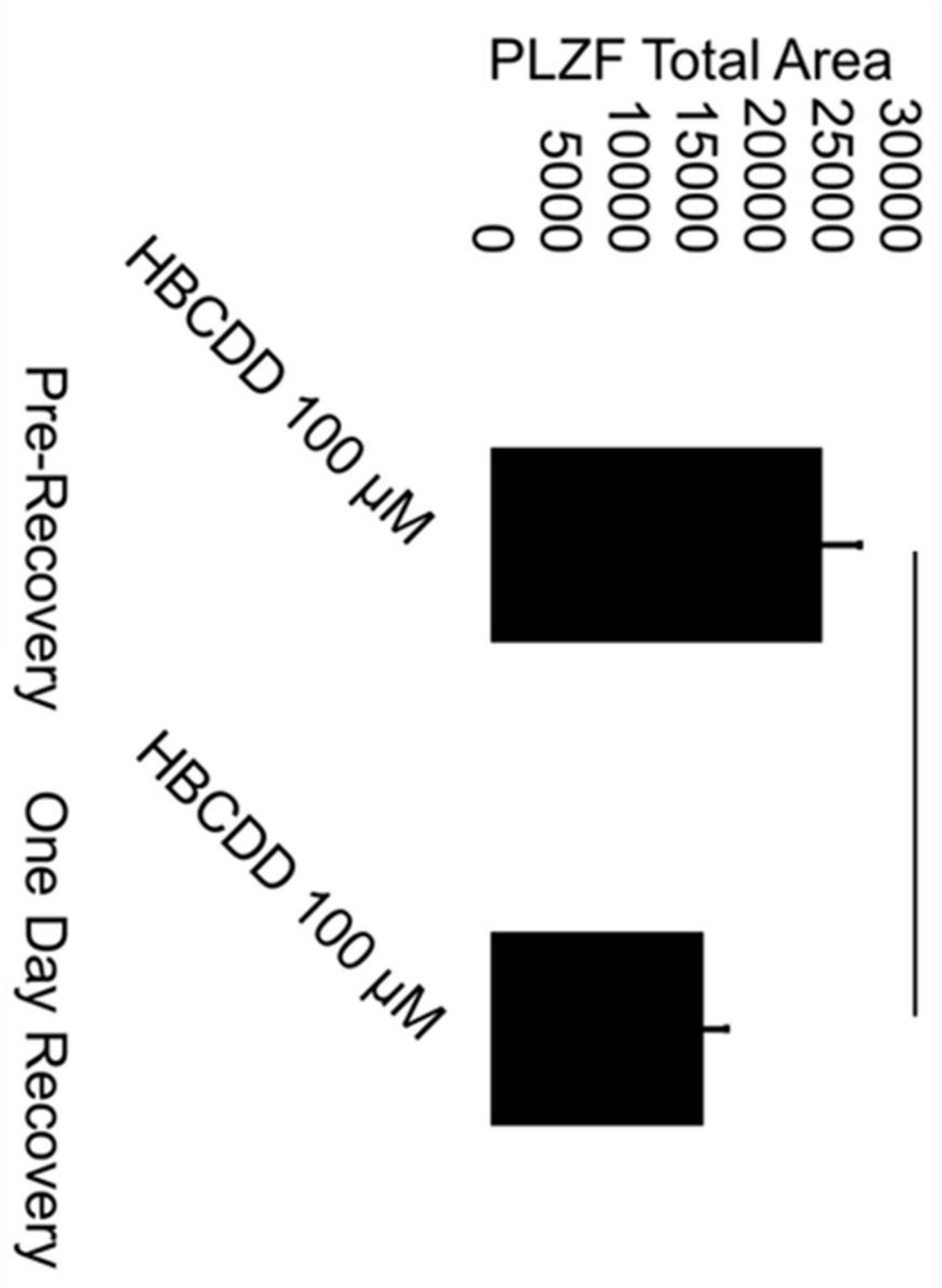
PLZF Total Area
30000
25000
20000
15000
10000
5000
0
HBCDD 100 µM
HBCDD 100 µM
***
Pre-Recovery
One Day Recovery

Figure 4.11. PLZF+ area in spermatogonia does not recover one day post-HBCDD exposure. Graphical representation showing that PLZF+ area is not capable of recovery following a twenty-four hour recovery period after 100 μM HBCDD exposure. Three replications were performed for each condition (n = 3). Differentiations were derived from H1 ESCs and compared to a 0.2% DMSO-only control. Significant changes in PLZF+ area were determined using a 1-way analysis of variance (1-way ANOVA) and validated via a Student's t-test, where * is $p<0.05$, ** is $p<0.01$, and *** is $p<0.001$. Data are represented as mean ± SEM.

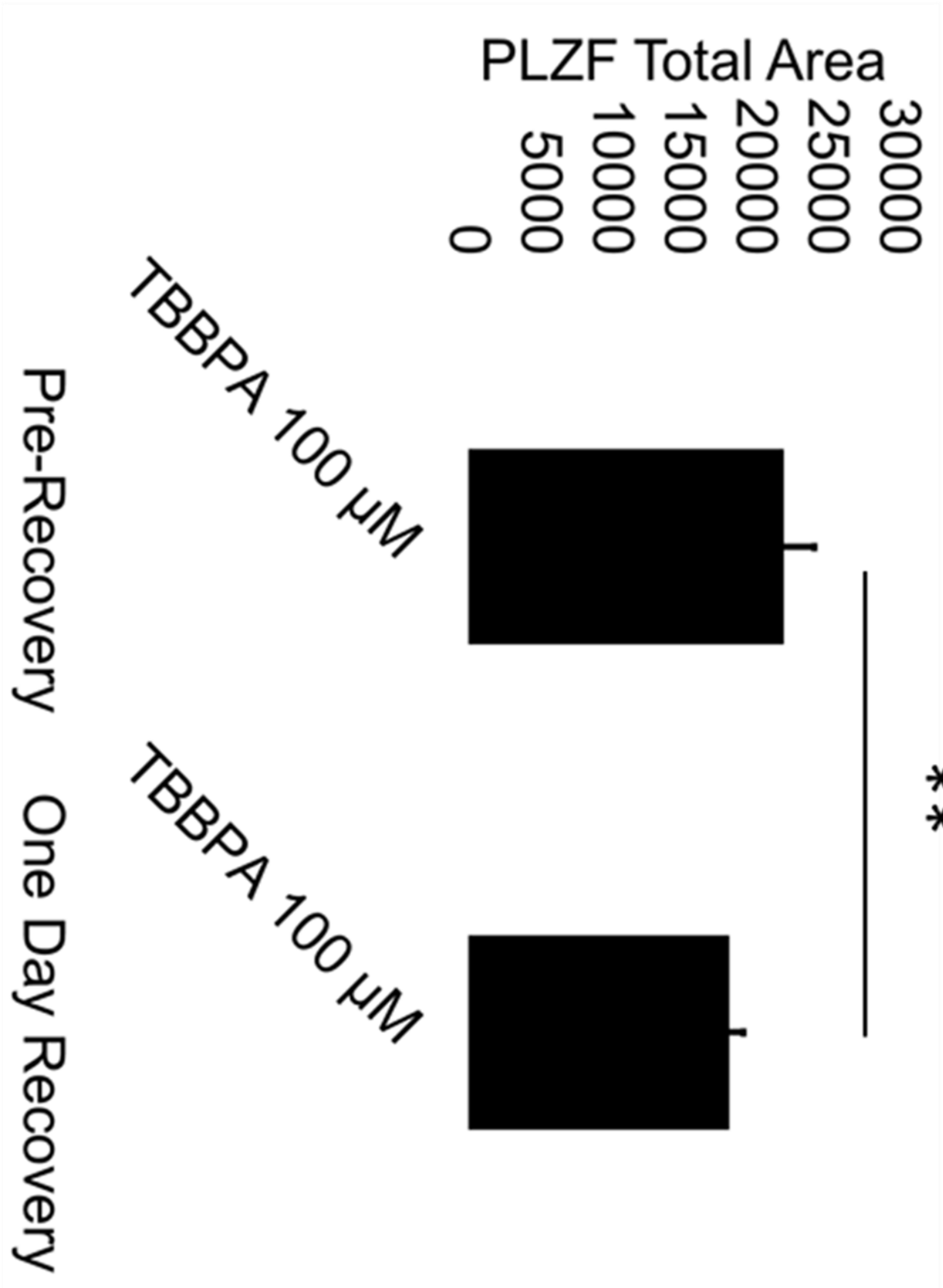
PLZF Total Area
30000
25000
20000
15000
10000
5000
0
**
TBBPA 100 μM
TBBPA 100 μM
Pre-Recovery
One Day Recovery

Figure 4.12. PLZF+ area in spermatogonia does not recover one day post-TBBPA exposure. Graphical representation showing that PLZF+ area is not capable of recovery following a twenty-four hour recovery period after 100 μM TBBPA exposure. Three replications were performed for each condition (n = 3). Differentiations were derived from H1 ESCs and compared to a 0.2% DMSO-only control. Significant changes in PLZF+ area were determined using a 1-way analysis of variance (1-way ANOVA) and validated via a Student's t-test, where * is $p<0.05$, ** is $p<0.01$, and *** is $p<0.001$. Data are represented as mean ± SEM.

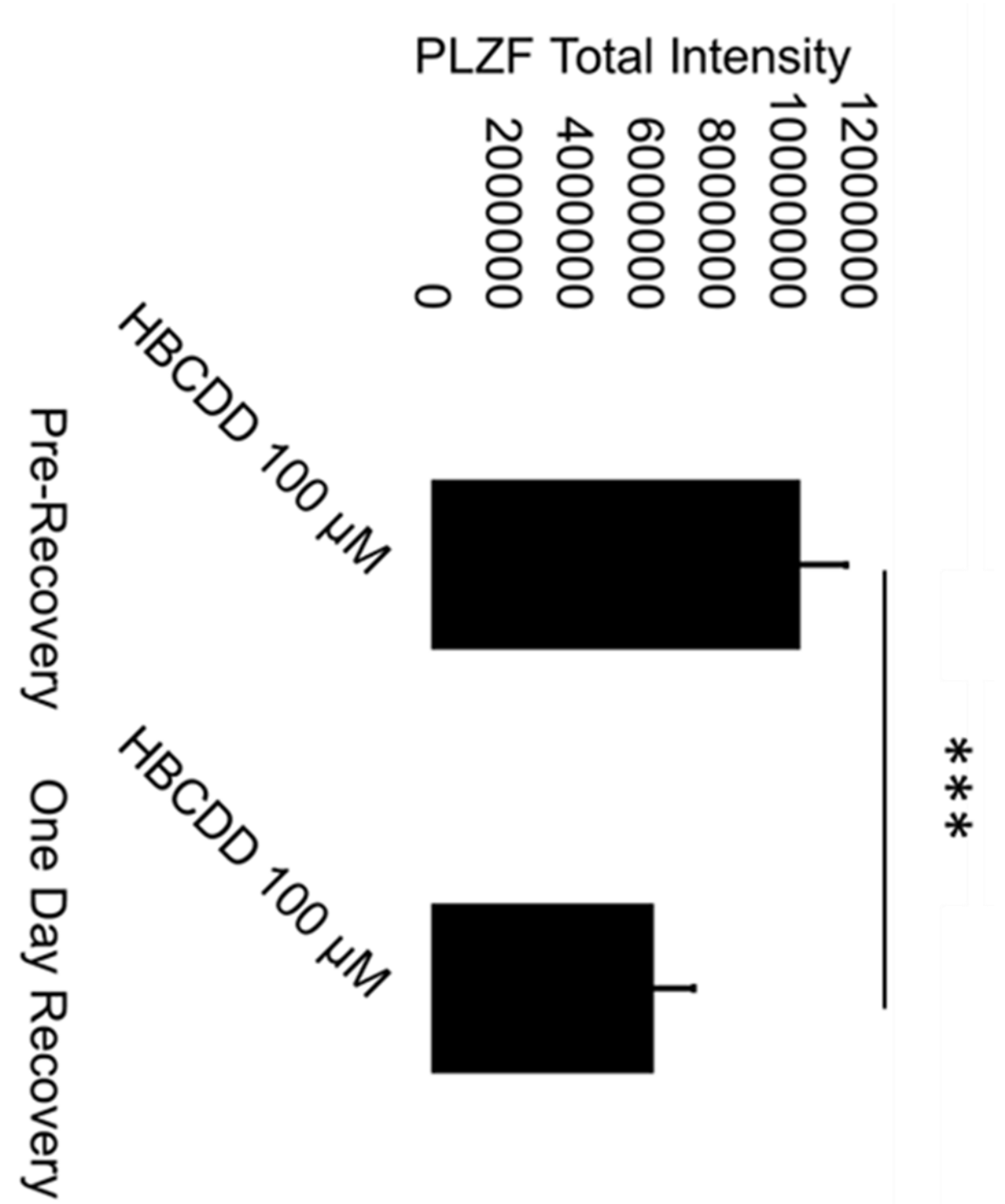
PLZF Total Intensity
12000000
10000000
8000000
6000000
4000000
2000000
0
HBCDD 100 μM
HBCDD 100 μM
***
Pre-Recovery
One Day Recovery

Figure 4.13. PLZF+ intensity in spermatogonia does not recover one day post-HBCDD exposure. Graphical representation showing that PLZF+ intensity is not capable of recovery following a twenty-four hour recovery period after 100 μM HBCDD exposure. Three replications were performed for each condition (n = 3). Differentiations were derived from H1 ESCs and compared to a 0.2% DMSO-only control. Significant changes in PLZF+ intensity were determined using a 1-way analysis of variance (1-way ANOVA) and validated via a Student's t-test, where * is $p<0.05$, ** is $p<0.01$, and *** is $p<0.001$. Data are represented as mean ± SEM.

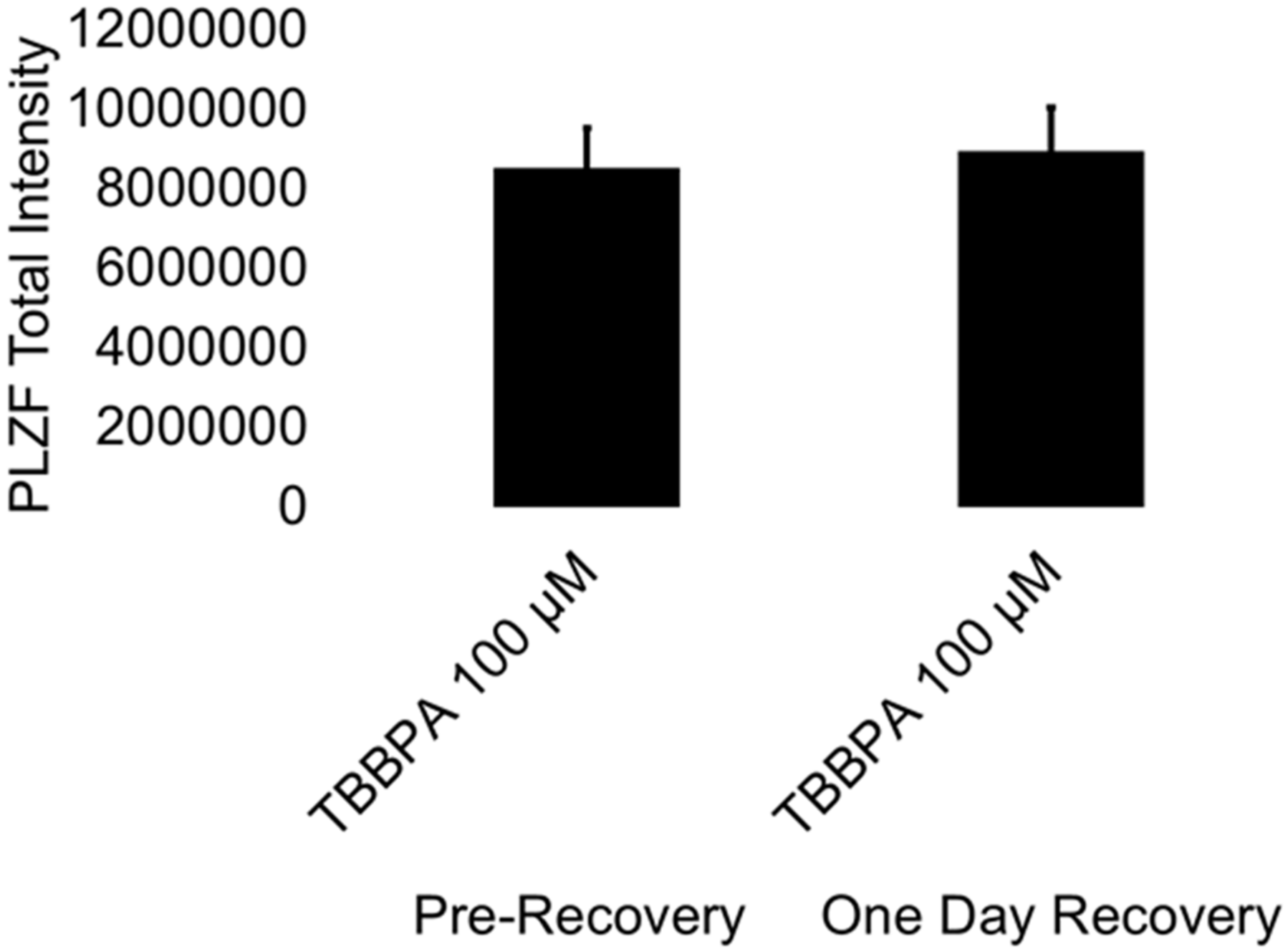
PLZF Total Intensity
12000000
10000000
8000000
6000000
4000000
2000000
0
TBBPA 100 µM
TBBPA 100 µM
Pre-Recovery
One Day Recovery

Figure 4.14. PLZF+ intensity in spermatogonia recovers one day post-TBBPA exposure. Graphical representation showing that PLZF+ intensity is capable of recovery following a twenty-four hour recovery period after 100 μM TBBPA exposure. Three replications were performed for each condition (n = 3). Differentiations were derived from H1 ESCs and compared to a 0.2% DMSO-only control. Significant changes in PLZF+ intensity were determined using a 1-way analysis of variance (1-way ANOVA) and validated via a Student's t-test, where * is $p<0.05$, ** is $p<0.01$, and *** is $p<0.001$. Data are represented as mean ± SEM.

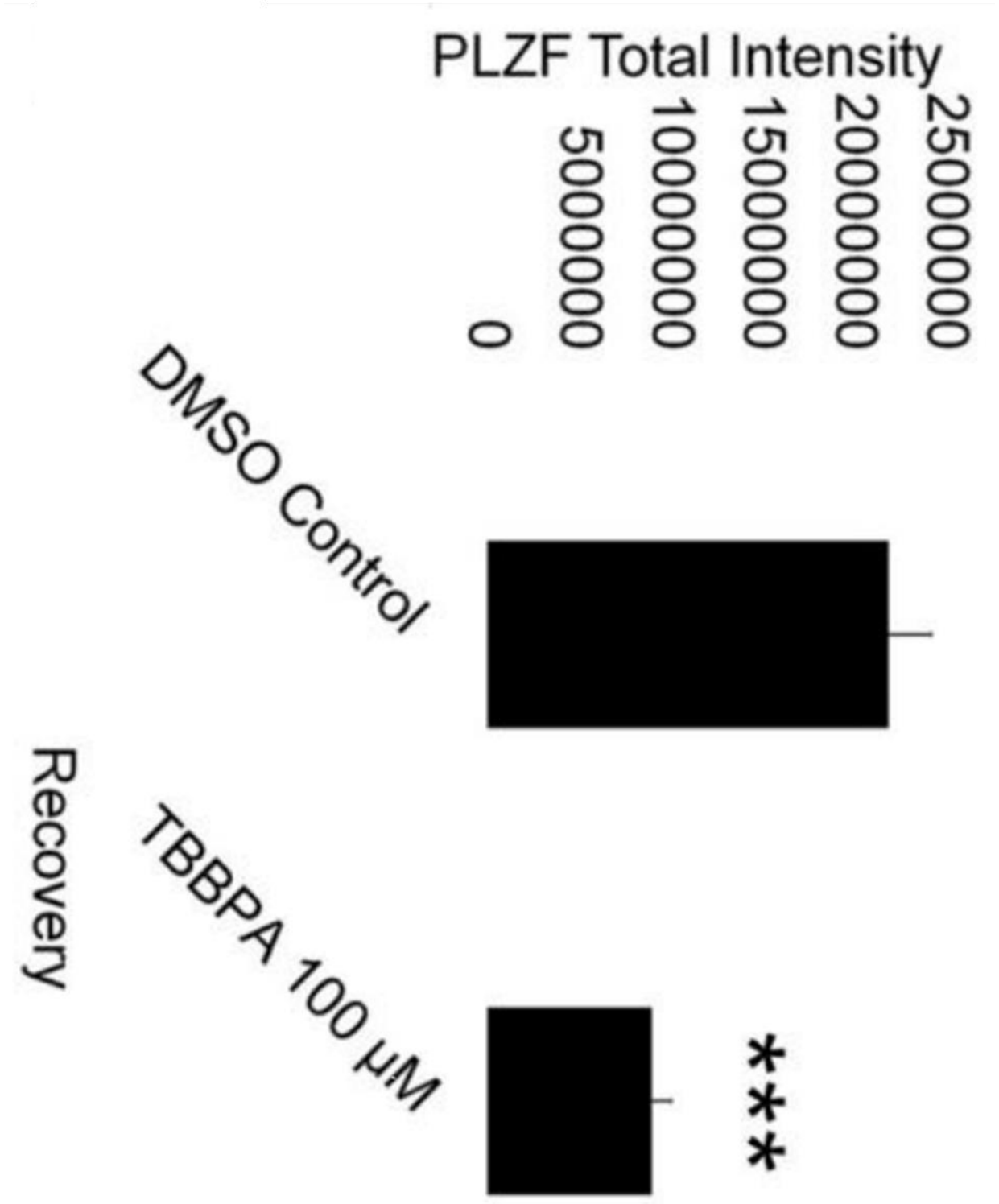
PLZF Total Intensity
25000000
20000000
15000000
10000000
5000000
0
DMSO Control
TBBPA 100 µM
***
Recovery

Figure 4.15. PLZF+ intensity in spermatogonia treated with TBBPA remains below control. Graphical representation showing that PLZF+ intensity in spermatogonia derived under *in vitro* spermatogenic conditions treated with 100 μM TBBPA remains below control levels following a twenty-four hour, chemical-free recovery period. Three replications were performed for each condition (n = 3). Differentiations were derived from H1 ESCs and compared to a 0.2% DMSO-only control. Significant changes in PLZF+ intensity were determined via a Student's t-test, where * is $p<0.05$, ** is $p<0.01$, and *** is $p<0.001$. Data are represented as mean ± SEM.

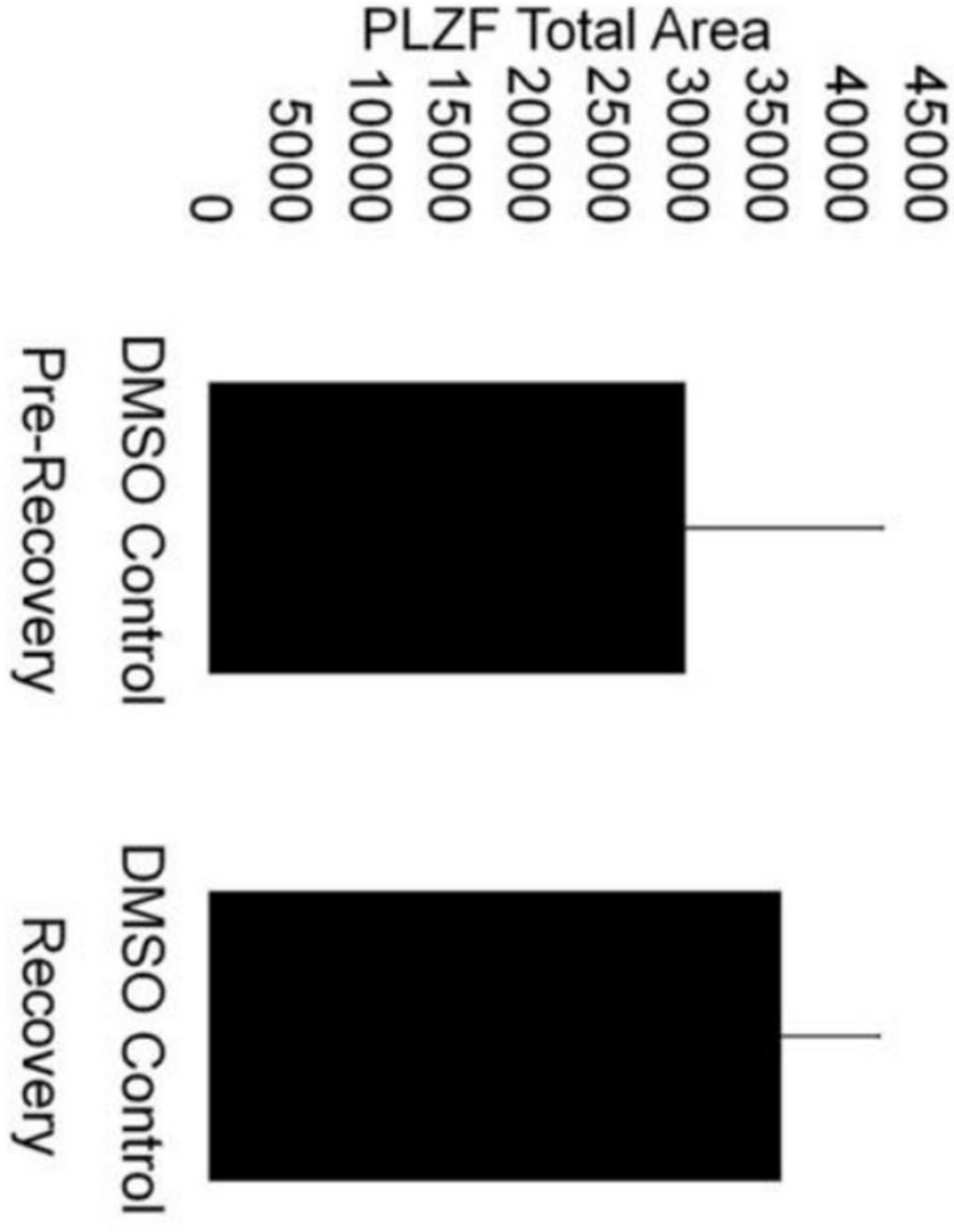
PLZF Total Area
45000
40000
35000
30000
25000
20000
15000
10000
5000
0
DMSO Control
Pre-Recovery
DMSO Control
Recovery

Figure 4.16. PLZF+ area remains unchanged in control spermatogonia during a twenty-four hour recovery period. Graphical representation showing that PLZF+ area in spermatogonia derived under *in vitro* spermatogenic control conditions remain statistically unchanged after a twenty four hour recovery period. Three replications were performed for each condition (n = 3). Differentiations were derived from H1 ESCs and compared to a 0.2% DMSO-only control. Significant changes in PLZF+ area were determined via a Student's t-test, where * is $p<0.05$, ** is $p<0.01$, and *** is $p<0.001$. Data are represented as mean ± SEM.

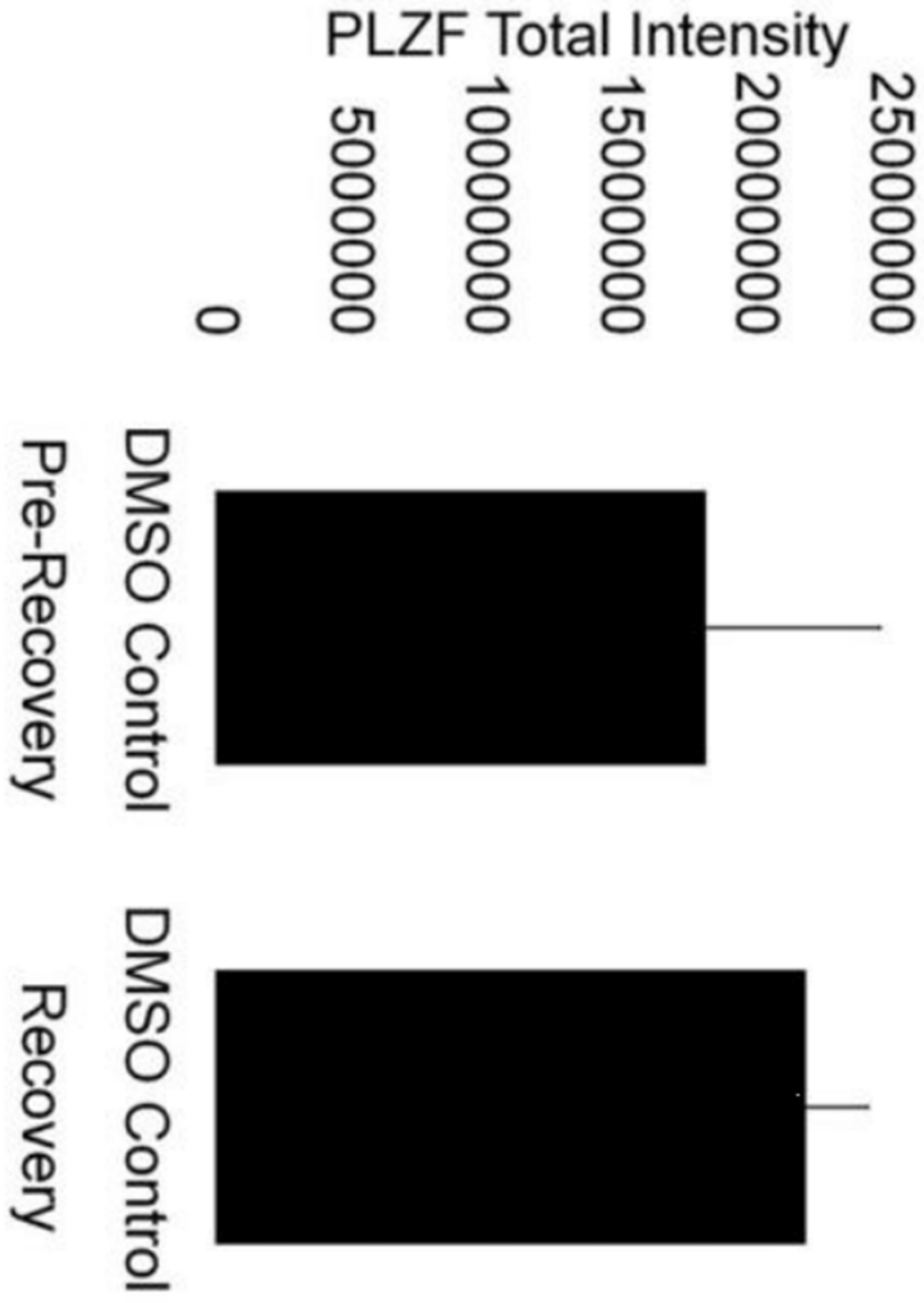
PLZF Total Intensity
25000000
20000000
15000000
10000000
5000000
0
DMSO Control
Pre-Recovery
DMSO Control
Recovery

Figure 4.17. PLZF+ intensity remains unchanged in control spermatogonia during a twenty-four hour recovery period. Graphical representation showing that PLZF+ intensity in spermatogonia derived under *in vitro* spermatogenic control conditions remain statistically unchanged after a twenty four hour recovery period. Three replications were performed for each condition (n = 3). Differentiations were derived from H1 ESCs and compared to a 0.2% DMSO-only control. Significant changes in PLZF+ intensity were determined via a Student's t-test, where * is $p<0.05$, ** is $p<0.01$, and *** is $p<0.001$. Data are represented as mean ± SEM.

PLZF Total Area
35000
30000
25000
20000
15000
10000
5000
0
DMSO Control
HBCDD 100 µM
Five Day Recovery

Figure 4.18. PLZF+ area in spermatogonia recovers five days post-HBCDD exposure. Graphical representation showing that PLZF+ area is capable of recovery following a five day recovery period after 100 μM HBCDD exposure. Three replications were performed for each condition (n = 3). Differentiations were derived from H1 ESCs and compared to a 0.2% DMSO-only control. Significant changes in PLZF+ area were determined using a 1-way analysis of variance (1-way ANOVA) and validated via a Student's t-test, where * is $p<0.05$, ** is $p<0.01$, and *** is $p<0.001$. Data are represented as mean ± SEM.

PLZF Total Area
35000
30000
25000
20000
15000
10000
5000
0
DMSO Control
TBBPA 100 µM
Five Day Recovery

Figure 4.19. PLZF+ area in spermatogonia recovers five days post-TBBPA exposure. Graphical representation showing that PLZF+ area is capable of recovery following a five day recovery period after 100 μM TBBPA exposure. Three replications were performed for each condition (n = 3). Differentiations were derived from H1 ESCs and compared to a 0.2% DMSO-only control. Significant changes in PLZF+ area were determined using a 1-way analysis of variance (1-way ANOVA) and validated via a Student's t-test, where * is $p<0.05$, ** is $p<0.01$, and *** is $p<0.001$. Data are represented as mean ± SEM.

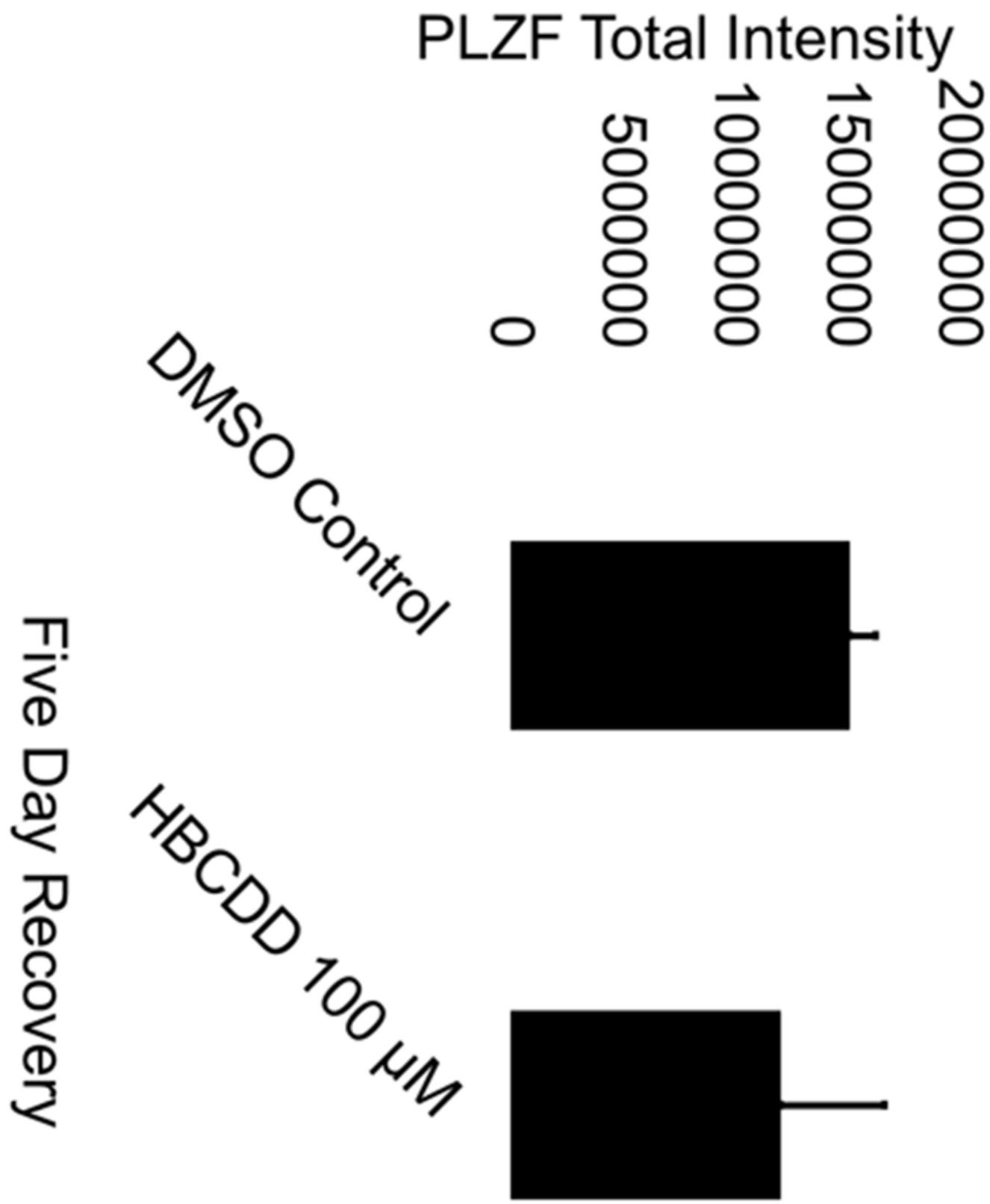
PLZF Total Intensity
0
5000000
10000000
15000000
20000000
DMSO Control
HBCDD 100 µM
Five Day Recovery

Figure 4.20. PLZF+ intensity in spermatogonia recovers five days post-HBCDD exposure. Graphical representation showing that PLZF+ intensity is capable of recovery following a five day recovery period after 100 μM HBCDD exposure. Three replications were performed for each condition (n = 3). Differentiations were derived from H1 ESCs and compared to a 0.2% DMSO-only control. Significant changes in PLZF+ intensity were determined using a 1-way analysis of variance (1-way ANOVA) and validated via a Student's t-test, where * is $p<0.05$, ** is $p<0.01$, and *** is $p<0.001$. Data are represented as mean ± SEM.

PLZF Total Intensity
0
5000000
10000000
15000000
20000000
DMSO Control
TBBPA 100 µM
Five Day Recovery

Figure 4.21. PLZF+ intensity in spermatogonia recovers five days post-TBBPA exposure. Graphical representation showing that PLZF+ intensity is capable of recovery following a five day recovery period after 100 μM TBBPA exposure. Three replications were performed for each condition (n = 3). Differentiations were derived from H1 ESCs and compared to a 0.2% DMSO-only control. Significant changes in PLZF+ intensity were determined using a 1-way analysis of variance (1-way ANOVA) and validated via a Student's t-test, where * is $p<0.05$, ** is $p<0.01$, and *** is $p<0.001$. Data are represented as mean ± SEM.

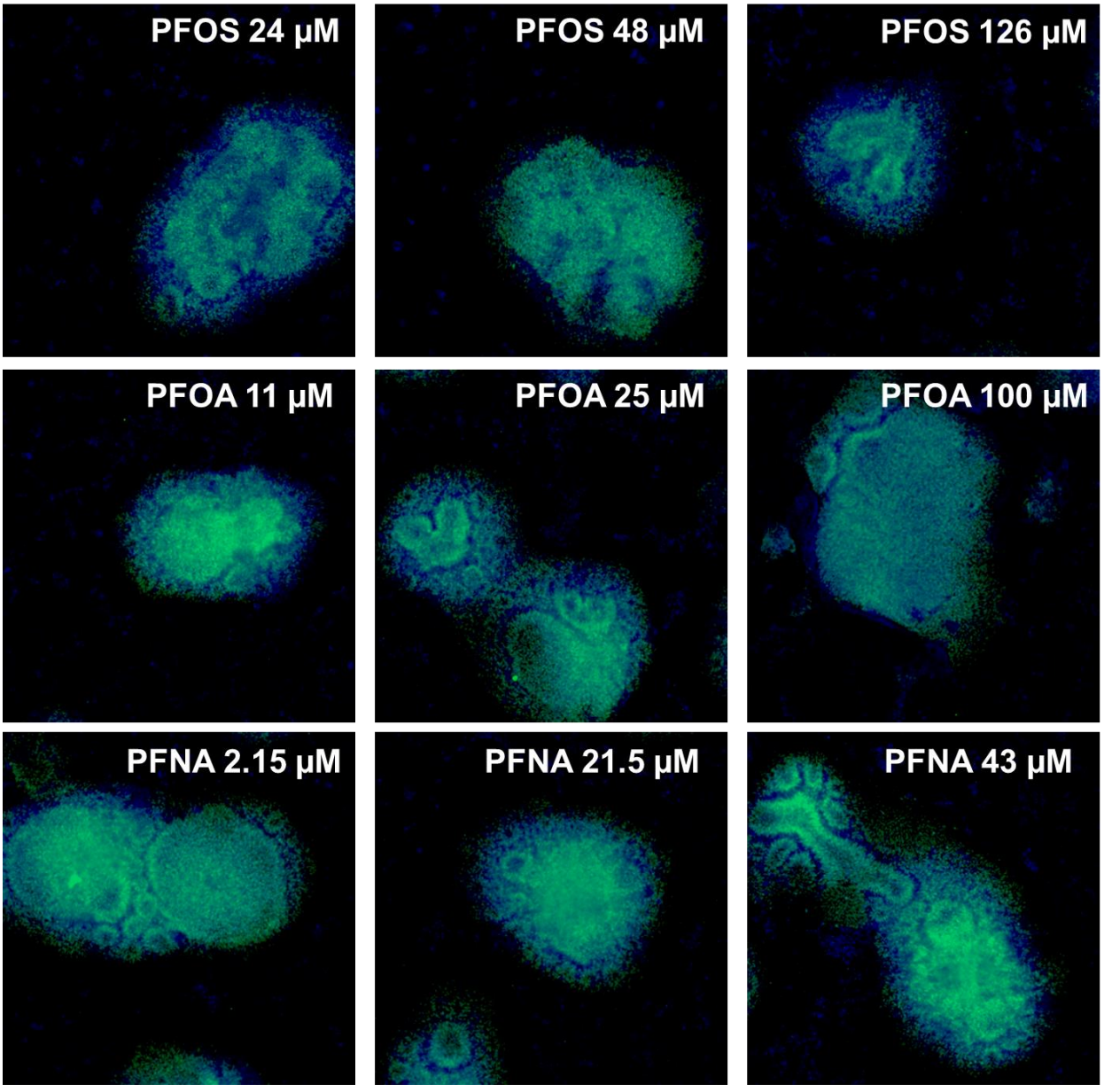
PFOS 24 µM
PFOS 48 µM
PFOS 126 µM
PFOA 11 µM
PFOA 25 µM
PFOA 100 µM
PFNA 2.15 µM
PFNA 21.5 µM
PFNA 43 µM

Figure 4.22. Persistent PFOS, PFOA, and PFNA exposure reduces PLZF+ area and intensity in spermatogonia in in vitro spermatogenic cultures derived from H1 ESCs. Representative 5X images obtained by the Cellomics ArrayScan VT1 of PLZF + (green) and DAPI (blue)-stained colonies treated with persistent doses of PFOS, PFOA, and PFNA from Day 1 to Day 10. Differentiations are derived from H1 ESCs. All images are taken under the same imaging conditions and parameters.

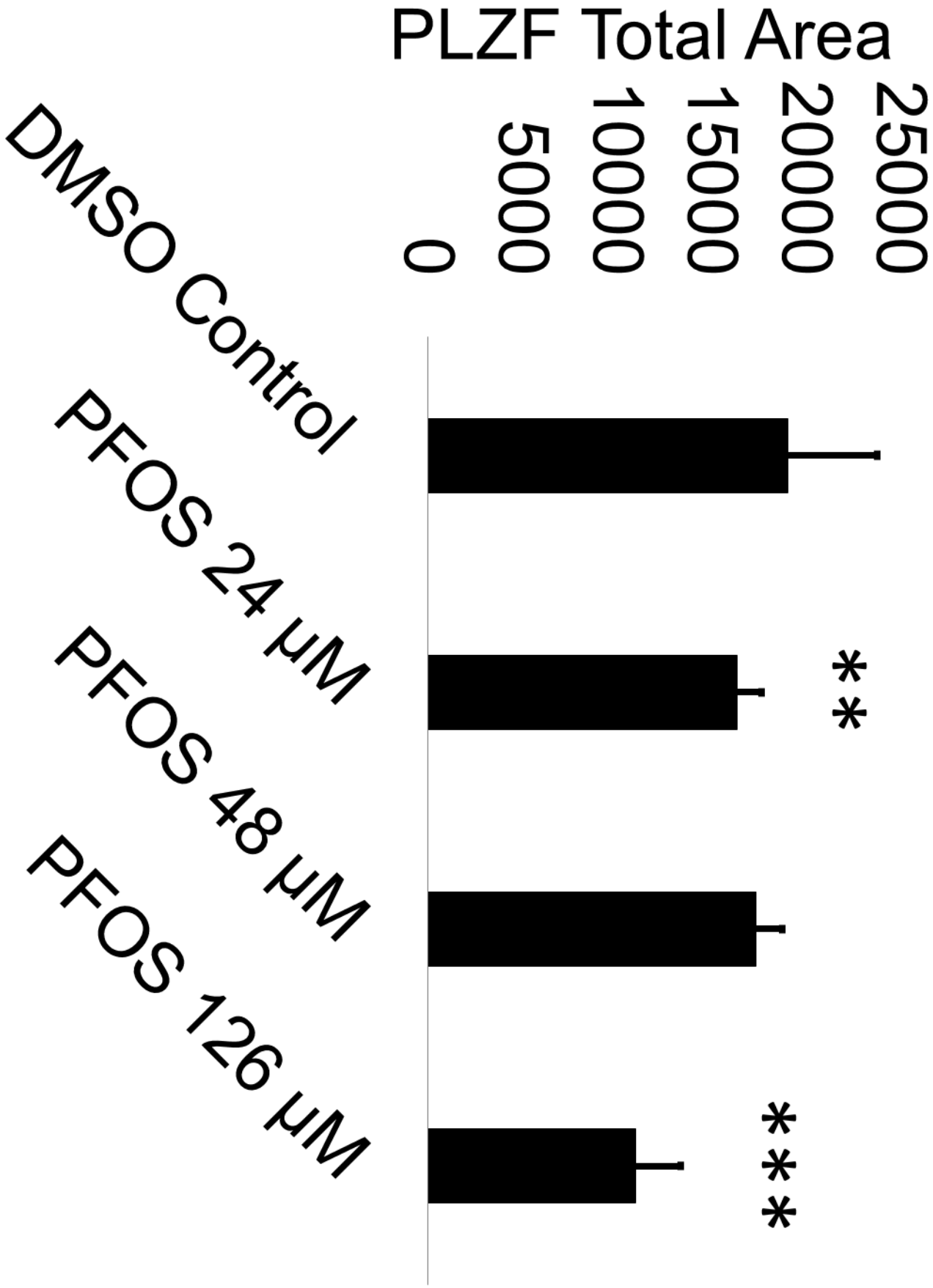
PLZF Total Area
0
5000
10000
15000
20000
25000
DMSO Control
PFOS 24 µM
PFOS 48 µM
PFOS 126 µM
**
***

Figure 4.23. Persistent PFOS exposure reduces PLZF+ area in spermatogonia in in vitro spermatogenic cultures derived from H1 ESCs. Graphical representation showing that persistent 24 μM and 126 μM PFOS exposure from Day 1 to Day 10 reduces average total PLZF+ area in spermatogonia derived under *in vitro* spermatogenic conditions in comparison to a 0.25% DMSO-only control. Three replications were performed for each condition, and spermatogenic cells were derived from H1 ESCs (n = 3). Significant changes in PLZF+ area were determined using a 1-way analysis of variance (1-way ANOVA) and validated via a Student's t-test, where * is $p<0.05$, ** is $p<0.01$, and *** is $p<0.001$. Data are represented as mean ± SEM.

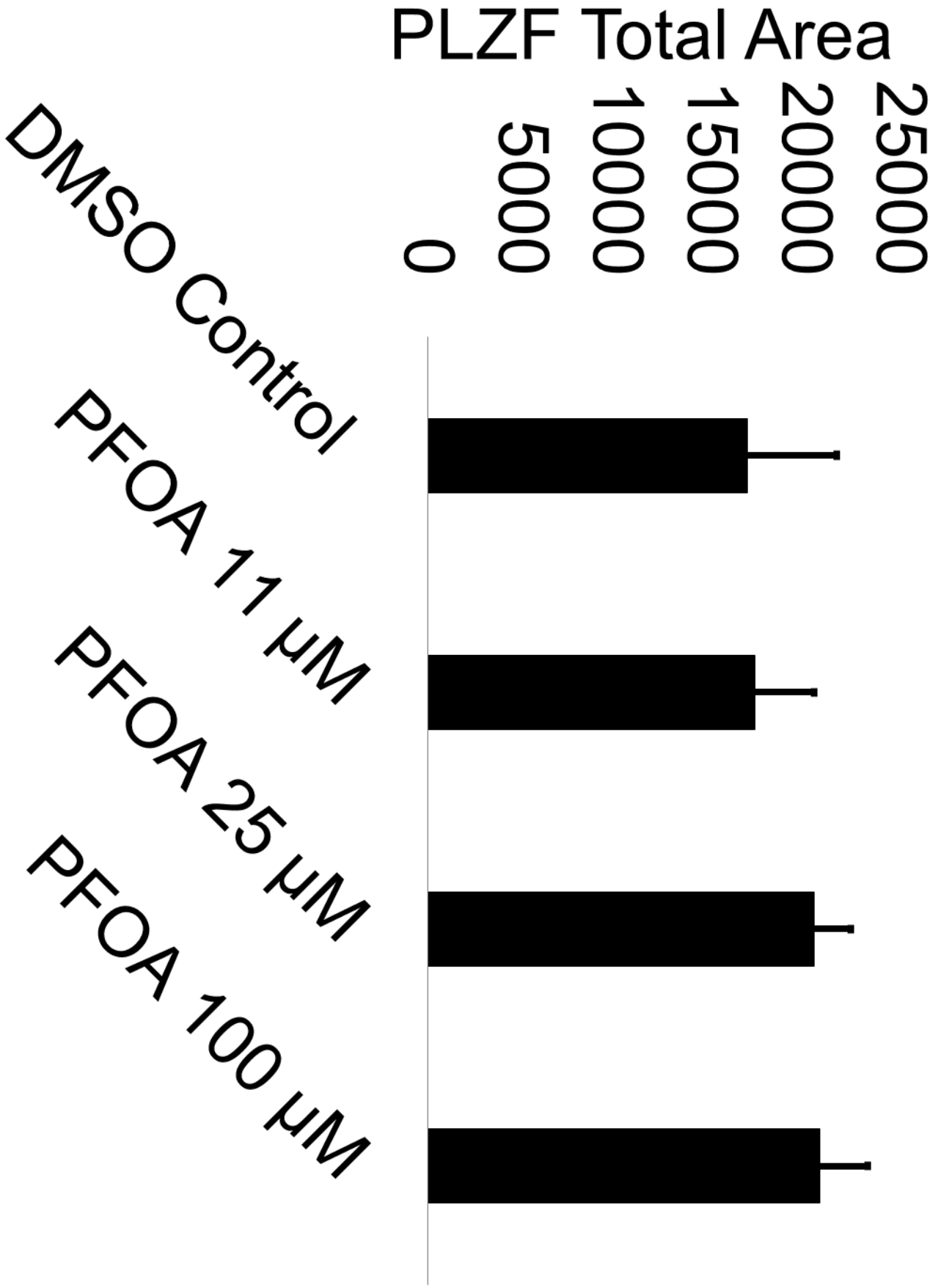
PLZF Total Area
0
5000
10000
15000
20000
25000
DMSO Control
PFOA 11 µM
PFOA 25 µM
PFOA 100 µM

Figure 4.24. Persistent PFOA exposure does not impact PLZF+ area in spermatogonia in in vitro spermatogenic cultures derived from H1 ESCs. Graphical representation showing that persistent 11 μM, 25 μM, and 100 μM PFOA exposure from Day 1 to Day 10 does not reduce average total PLZF+ area in spermatogonia derived under *in vitro* spermatogenic conditions in comparison to a 0.25% DMSO-only control. Three replications were performed for each condition, and spermatogenic cells were derived from H1 ESCs (n = 3). Significant changes in PLZF+ area were determined using a 1-way analysis of variance (1-way ANOVA) and validated via a Student's t-test, where * is $p<0.05$, ** is $p<0.01$, and *** is $p<0.001$. Data are represented as mean ± SEM.

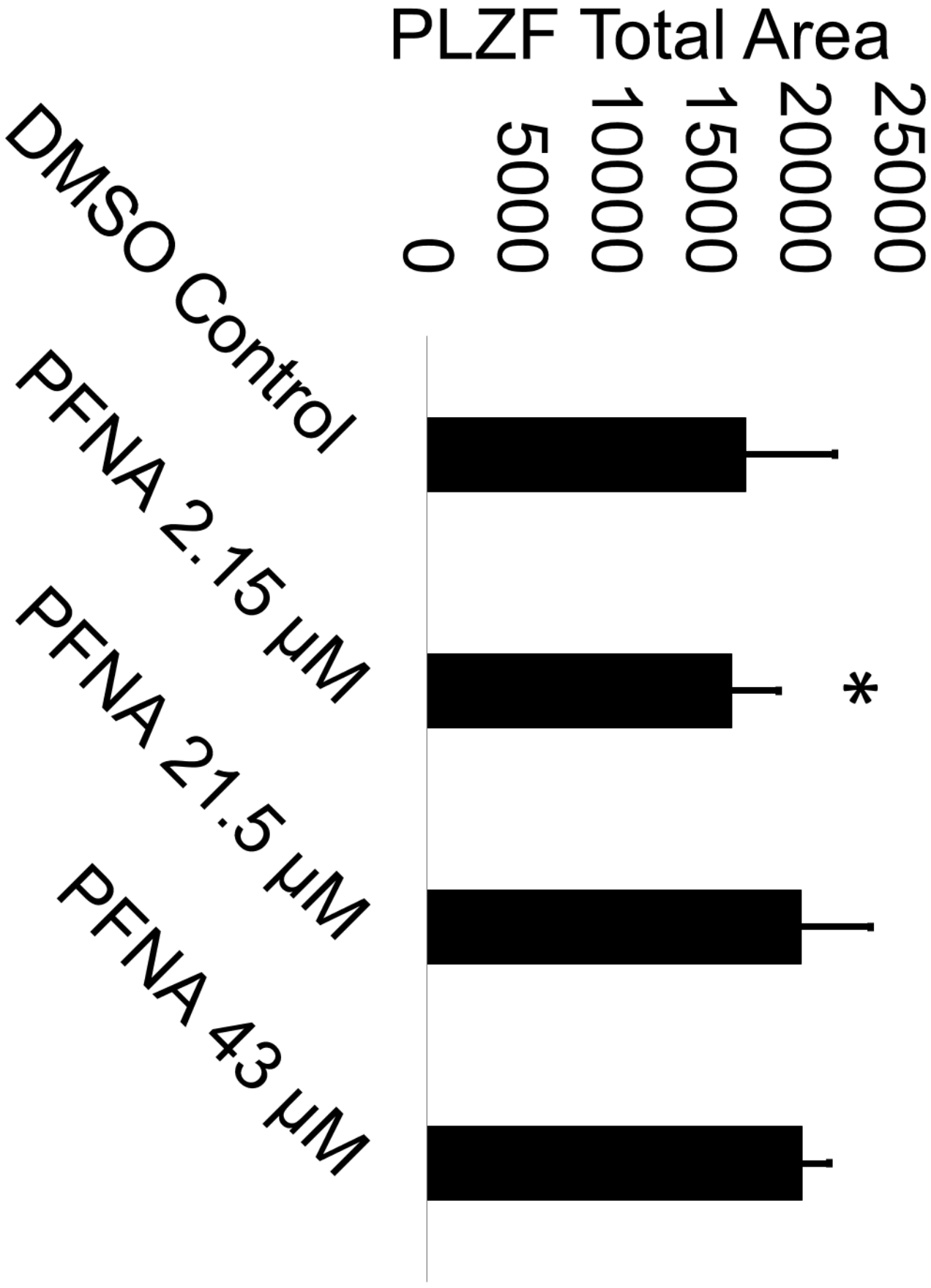
PLZF Total Area
0
5000
10000
15000
20000
25000
DMSO Control
PFNA 2.15 µM
PFNA 21.5 µM
PFNA 43 µM
*

Figure 4.25. Persistent PFNA exposure reduces PLZF+ area in spermatogonia in in vitro spermatogenic cultures derived from H1 ESCs. Graphical representation showing that persistent 2.15 μM PFNA exposure from Day 1 to Day 10 reduces average total PLZF+ area in spermatogonia derived under *in vitro* spermatogenic conditions in comparison to a 0.25% DMSO-only control. Three replications were performed for each condition, and spermatogenic cells were derived from H1 ESCs (n = 3). Significant changes in PLZF+ area were determined using a 1-way analysis of variance (1-way ANOVA) and validated via a Student's t-test, where * is $p<0.05$, ** is $p<0.01$, and *** is $p<0.001$. Data are represented as mean ± SEM.

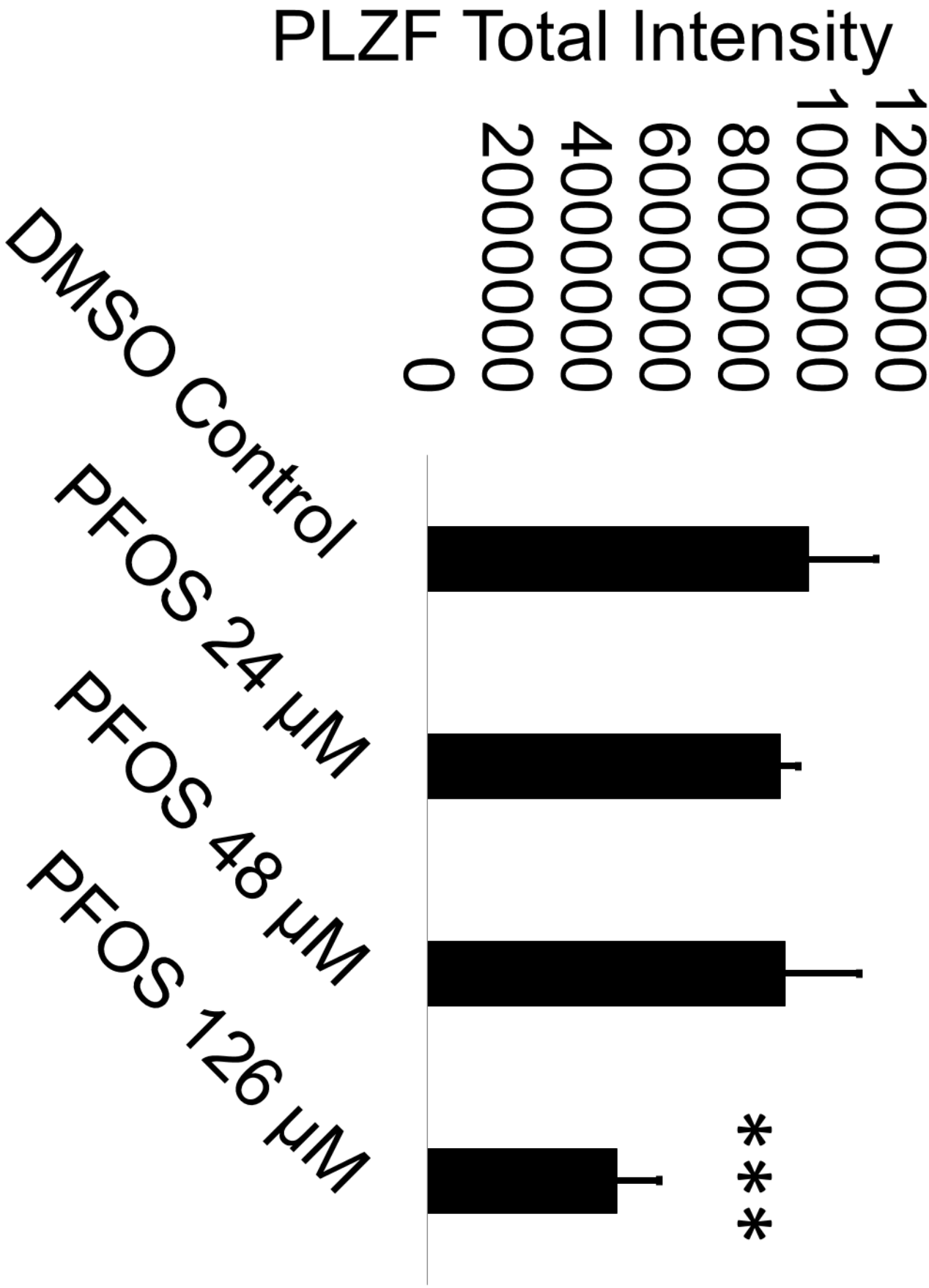
PLZF Total Intensity
0
2000000
4000000
6000000
8000000
10000000
12000000
DMSO Control
PFOS 24 µM
PFOS 48 µM
PFOS 126 µM
***

Figure 4.26. Persistent PFOS exposure reduces PLZF+ intensity in spermatogonia in in vitro spermatogenic cultures derived from H1 ESCs. Graphical representation showing that persistent 126 μM PFOS exposure from Day 1 to Day 10 reduces average total PLZF+ intensity in spermatogonia derived under *in vitro* spermatogenic conditions in comparison to a 0.25% DMSO-only control. Three replications were performed for each condition, and spermatogenic cells were derived from H1 ESCs (n = 3). Significant changes in PLZF+ intensity were determined using a 1-way analysis of variance (1-way ANOVA) and validated via a Student's t-test, where * is $p<0.05$, ** is $p<0.01$, and *** is $p<0.001$. Data are represented as mean ± SEM.

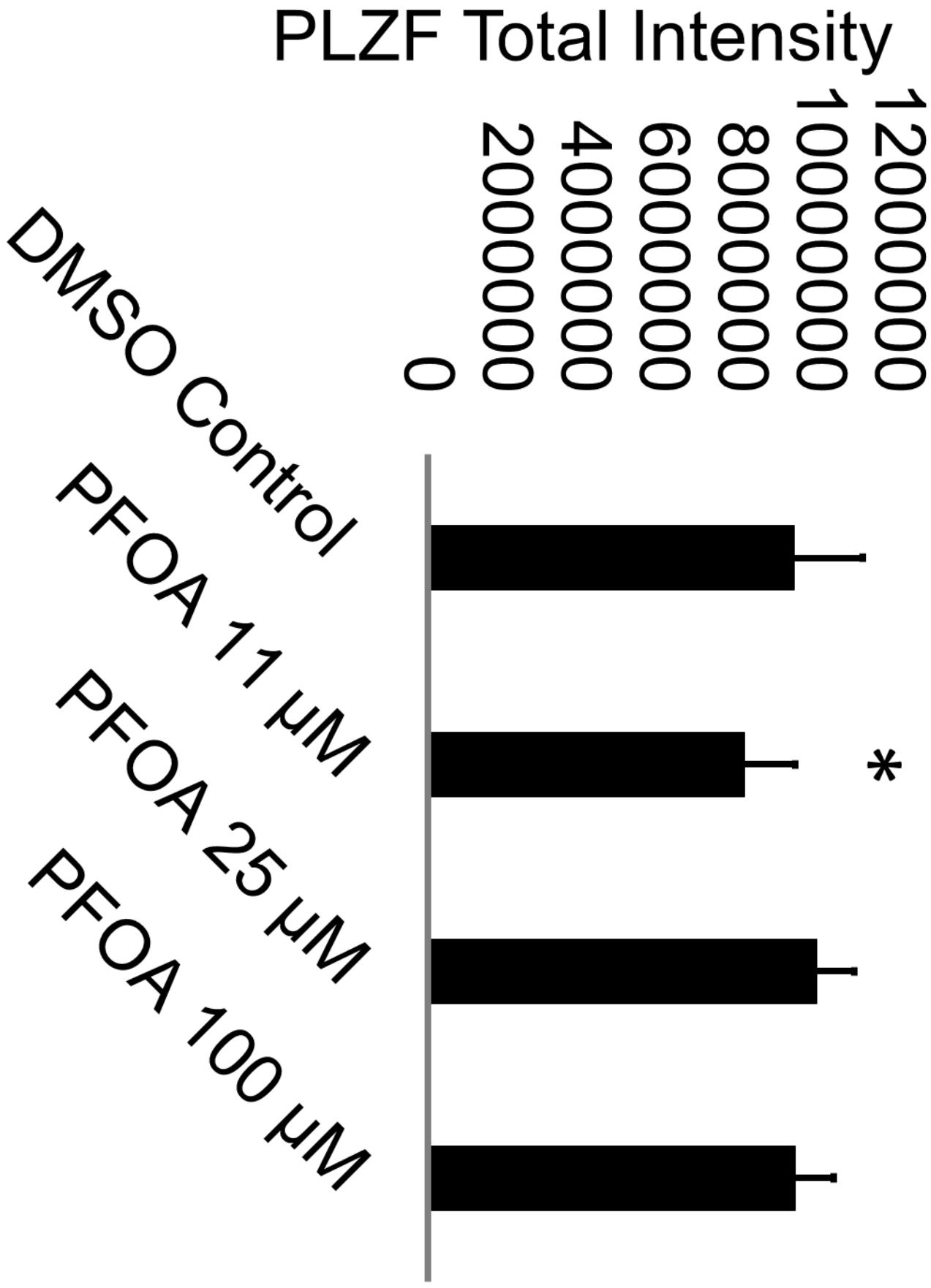
PLZF Total Intensity
0
2000000
4000000
6000000
8000000
10000000
12000000
DMSO Control
PFOA 11 µM
PFOA 25 µM
PFOA 100 µM
*

Figure 4.27. Persistent PFOA exposure reduces PLZF+ intensity in spermatogonia in in vitro spermatogenic cultures derived from H1 ESCs. Graphical representation showing that persistent 11 μM PFOA exposure from Day 1 to Day 10 reduces average total PLZF+ intensity in spermatogonia derived under *in vitro* spermatogenic conditions in comparison to a 0.25% DMSO-only control. Three replications were performed for each condition, and spermatogenic cells were derived from H1 ESCs (n = 3). Significant changes in PLZF+ intensity were determined using a 1-way analysis of variance (1-way ANOVA) and validated via a Student's t-test, where * is $p<0.05$, ** is $p<0.01$, and *** is $p<0.001$. Data are represented as mean ± SEM.

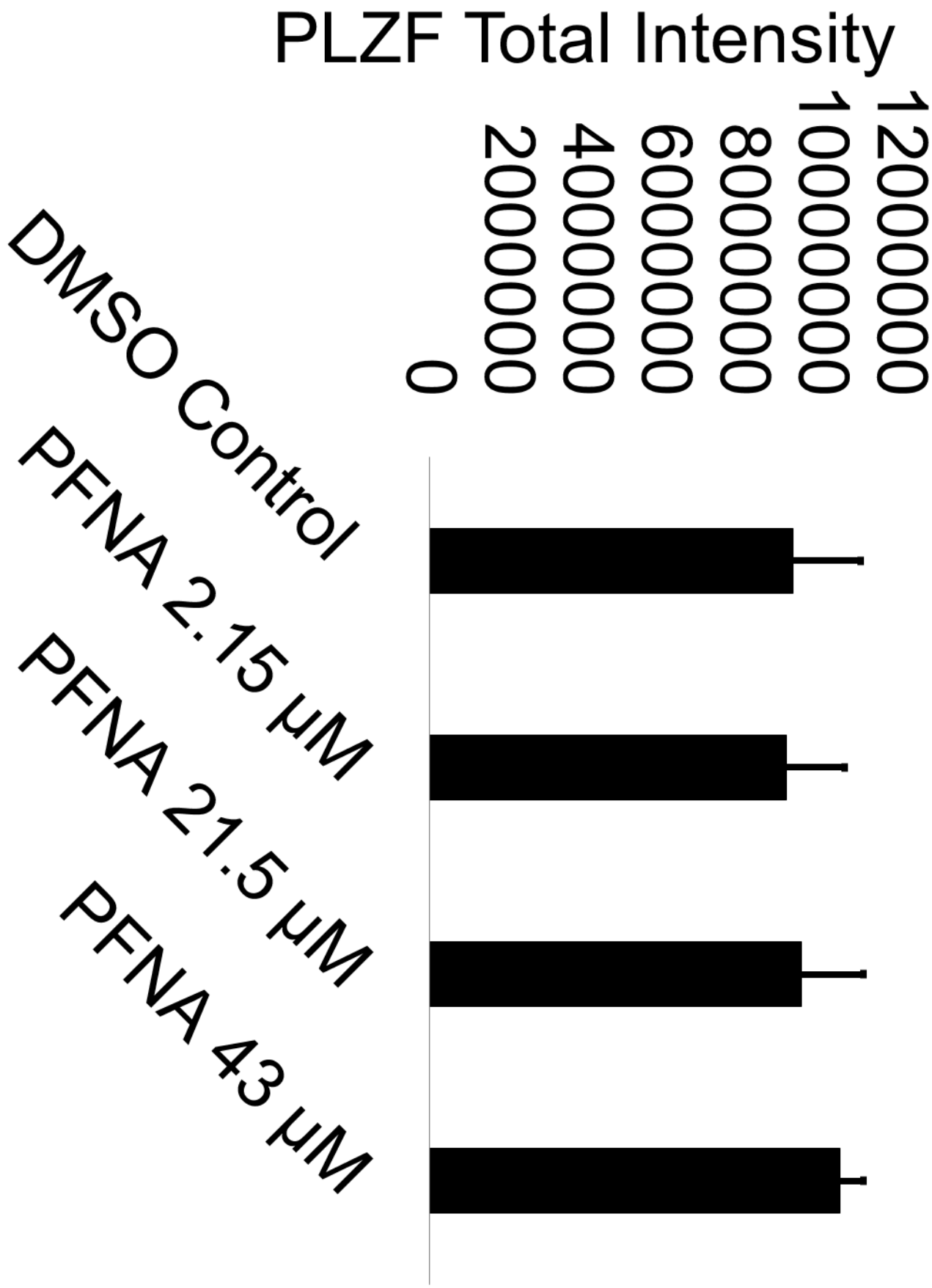
PLZF Total Intensity
0
2000000
4000000
6000000
8000000
10000000
12000000
DMSO Control
PFNA 2.15 µM
PFNA 21.5 µM
PFNA 43 µM

Figure 4.28. Persistent PFNA exposure does not reduce PLZF+ intensity in spermatogonia in in vitro spermatogenic cultures derived from H1 ESCs. Graphical representation showing that persistent 2.15 μM, 21.5 μM, and 43 μM PFNA exposure from Day 1 to Day 10 does not reduce average total PLZF+ intensity in spermatogonia derived under *in vitro* spermatogenic conditions in comparison to a 0.25% DMSO-only control. Three replications were performed for each condition, and spermatogenic cells were derived from H1 ESCs (n = 3). Significant changes in PLZF+ intensity were determined using a 1-way analysis of variance (1-way ANOVA) and validated via a Student's t-test, where * is $p<0.05$, ** is $p<0.01$, and *** is $p<0.001$. Data are represented as mean ± SEM.

2.5.3 Acute TDCPP, TDBPP, HBCDD, and TBBPA and persistent PFOS, PFOA, and PFNA exposure decreases the viability of primary spermatocytes derived from H1 ESCs

Spermatocytes are crucial to genome integrity as they undergo meiosis to give rise to haploid spermatids (Chen and Liu, 2015, Yan and McCarrey, 2009). Failures in meiosis, particularly failure of chromosomes to synapse or loss of sex chromosomes during meiosis, have implications in male fertility (Cloutier and Turner, 2010, Repping et al., 2002). Importantly, the repression of transposons and the regulation of genes critical to spermatogenesis are also occurring in primary spermatocytes (Juliano et al., 2011). Perturbation of any of these processes could result in meiotic arrest and failure to progress in differentiation or inducing cell death. To assess if primary spermatocytes are also cellular targets of our chemicals, we analyzed for expression of the primary spermatocyte marker piwi like RNA-mediated gene silencing 2 (HILI). Using high content imaging and quantification performed by the ThermoFisher Cellomics ArrayScan® VTI (ThermoFisher, Waltham, MA), we determined that TDCPP, TDBPP, HBCDD, and TBBPA all significantly increased HILI total area and total intensity beginning at 1 µM (Figures 5.1 – 5.9). TDCPP, TDBPP, HBCDD, and TBBPA all showed an initial significant increase in HILI+ area of 53%, 52%, 50%, and 50% in comparison to control, respectively (Figures 5.2 – 5.5). TDCPP, TDBPP, and TBBPA showed a steady, significant decline in HILI+ area with increasing concentration until levels decreased to roughly 30%, 30%, and 90%, of control, respectively (Figures 5.2 - 5.3, 5.5). Interestingly, HBCDD showed a steady, significant increase in HILI+ area until 25 µM, where HILI+ area is 85% above HILI+ total area in 0.2% DMSO-only control

(Figure 5.4). There was an abrupt, significant decline in HBCDD HILI+ area at 50 µM, ending with levels roughly 60% of control at 200 µM (Figure 5.4). Similarly, TDCPP, TDBPP, HBCDD, and TBBPA significantly increased HILI+ total intensity at 1 µM, with TDBPP and TBBPA showing a significant, steady decline in HILI total intensity (Figures 5.6 – 5.9). Initially, HILI total intensity was 67%, 65%, 80%, and 90% more than DMSO-only control (Figure 5.6 – 5.9). TDBPP and TBBPA HILI+ total intensity significantly declined to 13% and 9% of control levels at 200 µM, respectively, though total intensity was not statistically different from control levels at 200 µM TDBPP (Figure 5.7, 5.9). TDCPP HILI+ total intensity remained significantly elevated until 200 µM, where it declined to 50% of control levels (Figure 5.6). HBCDD HILI+ total intensity remained above control until 50 µM, where it significantly declined (Figure 5.8). HBCDD HILI+ levels were lowest at 200 µM, where they were roughly 50% of control levels (Figure 5.8). qRT-PCR results from the amplification of *PIWIL2* (HILI) transcripts in our *in vitro* model showed an increasing trend for 100 µM TDCPP, TDBPP, and TBBPA mRNA steady state levels compared to control, with a roughly 210%, 90%, and 80% increase, respectively (Figure 5.10). 100 µM HBCDD showed a slight decrease in HILI mRNA steady state levels that remained similar to control, with levels decreasing by roughly 8% (Figure 5.10). Together, these data suggest that low dose FR exposure increases HILI expression, while at higher doses, FR exposure reduces HILI expression by impacting spermatocyte viability.

Primary spermatocytes appear to fair better than spermatogonia following a twenty-four hour recovery period after 100 µM HBCDD and TBBPA exposure (Figures 5.11 – 5.12, 5.14 – 5.15). HBCDD-exposed primary spermatocytes show an

insignificant 17% increase in HILI area, while TBBPA-exposed cells show a 7% decline in area (Figures 5.11 – 5.12). Notably, DMSO-only treated cells show an insignificant 12% increase in HILI area (Figure 5.13). HBCDD-treated cells show a significant 39% increase in HILI intensity, and TBBPA-treated cells show a significant 32% increase in HILI intensity during the twenty-four hour recovery period (Figures 5.14 – 5.15). While the increases in HILI area and intensity observed may indicate a recovery of primary spermatocytes, both HBCDD and TBBPA do cause increases in HILI area and intensity at low levels. Possibly, the mechanism activated in low-level doses is similarly present in recovering cells, and this increase in area and intensity may also be a result of chemical exposure after the fact. This theory is highlighted by the fact that, while cells treated with 100 µM HBCDD recover following a five-day recovery period, cells treated with 100 µM TBBPA show a 36% decline in HILI total area and a 32% decline in HILI total intensity during the same time period (Figures 5.16 – 5.19). As such, it is possible that the increases in HILI seen are indicative of a toxic mechanism, with primary spermatocytes undergoing cell death at a time after this increase. Additionally, the differences in the recovery of TBBPA and HBCDD treated cells further highlights a difference in mechanisms of toxicity.

While the exact details remain unclear, these data suggest that low dose FR exposure increases HILI expression, while at higher doses, FR exposure may reduce HILI expression by impacting spermatocyte viability. Primary spermatocytes may be more capable of recovery following FR exposure, though the data could indicate irreversible damage in and other defects that could lead to later apoptosis.

Similar to TDCPP, TDBPP, HBCDD, and TBBPA, PFOS, PFOA, and PFNA impact primary spermatocytes (Figure 5.20). We determined that the area of HILI+ primary spermatocytes significantly decreased at all concentrations of PFOS and PFOA, with HILI+ area declining by as much as 60% and 56% at 126 µM PFOS and 100 µM PFOA, respectively (Figures 5.21 – 5.22). HILI+ area was not significantly affected by PFNA exposure (Figure 5.23). HILI intensity was similarly affected at all concentrations of PFOS and PFOA, with HILI intensity declining by as much as 63% and 55% at 126 µM PFOS and 100 µM PFOA, respectively (Figures 5.24 – 5.25). Interestingly, HILI intensity significantly increases at 43 µM PFNA by 14%, suggesting a similar mechanism to acute TDCCP, TDBPP, HBCDD, and TBBPA exposure (Figure 5.26).

Like PLZF expression, HILI expression is impacted by both halogenated flame retardants and PFASs. Unlike flame retardants, PFASs largely decrease HILI expression, though it is unclear if this would occur with flame retardants under persistent conditions. However, despite the differences in exposure length, halogenated flame retardants continue to exert the most toxic effects on primary spermatocytes, despite both classes of chemicals being highly lipophilic, halogenated compounds. It is unclear if the increased toxicity of halogenated flame retardants could be due to core structure, type of halogen, or number of halogens attached. Regardless, studies have shown that decreases in HILI expression lead to apoptosis arising from elevated transposition and increased double-stranded breaks (Juliano et al., 2011). While decreases in HILI expression for PFOS and PFOA are not matched by cell death, it is possible that this downregulation of HILI will ultimately lead to mutations and defects in

haploid spermatids, and it is likely that primary spermatocytes that do not undergo apoptosis from TDCPP, TDBPP, HBCDD, or TBBPA exposure will also carry DNA mutations. In cells exposed to lower concentrations of TDCPP, TDBBP, HBCDD, and TBBPA, as well as the highest concentration of PFNA, upregulation in HILI could be in response to increased activity of transposons. Increases in HILI could also be the result of increased crossing over events during meiosis, a process that could introduce mutations, translocations, and other chromosome abnormalities (Louis and Borts, 2003).

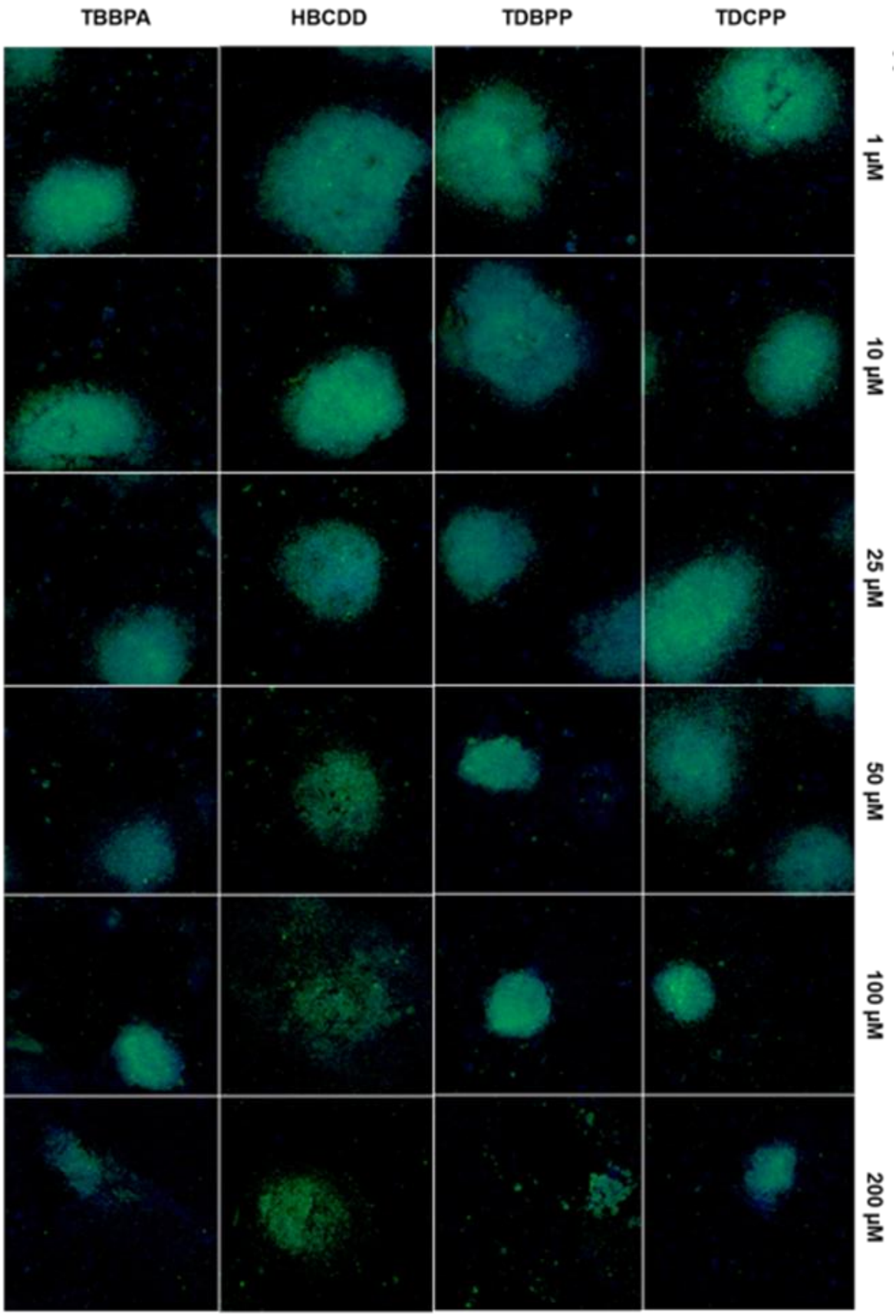
TBBPA
HBCDD
TDBPP
TDCPP
1 µM
10 µM
25 µM
50 µM
100 µM
200 µM

Figure 5.1. Acute TDCPP, TDBPP, HBCDD, and TBBPA exposure reduces HILI+ area and intensity in primary spermatocytes in in vitro spermatogenic cultures derived from H1 ESCs. Representative 5X images obtained by the Cellomics ArrayScan VT1 of HILI + (green) and DAPI (blue)-stained colonies treated with acute, twenty-four hour doses of 1 μM, 10 μM, 25 μM, 50 μM, 100 μM, and 200 μM TDCPP, TDBPP, HBCDD and TBBPA. Differentiations are derived from H1 ESCs. All images are taken under the same imaging conditions and parameters.

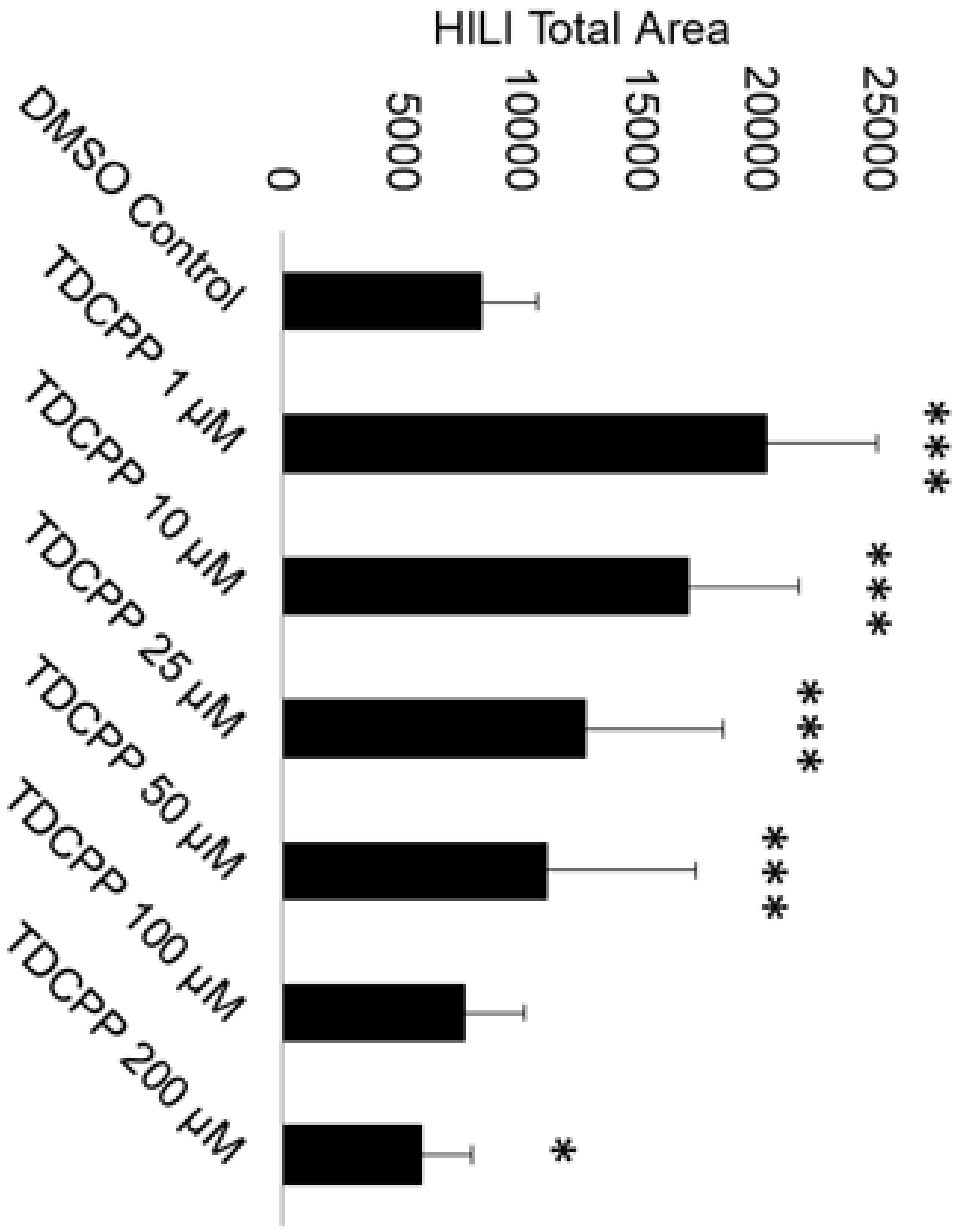
HILI Total Area
0
5000
10000
15000
20000
25000
DMSO Control
TDCPP 1 µM
TDCPP 10 µM
TDCPP 25 µM
TDCPP 50 µM
TDCPP 100 µM
TDCPP 200 µM
****
****
****
****
*

Figure 5.2. Acute TDCPP exposure impacts HILI+ area in primary spermatocytes in in vitro spermatogenic cultures derived from H1 ESCs. Graphical representation showing that acute, twenty-four hour exposure to 1 μM, 10 μM, 25 μM, 50 μM, 100 μM, and 200 μM TDCPP impacts average total HILI+ area in primary spermatocytes derived under *in vitro* spermatogenic conditions in comparison to a 0.2% DMSO-only control. Five replications were performed for each condition (n = 5). Significant changes in HILI+ area were determined using a 1-way analysis of variance (1-way ANOVA) and validated via a Student's t-test, where * is $p<0.05$, ** is $p<0.01$, and *** is $p<0.001$. Data are represented as mean ± SEM.

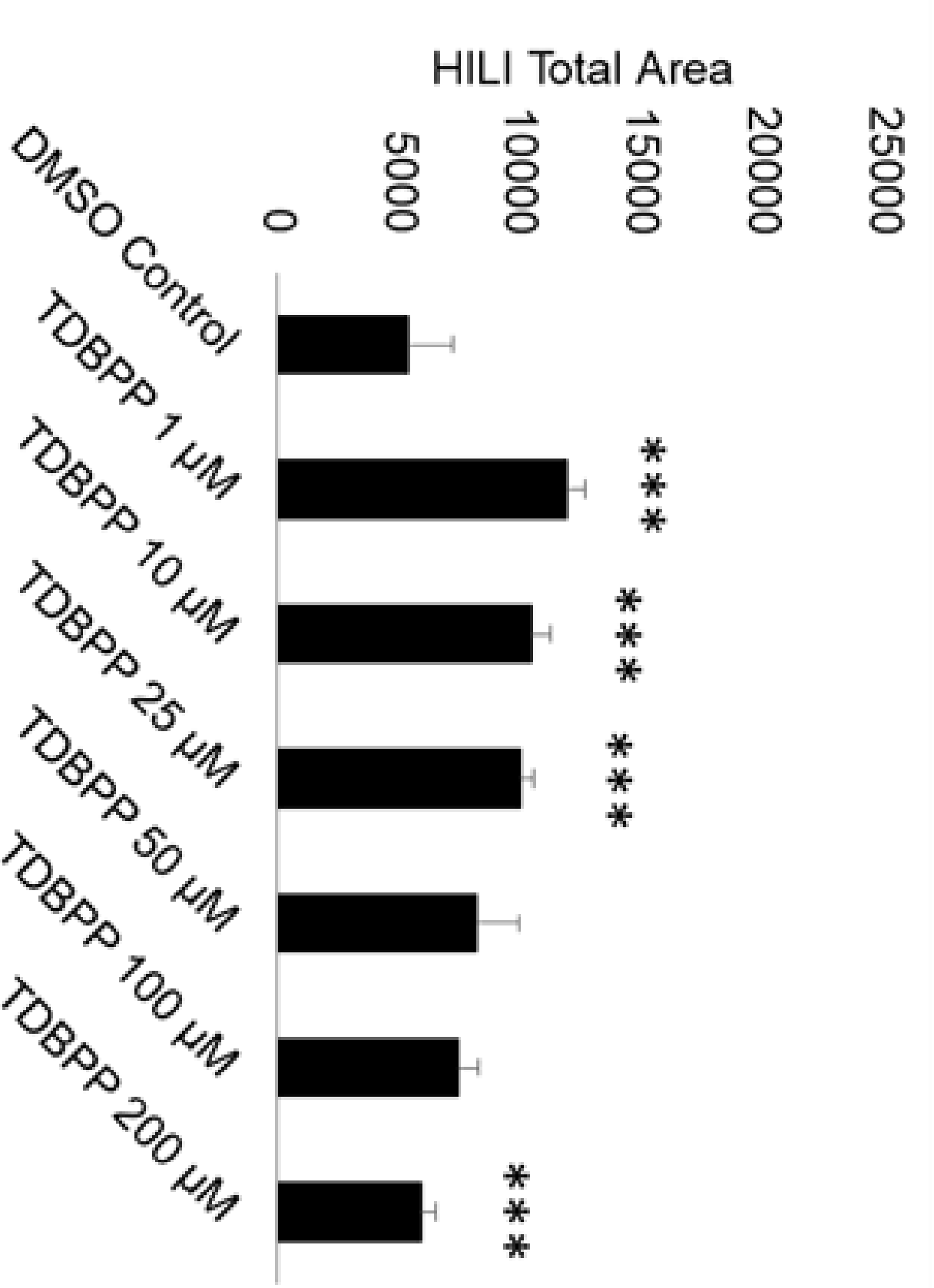
HILI Total Area
0
5000
10000
15000
20000
25000
DMSO Control
TDBPP 1 µM
TDBPP 10 µM
TDBPP 25 µM
TDBPP 50 µM
TDBPP 100 µM
TDBPP 200 µM
****
****
****
****

Figure 5.3. Acute TDBPP exposure impacts HILI+ area in primary spermatocytes in in vitro spermatogenic cultures derived from H1 ESCs. Graphical representation showing that acute, twenty-four hour exposure to 1 μM, 10 μM, 25 μM, 50 μM, 100 μM, and 200 μM TDBPP impacts average total HILI+ area in primary spermatocytes derived under *in vitro* spermatogenic conditions in comparison to a 0.2% DMSO-only control. Five replications were performed for each condition (n = 5). Significant changes in HILI+ area were determined using a 1-way analysis of variance (1-way ANOVA) and validated via a Student's t-test, where * is $p<0.05$, ** is $p<0.01$, and *** is $p<0.001$. Data are represented as mean ± SEM.

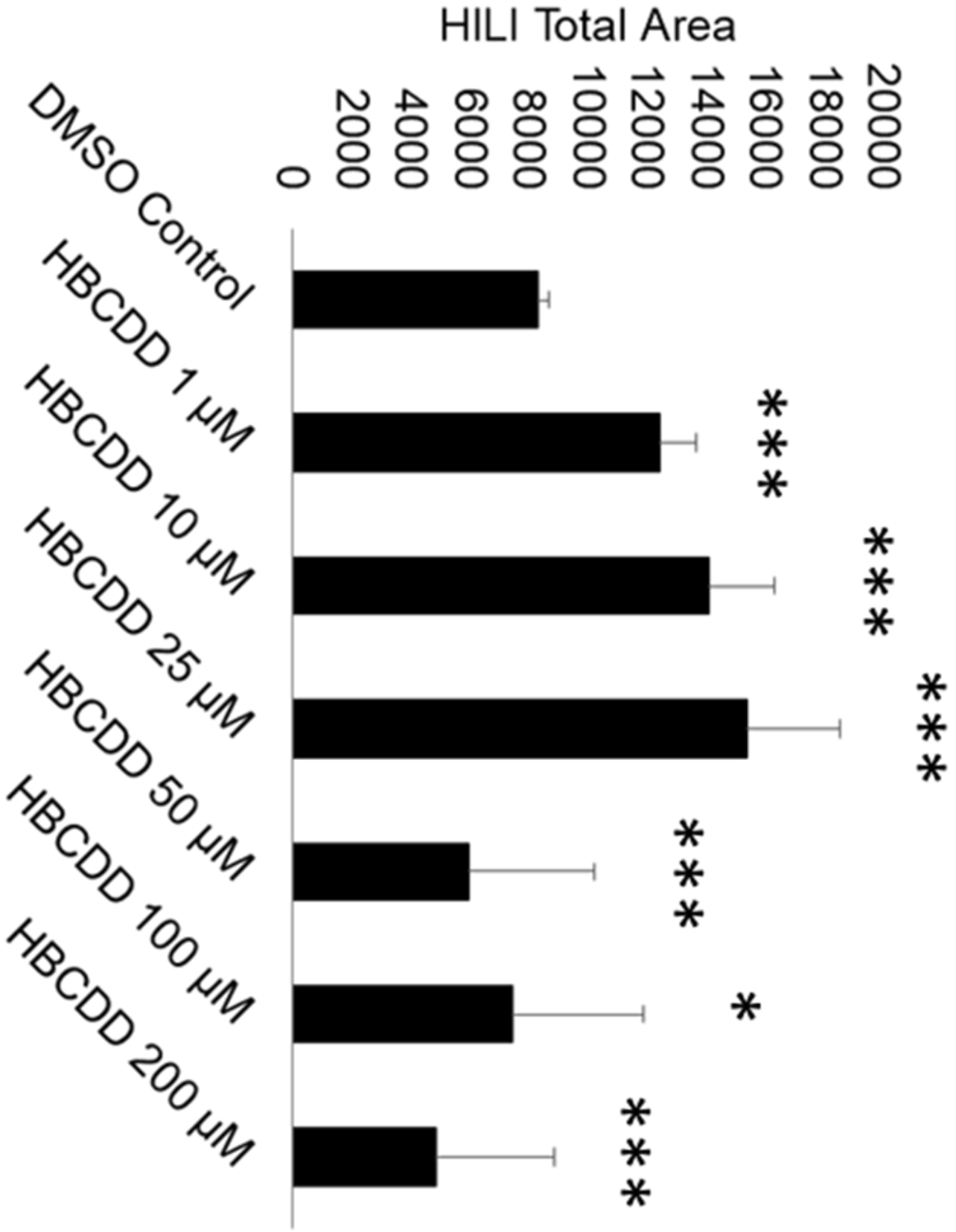
HILI Total Area
0
2000
4000
6000
8000
10000
12000
14000
16000
18000
20000
DMSO Control
HBCDD 1 µM
HBCDD 10 µM
HBCDD 25 µM
HBCDD 50 µM
HBCDD 100 µM
HBCDD 200 µM
****
****
****
****
*
***

Figure 5.4. Acute HBCDD exposure impacts HILI+ area in primary spermatocytes in in vitro spermatogenic cultures derived from H1 ESCs. Graphical representation showing that acute, twenty-four hour exposure to 1 μM, 10 μM, 25 μM, 50 μM, 100 μM, and 200 μM HBCDD impacts average total HILI+ area in primary spermatocytes derived under *in vitro* spermatogenic conditions in comparison to a 0.2% DMSO-only control. Five replications were performed for each condition (n = 5). Significant changes in HILI+ area were determined using a 1-way analysis of variance (1-way ANOVA) and validated via a Student's t-test, where * is $p<0.05$, ** is $p<0.01$, and *** is $p<0.001$. Data are represented as mean ± SEM.

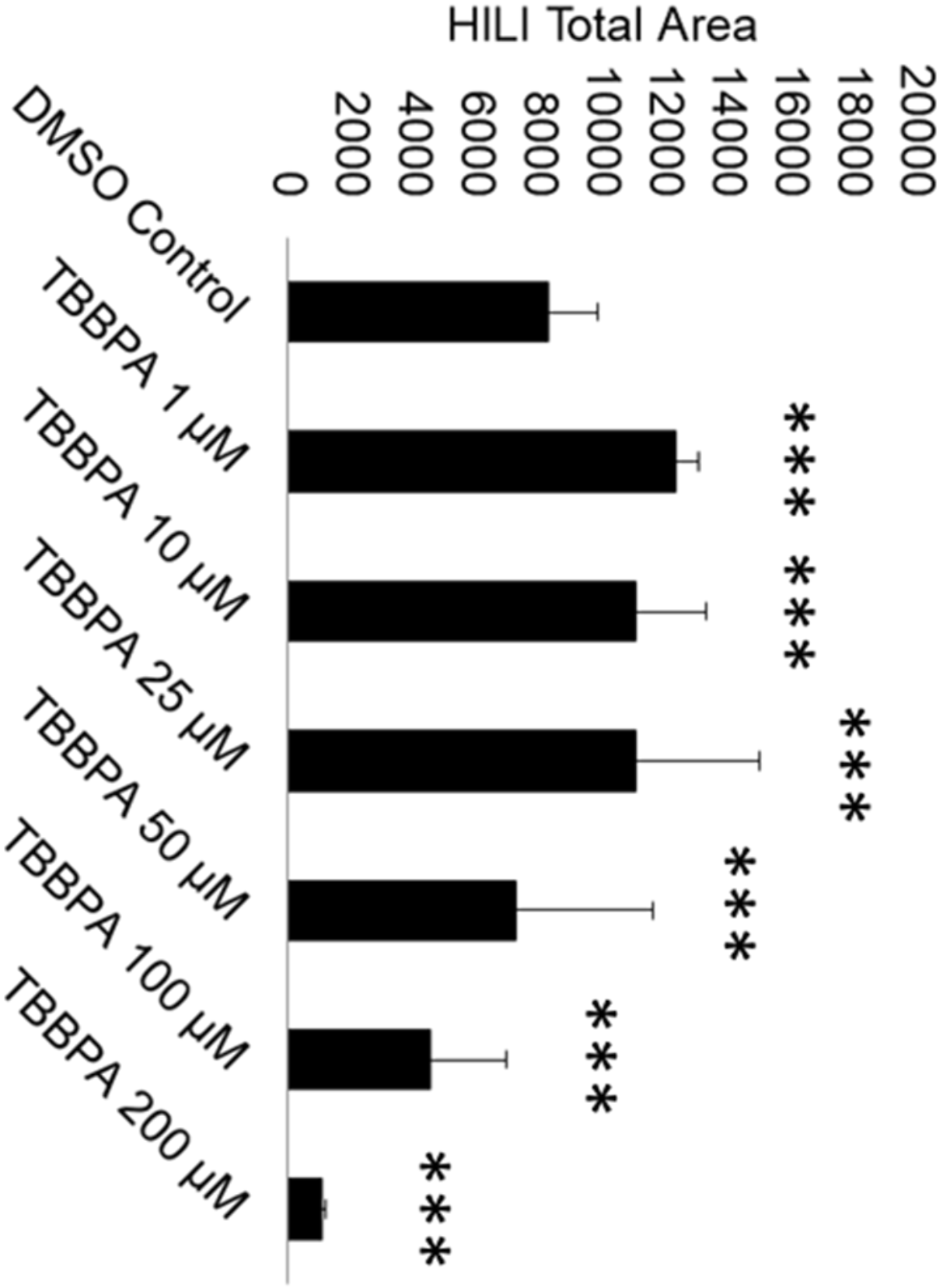
HILI Total Area
0
2000
4000
6000
8000
10000
12000
14000
16000
18000
20000
DMSO Control
TBBPA 1 µM
TBBPA 10 µM
TBBPA 25 µM
TBBPA 50 µM
TBBPA 100 µM
TBBPA 200 µM
****
****
****
****
****
****

Figure 5.5. Acute TBBPA exposure impacts HILI+ area in primary spermatocytes in in vitro spermatogenic cultures derived from H1 ESCs. Graphical representation showing that acute, twenty-four hour exposure to 1 μM, 10 μM, 25 μM, 50 μM, 100 μM, and 200 μM HBCDD impacts average total HILI+ area in primary spermatocytes derived under *in vitro* spermatogenic conditions in comparison to a 0.2% DMSO-only control. Five replications were performed for each condition (n = 5). Significant changes in HILI+ area were determined using a 1-way analysis of variance (1-way ANOVA) and validated via a Student's t-test, where * is $p<0.05$, ** is $p<0.01$, and *** is $p<0.001$. Data are represented as mean ± SEM.

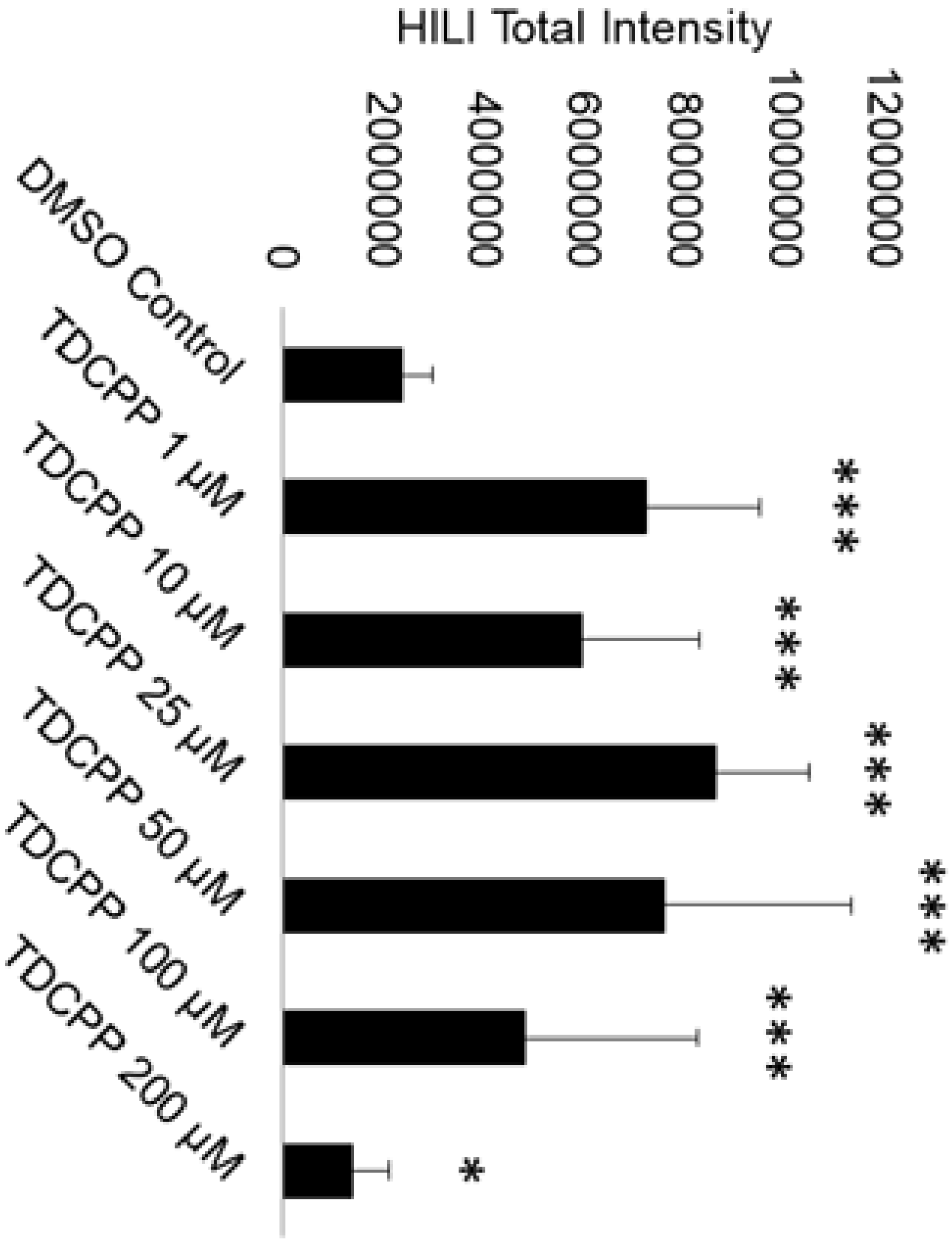
HILI Total Intensity
0
2000000
4000000
6000000
8000000
10000000
12000000
DMSO Control
TDCPP 1 µM
TDCPP 10 µM
TDCPP 25 µM
TDCPP 50 µM
TDCPP 100 µM
TDCPP 200 µM
****
****
****
****
****
*

Figure 5.6. Acute TDCPP exposure impacts HILI+ intensity in primary spermatocytes in in vitro spermatogenic cultures derived from H1 ESCs. Graphical representation showing that acute, twenty-four hour exposure to 1 μM, 10 μM, 25 μM, 50 μM, 100 μM, and 200 μM TDCPP impacts average total HILI+ intensity in primary spermatocytes derived under *in vitro* spermatogenic conditions in comparison to a 0.2% DMSO-only control. Five replications were performed for each condition (n = 5). Significant changes in HILI+ intensity were determined using a 1-way analysis of variance (1-way ANOVA) and validated via a Student's t-test, where * is $p<0.05$, ** is $p<0.01$, and *** is $p<0.001$. Data are represented as mean ± SEM.

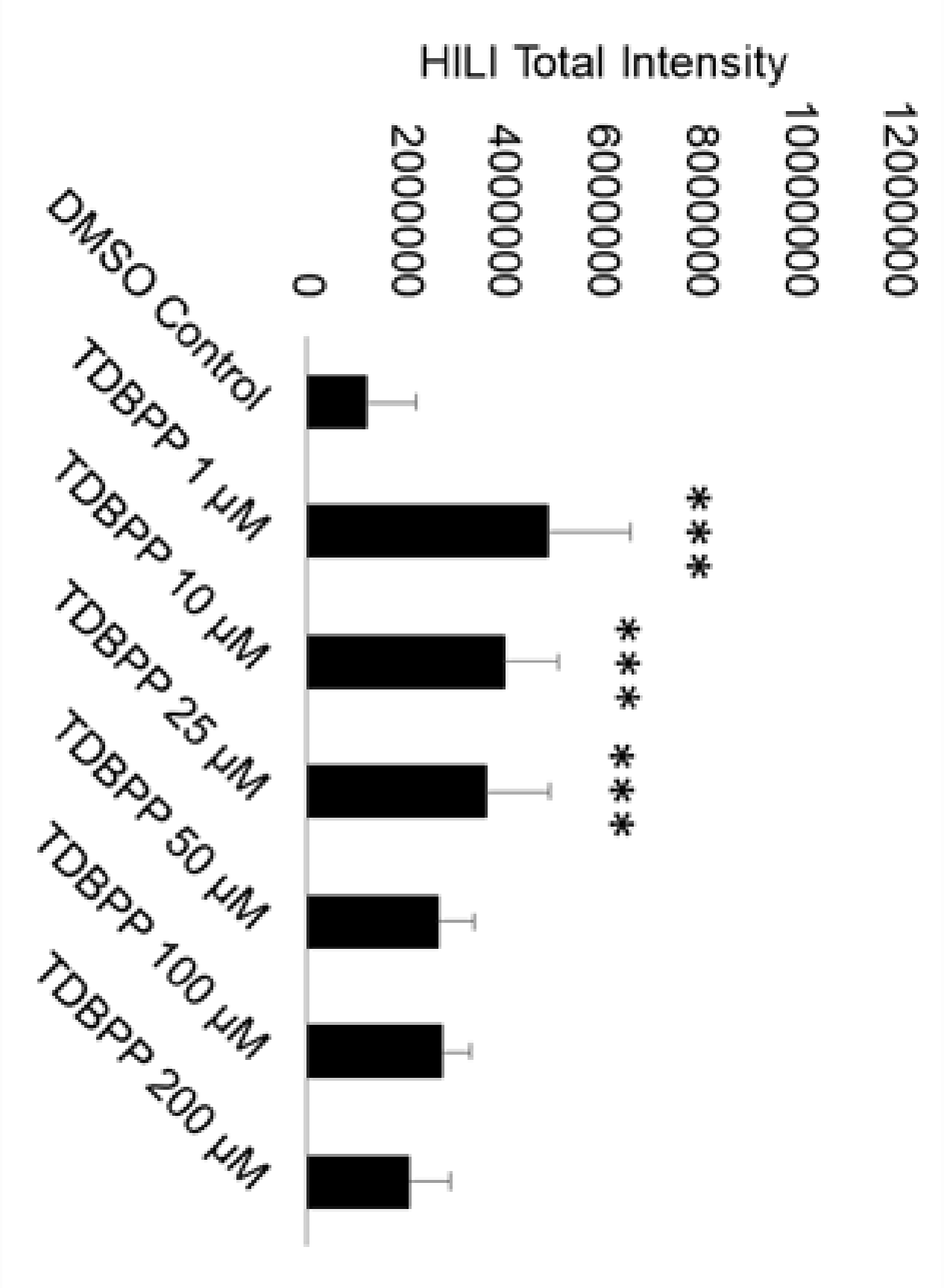
HILI Total Intensity
0
2000000
4000000
6000000
8000000
10000000
12000000
DMSO Control
TDBPP 1 µM
TDBPP 10 µM
TDBPP 25 µM
TDBPP 50 µM
TDBPP 100 µM
TDBPP 200 µM
****
****
****

Figure 5.7. Acute TDBPP exposure impacts HILI+ intensity in primary spermatocytes in in vitro spermatogenic cultures derived from H1 ESCs. Graphical representation showing that acute, twenty-four hour exposure to 1 μM, 10 μM, 25 μM, 50 μM, 100 μM, and 200 μM TDBPP impacts average total HILI+ intensity in primary spermatocytes derived under *in vitro* spermatogenic conditions in comparison to a 0.2% DMSO-only control. Five replications were performed for each condition (n = 5). Significant changes in HILI+ intensity were determined using a 1-way analysis of variance (1-way ANOVA) and validated via a Student's t-test, where * is $p<0.05$, ** is $p<0.01$, and *** is $p<0.001$. Data are represented as mean ± SEM.

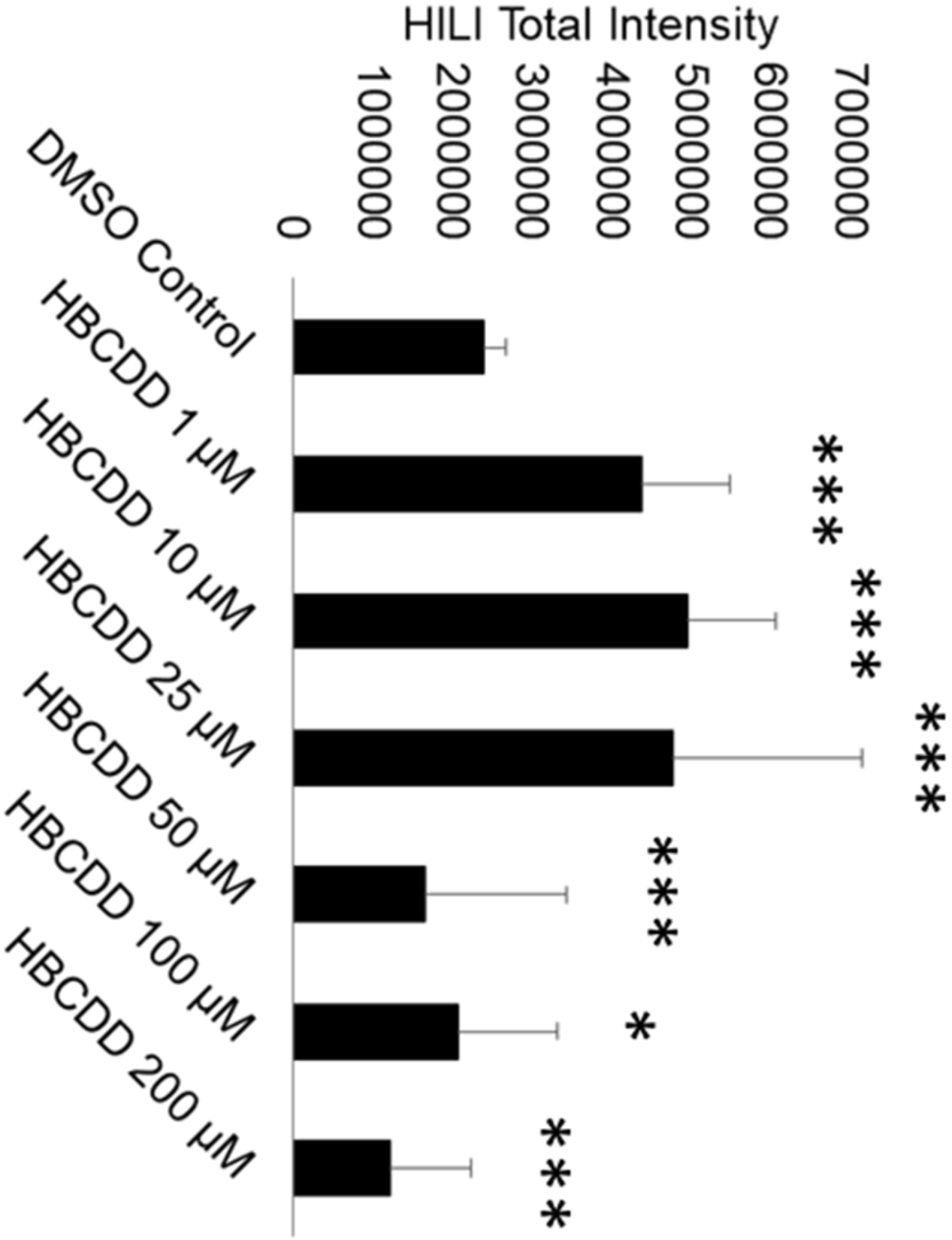
HILI Total Intensity
0
1000000
2000000
3000000
4000000
5000000
6000000
7000000
DMSO Control
HBCDD 1 μM
HBCDD 10 μM
HBCDD 25 μM
HBCDD 50 μM
HBCDD 100 μM
HBCDD 200 μM
****
****
****
***
*
***

Figure 5.8. Acute HBCDD exposure impacts HILI+ intensity in primary spermatocytes in in vitro spermatogenic cultures derived from H1 ESCs. Graphical representation showing that acute, twenty-four hour exposure to 1 μM, 10 μM, 25 μM, 50 μM, 100 μM, and 200 μM HBCDD impacts average total HILI+ intensity in primary spermatocytes derived under *in vitro* spermatogenic conditions in comparison to a 0.2% DMSO-only control. Five replications were performed for each condition (n = 5). Significant changes in HILI+ intensity were determined using a 1-way analysis of variance (1-way ANOVA) and validated via a Student's t-test, where * is $p<0.05$, ** is $p<0.01$, and *** is $p<0.001$. Data are represented as mean ± SEM.

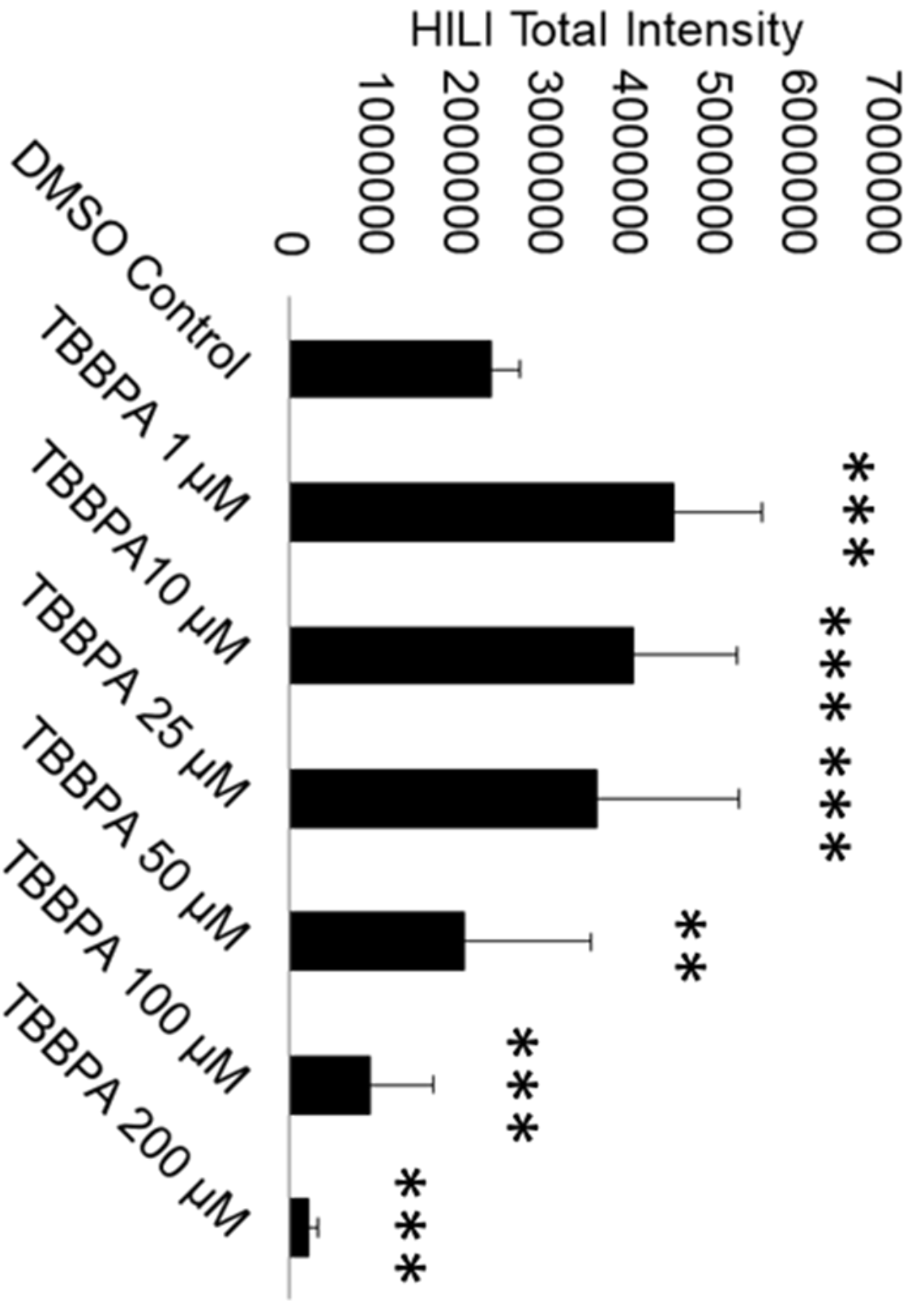
HILI Total Intensity
0
1000000
2000000
3000000
4000000
5000000
6000000
7000000
DMSO Control
TBBPA 1 µM
TBBPA10 µM
TBBPA 25 µM
TBBPA 50 µM
TBBPA 100 µM
TBBPA 200 µM
****
****
****
**
***
****

Figure 5.9. Acute TBBPA exposure impacts HILI+ intensity in primary spermatocytes in in vitro spermatogenic cultures derived from H1 ESCs. Graphical representation showing that acute, twenty-four hour exposure to 1 μM, 10 μM, 25 μM, 50 μM, 100 μM, and 200 μM TBBPA impacts average total HILI+ intensity in primary spermatocytes derived under *in vitro* spermatogenic conditions in comparison to a 0.2% DMSO-only control. Five replications were performed for each condition (n = 5). Significant changes in HILI+ intensity were determined using a 1-way analysis of variance (1-way ANOVA) and validated via a Student's t-test, where * is $p<0.05$, ** is $p<0.01$, and *** is $p<0.001$. Data are represented as mean ± SEM.

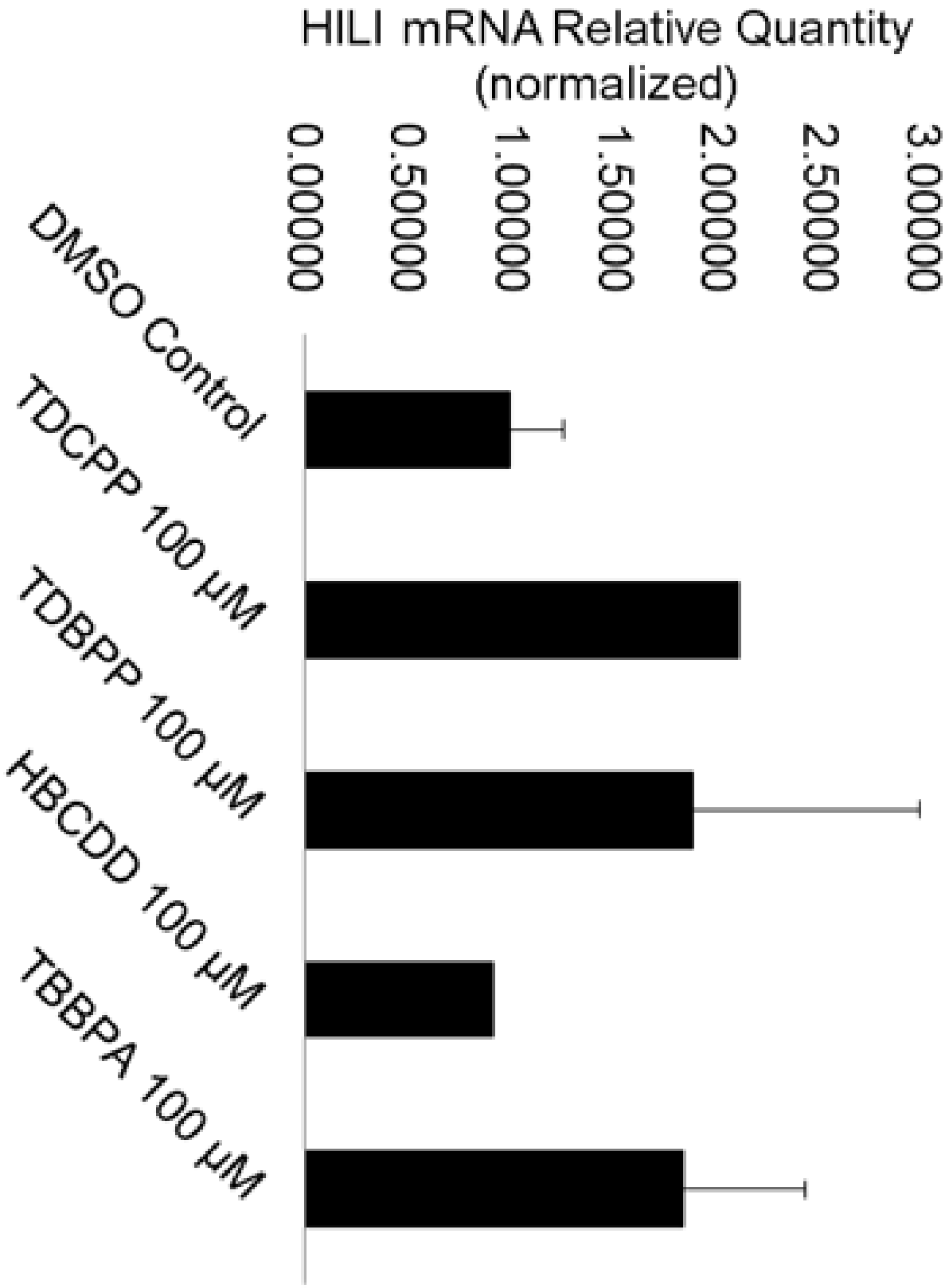
HILI mRNA Relative Quantity
(normalized)
0.00000
0.50000
1.00000
1.50000
2.00000
2.50000
3.00000
DMSO Control
TDCPP 100 µM
TDBPP 100 µM
HBCDD 100 µM
TBBPA 100 µM

Figure 5.10. Acute TDCPP, TDBPP, HBCDD, and TBBPA exposure does not significantly impact PIWIL2 (HILI) mRNA expression in spermatogonia in in vitro spermatogenic cultures derived from H1 ESCs. Graphical representation showing that acute, twenty-four hour exposure to 100 μM TDCPP, TDBPP, HBCDD, and TBBPA does not significantly impact average *PIWIL2* (HILI) mRNA expression in spermatogonia derived under *in vitro* spermatogenic conditions. Transcript levels were normalized to 0.2% DMSO-only control. Two separate replications were performed in duplicate (n=4) for each condition. Significant changes in mRNA steady state levels were determined using Bio-Rad CFX Manager™ Software (Bio-Rad, Hercules, CA).

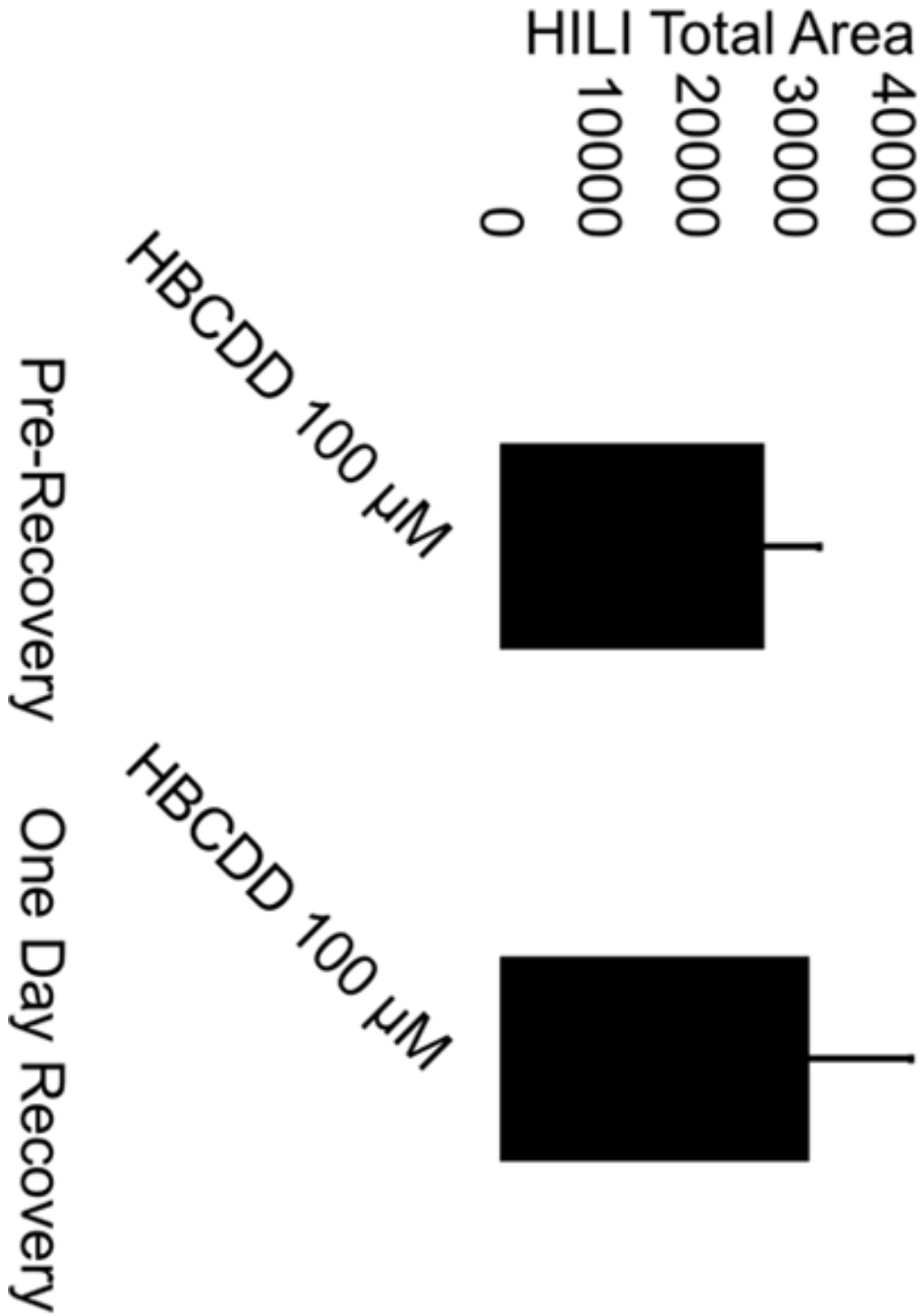
HILI Total Area
40000
30000
20000
10000
0
HBCDD 100 µM
HBCDD 100 µM
Pre-Recovery
One Day Recovery

Figure 5.11. HILI+ area in primary spermatocytes recovers one day post-HBCDD exposure. Graphical representation showing that HILI+ area is capable of recovery following a twenty-four hour recovery period after 100 μM HBCDD exposure. Three replications were performed for each condition (n = 3). Differentiations were derived from H1 ESCs and compared to a 0.2% DMSO-only control. Significant changes in HILI+ area were determined using a 1-way analysis of variance (1-way ANOVA) and validated via a Student's t-test, where * is $p<0.05$, ** is $p<0.01$, and *** is $p<0.001$. Data are represented as mean ± SEM.

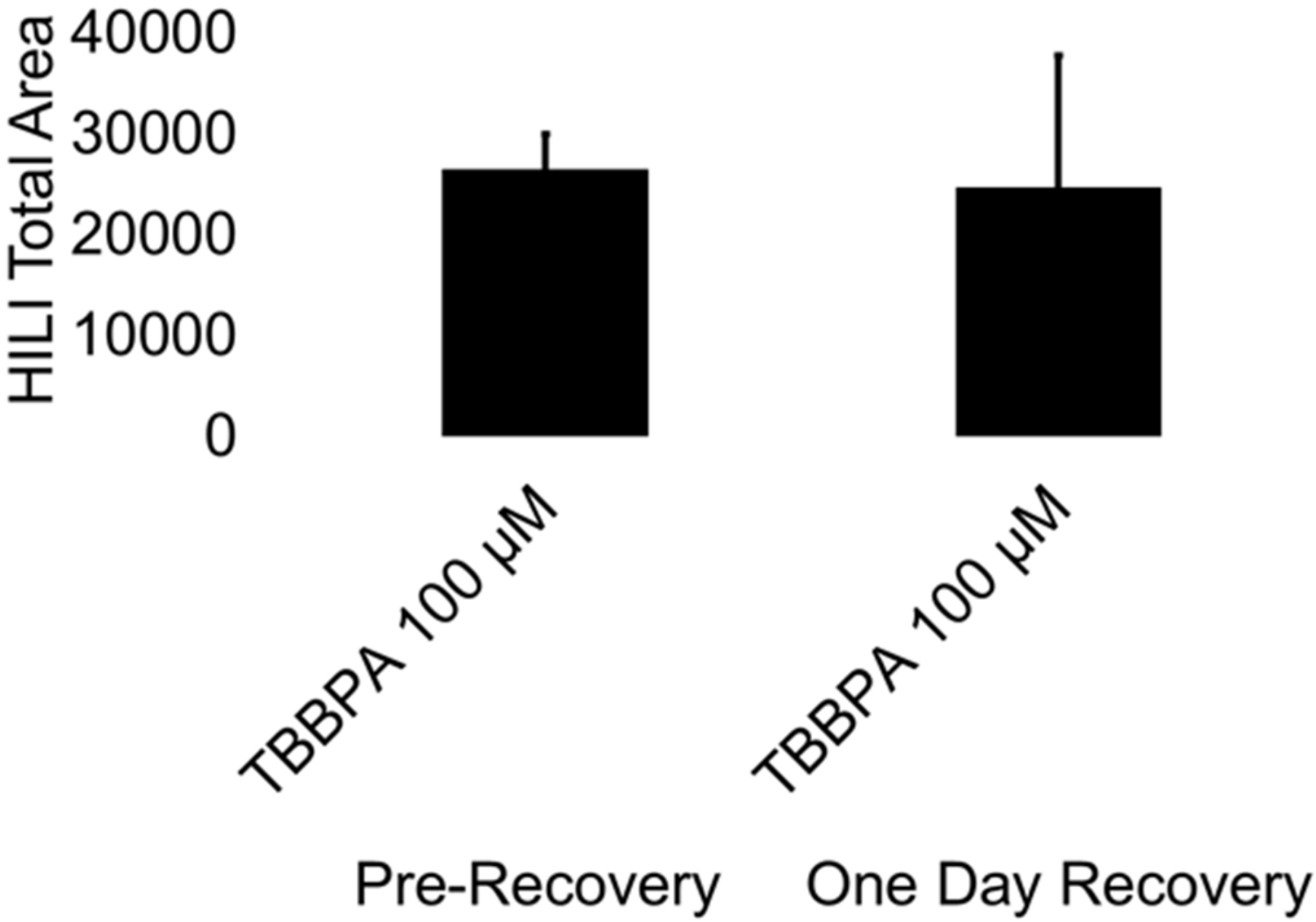
HILI Total Area
40000
30000
20000
10000
0
TBBPA 100 µM
TBBPA 100 µM
Pre-Recovery
One Day Recovery

Figure 5.12. HILI+ area in primary spermatocytes recovers one day post-TBBPA exposure. Graphical representation showing that HILI+ area is capable of recovery following a twenty-four hour recovery period after 100 μM TBBPA exposure. Three replications were performed for each condition (n = 3). Differentiations were derived from H1 ESCs and compared to a 0.2% DMSO-only control. Significant changes in HILI+ area were determined using a 1-way analysis of variance (1-way ANOVA) and validated via a Student's t-test, where * is $p<0.05$, ** is $p<0.01$, and *** is $p<0.001$. Data are represented as mean ± SEM.

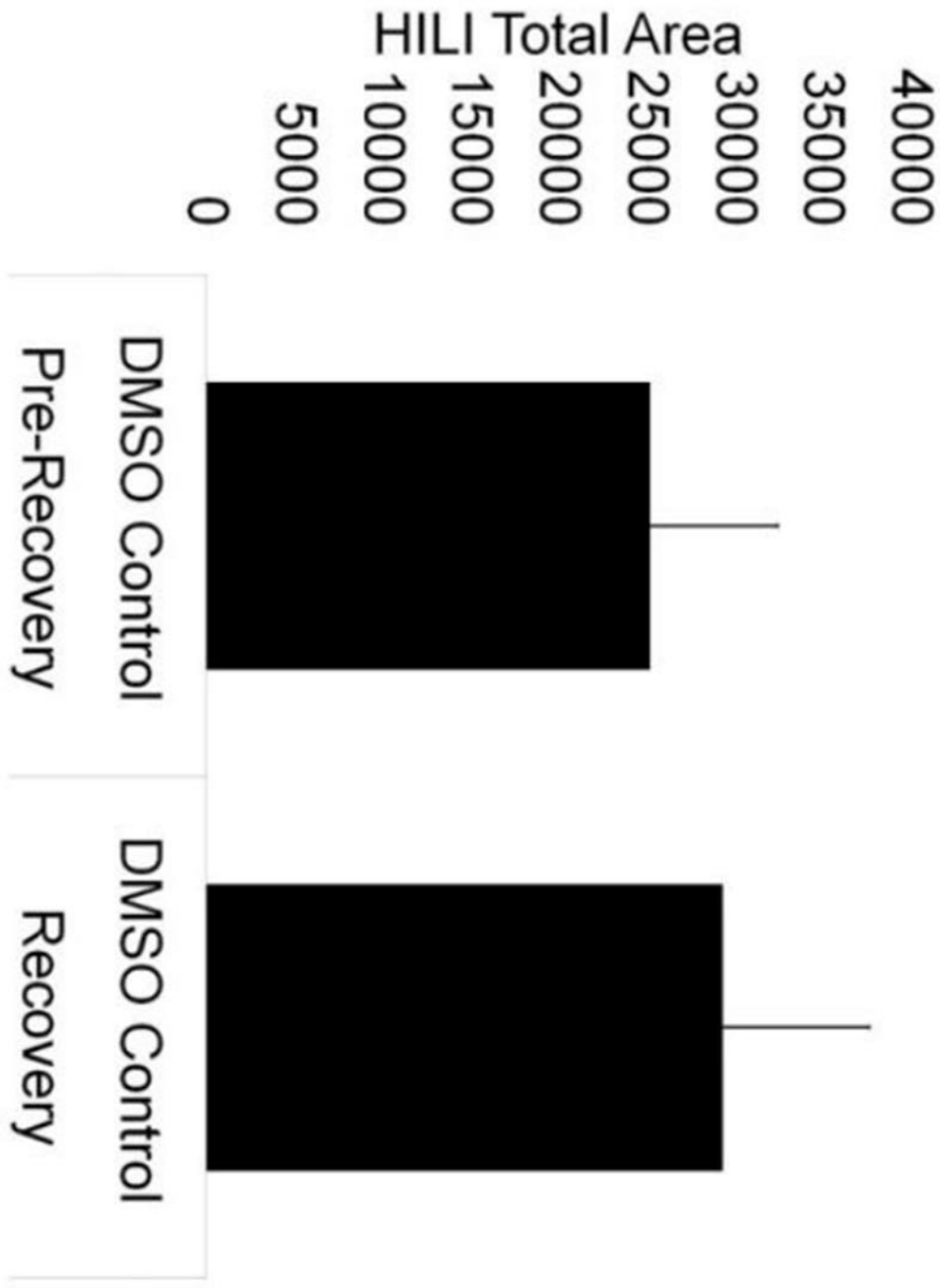
HILI Total Area
40000
35000
30000
25000
20000
15000
10000
5000
0
DMSO Control
Pre-Recovery
DMSO Control
Recovery

Figure 5.13. HILI+ area in primary spermatocytes remains statistically unchanged in control differentiations after twenty-four hours. Graphical representation showing that HILI+ area in primary spermatocytes derived under *in vitro* spermatogenic control conditions remain statistically the same after a twenty-four hour recovery period. Three replications were performed for each condition (n = 3). Differentiations were derived from H1 ESCs. Significant changes in HILI+ area were determined via a Student's t-test, where * is $p<0.05$, ** is $p<0.01$, and *** is $p<0.001$. Data are represented as mean ± SEM.

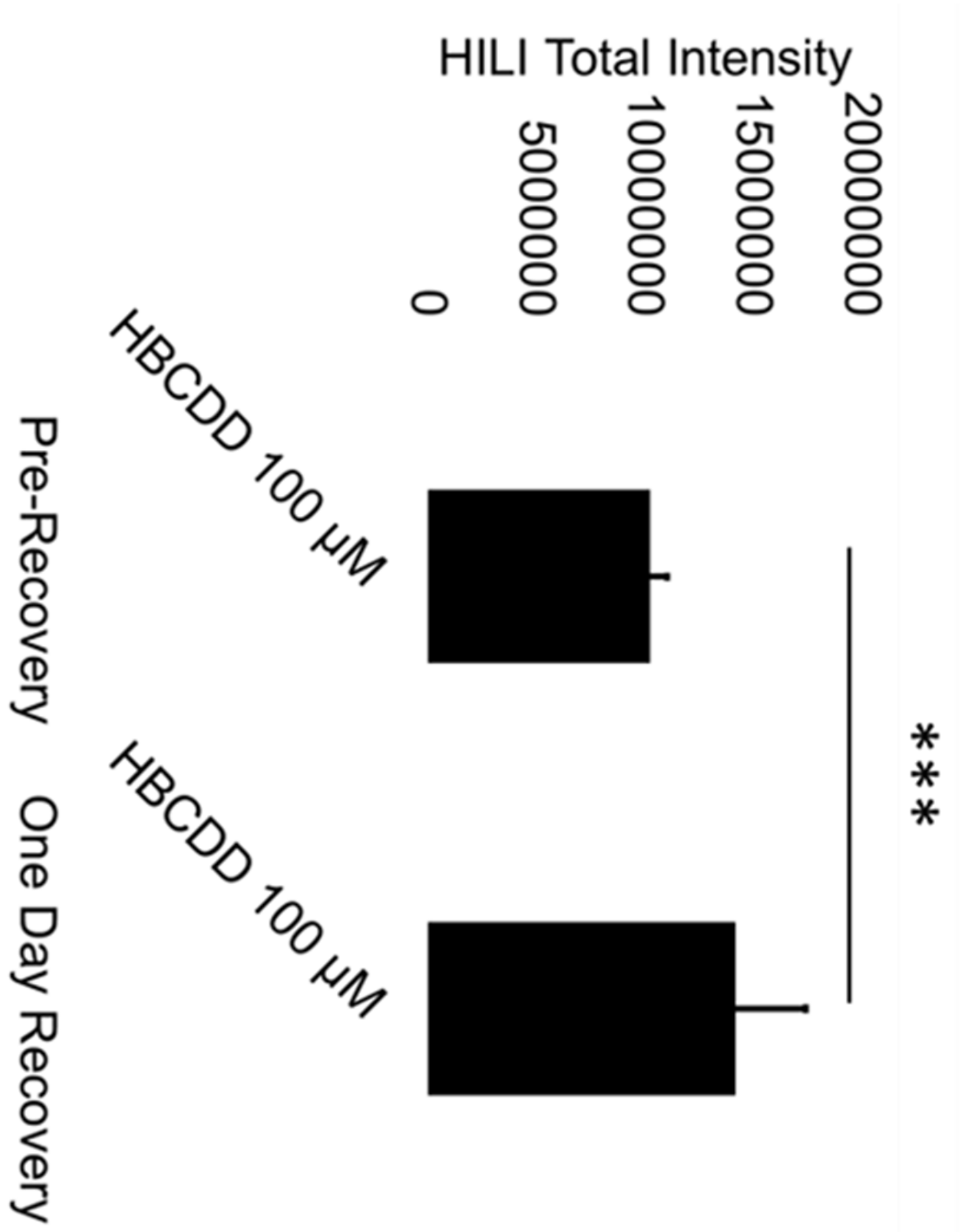
HILI Total Intensity
20000000
15000000
10000000
5000000
0
HBCDD 100 µM
HBCDD 100 µM
***
Pre-Recovery
One Day Recovery

Figure 5.14. HILI+ intensity in primary spermatocytes does not recover one day post-HBCDD exposure. Graphical representation showing that HILI+ intensity increases following a twenty-four hour recovery period after 100 μM HBCDD exposure. Three replications were performed for each condition (n = 3). Differentiations were derived from H1 ESCs and compared to a 0.2% DMSO-only control. Significant changes in HILI+ intensity were determined using a 1-way analysis of variance (1-way ANOVA) and validated via a Student's t-test, where * is $p<0.05$, ** is $p<0.01$, and *** is $p<0.001$. Data are represented as mean ± SEM.

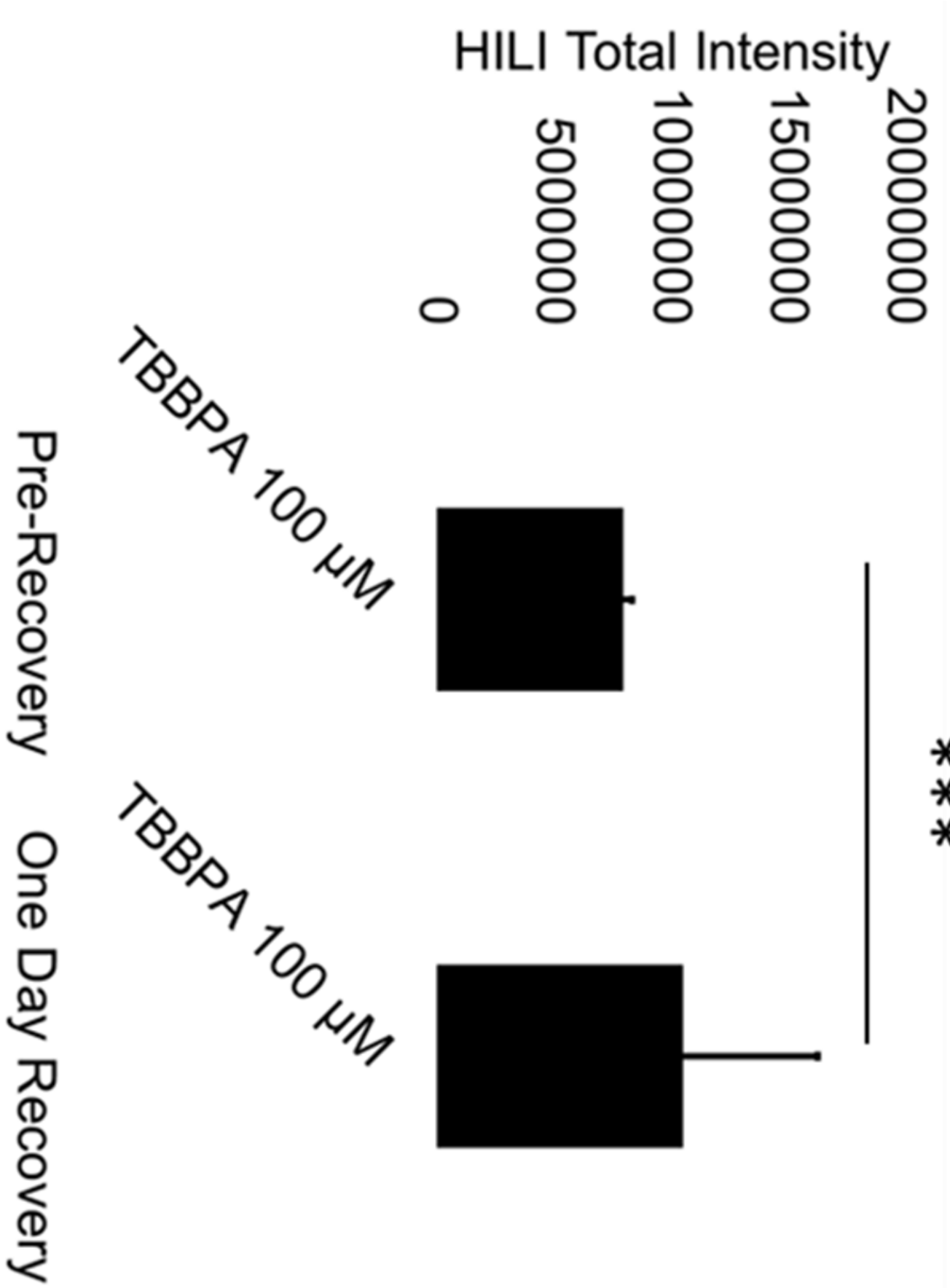
HILI Total Intensity
20000000
15000000
10000000
5000000
0
***
TBBPA 100 µM
TBBPA 100 µM
Pre-Recovery
One Day Recovery

Figure 5.15. HILI+ intensity in primary spermatocytes does not recover one day post-TBBPA exposure. Graphical representation showing that HILI+ intensity increases following a twenty-four hour recovery period after 100 μM TBBPA exposure. Three replications were performed for each condition (n = 3). Differentiations were derived from H1 ESCs and compared to a 0.2% DMSO-only control. Significant changes in HILI+ intensity were determined using a 1-way analysis of variance (1-way ANOVA) and validated via a Student's t-test, where * is $p<0.05$, ** is $p<0.01$, and *** is $p<0.001$. Data are represented as mean ± SEM.

HILI Total Area
40000
30000
20000
10000
0
DMSO Control
HBCDD 100 µM
Five Day Recovery

Figure 5.16. HILI+ area in primary spermatocytes recovers five days post-HBCDD exposure. Graphical representation showing that HILI+ area is capable of recovery following a five day recovery period after 100 μM HBCDD exposure. Three replications were performed for each condition (n = 3). Differentiations were derived from H1 ESCs and compared to a 0.2% DMSO-only control. Significant changes in HILI+ area were determined using a 1-way analysis of variance (1-way ANOVA) and validated via a Student's t-test, where * is $p<0.05$, ** is $p<0.01$, and *** is $p<0.001$. Data are represented as mean ± SEM.

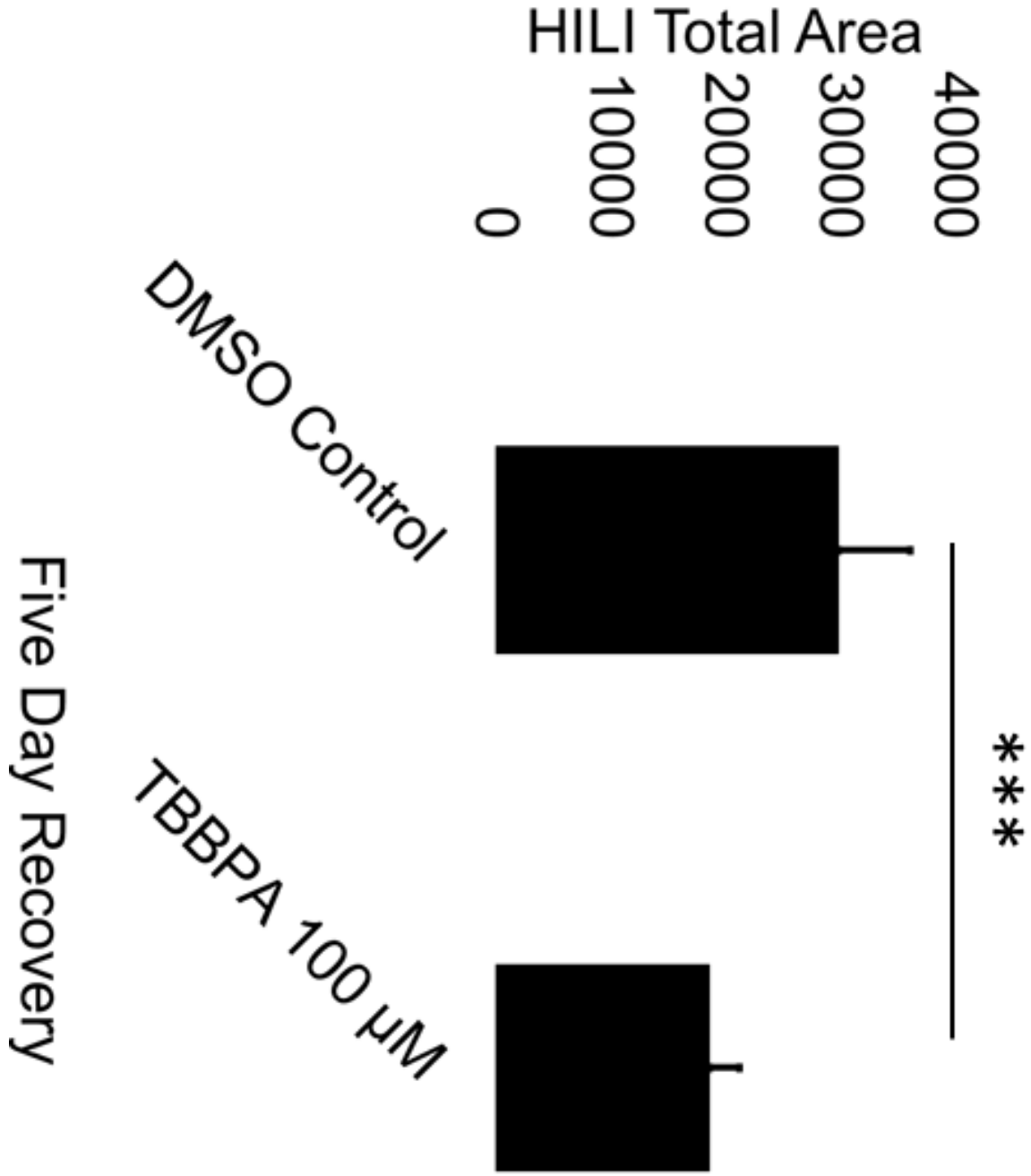
HILI Total Area
40000
30000
20000
10000
0
DMSO Control
TBBPA 100 µM
***
Five Day Recovery

Figure 5.17. HILI+ area in primary spermatocytes does not recover five days post-TBBPA exposure. Graphical representation showing that HILI+ area does not recover following a five day recovery period after 100 μM TBBPA exposure. Three replications were performed for each condition (n = 3). Differentiations were derived from H1 ESCs and compared to a 0.2% DMSO-only control. Significant changes in HILI+ area were determined using a 1-way analysis of variance (1-way ANOVA) and validated via a Student's t-test, where * is $p<0.05$, ** is $p<0.01$, and *** is $p<0.001$. Data are represented as mean ± SEM.

HLI Total Intensity
25000000
20000000
15000000
10000000
5000000
0
DMSO Control
HBCDD 100 µM
Five Day Recovery

Figure 5.18. HILI+ intensity in primary spermatocytes recovers five days post-HBCDD exposure. Graphical representation showing that HILI+ intensity recovers following a five day recovery period after 100 μM HBCDD exposure. Three replications were performed for each condition (n = 3). Differentiations were derived from H1 ESCs and compared to a 0.2% DMSO-only control. Significant changes in HILI+ intensity were determined using a 1-way analysis of variance (1-way ANOVA) and validated via a Student's t-test, where * is $p<0.05$, ** is $p<0.01$, and *** is $p<0.001$. Data are represented as mean ± SEM.

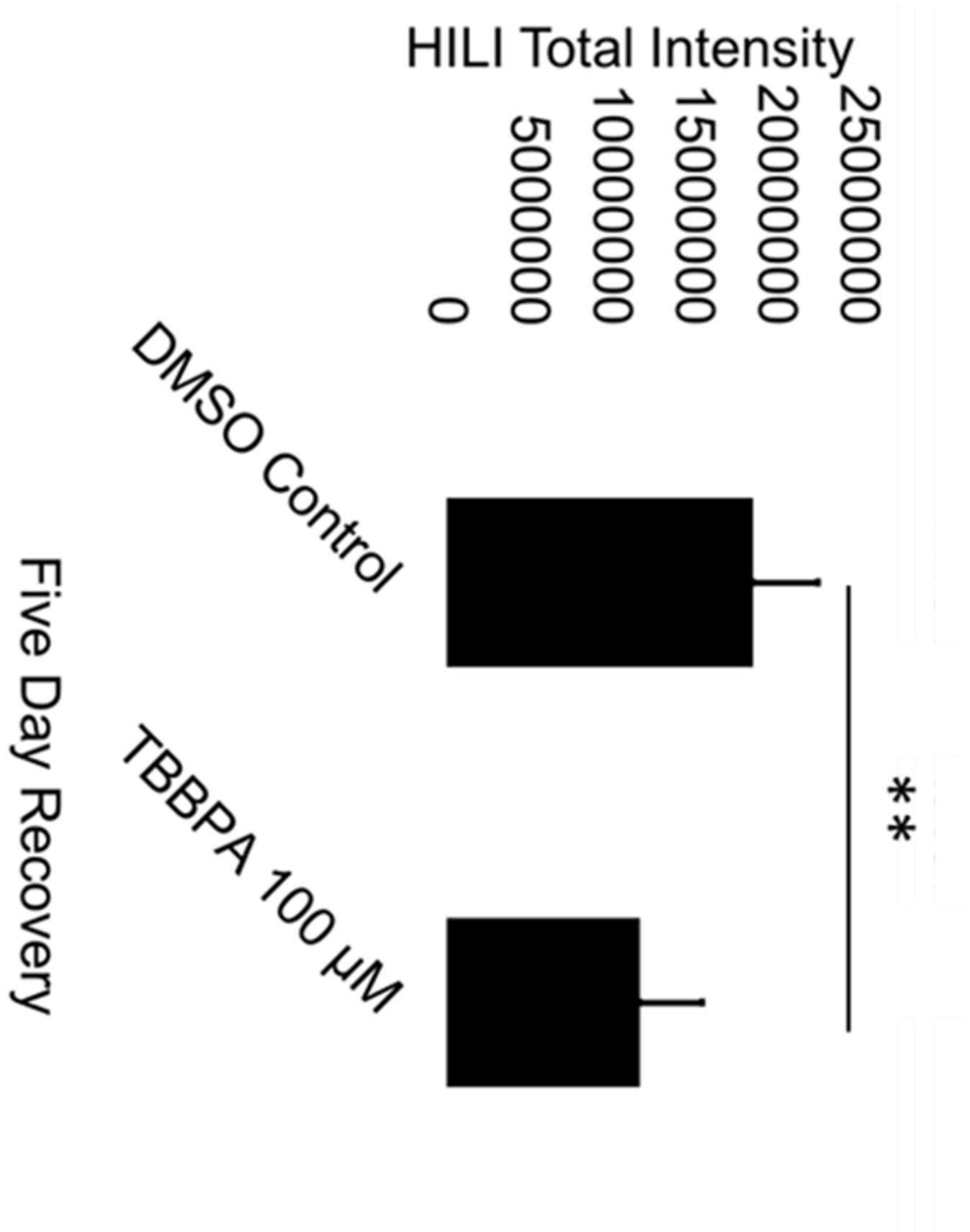
HILI Total Intensity
25000000
20000000
15000000
10000000
5000000
0
DMSO Control
TBBPA 100 µM
**
Five Day Recovery

Figure 5.19. HILI+ intensity in primary spermatocytes does not recover five days post-TBBPA exposure. Graphical representation showing that HILI+ intensity does not recover following a five day recovery period after 100 μM TBBPA exposure. Three replications were performed for each condition (n = 3). Differentiations were derived from H1 ESCs and compared to a 0.2% DMSO-only control. Significant changes in HILI+ intensity were determined using a 1-way analysis of variance (1-way ANOVA) and validated via a Student's t-test, where * is $p<0.05$, ** is $p<0.01$, and *** is $p<0.001$. Data are represented as mean ± SEM.

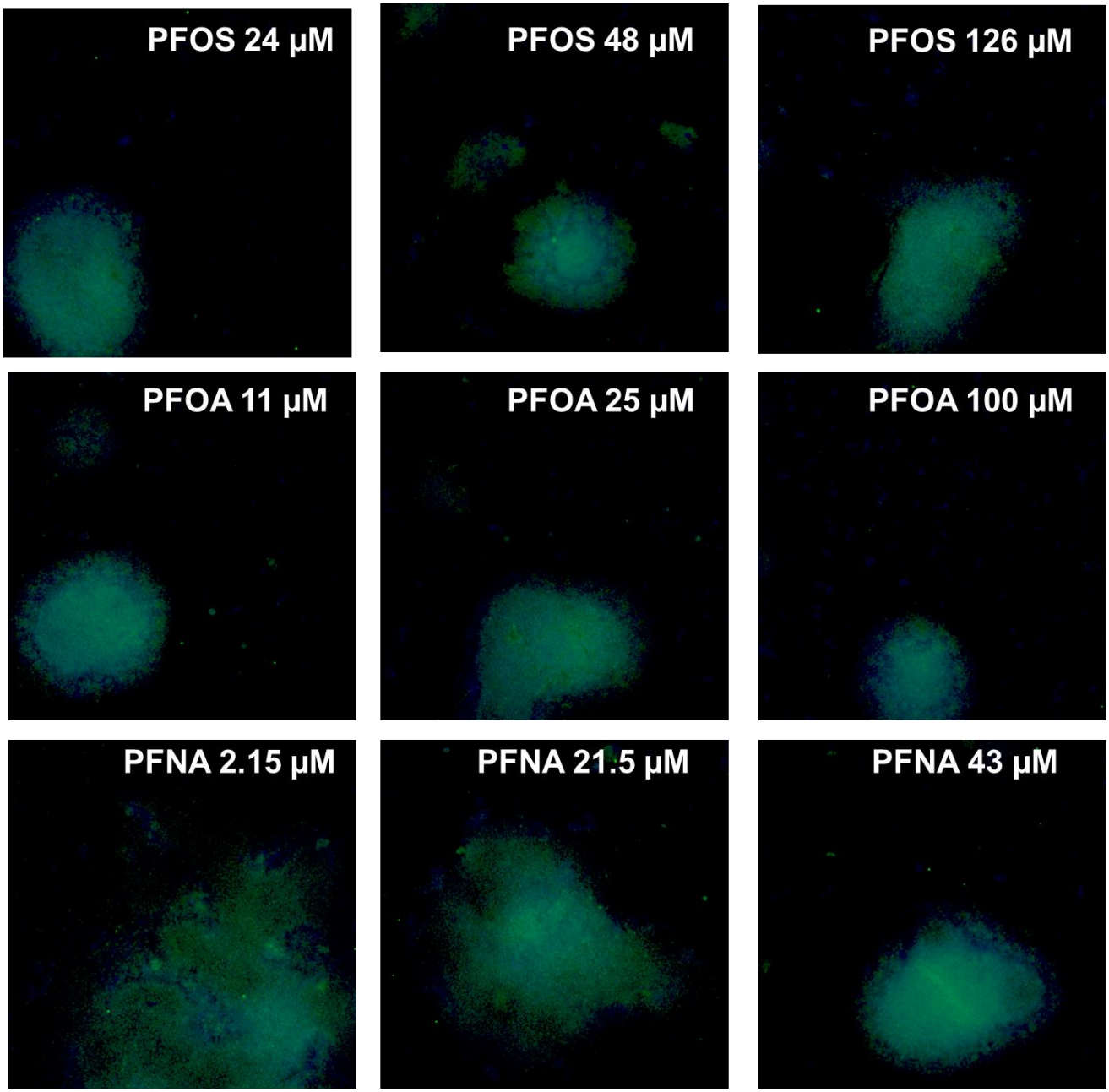
PFOS 24 µM
PFOS 48 µM
PFOS 126 µM
PFOA 11 µM
PFOA 25 µM
PFOA 100 µM
PFNA 2.15 µM
PFNA 21.5 µM
PFNA 43 µM

Figure 5.20. Persistent PFOS, PFOA, and PFNA exposure reduces HILI+ area and intensity in primary spermatocytes in in vitro spermatogenic cultures derived from H1 ESCs. Representative 5X images obtained by the Cellomics ArrayScan VT1 of HILI + (green) and DAPI (blue)-stained colonies treated with persistent doses of PFOS, PFOA, and PFNA from Day 1 to Day 10. Differentiations are derived from H1 ESCs. All images are taken under the same imaging conditions and parameters.

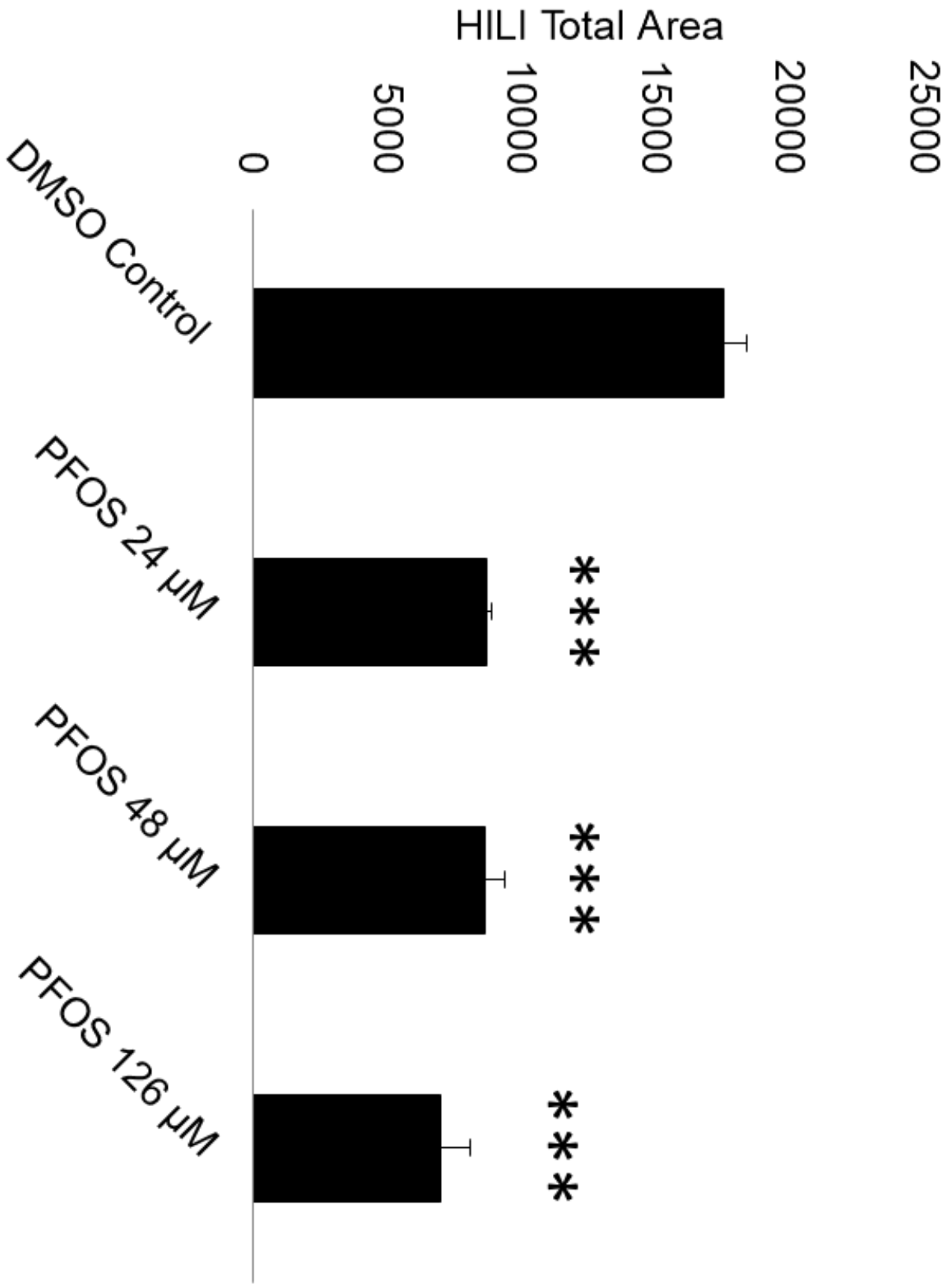
HILI Total Area
0
5000
10000
15000
20000
25000
DMSO Control
PFOS 24 µM
PFOS 48 µM
PFOS 126 µM
***
***
***

Figure 5.21. Persistent PFOS exposure reduces HILI+ area in primary spermatocytes in in vitro spermatogenic cultures derived from H1 ESCs. Graphical representation showing that persistent 24 μM, 48 μM, and 126 μM PFOS exposure from Day 1 to Day 10 reduces average total HILI+ area in primary spermatocytes derived under *in vitro* spermatogenic conditions in comparison to a 0.25% DMSO-only control. Three replications were performed for each condition, and spermatogenic cells were derived from H1 ESCs (n = 3). Significant changes in HILI+ area were determined using a 1-way analysis of variance (1-way ANOVA) and validated via a Student's t-test, where * is $p<0.05$, ** is $p<0.01$, and *** is $p<0.001$. Data are represented as mean ± SEM.

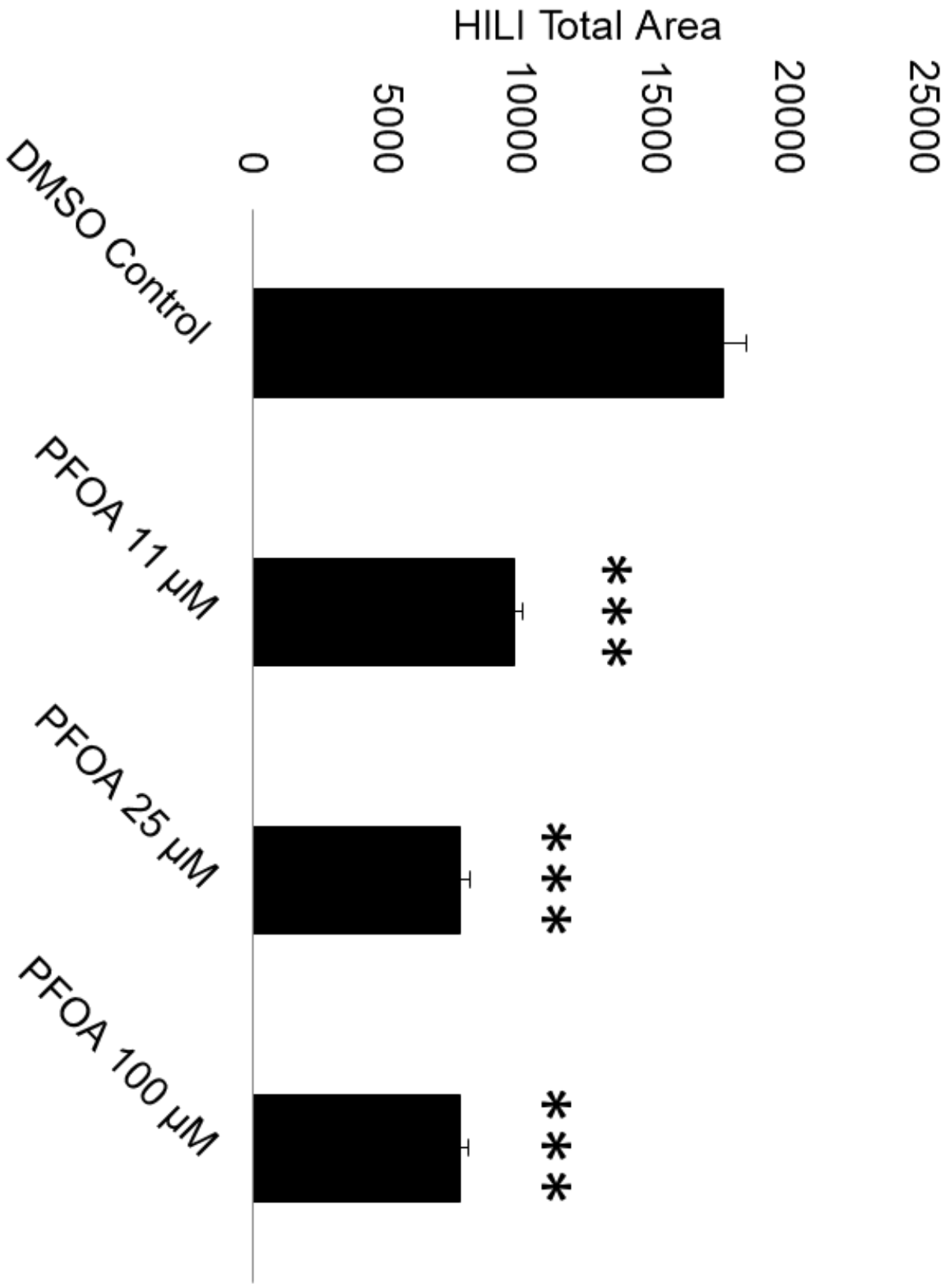
HILI Total Area
0
5000
10000
15000
20000
25000
DMSO Control
PFOA 11 µM
PFOA 25 µM
PFOA 100 µM
****
****
****

Figure 5.22. Persistent PFOA exposure reduces HILI+ area in primary spermatocytes in in vitro spermatogenic cultures derived from H1 ESCs. Graphical representation showing that persistent 11 μM, 25 μM, and 100 μM PFOA exposure from Day 1 to Day 10 reduces average total HILI+ area in primary spermatocytes derived under *in vitro* spermatogenic conditions in comparison to a 0.25% DMSO-only control. Three replications were performed for each condition, and spermatogenic cells were derived from H1 ESCs (n = 3). Significant changes in HILI+ area were determined using a 1-way analysis of variance (1-way ANOVA) and validated via a Student's t-test, where * is $p<0.05$, ** is $p<0.01$, and *** is $p<0.001$. Data are represented as mean ± SEM.

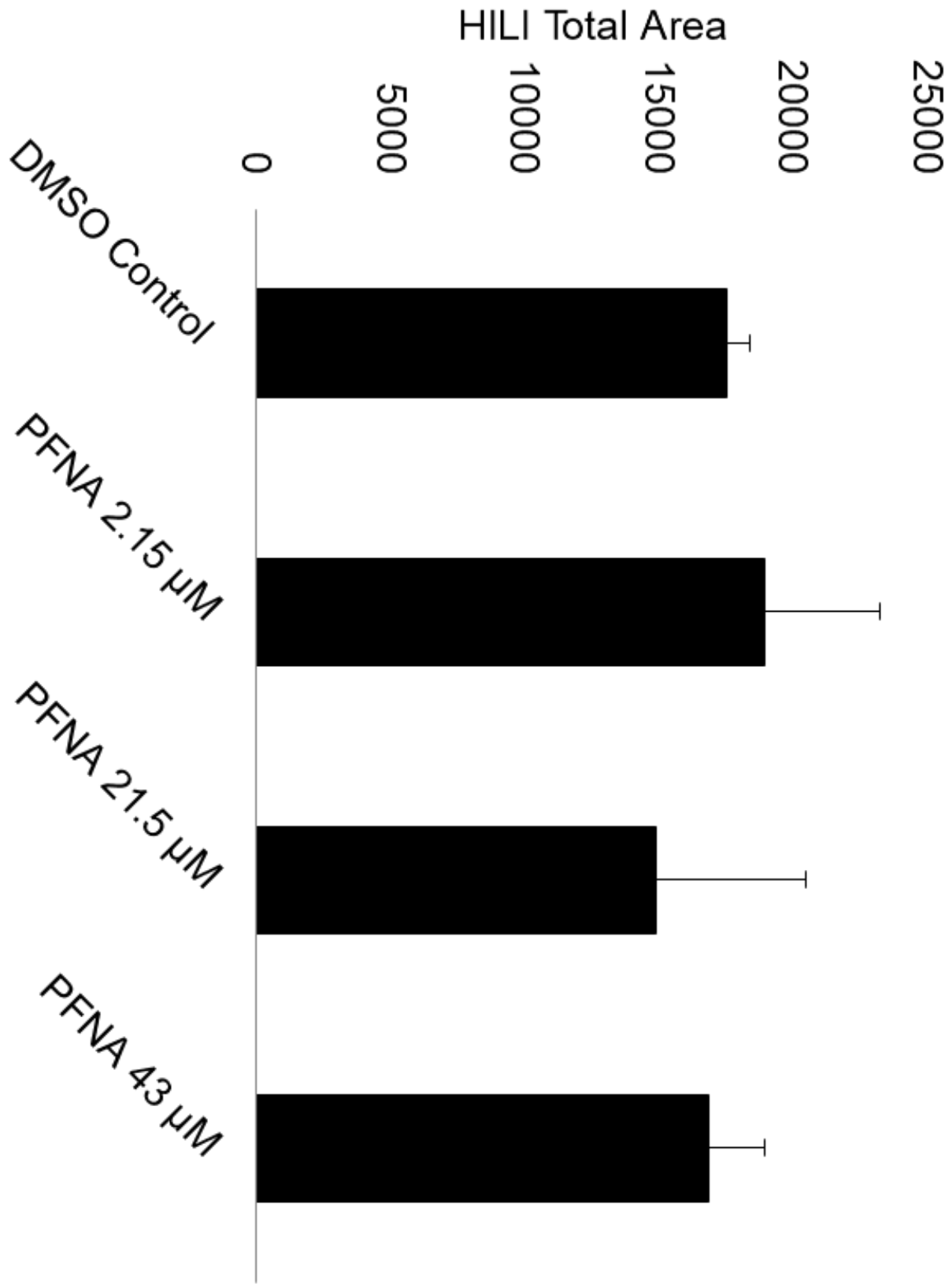
HILI Total Area
0
5000
10000
15000
20000
25000
DMSO Control
PFNA 2.15 µM
PFNA 21.5 µM
PFNA 43 µM

Figure 5.23. Persistent PFNA exposure does not impact HILI+ area in primary spermatocytes in in vitro spermatogenic cultures derived from H1 ESCs. Graphical representation showing that persistent 2.15 μM, 21.5 μM, and 43 μM PFNA exposure from Day 1 to Day 10 does not impact average total HILI+ area in primary spermatocytes derived under *in vitro* spermatogenic conditions in comparison to a 0.25% DMSO-only control. Three replications were performed for each condition, and spermatogenic cells were derived from H1 ESCs (n = 3). Significant changes in HILI+ area were determined using a 1-way analysis of variance (1-way ANOVA) and validated via a Student's t-test, where * is $p<0.05$, ** is $p<0.01$, and *** is $p<0.001$. Data are represented as mean ± SEM.

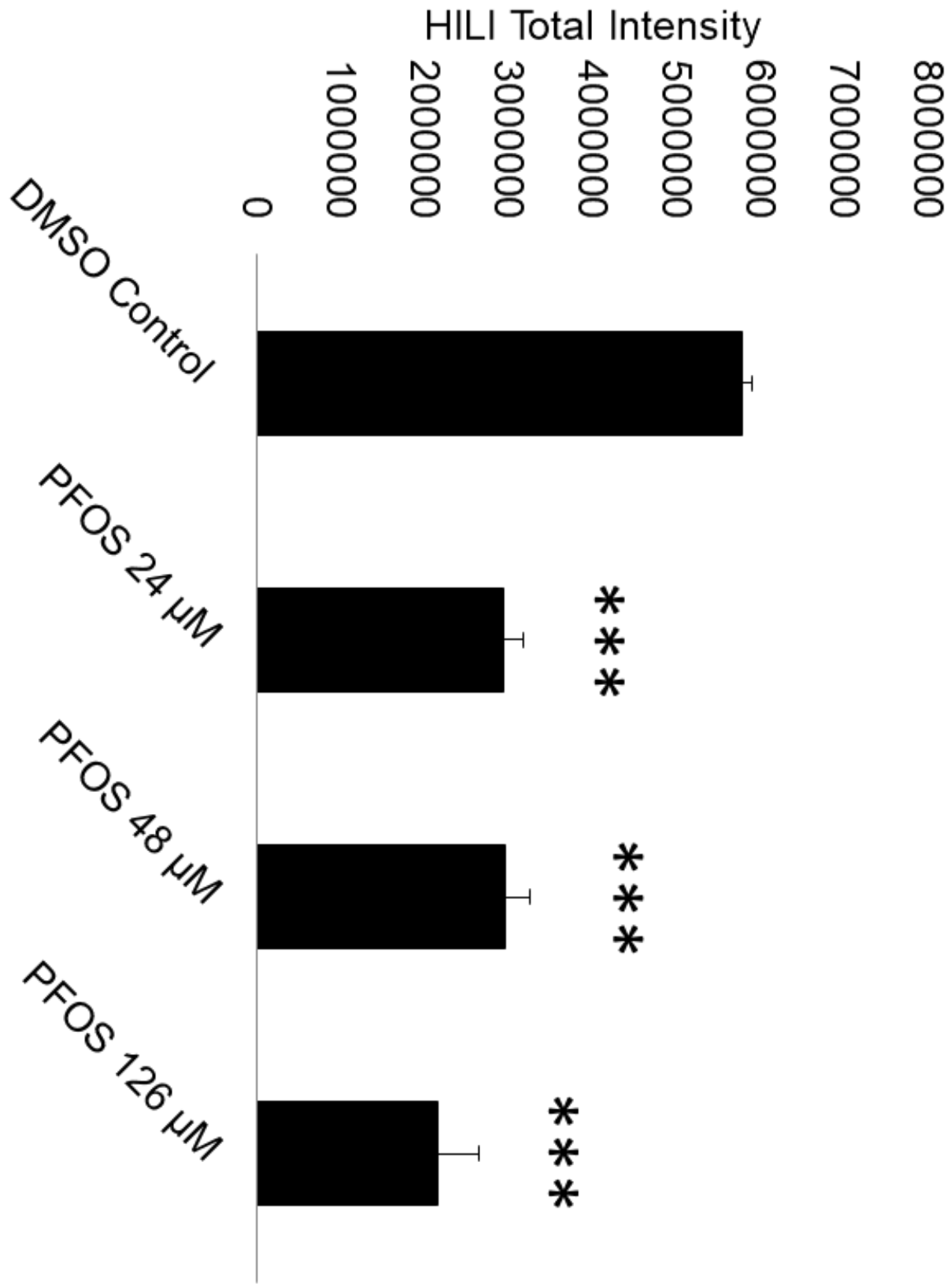
HILI Total Intensity
0
1000000
2000000
3000000
4000000
5000000
6000000
7000000
8000000
DMSO Control
PFOS 24 µM
PFOS 48 µM
PFOS 126 µM
***
***
***

Figure 5.24. Persistent PFOS exposure decreases HILI+ intensity in primary spermatocytes in in vitro spermatogenic cultures derived from H1 ESCs. Graphical representation showing that persistent 24 μM, 48 μM, and 126 μM PFOS exposure from Day 1 to Day 10 decreases average total HILI+ intensity in primary spermatocytes derived under *in vitro* spermatogenic conditions in comparison to a 0.25% DMSO-only control. Three replications were performed for each condition, and spermatogenic cells were derived from H1 ESCs (n = 3). Significant changes in HILI+ intensity were determined using a 1-way analysis of variance (1-way ANOVA) and validated via a Student's t-test, where * is $p<0.05$, ** is $p<0.01$, and *** is $p<0.001$. Data are represented as mean ± SEM.

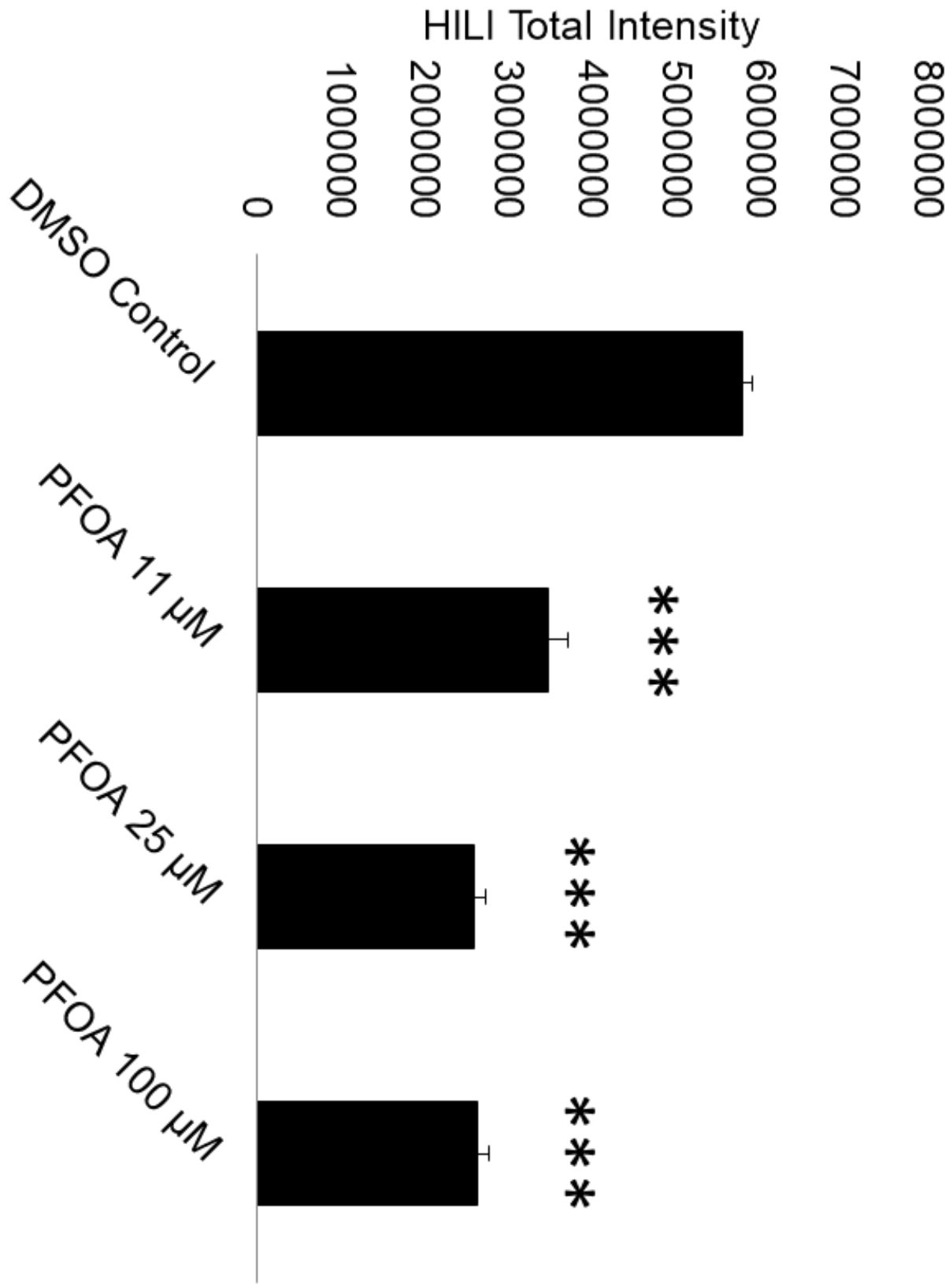
HILI Total Intensity
0
1000000
2000000
3000000
4000000
5000000
6000000
7000000
8000000
DMSO Control
PFOA 11 µM
PFOA 25 µM
PFOA 100 µM
***
***
***

Figure 5.25. Persistent PFOA exposure decreases HILI+ intensity in primary spermatocytes in in vitro spermatogenic cultures derived from H1 ESCs. Graphical representation showing that persistent 11 μM, 25 μM, and 100 μM PFOA exposure from Day 1 to Day 10 decreases average total HILI+ intensity in primary spermatocytes derived under *in vitro* spermatogenic conditions in comparison to a 0.25% DMSO-only control. Three replications were performed for each condition, and spermatogenic cells were derived from H1 ESCs (n = 3). Significant changes in HILI+ intensity were determined using a 1-way analysis of variance (1-way ANOVA) and validated via a Student's t-test, where * is $p<0.05$, ** is $p<0.01$, and *** is $p<0.001$. Data are represented as mean ± SEM.

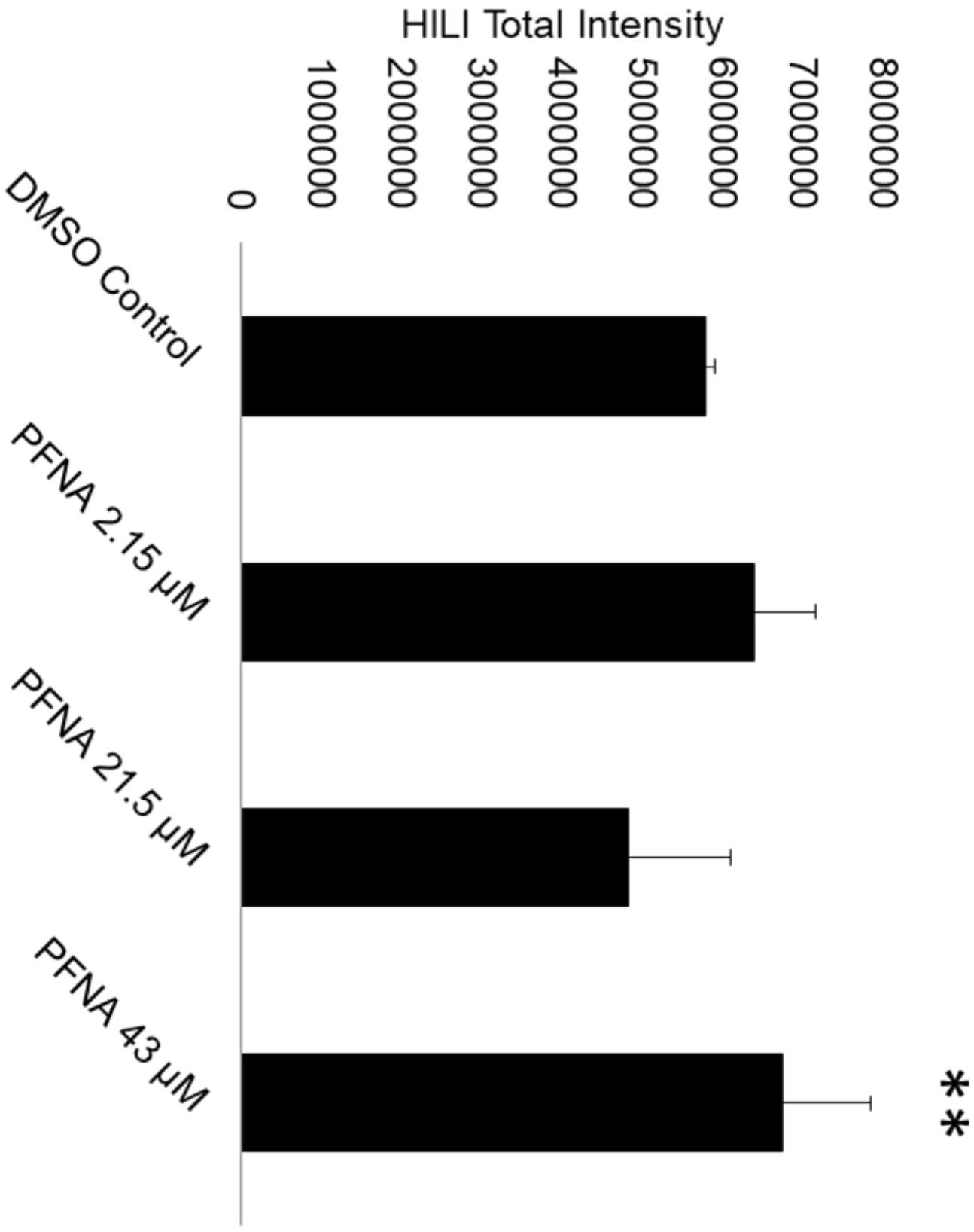
HILI Total Intensity
0
1000000
2000000
3000000
4000000
5000000
6000000
7000000
8000000
DMSO Control
PFNA 2.15 µM
PFNA 21.5 µM
PFNA 43 µM
**

Figure 5.26. Persistent PFNA exposure decreases HILI+ intensity in primary spermatocytes in in vitro spermatogenic cultures derived from H1 ESCs. Graphical representation showing that persistent 43 μM PFNA exposure from Day 1 to Day 10 decreases average total HILI+ intensity in primary spermatocytes derived under *in vitro* spermatogenic conditions in comparison to a 0.25% DMSO-only control. Three replications were performed for each condition, and spermatogenic cells were derived from H1 ESCs (n = 3). Significant changes in HILI+ intensity were determined using a 1-way analysis of variance (1-way ANOVA) and validated via a Student's t-test, where * is $p<0.05$, ** is $p<0.01$, and *** is $p<0.001$. Data are represented as mean ± SEM.

2.5.4 Acute TDCCP, TDBPP, HBCDD, and TBBPA exposure impairs cell cycle progression in in vitro cultures but does not affect haploid sperm viability, and persistent PFAS exposure does not impact cell cycle or haploid cells

Spermatogenic cells work to guarantee genome integrity through cell cycle checkpoints, as infidelity in DNA replication, mistakes in chromosome segregation, and other forms of DNA mutations can occur. Therefore, toxicants that disturb these processes may impact the cell cycle, making cell cycle profiles vital indicators of germ cell health (Shackelford et al., 1999). Cell cycle information in regard to flame retardant exposure during spermatogenesis is limited. In somatic cells, TDCPP has been shown to downregulate the pathways required for cell proliferation in HepG2/C3A and A549 cells (Zhang et al., 2016). Additionally, TDBPP decreases cell growth *in vitro* in rat hepatoma cells (Soderlund and Dybing, 1979). HBCDD has been shown to upregulate cell cycle-related genes in LNCaP cells and may act to increase cell proliferation (Kim et al., 2016). In germ cells, TBBPA has been shown to have an adverse effect on the cell cycle in mouse spermatogonial stem cells (Liang et al., 2017). To determine how these toxicants impact *in vitro* spermatogenesis in a mixed population of spermatogonia, primary and secondary spermatocytes, and spermatids, cell cycle profiles of flame retardant exposed cells were generated by staining with propidium iodide. Flow cytometry plots were generated showing the percentage of haploid cells and cells in G0/G1, S phase, and G2 in our cultures (Figure 6.1). While TDBPP, HBCDD, and TBBPA did not affect G0/G1, TDCPP significantly decreased the percentage of cells in G0/G1 at 10 µM by roughly 11% and significantly increased cells in G0/G1 by nearly 16% at 100 µM (Figures 6.2 – 6.5). Similarly, TDCPP significantly decreased the

percentage of cells in S phase at 100 µM by 22% (Figure 6.2). TDBPP significantly increased cells in S phase at 10 µM and 25 µM by 13%, but cells in S phase decreased beginning at 50 µM with a nearly 33% decrease at 200 µM (Figure 6.3). HBCDD also significantly increased cells in S phase at 25 µM by 13%, with a decrease in cells in S phase at 100 µM and 200 µM by 36% and 22%, respectively (Figure 6.4). All flame retardants had a significant impact on G2 (Figures 6.2 – 6.5). TDCPP, TDBPP, HBCDD, and TBBPA significantly decreased the percentage of cells in G2 beginning at 50 µM, 50 µM, 10 µM, and 100 µM by nearly 18%, 49%, 56%, and 53%, respectively (Figures 6.2 – 6.5). TBBPA significantly increased the percentage of cells in G2 at 1 µM by nearly 25% (Figure 6.5). This suggests that spermatogonia, primary spermatocytes, or secondary spermatocytes in our cultures are likely targets of our flame retardant toxicants, as they are the cell populations actively undergoing cell division. As such, these cell cycle profiles validate our PLZF and HILI staining data.

However, the end product of spermatogenesis is the production of haploid spermatids. Numerous environmental factors have been shown to reduce sperm counts (Wong and Cheng, 2011), and some toxicants are known to target haploid spermatids (Easley et al., 2015). However, the halogenated flame retardants TDCPP, TDBPP, HBCDD, and TBBPA all significantly increased the percentage of haploid spermatids in our cultures beginning at 100 µM, 50 µM, 50 µM, and 100 µM, respectively (Figures 6.6 – 6.9). 200 µM TDCPP and TDBPP significantly increased the percentage of haploid cells in our cultures by 46% and 73%, respectively (Figures 6.6 – 6.7). 100 µM HBCDD and TBBPA significantly increased the percentage of spermatids in our cultures at by 67% and 63%, respectively (Figures 6.8 – 6.9). HBCDD treatment caused a significant

decrease in haploid spermatids at 200 µM versus 100 µM by roughly 17%; however, the percentage of haploid spermatids was still greater than control (Figure 6.8).

Importantly, the increases in haploid cells seen in these assays were likely not due to increases in meiosis that drove the generation of more spermatids. Because chemical exposure occurred under acute conditions over twenty-four hours, percentages of haploid cells likely increased due to spermatogonia and primary spermatocytes undergoing cell death, leaving more haploid cells present in our mixed cell cultures. As such, these results again indicate that the direct targets of these toxicants are likely the actively dividing spermatogonia and primary spermatocytes undergoing meiosis. These results are of critical importance. Though spermatids are not directly targeted, thus not causing immediate infertility in an adult male, evidence suggests that exposure to these flame retardants at physiologically relevant concentrations could be impacting the pool of spermatogonia responsible for generating spermatids/sperm. Additionally, spermatogonia and primary spermatocytes continue to be impacted by HBCDD and TBBPA even after removal during recovery experiments. As such, exposure could lead to reduced fertility in populations exposed, though the potential for abnormalities in the surviving spermatids also exists.

Reports on the impacts of PFASs on the cell cycle of germ cells are limited, though *C. elegans* exposed to PFOS have experienced mitotic cell arrest in germ cells (Guo et al., 2016). Similarly, one study that examined the impacts of various per- and polyfluoroalkyl substances found that PFOA was able to disrupt the cell cycle of human hepatoblastoma HepG2 cells, and another study reported cell cycle arrest in the spleen and thymus of BALB/c mice upon exposure to PFNA (Fang et al., 2008) (Mulkiewicz,

Jastorff, Skladanowski, Kleszczynski, & Stepnowski, 2007). To determine how these toxicants can impact *in vitro* spermatogenesis, cell cycle profiles of PFAS exposed cells and DMSO-only treated cells were generated. Flow cytometry plots were generated showing the percentage of haploid cells and cells in G0/G1, S phase, and G2 in our cultures (Figure 6.10). Neither PFOS, PFOA, nor PFNA displayed a significant ability to alter the percentages of haploid, G0/G1, S, or G2 cells undergoing spermatogenesis at any of the concentrations tested (Figure 6.11 – 6.13). Notably, PFOA exposure resulted in an increasing number of germ cells in G2 phase upon increasing concentration, with a roughly 15% increase in cells in G2 at 100 µM, but this trend was not statistically significant (Figure 6.12).

Remarkably, exposure to PFOS, PFOA, and PFNA also did not impact haploid cell production in our model at any concentration tested (Figures 6.14 – 6.16) consistent with human studies. PFOA exposure did result in a decreasing percentage of haploid cells with increasing concentration of PFOA, with a roughly 25% decline at 100 µM, though this decline was not statistically significant (Figure 6.15). These results indicate that these chemicals are not toxic to even the most sensitive of our mixed population of germ cells.

The results from these analyses confirm that halogenated flame retardants and PFASs, despite having lyophilic properties and halogenation, have differing toxicities, with flame retardants directly impacting cell viability and cell cycle progression. PFASs may impact gene expression and subcellular processes, but differences in these compound’s structures mitigates toxic effects. As such, it would be beneficial for future studies to assess how timing, differences in core structure, differences in type of

halogenation, and differences in number of halogens may reduce the toxicity of flame retardants.

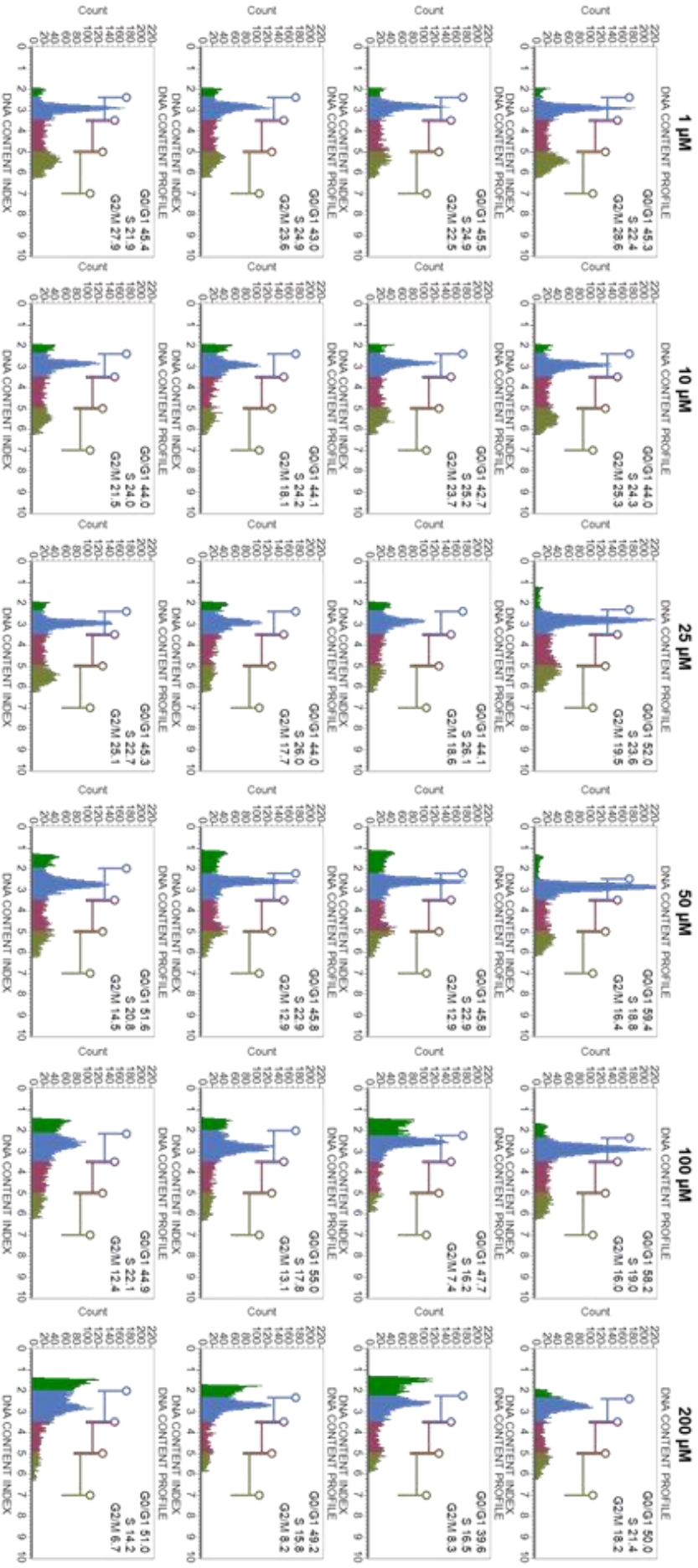
TDCPP
TDBPP
HBCDD
TBBPA
1 µM
10 µM
25 µM
50 µM
100 µM
200 µM
DNA CONTENT PROFILE
DNA CONTENT INDEX
Count
G0/G1 45.3
S 22.4
G2/M 28.6
G0/G1 44.0
S 24.3
G2/M 25.3
G0/G1 52.0
S 23.6
G2/M 19.5
G0/G1 59.4
S 18.8
G2/M 16.4
G0/G1 58.2
S 19.0
G2/M 16.0
G0/G1 50.0
S 21.4
G2/M 18.2
G0/G1 45.5
S 24.9
G2/M 22.5
G0/G1 42.7
S 25.2
G2/M 23.7
G0/G1 44.1
S 26.1
G2/M 18.6
G0/G1 45.8
S 22.9
G2/M 12.9
G0/G1 47.7
S 16.2
G2/M 17.4
G0/G1 39.6
S 16.5
G2/M 8.3
G0/G1 43.0
S 24.9
G2/M 23.6
G0/G1 44.1
S 24.2
G2/M 18.1
G0/G1 44.0
S 26.0
G2/M 17.7
G0/G1 45.8
S 22.9
G2/M 12.9
G0/G1 55.0
S 17.8
G2/M 13.1
G0/G1 49.2
S 15.8
G2/M 8.2
G0/G1 45.4
S 21.9
G2/M 27.9
G0/G1 44.0
S 24.0
G2/M 21.5
G0/G1 45.3
S 22.7
G2/M 25.1
G0/G1 51.6
S 20.8
G2/M 14.5
G0/G1 44.9
S 22.1
G2/M 12.4
G0/G1 51.0
S 14.2
G2/M 6.7

Figure 6.1. Acute TDCPP, TDBPP, HBCDD, and TBBPA exposure impact the cell cycle in spermatogenic cells derived from H1 ESCs without impacting haploid cell viability. Flow cytometry analyses of cell cycle profiles following acute twenty-four hour treatment of 1 μM, 10 μM, 25 μM, 50 μM, 100 μM, and 200 μM TDCPP, TDBPP, HBCDD, and TBBPA. Green, blue, purple, and beige populations on flow cytometry correspond to haploid, G0/G1, S, and G2 phases, respectively.

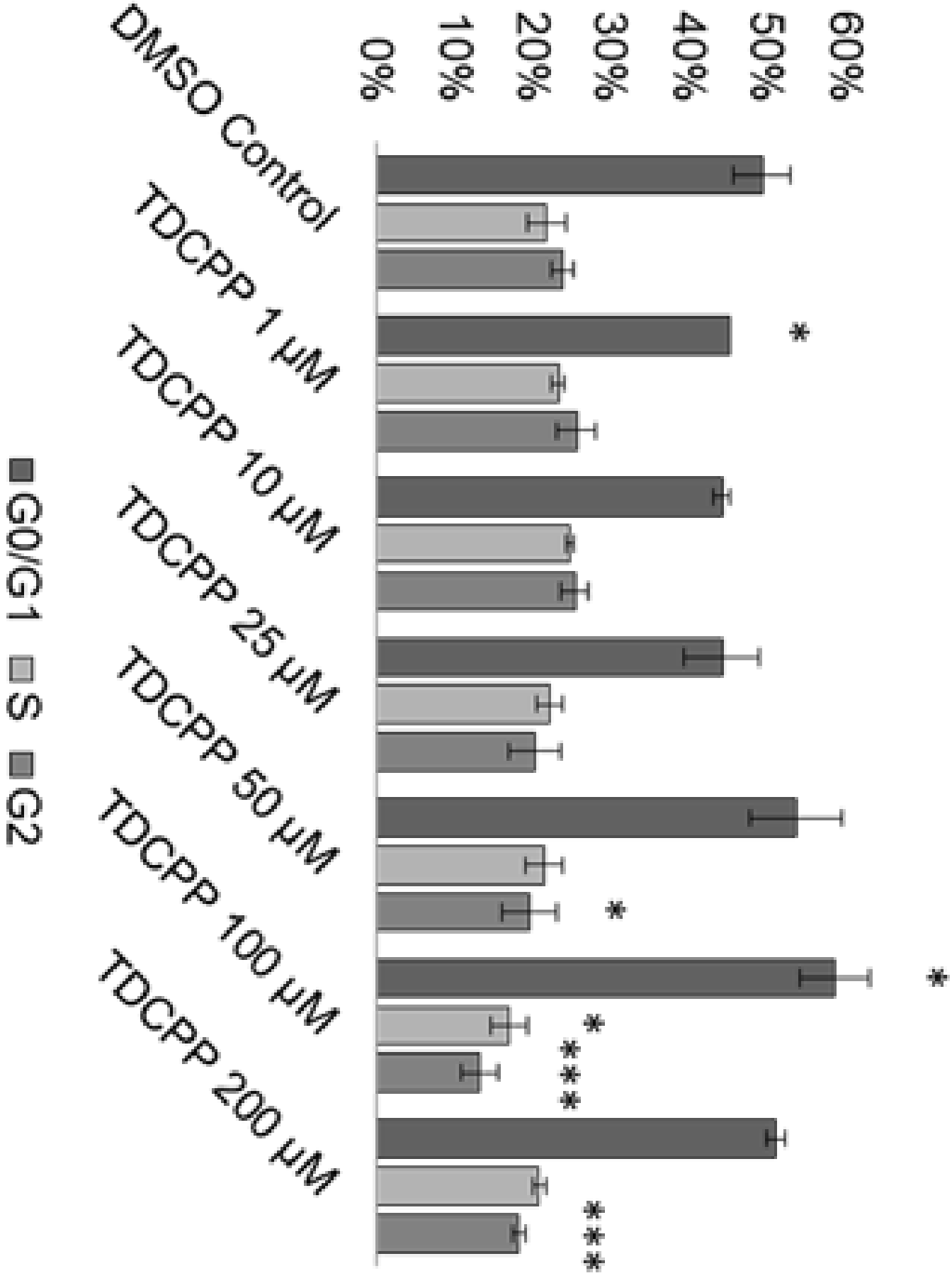
DMSO Control
TDCPP 1 µM
TDCPP 10 µM
TDCPP 25 µM
TDCPP 50 µM
TDCPP 100 µM
TDCPP 200 µM
0%
10%
20%
30%
40%
50%
60%
G0/G1
S
G2

Figure 6.2. Acute TDCPP exposure affects the cell cycle in spermatogenic cells derived from H1 ESCs. Graphical representation showing that 1 μM, 50 μM, 100 μM, and 200 μM TDCPP affects the cell cycle of actively dividing H1 ESCS differentiated in *in vitro* spermatogenic conditions in comparison to a 0.2% DMSO-only control. 5,000 events were analyzed, with five replications performed for each condition (n = 5). Significant changes in percentages of cells in G0/G1, S phase, and G2 were determined using a 1-way analysis of variance (1-way ANOVA) and validated via a Student's t-test, where * is $p<0.05$, ** is $p<0.01$, and *** is $p<0.001$. Data are represented as mean ± SEM.

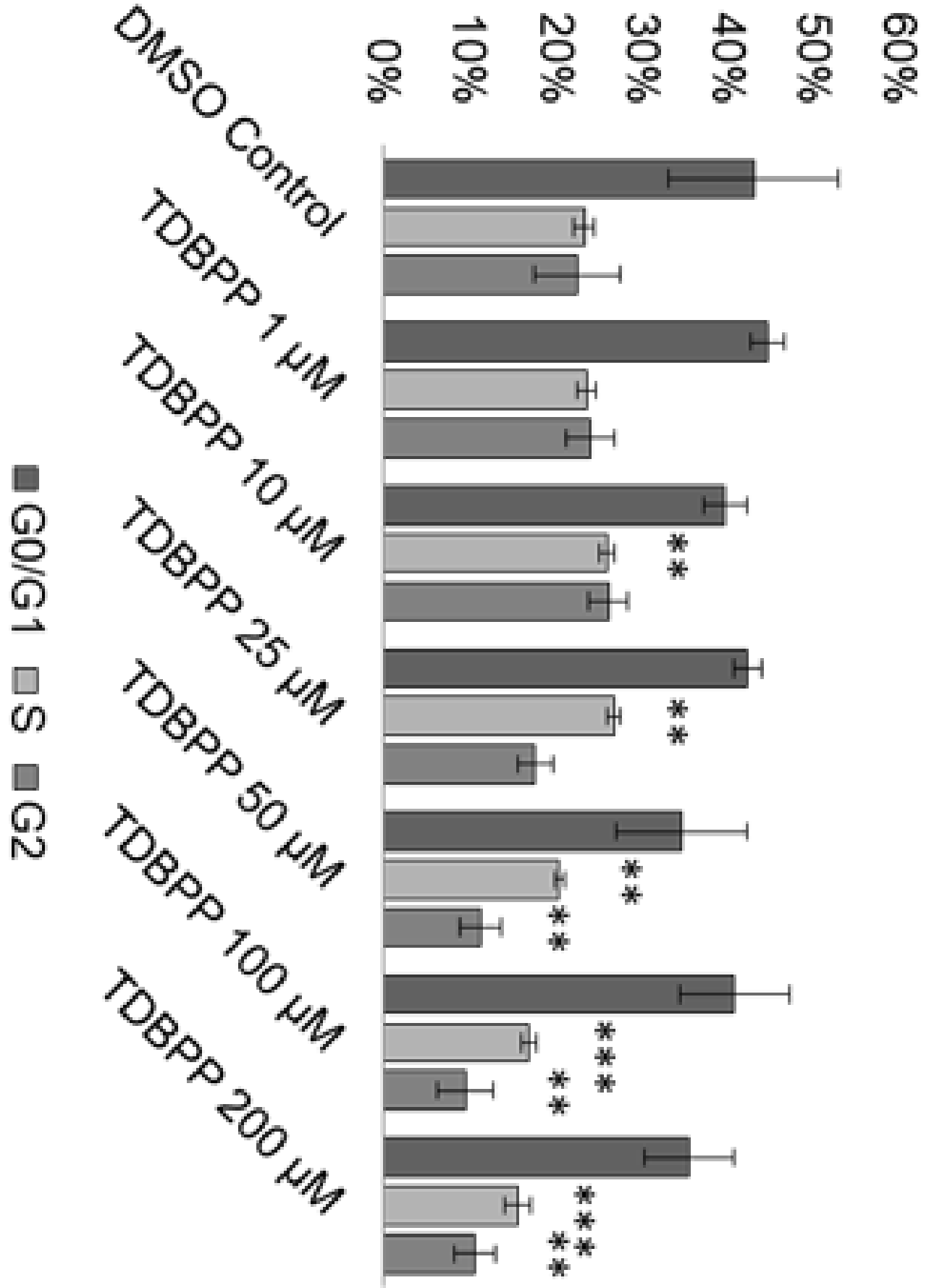
60%
50%
40%
30%
20%
10%
0%
DMSO Control
TDBPP 1 µM
TDBPP 10 µM
TDBPP 25 µM
TDBPP 50 µM
TDBPP 100 µM
TDBPP 200 µM
G0/G1
S
G2

Figure 6.3. Acute TDBPP exposure affects the cell cycle in spermatogenic cells derived from H1 ESCs. Graphical representation showing that 10 μM, 25 μM, 50 μM, 100 μM, and 200 μM TDBPP affects the cell cycle of actively dividing H1 ESCS differentiated in *in vitro* spermatogenic conditions in comparison to a 0.2% DMSO-only control. 5,000 events were analyzed, with five replications performed for each condition (n = 5). Significant changes in percentages of cells in G0/G1, S phase, and G2 were determined using a 1-way analysis of variance (1-way ANOVA) and validated via a Student's t-test, where * is $p<0.05$, ** is $p<0.01$, and *** is $p<0.001$. Data are represented as mean ± SEM.

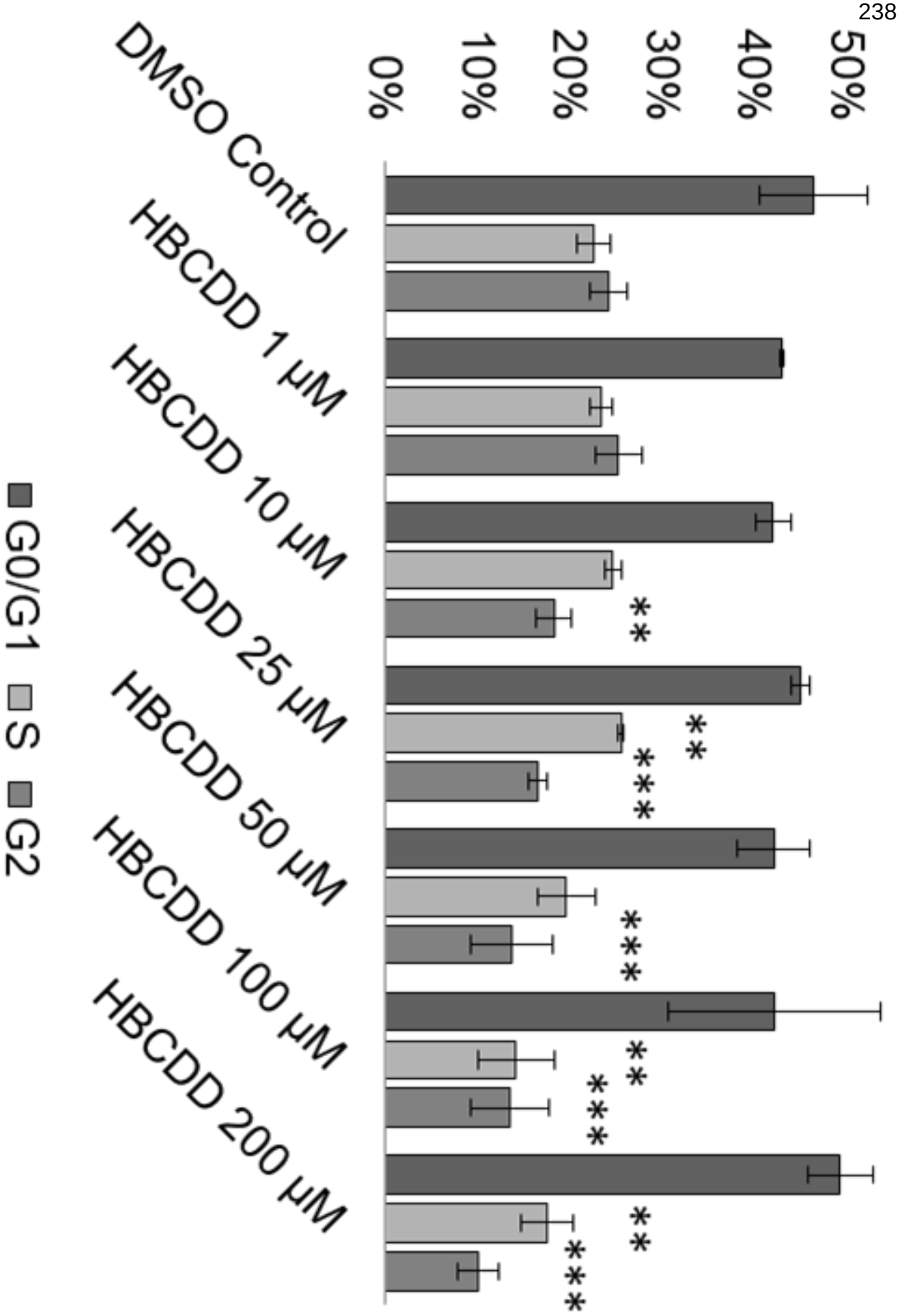
50%
40%
30%
20%
10%
0%
DMSO Control
HBCDD 1 μM
HBCDD 10 μM
HBCDD 25 μM
HBCDD 50 μM
HBCDD 100 μM
HBCDD 200 μM
G0/G1
S
G2

Figure 6.4. Acute HBCDD exposure affects the cell cycle in spermatogenic cells derived from H1 ESCs. Graphical representation showing that 10 μM, 25 μM, 50 μM, 100 μM, and 200 μM HBCDD affects the cell cycle of actively dividing H1 ESCS differentiated in *in vitro* spermatogenic conditions in comparison to a 0.2% DMSO-only control. 5,000 events were analyzed, with five replications performed for each condition (n = 5). Significant changes in percentages of cells in G0/G1, S phase, and G2 were determined using a 1-way analysis of variance (1-way ANOVA) and validated via a Student's t-test, where * is $p<0.05$, ** is $p<0.01$, and *** is $p<0.001$. Data are represented as mean ± SEM.

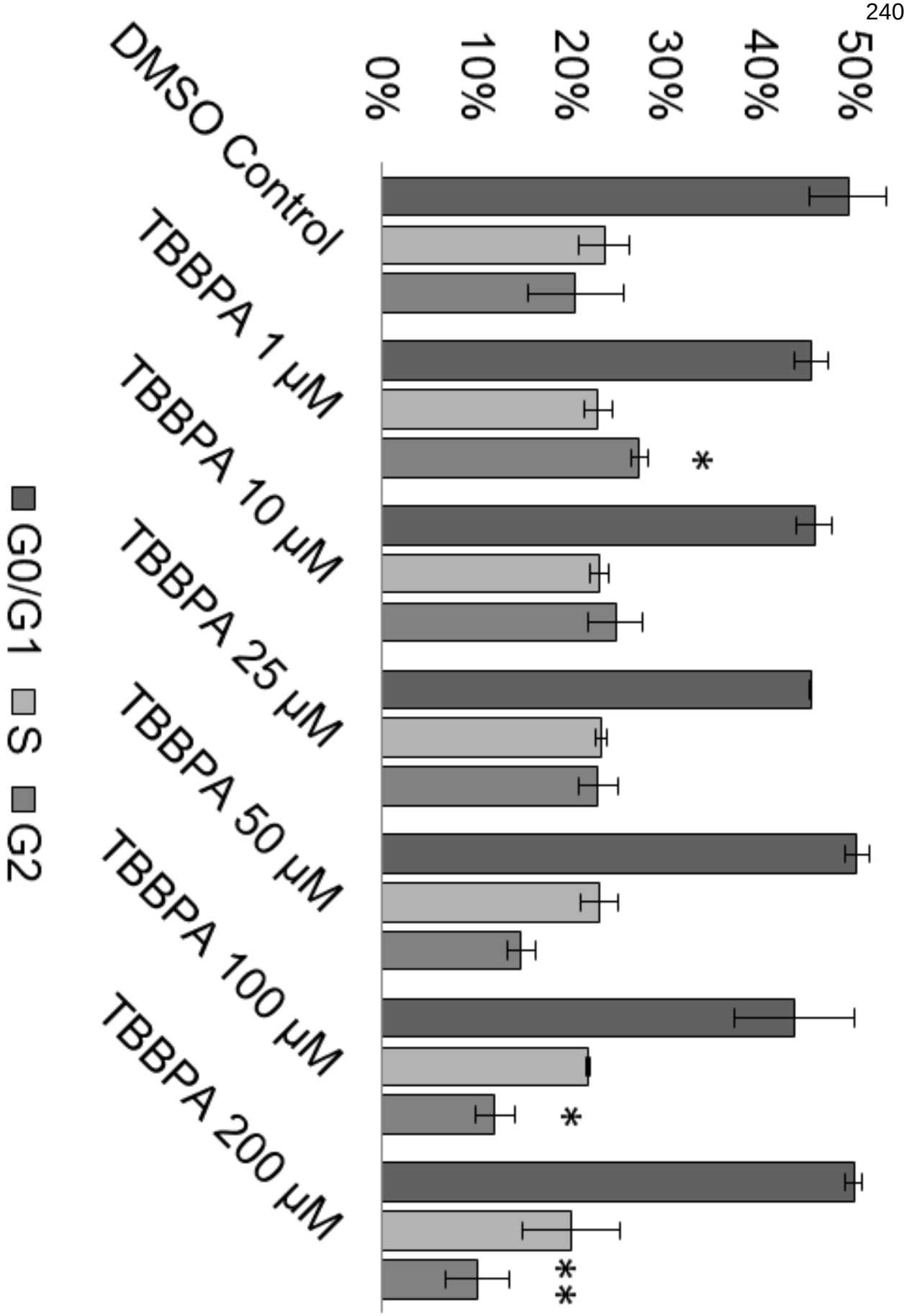
50%
40%
30%
20%
10%
0%
DMSO Control
TBBPA 1 µM
TBBPA 10 µM
TBBPA 25 µM
TBBPA 50 µM
TBBPA 100 µM
TBBPA 200 µM
G0/G1
S
G2
*
*
*
*

Figure 6.5. Acute TBBPA exposure affects the cell cycle in spermatogenic cells derived from H1 ESCs. Graphical representation showing that 1 μM, 100 μM, and 200 μM TBBPA affects the cell cycle of actively dividing H1 ESCS differentiated in *in vitro* spermatogenic conditions in comparison to a 0.2% DMSO-only control. 5,000 events were analyzed, with five replications performed for each condition (n = 5). Significant changes in percentages of cells in G0/G1, S phase, and G2 were determined using a 1-way analysis of variance (1-way ANOVA) and validated via a Student's t-test, where * is $p<0.05$, ** is $p<0.01$, and *** is $p<0.001$. Data are represented as mean ± SEM.

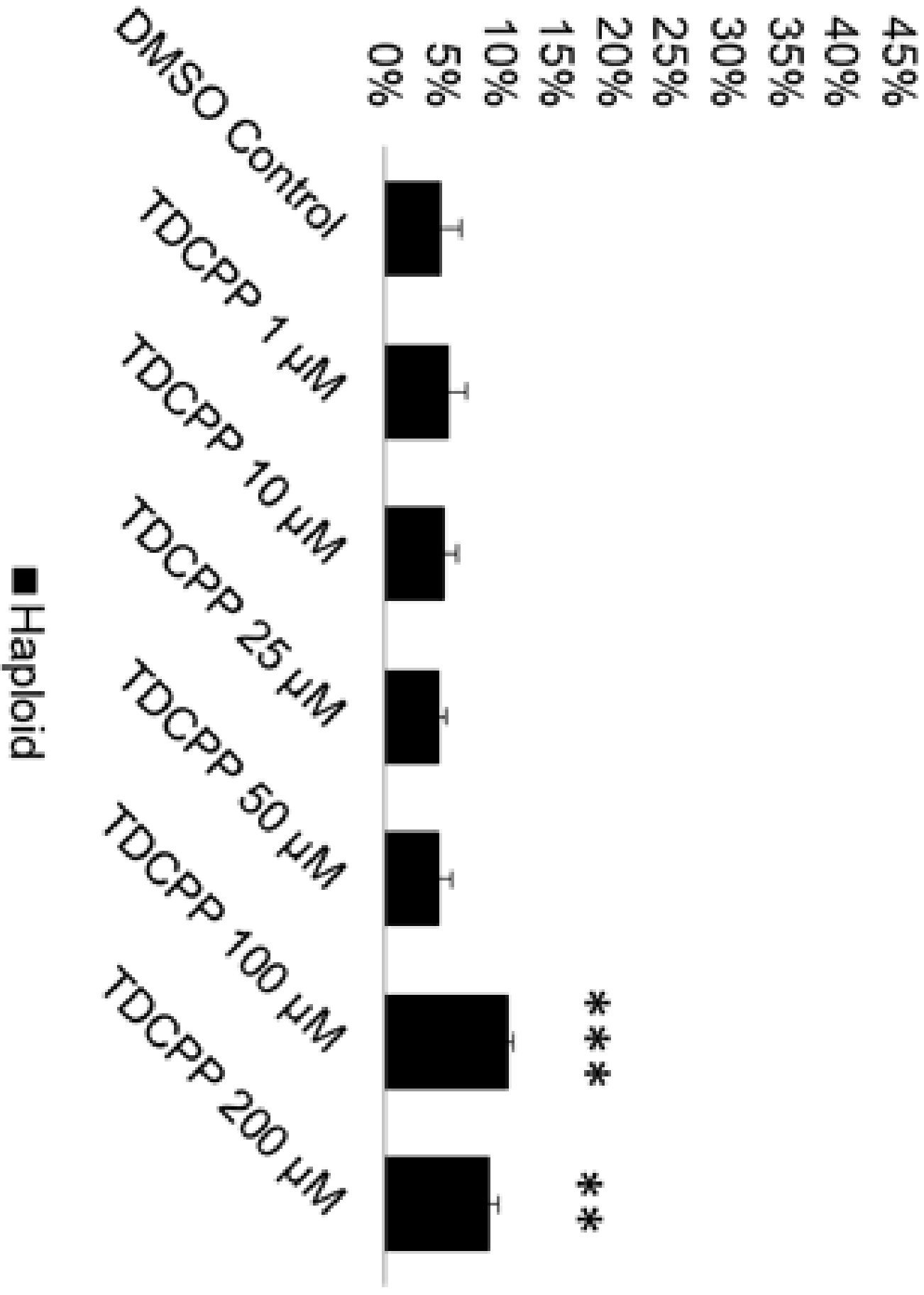
45%
40%
35%
30%
25%
20%
15%
10%
5%
0%
DMSO Control
TDCPP 1 µM
TDCPP 10 µM
TDCPP 25 µM
TDCPP 50 µM
TDCPP 100 µM
TDCPP 200 µM
***
**
■Haploid

Figure 6.6. Acute TDCPP exposure does not impact the viability of haploid cells in spermatogenic cells derived from H1 ESCs. Graphical representation showing that 100 μM and 200 μM TDCPP increases the percentage of haploid cells in H1 ESCS differentiated in *in vitro* spermatogenic conditions in comparison to a 0.2% DMSO-only control. 5,000 events were analyzed, with five replications performed for each condition (n = 5). Significant changes in percentages of haploid cells were determined using a 1-way analysis of variance (1-way ANOVA) and validated via a Student's t-test, where * is $p<0.05$, ** is $p<0.01$, and *** is $p<0.001$. Data are represented as mean ± SEM.

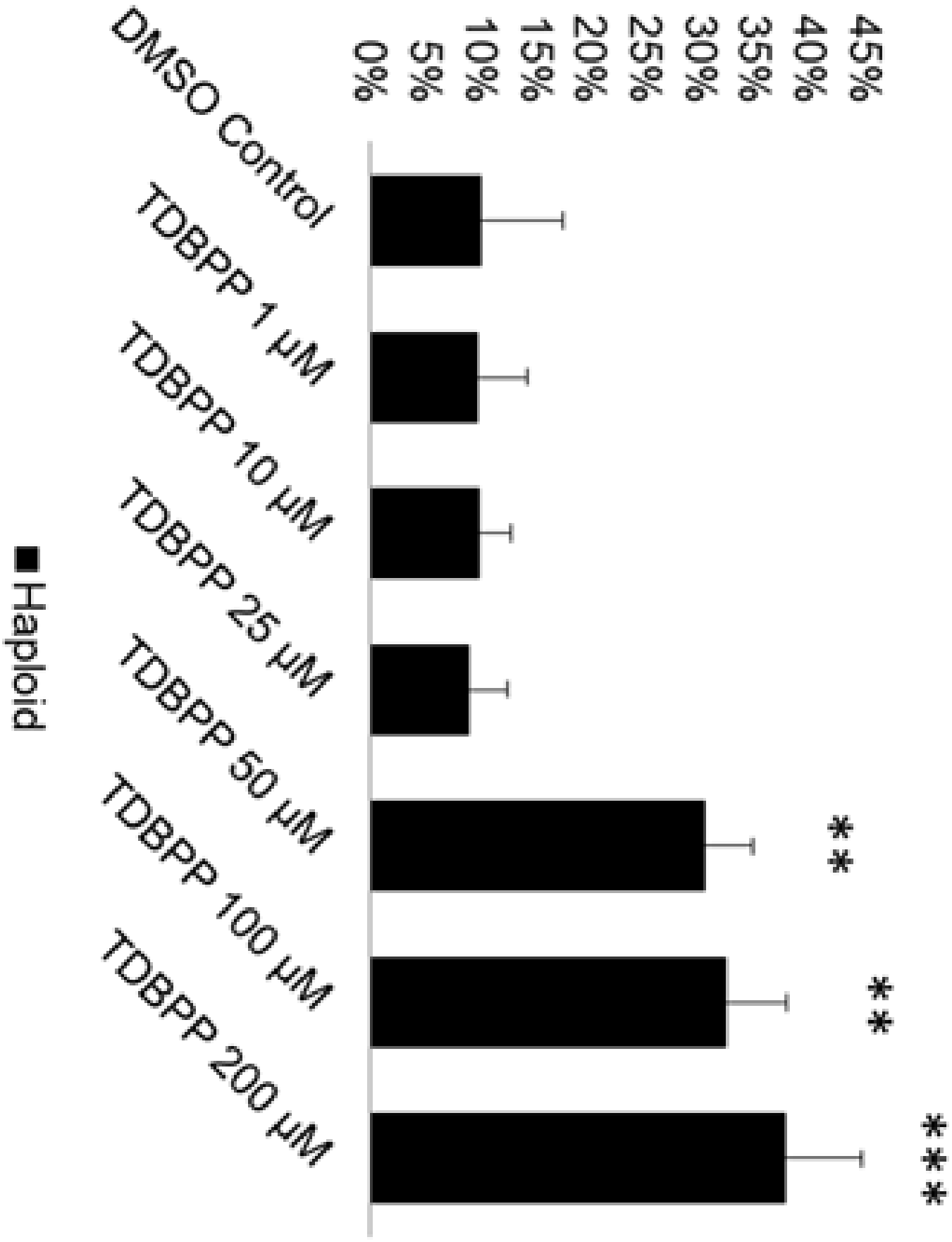
45%
40%
35%
30%
25%
20%
15%
10%
5%
0%
DMSO Control
TDBPP 1 µM
TDBPP 10 µM
TDBPP 25 µM
TDBPP 50 µM
TDBPP 100 µM
TDBPP 200 µM
**
**
***
■Haploid

Figure 6.7. Acute TDBPP exposure does not impact the viability of haploid cells in spermatogenic cells derived from H1 ESCs. Graphical representation showing that 50 μM, 100 μM, and 200 μM TDBPP increases the percentage of haploid cells in H1 ESCS differentiated in *in vitro* spermatogenic conditions in comparison to a 0.2% DMSO-only control. 5,000 events were analyzed, with five replications performed for each condition (n = 5). Significant changes in percentages of haploid cells were determined using a 1-way analysis of variance (1-way ANOVA) and validated via a Student's t-test, where * is $p<0.05$, ** is $p<0.01$, and *** is $p<0.001$. Data are represented as mean ± SEM.

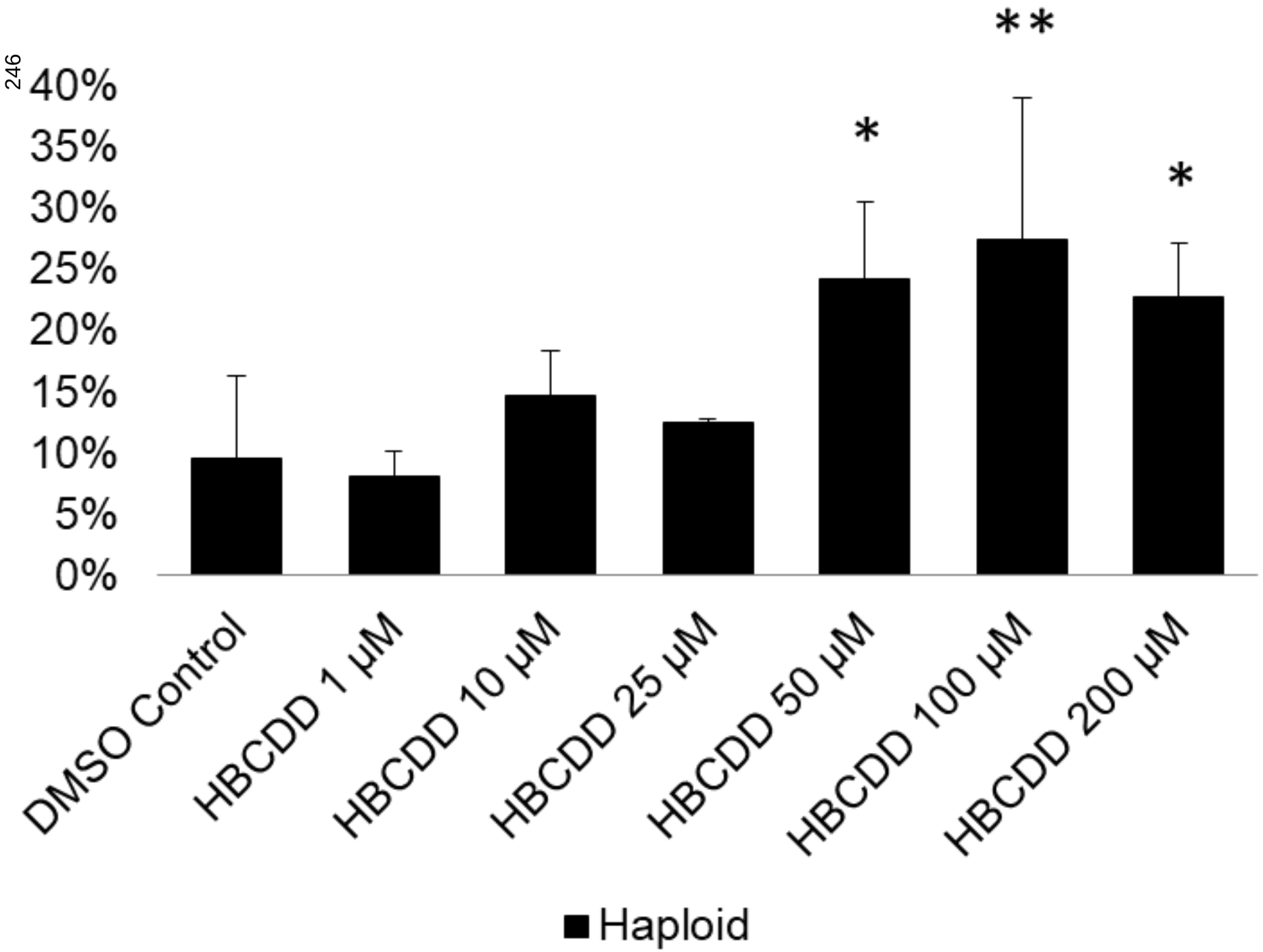
40%
35%
30%
25%
20%
15%
10%
5%
0%
*
**
*
DMSO Control
HBCDD 1 µM
HBCDD 10 µM
HBCDD 25 µM
HBCDD 50 µM
HBCDD 100 µM
HBCDD 200 µM
Haploid

Figure 6.8. Acute HBCDD exposure does not impact the viability of haploid cells in spermatogenic cells derived from H1 ESCs. Graphical representation showing that 50 μM, 100 μM, and 200 μM HBCDD increases the percentage of haploid cells in H1 ESCS differentiated in *in vitro* spermatogenic conditions in comparison to a 0.2% DMSO-only control. 5,000 events were analyzed, with five replications performed for each condition (n = 5). Significant changes in percentages of haploid cells were determined using a 1-way analysis of variance (1-way ANOVA) and validated via a Student's t-test, where * is $p<0.05$, ** is $p<0.01$, and *** is $p<0.001$. Data are represented as mean ± SEM.

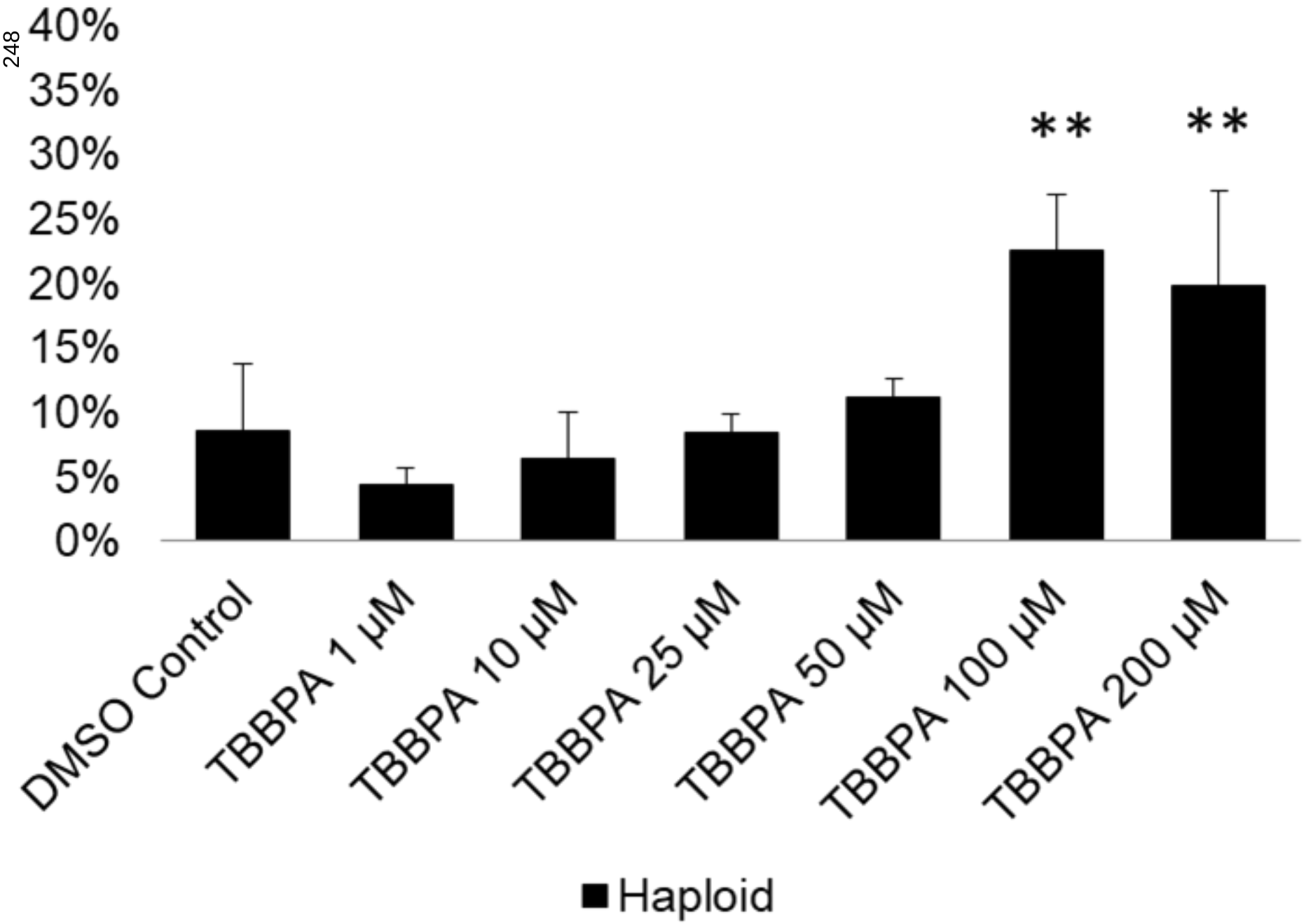
40%
35%
30%
25%
20%
15%
10%
5%
0%
**
**
DMSO Control
TBBPA 1 µM
TBBPA 10 µM
TBBPA 25 µM
TBBPA 50 µM
TBBPA 100 µM
TBBPA 200 µM
Haploid

Figure 6.9. Acute TBBPA exposure does not impact the viability of haploid cells in spermatogenic cells derived from H1 ESCs. Graphical representation showing that 100 μM and 200 μM TBBPA increases the percentage of haploid cells in H1 ESCS differentiated in *in vitro* spermatogenic conditions in comparison to a 0.2% DMSO-only control. 5,000 events were analyzed, with five replications performed for each condition (n = 5). Significant changes in percentages of haploid cells were determined using a 1-way analysis of variance (1-way ANOVA) and validated via a Student's t-test, where * is $p<0.05$, ** is $p<0.01$, and *** is $p<0.001$. Data are represented as mean ± SEM.

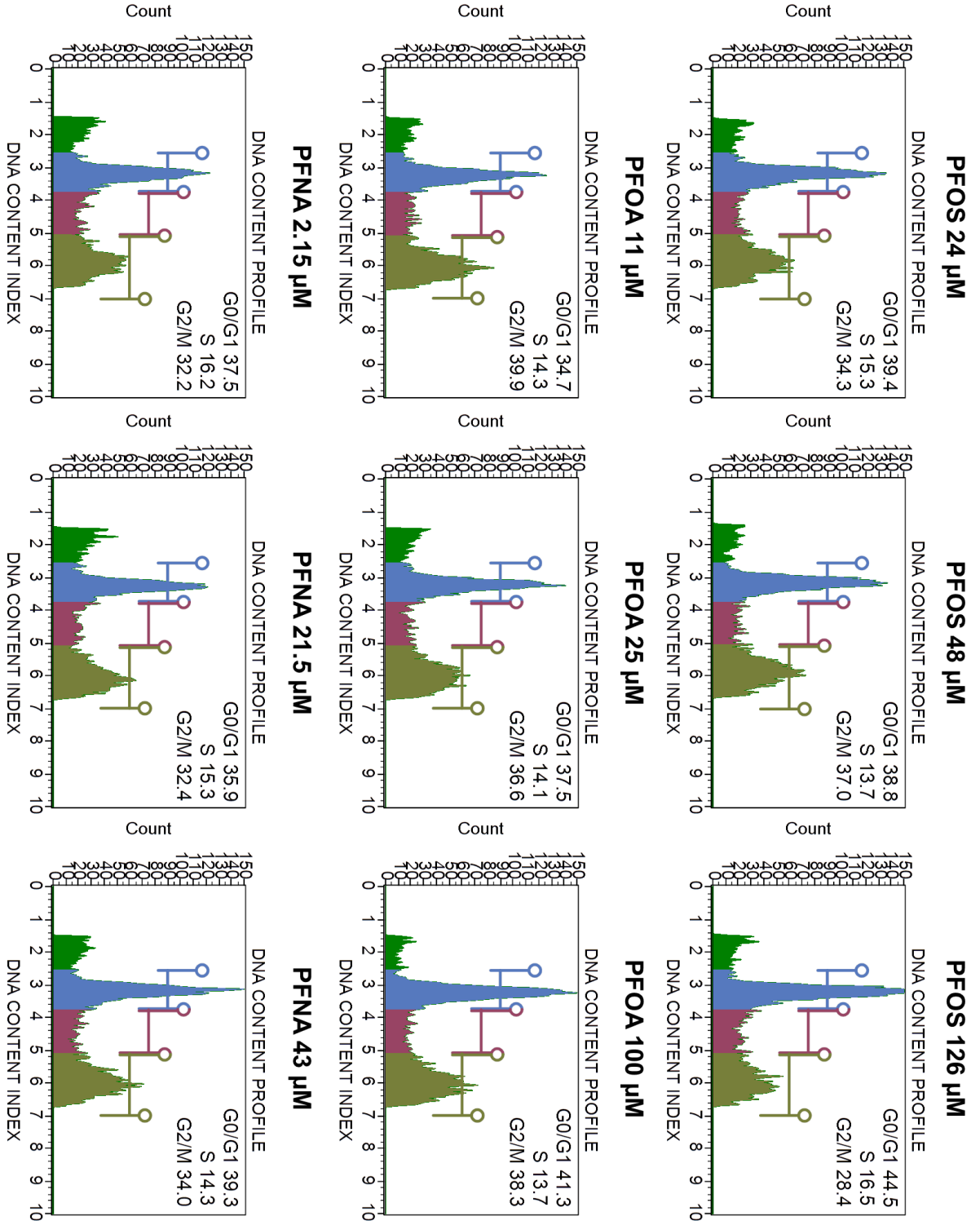
PFOS 24 µM
DNA CONTENT PROFILE
G0/G1 39.4
S 15.3
G2/M 34.3
Count
DNA CONTENT INDEX
PFOS 48 µM
DNA CONTENT PROFILE
G0/G1 38.8
S 13.7
G2/M 37.0
Count
DNA CONTENT INDEX
PFOS 126 µM
DNA CONTENT PROFILE
G0/G1 44.5
S 16.5
G2/M 28.4
Count
DNA CONTENT INDEX
PFOA 11 µM
DNA CONTENT PROFILE
G0/G1 34.7
S 14.3
G2/M 39.9
Count
DNA CONTENT INDEX
PFOA 25 µM
DNA CONTENT PROFILE
G0/G1 37.5
S 14.1
G2/M 36.6
Count
DNA CONTENT INDEX
PFOA 100 µM
DNA CONTENT PROFILE
G0/G1 41.3
S 13.7
G2/M 38.3
Count
DNA CONTENT INDEX
PFNA 2.15 µM
DNA CONTENT PROFILE
G0/G1 37.5
S 16.2
G2/M 32.2
Count
DNA CONTENT INDEX
PFNA 21.5 µM
DNA CONTENT PROFILE
G0/G1 35.9
S 15.3
G2/M 32.4
Count
DNA CONTENT INDEX
PFNA 43 µM
DNA CONTENT PROFILE
G0/G1 39.3
S 14.3
G2/M 34.0
Count
DNA CONTENT INDEX

Figure 6.10. Persistent PFOS, PFOA, and PFNA exposure does not impact the cell cycle or haploid viability in spermatogenic cells derived from H1 ESCs. Flow cytometry analyses of cell cycle profiles following persistent treatment of PFOS. PFOA, and PFNA from Day 1 to Day 10. Green, blue, purple, and beige populations on flow cytometry correspond to haploid, G0/G1, S, and G2 phases, respectively.

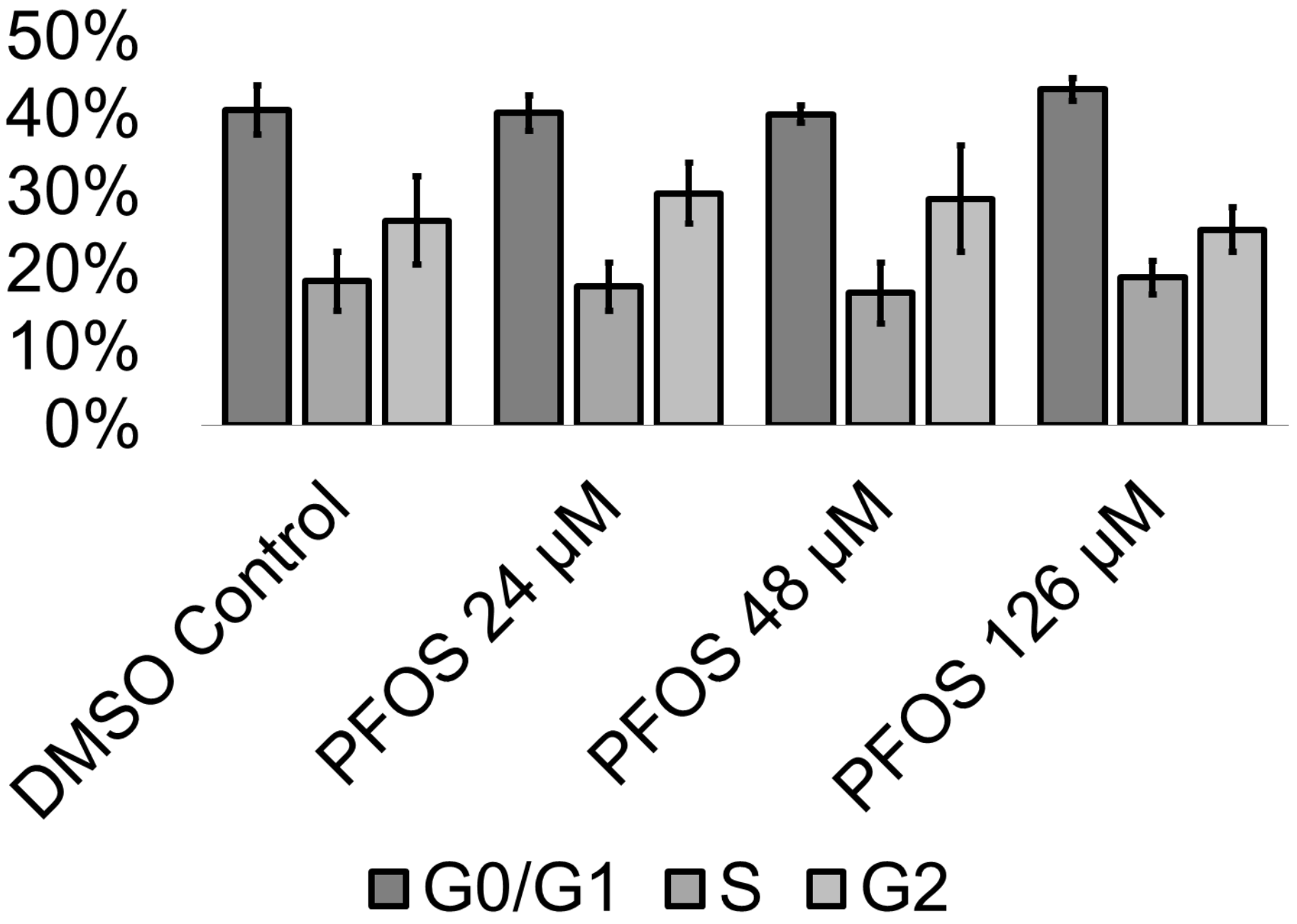
50%
40%
30%
20%
10%
0%
DMSO Control
PFOS 24 µM
PFOS 48 µM
PFOS 126 µM
G0/G1
S
G2

Figure 6.11. Persistent PFOS exposure does not impact the cell cycle of spermatogenic cells derived from H1 ESCs. Graphical representation showing that persistent exposure to 24 μM, 48 μM, and 126 μM PFOS from Day 1 to Day 10 does not impact the cell cycle of H1 ESCS differentiated in *in vitro* spermatogenic conditions in comparison to a 0.25% DMSO-only control. 5,000 events were analyzed, with three replications performed for each condition (n = 3). Significant changes in the percentage of cells in G0/G1, S phase, and G2 were determined using a 1-way analysis of variance (1-way ANOVA) and validated via a Student's t-test, where * is $p<0.05$, ** is $p<0.01$, and *** is $p<0.001$. Data are represented as mean ± SEM.

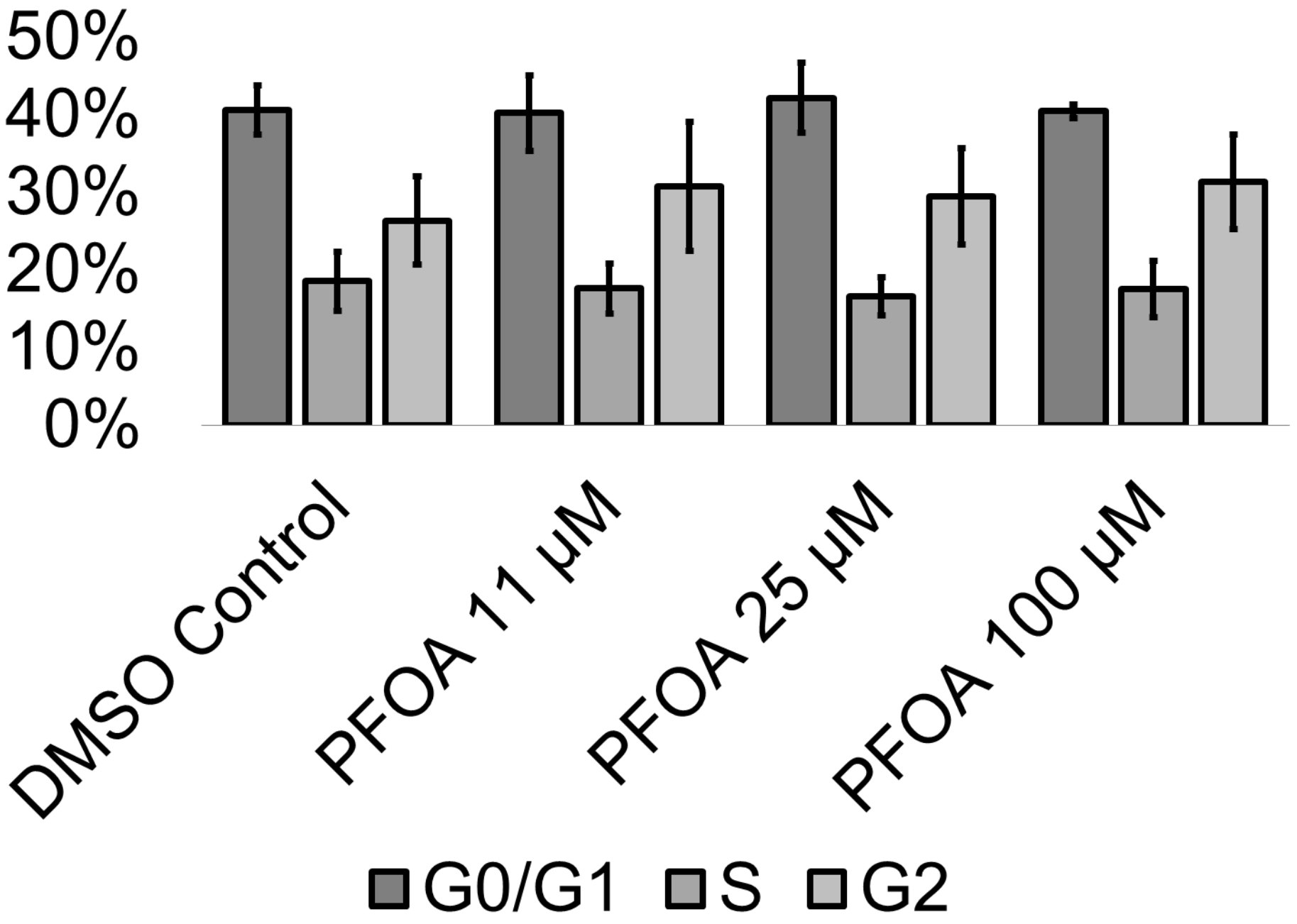
50%
40%
30%
20%
10%
0%
DMSO Control
PFOA 11 µM
PFOA 25 µM
PFOA 100 µM
G0/G1
S
G2

Figure 6.12. Persistent PFOA exposure does not impact the cell cycle of spermatogenic cells derived from H1 ESCs. Graphical representation showing that persistent exposure to 11 μM, 25 μM, and 100 μM PFOA from Day 1 to Day 10 does not impact the cell cycle of H1 ESCS differentiated in *in vitro* spermatogenic conditions in comparison to a 0.25% DMSO-only control. 5,000 events were analyzed, with three replications performed for each condition (n = 3). Significant changes in the percentage of cells in G0/G1, S phase, and G2 were determined using a 1-way analysis of variance (1-way ANOVA) and validated via a Student's t-test, where * is $p<0.05$, ** is $p<0.01$, and *** is $p<0.001$. Data are represented as mean ± SEM.

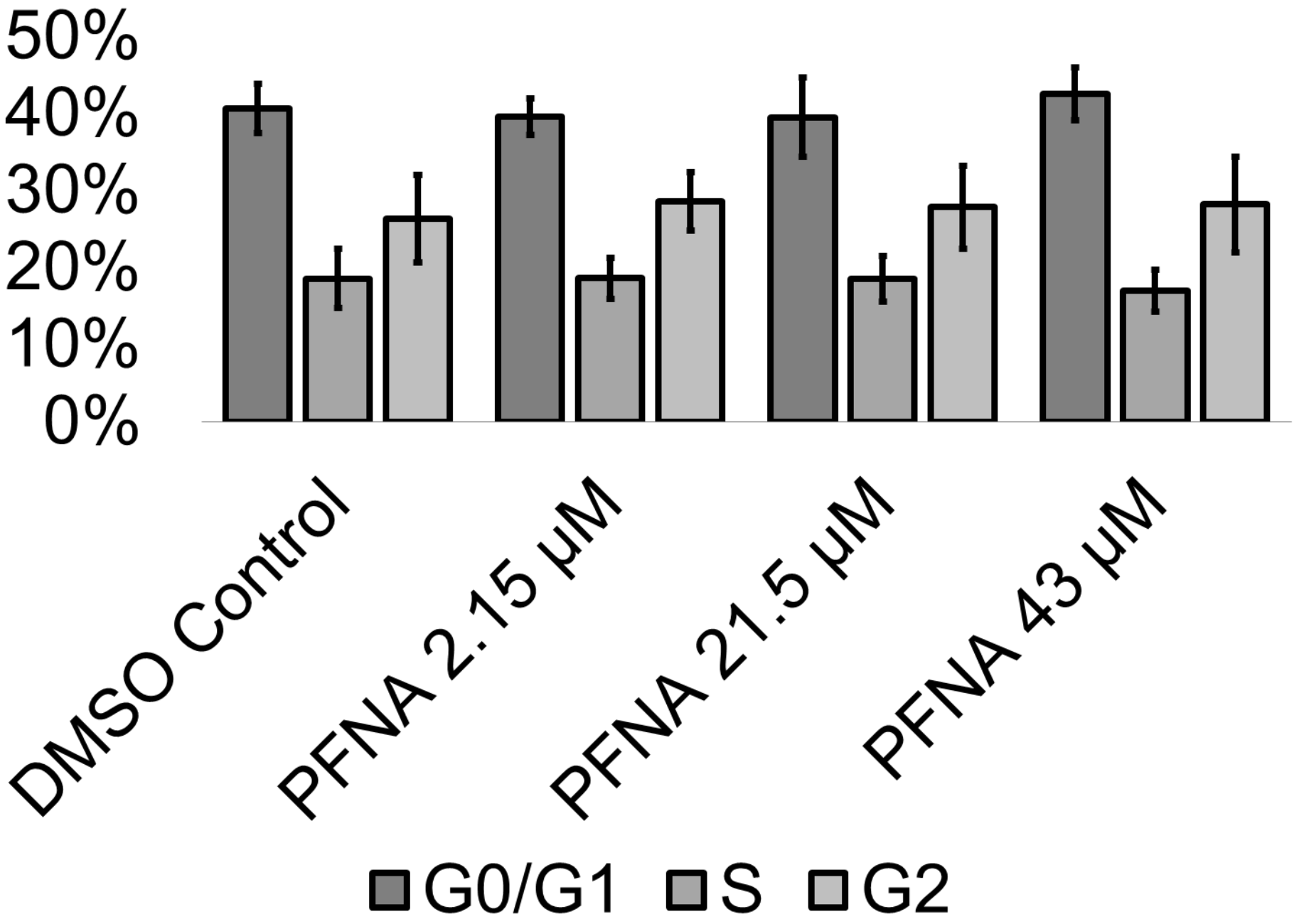
50%
40%
30%
20%
10%
0%
DMSO Control
PFNA 2.15 µM
PFNA 21.5 µM
PFNA 43 µM
G0/G1
S
G2

Figure 6.13. Persistent PFNA exposure does not impact the cell cycle of spermatogenic cells derived from H1 ESCs. Graphical representation showing that persistent exposure to 2.15 μM, 21.5 μM, and 43 μM PFNA from Day 1 to Day 10 does not impact the cell cycle of H1 ESCS differentiated in *in vitro* spermatogenic conditions in comparison to a 0.25% DMSO-only control. 5,000 events were analyzed, with three replications performed for each condition (n = 3). Significant changes in the percentage of cells in G0/G1, S phase, and G2 were determined using a 1-way analysis of variance (1-way ANOVA) and validated via a Student's t-test, where * is $p<0.05$, ** is $p<0.01$, and *** is $p<0.001$. Data are represented as mean ± SEM.

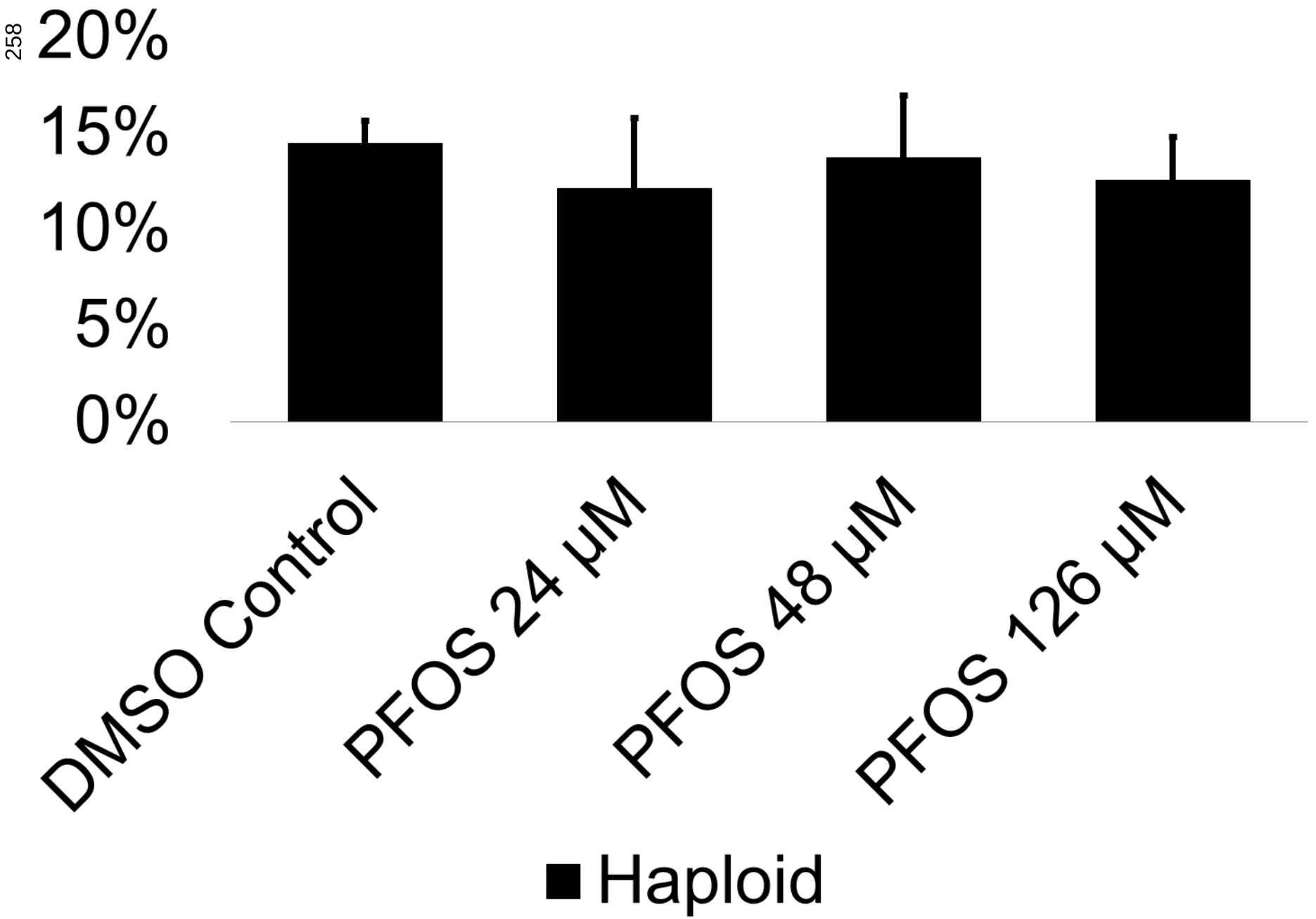
20%
15%
10%
5%
0%
DMSO Control
PFOS 24 µM
PFOS 48 µM
PFOS 126 µM
Haploid

Figure 6.14. Persistent PFOS exposure does not impact haploid cell viability of spermatogenic cells derived from H1 ESCs. Graphical representation showing that persistent exposure to 24 μM, 48 μM, and 126 μM PFOS from Day 1 to Day 10 does not impact the viability of haploid cells of H1 ESCS differentiated in *in vitro* spermatogenic conditions in comparison to a 0.25% DMSO-only control. 5,000 events were analyzed, with three replications performed for each condition (n = 3). Significant changes in the percentages of haploid cells were determined using a 1-way analysis of variance (1-way ANOVA) and validated via a Student's t-test, where * is $p<0.05$, ** is $p<0.01$, and *** is $p<0.001$. Data are represented as mean ± SEM.

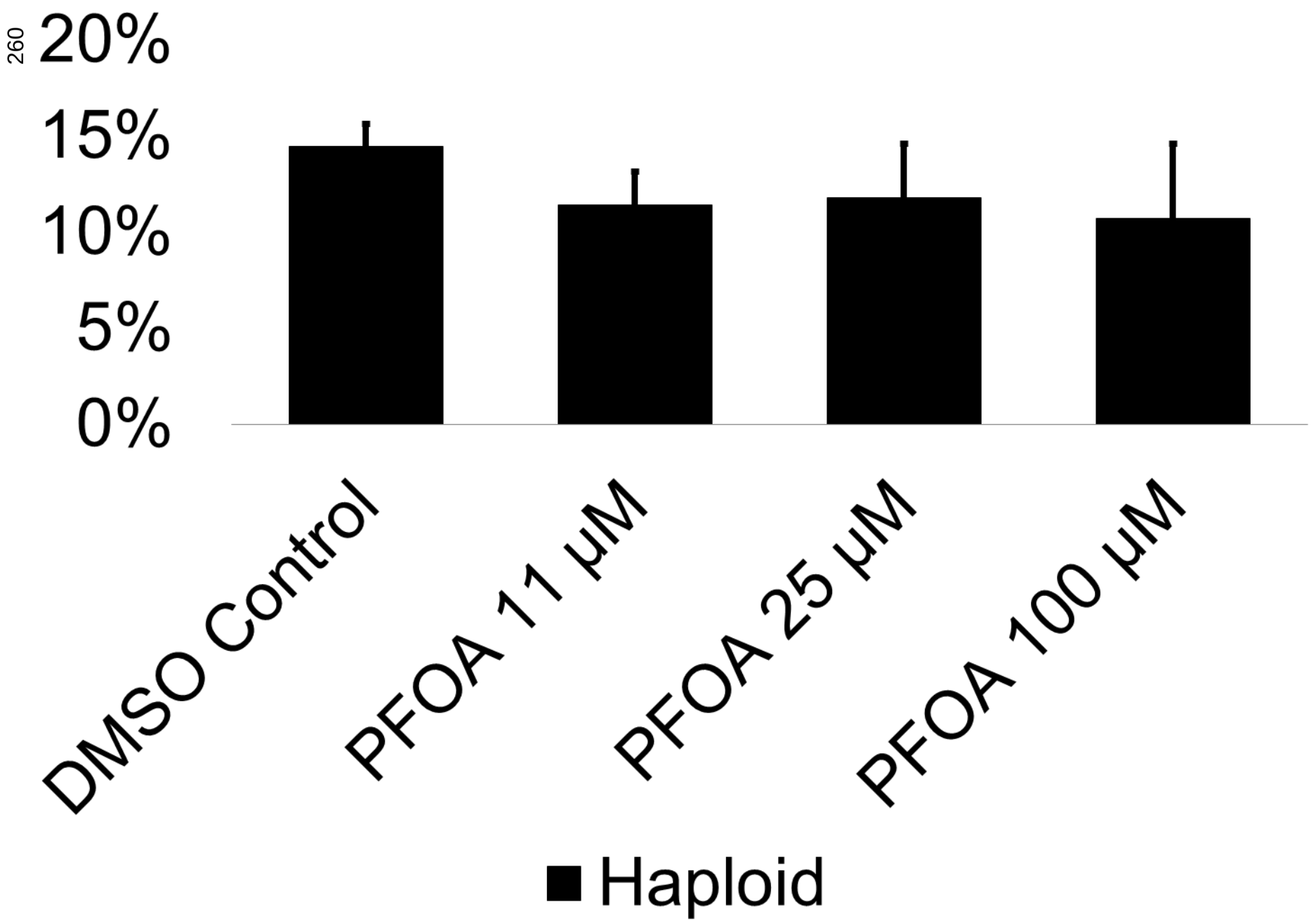
20%
15%
10%
5%
0%
DMSO Control
PFOA 11 µM
PFOA 25 µM
PFOA 100 µM
Haploid

Figure 6.15. Persistent PFOA exposure does not impact haploid cell viability of spermatogenic cells derived from H1 ESCs. Graphical representation showing that persistent exposure to 11 μM, 25 μM, and 100 μM PFOA from Day 1 to Day 10 does not impact the viability of haploid cells of H1 ESCS differentiated in *in vitro* spermatogenic conditions in comparison to a 0.25% DMSO-only control. 5,000 events were analyzed, with three replications performed for each condition (n = 3). Significant changes in the percentages of haploid cells were determined using a 1-way analysis of variance (1-way ANOVA) and validated via a Student's t-test, where * is $p<0.05$, ** is $p<0.01$, and *** is $p<0.001$. Data are represented as mean ± SEM.

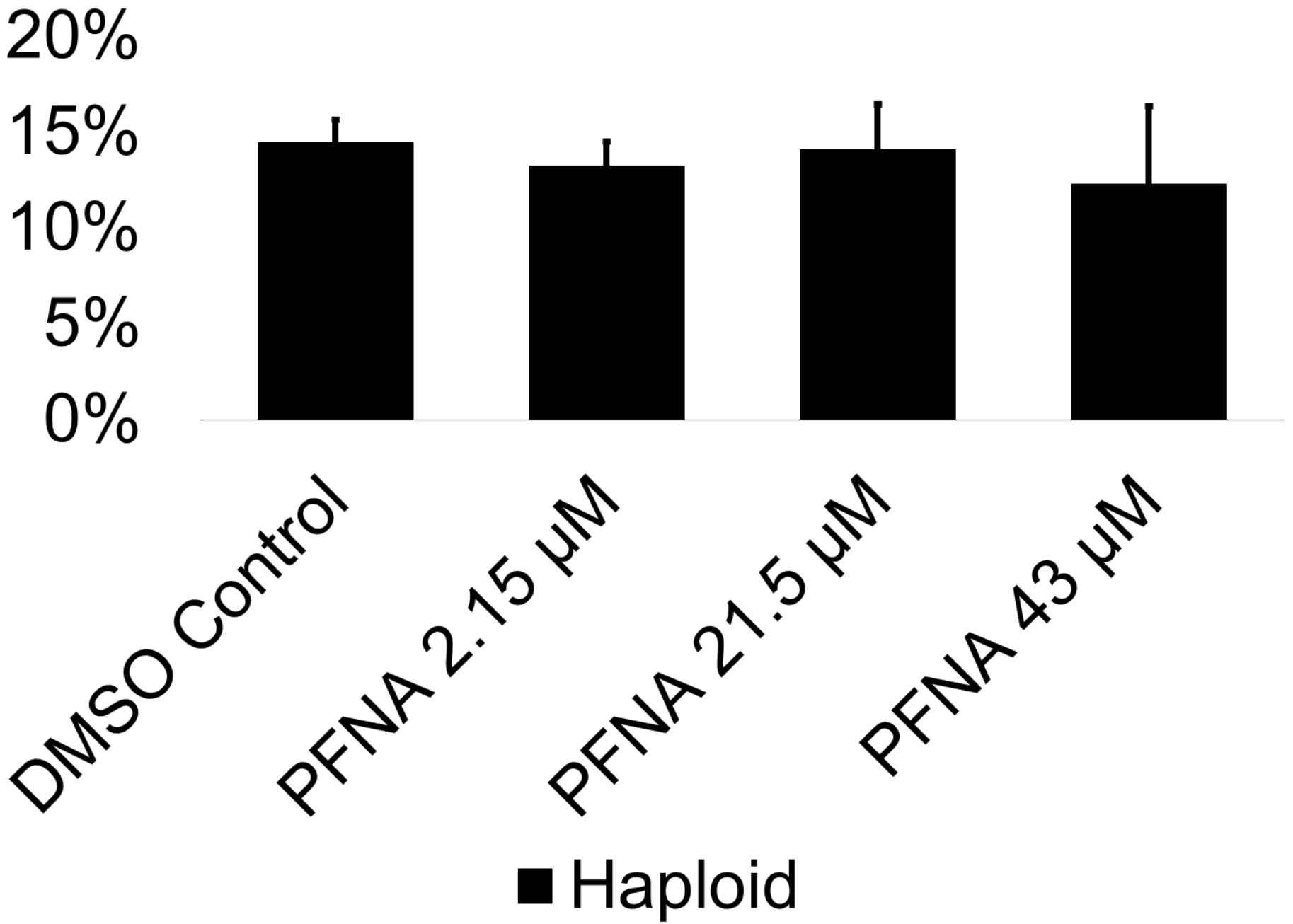
20%
15%
10%
5%
0%
DMSO Control
PFNA 2.15 µM
PFNA 21.5 µM
PFNA 43 µM
Haploid

Figure 6.16. Persistent PFNA exposure does not impact haploid cell viability of spermatogenic cells derived from H1 ESCs. Graphical representation showing that persistent exposure to 2.15 μM, 21.5 μM, and 43 μM PFNA from Day 1 to Day 10 does not impact the viability of haploid cells of H1 ESCS differentiated in *in vitro* spermatogenic conditions in comparison to a 0.25% DMSO-only control. 5,000 events were analyzed, with three replications performed for each condition (n = 3). Significant changes in the percentages of haploid cells were determined using a 1-way analysis of variance (1-way ANOVA) and validated via a Student's t-test, where * is $p<0.05$, ** is $p<0.01$, and *** is $p<0.001$. Data are represented as mean ± SEM.

2.5.5 Acute TDCPP, TDBPP, TBBPA, and HBCDD exposure decreases GSH/GSSG ratios while TBBPA exposure increases reactive oxygen species levels in in vitro spermatogenesis, but persistent PFAS exposure decreases ROS production

Known reproductive toxicants have been shown to induce oxidative stress (Aly, 2013, Erkekoglu and Kocer-Gumusel, 2014, Maiorino and Ursini, 2002) even in our *in vitro* model (Easley et al., 2015). The mammalian testis is susceptible to toxic assault by reactive oxygen species (ROS) (Agarwal et al., 2014), with ROS causing cell death through necrotic and apoptotic pathways (Ryter et al., 2007). As such, ROS induced cell death in testis cells could lead to impaired male fertility. However, ROS production does not always induce cell death (Matic, 2017). Reactive oxygen species are extremely volatile genotoxic agents capable of damaging DNA and oxidizing proteins (Matic, 2017). An increase in ROS could lead to DNA mutations capable of being transmitted to future generations. Increased ROS generation may provide a mechanism for increased germ cell death in response to halogenated flame retardant exposure, as well as changes in cell cycle progression and alterations in HILI expression. TDCPP, HBCDD, and TBBPA have been shown to increase oxidative stress in in vitro assays (Dishaw et al., 2014; Huang et al., 2016; Suh et al., 2017). TBBPA has been shown to increase oxidative stress in *in vitro* assays and to increase ROS in fish sperm (Dishaw et al., 2014, Huang et al., 2016, Linhartova et al., 2015); however, there is no information on the effects of TDCPP, TDBPP, and HBCDD on ROS generation during spermatogenesis. TDCPP has been shown to increase ROS generation in a neuroblastoma cell line (Li et al., 2017a), and Chinese rare minnows exposed to HBCDD have shown an increase in ROS production (Zhang et al., 2008). We examined

whether TDCPP, TDBPP, HBCDD, and TBPPA in comparison to 0.2% DMSO-only negative control can increase ROS generation in our *in vitro* spermatogenesis model using dihydroethidium (DHE) staining. Flow cytometry profiles were generated showing the percentage of ROS positive (ROS+; red) and ROS negative (ROS-; blue) cells in our cultures (Figure 7.1). TDCPP, TDBPP, and HBCDD treatment did not cause a statistically significant increase in ROS generation at any concentration (Figures 7.2 – 7.4). However, TBBPA treatment caused a statistically significant increase in ROS generation (ROS+ cells) beginning at 10 µM, consistent with published data and relevant to occupationally exposed populations (Figure 7.5). TBBPA showed the most significant increase in ROS+ cells at 25 µM, with ROS+ cells increasing by 10% (Figure 7.5).

When assessed over the course of twelve hours, ROS production appears to decrease in cells treated with 100 µM HBCDD beginning within the first half hour and persisting for the entirety of the twelve hour assay (Figure 7.6). During a twelve hour-exposure, cells treated with 100 µM TBBPA experience a significant 46% increase in ROS at nine hours (Figure 7.7). ROS levels return to normal at twelve hours, suggesting that our *in vitro* cultures are still capable of processing the ROS generated by TBBPA exposure at that time (Figure 7.7). However, ROS generation does still appear to be the main mechanism of cell death in TBBPA treated cells. Following treatment of our *in vitro* cultures with 1 µM of the antioxidant *l*-sulforaphane for twelve hours, cells that were treated with 100 µM TBBPA show live cell and late apoptotic/dead cell populations similar to control (Figures 7.9 and 7.11). However, *l*-sulforaphane pre-treatment does not rescue cell death caused by 100 µM HBCDD treatment, with cells showing a 6%

decrease in live cells and a 135% increase in late apoptotic/dead cells (Figures 7.8 and 7.10). This increase in apoptosis remains similar to non-rescued cells treated with 100 µM HBCDD, suggesting that ROS does not play a role in HBCDD induced cell death (Figures 3.5 and 3.9). We have previously used this method to rescue our *in vitro* cultures following exposure to the known male reproductive toxicants 2-BP and DBCP (Easley et al., 2015). These results suggest that HBCDD's mechanism of toxicity is distinctly different from known reproductive toxicants, which classically induce cell death through ROS assault, as well as TBBPA.

Results from the Muse® Oxidative Stress Assay Kit were validated by assessing changes in the GSH/GSSG ratios in TDCPP, TDBPP, HBCDD, and TBBPA treatment groups as per manufacturer's instructions by the Promega GSH/GSSG-Glo^{TM} Assay (Promega, Madison, WI). TDCPP, TDBPP, HBCDD, and TBBPA all decrease GSH/GSSG ratios, indicating increased ROS generation, at as little as 1 µM (Figures 7.12 – 7.15). Though TDCPP, TDBPP, HBCDD, and TBBPA both increase ROS as indicated by decreases in GSH/GSSG ratios, the results suggest that only TBBPA is capable of generating sufficient ROS to overwhelm the cell's defenses in response to exposure *in vitro*. These results may explain why these chemicals have little impact on spermatids in our *in vitro* model, as spermatids are most sensitive to ROS generation (Agarwal et al., 2014, Maiorino and Ursini, 2002). Similarly, these results again highlight the class-wide effects these chemicals have on *in vitro* spermatogenic cells and also further elucidate the different mechanisms of action between TDCPP, TDBPP, HBCDD, and TBBPA.

Per- and polyfluoroalkyl substances, including PFOS, PFOA, and PFNA have been shown to increase ROS in a dose-dependent manner (Wielsoe et al., 2015). Specifically, PFOS has been shown to increase production of ROS in the *C. elegans* germline, while PFOA has been shown to induce testicular damage in male mice, with exposure resulting in a significant increase of oxidative stress (Liu et al., 2015, Guo et al., 2016). While the generation of ROS in the germline due to PFNA exposure has not been examined, PFNA exposure has been connected to the formation of ROS in the spleen cells of rats, resulting in cell-mediated death through apoptotic pathways (Fang et al., 2010). We examined whether PFOS, PFOA, PFNA, and a mixture of 48 µM PFOS, 25 µM PFOA, and 21.5 µM of PFNA could increase ROS levels in comparison to a 0.25% DMSO-only negative control (Figure 7.16). As a positive control, cells were treated with 200 µM hydrogen peroxide (H_2O_2) (Figure 7.17). While PFOA exposure resulted in no significant changes to ROS production at any concentration tested, PFOS and PFNA both showed significantly less ROS levels compared to the 0.25% DMSO-only control by as much as 55% and 28% at the lowest concentrations tested, respectively (Figures 7.18 – 7.20). A PFAS mixture with 48 µM PFOS, 25 µM PFOA, and 21.5 µM of PFNA similarly showed a 33% reduction in reactive oxygen species (Figure 7.21). Interestingly, PFOS and PFOA both increased ROS in a dose-wise manner (although not statistically significant), with an 18% and 41% difference between the lowest and highest concentrations of PFOS and PFOA tested, respectively (Figures 7.18 – 7.19). Consistent with our viability results, it is unlikely that ROS produced by PFAS exposure is influencing the viability of spermatogenic cells *in vitro*. These results indicate that PFAS exposure may be protective against ROS in our *in vitro* cultures at

lower concentrations; however, higher concentrations may increase the production of ROS.

These results once again highlight the different mechanisms between halogenated flame retardants and PFASs, despite similarities in properties. TBBPA's structure consists of two hydroxyphenyl rings with four bonded bromine molecules, making it the least halogenated compound assessed in this study. TBBPA was the only compound to increase reactive oxygen species production that could surpass spermatogenic cells' defensive capabilities, suggesting that less halogenated compounds may be more capable of inflicting damage. However, TDCPP, TDBPP, HBCDD, and the PFASs do not have comparable structures, so backbone structure cannot be ruled out. In future studies, it would be worthwhile to assess other hydroxyphenyl structures with increasing number and differing types of halogens.

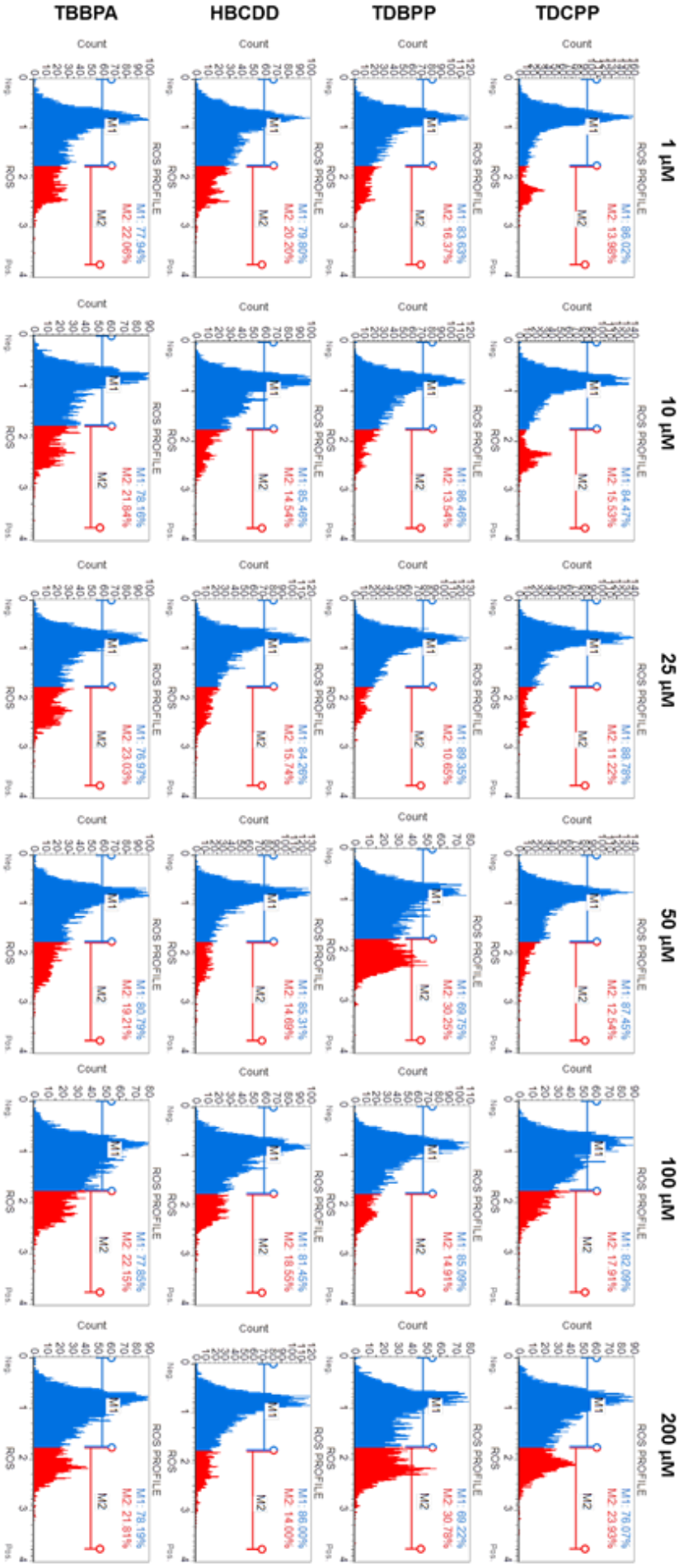
TDCPP
TDBPP
HBCDD
TBBPA
1 µM
10 µM
25 µM
50 µM
100 µM
200 µM
Count
ROS PROFILE
ROS
M1
M2

Figure 7.1. Acute TDCPP, TDBPP, HBCDD, and TBBPA exposure increase ROS production in spermatogenic cells derived from H1 ESCs. Flow cytometry based analysis of DHE labeling. Blue indicates ROS- cells. Red indicates ROS+ cells.

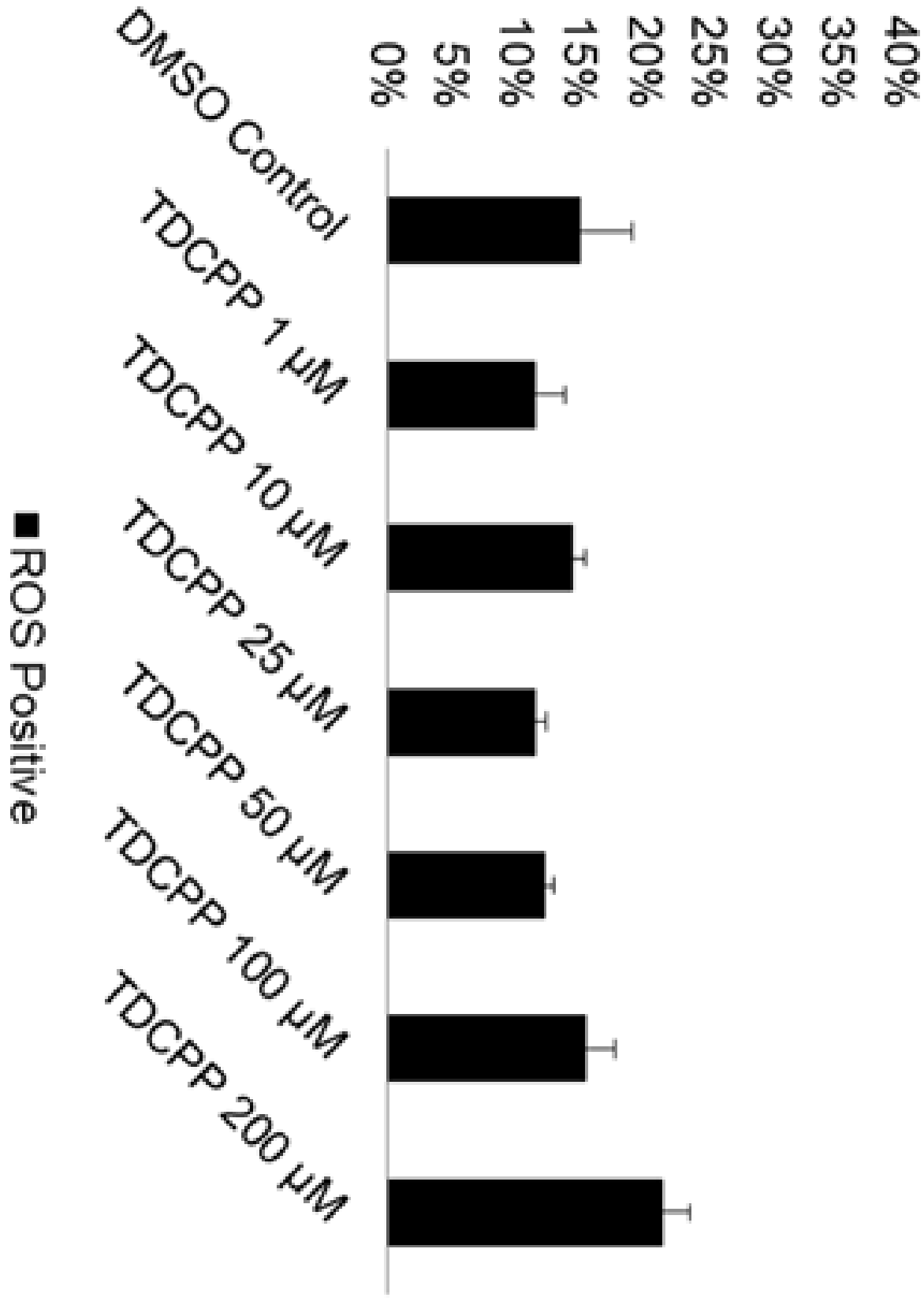
40%
35%
30%
25%
20%
15%
10%
5%
0%
DMSO Control
TDCPP 1 µM
TDCPP 10 µM
TDCPP 25 µM
TDCPP 50 µM
TDCPP 100 µM
TDCPP 200 µM
ROS Positive

Figure 7.2. Acute TDCPP exposure does not impact ROS production in spermatogenic cells derived from H1 ESCs. Graphical representation showing that acute, twenty-four hour 1 μM, 10 μM, 25 μM, 50 μM, 100 μM, and 200 μM TDCPP exposure does not impact ROS generation in H1 ESCs differentiated in *in vitro* spermatogenic conditions in comparison to a 0.2% DMSO-only control. 5,000 events were analyzed, with three replications performed for each condition (n = 3). Significant changes in ROS production were determined using a 1-way analysis of variance (1-way ANOVA) and validated via a Student's t-test, where * is $p<0.05$, ** is $p<0.01$, and *** is $p<0.001$. Data are represented as mean ± SEM.

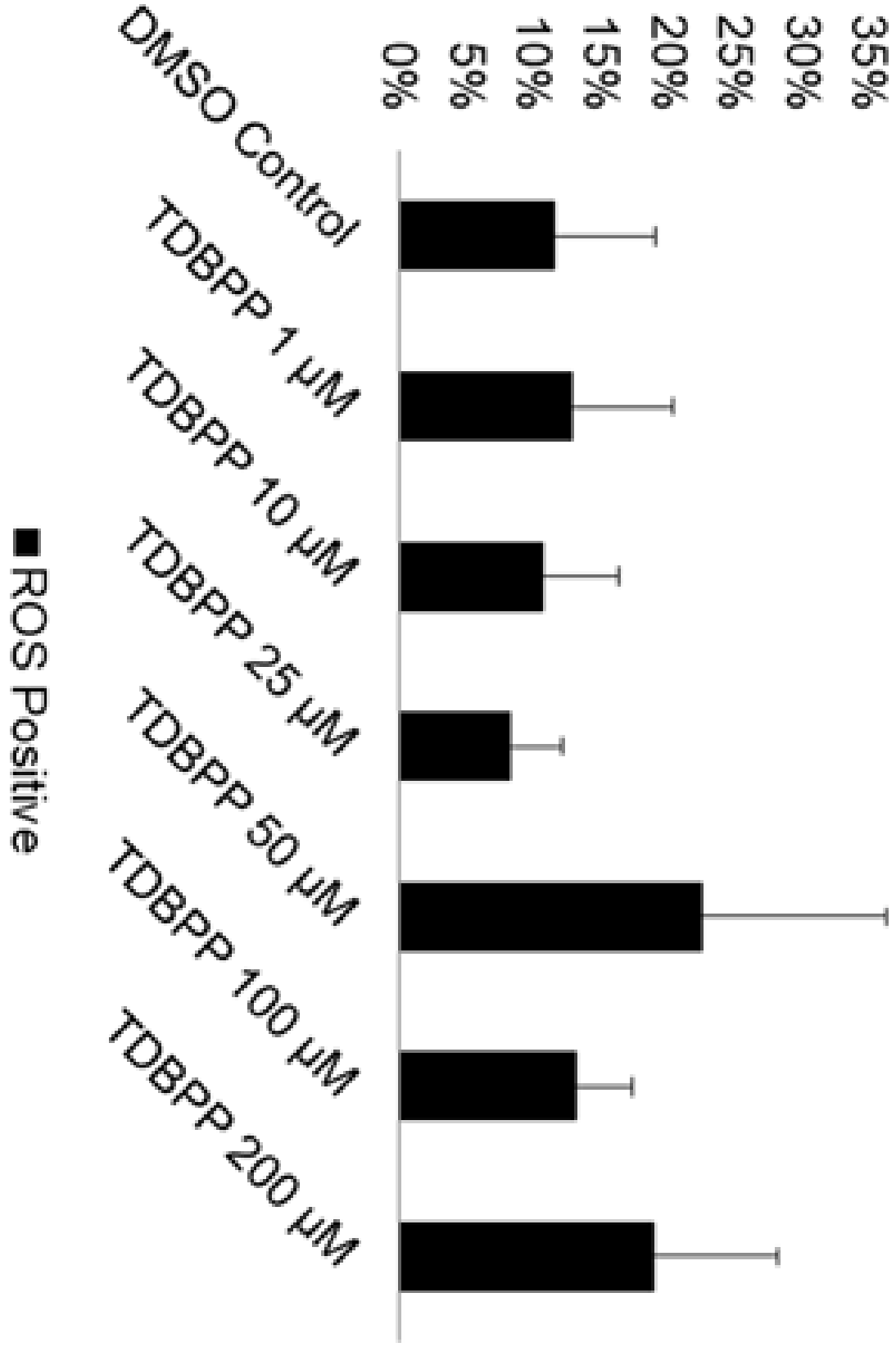
40%
35%
30%
25%
20%
15%
10%
5%
0%
DMSO Control
TDBPP 1 µM
TDBPP 10 µM
TDBPP 25 µM
TDBPP 50 µM
TDBPP 100 µM
TDBPP 200 µM
ROS Positive

Figure 7.3. Acute TDBPP exposure does not impact ROS production in spermatogenic cells derived from H1 ESCs. Graphical representation showing that acute, twenty-four hour 1 μM, 10 μM, 25 μM, 50 μM, 100 μM, and 200 μM TDBPP exposure does not impact ROS generation in H1 ESCs differentiated in *in vitro* spermatogenic conditions in comparison to a 0.2% DMSO-only control. 5,000 events were analyzed, with three replications performed for each condition (n = 3). Significant changes in ROS production were determined using a 1-way analysis of variance (1-way ANOVA) and validated via a Student's t-test, where * is $p<0.05$, ** is $p<0.01$, and *** is $p<0.001$. Data are represented as mean ± SEM.

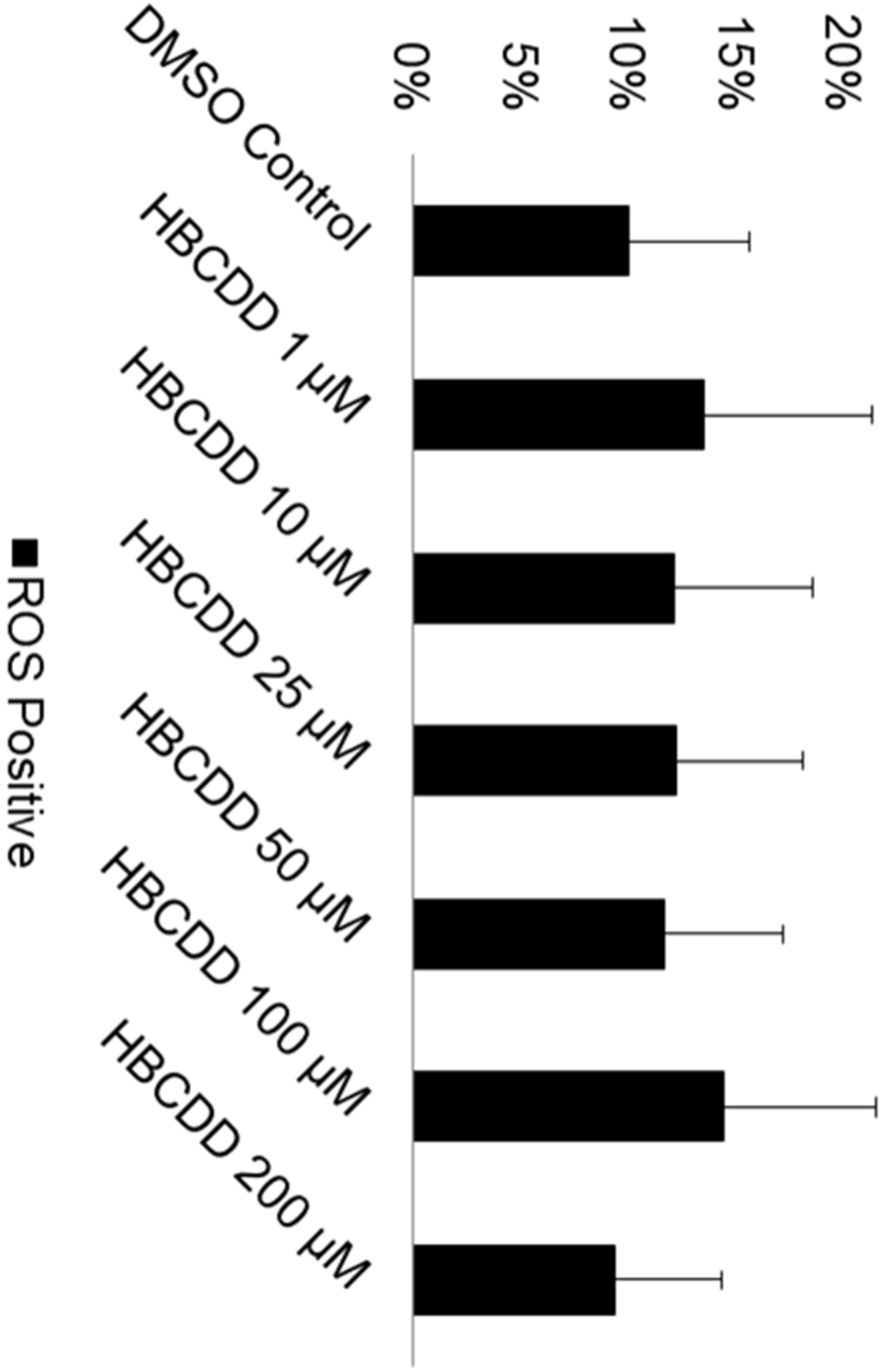
25%
20%
15%
10%
5%
0%
DMSO Control
HBCDD 1 μM
HBCDD 10 μM
HBCDD 25 μM
HBCDD 50 μM
HBCDD 100 μM
HBCDD 200 μM
ROS Positive

Figure 7.4. Acute HBCDD exposure does not impact ROS production in spermatogenic cells derived from H1 ESCs. Graphical representation showing that acute, twenty-four hour 1 μM, 10 μM, 25 μM, 50 μM, 100 μM, and 200 μM HBCDD exposure does not impact ROS generation in H1 ESCs differentiated in *in vitro* spermatogenic conditions in comparison to a 0.2% DMSO-only control. 5,000 events were analyzed, with three replications performed for each condition (n = 3). Significant changes in ROS production were determined using a 1-way analysis of variance (1-way ANOVA) and validated via a Student's t-test, where * is $p<0.05$, ** is $p<0.01$, and *** is $p<0.001$. Data are represented as mean ± SEM.

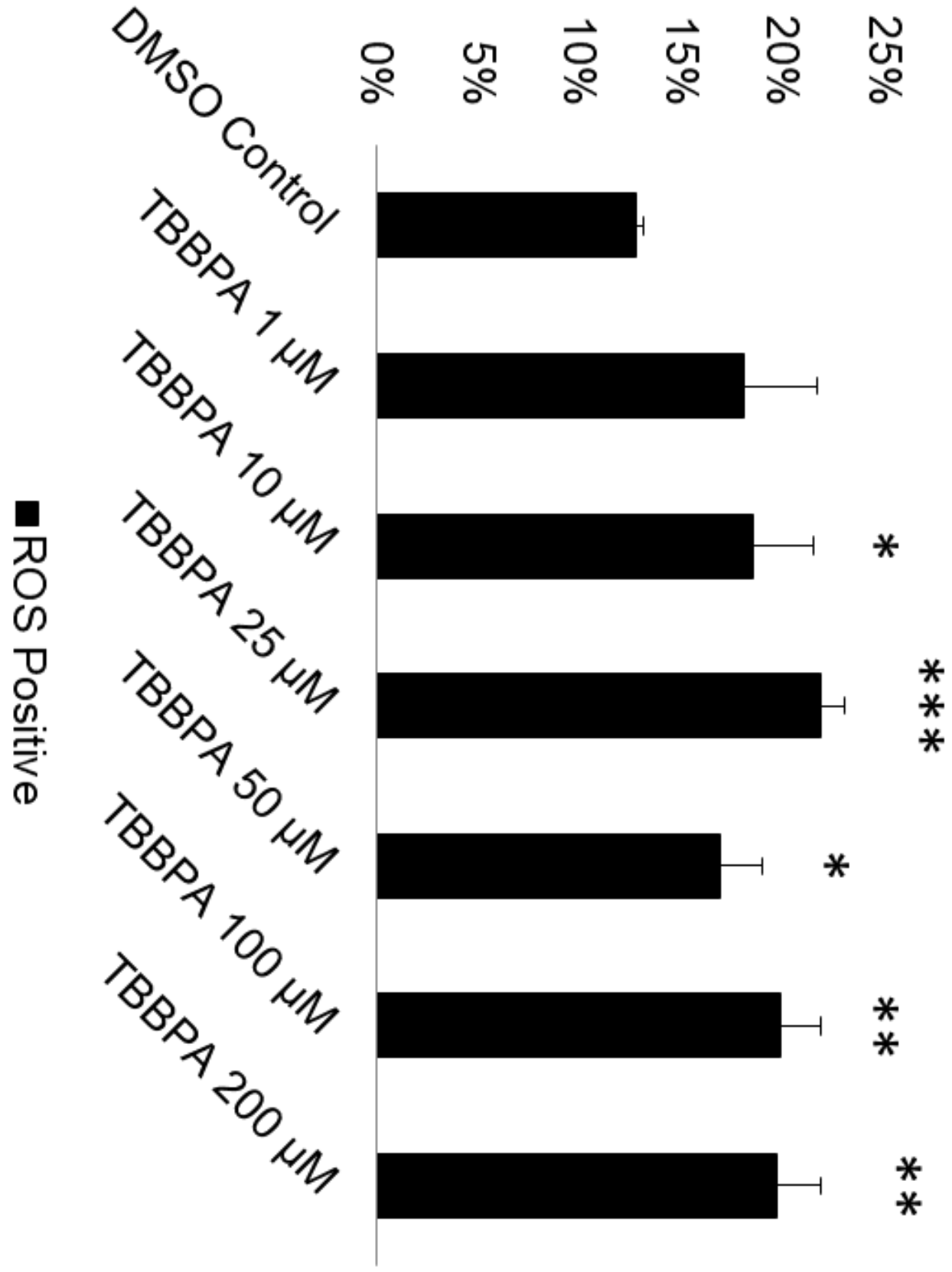
25%
20%
15%
10%
5%
0%
DMSO Control
TBBPA 1 µM
TBBPA 10 µM
TBBPA 25 µM
TBBPA 50 µM
TBBPA 100 µM
TBBPA 200 µM
*
***
*
**
**
■ROS Positive

Figure 7.5. Acute TBBPA exposure increases ROS production in spermatogenic cells derived from H1 ESCs. Graphical representation showing that acute, twenty-four hour 10 μM, 25 μM, 50 μM, 100 μM, and 200 μM TBBPA exposure increases ROS generation in H1 ESCs differentiated in *in vitro* spermatogenic conditions in comparison to a 0.2% DMSO-only control. 5,000 events were analyzed, with three replications performed for each condition (n = 3). Significant changes in ROS production were determined using a 1-way analysis of variance (1-way ANOVA) and validated via a Student's t-test, where * is $p<0.05$, ** is $p<0.01$, and *** is $p<0.001$. Data are represented as mean ± SEM.

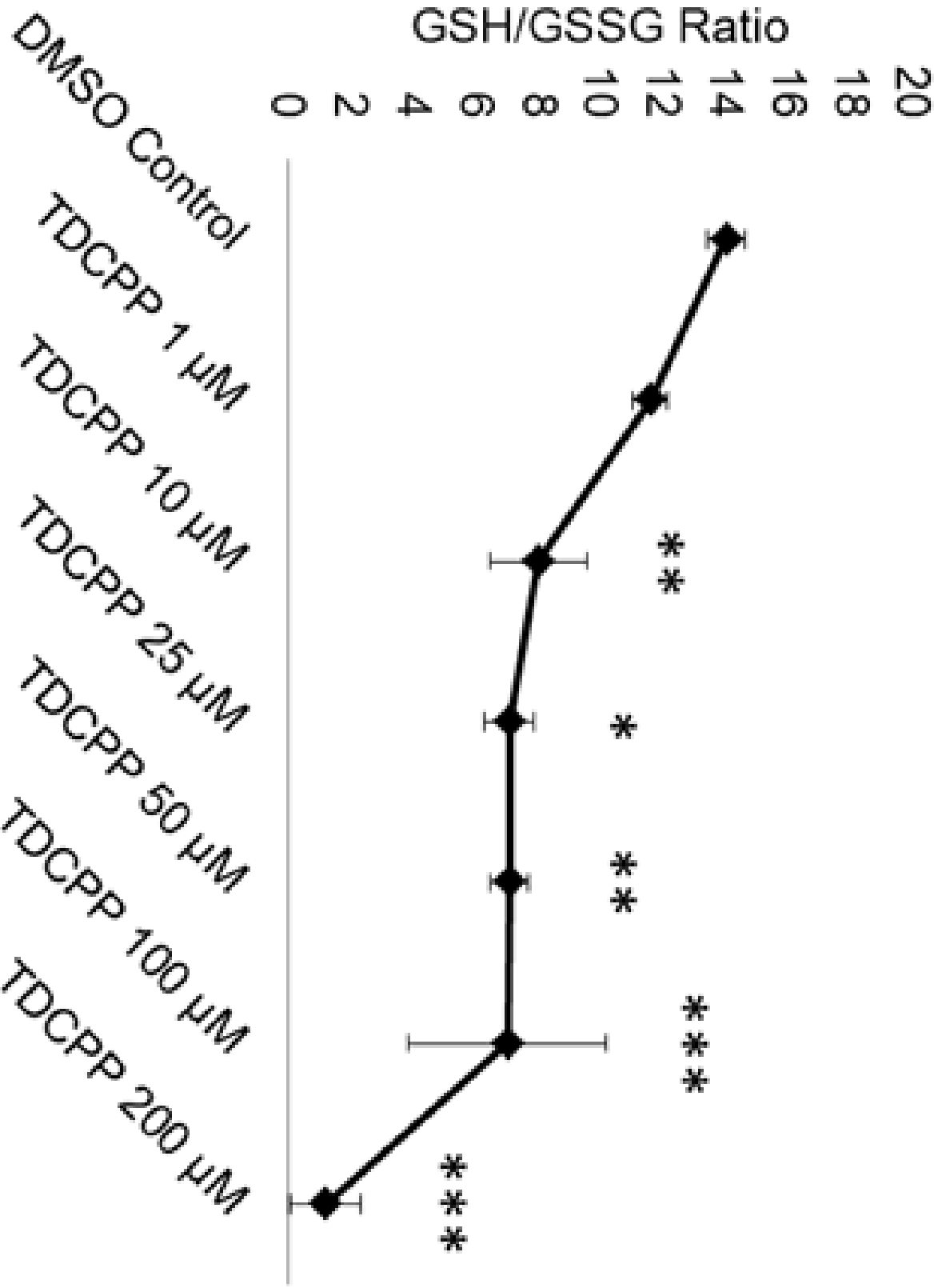
GSH/GSSG Ratio
0
2
4
6
8
10
12
14
16
18
20
DMSO Control
TDCPP 1 µM
TDCPP 10 µM
TDCPP 25 µM
TDCPP 50 µM
TDCPP 100 µM
TDCPP 200 µM
**
*
**
***
***

Figure 7.6. Acute TDCPP exposure decreases the GSH/GSSG ratio in spermatogenic cells derived from H1 ESCs. Graphical representation showing that acute, twenty-four hour 10 μM, 25 μM, 50 μM, 100 μM, and 200 μM TDCPP exposure decreases the GSH/GSSG ratio in H1 ESCs differentiated in *in vitro* spermatogenic conditions in comparison to a 0.2% DMSO-only control. Three replications were performed for each condition (n = 3). Significant changes in GSH/GSSG ratio were determined using a 1-way analysis of variance (1-way ANOVA) and validated via a Student's t-test, where * is $p<0.05$, ** is $p<0.01$, and *** is $p<0.001$. Data are represented as mean ± SEM.

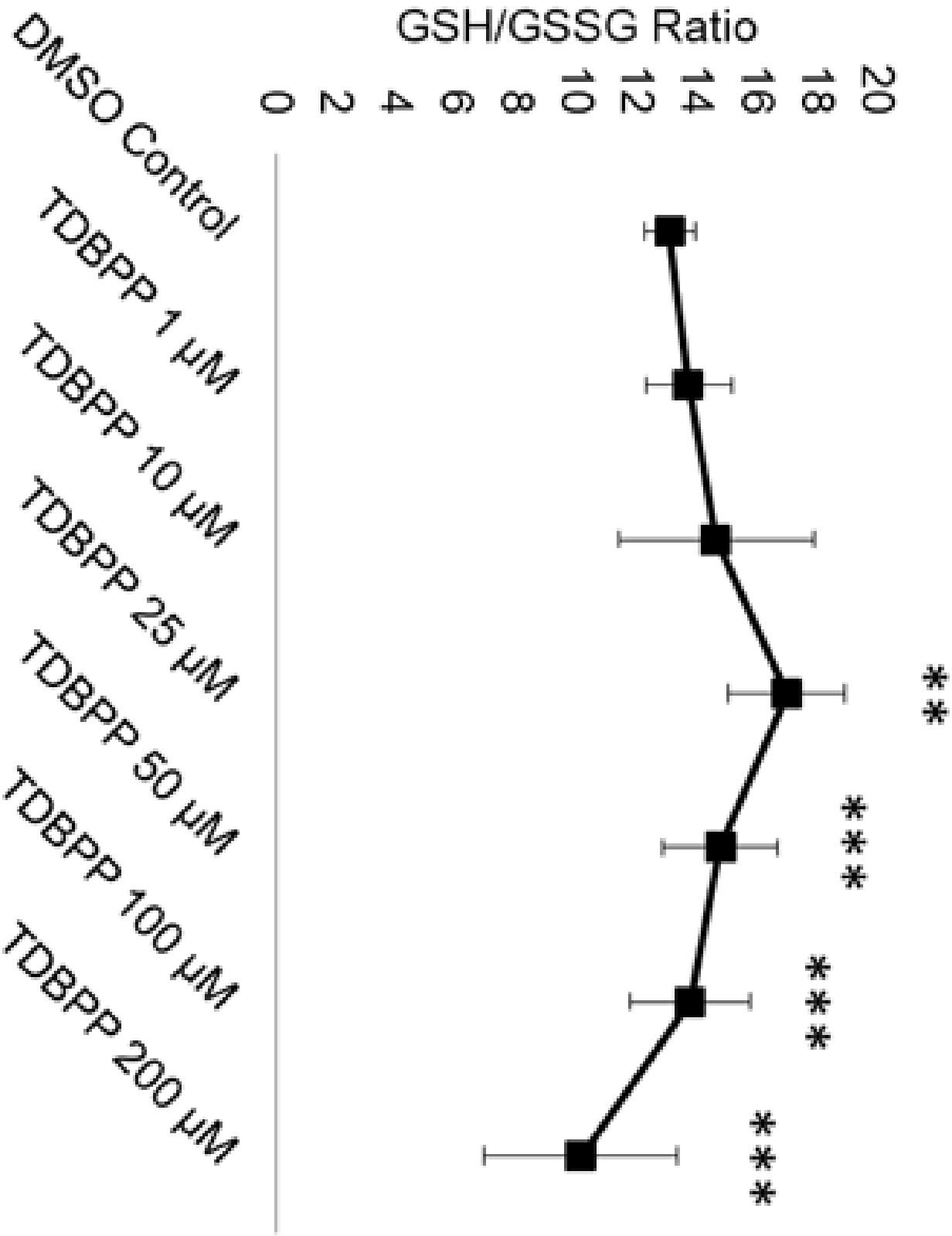
GSH/GSSG Ratio
0
2
4
6
8
10
12
14
16
18
20
DMSO Control
TDBPP 1 µM
TDBPP 10 µM
TDBPP 25 µM
TDBPP 50 µM
TDBPP 100 µM
TDBPP 200 µM
**
***
***
***

Figure 7.7. Acute TDBPP exposure decreases the GSH/GSSG ratio in spermatogenic cells derived from H1 ESCs. Graphical representation showing that acute, twenty-four hour 25 μM, 50 μM, 100 μM, and 200 μM TDBPP exposure decreases the GSH/GSSG ratio in H1 ESCs differentiated in *in vitro* spermatogenic conditions in comparison to a 0.2% DMSO-only control. Three replications were performed for each condition (n = 3). Significant changes in GSH/GSSG ratio were determined using a 1-way analysis of variance (1-way ANOVA) and validated via a Student's t-test, where * is $p<0.05$, ** is $p<0.01$, and *** is $p<0.001$. Data are represented as mean ± SEM.

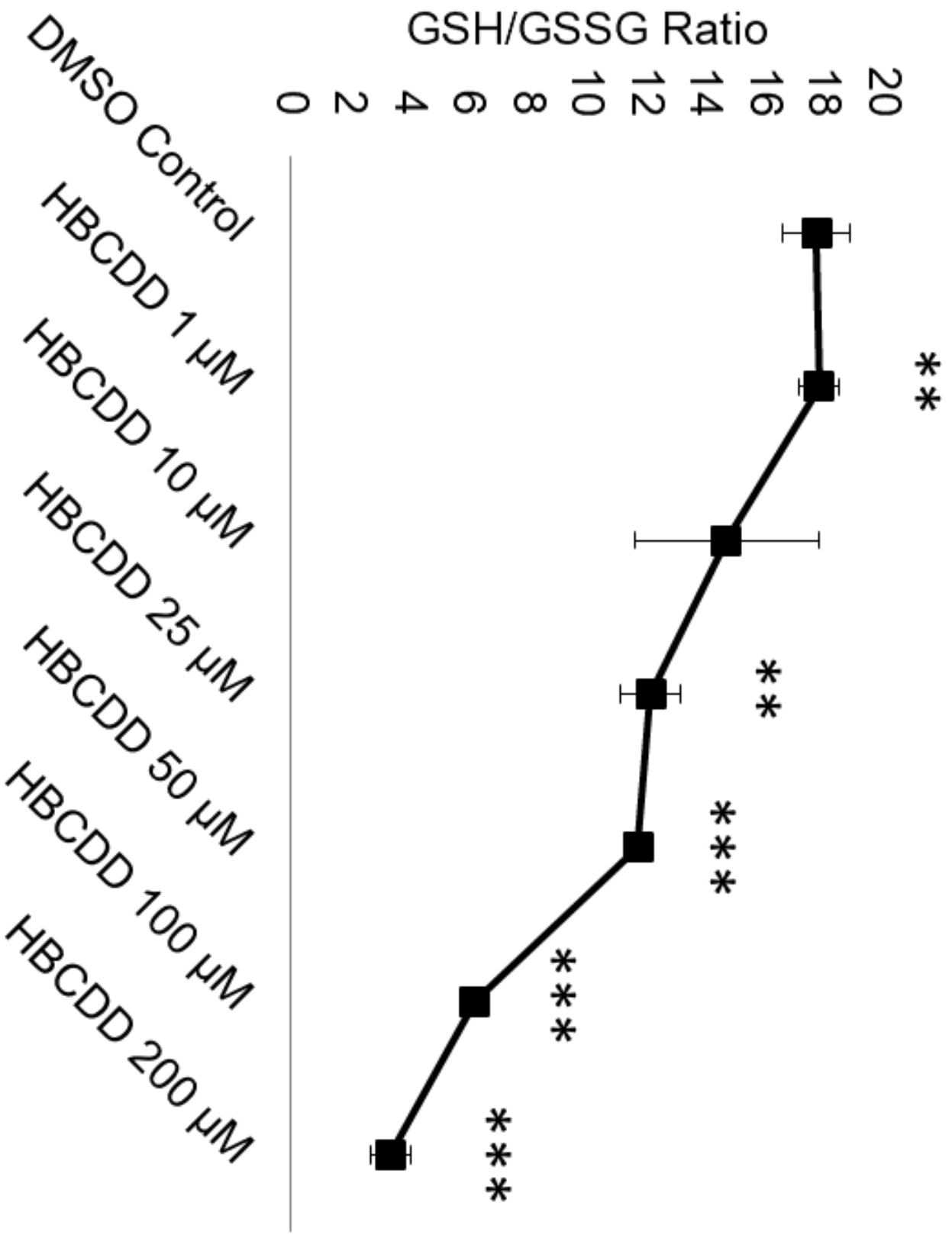
GSH/GSSG Ratio
0
2
4
6
8
10
12
14
16
18
20
DMSO Control
HBCDD 1 µM
HBCDD 10 µM
HBCDD 25 µM
HBCDD 50 µM
HBCDD 100 µM
HBCDD 200 µM
**
**
****
****
****

Figure 7.8. Acute HBCDD exposure decreases the GSH/GSSG ratio in spermatogenic cells derived from H1 ESCs. Graphical representation showing that acute, twenty-four hour 1 μM, 25 μM, 50 μM, 100 μM, and 200 μM HBCDD exposure decreases the GSH/GSSG ratio in H1 ESCs differentiated in *in vitro* spermatogenic conditions in comparison to a 0.2% DMSO-only control. Three replications were performed for each condition (n = 3). Significant changes in GSH/GSSG ratio were determined using a 1-way analysis of variance (1-way ANOVA) and validated via a Student's t-test, where * is $p<0.05$, ** is $p<0.01$, and *** is $p<0.001$. Data are represented as mean ± SEM.

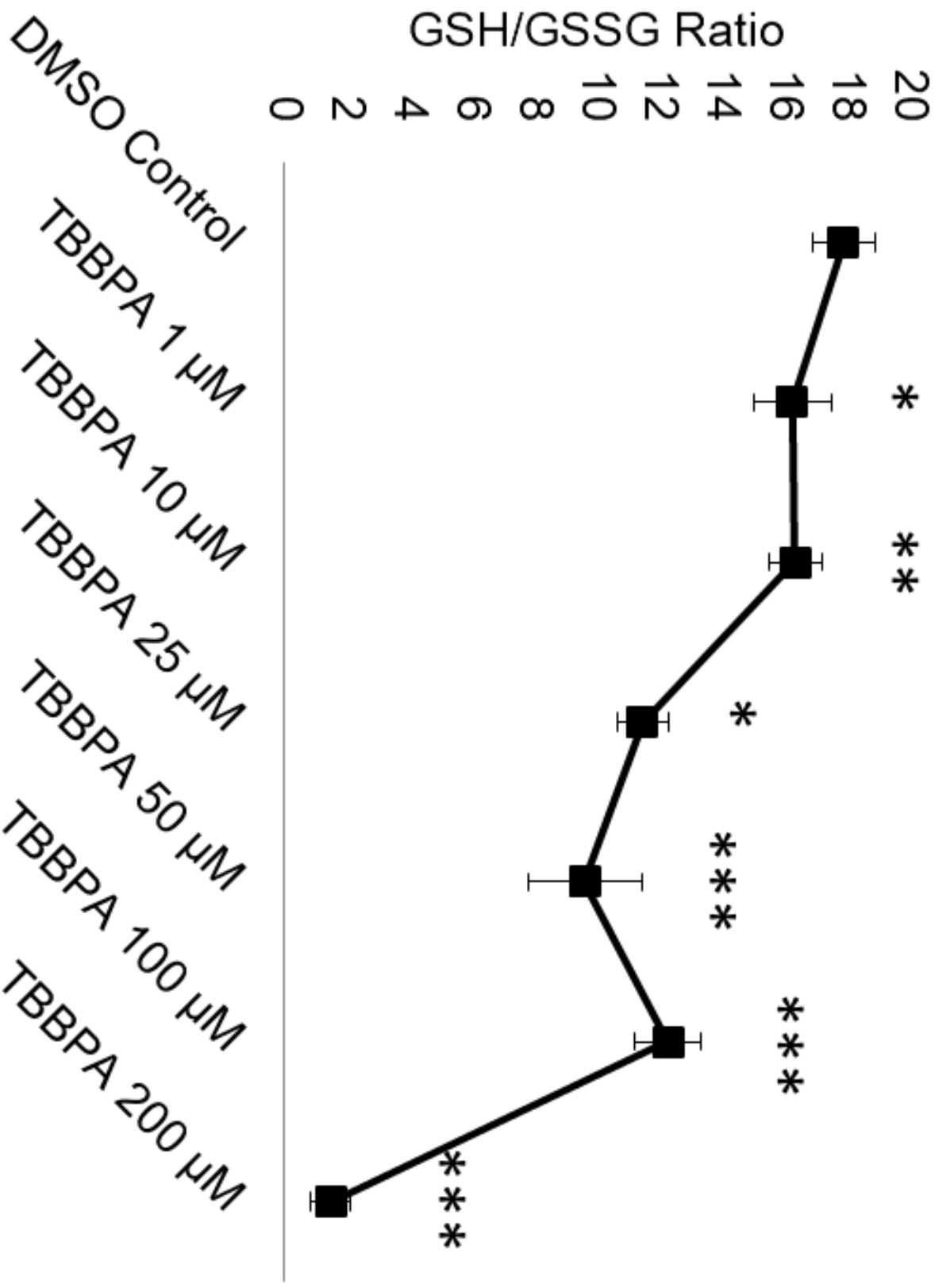
GSH/GSSG Ratio
0
2
4
6
8
10
12
14
16
18
20
DMSO Control
TBBPA 1 µM
TBBPA 10 µM
TBBPA 25 µM
TBBPA 50 µM
TBBPA 100 µM
TBBPA 200 µM
*
**
*
***
***
***

Figure 7.9. Acute TBBPA exposure decreases the GSH/GSSG ratio in spermatogenic cells derived from H1 ESCs. Graphical representation showing that acute, twenty-four hour 1 μM, 10 μM, 25 μM, 50 μM, 100 μM, and 200 μM TBBPA exposure decreases the GSH/GSSG ratio in H1 ESCs differentiated in *in vitro* spermatogenic conditions in comparison to a 0.2% DMSO-only control. Three replications were performed for each condition (n = 3). Significant changes in GSH/GSSG ratio were determined using a 1-way analysis of variance (1-way ANOVA) and validated via a Student's t-test, where * is $p<0.05$, ** is $p<0.01$, and *** is $p<0.001$. Data are represented as mean ± SEM.

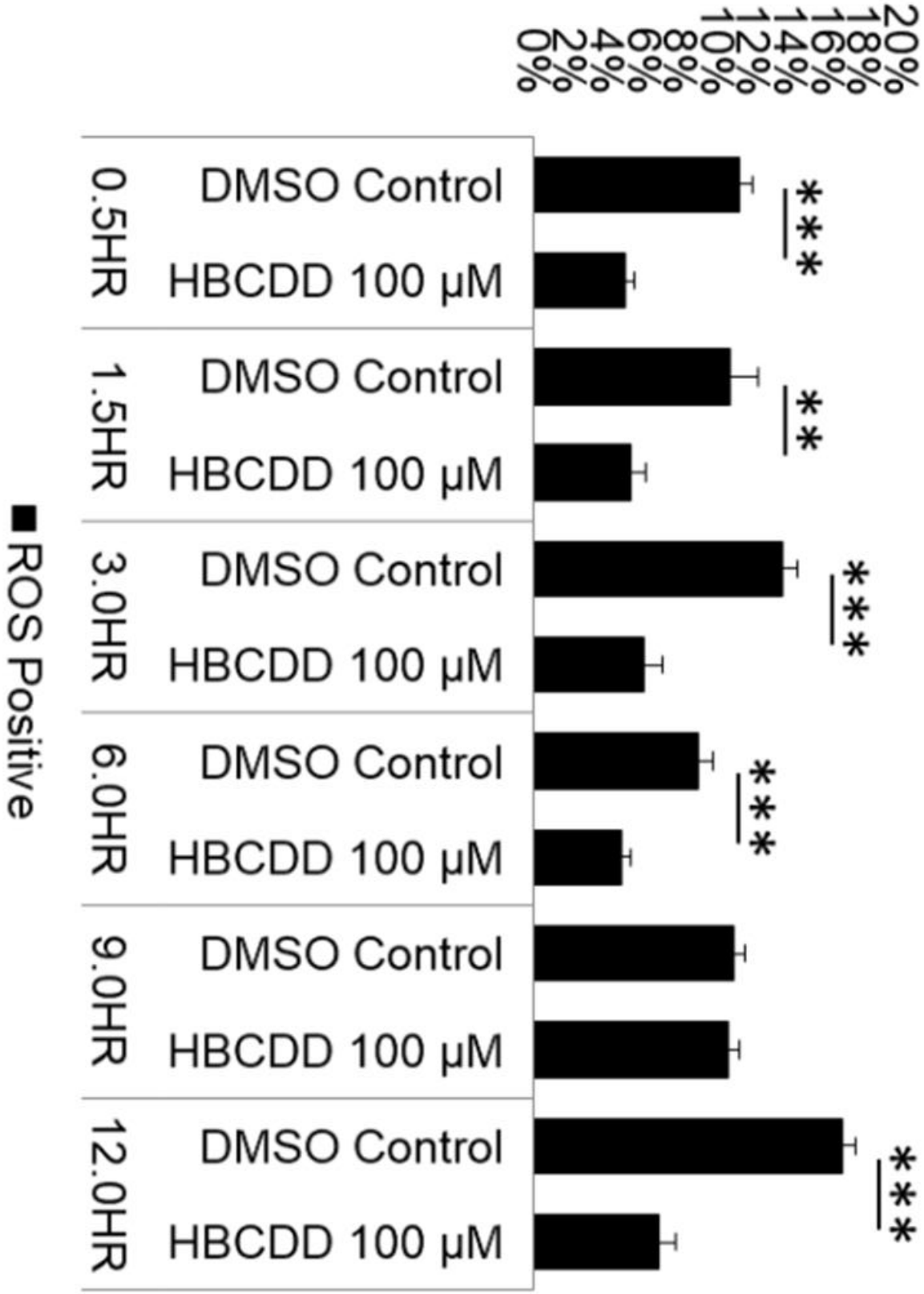
20%
18%
16%
14%
12%
10%
8%
6%
4%
2%
0%
■ ROS Positive
0.5HR
DMSO Control
HBCDD 100 μM
***
1.5HR
DMSO Control
HBCDD 100 μM
**
3.0HR
DMSO Control
HBCDD 100 μM
***
6.0HR
DMSO Control
HBCDD 100 μM
***
9.0HR
DMSO Control
HBCDD 100 μM
12.0HR
DMSO Control
HBCDD 100 μM
***

Figure 7.10. Acute HBCDD exposure initially decreases ROS production in spermatogenic cells derived from H1 ESCs. Graphical representation showing that acute 100 μM HBCDD exposure decreases the production of ROS in H1 ESCs differentiated in *in vitro* spermatogenic conditions in comparison to a 0.2% DMSO-only control in as little as 0.5 hours. Three replications were performed for each condition (n = 3). Significant changes in ROS production were determined via a Student's t-test, where * is $p<0.05$, ** is $p<0.01$, and *** is $p<0.001$. Data are represented as mean ± SEM.

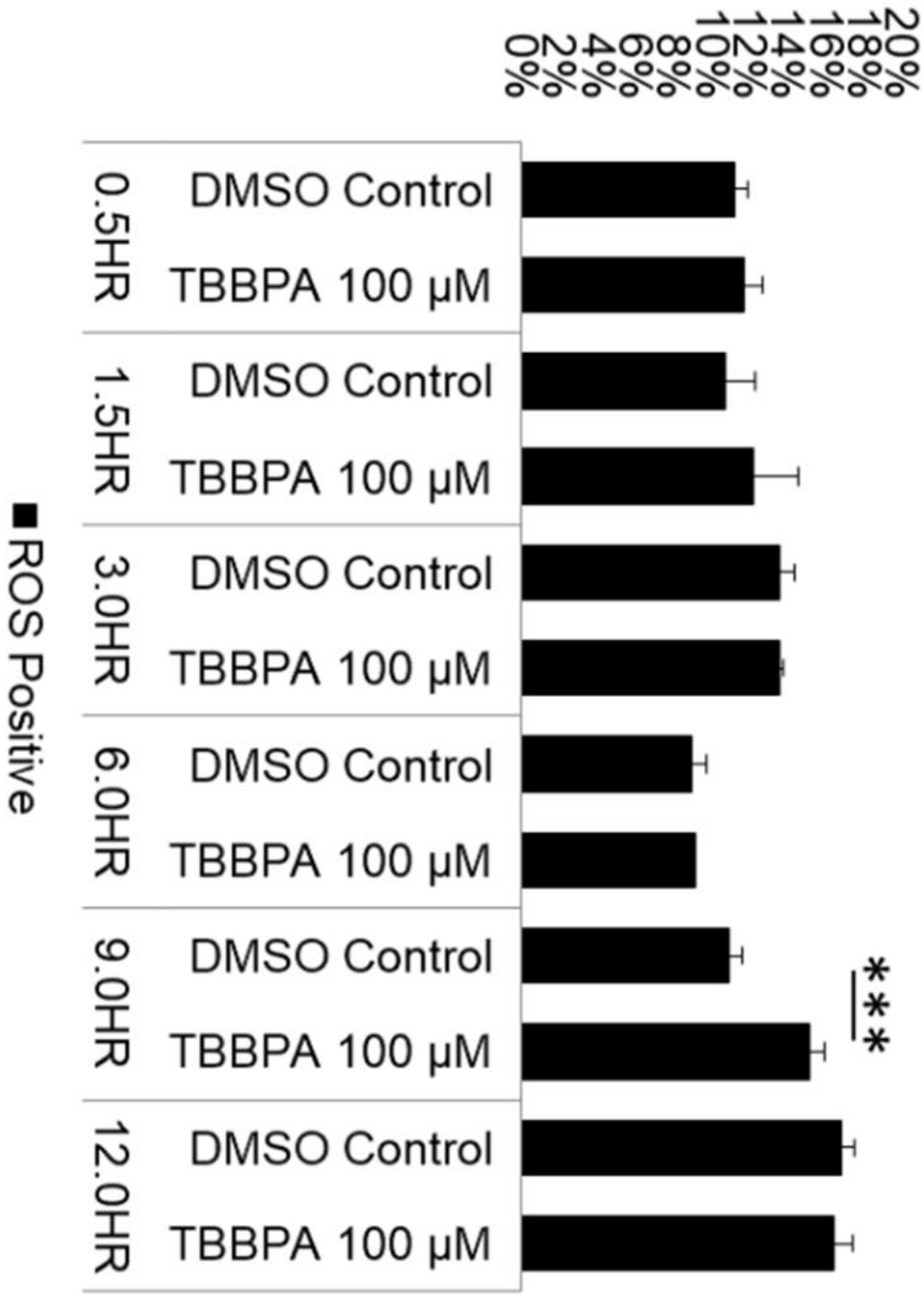
20%
18%
16%
14%
12%
10%
8%
6%
4%
2%
0%
■ROS Positive
0.5HR
DMSO Control
TBBPA 100 μM
1.5HR
DMSO Control
TBBPA 100 μM
3.0HR
DMSO Control
TBBPA 100 μM
6.0HR
DMSO Control
TBBPA 100 μM
9.0HR
DMSO Control
TBBPA 100 μM
12.0HR
DMSO Control
TBBPA 100 μM
***

Figure 7.11. Acute TBBPA exposure increases ROS production in spermatogenic cells derived from H1 ESCs. Graphical representation showing that acute 100 μM TBBPA exposure increases the production of ROS in H1 ESCs differentiated in *in vitro* spermatogenic conditions in comparison to a 0.2% DMSO-only control beginning at 9.0 hours. Three replications were performed for each condition (n = 3). Significant changes in ROS production were determined via a Student's t-test, where * is $p<0.05$, ** is $p<0.01$, and *** is $p<0.001$. Data are represented as mean ± SEM.

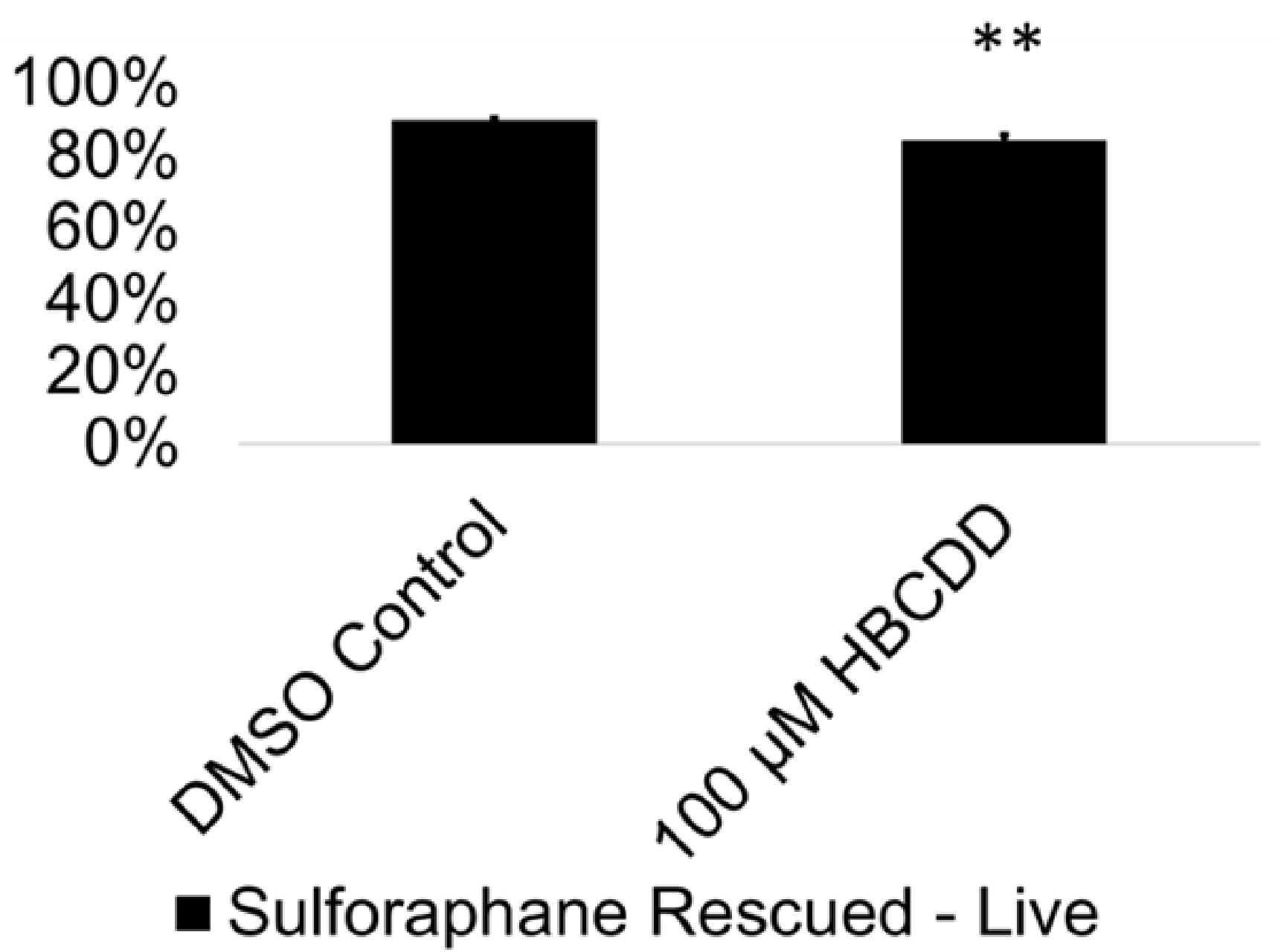
**
100%
80%
60%
40%
20%
0%
DMSO Control
100 µM HBCDD
Sulforaphane Rescued - Live

Figure 7.12. 1 μM l-Sulforaphane pre-treatment does not rescue acute HBCDD-mediated cell death in spermatogenic cells derived from H1 ESCs. Graphical representation showing that a twelve hour pre-treatment with 1 μM *l*-Sulforaphane does not rescue cell death caused by exposure to 100 μM HBCDD in H1 ESCs differentiated in *in vitro* spermatogenic conditions in comparison to a 0.2% DMSO-only control. Three replications were performed for each condition (n = 3). Significant changes in live cell percentages were determined using a 1-way analysis of variance (1-way ANOVA) and validated via a Student's t-test, where * is $p<0.05$, ** is $p<0.01$, and *** is $p<0.001$. Data are represented as mean ± SEM.

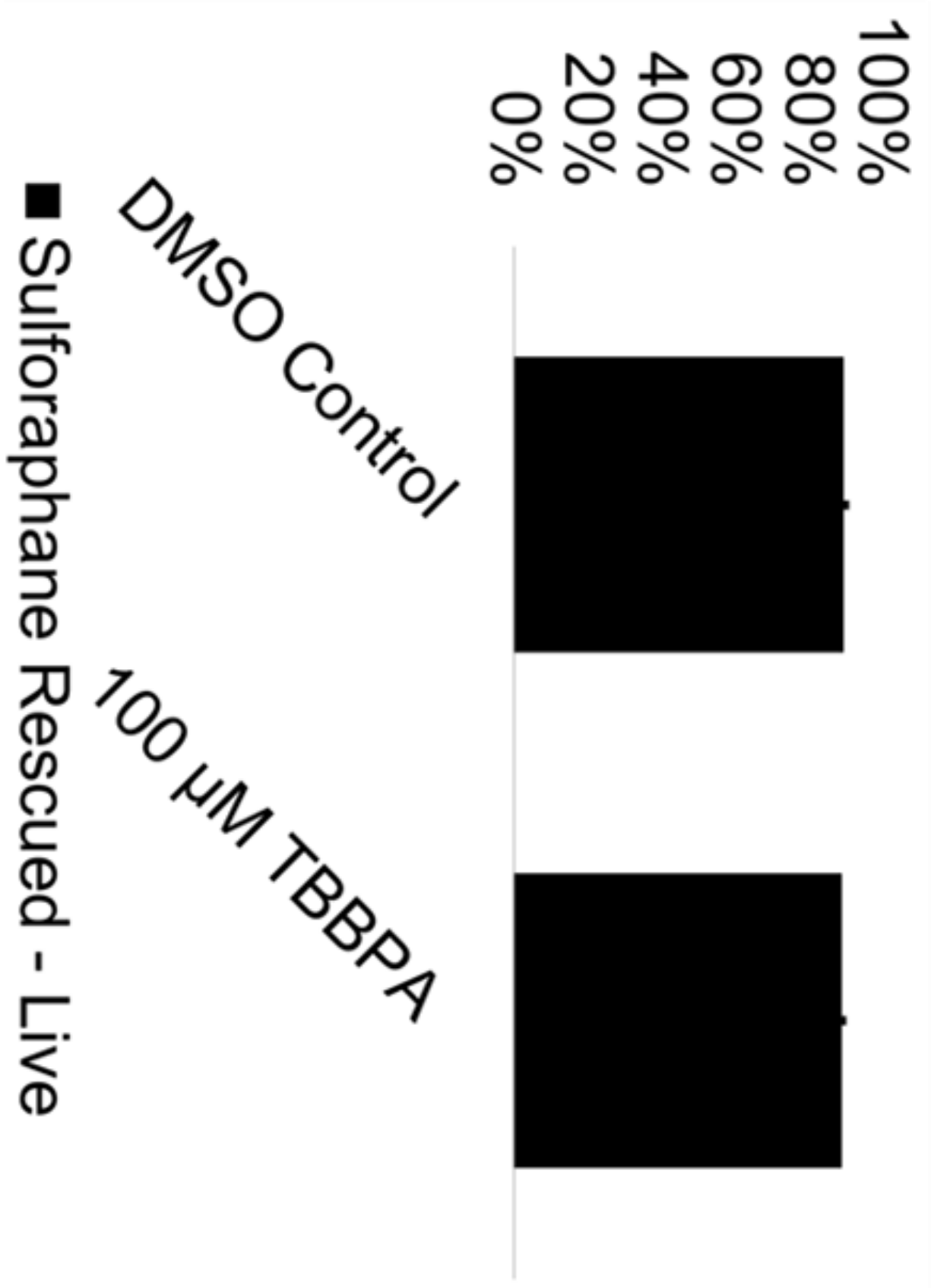
100%
80%
60%
40%
20%
0%
DMSO Control
100 µM TBBPA
Sulforaphane Rescued - Live

Figure 7.13. 1 μM l-Sulforaphane pre-treatment rescues acute TBBPA-mediated cell death in spermatogenic cells derived from H1 ESCs. Graphical representation showing that a twelve hour pre-treatment with 1 μM *l*-Sulforaphane rescues cell death caused by exposure to 100 μM TBBPA in H1 ESCs differentiated in *in vitro* spermatogenic conditions in comparison to a 0.2% DMSO-only control. Three replications were performed for each condition (n = 3). Significant changes in live cell percentages were determined using a 1-way analysis of variance (1-way ANOVA) and validated via a Student's t-test, where * is $p<0.05$, ** is $p<0.01$, and *** is $p<0.001$. Data are represented as mean ± SEM.

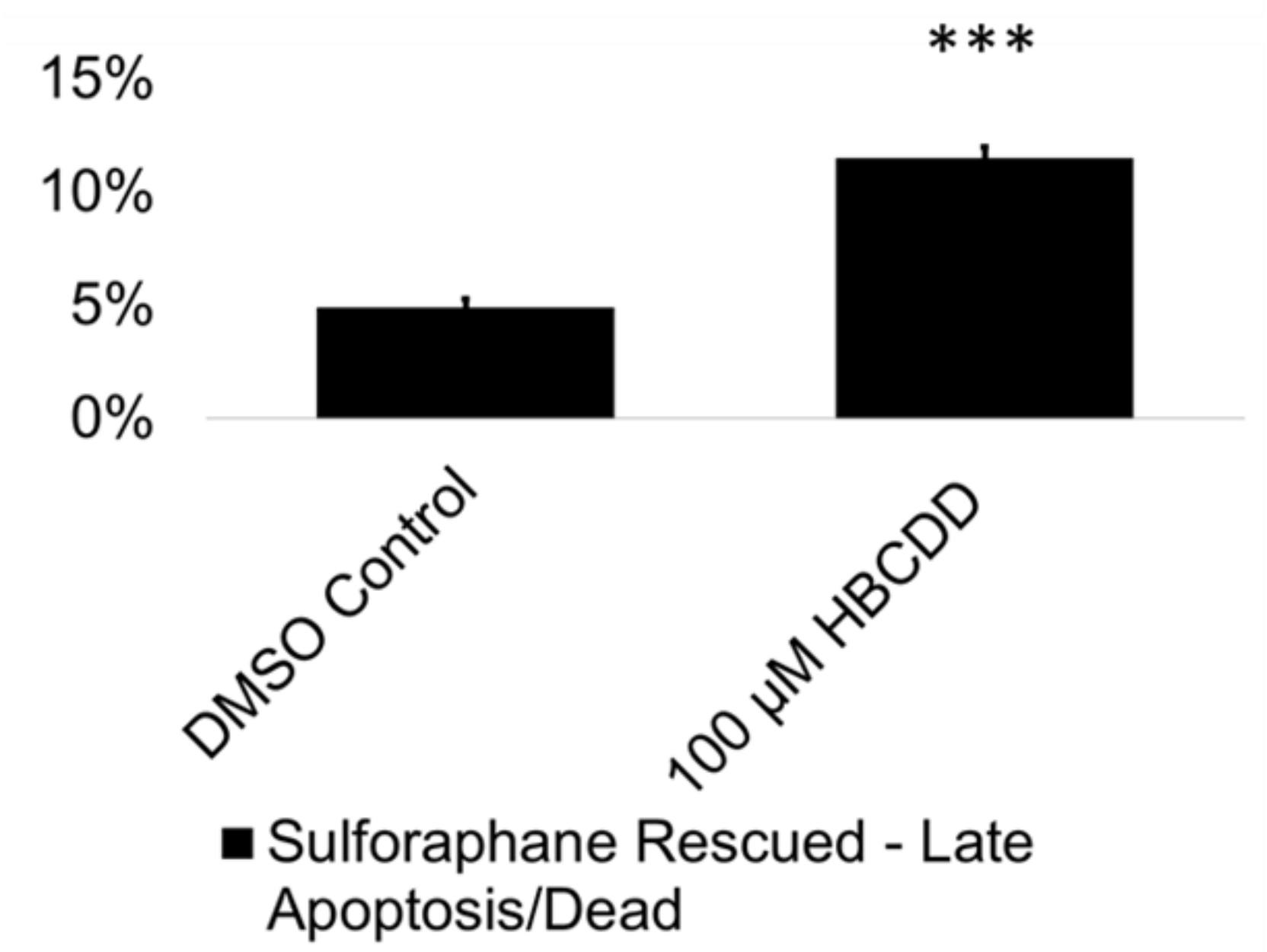
***
15%
10%
5%
0%
DMSO Control
100 µM HBCDD
Sulforaphane Rescued - Late Apoptosis/Dead

Figure 7.14. 1 μM l-Sulforaphane pre-treatment does not impact apoptosis in acute HBCDD exposed spermatogenic cells derived from H1 ESCs. Graphical representation showing that a twelve hour pre-treatment with 1 μM *l*-Sulforaphane does not impact apoptosis caused by exposure to 100 μM HBCDD in H1 ESCs differentiated in *in vitro* spermatogenic conditions in comparison to a 0.2% DMSO-only control. Three replications were performed for each condition (n = 3). Significant changes in the percentage of cells undergoing apoptosis were determined using a 1-way analysis of variance (1-way ANOVA) and validated via a Student's t-test, where * is $p<0.05$, ** is $p<0.01$, and *** is $p<0.001$. Data are represented as mean ± SEM.

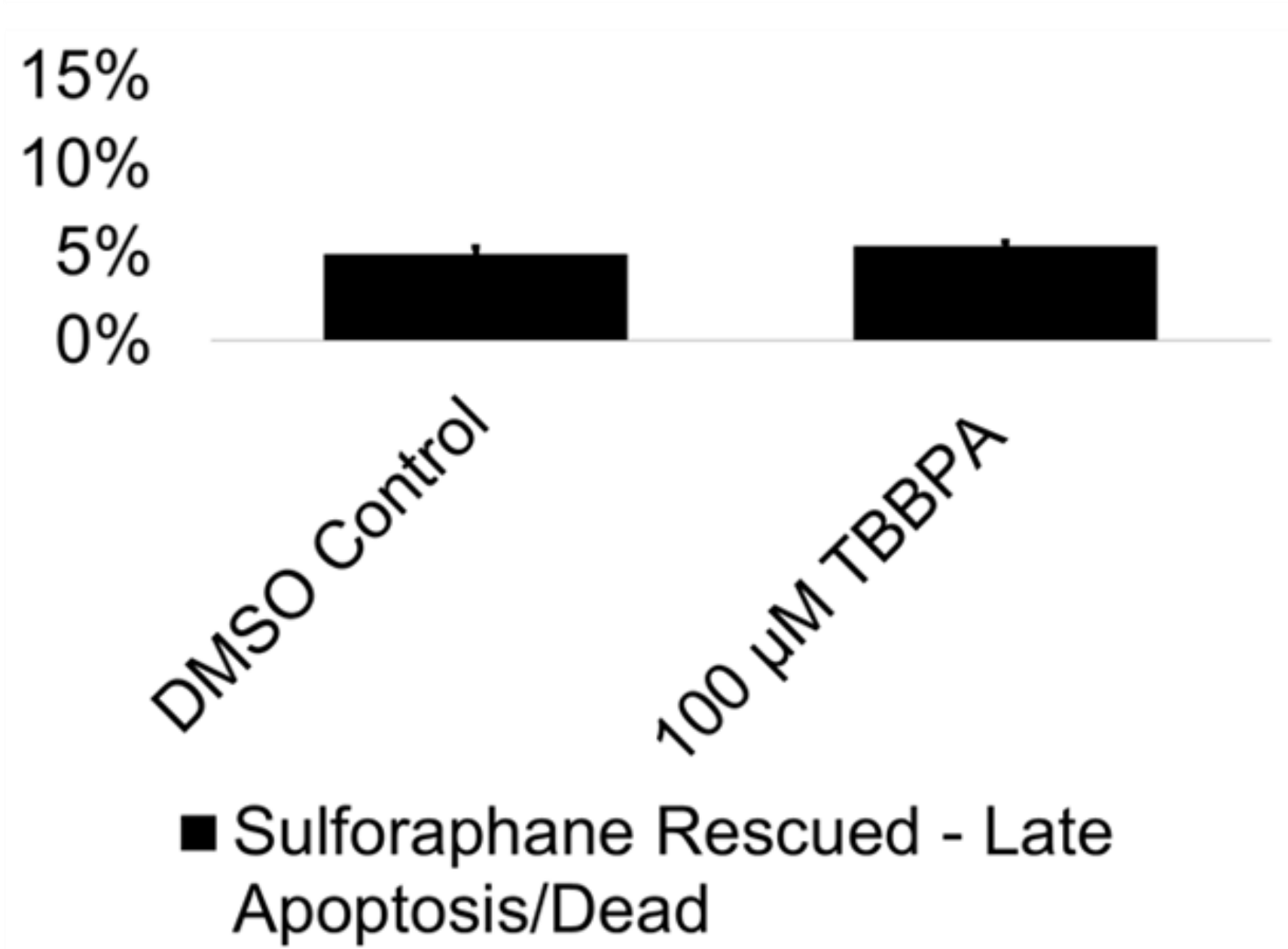
15%
10%
5%
0%
DMSO Control
100 µM TBBPA
Sulforaphane Rescued - Late Apoptosis/Dead

Figure 7.15. 1 μM l-Sulforaphane pre-treatment prevents apoptosis in acute TBBPA exposed spermatogenic cells derived from H1 ESCs. Graphical representation showing that a twelve hour pre-treatment with 1 μM *l*-Sulforaphane prevents apoptosis caused by exposure to 100 μM TBBPA in H1 ESCs differentiated in *in vitro* spermatogenic conditions in comparison to a 0.2% DMSO-only control. Three replications were performed for each condition (n = 3). Significant changes in the percentage of cells undergoing apoptosis were determined using a 1-way analysis of variance (1-way ANOVA) and validated via a Student's t-test, where * is $p<0.05$, ** is $p<0.01$, and *** is $p<0.001$. Data are represented as mean ± SEM.

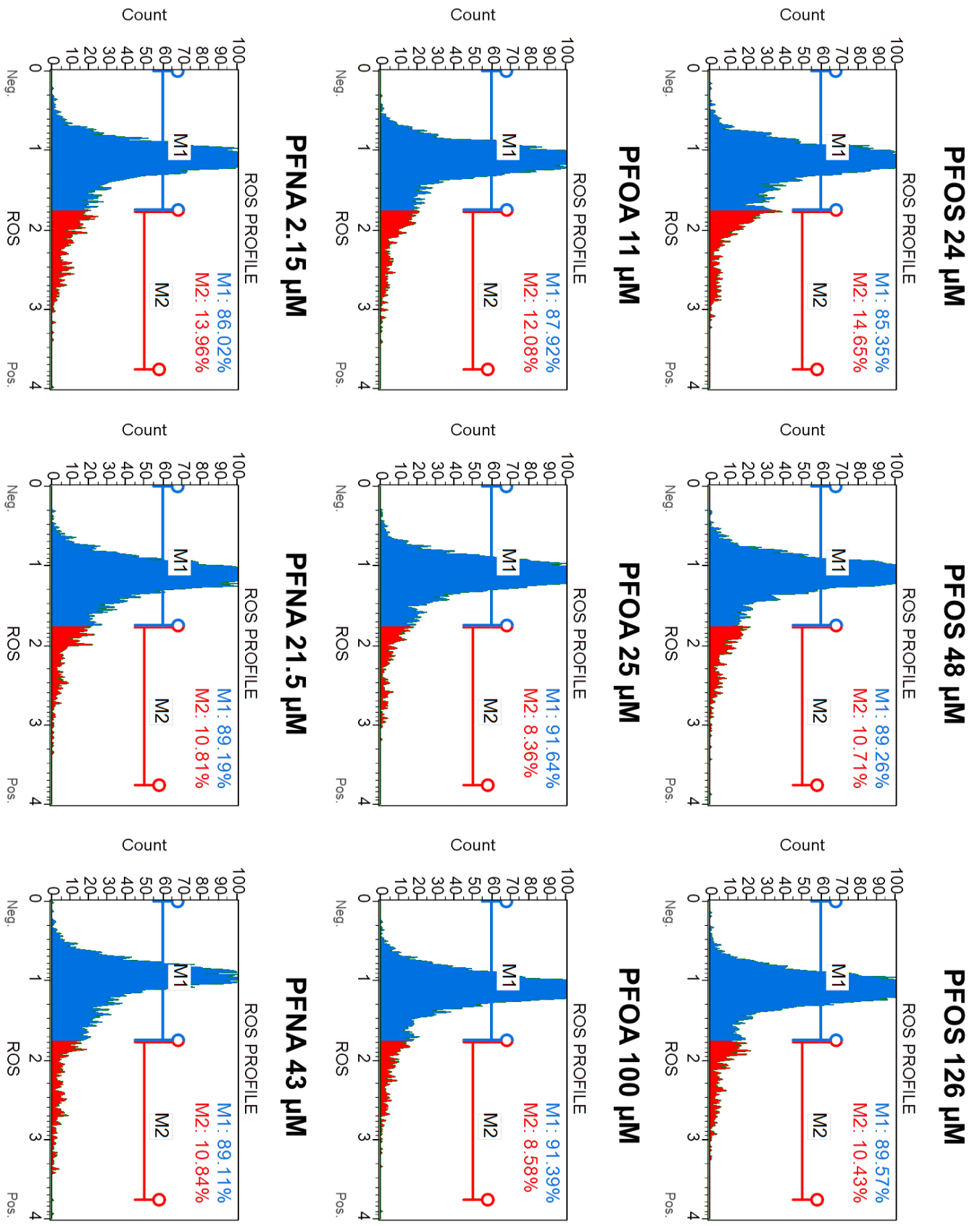
PFOS 24 µM
PFOS 48 µM
PFOS 126 µM
PFOA 11 µM
PFOA 25 µM
PFOA 100 µM
PFNA 2.15 µM
PFNA 21.5 µM
PFNA 43 µM
ROS PROFILE
M1: 85.35%
M2: 14.65%
M1: 89.26%
M2: 10.71%
M1: 89.57%
M2: 10.43%
M1: 87.92%
M2: 12.08%
M1: 91.64%
M2: 8.36%
M1: 91.39%
M2: 8.58%
M1: 86.02%
M2: 13.96%
M1: 89.19%
M2: 10.81%
M1: 89.11%
M2: 10.84%
M1
M2
Count
ROS
Neg.
Pos.

Figure 7.16. Persistent PFOS, PFOA, and PFNA exposure decreases ROS production in spermatogenic cells derived from H1 ESCs. Flow cytometry based analysis of DHE labeling. Blue indicates ROS- cells. Red indicates ROS+ cells.

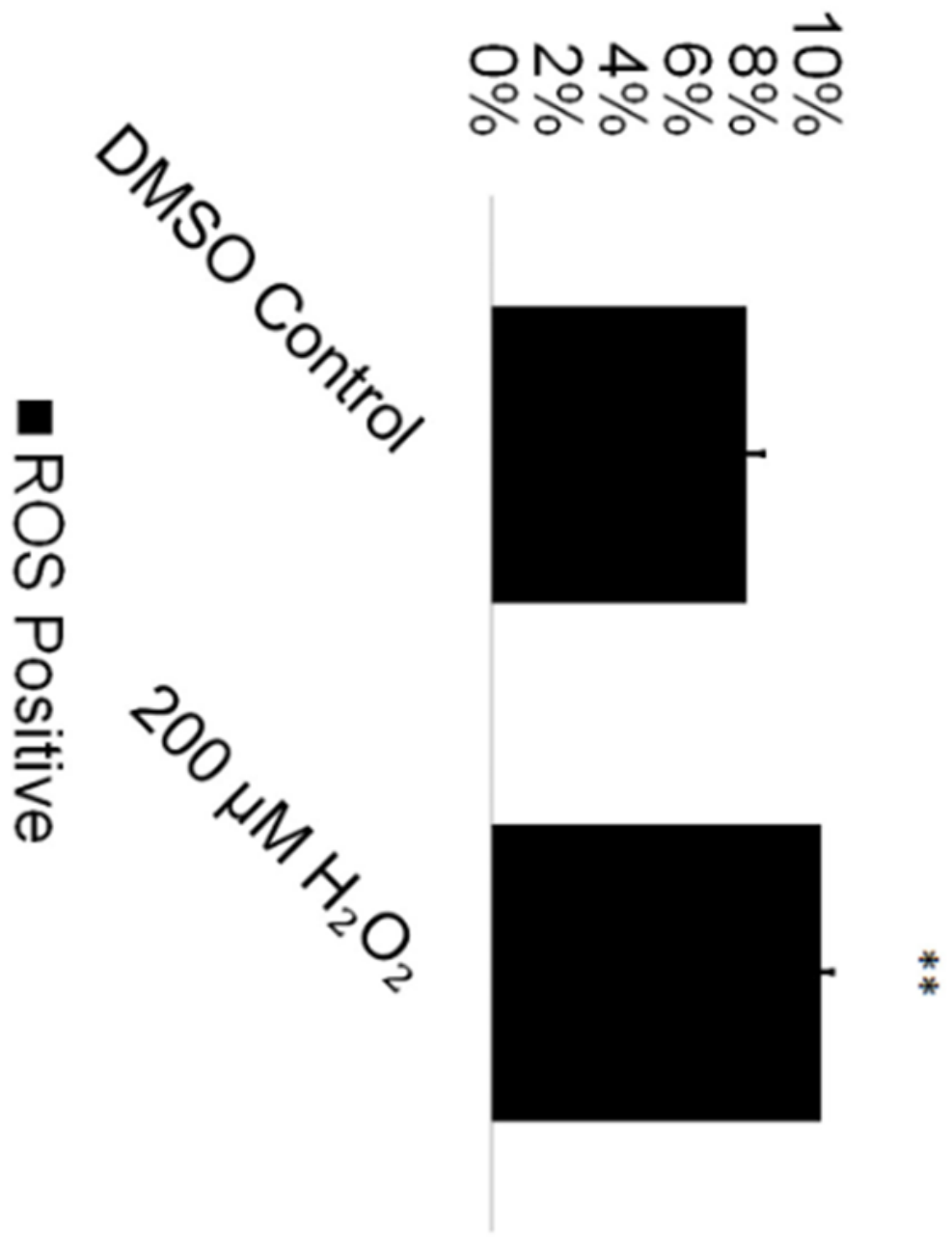
10%
8%
6%
4%
2%
0%
DMSO Control
200 μM H_2O_2
**
■ROS Positive

Figure 7.17. 200 μM H_2O_2 exposure increases ROS generation in spermatogenic cells derived from H1 ESCs. Graphical representation showing that ROS generation increases in H1 SSCs exposed to 200 μM H_2O_2 for six hours. 5,000 events were analyzed, with three replications performed for each condition (n = 3). Significant changes in ROS production were determined using a 1-way analysis of variance (1-way ANOVA) and validated via a Student's t-test, where * is $p<0.05$, ** is $p<0.01$, and *** is $p<0.001$. Data are represented as mean ± SEM.

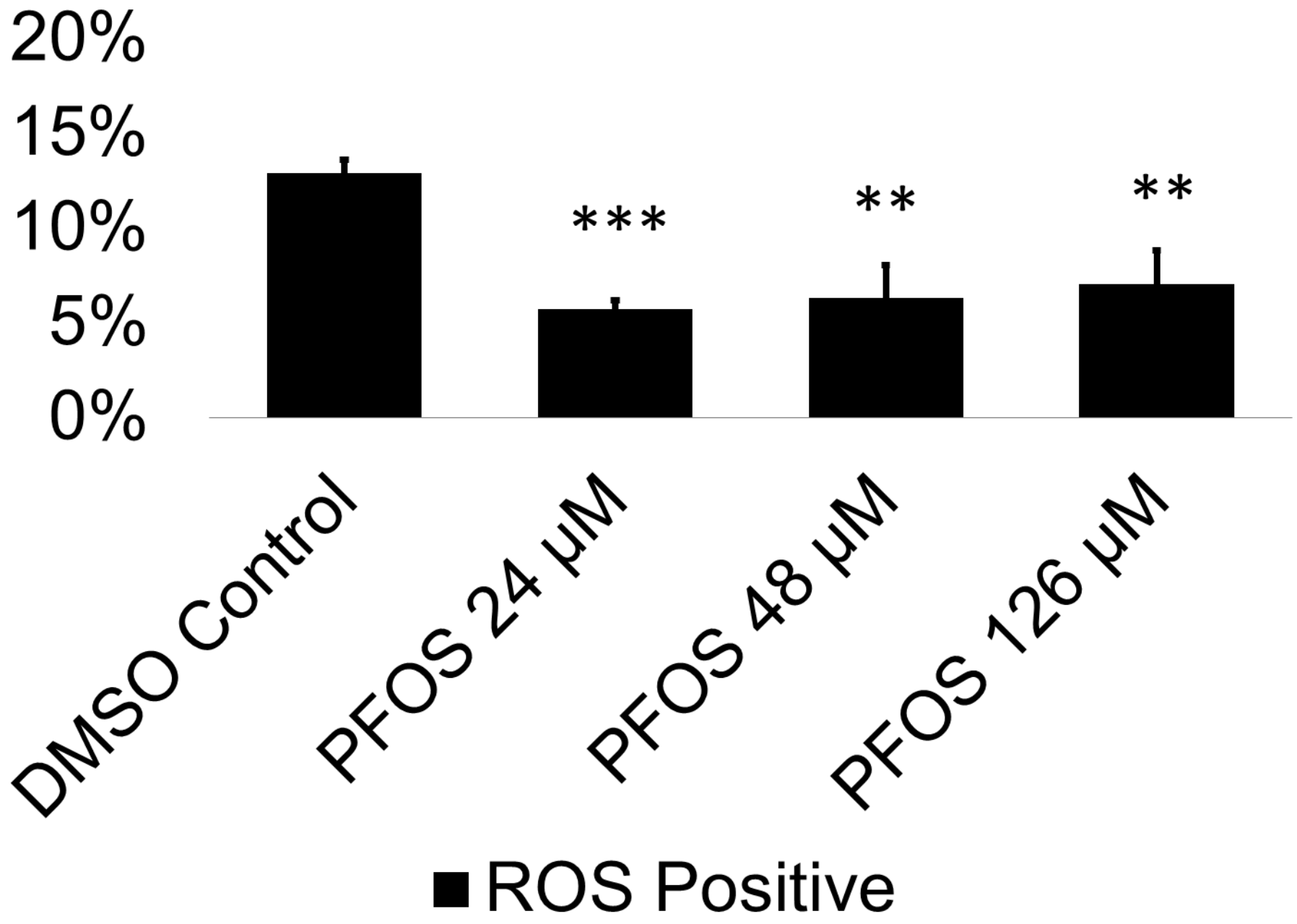
20%
15%
10%
5%
0%
***
**
**
DMSO Control
PFOS 24 µM
PFOS 48 µM
PFOS 126 µM
ROS Positive

Figure 7.18. Persistent PFOS exposure decreases ROS production in spermatogenic cells derived from H1 ESCs. Graphical representation showing that exposure to 24 μM, 48 μM, and 126 μM PFOS from Day 1 to Day 10 decreases ROS production in H1 ESCs differentiated in *in vitro* spermatogenic conditions in comparison to a 0.25% DMSO-only control. 5,000 events were analyzed, with five replications performed for each condition (n = 5). Significant changes in ROS production were determined using a 1-way analysis of variance (1-way ANOVA) and validated via a Student's t-test, where * is $p<0.05$, ** is $p<0.01$, and *** is $p<0.001$. Data are represented as mean ± SEM.

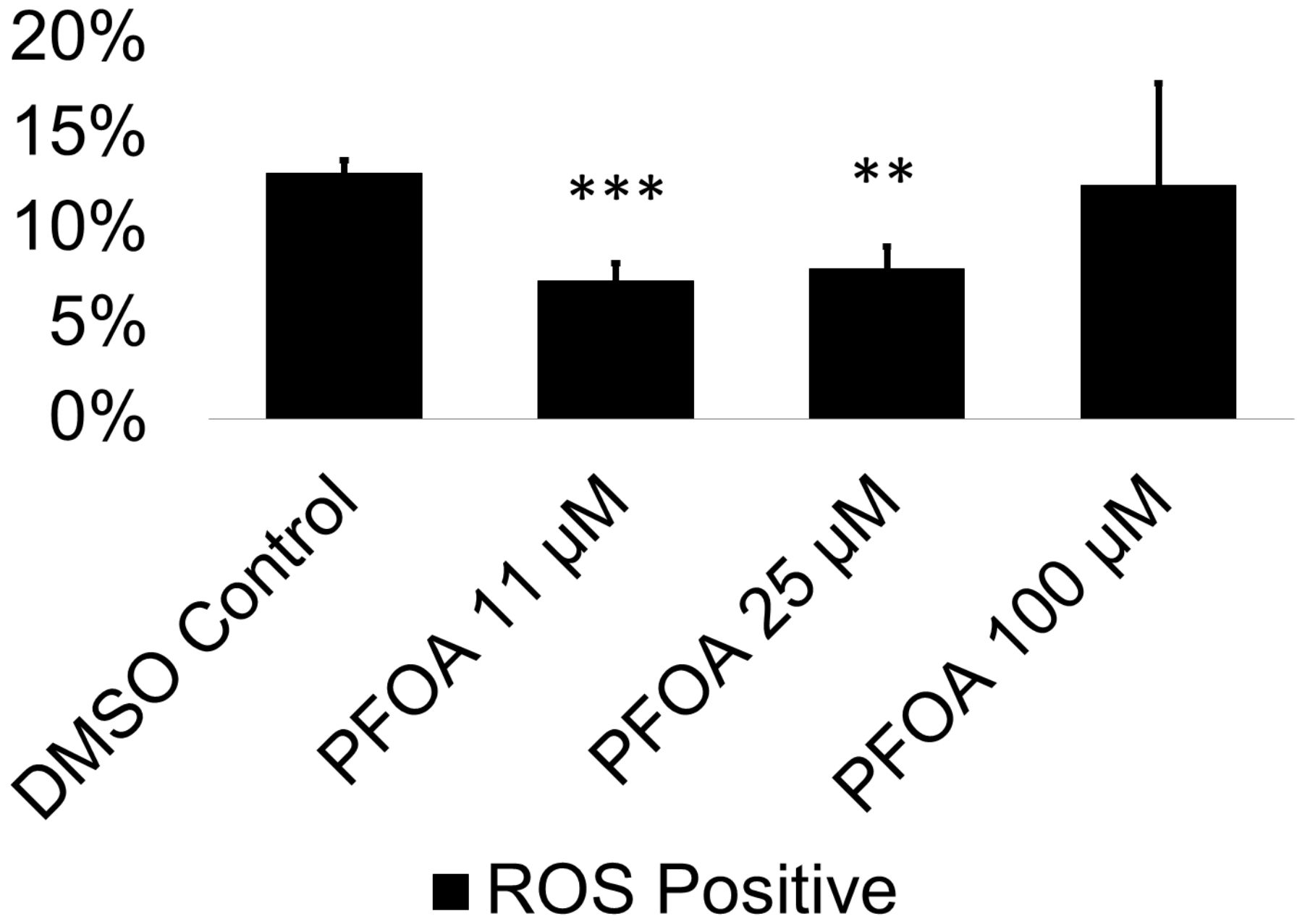
20%
15%
10%
5%
0%
***
**
DMSO Control
PFOA 11 µM
PFOA 25 µM
PFOA 100 µM
ROS Positive

Figure 7.19. Persistent PFOA exposure decreases ROS production in spermatogenic cells derived from H1 ESCs. Graphical representation showing that exposure to 11 μM and 25 μM PFOA from Day 1 to Day 10 decreases ROS production in H1 ESCs differentiated in *in vitro* spermatogenic conditions in comparison to a 0.25% DMSO-only control. 5,000 events were analyzed, with five replications performed for each condition (n = 5). Significant changes in ROS production were determined using a 1-way analysis of variance (1-way ANOVA) and validated via a Student's t-test, where * is $p<0.05$, ** is $p<0.01$, and *** is $p<0.001$. Data are represented as mean ± SEM.

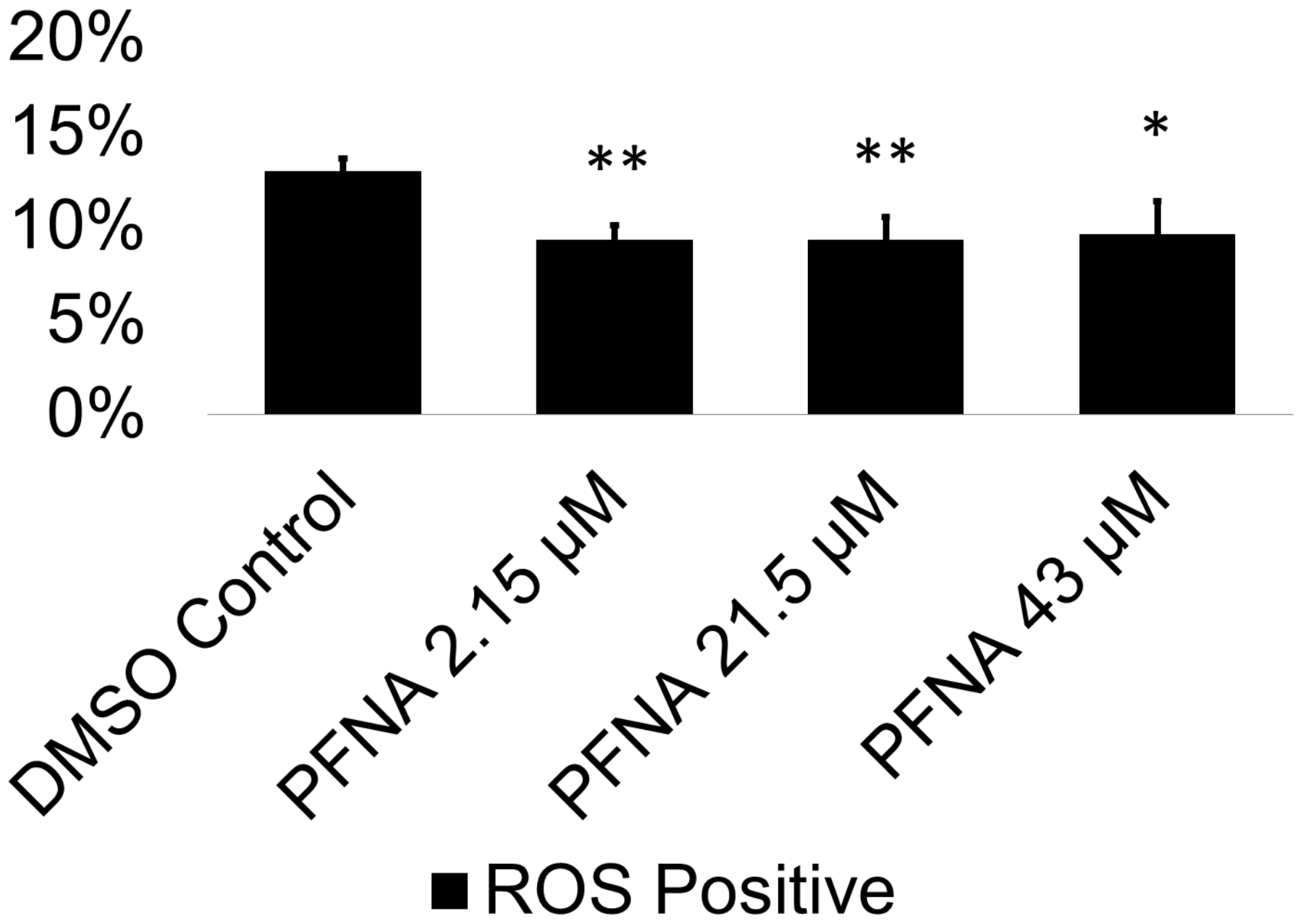
20%
15%
10%
5%
0%
**
**
*
DMSO Control
PFNA 2.15 µM
PFNA 21.5 µM
PFNA 43 µM
ROS Positive

Figure 7.20. Persistent PFNA exposure decreases ROS production in spermatogenic cells derived from H1 ESCs. Graphical representation showing that exposure to 2.15 μM, 21.5 μM, and 43 μM PFNA from Day 1 to Day 10 decreases ROS production in H1 ESCs differentiated in *in vitro* spermatogenic conditions in comparison to a 0.25% DMSO-only control. 5,000 events were analyzed, with five replications performed for each condition (n = 5). Significant changes in ROS production were determined using a 1-way analysis of variance (1-way ANOVA) and validated via a Student's t-test, where * is $p<0.05$, ** is $p<0.01$, and *** is $p<0.001$. Data are represented as mean ± SEM.

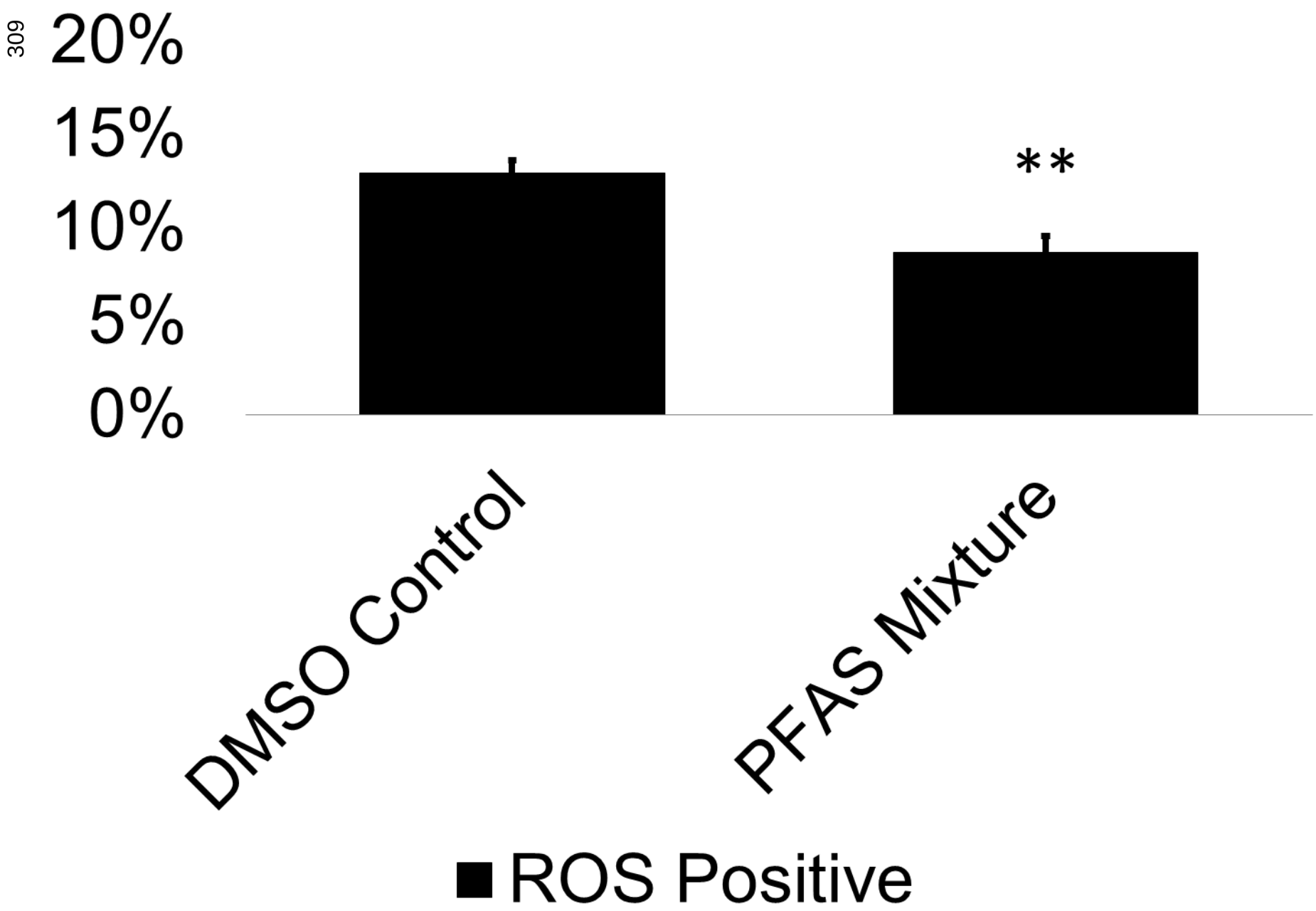
20%
15%
10%
5%
0%
**
DMSO Control
PFAS Mixture
ROS Positive

Figure 7.21. Persistent PFAS mixture exposure decreases ROS production in spermatogenic cells derived from H1 ESCs. Graphical representation showing that exposure to a mixture of 48 μM PFOS, 25 μM PFOA, and 21.5 μM of PFNA from Day 1 to Day 10 decreases ROS production in H1 ESCs differentiated in *in vitro* spermatogenic conditions in comparison to a 0.25% DMSO-only control. 5,000 events were analyzed, with five replications performed for each condition (n = 5). Significant changes in ROS production were determined using a 1-way analysis of variance (1-way ANOVA) and validated via a Student's t-test, where * is $p<0.05$, ** is $p<0.01$, and *** is $p<0.001$. Data are represented as mean ± SEM.

2.5.6 Acute TDCPP, TDBPP, HBCDD, and TBPPA exposure decreases mitochondrial membrane potential in in vitro spermatogenesis cultures, but persistent PFAS exposure does not impact mitochondrial membrane potential

The mitochondria are one of the most essential organelles in a cell, with functions including the generation of cellular energy in the form of ATP, cell signaling, calcium homeostasis, and cell cycle regulation, among other functions (Attene-Ramos et al., 2013). As such, the inhibition of mitochondrial function is detrimental. Mitochondria have been shown to be susceptible to early-stage effects of chemical toxicity, and multiple chemicals have been shown to cause mitochondrial dysfunction (Schmidt, 2010). As such, assessing mitochondrial membrane potential could act as a valid, early assessment for cell health in our *in vitro* cultures. TDCPP, HBCDD, and TBBPA have been shown to negatively impact mitochondria or impair oxidative phosphorylation in HepG2/C3A, A549, and pancreatic beta-cells *in vitro* (An et al., 2014, Suh et al., 2017, Zhang et al., 2016a). Here we examined whether TDCCP, TDBPP, HBCDD, and TBPPA negatively affected mitochondrial membrane potential in our *in vitro* spermatogenesis model using a cationic, lipophilic dye and 7-AAD supplied by the Muse® MitoPotential Kit (MilliporeSigma, Billerica, MA) to assess membrane depolarization. Flow cytometry plots were generated showing the percentage of live, depolarized/ live, depolarized/ dead, and dead cells in our cultures (Figure 8.1). TDCPP significantly increased mitochondrial membrane depolarization beginning 10 µM, with a nearly 250% increase in mitochondrial membrane depolarization and cell death at 200 µM (Figure 8.2). TDBPP significantly decreased membrane potential beginning at 25 µM and also showed a 205% increase in membrane depolarization and death at 100

μM (Figure 8.3). HBCDD significantly increased mitochondrial dysfunction beginning at 1 μM and showed at 190% increase in mitochondrial membrane depolarization and death at 200 μM (Figure 8.4). TBBPA significantly increased mitochondrial dysfunction at a concentration of 10 μM and had nearly 250% more membrane depolarization and cell death compared to control at 200 μM (Figure 8.5).

Similar to our apoptosis data, TDCPP, TDBPP, and HBCDD significantly decreased healthy, live cell populations beginning at 10 μM, and TBBPA significantly decreased healthy, live cell populations beginning at and 25 μM (Figures 8.6 – 8.9). TDCPP significantly decreased healthy, live cells at 200 μM by 99% (Figure 8.6). TDBPP significantly decreased healthy, live cells at 200 μM by 89% (Figure 8.7). HBCDD and TBBPA significantly decreased healthy, live cells at 200 μM by 83% and 98%, respectively (Figures 8.8 – 8.9).

The mechanism by which HBCDD and TBBPA cause mitochondrial dysfunction appears to be drastically different, consistent with PLZF, HILI, and ROS assays. A shift toward live cells by 162% can be seen within half an hour of treating cells with 100 μM HBCDD (Figure 8.10). As it is unlikely that HBCDD exposure drastically increases cell viability after half an hour, this shift from the norm is likely the result of mitochondrial hyperpolarization. This hyperpolarizing event occurs for approximately nine hours post-exposure, with depolarization significantly shifting cells toward the depolarized/live quadrant at six and twelve hours (Figure 8.12). Because mitochondria produce ROS during oxidative phosphorylation, this acute perturbation of the mitochondria may be another potential explanation for the decrease in ROS seen in HBCDD treated cells. The viability of TBBPA-exposed cells begins decreasing at 1.5 hours post-exposure,

though significant depolarization of the mitochondrial membrane and cell death occurs as quickly as 0.5 hours after TBBPA exposure (Figures 8.11, 8.13). This increase in depolarized/dead cells becomes more dramatic at nine hours (Figures 8.11, 8.13). Because mitochondria are sensitive to ROS, it is likely that the abrupt mitochondrial membrane depolarization seen following TBBPA exposure is likely due to assault by ROS (Balaban et al., 2005). These results indicate that mitochondria are a direct target of halogenated flame retardants in our *in vitro* cultures at concentrations that are physiologically relevant, with exposure resulting in mitochondrial membrane dysfunction and increased cell death. TBBPA likely causes mitochondrial dysfunction due to ROS generation, though the mechanism by which HBCDD impacts the mitochondria is less clear. Possibly, HBCDD's unique mechanism of toxicity involves directly targeting mitochondria in spermatogenic cells. TDCPP and TDBPP's mechanisms were not examined in this study and remain unclear.

PFOS has been shown to decrease the mitochondrial membrane potential of mouse Leydig cells, ultimately leading to apoptosis through mitochondrially-mediated pathways (Zhang et al., 2015). PFOS was found to impact mitochondrial membrane potential at concentrations below those associated with other adverse outcomes, indicating that the mitochondria may be particularly sensitive to PFOS exposure (Hu et al., 2003). Similarly, in a study assessing the effects of PFNA on rat Sertoli cells, PFNA exposure was associated with a decline in mitochondrial integrity and an increase in cell death (Feng et al., 2010). While no studies of the effects of PFOA on the mitochondria of testicular tissue exist, PFOA has been shown to induce mitochondrial dysfunction in mouse derived osteoblast cells, with the introduction of PFOA resulting in a collapse of

mitochondrial membrane potential (Choi et al., 2017). No studies on PFAS exposure and the mitochondria of germ cells have been conducted. We assessed whether exposure to the per- and polyfluoroalkyl substances PFOS, PFOA, and PFNA in comparison to a DMSO-only control results in decreases in mitochondrial membrane potential. Flow cytometry plots were created showing percentages of live, depolarized/live, depolarized/dead, and dead cells in our *in vitro* cell cultures (Figure 8.14). Neither PFOS, PFOA, nor PFNA exposure significantly decreased mitochondrial membrane potential or increased cell death, consistent with the cell viability results (Figures 8.15 – 8.17). Similarly, exposure to a mixture of 48 µM PFOS, 25 µM PFOA, and 21.5 µM of PFNA did not decrease mitochondrial membrane potential or increase cell death in our cell cultures (Figure 8.18). As such, these results, combined with our other data, provide firm evidence that PFOS, PFOA, and PFNA do not affect the viability of spermatogenic cells in our human *in vitro* cultures.

The mitochondrial potential assay confirms the stark differences between halogenated flame retardants and PFASs. Despite having ten times the exposure length at similar or higher concentrations, PFASs do not cause cell death, though they may impact subcellular processes. These studies undoubtedly reveal the severely toxic effects of halogenated flame retardants on human spermatogenesis. Though only four halogenated FRs were assessed, the results of these studies suggest that these toxic effects may be class wide.

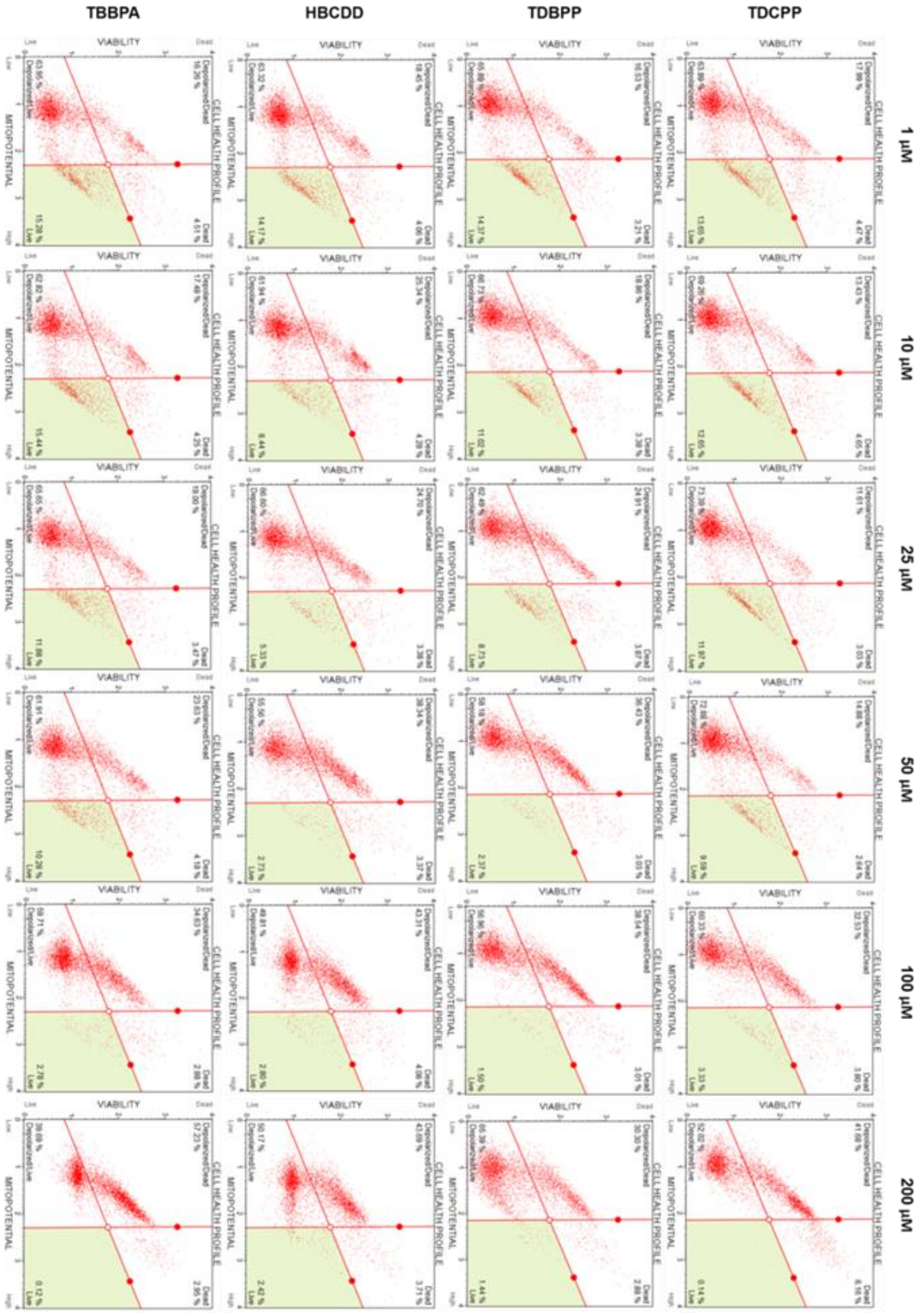
TDCPP
TDBPP
HBCDD
TBBPA
1 µM
10 µM
25 µM
50 µM
100 µM
200 µM
VIABILITY
MITOPOTENTIAL
CELL HEALTH PROFILE

Figure 8.1. Acute TDCPP, TDBPP, HBCDD, and TBBPA exposure depolarizes the mitochondrial membrane and increases cell death in spermatogenic cells derived from H1 ESCs. Flow cytometry analyses for indicating percent live cells, percent depolarized/live cells, percent depolarized/dead cells, and percent dead cells. Lower right quadrant represents viable cells, lower left quadrant represents depolarized/live cells, upper right quadrant is depolarized/dead cells, and the upper right quadrant is dead cells.

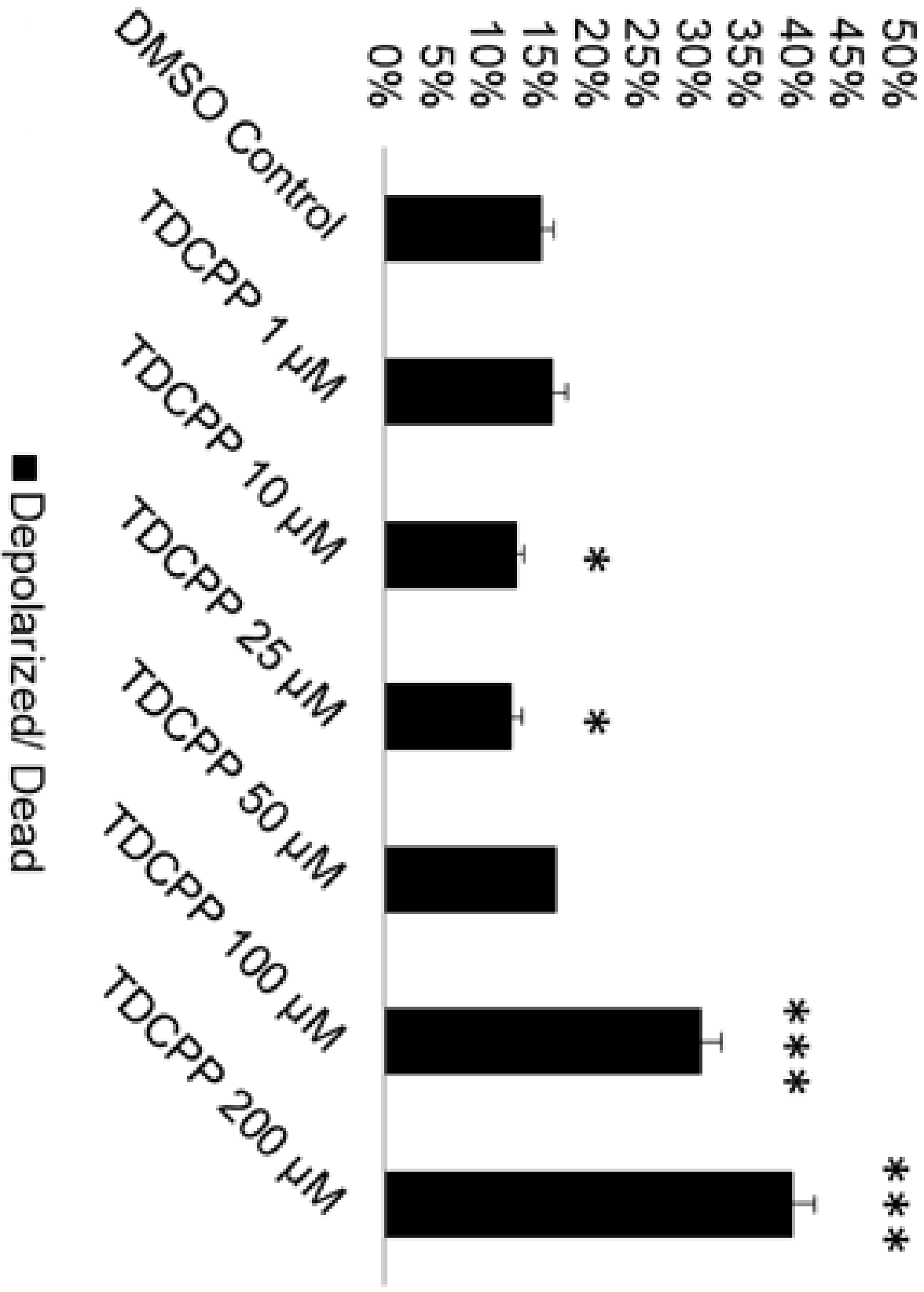
50%
45%
40%
35%
30%
25%
20%
15%
10%
5%
0%
DMSO Control
TDCPP 1 µM
TDCPP 10 µM
TDCPP 25 µM
TDCPP 50 µM
TDCPP 100 µM
TDCPP 200 µM
*
*
***
***
■ Depolarized/ Dead

Figure 8.2. Acute TDCPP exposure depolarizes the mitochondrial membrane and increases cell death in spermatogenic cells derived from H1 ESCs. Graphical representation showing that acute, twenty-four hour 100 μM and 200 μM TDCPP exposure increases membrane depolarization and cell death in H1 ESCS differentiated in *in vitro* spermatogenic conditions in comparison to a 0.2% DMSO-only control. 5,000 events were analyzed, with three replications performed for each condition (n = 3). Significant changes in mitochondrial membrane potential and cell death were determined using a 1-way analysis of variance (1-way ANOVA) and validated via a Student's t-test, where * is $p<0.05$, ** is $p<0.01$, and *** is $p<0.001$. Data are represented as mean ± SEM.

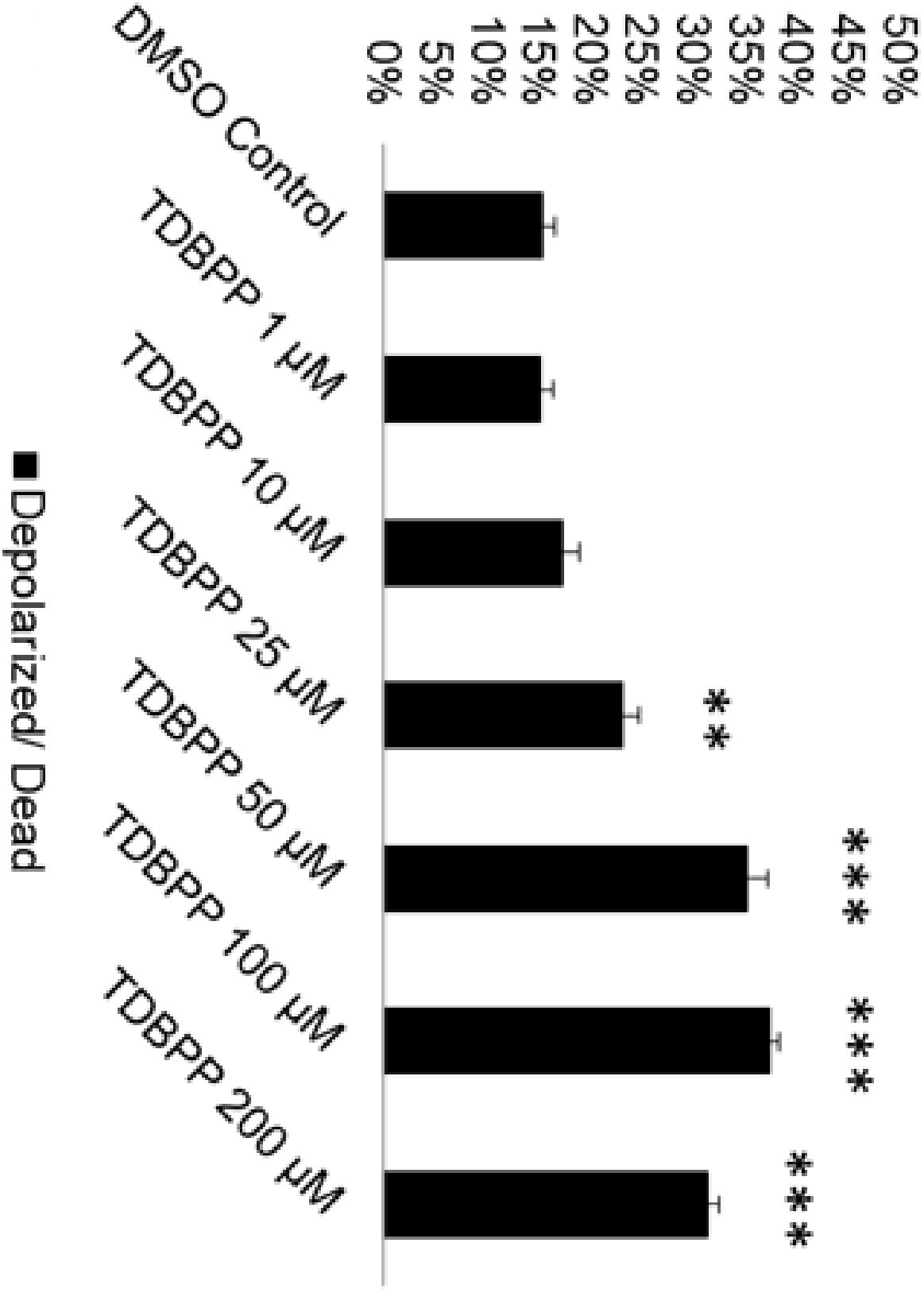
50%
45%
40%
35%
30%
25%
20%
15%
10%
5%
0%
DMSO Control
TDBPP 1 µM
TDBPP 10 µM
TDBPP 25 µM
TDBPP 50 µM
TDBPP 100 µM
TDBPP 200 µM
**
****
****
****
■ Depolarized/ Dead

Figure 8.3. Acute TDBPP exposure depolarizes the mitochondrial membrane and increases cell death in spermatogenic cells derived from H1 ESCs. Graphical representation showing that acute, twenty-four hour 25 μM, 100 μM, and 200 μM TDBPP exposure increases membrane depolarization and cell death in H1 ESCS differentiated in *in vitro* spermatogenic conditions in comparison to a 0.2% DMSO-only control. 5,000 events were analyzed, with three replications performed for each condition (n = 3). Significant changes in mitochondrial membrane potential and cell death were determined using a 1-way analysis of variance (1-way ANOVA) and validated via a Student's t-test, where * is $p<0.05$, ** is $p<0.01$, and *** is $p<0.001$. Data are represented as mean ± SEM.

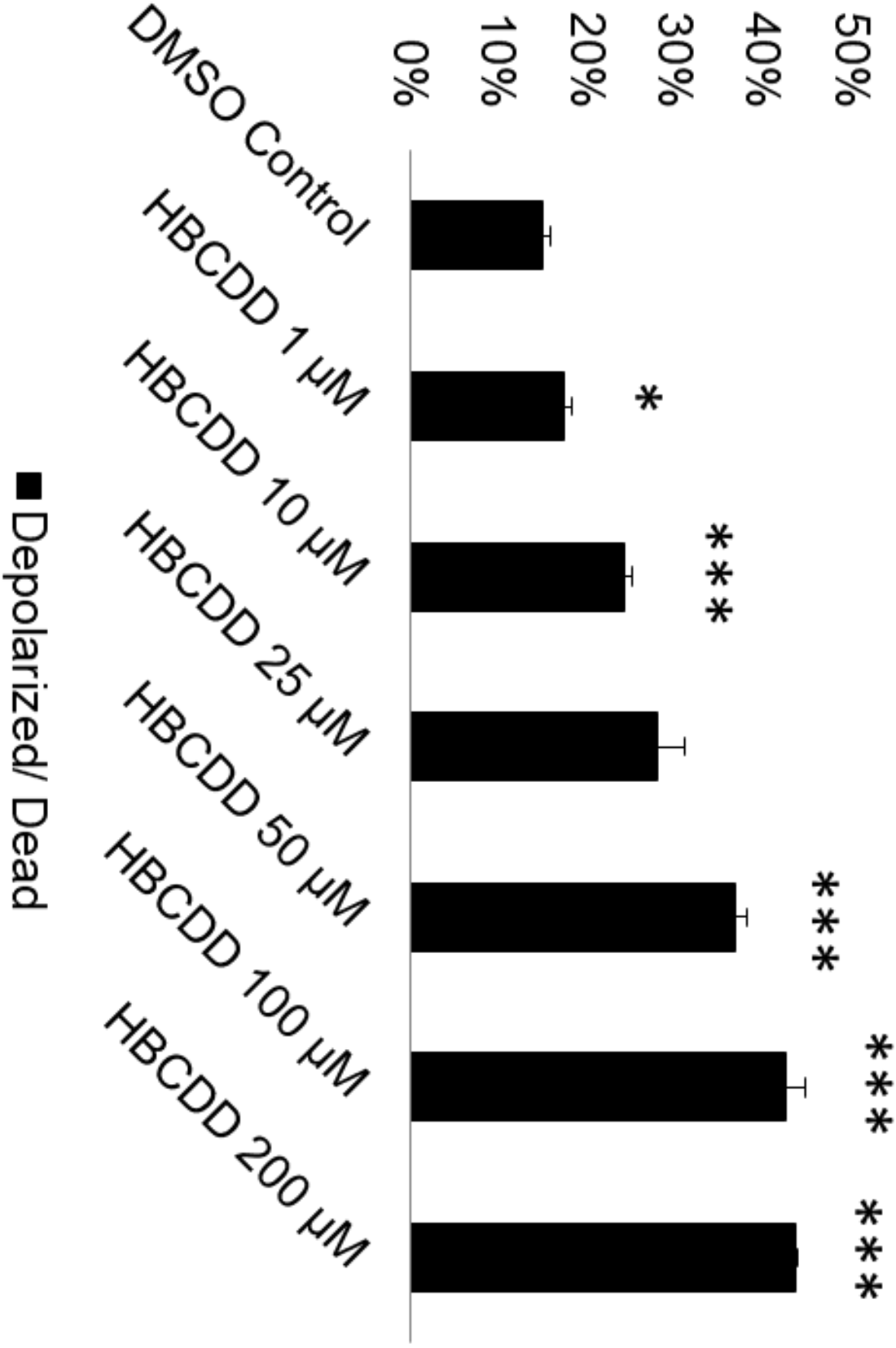
60%
50%
40%
30%
20%
10%
0%
DMSO Control
HBCDD 1 µM
HBCDD 10 µM
HBCDD 25 µM
HBCDD 50 µM
HBCDD 100 µM
HBCDD 200 µM
*
***
***
***
***
■Depolarized/ Dead

Figure 8.4. Acute HBCDD exposure depolarizes the mitochondrial membrane and increases cell death in spermatogenic cells derived from H1 ESCs. Graphical representation showing that acute, twenty-four hour 1 μM, 10 μM, 50 μM, 100 μM, and 200 μM TDBPP exposure increases membrane depolarization and cell death in H1 ESCS differentiated in *in vitro* spermatogenic conditions in comparison to a 0.2% DMSO-only control. 5,000 events were analyzed, with three replications performed for each condition (n = 3). Significant changes in mitochondrial membrane potential and cell death were determined using a 1-way analysis of variance (1-way ANOVA) and validated via a Student's t-test, where * is $p<0.05$, ** is $p<0.01$, and *** is $p<0.001$. Data are represented as mean ± SEM.

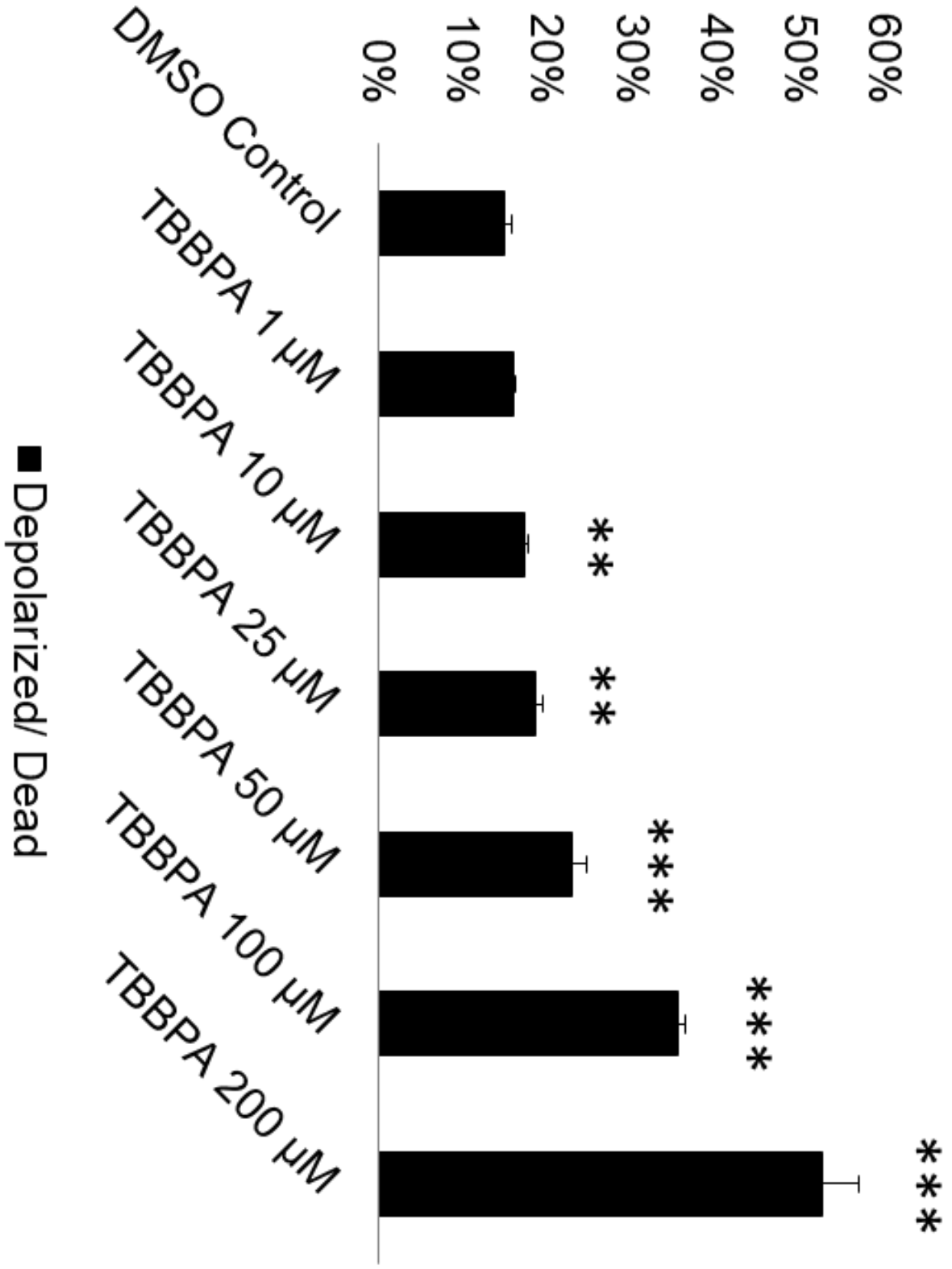
60%
50%
40%
30%
20%
10%
0%
DMSO Control
TBBPA 1 µM
TBBPA 10 µM
TBBPA 25 µM
TBBPA 50 µM
TBBPA 100 µM
TBBPA 200 µM
**
**
***
***
****
■Depolarized/ Dead

Figure 8.5. Acute TBBPA exposure depolarizes the mitochondrial membrane and increases cell death in spermatogenic cells derived from H1 ESCs. Graphical representation showing that acute, twenty-four hour 10 μM, 25 μM, 50 μM, 100 μM, and 200 μM TBBPA exposure increases membrane depolarization and cell death in H1 ESCS differentiated in *in vitro* spermatogenic conditions in comparison to a 0.2% DMSO-only control. 5,000 events were analyzed, with three replications performed for each condition (n = 3). Significant changes in mitochondrial membrane potential and cell death were determined using a 1-way analysis of variance (1-way ANOVA) and validated via a Student's t-test, where * is $p<0.05$, ** is $p<0.01$, and *** is $p<0.001$. Data are represented as mean ± SEM.

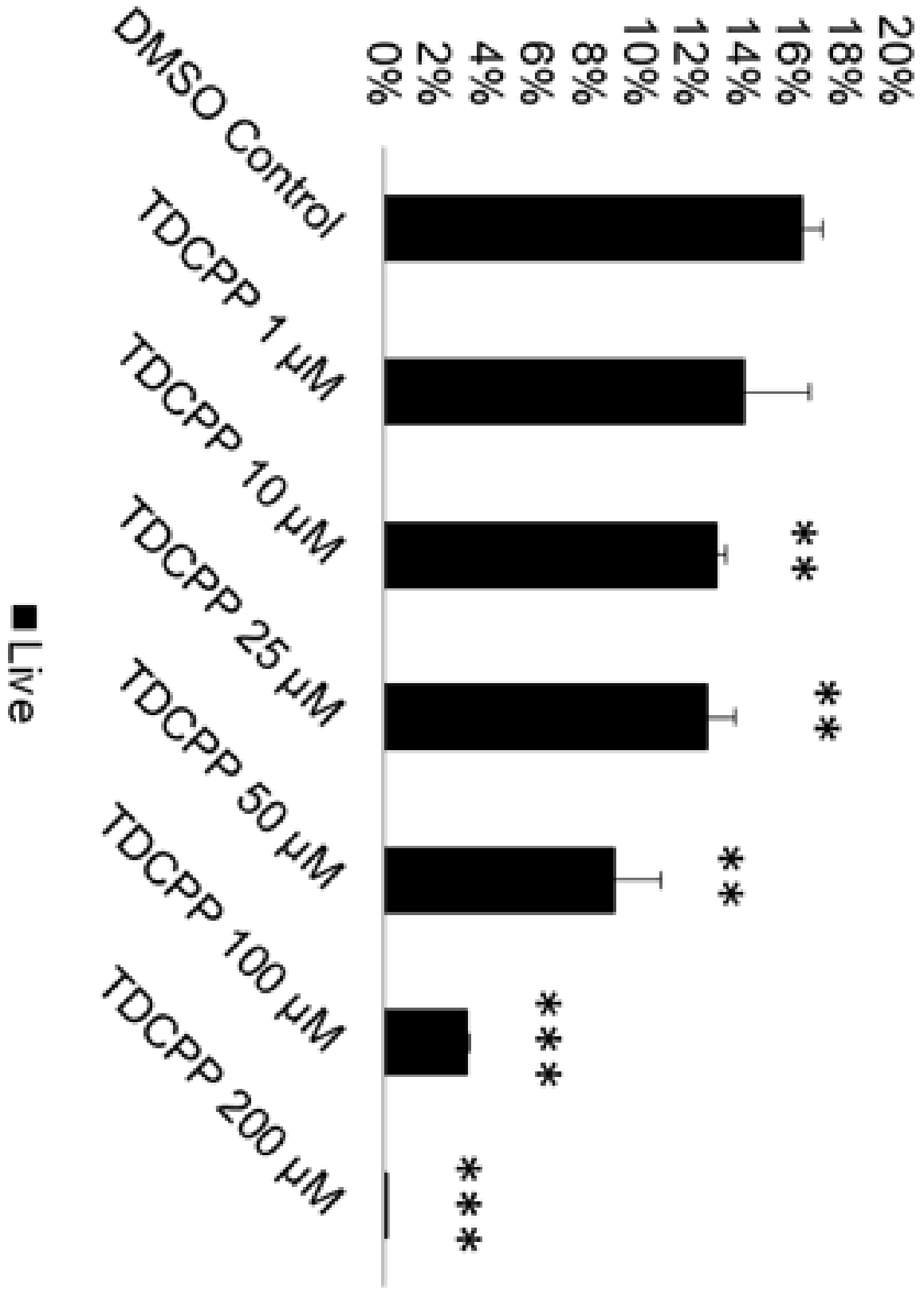
20%
18%
16%
14%
12%
10%
8%
6%
4%
2%
0%
DMSO Control
TDCPP 1 µM
TDCPP 10 µM
TDCPP 25 µM
TDCPP 50 µM
TDCPP 100 µM
TDCPP 200 µM
**
**
**
***
***
■Live

Figure 8.6. Acute TDCPP exposure decreases cell viability in spermatogenic cells derived from H1 ESCs in a mitochondrial potential assay. Graphical representation showing that acute, twenty-four hour 10 μM, 25 μM, 50 μM, 100 μM, and 200 μM TDCPP exposure decreases cell viability in H1 ESCS differentiated in *in vitro* spermatogenic conditions in comparison to a 0.2% DMSO-only control. 5,000 events were analyzed, with three replications performed for each condition (n = 3). Significant changes in cell viability were determined using a 1-way analysis of variance (1-way ANOVA) and validated via a Student's t-test, where * is $p<0.05$, ** is $p<0.01$, and *** is $p<0.001$. Data are represented as mean ± SEM.

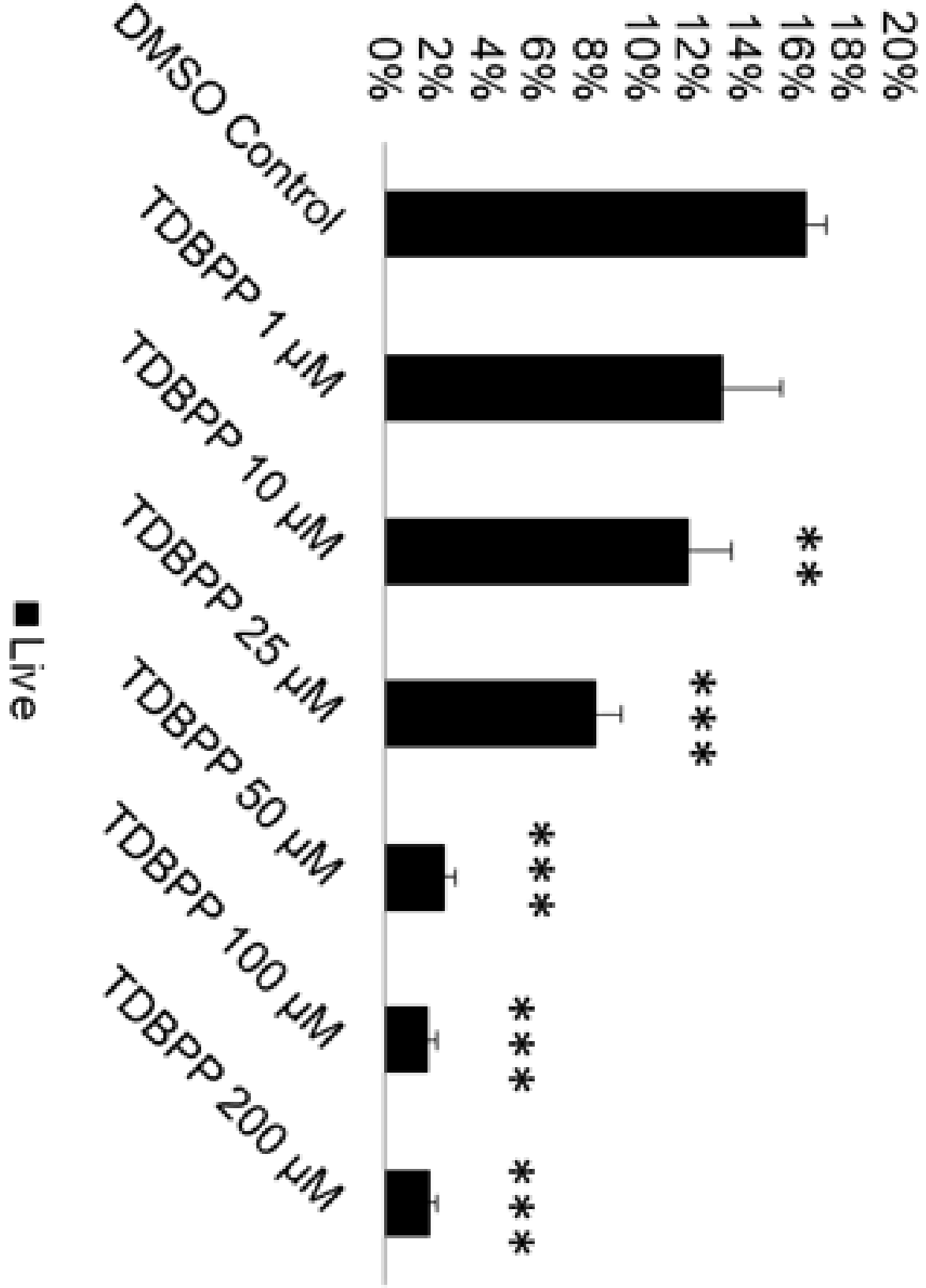
20%
18%
16%
14%
12%
10%
8%
6%
4%
2%
0%
DMSO Control
TDBPP 1 µM
TDBPP 10 µM
TDBPP 25 µM
TDBPP 50 µM
TDBPP 100 µM
TDBPP 200 µM
**
***
****
****
****
■Live

Figure 8.7. Acute TDBPP exposure decreases cell viability in spermatogenic cells derived from H1 ESCs in a mitochondrial potential assay. Graphical representation showing that acute, twenty-four hour 10 μM, 25 μM, 50 μM, 100 μM, and 200 μM TDBPP exposure decreases cell viability in H1 ESCS differentiated in *in vitro* spermatogenic conditions in comparison to a 0.2% DMSO-only control. 5,000 events were analyzed, with three replications performed for each condition (n = 3). Significant changes in cell viability were determined using a 1-way analysis of variance (1-way ANOVA) and validated via a Student's t-test, where * is $p<0.05$, ** is $p<0.01$, and *** is $p<0.001$. Data are represented as mean ± SEM.

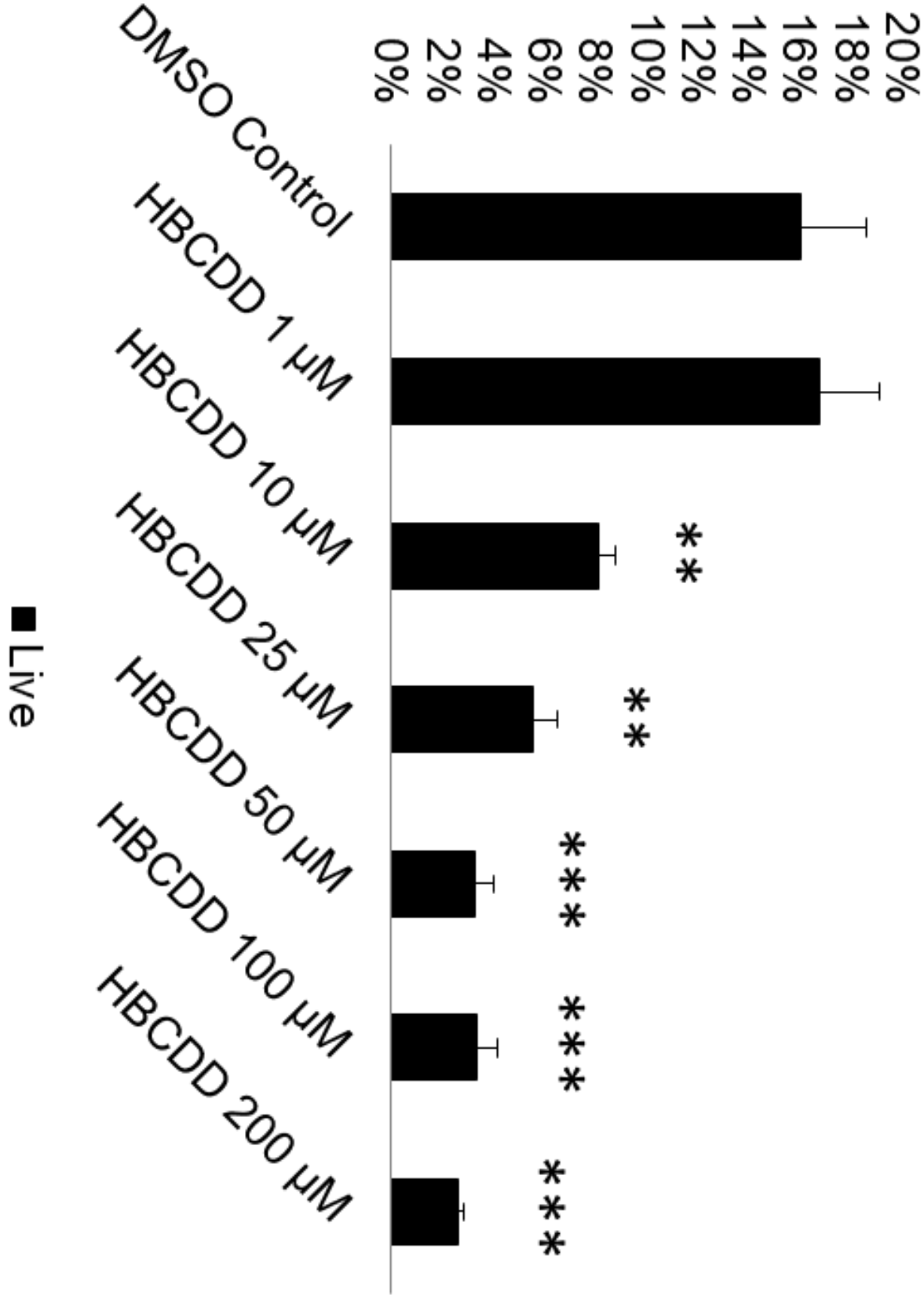
20%
18%
16%
14%
12%
10%
8%
6%
4%
2%
0%
DMSO Control
HBCDD 1 μM
HBCDD 10 μM
HBCDD 25 μM
HBCDD 50 μM
HBCDD 100 μM
HBCDD 200 μM
**
**
***
***
***
Live

Figure 8.8. Acute HBCDD exposure decreases cell viability in spermatogenic cells derived from H1 ESCs in a mitochondrial potential assay. Graphical representation showing that acute, twenty-four hour 10 μM, 25 μM, 50 μM, 100 μM, and 200 μM HBCDD exposure decreases cell viability in H1 ESCS differentiated in *in vitro* spermatogenic conditions in comparison to a 0.2% DMSO-only control. 5,000 events were analyzed, with three replications performed for each condition (n = 3). Significant changes in cell viability were determined using a 1-way analysis of variance (1-way ANOVA) and validated via a Student's t-test, where * is $p<0.05$, ** is $p<0.01$, and *** is $p<0.001$. Data are represented as mean ± SEM.

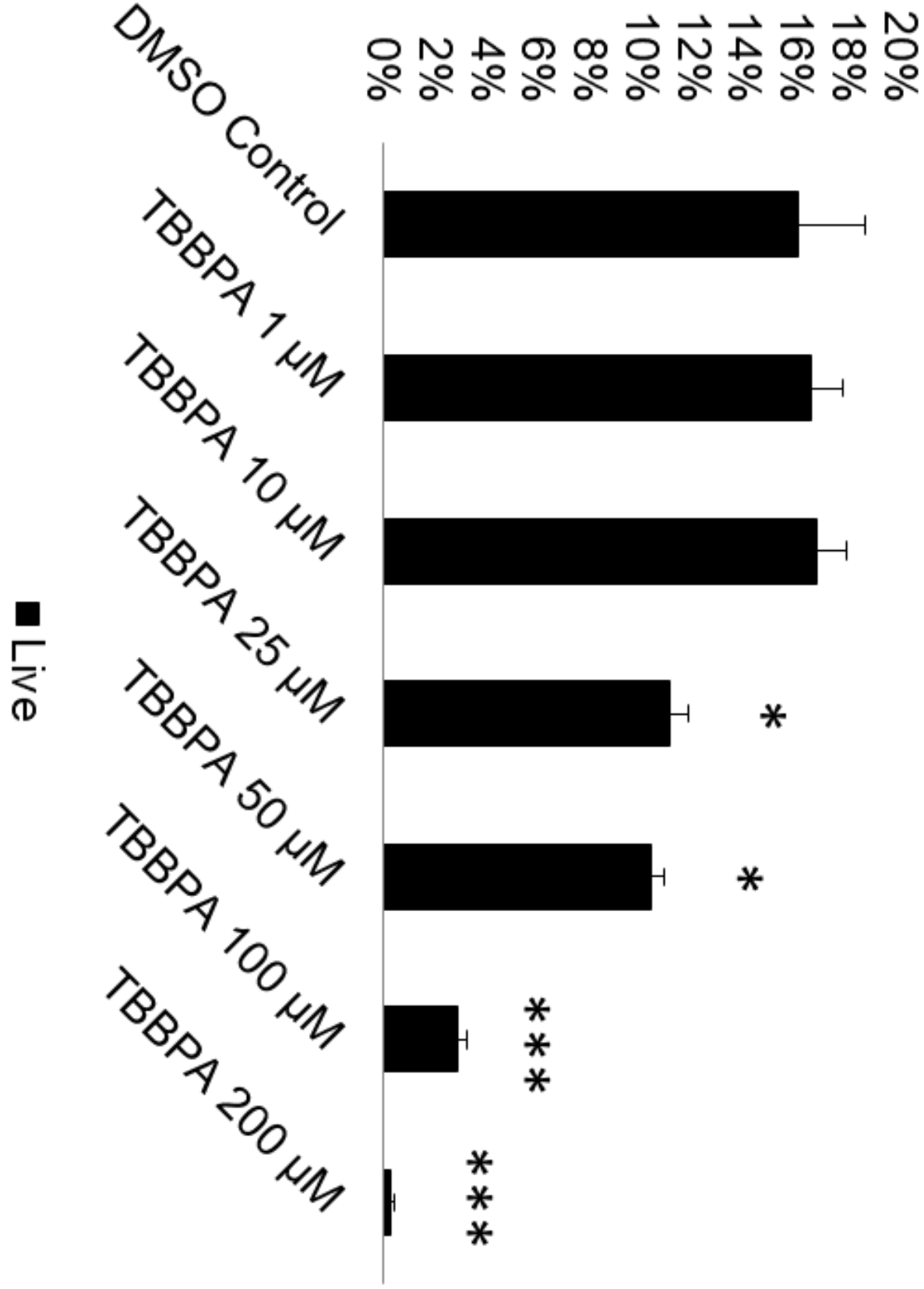
20%
18%
16%
14%
12%
10%
8%
6%
4%
2%
0%
DMSO Control
TBBPA 1 µM
TBBPA 10 µM
TBBPA 25 µM
TBBPA 50 µM
TBBPA 100 µM
TBBPA 200 µM
*
*
***
***
Live

Figure 8.9. Acute TBBPA exposure decreases cell viability in spermatogenic cells derived from H1 ESCs in a mitochondrial potential assay. Graphical representation showing that acute, twenty-four hour 25 μM, 50 μM, 100 μM, and 200 μM TBBPA exposure decreases cell viability in H1 ESCS differentiated in *in vitro* spermatogenic conditions in comparison to a 0.2% DMSO-only control. 5,000 events were analyzed, with three replications performed for each condition (n = 3). Significant changes in cell viability were determined using a 1-way analysis of variance (1-way ANOVA) and validated via a Student's t-test, where * is $p<0.05$, ** is $p<0.01$, and *** is $p<0.001$. Data are represented as mean ± SEM.

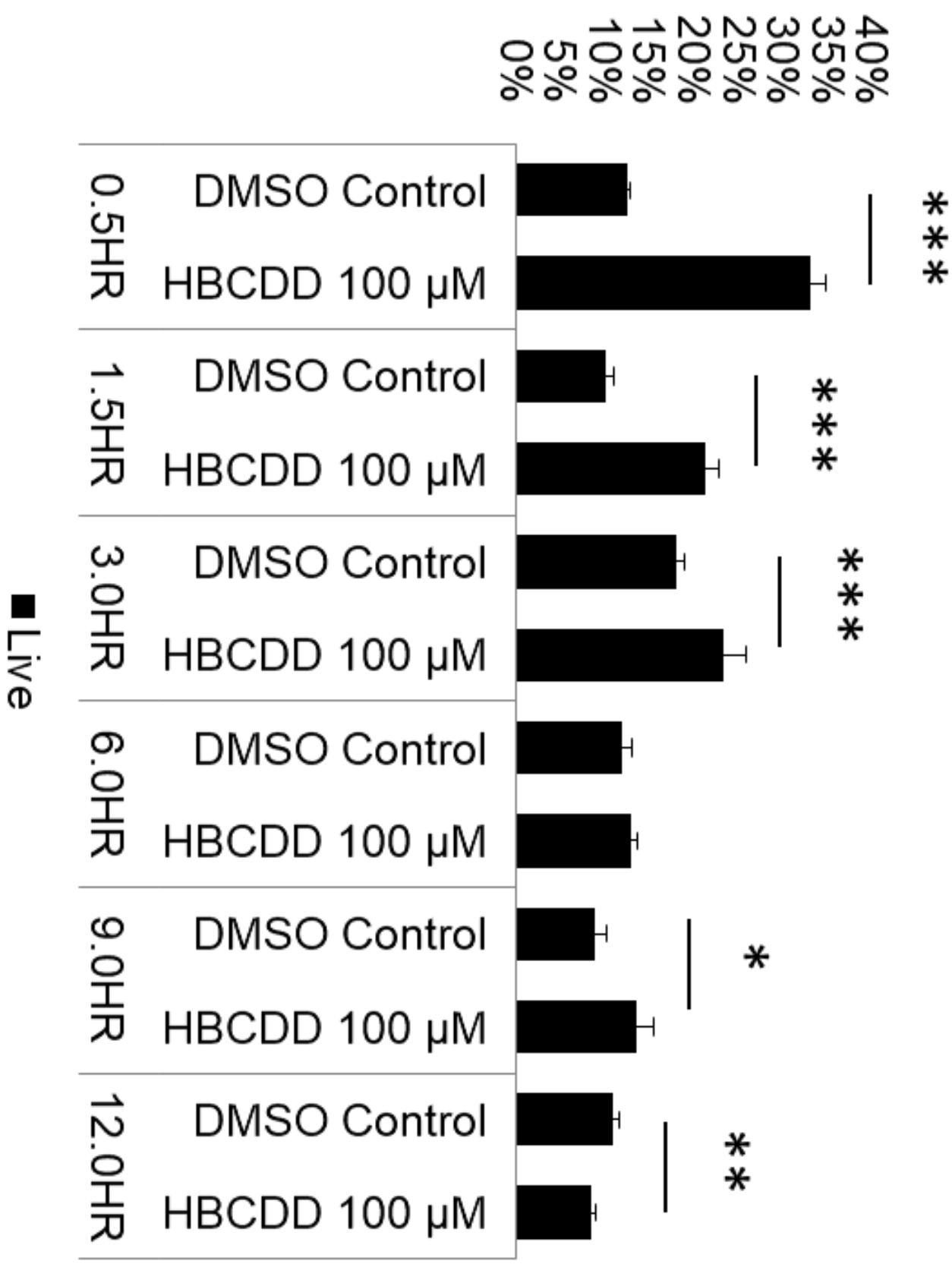
40%
35%
30%
25%
20%
15%
10%
5%
0%
■Live
0.5HR
DMSO Control
HBCDD 100 μM
1.5HR
DMSO Control
HBCDD 100 μM
3.0HR
DMSO Control
HBCDD 100 μM
6.0HR
DMSO Control
HBCDD 100 μM
9.0HR
DMSO Control
HBCDD 100 μM
12.0HR
DMSO Control
HBCDD 100 μM
***
***
***
*
**

Figure 8.10. Acute HBCDD exposure hyperpolarizes the mitochondrial membrane in cells before decreasing cell viability in spermatogenic cells derived from H1 ESCs. Graphical representation showing that acute, twenty-four hour 100 μM HBCDD hyperpolarizes the mitochondrial membrane in H1 ESCS differentiated in *in vitro* spermatogenic conditions in comparison to a 0.2% DMSO-only control. Live cell assessment was performed over twelve hours. 5,000 events were analyzed, with three replications performed for each condition (n = 3). Significant changes in live cell percentages were determined using a 1-way analysis of variance (1-way ANOVA) and validated via a Student's t-test, where * is $p<0.05$, ** is $p<0.01$, and *** is $p<0.001$. Data are represented as mean ± SEM.

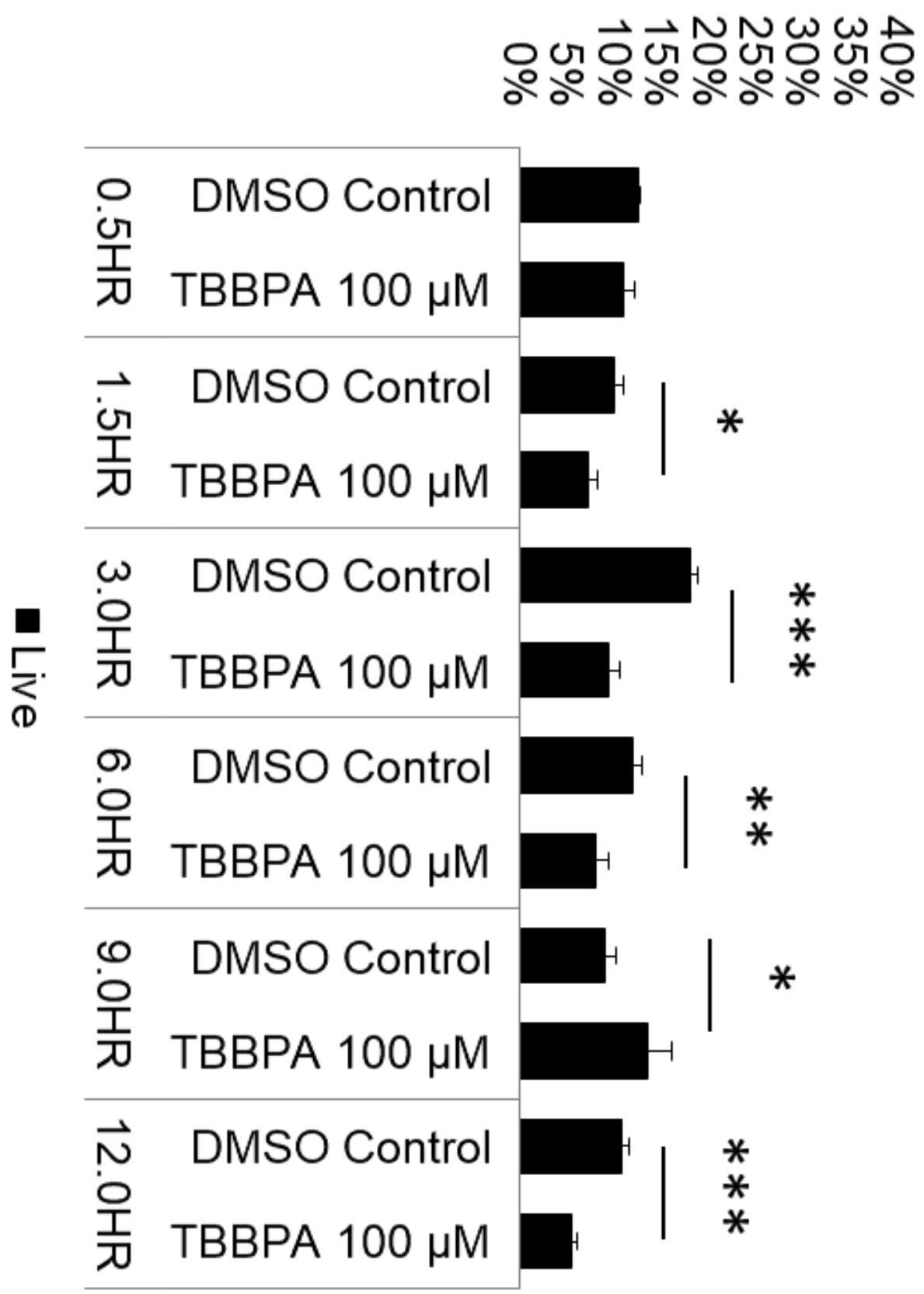
40%
35%
30%
25%
20%
15%
10%
5%
0%
■ Live
0.5HR
DMSO Control
TBBPA 100 µM
1.5HR
DMSO Control
TBBPA 100 µM
*
3.0HR
DMSO Control
TBBPA 100 µM
***
6.0HR
DMSO Control
TBBPA 100 µM
**
9.0HR
DMSO Control
TBBPA 100 µM
*
12.0HR
DMSO Control
TBBPA 100 µM
***

Figure 8.11. Acute TBBPA exposure rapidly decreases cell viability in spermatogenic cells derived from H1 ESCs in a twelve-hour assessment. Graphical representation showing that acute, twenty-four hour 100 μM TBBPA decreases live cell viability in as little as 1.5 hours in H1 ESCS differentiated in *in vitro* spermatogenic conditions in comparison to a 0.2% DMSO-only control. Live cell assessment was performed over twelve hours. 5,000 events were analyzed, with three replications performed for each condition (n = 3). Significant changes in live cell percentages were determined using a 1-way analysis of variance (1-way ANOVA) and validated via a Student's t-test, where * is $p<0.05$, ** is $p<0.01$, and *** is $p<0.001$. Data are represented as mean ± SEM.

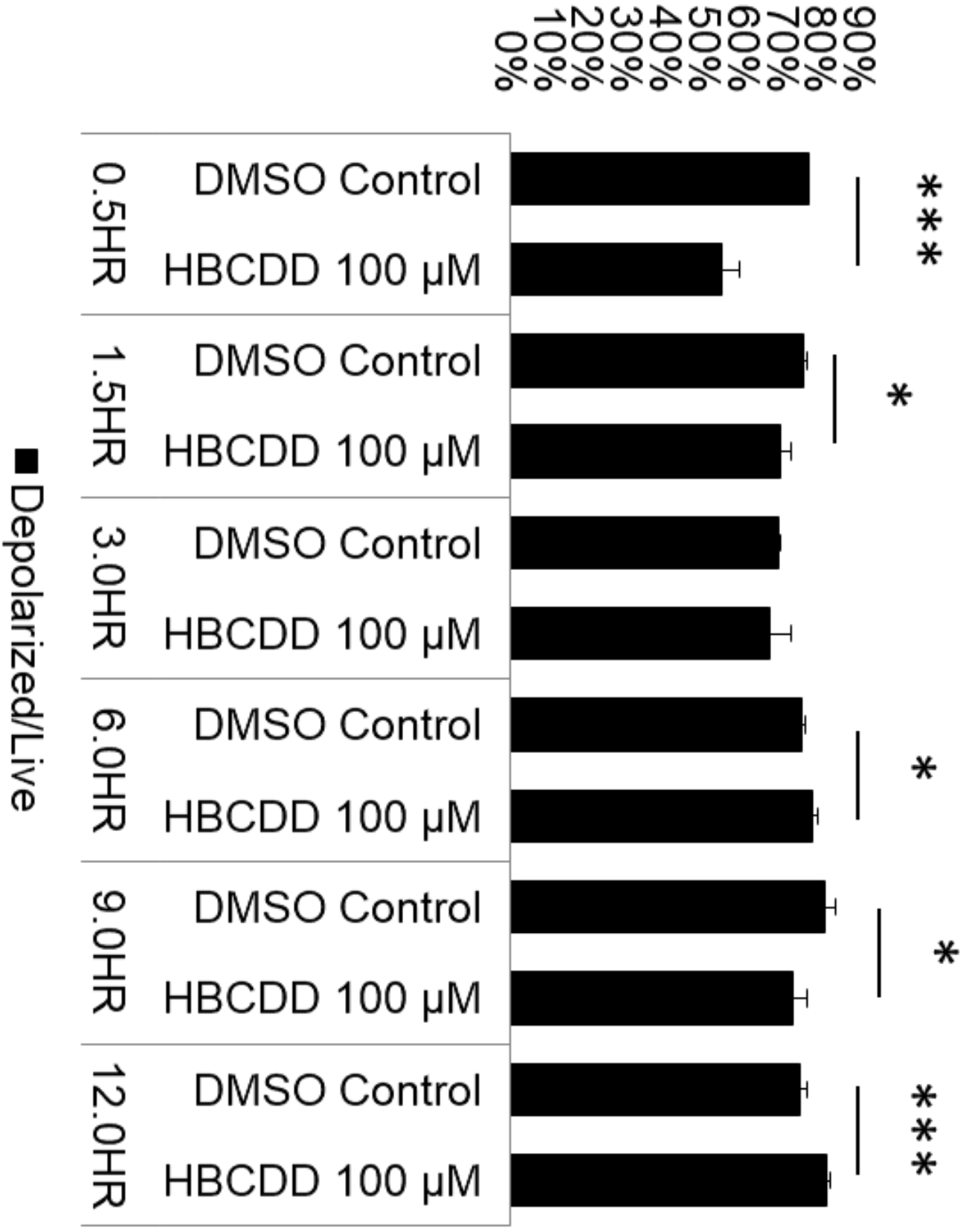
90%
80%
70%
60%
50%
40%
30%
20%
10%
0%
■ Depolarized/Live
0.5HR
DMSO Control
HBCDD 100 µM
1.5HR
DMSO Control
HBCDD 100 µM
3.0HR
DMSO Control
HBCDD 100 µM
6.0HR
DMSO Control
HBCDD 100 µM
9.0HR
DMSO Control
HBCDD 100 µM
12.0HR
DMSO Control
HBCDD 100 µM
***
*
*
*
***

Figure 8.12. Acute HBCDD exposure depolarizes the mitochondrial membrane before causing death in spermatogenic cells derived from H1 ESCs in a twelve-hour assessment. Graphical representation showing that acute, twenty-four hour 100 μM HBCDD decreases mitochondrial membrane potential in approximately 6.0 hours in H1 ESCS differentiated in *in vitro* spermatogenic conditions in comparison to a 0.2% DMSO-only control. Depolarized/live cell assessment was performed over twelve hours. 5,000 events were analyzed, with three replications performed for each condition (n = 3). Significant changes in depolarized/live cell percentages were determined using a 1-way analysis of variance (1-way ANOVA) and validated via a Student's t-test, where * is $p<0.05$, ** is $p<0.01$, and *** is $p<0.001$. Data are represented as mean ± SEM.

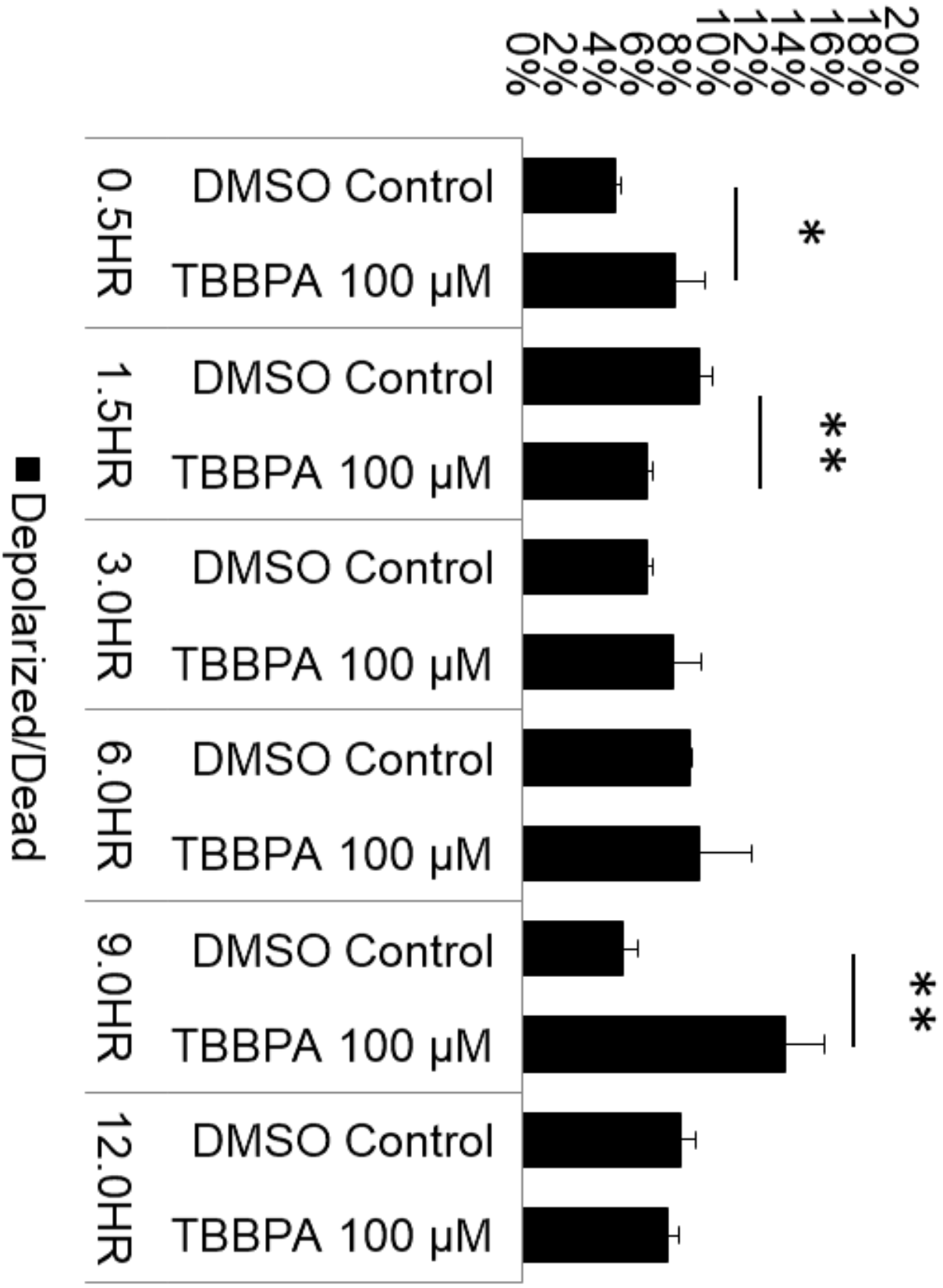
20%
18%
16%
14%
12%
10%
8%
6%
4%
2%
0%
■ Depolarized/Dead
0.5HR
1.5HR
3.0HR
6.0HR
9.0HR
12.0HR
DMSO Control
TBBPA 100 µM
*
**
**

Figure 8.13. Acute TBBPA exposure rapidly depolarizes the mitochondrial membrane before causing death in spermatogenic cells derived from H1 ESCs in a twelve-hour assessment. Graphical representation showing that acute, twenty-four hour 100 μM TBBPA increases mitochondrial membrane depolarization in as little as 0.5 hours in H1 ESCS differentiated in *in vitro* spermatogenic conditions in comparison to a 0.2% DMSO-only control. Depolarized/dead cell assessment was performed over twelve hours. 5,000 events were analyzed, with three replications performed for each condition (n = 3). Significant changes in depolarized/dead cell percentages were determined using a 1-way analysis of variance (1-way ANOVA) and validated via a Student's t-test, where * is $p<0.05$, ** is $p<0.01$, and *** is $p<0.001$. Data are represented as mean ± SEM.

PFOS 24 µM

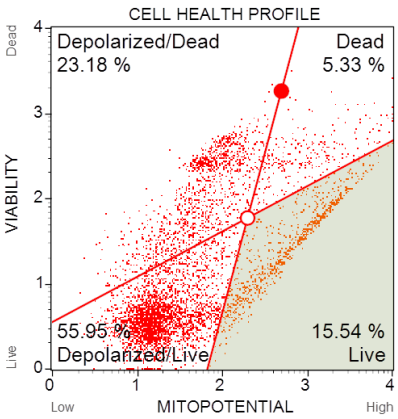

PFOS 48 µM

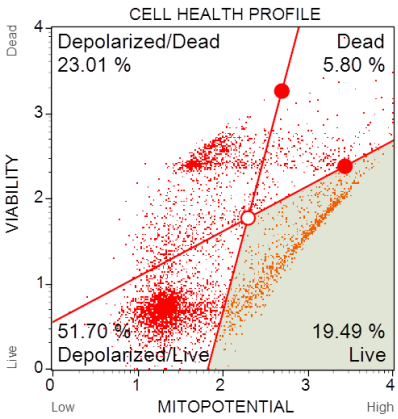

PFOS 126 µM

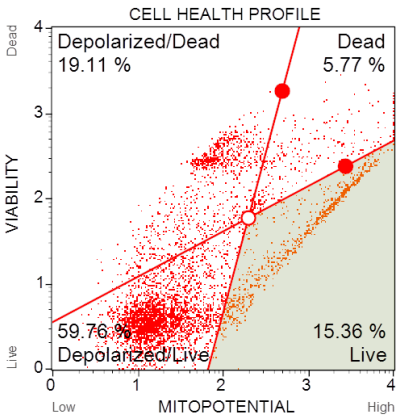

PFOA 11 µM

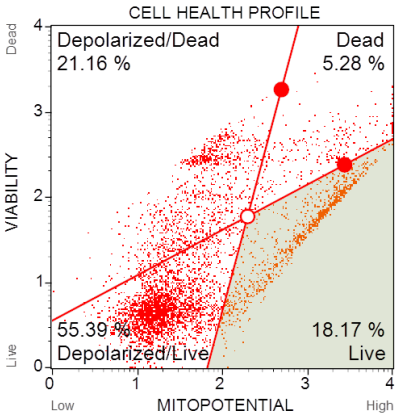

PFOA 25 µM

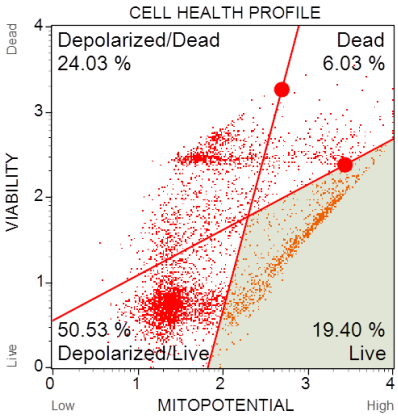

PFOA 100 µM

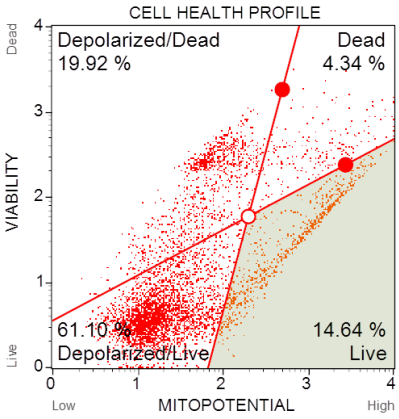

PFNA 2.15 µM

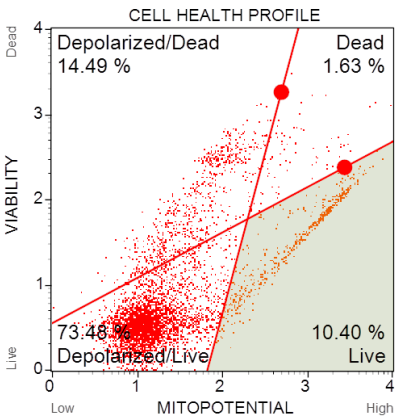

PFNA 21.5 µM

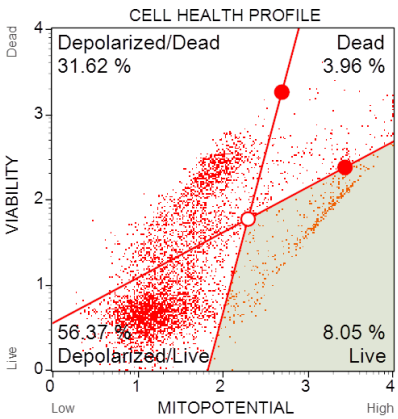

PFNA 43 µM

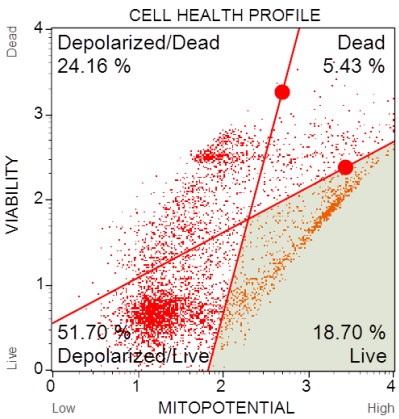

Figure 8.14. Persistent PFOS, PFOA, and PFNA exposure does not impact mitochondrial membrane polarization in spermatogenic cells derived from H1 ESCs. Flow cytometry analyses for indicating percent live cells, percent depolarized/live cells, percent depolarized/dead cells, and percent dead cells. Lower right quadrant represents viable cells, lower left quadrant represents depolarized/live cells, upper right quadrant is depolarized/dead cells, and the upper right quadrant is dead cells.

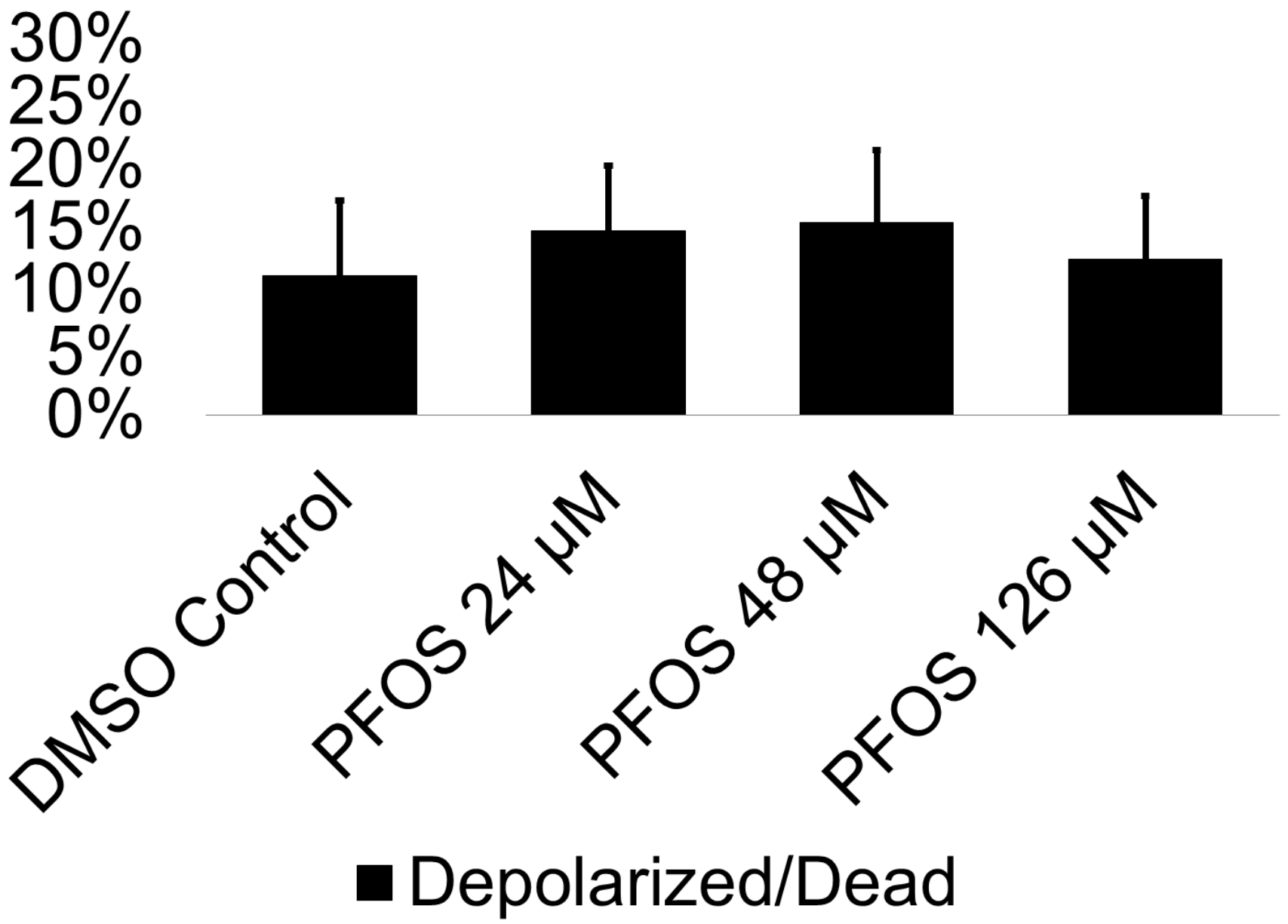
30%
25%
20%
15%
10%
5%
0%
DMSO Control
PFOS 24 µM
PFOS 48 µM
PFOS 126 µM
Depolarized/Dead

Figure 8.15. Persistent PFOS exposure does not impact mitochondrial membrane polarization in spermatogenic cells derived from H1 ESCs. Graphical representation showing that exposure to 24 μM, 48 μM , and 126 μM PFOS from Day 1 to Day 10 does not impact mitochondrial membrane potential or cell viability in H1 ESCS differentiated in *in vitro* spermatogenic conditions in comparison to a 0.25% DMSO-only control. 5,000 events were analyzed, with four replications performed for each condition (n = 4). Significant changes in the percentage of depolarized/dead cells were determined using a 1-way analysis of variance (1-way ANOVA) and validated via a Student's t-test, where * is $p<0.05$, ** is $p<0.01$, and *** is $p<0.001$.

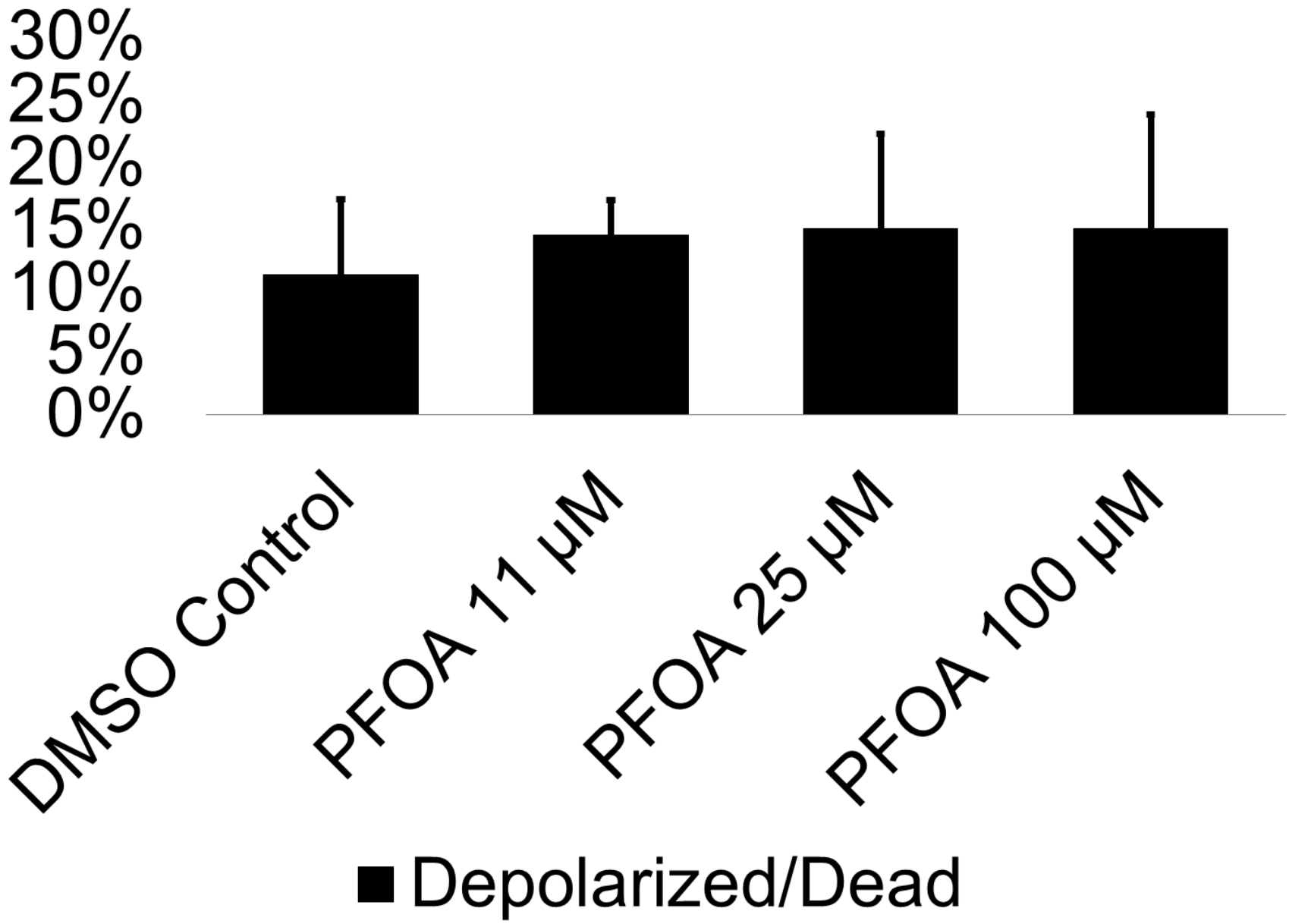
30%
25%
20%
15%
10%
5%
0%
DMSO Control
PFOA 11 µM
PFOA 25 µM
PFOA 100 µM
Depolarized/Dead

Figure 8.16. Persistent PFOA exposure does not impact mitochondrial membrane polarization in spermatogenic cells derived from H1 ESCs. Graphical representation showing that exposure to 11 µM, 25 µM , and 100 µM PFOA from Day 1 to Day 10 does not impact mitochondrial membrane potential or cell viability in H1 ESCS differentiated in *in vitro* spermatogenic conditions in comparison to a 0.25% DMSO-only control. 5,000 events were analyzed, with four replications performed for each condition (n = 4). Significant changes in the percentage of depolarized/dead cells were determined using a 1-way analysis of variance (1-way ANOVA) and validated via a Student's t-test, where * is $p<0.05$, ** is $p<0.01$, and *** is $p<0.001$.

30%
25%
20%
15%
10%
5%
0%
DMSO Control
PFNA 2.15 µM
PFNA 21.5 µM
PFNA 43 µM
Depolarized/Dead

Figure 8.17. Persistent PFNA exposure does not impact mitochondrial membrane polarization in spermatogenic cells derived from H1 ESCs. Graphical representation showing that exposure to 2.15 μM, 21.5 μM , and 43 μM PFNA from Day 1 to Day 10 does not impact mitochondrial membrane potential or cell viability in H1 ESCS differentiated in *in vitro* spermatogenic conditions in comparison to a 0.25% DMSO-only control. 5,000 events were analyzed, with four replications performed for each condition (n = 4). Significant changes in the percentage of depolarized/dead cells were determined using a 1-way analysis of variance (1-way ANOVA) and validated via a Student's t-test, where * is $p<0.05$, ** is $p<0.01$, and *** is $p<0.001$.

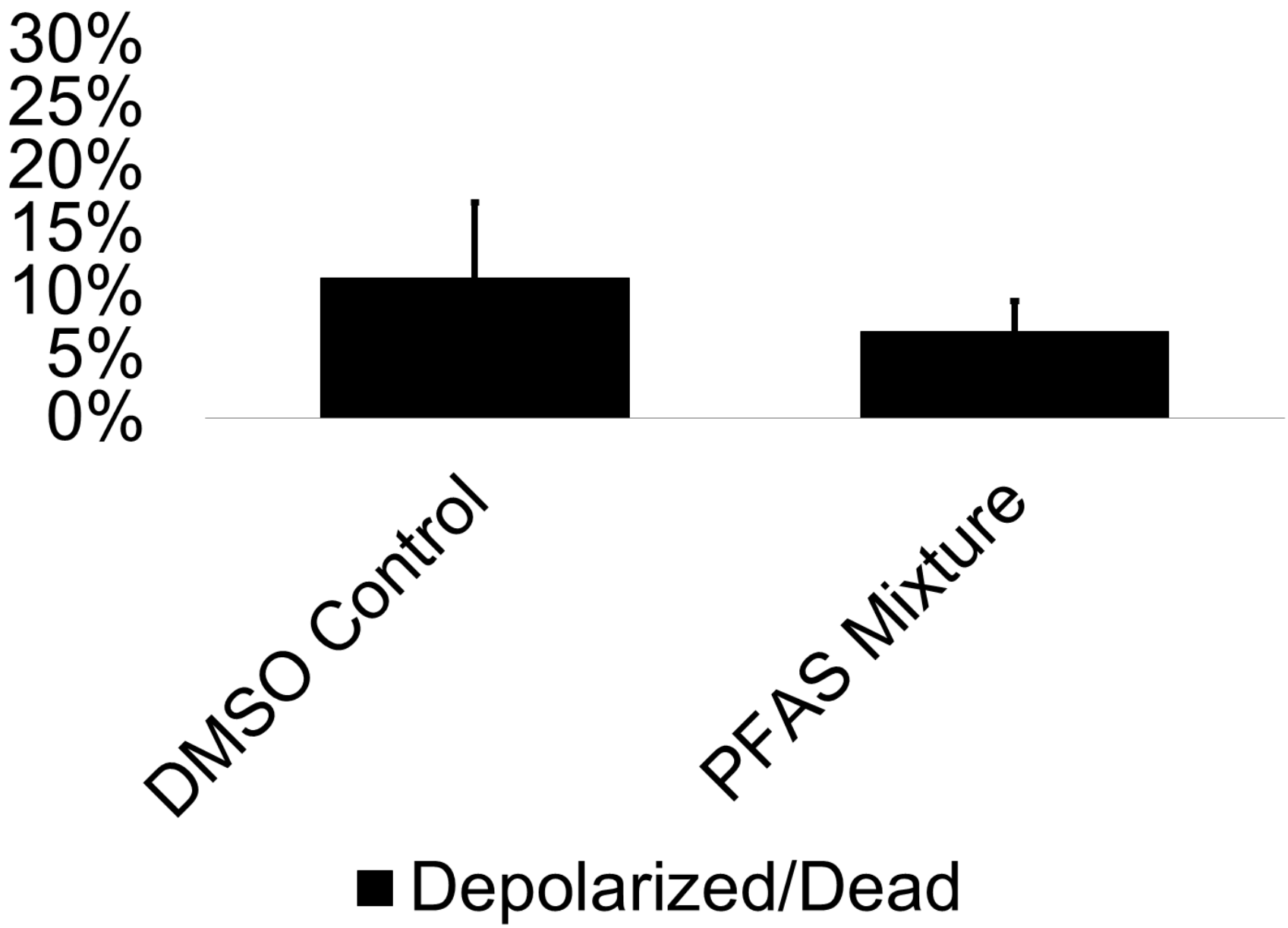
30%
25%
20%
15%
10%
5%
0%
DMSO Control
PFAS Mixture
Depolarized/Dead

Figure 8.18. Persistent PFAS mixture does not impact mitochondrial membrane polarization or cell viability in spermatogenic cells derived from H1 ESCs. Graphical representation showing that exposure to a mixture of 48 μM PFOS, 25 μM PFOA, and 21.5 μM of PFNA from Day 1 to Day 10 does not impact mitochondrial membrane potential or cell viability in H1 ESCs differentiated in *in vitro* spermatogenic conditions in comparison to a 0.25% DMSO-only control. 5,000 events were analyzed, with four replications performed for each condition (n = 4). Significant changes in the percentage of depolarized/ dead cells were determined using a 1-way analysis of variance (1-way ANOVA) and validated via a Student's t-test, where * is $p<0.05$, ** is $p<0.01$, and *** is $p<0.001$.

2.6 Discussion

Few studies on the potential human health effects resulting from halogenated flame retardant exposure exist despite evidence of widespread, everyday exposure to these compounds through direct contact or from ingestion of house dust and other contaminated sources (Weissman and Pan, 2015, Dishaw et al., 2014). In studies that have directly assessed relationships between flame retardants and human male fertility, some flame retardants have been associated with changes in male hormones, though no effects on sperm quantity or quality have ever been reported, and direct changes in spermatogenesis have not been investigated (Cooper et al., 2011, Johnson et al., 2013, Meeker and Stapleton, 2010, Yard et al., 2011). Here, we show that TDCPP, TDBPP, HBCDD, and TBBPA negatively impact the viability of human spermatogenic cell lineages *in vitro* at as little as 1 μM during twenty-four hours of treatment. Specifically, the acute targets of these chemicals appear to be the spermatogonia and primary spermatocytes.

Spermatogonia are the progenitors of primary and secondary spermatocytes and ultimately spermatids and sperm (Neto et al., 2016). Their function involves producing sperm during a male's post-pubertal lifetime by undergoing mitosis to replenish their own population as well as meiosis to produce male gametes (Neto et al., 2016). Spermatogonia are direct targets of the flame retardants we tested, with populations reduced at the lowest concentrations assessed during a twenty-four hour exposure. This finding suggests that males who experience long-term or acute exposure in an occupational setting could experience a depletion of their spermatogonia that could render them infertile over time, yet to date no clinical studies have been undertaken to

examine at-risk populations. Notably, occupational workers could be exposed to concentrations of TDCPP, TDBPP, HBCDD, and TBBPA assessed in this study on a daily basis. The results shown in this study are the result of acute exposure, and occupationally exposed workers may see more detrimental impacts over time. These results also highlight changes that may not be visible in epidemiological data, as sperm, the most common cell type assessed in epidemiological studies, are not the direct targets of these chemicals, and it is unclear how long exposure would have to occur before sperm would be directly affected. Infertility and sterility resulting from reduced populations of spermatogonia may occur long after the exposure occurs and may not be linked to this exposure, thus making these results even more relevant for assessments on occupational workers in the future. Importantly, spermatogonia are also the only spermatogenic cell lineage to exist before puberty. It has been reported that young children are exposed to higher than average concentrations of flame retardants, and reports indicate that this early exposure can lead to low sperm count and other reproductive disorders later in life (Bonde et al., 2016). As such, this research also has implications for childhood exposures to chemicals that could have impacts on fertility during adulthood. It is also notable that spermatogonia exhibited a delayed recovery following removal of the flame retardants tested. While spermatogonia did recover over time, occupational workers are exposed to these toxicants on a daily basis. As such, these chemicals may not be eliminated from their bodies long enough for recovery to occur. This finding suggests that those who have been exposed to higher concentrations of HBCDD and TBBPA may suffer irreversible damage to their fertility. Similar work with TDCPP and TDBPP remains.

Similar to the results with halogenated flame retardants, PFASs also impacted spermatogonia. Most studies examining the impacts PFOS, PFOA, and PFNA on semen parameters do not report declines in semen volume or sperm number (Vested et al., 2013, Toft et al., 2012, Raymer et al., 2012, Kvist et al., 2012, Joensen et al., 2013, Louis et al., 2015, Governini et al., 2015, Specht et al., 2012). Studies in rodents assessing the impact PFASs have on spermatogenesis have shown significant declines in sperm count, in stark contrast to the results found in human studies (Liu et al., 2015, Fan et al., 2005, Kato et al., 2015). Rodent studies have identified Sertoli cells, seminiferous tubules, and the epididymis as targets of PFASs (Liu et al., 2015, Zhang et al., 2014, Kato et al., 2015, Wan et al., 2014, Lu et al., 2016, Qiu et al., 2016). Specifically, PFOS exposure in male CD-1 mice led to decreases in testicular gonadotropin receptors and decreased expression of growth hormone receptor (GHR), insulin-like growth factor 1 receptor precursor (IGF1R), inhibins, and activins (Wan et al., 2011). These impacts were associated with impairment of testicular steroidogenesis resulting in less testosterone and less sperm in the epididymis (Wan et al., 2011). PFAS exposure has similarly been shown to inhibit aromatase in a human placental cell line, further suggesting that they interfere with steroidogenesis (Gorrochategui et al., 2014). While effects of PFAS exposure on steroidogenesis and somatic support cell viability were not tested in this study, our study provides information on the impacts of PFOS, PFOA, and PFNA exposure directly on spermatogenic cells.

Here we report that exposure to PFOS, PFOA, PFNA, and a mixture of PFOS, PFOA, and PFNA do not increase ROS production or cause mitochondrial dysfunction that may lead to germ cell death. Additionally, PFOS, PFOA, and PFNA exposure does

not induce apoptosis of spermatogenic cells or have impacts on the cell cycle or haploid spermatid production. Therefore, our *in vitro* human spermatogenesis model recapitulates the results reported in human cohort studies. This is an important result that further validates our model as a high throughput system for examining direct impacts on human male germ cells. PFOS, PFOA, and PFNA exposure did have impacts on spermatogonia in our *in vitro* model by decreasing PLZF area and intensity at certain concentrations. Though further studies are needed, it is possible that exposure to PFASs inhibits the ability of spermatogonia to maintain their own population. The results of our cell cycle analyses indicate that, in such a case, spermatogonia are still capable of differentiation, but these cells do not continue to self-renew, suggesting terminal differentiation and a potential exhaustion of the spermatogonial stem cell pool.

Similarly, primary spermatocytes are also impacted by exposure to TDCPP, TDCPP, HBCDD, and TBBPA, though the exact impacts these chemicals have on primary spermatocytes is less clear. Primary spermatocytes express HILI, which functions in the male germline to repress transposons, regulate gene expression at the epigenetic, post-transcriptional, and translational levels, and has been implicated in chromosome synapsis during meiosis, among other important processes (Juliano et al., 2011). Significantly, HILI levels are upregulated upon exposure to our halogenated flame retardants at low to moderate levels. HILI levels do decrease at higher chemical concentrations for both chemicals assessed, and studies have shown that decreases in HILI expression lead to apoptosis in primary spermatocytes (Juliano et al., 2011). Perhaps most importantly, the results of this study do not suggest that primary

spermatocytes undergo cell death in response to chemical exposure to the same extent as spermatogonia. Spermatogonia are capable of recovery following HBCDD and TBBPA exposure, though primary spermatocytes do not recover from TBBPA exposure, even after a five day recovery.

Additionally, HILI area and intensity decreased upon exposure to PFOS and PFOA, though this decrease is likely not due to death of primary spermatocytes or cell cycle arrest. Specific transcription factors for HILI expression in male germ cells have not been identified, and it is unclear how exposure to PFASs could impact HILI expression. Importantly, HILI maintains germline integrity by repressing transposable elements during meiosis, regulating gene expression at the epigenetic, post-transcriptional, and translational levels in primary spermatocytes, and through involvement in chromosome synapsis during meiosis (Juliano et al., 2011). A decrease in HILI expression could result in activated retrotransposons, aberrant gene expression, and failure of cells to undergo meiosis properly.

Decreased viability of spermatogonia and primary spermatocytes occurred via apoptosis at higher halogenated flame retardant concentrations, highlighting a disconnect between apoptotic data and immunostaining results for PLZF, where cell populations were decreased at even the lowest concentration. Mitochondrial membrane potential data suggests that our *in vitro* cultures are sensitive to flame retardant toxicants at lower concentrations, which have implications for occupationally exposed workers. Mitochondria have been called the “canary” of cell health, and our results indicate that they may be susceptible to toxicants earlier than other processes and act as an early warning system for cell health in contrast to apoptotic and ROS markers.

Decreasing mitochondrial function is often paired with increasing ROS generation, though only TBBPA showed increases in ROS capable of overwhelming the cell's defense mechanisms, with the first signs of ROS beginning to overwhelm cell defenses at nine hours post-exposure. The mitochondrial membrane depolarization data suggest different mechanisms of toxicity for HBCDD and TBBPA despite having similar end results. HBCDD exposure causes an immediate shift to a more negative, hyperpolarized mitochondrial state that inevitably leads to depolarization and death. The results of this study point to HBCDD utilizing a mechanism of toxicity that is distinctly different from recognized male reproductive toxicants, such as 2-BP and DBCP. Possibly, mitochondria may be the direct target of HBCDD, though further studies are required. TBBPA exposure, however, shows an opposite mechanism to HBCDD, with depolarization occurring in the first 1.5 hours followed by death. This depolarization is likely due to assault by ROS, as this was identified as the main mechanism of cell death for TBBPA following *l*-sulforaphane rescue. However, cell death, whether it is through mitochondrial dysfunction or another mechanism, may not be the only explanation for decreases in spermatogonia and primary spermatocyte populations. Though this was a twenty-four hour exposure, cell cycle profiles revealed that our chemicals can arrest our cultures during cell division. Alternatively, or perhaps in conjunction with cell death, it is possible that our chemicals at higher concentrations block differentiation from spermatogonia to primary and secondary spermatocytes and spermatids by arresting cells during mitosis and meiosis, although longer term studies will need to be conducted to fully elucidate this mechanism. Further studies are needed to elucidate mechanisms for TDCPP and TDBPP.

Our *in vitro* human stem cell model of spermatogenesis has revealed for the first time that the flame retardants TDCPP, TDBPP, HBCDD and TBBPA can directly impact human spermatogenesis. These results highlight the need for more data regarding the prevalence of these toxicants in the human system and the need for additional experiments to understand how TDCPP, TDBPP, HBCDD, and TBBPA may alter spermatogenesis and male fertility, especially at persistent concentrations that are relevant to occupationally exposed workers. It must be stressed that spermatogonia and primary spermatocytes were impacted at occupationally relevant concentrations after only one day of exposure *in vitro*. Additionally, as semen parameters continue to plummet in the Western male with no definitive cause, further investigation into TDCPP, TDBPP, HBCDD, and TBBPA's potential to impact male fertility is highly recommended, as the average person is also exposed to these chemicals on a daily basis. Finally, though they have different core structures, the halogenated flame retardants TDCPP, TDBPP, HBCDD, and TBBPA had similar impacts on human spermatogenesis. This suggests that this class of chemicals could be as detrimental as their PCB and PBDE predecessors and stresses the need for continued studies on their potential health impacts. However, despite having similar properties, the PFASs used in this study, despite being present for ten times longer, were nowhere near as detrimental as halogenated flame retardants on *in vitro* spermatogenesis. PFOS, PFOA, and PFNA are distinctly different from TDCPP, TDBPP, HBCDD, and TBBPA in not only structure, but also type and number of halogens. It is possible the fluorine may be less toxic than bromine or chlorine halogens. Alternatively, increasing the number of halogens on a

structure may decrease a compound’s toxicity. Future studies are needed to assess these theories.

Chapter 3: General Discussion and Future Directions

3.1 Introduction

Spermatogonia are the foundation for spermatogenesis, serving as progenitor cells for primary spermatocytes, secondary spermatocytes, and ultimately, spermatids capable of fertilization while simultaneously maintaining their own population through self-renewing divisions (Valli et al., 2014). Balance between differentiation versus self-renewal is maintained through asymmetric division of spermatogonia by promyelocytic leukemia zinc finger (PLZF), GDNF family receptor alpha-1 (GFRα1), and undifferentiated embryonic cell transcription factor 1 (UTF1) (Zhou et al., 2015). PLZF and GFRα1 are required for the self-renewal of spermatogonia, while loss of PLZF and expression of UTF1 occurs in the subset of spermatogonia that will differentiate (Zhou et al., 2015).

PLZF is a transcription factor belonging to the POZ-Krüppel-like (POK) zinc finger family of proteins (Liu et al., 2016c). PLZF is expressed in a tissue- and age-specific fashion and plays a role in cell proliferation, differentiation, and development in processes ranging from embryonic limb patterning, spermatogenesis, and neurogenesis (Pearson et al., 2008, Cook et al., 1995, Liu et al., 2016c). PLZF associates with the Polycomb protein BMI1, as well as nuclear co-repressors SMRT, N-CoR, Sin-3, and class I and II histone acetylases, to regulate the epigenetic repression of target chromatin domains (Barna et al., 2002, Hong et al., 1997, He et al., 1998, David et al., 1998, Buaas et al., 2004). PLZF is thought to regulate the epigenetic repression of chromatin domains required for cell differentiation (Buaas et al., 2004). PLZF additionally acts as a transcriptional activator (Labbaye et al., 2002, Kolesnichenko and

Vogt, 2011). PLZF activates the transcription of Regulated in Development and DNA Damage responses 1 (REDD1), which inhibits activation of TORC1 by disruption of the TSC1/TSC2 complex and inhibition of RHEB-mediated activation (Brugarolas et al., 2004, Kolesnichenko and Vogt, 2011). This positive regulation of REDD1 enables the maintenance of pluripotency in spermatogonia (Kolesnichenko and Vogt, 2011, Hobbs et al., 2010).

Loss of PLZF has been shown to lead to a loss of spermatogonia, and thus an increased incidence of male infertility (Dadoune, 2007, Buaas et al., 2004, Costoya et al., 2004, Kotaja and Sassone-Corsi, 2004). Male mice homozygous for the luxoid mutation, a nonsense mutation in *Zfp145*, which encodes *Plzf* in mice, produce limited numbers of sperm and become infertile through progressive germ cell loss (Buaas et al., 2004). Similarly, the generation of *Zfp145*$^{-/-}$ null mice results in gradual germ cell loss with increasing age (Costoya et al., 2004). Defects in *Zfp145*$^{-/-}$ resemble the clinical characteristics of male infertility (Costoya et al., 2004). On the genetic level, *Zfp145*$^{-/-}$ mice show changes in the expression of genes required for spermatogenesis, including the genes required for spermatogonia differentiation (Costoya et al., 2004).

We have identified PLZF as a target of the halogenated flame retardants (FRs) tris(1,3-dichloro-2-propyl) phosphate (TDCPP), tris(2,3-dibromopropyl) phosphate (TDBPP), hexabromocyclododecane (HBCDD), and tetrabromobisphenol A (TBBPA) . Under acute conditions relevant to occupational exposure conditions, exposure to FRs at concentrations at as little as 1 µM can decrease PLZF expression by over 20% (Figures 4.1 – 4.9) (Steves et al., 2018a). This decline in PLZF is not matched by cell

death, indicating that the decline in PLZF expression is not from the loss of spermatogonia but due to direct effects on PLZF expression itself (Steves et al., 2018a).

The results from these experiments indicate that the halogenated FRs TDCPP, TDBPP, HBCDD, and TBBPA impact PLZF expression in multiple, distinctly different genetic backgrounds. However, results for some chemicals in some genetic backgrounds do not match the results from acute studies, and different genetic backgrounds may also have different responses to the same chemicals, highlighting how genetics plays an important role in processing chemical toxicity.

We have previously identified spermatogonia as targets of TDCPP, TDBPP, HBCDD, and TBBPA under acute, occupationally relevant conditions in a mixed population of spermatogonia, primary spermatocytes, secondary spermatocytes, and spermatids *in vitro* (Figures 4.1 – 4.9) (Steves et al., 2018a). TDCPP, TDBPP, HBCDD, and TBBPA decrease PLZF, a marker for spermatogonia, by as much as 20% at 1 μM during a twenty-four hour exposure (Figures 4.1 – 4.9) (Steves et al., 2018a). However, this decline in PLZF was not matched by increases in apoptosis, indicating that spermatogonia may be impacted by halogenated FR exposure via mechanisms that do not result in cell death (Figures 3.1 – 3.17) (Steves et al., 2018a). Because PLZF is critical to the balance between self-renewal and differentiation in spermatogonia, decreases in PLZF expression could block differentiation, or alternatively, skew the balance of self-renewal versus differentiation to a terminally differentiated fate (Kolesnichenko and Vogt, 2011, Hobbs et al., 2010, Buaas et al., 2004). To investigate the mechanism by which flame retardant exposure impacts PLZF expression, stem cell lines H1, H13, and H23 were differentiated into spermatogonia, primary and secondary

spermatocytes, and haploid spermatids. Including two additional, distinctly different genetic backgrounds for these experiments allows for the investigation into how genetics may influence this process. SSC differentiations were treated with chemicals beginning on Day 3. This treatment more accurately recapitulates adult spermatogenesis, as spermatogenesis has been initiated at this point. Treatment with 10 nM, 100 nM, 500 nM, 1 μM, and 5 μM TDCPP, TDBPP, HBCDD, and TBBPA began on Day 3 and continued for an additional ten days to Day 12, representing a chronic exposure to these FRs at concentrations found in the blood of the general population as well as occupationally exposed workers (Thomsen et al., 2007, Li et al., 2014b, Jakobsson et al., 2002, Cariou et al., 2008, Liu et al., 2016b). Treatment groups were compared to a 0.2% DMSO-only negative control.

3.2 Methods

Methods are described in section 2.4, page 43.

3.3 Results

Persistent exposure to 10 nM, 100 nM, 500 nM, 1 μM, and 5 μM from Day 3 to Day 12 in H1 SSCs began impacting PLZF area and expression at as little as 100 nM, though intensity was not impacted until 1 μM, suggesting that persistent TDCPP exposure may be impacting the cell cycle of spermatogonia in this genetic background, not PLZF expression (Figures 9.1 and 9.5). PLZF area decreased by as much as 16% at 5 μM (Figure 9.1) Persistent exposure to TDBPP in the H1 genetic background decreased area beginning at 10 nM and intensity beginning at 500 nM, suggesting the potential for both a cell cycle issue and direct impacts on PLZF expression (Figures 9.2 and 9.6). PLZF area decreased by as much as 27% at 500 nM, and PLZF intensity

decreased by 13% (Figures 9.2 and 9.6). In the H1 genetic background, PLZF area displayed an S-phase non-monotonic dose response in response to HBCDD exposure beginning at 10 nM, with a 12% increase in PLZF area (Figure 9.3). HBCDD intensity began increasing at 10 nM, with a 32% increase in intensity that could suggest that HBCDD exposure could drive expression of PLZF in this genetic background (Figure 9.7). Similarly, TBBPA area and intensity began increasing at as little as 100 nM and 10 nM, respectively, with respective 15% and 17% increases at 5 μM (Figures 9.4 and 9.8).

In contrast with the H1 SSC genetic background, exposure to persistent TDCPP in the H23 SSC genetic background decreases PLZF area and intensity beginning at 500 nM and 100 nM, respectively (Figures 9.9 and 9.13). PLZF area and intensity decrease by as much as 32% and 12% at 5 μM (Figures 9.9 and 9.13). TDBPP exposure also decreases PLZF area and intensity beginning at 10 nM and 500 nM, respectively, with 14% and 13% at 5 μM and 1 μM, respectively (Figures 9.10 and 9.14). In the H23 SSC background, HBCDD exposure increases PLZF area only at 100 nM and may have a U-shaped non-monotonic dose response on PLZF intensity (Figures 9.11 and 9.15). HBCDD increases PLZF area at 100 nM by 20% (Figure 9.11). TBBPA exposure decreases PLZF area in the H23 SSC genetic background at 10 nM by 10% but increases intensity at 100 nM by 11%, suggesting dose-specific responses (Figures 9.12 and 9.16).

The H13 SSC genetic background also exhibits unique responses to chronic halogenated FR exposure. TDCPP and TBBPA exposure does not impact PLZF area or intensity at any concentration, suggesting a more robust anti-oxidant response system in this genetic background (Figures 9.17, 9.20, 9.21, and 9.24). Additionally, TDBPP

only impacts PLZF area and intensity at 5 μM, decreasing area and intensity by 14% and 15%, respectively (Figures 9.18 and 9.22). PLZF area exhibits a non-monotonic dose response in response to HBCDD exposure, with area decreasing beginning at 10 nM (Figure 9.19). HBCDD intensity decreases on at 5 μM (Figure 9.23). PLZF area and intensity decrease by 41% and 37%, respectively (Figures 9.19 and 9.23).

3.4 Discussion

Results from the persistent exposure experiments reveal that TDCPP, TDBPP, HBCDD, and TBBPA have different mechanisms depending on exposure type. Acute TDCPP, TDBPP, HBCDD, and TBBPA had shown that spermatogonia were the targets of each chemical; however, each chemical had different impacts on PLZF expression in spermatogonia under persistent conditions. These differences indicated cell cycle arrest, decreases in PLZF expression that may be consistent with the initial hypothesis, and evidence that some chemicals may drive PLZF depending on cell line used. Because each cell line was derived from a uniquely different blastocyst, this result suggests that genetics may factor into how flame retardant exposure impacts PLZF exposure. Impacts each chemical had on PLZF expression were also concentration dependent, with some chemicals eliciting changes only at low doses, only at high doses, in a dose-dependent manner, or following a non-monotonic dose response. Additionally, genetic background greatly influenced how TDCPP, TDBPP, HBCDD, and TBBPA impacted PLZF expression. H13 ESCs showed largely no response to TDCPP and TBBPA, but higher concentrations of HBCDD impacted PLZF expression in this genetic background. In the H1 SSC genetic background, HBCDD also appeared to impact PLZF expression, though whereas PLZF expression decreased in H13, PLZF

expression increased in the H1 SSC genetic background at the highest concentration of PLZF. In the H23 genetic background, TDCPP had the most impact on PLZF expression, decreasing both PLZF area and intensity. Because H1 and H13 were derived at the same time and under the same conditions, it is unlikely that differences between these two lines are the result of age or derivation methods, further suggesting that genetics may explain the different results between these two genetic backgrounds (Thomson et al., 1998). However, H23 was not derived under the same conditions as H1 and H13 and leaves open the possibility that differences in how and when this line was derived could explain some of the differences in PLZF expression seen.

While the acute flame retardant results had begun to tease apart mechanistic differences between flame retardants, these results indicate that halogenated flame retardants, despite being the same class of chemicals, have radically different impacts on PLZF expression and spermatogonia. Perhaps alarmingly, these impacts are not dose dependent, though they are also genetic background dependent. The implications this has for epidemiological studies are troubling. These results indicate that different concentrations can have radically different results. It also indicates that there may be a fine line when determining exposure groups (i.e. low-, medium-, and high-risk groups). The non-monotonic dose responses indicate that the wrong categorization of individuals can have detrimental impacts on results. Additionally, generalizations cannot be made on groups of people because of genetic variation. It is critical that we identify the genes responsible for attenuating reproductive toxicity, and we must analyze people accordingly.

Finally, these experiments focused on the impacts of TDCPP, TDBPP, HBCDD, and TBBPA on adult spermatogenesis. However, the literature suggests that exposures that happen *in utero* can have more severe results on spermatogenesis. In the future, it would be worthwhile to worthwhile to examine the window of exposure where ESCs give rise to spermatogonia to simulate *in utero* impacts of FR exposure.

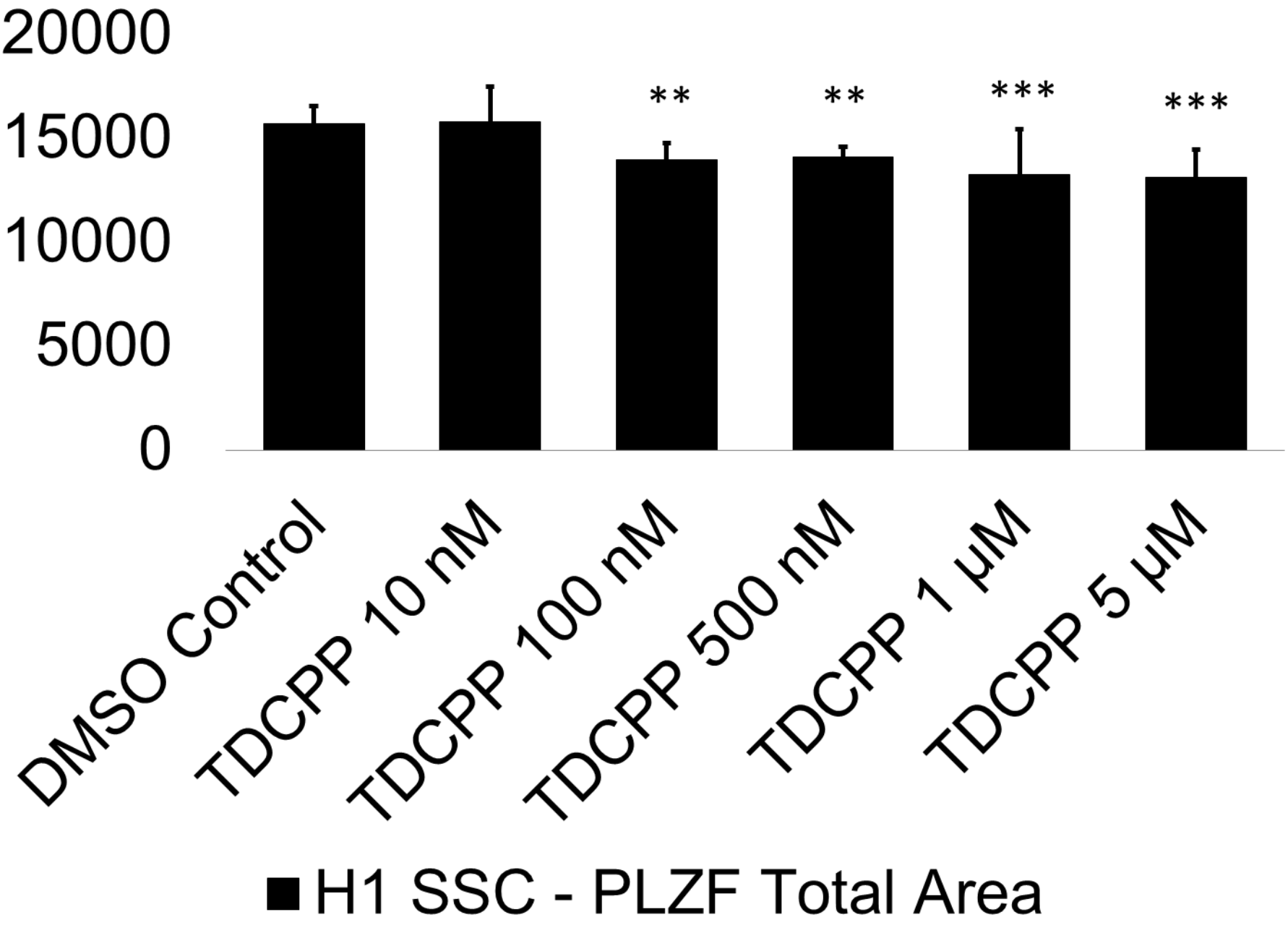
20000
15000
10000
5000
0
**
**
***
***
DMSO Control
TDCPP 10 nM
TDCPP 100 nM
TDCPP 500 nM
TDCPP 1 µM
TDCPP 5 µM
H1 SSC - PLZF Total Area

Figure 9.1. Persistent TDCPP exposure decreases PLZF+ area in in vitro-derived spermatogenic cells (H1 SSC). Graphical representation showing declines in average PLZF+ area in comparison to 0.2 % DMSO-only control in spermatogonia derived under *in vitro* spermatogenic conditions from H1 ESCs and treated with 100nM, 500 nM, 1 μM, and 5 μM TDCPP from Day 3 to Day 12. Three replications were performed for each condition. Significant changes in PLZF+ area were determined using a 1-way analysis of variance (1-way ANOVA) and validated via a Student's t-test, where * is $p<0.05$, ** is $p<0.01$, and *** is $p<0.001$. Data are represented as mean ± SEM.

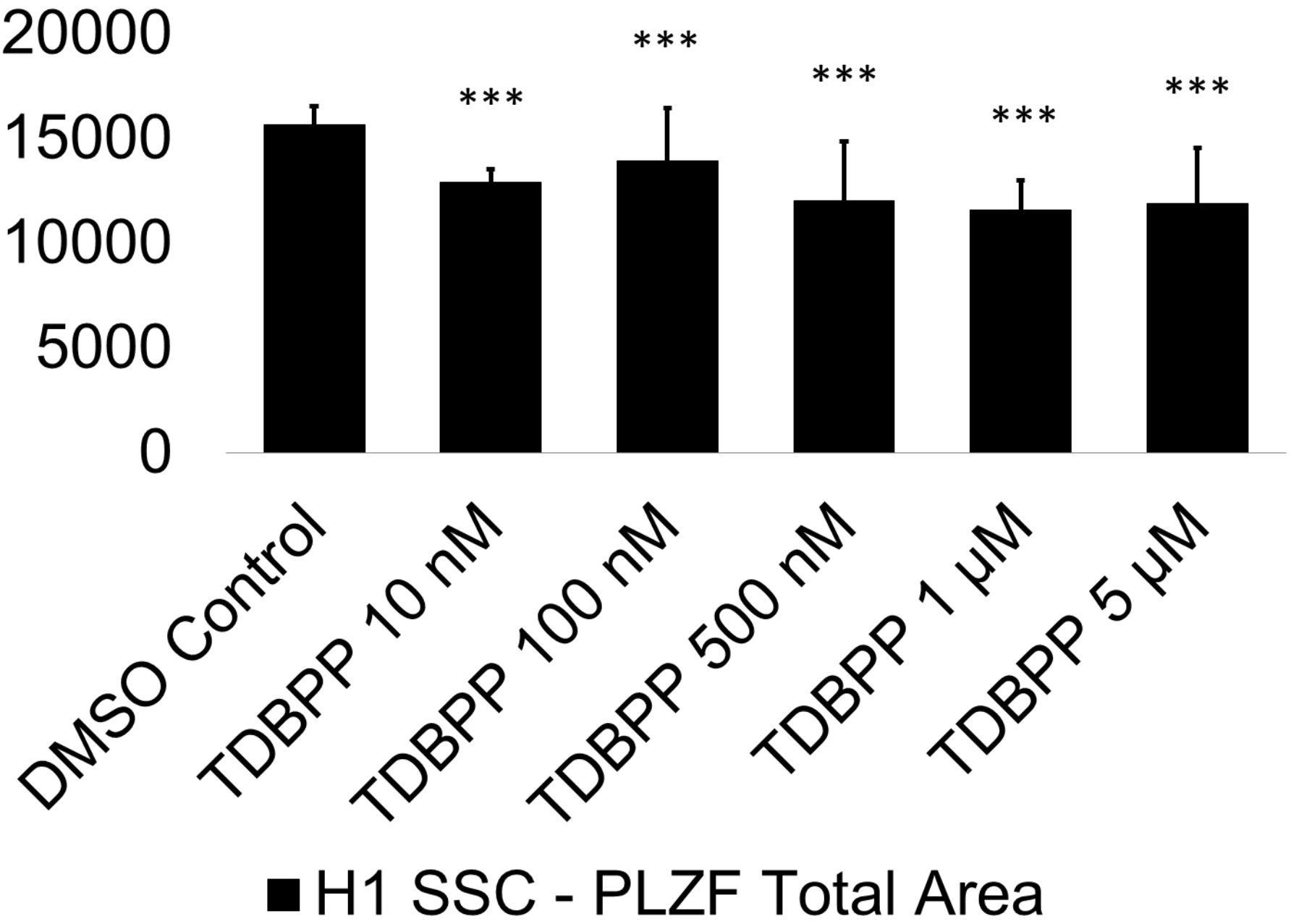
20000
15000
10000
5000
0
***
***
***
***
***
DMSO Control
TDBPP 10 nM
TDBPP 100 nM
TDBPP 500 nM
TDBPP 1 µM
TDBPP 5 µM
H1 SSC - PLZF Total Area

Figure 9.2. Persistent TDBPP exposure decreases PLZF+ area in in vitro-derived spermatogenic cells (H1 SSC). Graphical representation showing declines in average PLZF+ area in comparison to 0.2 % DMSO-only control in spermatogonia derived under *in vitro* spermatogenic conditions from H1 ESCs and treated with 10 nM, 100nM, 500 nM, 1 μM, and 5 μM TDBPP from Day 3 to Day 12. Three replications were performed for each condition. Significant changes in PLZF+ area were determined using a 1-way analysis of variance (1-way ANOVA) and validated via a Student's t-test, where * is $p<0.05$, ** is $p<0.01$, and *** is $p<0.001$. Data are represented as mean ± SEM.

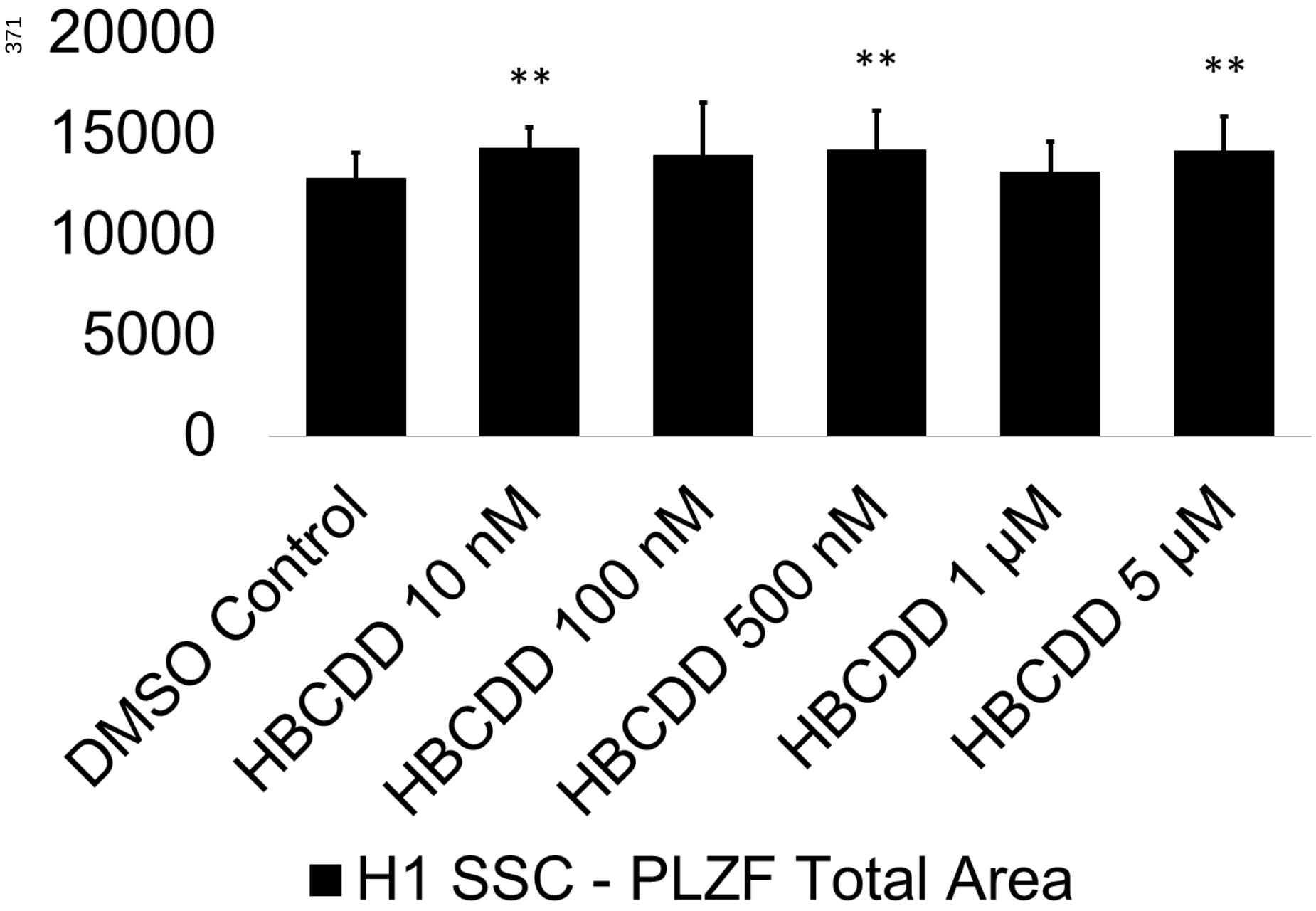
20000
15000
10000
5000
0
**
**
**
DMSO Control
HBCDD 10 nM
HBCDD 100 nM
HBCDD 500 nM
HBCDD 1 µM
HBCDD 5 µM
H1 SSC - PLZF Total Area

Figure 9.3. Persistent HBCDD exposure impacts PLZF+ area in in vitro-derived spermatogenic cells (H1 SSC). Graphical representation showing S-phase non-monotonic dose response increases in average PLZF+ area in comparison to 0.2 % DMSO-only control in spermatogonia derived under *in vitro* spermatogenic conditions from H1 ESCs and treated with 10 nM, 100nM, 500 nM, 1 μM, and 5 μM HBCDD from Day 3 to Day 12. Three replications were performed for each condition. Significant changes in PLZF+ area were determined using a 1-way analysis of variance (1-way ANOVA) and validated via a Student's t-test, where * is $p<0.05$, ** is $p<0.01$, and *** is $p<0.001$. Data are represented as mean ± SEM.

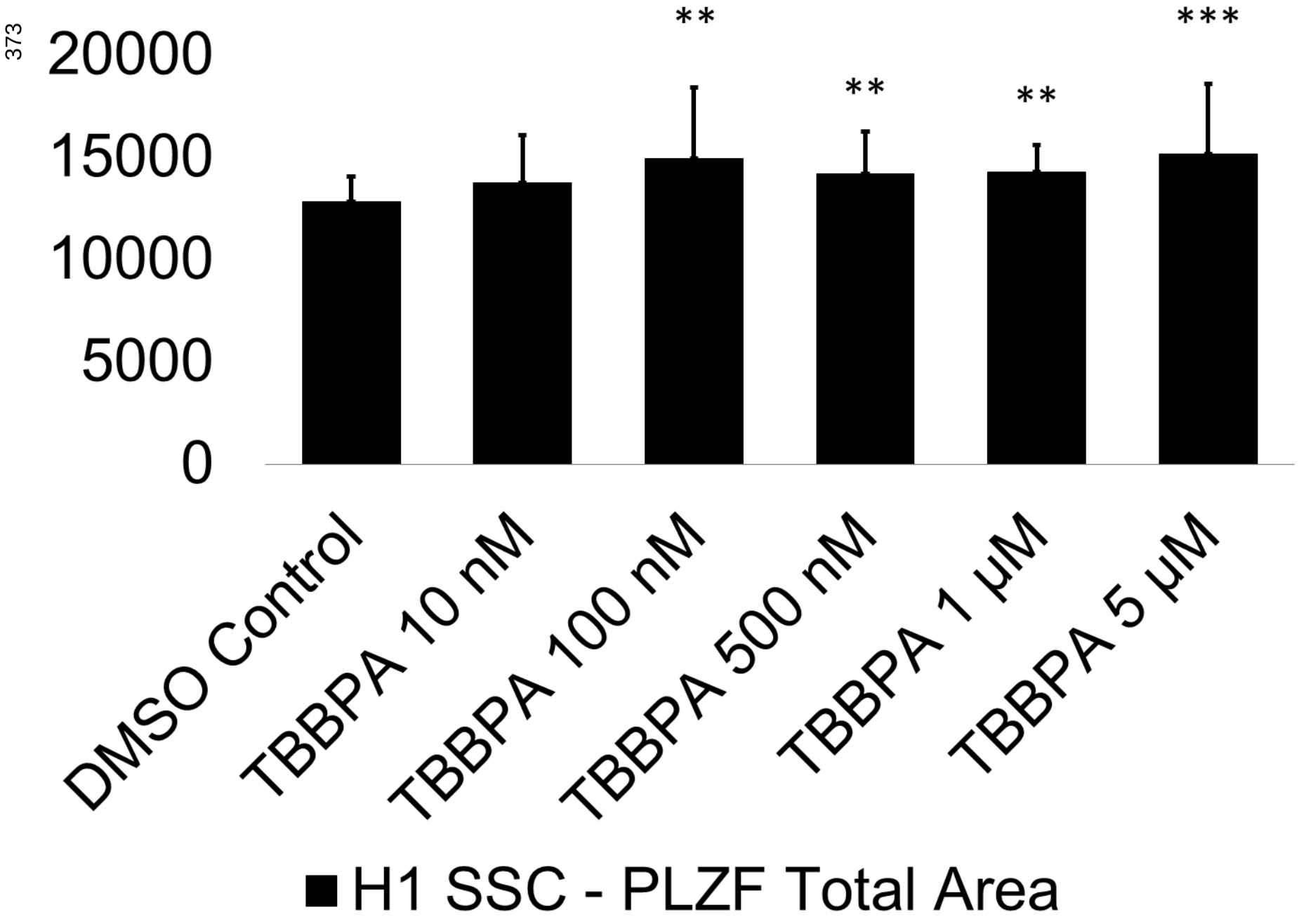
20000
15000
10000
5000
0
**
**
**
***
DMSO Control
TBBPA 10 nM
TBBPA 100 nM
TBBPA 500 nM
TBBPA 1 µM
TBBPA 5 µM
H1 SSC - PLZF Total Area

Figure 9.4. Persistent TBBPA exposure increases PLZF+ area in in vitro-derived spermatogenic cells (H1 SSC). Graphical representation showing increases in average PLZF+ area in comparison to 0.2 % DMSO-only control in spermatogonia derived under *in vitro* spermatogenic conditions from H1 ESCs and treated with 100nM, 500 nM, 1 μM, and 5 μM TBBPA from Day 3 to Day 12. Three replications were performed for each condition. Significant changes in PLZF+ area were determined using a 1-way analysis of variance (1-way ANOVA) and validated via a Student's t-test, where * is $p<0.05$, ** is $p<0.01$, and *** is $p<0.001$. Data are represented as mean ± SEM.

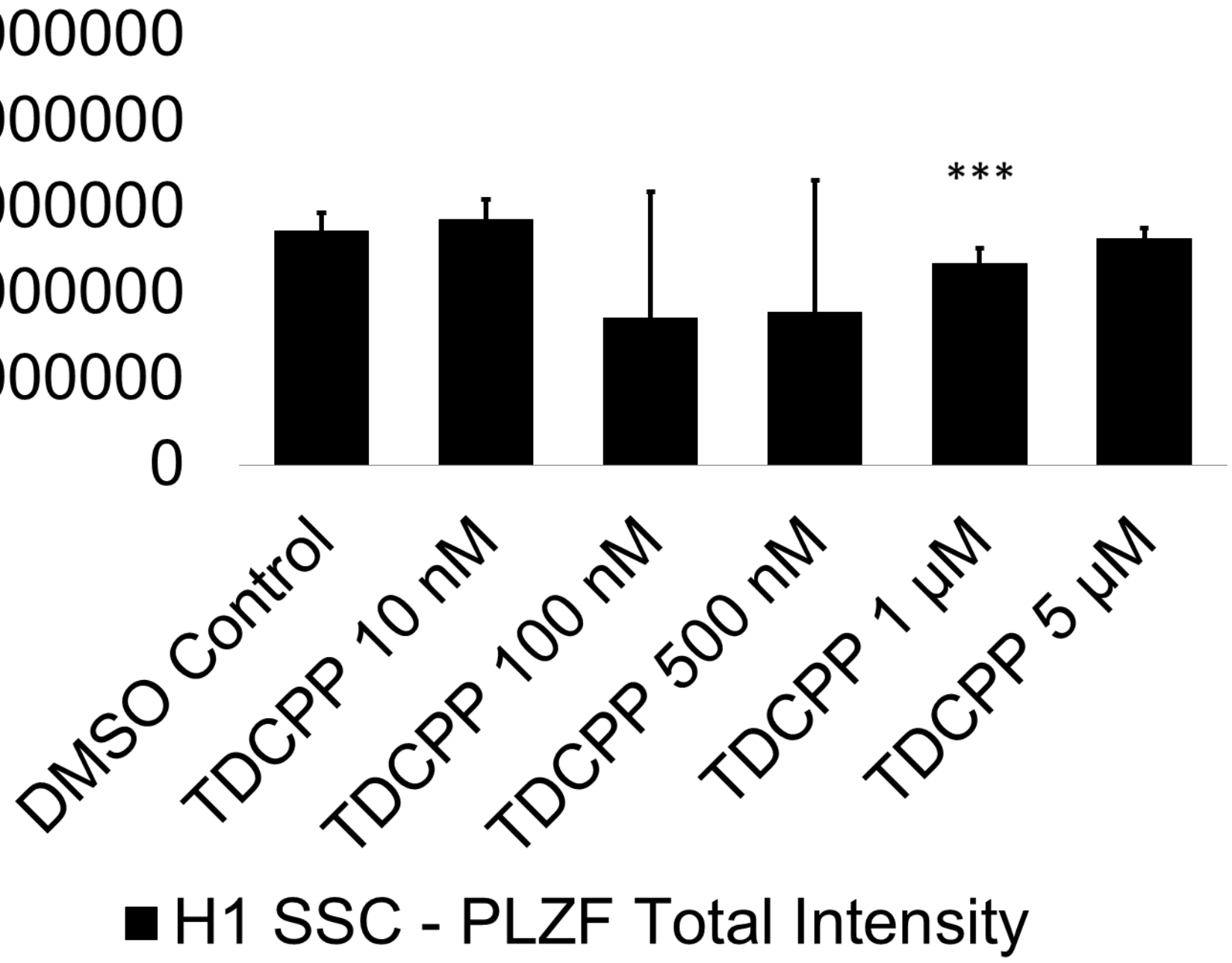
25000000
20000000
15000000
10000000
5000000
0
***
DMSO Control
TDCPP 10 nM
TDCPP 100 nM
TDCPP 500 nM
TDCPP 1 µM
TDCPP 5 µM
H1 SSC - PLZF Total Intensity

Figure 9.5. Persistent TDCPP exposure decreases PLZF+ intensity in in vitro-derived spermatogenic cells (H1 SSC). Graphical representation showing decreases in average PLZF+ intensity in comparison to 0.2 % DMSO-only control in spermatogonia derived under *in vitro* spermatogenic conditions from H1 ESCs and treated with 1 μM TDCPP from Day 3 to Day 12. Three replications were performed for each condition. Significant changes in PLZF+ area were determined using a 1-way analysis of variance (1-way ANOVA) and validated via a Student's t-test, where * is $p<0.05$, ** is $p<0.01$, and *** is $p<0.001$. Data are represented as mean ± SEM.

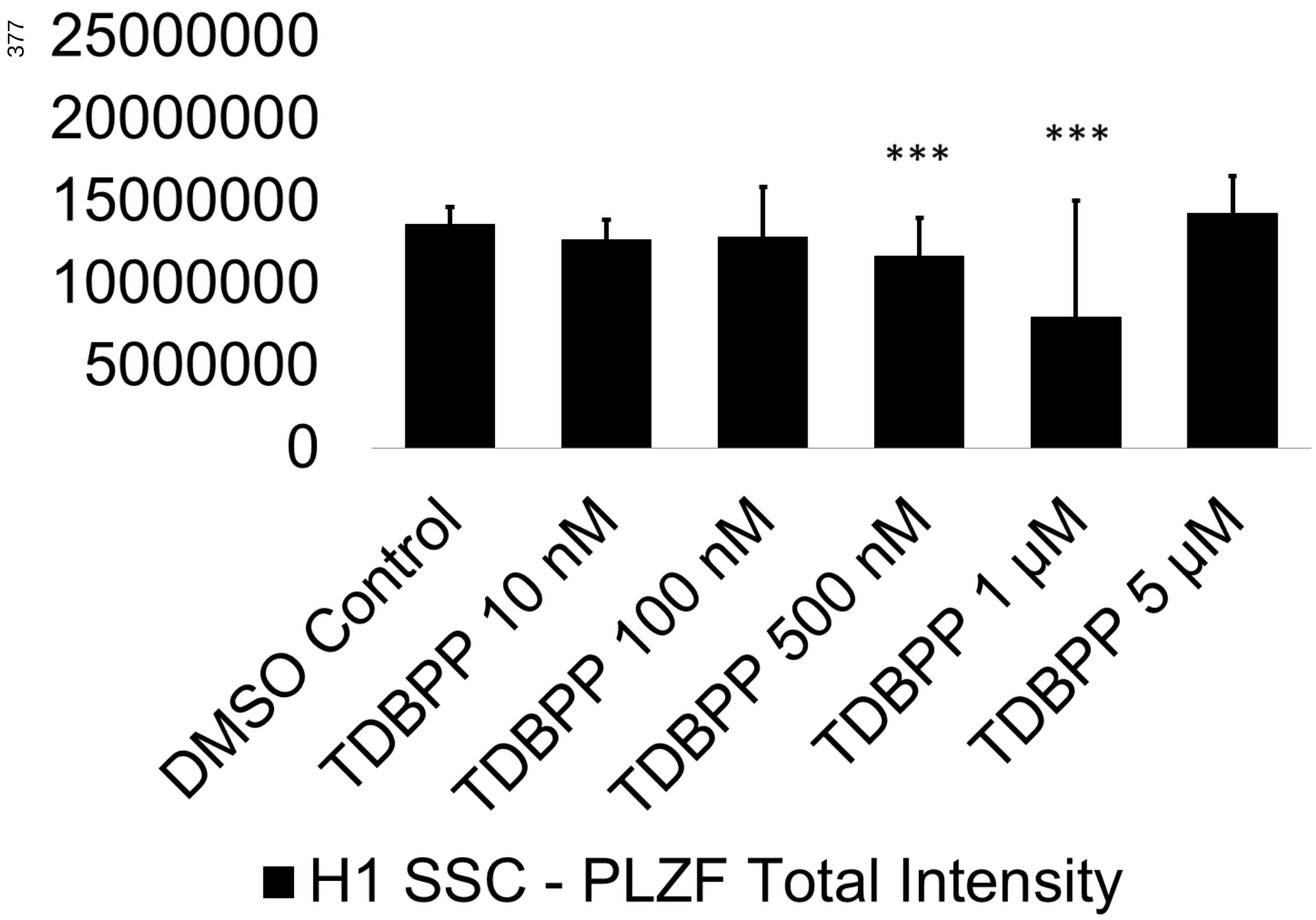
25000000
20000000
15000000
10000000
5000000
0
***
***
DMSO Control
TDBPP 10 nM
TDBPP 100 nM
TDBPP 500 nM
TDBPP 1 µM
TDBPP 5 µM
H1 SSC - PLZF Total Intensity

Figure 9.6. Persistent TDBPP exposure decreases PLZF+ intensity in in vitro-derived spermatogenic cells (H1 SSC). Graphical representation showing decreases in average PLZF+ intensity in comparison to 0.2 % DMSO-only control in spermatogonia derived under *in vitro* spermatogenic conditions from H1 ESCs and treated with 500 nM and 1 μM TDBPP from Day 3 to Day 12. Three replications were performed for each condition. Significant changes in PLZF+ area were determined using a 1-way analysis of variance (1-way ANOVA) and validated via a Student's t-test, where * is $p<0.05$, ** is $p<0.01$, and *** is $p<0.001$. Data are represented as mean ± SEM.

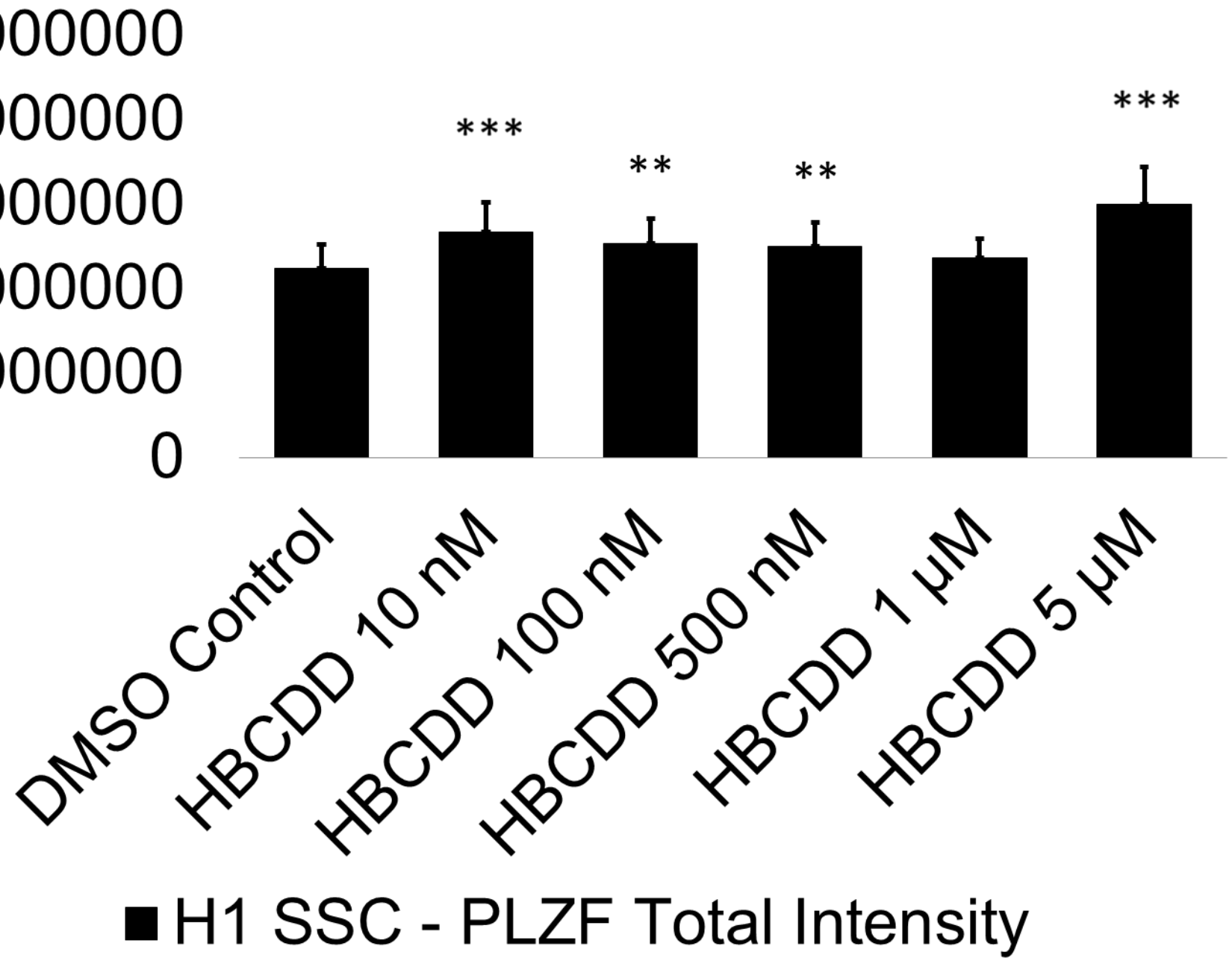
25000000
20000000
15000000
10000000
5000000
0
***
**
**
***
DMSO Control
HBCDD 10 nM
HBCDD 100 nM
HBCDD 500 nM
HBCDD 1 µM
HBCDD 5 µM
H1 SSC - PLZF Total Intensity

Figure 9.7. Persistent HBCDD exposure increases PLZF+ intensity in in vitro-derived spermatogenic cells (H1 SSC). Graphical representation showing increases in average PLZF+ intensity in comparison to 0.2 % DMSO-only control in spermatogonia derived under *in vitro* spermatogenic conditions from H1 ESCs and treated with 10 nM, 100 nM, 500 nM, and 5 μM TDBPP from Day 3 to Day 12. Three replications were performed for each condition. Significant changes in PLZF+ area were determined using a 1-way analysis of variance (1-way ANOVA) and validated via a Student's t-test, where * is $p<0.05$, ** is $p<0.01$, and *** is $p<0.001$. Data are represented as mean ± SEM.

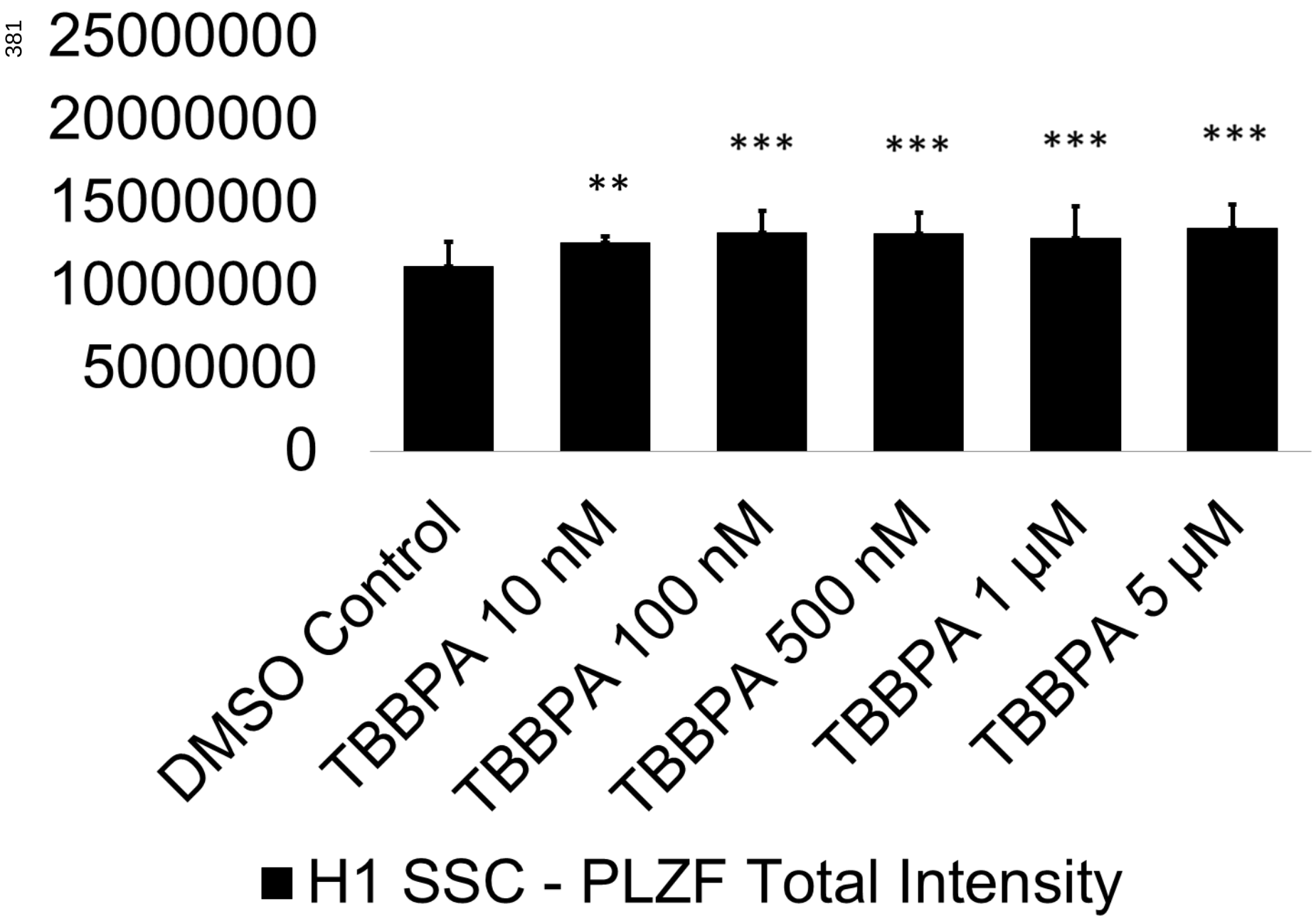
25000000
20000000
15000000
10000000
5000000
0
**
***
***
***
***
DMSO Control
TBBPA 10 nM
TBBPA 100 nM
TBBPA 500 nM
TBBPA 1 µM
TBBPA 5 µM
H1 SSC - PLZF Total Intensity

Figure 9.8. Persistent TBBPA exposure increases PLZF+ intensity in in vitro-derived spermatogenic cells (H1 SSC). Graphical representation showing increases in average PLZF+ intensity in comparison to 0.2 % DMSO-only control in spermatogonia derived under *in vitro* spermatogenic conditions from H1 ESCs and treated with 10 nM, 100 nM, 500 nM, 1 μM, and 5 μM TBBPA from Day 3 to Day 12. Three replications were performed for each condition. Significant changes in PLZF+ area were determined using a 1-way analysis of variance (1-way ANOVA) and validated via a Student's t-test, where * is $p<0.05$, ** is $p<0.01$, and *** is $p<0.001$. Data are represented as mean ± SEM.

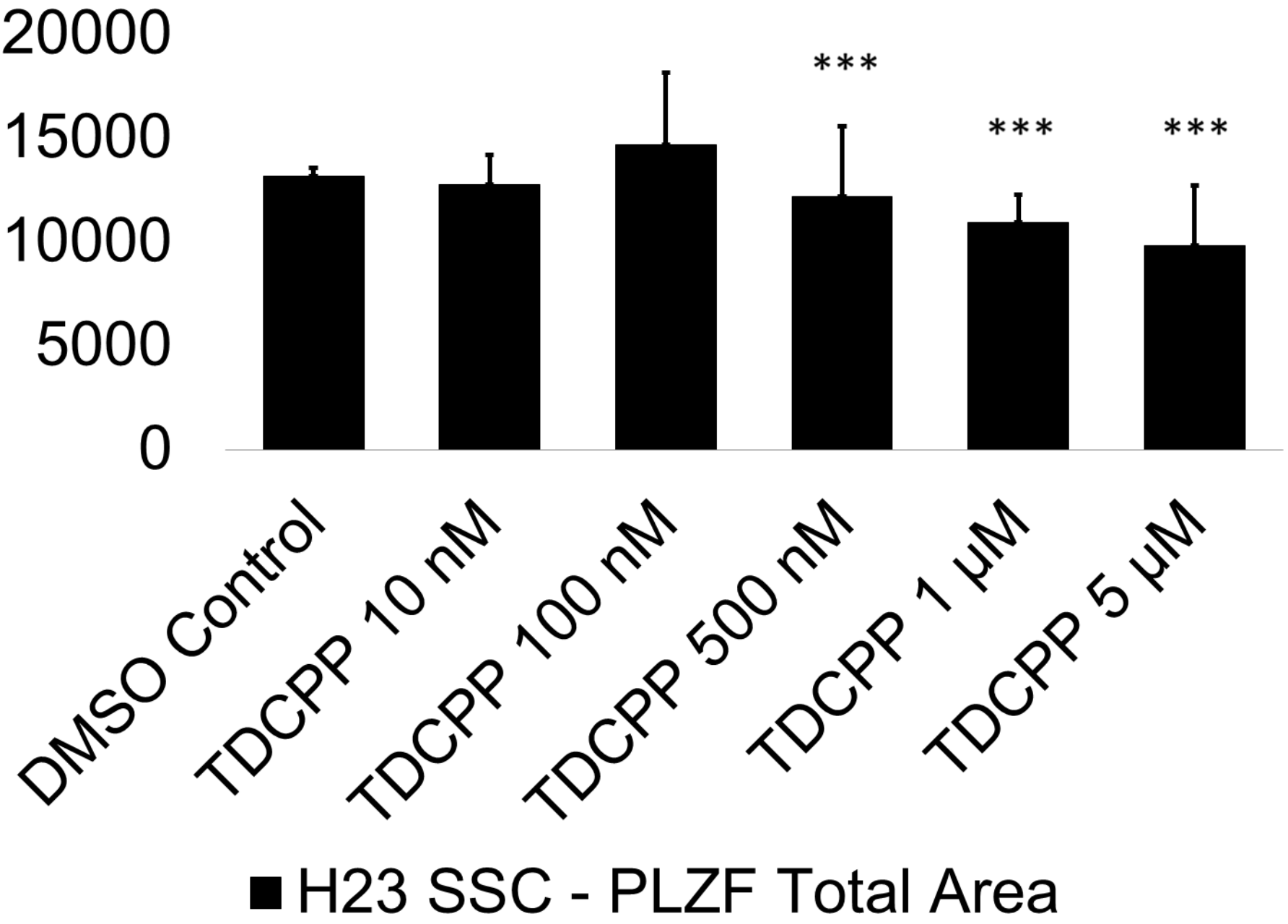
20000
15000
10000
5000
0
***
***
***
DMSO Control
TDCPP 10 nM
TDCPP 100 nM
TDCPP 500 nM
TDCPP 1 µM
TDCPP 5 µM
H23 SSC - PLZF Total Area

Figure 9.9. Persistent TDCPP exposure decreases PLZF+ area in in vitro-derived spermatogenic cells (H23 SSC). Graphical representation showing decreases in average PLZF+ area in comparison to 0.2% DMSO-only control in spermatogonia derived under *in vitro* spermatogenic conditions from H23 ESCs and treated with 500 nM, 1 μM, and 5 μM TDCPP from Day 3 to Day 12. Three replications were performed for each condition. Significant changes in PLZF+ area were determined using a 1-way analysis of variance (1-way ANOVA) and validated via a Student's t-test, where * is $p<0.05$, ** is $p<0.01$, and *** is $p<0.001$. Data are represented as mean ± SEM.

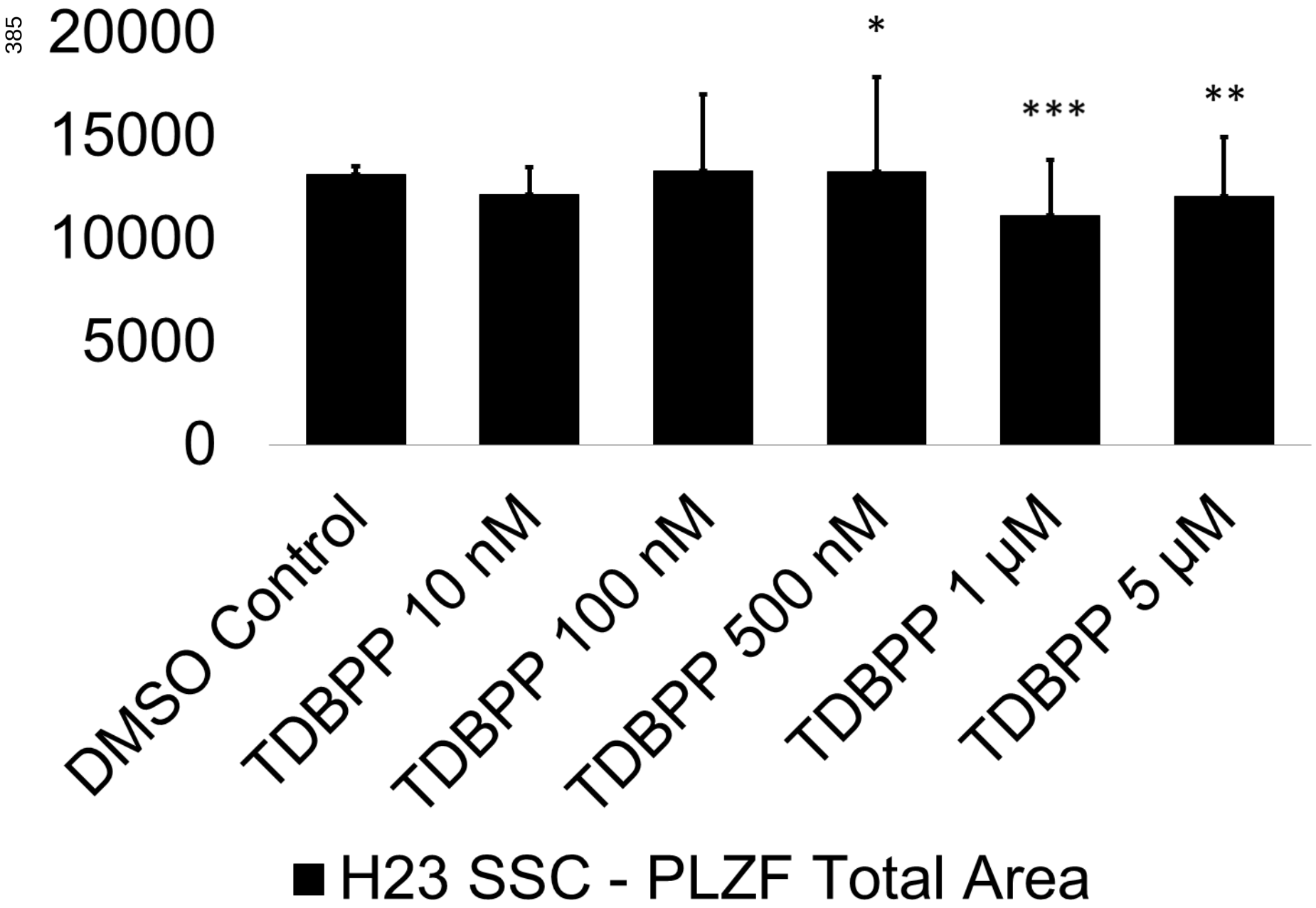
20000
15000
10000
5000
0
*
***
**
DMSO Control
TDBPP 10 nM
TDBPP 100 nM
TDBPP 500 nM
TDBPP 1 µM
TDBPP 5 µM
H23 SSC - PLZF Total Area

Figure 9.10. Persistent TDCPP exposure impacts PLZF+ area in in vitro-derived spermatogenic cells (H23 SSC). Graphical representation showing S-phase non-monotonic dose response changes in average PLZF+ area in comparison to 0.2% DMSO-only control in spermatogonia derived under *in vitro* spermatogenic conditions from H23 ESCs and treated with 10 nM, 100 nM 500 nM, 1 μM, and 5 μM TDBPP from Day 3 to Day 12. Three replications were performed for each condition. Significant changes in PLZF+ area were determined using a 1-way analysis of variance (1-way ANOVA) and validated via a Student's t-test, where * is $p<0.05$, ** is $p<0.01$, and *** is $p<0.001$. Data are represented as mean ± SEM.

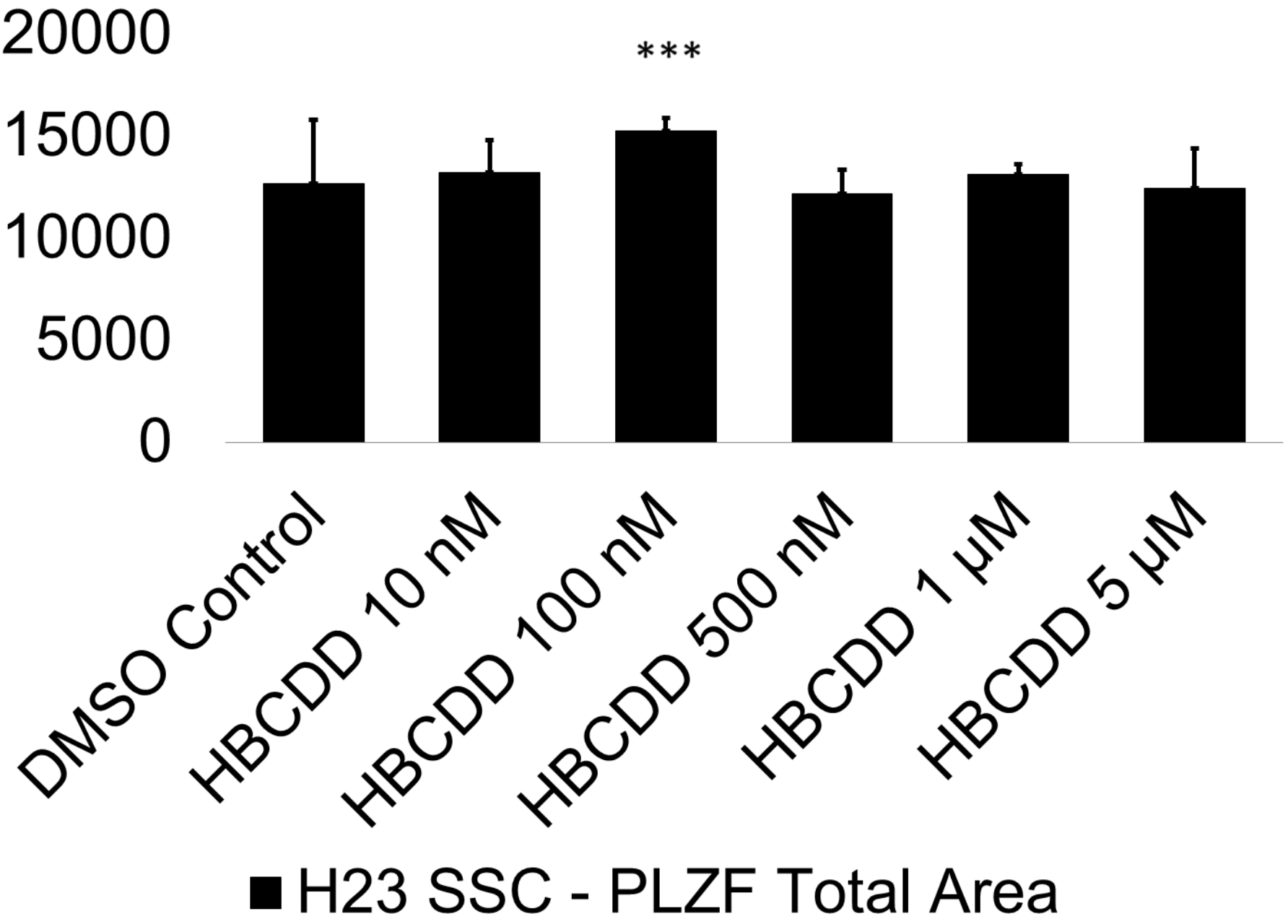
20000
15000
10000
5000
0
***
DMSO Control
HBCDD 10 nM
HBCDD 100 nM
HBCDD 500 nM
HBCDD 1 µM
HBCDD 5 µM
H23 SSC - PLZF Total Area

Figure 9.11. Persistent HBCDD exposure increases PLZF+ area in in vitro-derived spermatogenic cells (H23 SSC). Graphical representation showing increases in average PLZF+ area in comparison to 0.2% DMSO-only control in spermatogonia derived under *in vitro* spermatogenic conditions from H23 ESCs and treated with 100 nM HBCDD from Day 3 to Day 12. Three replications were performed for each condition. Significant changes in PLZF+ area were determined using a 1-way analysis of variance (1-way ANOVA) and validated via a Student's t-test, where * is $p<0.05$, ** is $p<0.01$, and *** is $p<0.001$. Data are represented as mean ± SEM.

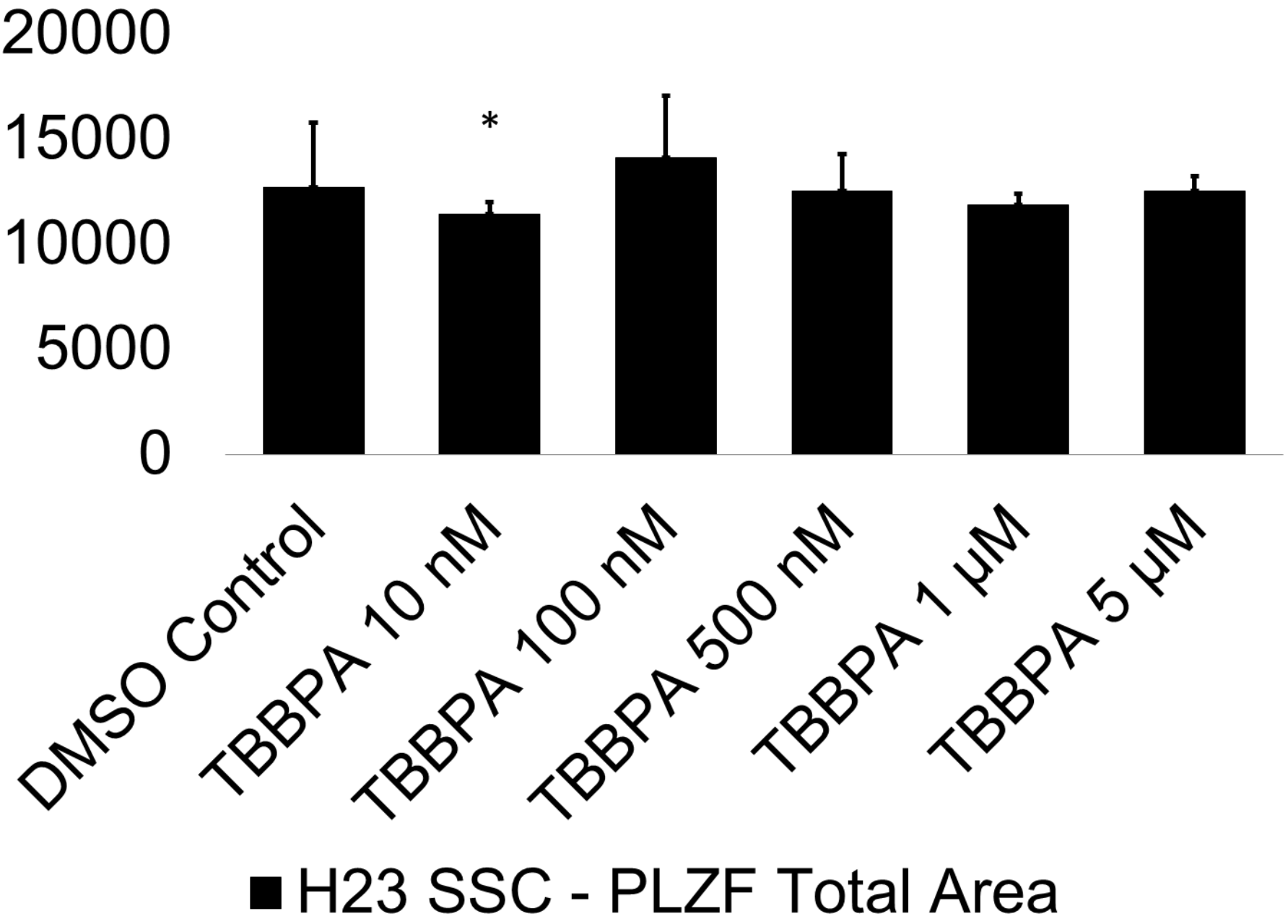
20000
15000
10000
5000
0
*
DMSO Control
TBBPA 10 nM
TBBPA 100 nM
TBBPA 500 nM
TBBPA 1 µM
TBBPA 5 µM
H23 SSC - PLZF Total Area

Figure 9.12. Persistent TBBPA exposure decreases PLZF+ area in in vitro-derived spermatogenic cells (H23 SSC). Graphical representation showing decreases in average PLZF+ area in comparison to 0.2% DMSO-only control in spermatogonia derived under *in vitro* spermatogenic conditions from H23 ESCs and treated with 10 nM TBBPA from Day 3 to Day 12. Three replications were performed for each condition. Significant changes in PLZF+ area were determined using a 1-way analysis of variance (1-way ANOVA) and validated via a Student's t-test, where * is $p<0.05$, ** is $p<0.01$, and *** is $p<0.001$. Data are represented as mean ± SEM.

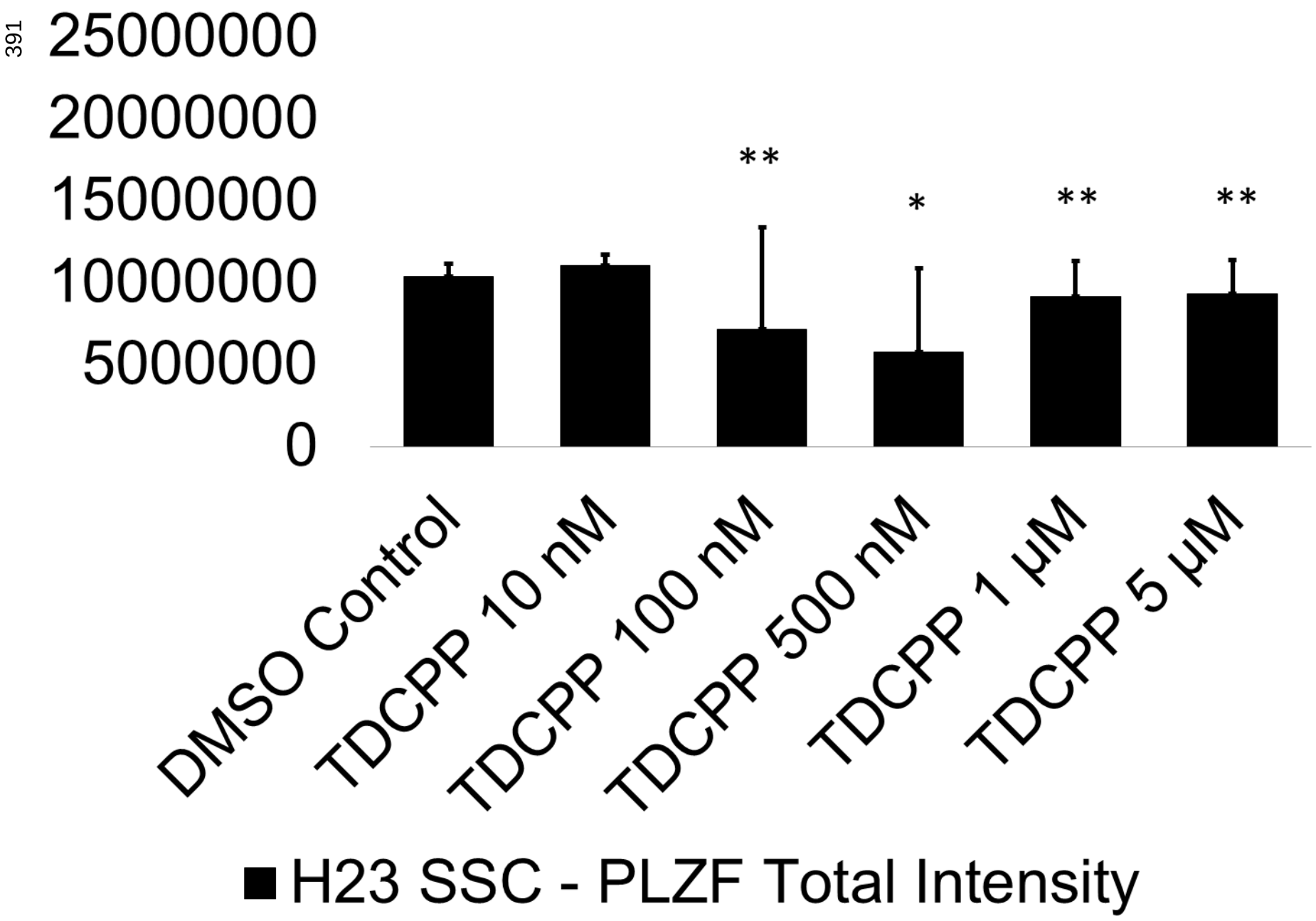
25000000
20000000
15000000
10000000
5000000
0
**
*
**
**
DMSO Control
TDCPP 10 nM
TDCPP 100 nM
TDCPP 500 nM
TDCPP 1 µM
TDCPP 5 µM
H23 SSC - PLZF Total Intensity

Figure 9.13. Persistent TDCPP exposure decreases PLZF+ intensity in in vitro-derived spermatogenic cells (H23 SSC). Graphical representation showing decreases in average PLZF+ intensity in comparison to 0.2% DMSO-only control in spermatogonia derived under *in vitro* spermatogenic conditions from H23 ESCs and treated with 100 nM, 500 nM, 1 μM, and 5 μM TDCPP from Day 3 to Day 12. Three replications were performed for each condition. Significant changes in PLZF+ area were determined using a 1-way analysis of variance (1-way ANOVA) and validated via a Student's t-test, where * is $p<0.05$, ** is $p<0.01$, and *** is $p<0.001$. Data are represented as mean ± SEM.

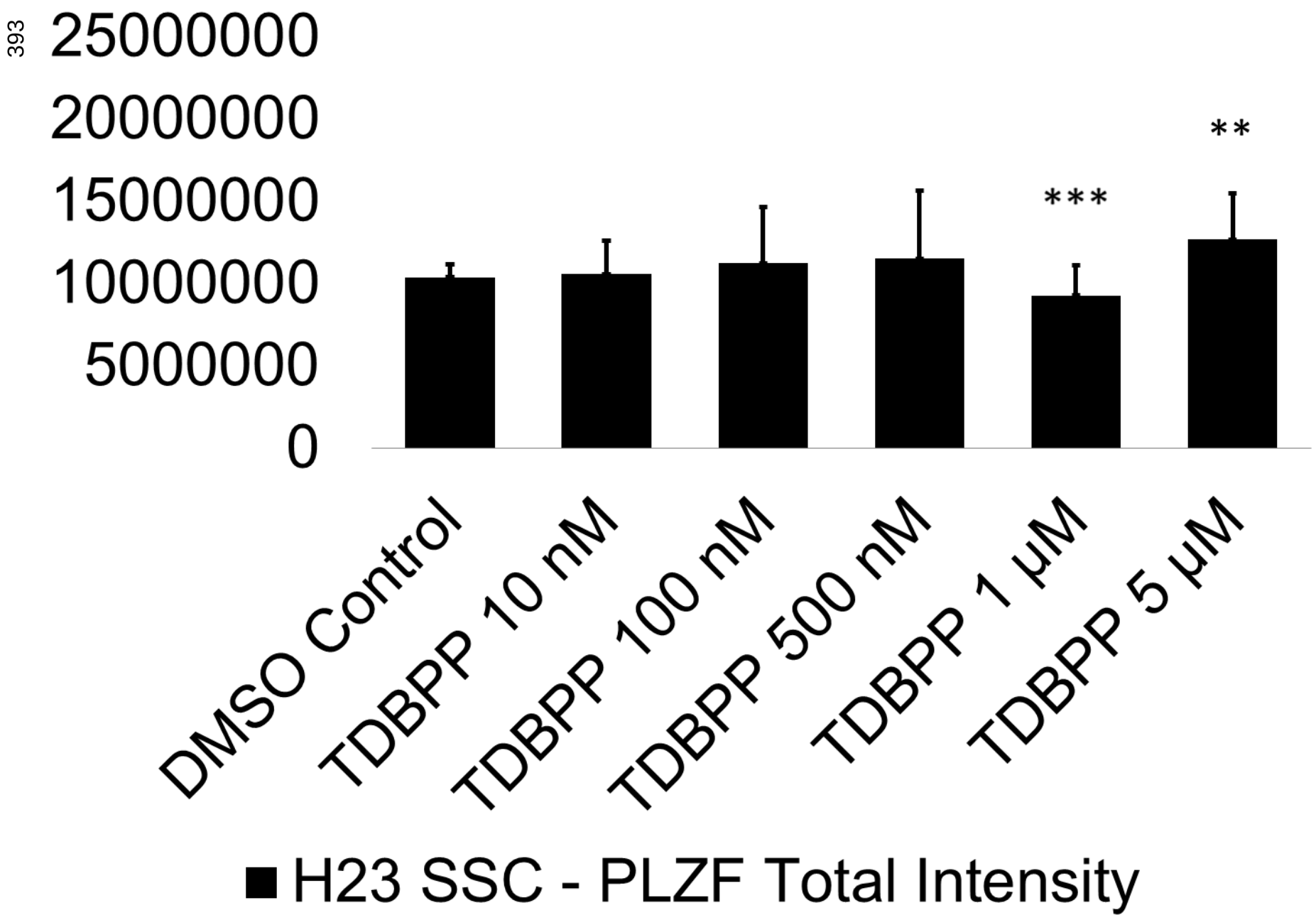
25000000
20000000
15000000
10000000
5000000
0
***
**
DMSO Control
TDBPP 10 nM
TDBPP 100 nM
TDBPP 500 nM
TDBPP 1 µM
TDBPP 5 µM
H23 SSC - PLZF Total Intensity

Figure 9.14. Persistent TDBPP exposure impacts PLZF+ intensity in in vitro-derived spermatogenic cells (H23 SSC). Graphical representation showing a U-shaped non-monotonic dose response change in average PLZF+ intensity in comparison to 0.2% DMSO-only control in spermatogonia derived under *in vitro* spermatogenic conditions from H23 ESCs and treated with 1 μM and 5 μM TDBPP from Day 3 to Day 12. Three replications were performed for each condition. Significant changes in PLZF+ area were determined using a 1-way analysis of variance (1-way ANOVA) and validated via a Student's t-test, where * is $p<0.05$, ** is $p<0.01$, and *** is $p<0.001$. Data are represented as mean ± SEM.

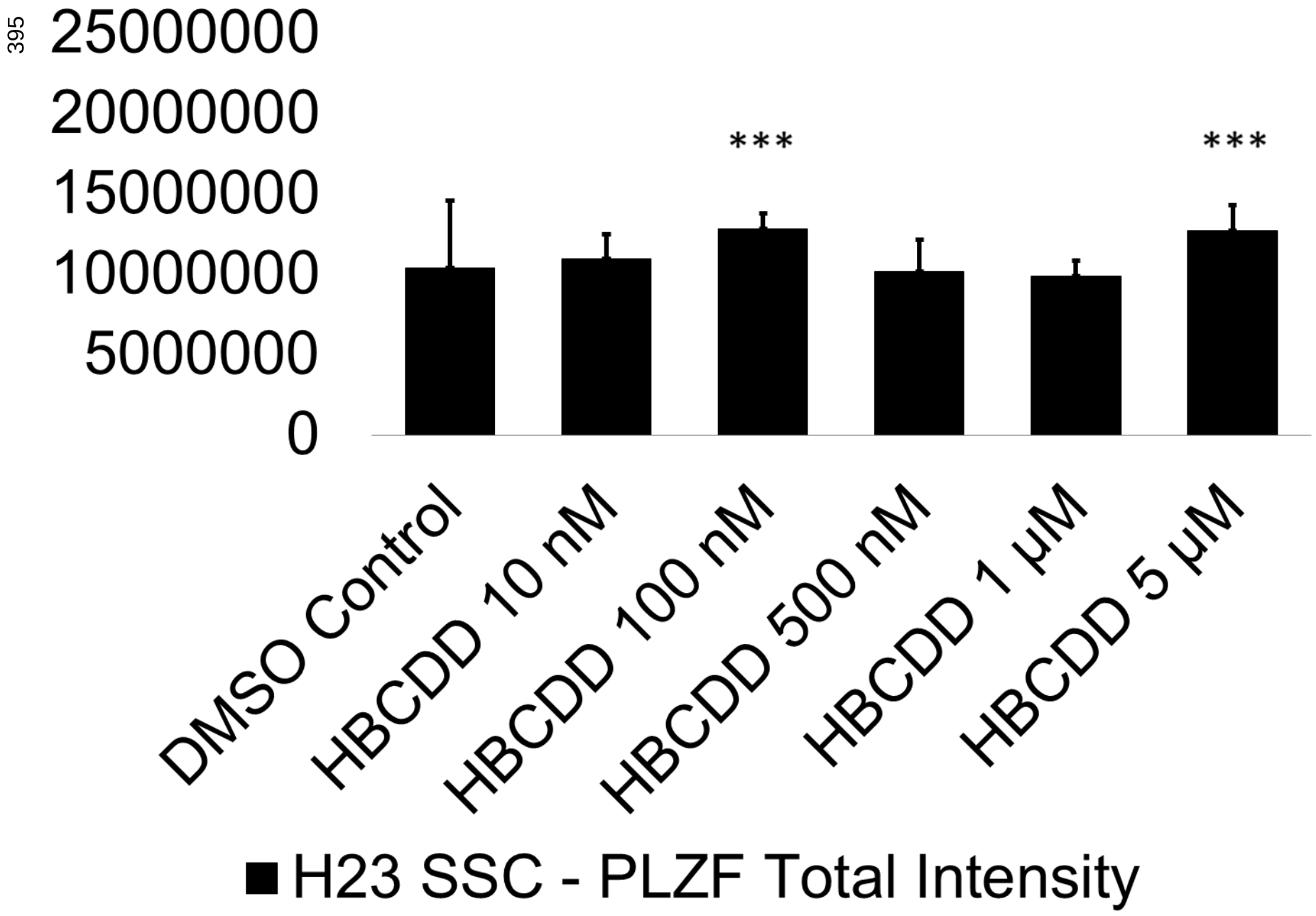
25000000
20000000
15000000
10000000
5000000
0
***
***
DMSO Control
HBCDD 10 nM
HBCDD 100 nM
HBCDD 500 nM
HBCDD 1 µM
HBCDD 5 µM
H23 SSC - PLZF Total Intensity

Figure 9.15. Persistent HBCDD exposure increases PLZF+ intensity in in vitro-derived spermatogenic cells (H23 SSC). Graphical representation showing increases in average PLZF+ intensity in comparison to 0.2% DMSO-only control in spermatogonia derived under *in vitro* spermatogenic conditions from H23 ESCs and treated with 100 nM and 5 μM HBCDD from Day 3 to Day 12. Three replications were performed for each condition. Significant changes in PLZF+ area were determined using a 1-way analysis of variance (1-way ANOVA) and validated via a Student's t-test, where * is $p<0.05$, ** is $p<0.01$, and *** is $p<0.001$. Data are represented as mean ± SEM.

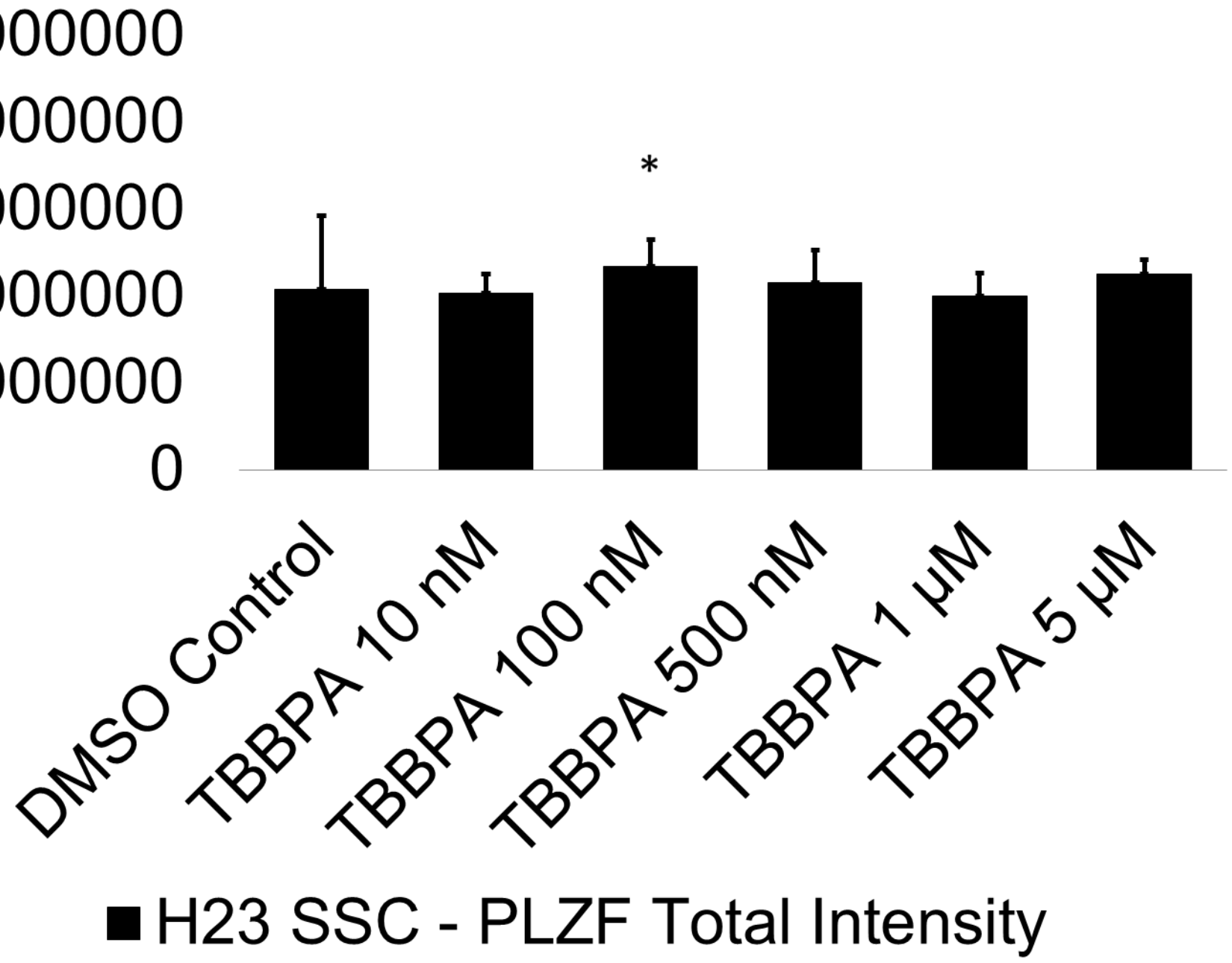
25000000
20000000
15000000
10000000
5000000
0
*
DMSO Control
TBBPA 10 nM
TBBPA 100 nM
TBBPA 500 nM
TBBPA 1 µM
TBBPA 5 µM
H23 SSC - PLZF Total Intensity

Figure 9.16. Persistent TBBPA exposure increases PLZF+ intensity in in vitro-derived spermatogenic cells (H23 SSC). Graphical representation showing increases in average PLZF+ intensity in comparison to 0.2% DMSO-only control in spermatogonia derived under *in vitro* spermatogenic conditions from H23 ESCs and treated with 100 nM TBBPA from Day 3 to Day 12. Three replications were performed for each condition. Significant changes in PLZF+ area were determined using a 1-way analysis of variance (1-way ANOVA) and validated via a Student's t-test, where * is $p<0.05$, ** is $p<0.01$, and *** is $p<0.001$. Data are represented as mean ± SEM.

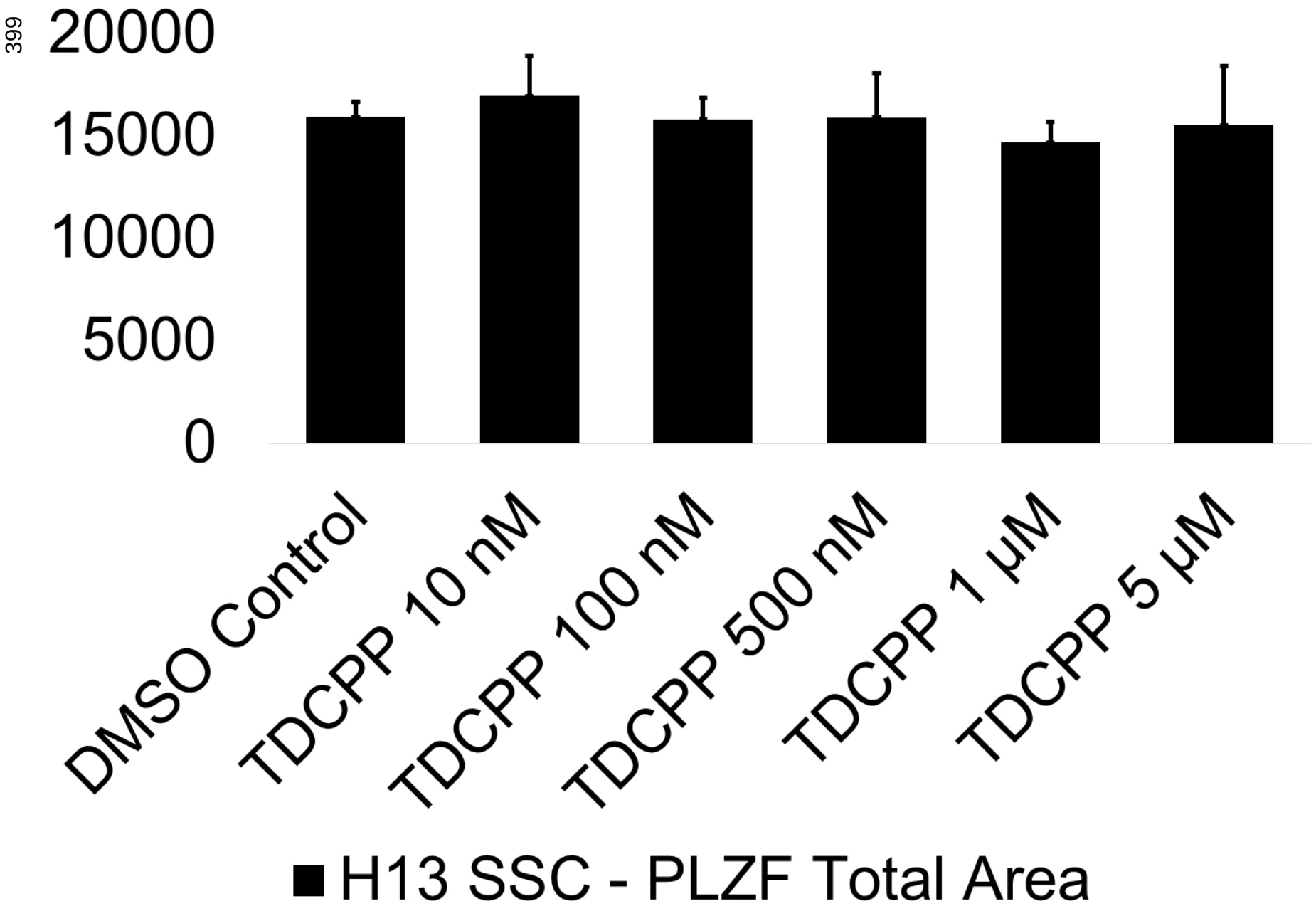
20000
15000
10000
5000
0
DMSO Control
TDCPP 10 nM
TDCPP 100 nM
TDCPP 500 nM
TDCPP 1 µM
TDCPP 5 µM
H13 SSC - PLZF Total Area

Figure 9.17. Persistent TDCPP exposure does not impact PLZF+ area in in vitro-derived spermatogenic cells (H13 SSC). Graphical representation showing no impact on average PLZF+ area in comparison to 0.2% DMSO-only control in spermatogonia derived under *in vitro* spermatogenic conditions from H13 ESCs and treated with 10 nM, 100 nM, 500 nM, 1 μM, 5 μM TDCPP from Day 3 to Day 12. Three replications were performed for each condition. Significant changes in PLZF+ area were determined using a 1-way analysis of variance (1-way ANOVA) and validated via a Student's t-test, where * is $p<0.05$, ** is $p<0.01$, and *** is $p<0.001$. Data are represented as mean ± SEM.

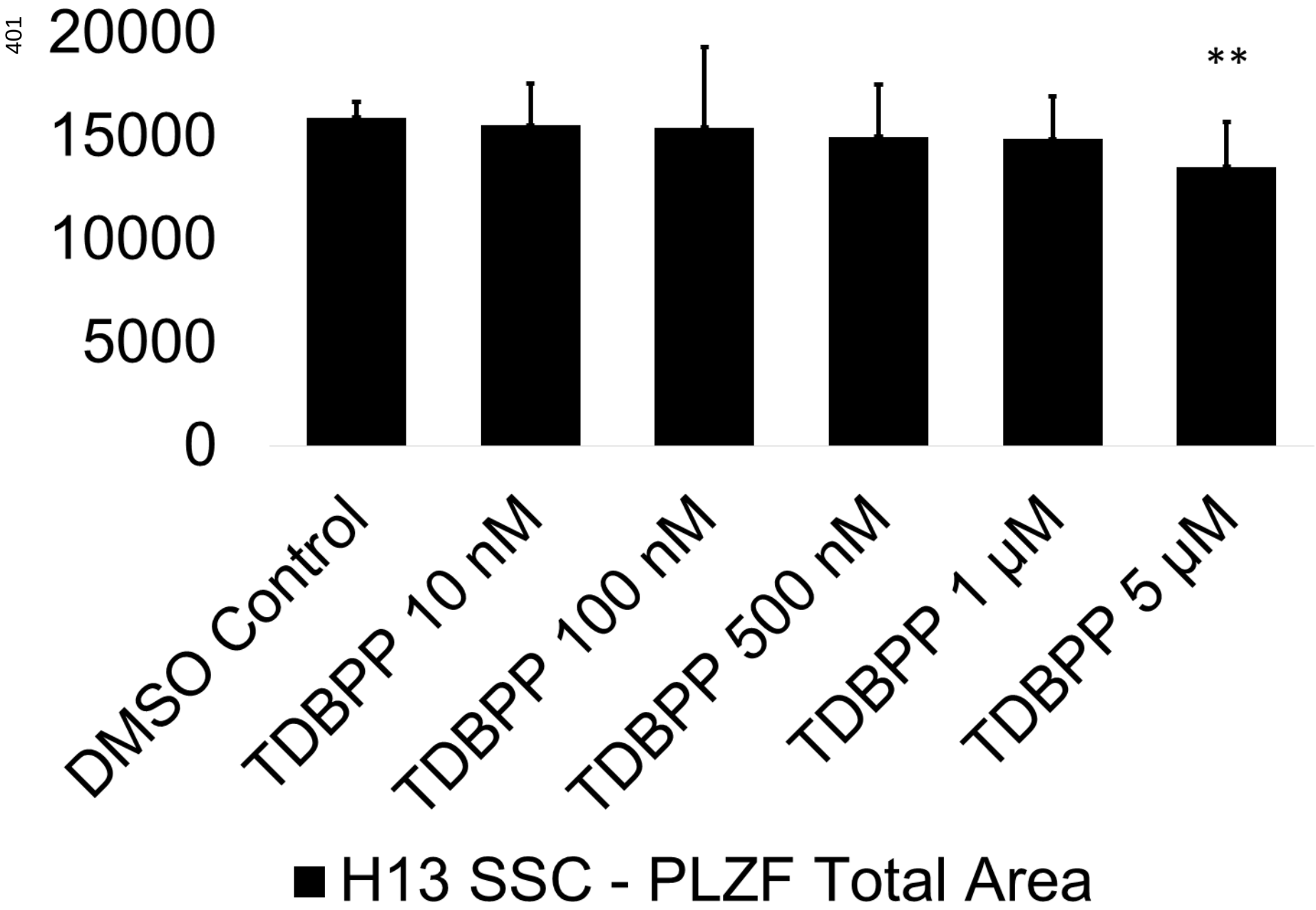
20000
15000
10000
5000
0
**
DMSO Control
TDBPP 10 nM
TDBPP 100 nM
TDBPP 500 nM
TDBPP 1 µM
TDBPP 5 µM
H13 SSC - PLZF Total Area

Figure 9.18. Persistent TDBPP exposure decreases PLZF+ area in in vitro-derived spermatogenic cells (H13 SSC). Graphical representation showing decreases in average PLZF+ area in comparison to 0.2% DMSO-only control in spermatogonia derived under *in vitro* spermatogenic conditions from H13 ESCs and treated with 5 μM TDBPP from Day 3 to Day 12. Three replications were performed for each condition. Significant changes in PLZF+ area were determined using a 1-way analysis of variance (1-way ANOVA) and validated via a Student's t-test, where * is $p<0.05$, ** is $p<0.01$, and *** is $p<0.001$. Data are represented as mean ± SEM.

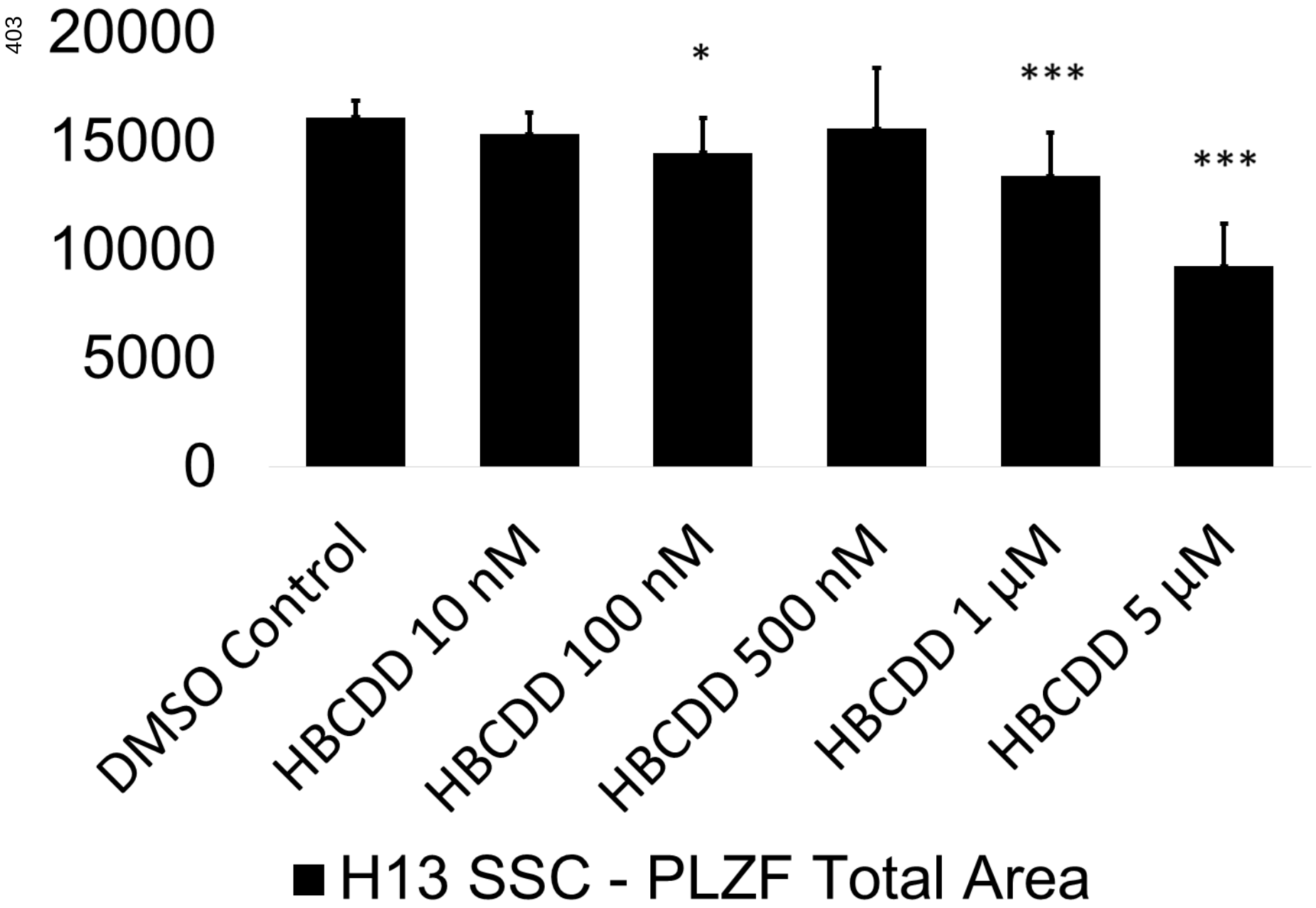
20000
15000
10000
5000
0
*
***
***
DMSO Control
HBCDD 10 nM
HBCDD 100 nM
HBCDD 500 nM
HBCDD 1 µM
HBCDD 5 µM
H13 SSC - PLZF Total Area

Figure 9.19. Persistent HBCDD exposure decreases PLZF+ area in in vitro-derived spermatogenic cells (H13 SSC). Graphical representation showing decreases in average PLZF+ area in comparison to 0.2% DMSO-only control in spermatogonia derived under *in vitro* spermatogenic conditions from H13 ESCs and treated with 100 nM, 1 μM, and 5 μM HBCDD from Day 3 to Day 12. Three replications were performed for each condition. Significant changes in PLZF+ area were determined using a 1-way analysis of variance (1-way ANOVA) and validated via a Student's t-test, where * is $p<0.05$, ** is $p<0.01$, and *** is $p<0.001$. Data are represented as mean ± SEM.

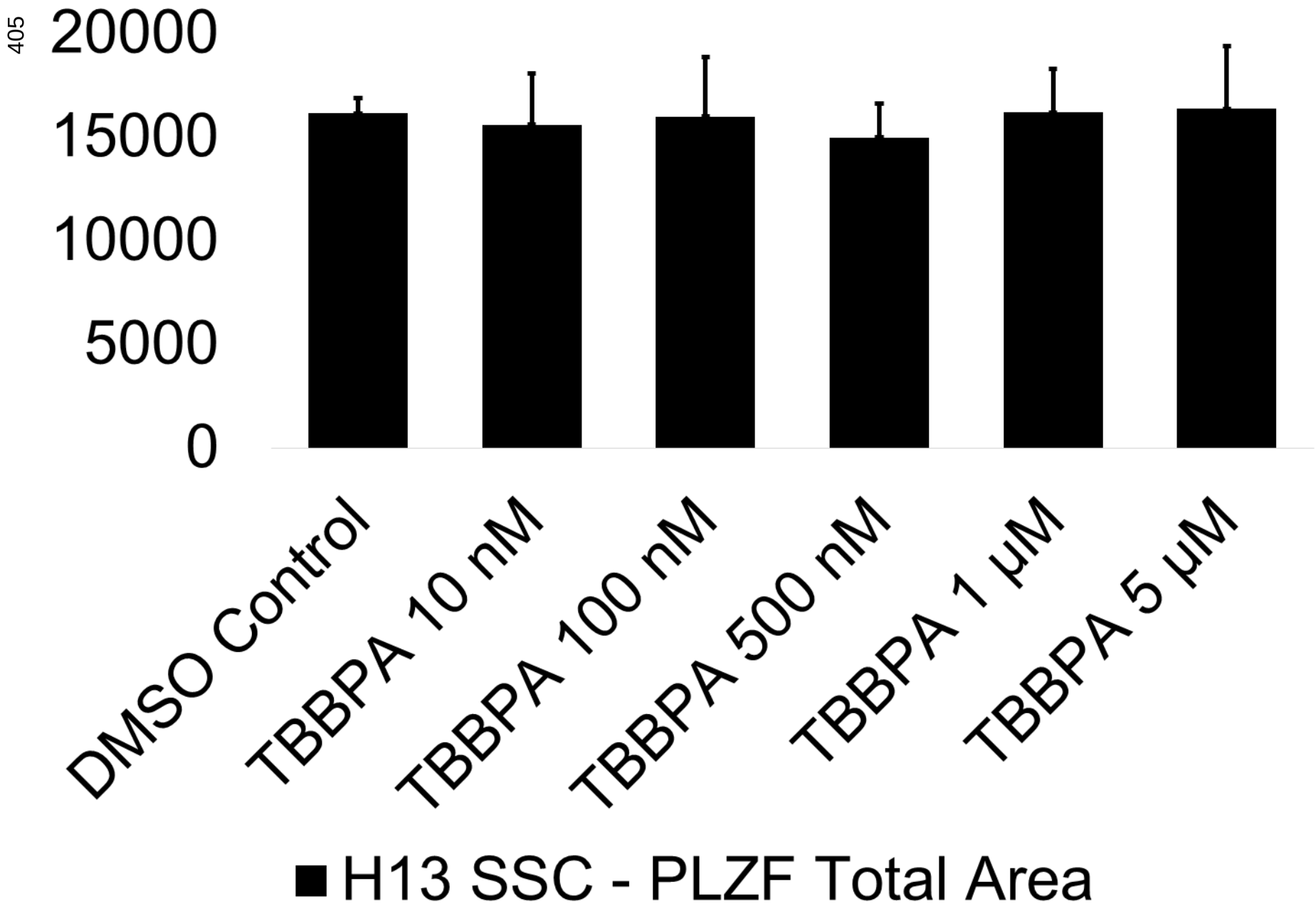
405
20000
15000
10000
5000
0
DMSO Control
TBBPA 10 nM
TBBPA 100 nM
TBBPA 500 nM
TBBPA 1 µM
TBBPA 5 µM
H13 SSC - PLZF Total Area

Figure 9.20. Persistent TBBPA exposure has no impact on PLZF+ area in in vitro-derived spermatogenic cells (H13 SSC). Graphical representation showing no impact on average PLZF+ area in comparison to 0.2% DMSO-only control in spermatogonia derived under *in vitro* spermatogenic conditions from H13 ESCs and treated with 10 nM, 100 nM, 500 nM, 1 μM, and 5 μM TBBPA from Day 3 to Day 12. Three replications were performed for each condition. Significant changes in PLZF+ area were determined using a 1-way analysis of variance (1-way ANOVA) and validated via a Student's t-test, where * is $p<0.05$, ** is $p<0.01$, and *** is $p<0.001$. Data are represented as mean ± SEM.

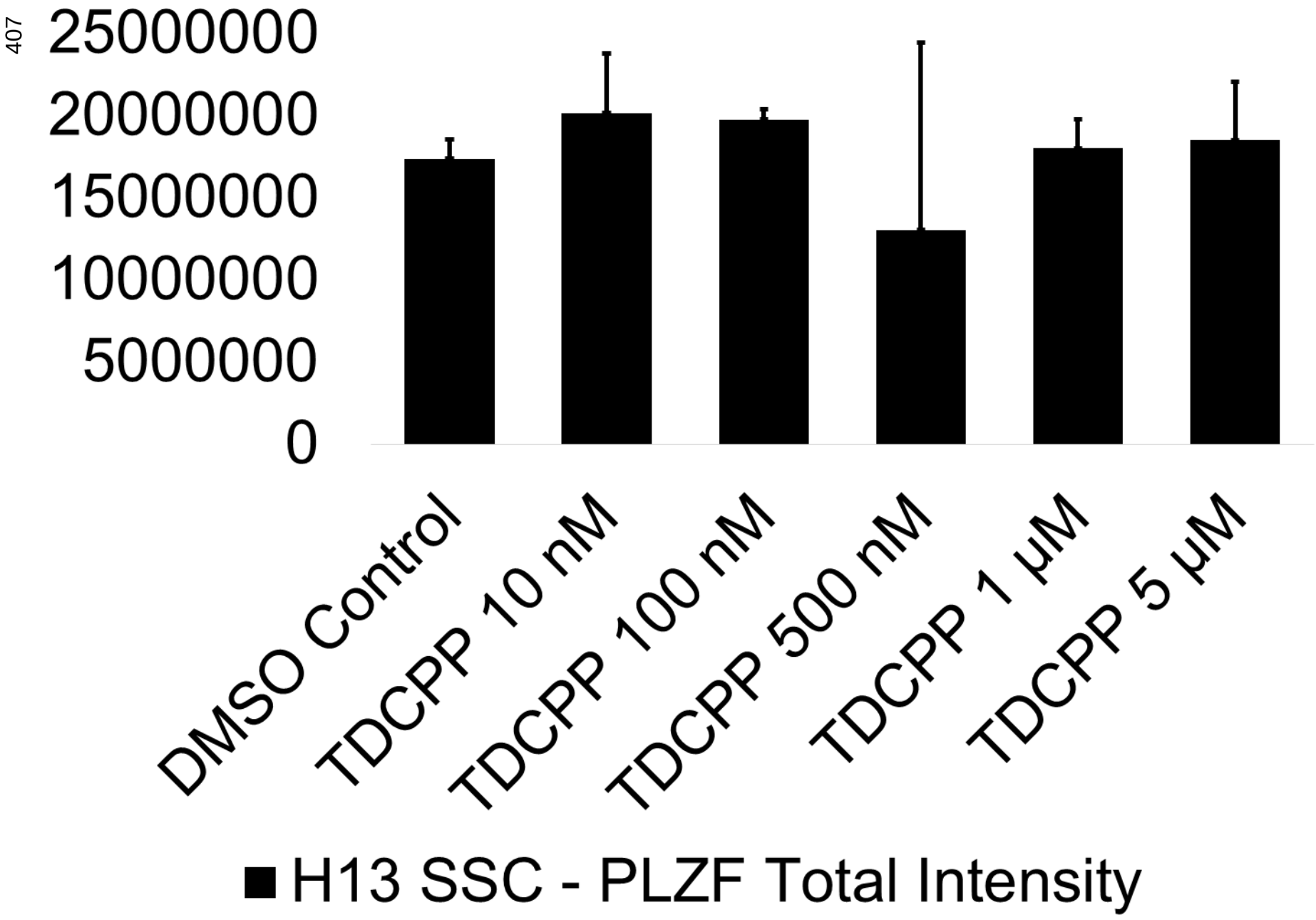
25000000
20000000
15000000
10000000
5000000
0
DMSO Control
TDCPP 10 nM
TDCPP 100 nM
TDCPP 500 nM
TDCPP 1 µM
TDCPP 5 µM
H13 SSC - PLZF Total Intensity

Figure 9.21. Persistent TDCPP exposure has no impact on PLZF+ intensity in in vitro-derived spermatogenic cells (H13 SSC). Graphical representation showing no impact on average PLZF+ intensity in comparison to 0.2% DMSO-only control in spermatogonia derived under *in vitro* spermatogenic conditions from H13 ESCs and treated with 10 nM, 100 nM, 500 nM, 1 μM, and 5 μM TDCPP from Day 3 to Day 12. Three replications were performed for each condition. Significant changes in PLZF+ area were determined using a 1-way analysis of variance (1-way ANOVA) and validated via a Student's t-test, where * is $p<0.05$, ** is $p<0.01$, and *** is $p<0.001$. Data are represented as mean ± SEM.

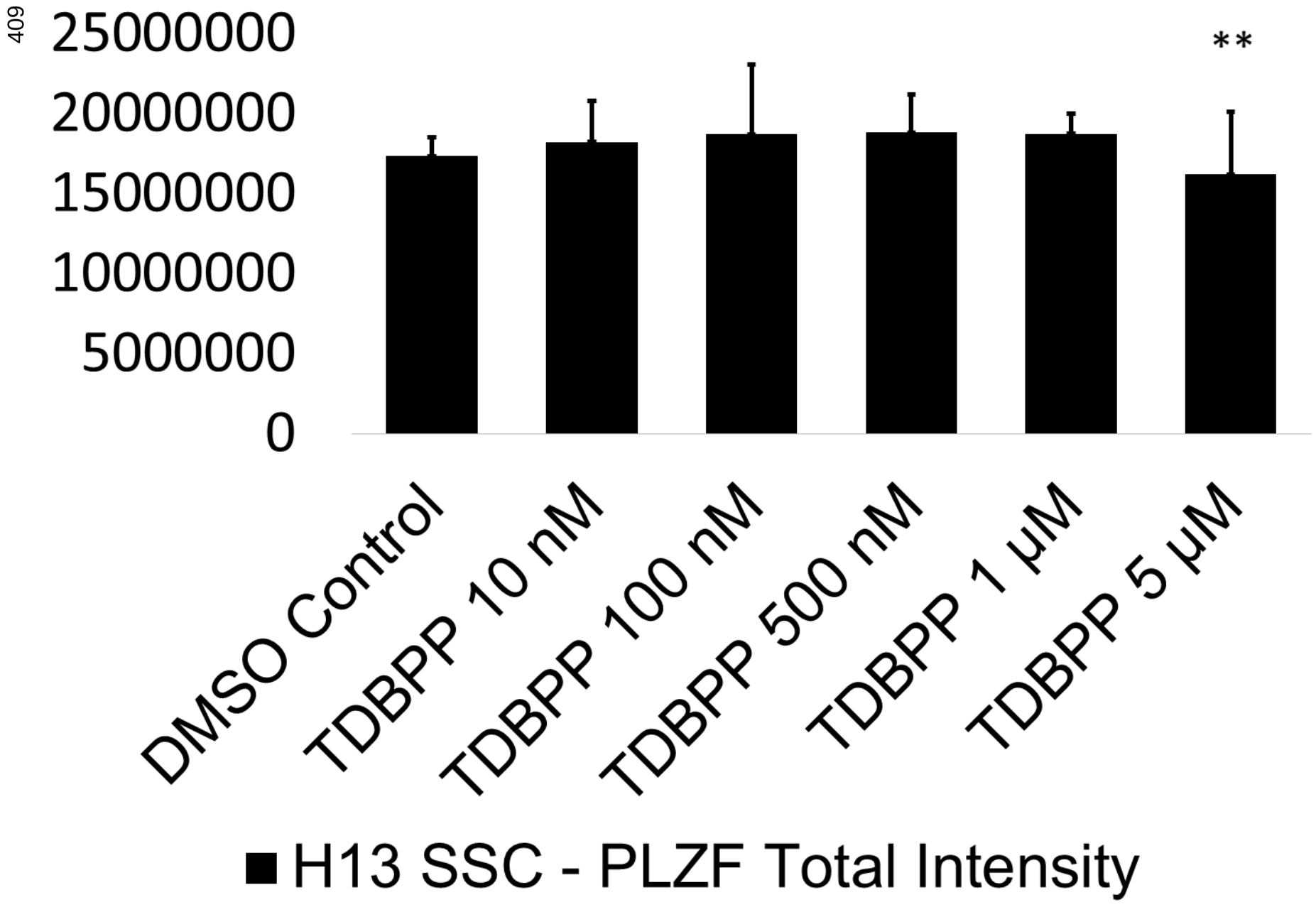
25000000
20000000
15000000
10000000
5000000
0
**
DMSO Control
TDBPP 10 nM
TDBPP 100 nM
TDBPP 500 nM
TDBPP 1 µM
TDBPP 5 µM
H13 SSC - PLZF Total Intensity

Figure 9.22. Persistent TDBPP exposure decreases PLZF+ intensity in in vitro-derived spermatogenic cells (H13 SSC). Graphical representation showing decreases in average PLZF+ intensity in comparison to 0.2% DMSO-only control in spermatogonia derived under *in vitro* spermatogenic conditions from H13 ESCs and treated with 5 μM TDBPP from Day 3 to Day 12. Three replications were performed for each condition. Significant changes in PLZF+ area were determined using a 1-way analysis of variance (1-way ANOVA) and validated via a Student's t-test, where * is $p<0.05$, ** is $p<0.01$, and *** is $p<0.001$. Data are represented as mean ± SEM.

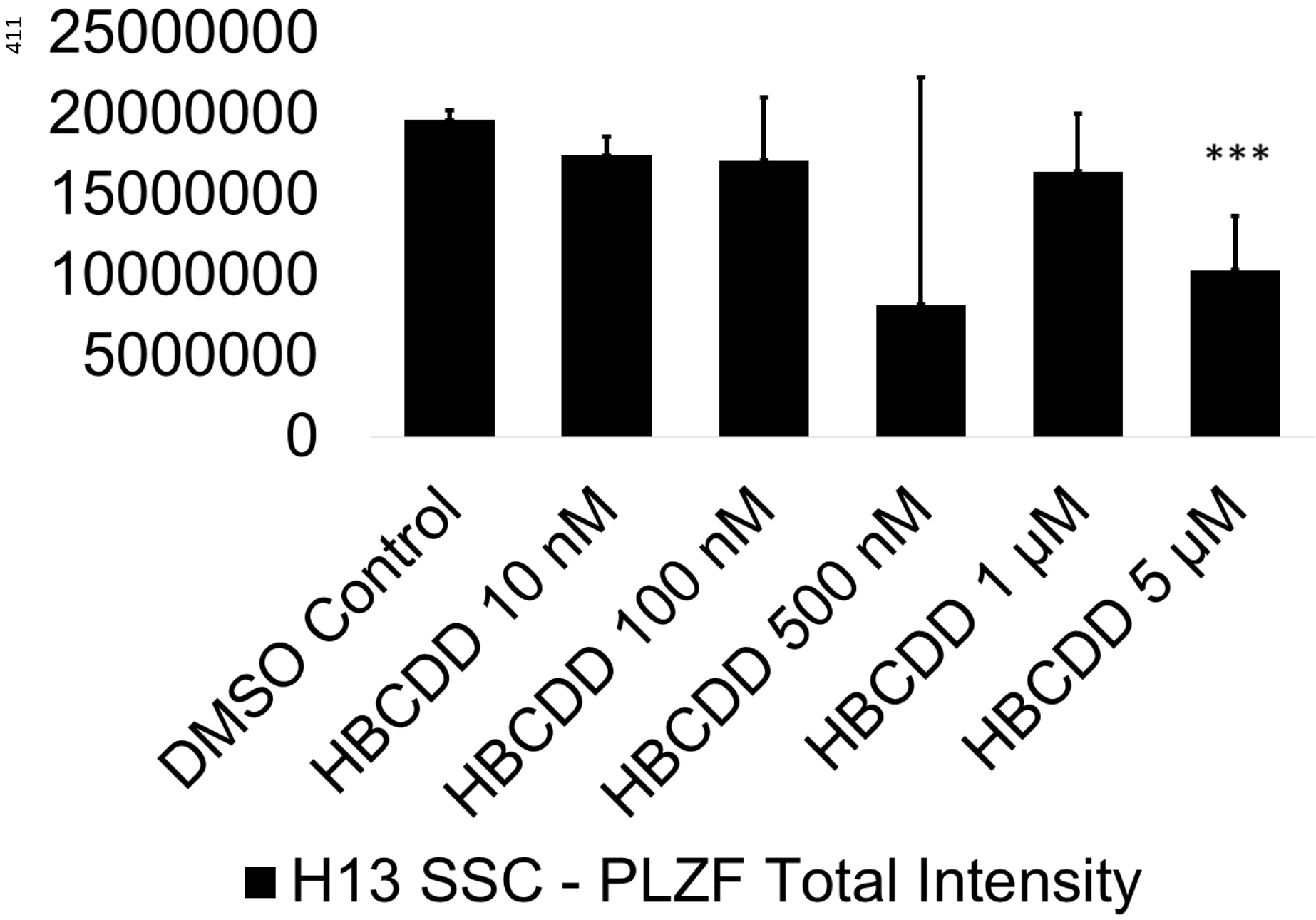
25000000
20000000
15000000
10000000
5000000
0
***
DMSO Control
HBCDD 10 nM
HBCDD 100 nM
HBCDD 500 nM
HBCDD 1 µM
HBCDD 5 µM
H13 SSC - PLZF Total Intensity

Figure 9.23. Persistent HBCDD exposure decreases PLZF+ intensity in in vitro-derived spermatogenic cells (H13 SSC). Graphical representation showing decreases in average PLZF+ intensity in comparison to 0.2% DMSO-only control in spermatogonia derived under *in vitro* spermatogenic conditions from H13 ESCs and treated with 5 μM HBCDD from Day 3 to Day 12. Three replications were performed for each condition. Significant changes in PLZF+ area were determined using a 1-way analysis of variance (1-way ANOVA) and validated via a Student's t-test, where * is $p<0.05$, ** is $p<0.01$, and *** is $p<0.001$. Data are represented as mean ± SEM.

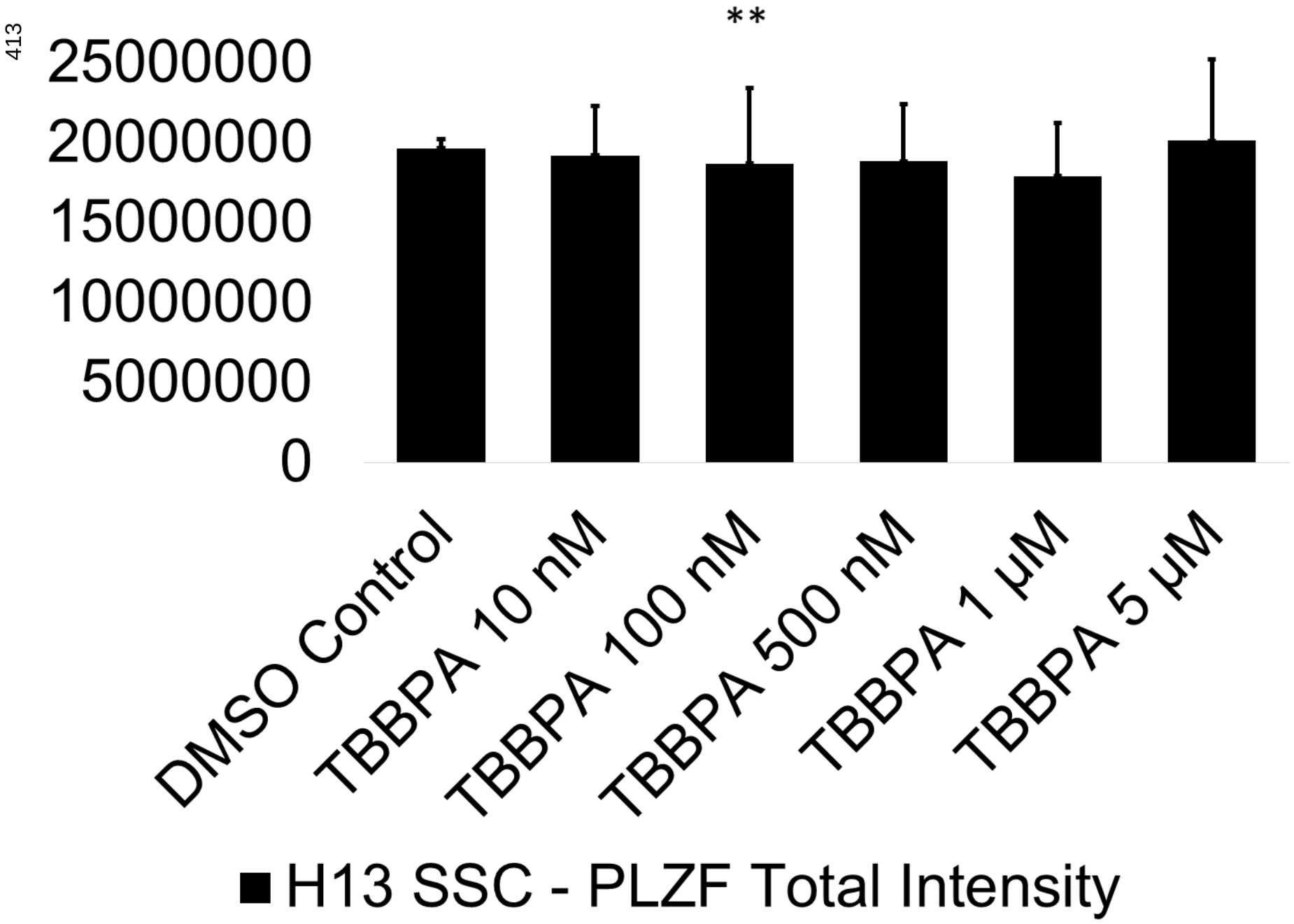
**
25000000
20000000
15000000
10000000
5000000
0
DMSO Control
TBBPA 10 nM
TBBPA 100 nM
TBBPA 500 nM
TBBPA 1 µM
TBBPA 5 µM
H13 SSC - PLZF Total Intensity

Figure 9.24. Persistent TBBPA exposure decreases PLZF+ intensity in in vitro-derived spermatogenic cells (H13 SSC). Graphical representation showing decreases in average PLZF+ intensity in comparison to 0.2% DMSO-only control in spermatogonia derived under *in vitro* spermatogenic conditions from H13 ESCs and treated with 100 nM TBBPA from Day 3 to Day 12. Three replications were performed for each condition. Significant changes in PLZF+ area were determined using a 1-way analysis of variance (1-way ANOVA) and validated via a Student's t-test, where * is $p<0.05$, ** is $p<0.01$, and *** is $p<0.001$. Data are represented as mean ± SEM.

Chapter 4: References

ABAFE, O. A. & MARTINCIGH, B. S. 2016. Determination and human exposure assessment of polybrominated diphenyl ethers and tetrabromobisphenol A in indoor dust in South Africa. *Environ Sci Pollut Res Int,* 23**,** 7038-49.

ABDELOUAHAB, N., AINMELK, Y. & TAKSER, L. 2011. Polybrominated diphenyl ethers and sperm quality. *Reprod Toxicol,* 31**,** 546-50.

AGARWAL, A., VIRK, G., ONG, C. & DU PLESSIS, S. S. 2014. Effect of oxidative stress on male reproduction. *World J Mens Health,* 32**,** 1-17.

AGENCY, U. S. E. P. Supplemental File 1: TBBPA Human Biomonitoring Data.

AGENCY, U. S. E. P. 2014. FLAME RETARDANT ALTERNATIVES FOR HEXABROMOCYCLODODECANE (HBCD).

AITKEN, R. J. & BAKER, M. A. 2013. Causes and consequences of apoptosis in spermatozoa; contributions to infertility and impacts on development. *Int J Dev Biol,* 57**,** 265-72.

AKUTSU, K., TAKATORI, S., NOZAWA, S., YOSHIIKE, M., NAKAZAWA, H., HAYAKAWA, K., MAKINO, T. & IWAMOTO, T. 2008. Polybrominated diphenyl ethers in human serum and sperm quality. *Bull Environ Contam Toxicol,* 80**,** 345-50.

AL-MOUSA, F. & MICHELANGELI, F. 2014. The sarcoplasmic-endoplasmic reticulum Ca(2+)-ATPase (SERCA) is the likely molecular target for the acute toxicity of the brominated flame retardant hexabromocyclododecane (HBCD). *Chem Biol Interact,* 207**,** 1-6.

ALLEN, J. G., GALE, S., ZOELLER, R. T., SPENGLER, J. D., BIRNBAUM, L. & MCNEELY, E. 2016. PBDE flame retardants, thyroid disease, and menopausal status in U.S. women. *Environ Health,* 15**,** 60.

ALY, H. A. 2013. Aroclor 1254 induced oxidative stress and mitochondria mediated apoptosis in adult rat sperm in vitro. *Environ Toxicol Pharmacol,* 36**,** 274-83.

AN, J., CHEN, C., WANG, X., ZHONG, Y., ZHANG, X., YU, Y. & YU, Z. 2014. Oligomeric proanthocyanidins alleviate hexabromocyclododecane-induced cytotoxicity in HepG2 cells through regulation on ROS formation and mitochondrial pathway. *Toxicol In Vitro,* 28**,** 319-26.

ANDRADE, A. J., GRANDE, S. W., TALSNESS, C. E., GROTE, K., GOLOMBIEWSKI, A., STERNER-KOCK, A. & CHAHOUD, I. 2006. A dose-response study following in utero and lactational exposure to di-(2-ethylhexyl) phthalate (DEHP): effects on androgenic status, developmental landmarks and testicular histology in male offspring rats. *Toxicology,* 225**,** 64-74.

ANIAGU, S. O., WILLIAMS, T. D., ALLEN, Y., KATSIADAKI, I. & CHIPMAN, J. K. 2008. Global genomic methylation levels in the liver and gonads of the three-spine stickleback (Gasterosteus aculeatus) after exposure to hexabromocyclododecane and 17-beta oestradiol. *Environ Int,* 34**,** 310-7.

ARVANITI, O. S. & STASINAKIS, A. S. 2015. Review on the occurrence, fate and removal of perfluorinated compounds during wastewater treatment. *Sci Total Environ,* 524-525**,** 81-92.

BALABAN, R. S., NEMOTO, S. & FINKEL, T. 2005. Mitochondria, oxidants, and aging. *Cell,* 120**,** 483-95.

BALHORN, R. 2007. The protamine family of sperm nuclear proteins. *Genome Biol,* 8**,** 227.

BARNA, M., MERGHOUB, T., COSTOYA, J. A., RUGGERO, D., BRANFORD, M., BERGIA, A., SAMORI, B. & PANDOLFI, P. P. 2002. Plzf mediates transcriptional repression of HoxD gene expression through chromatin remodeling. *Dev Cell,* 3**,** 499-510.

BERGER, R. G., LEFEVRE, P. L., ERNEST, S. R., WADE, M. G., MA, Y. Q., RAWN, D. F., GAERTNER, D. W., ROBAIRE, B. & HALES, B. F. 2014. Exposure to an environmentally relevant mixture of brominated flame retardants affects fetal development in Sprague-Dawley rats. *Toxicology,* 320**,** 56-66.

BETTS, K. S. 2010a. Endocrine damper? Flame retardants linked to male hormone, sperm count changes. *Environ Health Perspect,* 118**,** A 130.

BETTS, K. S. 2010b. Thyroid insult: flame retardants linked to alterations in pregnant women's TSH levels. *Environ Health Perspect,* 118**,** A445.

BETTS, K. S. 2013. Exposure to TDCPP appears widespread. *Environ Health Perspect,* 121**,** a150.

BIAVA, C. G., SMUCKLER, E. A. & WHORTON, D. 1978. The testicular morphology of individuals exposed to dibromochloropropane. *Exp Mol Pathol,* 29**,** 448-58.

BIRNBAUM, L. S., MORRISSEY, R. E. & HARRIS, M. W. 1991. Teratogenic effects of 2,3,7,8-tetrabromodibenzo-p-dioxin and three polybrominated dibenzofurans in C57BL/6N mice. *Toxicol Appl Pharmacol,* 107**,** 141-52.

BJERMO, H., AUNE, M., CANTILLANA, T., GLYNN, A., LIND, P. M., RIDEFELT, P. & DARNERUD, P. O. 2017. Serum levels of brominated flame retardants (BFRs: PBDE, HBCD) and influence of dietary factors in a population-based study on Swedish adults. *Chemosphere,* 167**,** 485-491.

BLANCK, H. M., MARCUS, M., TOLBERT, P. E., RUBIN, C., HENDERSON, A. K., HERTZBERG, V. S., ZHANG, R. H. & CAMERON, L. 2000. Age at menarche and tanner stage in girls exposed in utero and postnatally to polybrominated biphenyl. *Epidemiology,* 11**,** 641-7.

BLOOM, M. S., WHITCOMB, B. W., CHEN, Z., YE, A., KANNAN, K. & BUCK LOUIS, G. M. 2015. Associations between urinary phthalate concentrations and semen quality parameters in a general population. *Hum Reprod,* 30**,** 2645-57.

BLUM, A., GOLD, M. D., AMES, B. N., JONES, F. R., HETT, E. A., DOUGHERTY, R. C., HORNING, E. C., DZIDIC, I., CARROLL, D. I., STILLWELL, R. N. & THENOT, J. P. 1978. Children absorb tris-BP flame retardant from sleepwear: urine contains the mutagenic metabolite, 2,3-dibromopropanol. *Science,* 201**,** 1020-3.

BOEKELHEIDE, K., DARNEY, S. P., DASTON, G. P., DAVID, R. M., LUDERER, U., OLSHAN, A. F., SANDERSON, W. T., WILLHITE, C. C., WOSKIE, S. & PANEL, N. T. P. C. F. T. E. O. R. T. H. R. B. E. 2004. NTP-CERHR Expert Panel Report on the reproductive and developmental toxicity of 2-bromopropane. *Reprod Toxicol,* 18**,** 189-217.

BONDE, J. P., FLACHS, E. M., RIMBORG, S., GLAZER, C. H., GIWERCMAN, A., RAMLAU-HANSEN, C. H., HOUGAARD, K. S., HOYER, B. B., HAERVIG, K. K., PETERSEN, S. B., RYLANDER, L., SPECHT, I. O., TOFT, G. & BRAUNER, E. V. 2016. The epidemiologic evidence linking prenatal and postnatal exposure to endocrine disrupting chemicals with male reproductive disorders: a systematic review and meta-analysis. *Hum Reprod Update,* 23**,** 104-125.

BRAUN, J. M., KALKBRENNER, A. E., JUST, A. C., YOLTON, K., CALAFAT, A. M., SJODIN, A., HAUSER, R., WEBSTER, G. M., CHEN, A. & LANPHEAR, B. P. 2014. Gestational exposure to endocrine-disrupting chemicals and reciprocal social, repetitive, and stereotypic behaviors in 4- and 5-year-old children: the HOME study. *Environ Health Perspect,* 122**,** 513-20.

BRUGAROLAS, J., LEI, K., HURLEY, R. L., MANNING, B. D., REILING, J. H., HAFEN, E., WITTERS, L. A., ELLISEN, L. W. & KAELIN, W. G., JR. 2004. Regulation of mTOR function in response to hypoxia by REDD1 and the TSC1/TSC2 tumor suppressor complex. *Genes Dev,* 18**,** 2893-904.

BUAAS, F. W., KIRSH, A. L., SHARMA, M., MCLEAN, D. J., MORRIS, J. L., GRISWOLD, M. D., DE ROOIJ, D. G. & BRAUN, R. E. 2004. Plzf is required in adult male germ cells for stem cell self-renewal. *Nat Genet,* 36**,** 647-52.

BUHRKE, T., KIBELLUS, A. & LAMPEN, A. 2013. In vitro toxicological characterization of perfluorinated carboxylic acids with different carbon chain lengths. *Toxicol Lett,* 218**,** 97-104.

CALAFAT, A. M., WONG, L. Y., KUKLENYIK, Z., REIDY, J. A. & NEEDHAM, L. L. 2007. Polyfluoroalkyl chemicals in the U.S. population: data from the National Health and Nutrition Examination Survey (NHANES) 2003-2004 and comparisons with NHANES 1999-2000. *Environ Health Perspect,* 115**,** 1596-602.

CAMPION, S., CATLIN, N., HEGER, N., MCDONNELL, E. V., PACHECO, S. E., SAFFARINI, C., SANDROF, M. A. & BOEKELHEIDE, K. 2012. Male reprotoxicity and endocrine disruption. *EXS,* 101**,** 315-60.

CANNON, S. B., VEAZEY, J. M., JR., JACKSON, R. S., BURSE, V. W., HAYES, C., STRAUB, W. E., LANDRIGAN, P. J. & LIDDLE, J. A. 1978. Epidemic kepone poisoning in chemical workers. *Am J Epidemiol,* 107**,** 529-37.

CARIGNAN, C. C., MCCLEAN, M. D., COOPER, E. M., WATKINS, D. J., FRASER, A. J., HEIGER-BERNAYS, W., STAPLETON, H. M. & WEBSTER, T. F. 2013. Predictors of tris(1,3-dichloro-2-propyl) phosphate metabolite in the urine of office workers. *Environ Int,* 55**,** 56-61.

CARIGNAN, C. C., MINGUEZ-ALARCON, L., BUTT, C. M., WILLIAMS, P. L., MEEKER, J. D., STAPLETON, H. M., TOTH, T. L., FORD, J. B., HAUSER, R. & TEAM, E. S. 2017. Urinary Concentrations of Organophosphate Flame Retardant Metabolites and Pregnancy Outcomes among Women Undergoing in Vitro Fertilization. *Environ Health Perspect,* 125**,** 087018.

CARIGNAN, C. C., MINGUEZ-ALARCON, L., WILLIAMS, P. L., MEEKER, J. D., STAPLETON, H. M., BUTT, C. M., TOTH, T. L., FORD, J. B., HAUSER, R. & TEAM, E. S. 2018. Paternal urinary concentrations of organophosphate flame retardant metabolites, fertility measures, and pregnancy outcomes among couples undergoing in vitro fertilization. *Environ Int,* 111**,** 232-238.

CARIOU, R., ANTIGNAC, J. P., ZALKO, D., BERREBI, A., CRAVEDI, J. P., MAUME, D., MARCHAND, P., MONTEAU, F., RIU, A., ANDRE, F. & LE BIZEC, B. 2008. Exposure assessment of French women and their newborns to tetrabromobisphenol-A: occurrence measurements in maternal adipose tissue, serum, breast milk and cord serum. *Chemosphere,* 73**,** 1036-41.

CHAUVIGNE, F., MENUET, A., LESNE, L., CHAGNON, M. C., CHEVRIER, C., REGNIER, J. F., ANGERER, J. & JEGOU, B. 2009. Time- and dose-related effects of di-(2-ethylhexyl) phthalate and its main metabolites on the function of the rat fetal testis in vitro. *Environ Health Perspect,* 117**,** 515-21.

CHEN, J., MA, X., TIAN, L., KONG, A., WANG, N., HUANG, C. & YANG, D. 2018a. Chronic co-exposure to low levels of brominated flame retardants and heavy metals induces reproductive toxicity in zebrafish. *Toxicol Ind Health***,** 748233718779478.

CHEN, L., WANG, C., ZHANG, Y., ZHOU, Y., SHI, R., CUI, C., GAO, Y. & TIAN, Y. 2018b. Polybrominated diphenyl ethers in cord blood and perinatal outcomes from Laizhou Wan Birth Cohort, China. *Environ Sci Pollut Res Int,* 25**,** 20802-20808.

CHEN, S. R. & LIU, Y. X. 2015. Regulation of spermatogonial stem cell self-renewal and spermatocyte meiosis by Sertoli cell signaling. *Reproduction,* 149**,** R159-67.

CHEN ZEE, E., CORNET, P., LAZIMI, G., RONDET, C., LOCHARD, M., MAGNIER, A. M. & IBANEZ, G. 2013. [Impact of endocrine disrupting chemicals on birth outcomes]. *Gynecol Obstet Fertil,* 41**,** 601-10.

CHOI, E. M., SUH, K. S., RHEE, S. Y., OH, S., WOO, J. T., KIM, S. W., KIM, Y. S., PAK, Y. K. & CHON, S. 2017. Perfluorooctanoic acid induces mitochondrial dysfunction in MC3T3-E1 osteoblast cells. *J Environ Sci Health A Tox Hazard Subst Environ Eng,* 52**,** 281-289.

CHOI, J. S., LEE, Y. J., KIM, T. H., LIM, H. J., AHN, M. Y., KWACK, S. J., KANG, T. S., PARK, K. L., LEE, J., KIM, N. D., JEONG, T. C., KIM, S. G., JEONG, H. G., LEE, B. M. & KIM, H. S. 2011. Molecular Mechanism of Tetrabromobisphenol A (TBBPA)-induced Target Organ Toxicity in Sprague-Dawley Male Rats. *Toxicol Res,* 27**,** 61-70.

CLOUTIER, J. M. & TURNER, J. M. 2010. Meiotic sex chromosome inactivation. *Curr Biol,* 20**,** R962-3.

COOK, M., GOULD, A., BRAND, N., DAVIES, J., STRUTT, P., SHAKNOVICH, R., LICHT, J., WAXMAN, S., CHEN, Z., GLUECKSOHN-WAELSCH, S. & ET AL. 1995. Expression of the zinc-finger gene PLZF at rhombomere boundaries in the vertebrate hindbrain. *Proc Natl Acad Sci U S A,* 92**,** 2249-53.

COOPER, E. M., COVACI, A., VAN NUIJS, A. L., WEBSTER, T. F. & STAPLETON, H. M. 2011. Analysis of the flame retardant metabolites bis(1,3-dichloro-2-propyl) phosphate (BDCPP) and diphenyl phosphate (DPP) in urine using liquid chromatography-tandem mass spectrometry. *Anal Bioanal Chem,* 401**,** 2123-32.

COSTOYA, J. A., HOBBS, R. M., BARNA, M., CATTORETTI, G., MANOVA, K., SUKHWANI, M., ORWIG, K. E., WOLGEMUTH, D. J. & PANDOLFI, P. P. 2004. Essential role of Plzf in maintenance of spermatogonial stem cells. *Nat Genet,* 36**,** 653-9.

COVACI, A., GERECKE, A. C., LAW, R. J., VOORSPOELS, S., KOHLER, M., HEEB, N. V., LESLIE, H., ALLCHIN, C. R. & DE BOER, J. 2006. Hexabromocyclododecanes (HBCDs) in the environment and humans: a review. *Environ Sci Technol,* 40**,** 3679-88.

COVACI, A., HARRAD, S., ABDALLAH, M. A., ALI, N., LAW, R. J., HERZKE, D. & DE WIT, C. A. 2011. Novel brominated flame retardants: a review of their analysis, environmental fate and behaviour. *Environ Int,* 37**,** 532-56.

CRUMP, D., CHIU, S. & KENNEDY, S. W. 2012. Effects of tris(1,3-dichloro-2-propyl) phosphate and tris(1-chloropropyl) phosphate on cytotoxicity and mRNA expression in primary cultures of avian hepatocytes and neuronal cells. *Toxicol Sci,* 126**,** 140-8.

CZERSKA, M., ZIELINSKI, M., KAMINSKA, J. & LIGOCKA, D. 2013. Effects of polybrominated diphenyl ethers on thyroid hormone, neurodevelopment and fertility in rodents and humans. *Int J Occup Med Environ Health,* 26**,** 498-510.

DADOUNE, J. P. 2007. New insights into male gametogenesis: what about the spermatogonial stem cell niche? *Folia Histochem Cytobiol,* 45**,** 141-7.

DAO, T., HONG, X., WANG, X. & TANG, W. Y. 2015. Aberrant 5'-CpG Methylation of Cord Blood TNFalpha Associated with Maternal Exposure to Polybrominated Diphenyl Ethers. *PLoS One,* 10**,** e0138815.

DARNERUD, P. O., AUNE, M., LARSSON, L., LIGNELL, S., MUTSHATSHI, T., OKONKWO, J., BOTHA, B. & AGYEI, N. 2011. Levels of brominated flame retardants and other pesistent organic pollutants in breast milk samples from Limpopo Province, South Africa. *Sci Total Environ,* 409**,** 4048-53.

DAVID, G., ALLAND, L., HONG, S. H., WONG, C. W., DEPINHO, R. A. & DEJEAN, A. 1998. Histone deacetylase associated with mSin3A mediates repression by the acute promyelocytic leukemia-associated PLZF protein. *Oncogene,* 16**,** 2549-56.

DE ESCOBAR, G. M., OBREGON, M. J. & DEL REY, F. E. 2004. Maternal thyroid hormones early in pregnancy and fetal brain development. *Best Pract Res Clin Endocrinol Metab,* 18**,** 225-48.

DE WIT, C. A. 2002. An overview of brominated flame retardants in the environment. *Chemosphere,* 46**,** 583-624.

DEN HOND, E., TOURNAYE, H., DE SUTTER, P., OMBELET, W., BAEYENS, W., COVACI, A., COX, B., NAWROT, T. S., VAN LAREBEKE, N. & D'HOOGHE, T. 2015. Human exposure to endocrine disrupting chemicals and fertility: A case-control study in male subfertility patients. *Environ Int,* 84**,** 154-60.

DENG, J., GUO, J., ZHOU, X., ZHOU, P., FU, X., ZHANG, W. & LIN, K. 2014. Hazardous substances in indoor dust emitted from waste TV recycling facility. *Environ Sci Pollut Res Int,* 21**,** 7656-67.

DENG, J., YU, L., LIU, C., YU, K., SHI, X., YEUNG, L. W., LAM, P. K., WU, R. S. & ZHOU, B. 2009. Hexabromocyclododecane-induced developmental toxicity and apoptosis in zebrafish embryos. *Aquat Toxicol,* 93**,** 29-36.

DEODATI, A., SALLEMI, A., MARANGHI, F., GERMANI, D., PUGLIANIELLO, A., BALDARI, F., BUSANI, L., MANCINI, F. R., TASSINARI, R., MANTOVANI, A. & CIANFARANI, S. 2016. Serum Levels of Polybrominated Diphenyl Ethers in Girls with Premature Thelarche. *Horm Res Paediatr,* 86**,** 233-239.

DEONANDAN, R. & JALEEL, M. 2012. Global decline in semen quality: ignoring the developing world introduces selection bias. *Int J Gen Med,* 5**,** 303-6.

DISHAW, L. V., MACAULAY, L. J., ROBERTS, S. C. & STAPLETON, H. M. 2014. Exposures, mechanisms, and impacts of endocrine-active flame retardants. *Curr Opin Pharmacol,* 19**,** 125-33.

DODSON, R. E., PEROVICH, L. J., COVACI, A., VAN DEN EEDE, N., IONAS, A. C., DIRTU, A. C., BRODY, J. G. & RUDEL, R. A. 2012. After the PBDE phase-out: a broad suite of flame retardants in repeat house dust samples from California. *Environ Sci Technol,* 46**,** 13056-66.

E.C.B. EUROPEAN COMMISSION DIRECTRATE-GENERAL JOINT RESEARCH CENTER, I. F. H. A. C. P. E., EUROPEAN UNION RISK ASSESSMENT REPORT, EUROPEAN CHEMICALS BUREAU, UNITED KINGDOM 2006. European union risk assessment report. 2,2',6,6'-Tetrabromo-4,4'-isopropylidenediphenol (tetrabromobisphenol-A or TBBP-A). Part II – Human health.

EASLEY, C. A. T., BRADNER, J. M., MOSER, A., RICKMAN, C. A., MCEACHIN, Z. T., MERRITT, M. M., HANSEN, J. M. & CAUDLE, W. M. 2015. Assessing reproductive toxicity of two environmental toxicants with a novel in vitro human spermatogenic model. *Stem Cell Res,* 14**,** 347-55.

EASLEY, C. A. T., PHILLIPS, B. T., MCGUIRE, M. M., BARRINGER, J. M., VALLI, H., HERMANN, B. P., SIMERLY, C. R., RAJKOVIC, A., MIKI, T., ORWIG, K. E. & SCHATTEN, G. P. 2012. Direct differentiation of human pluripotent stem cells into haploid spermatogenic cells. *Cell Rep,* 2**,** 440-6.

EHMCKE, J., WISTUBA, J. & SCHLATT, S. 2006. Spermatogonial stem cells: questions, models and perspectives. *Hum Reprod Update,* 12**,** 275-82.

EL-HELALY, M., AWADALLA, N., MANSOUR, M. & EL-BIOMY, Y. 2010. Workplace exposures and male infertility - a case-control study. *Int J Occup Med Environ Health,* 23**,** 331-8.

ERKEKOGLU, P. & KOCER-GUMUSEL, B. 2014. Genotoxicity of phthalates. *Toxicol Mech Methods,* 24**,** 616-26.

ESKENAZI, B., RAUCH, S. A., TENERELLI, R., HUEN, K., HOLLAND, N. T., LUSTIG, R. H., KOGUT, K., BRADMAN, A., SJODIN, A. & HARLEY, K. G. 2017. In utero and childhood DDT, DDE, PBDE and PCBs exposure and sex hormones in adolescent boys: The CHAMACOS study. *Int J Hyg Environ Health,* 220**,** 364-372.

FAN, Y. O., JIN, Y. H., MA, Y. X. & ZHANG, Y. H. 2005. [Effects of perfluorooctane sulfonate on spermiogenesis function of male rats]. *Wei Sheng Yan Jiu,* 34**,** 37-9.

FANG, X., FENG, Y., WANG, J. & DAI, J. 2010. Perfluorononanoic acid-induced apoptosis in rat spleen involves oxidative stress and the activation of caspase-independent death pathway. *Toxicology,* 267**,** 54-9.

FANG, X., ZHANG, L., FENG, Y., ZHAO, Y. & DAI, J. 2008. Immunotoxic effects of perfluorononanoic acid on BALB/c mice. *Toxicol Sci,* 105**,** 312-21.

FARHAT, A., BUICK, J. K., WILLIAMS, A., YAUK, C. L., O'BRIEN, J. M., CRUMP, D., WILLIAMS, K. L., CHIU, S. & KENNEDY, S. W. 2014. Tris(1,3-dichloro-2-propyl) phosphate perturbs the expression of genes involved in immune response and lipid and steroid metabolism in chicken embryos. *Toxicol Appl Pharmacol,* 275**,** 104-12.

FAYOMI, A. P. & ORWIG, K. E. 2018. Spermatogonial stem cells and spermatogenesis in mice, monkeys and men. *Stem Cell Res,* 29**,** 207-214.

FENG, Y., FANG, X., SHI, Z., XU, M. & DAI, J. 2010. Effects of PFNA exposure on expression of junction-associated molecules and secretory function in rat Sertoli cells. *Reprod Toxicol,* 30**,** 429-37.

FENG, Y., SHI, Z., FANG, X., XU, M. & DAI, J. 2009. Perfluorononanoic acid induces apoptosis involving the Fas death receptor signaling pathway in rat testis. *Toxicol Lett,* 190**,** 224-30.

FOSTER, W. G., NEAL, M. S., HAN, M. S. & DOMINGUEZ, M. M. 2008. Environmental contaminants and human infertility: hypothesis or cause for concern? *J Toxicol Environ Health B Crit Rev,* 11**,** 162-76.

FROMME, H., BECHER, G., HILGER, B. & VOLKEL, W. 2016a. Brominated flame retardants - Exposure and risk assessment for the general population. *Int J Hyg Environ Health,* 219**,** 1-23.

FROMME, H., HILGER, B., ALBRECHT, M., GRIES, W., LENG, G. & VOLKEL, W. 2016b. Occurrence of chlorinated and brominated dioxins/furans, PCBs, and brominated flame retardants in blood of German adults. *Int J Hyg Environ Health,* 219**,** 380-8.

FU, J., GAO, Y., CUI, L., WANG, T., LIANG, Y., QU, G., YUAN, B., WANG, Y., ZHANG, A. & JIANG, G. 2016. Occurrence, temporal trends, and half-lives of perfluoroalkyl acids (PFAAs) in occupational workers in China. *Sci Rep,* 6**,** 38039.

GAO, Y., CHEN, L., WANG, C., ZHOU, Y., WANG, Y., ZHANG, Y., HU, Y., JI, L., SHI, R., CUI, C., DING, G., JIN, J. & TIAN, Y. 2016. Exposure to polybrominated diphenyl ethers and female reproductive function: A study in the production area of Shandong, China. *Sci Total Environ,* 572**,** 9-15.

GEYER HJ, S. K., DARNERUD PO, AUNE M, EA FEICHT, FRIED KW, HENKELMANN B, LENOIR D, SCHMID P, MCDONALD TA 2004. Terminal elimination half-lives of the brominated flame retardants TBBPA, HBCD, and lower brominated PBDEs in humans *Organohalogen Compounds,* 66.

GOLD, M. D., BLUM, A. & AMES, B. N. 1978. Another flame retardant, tris-(1,3-dichloro-2-propyl)-phosphate, and its expected metabolites are mutagens. *Science,* 200**,** 785-7.

GOODYER, C. G., POON, S., ALEKSA, K., HOU, L., ATEHORTUA, V., CARNEVALE, A., JEDNAK, R., EMIL, S., BAGLI, D., DAVE, S., HALES, B. F. & CHEVRIER, J. 2017. A Case-Control Study of Maternal Polybrominated Diphenyl Ether (PBDE) Exposure and Cryptorchidism in Canadian Populations. *Environ Health Perspect,* 125**,** 057004.

GORROCHATEGUI, E., LACORTE, S., TAULER, R. & MARTIN, F. L. 2016. Perfluoroalkylated Substance Effects in Xenopus laevis A6 Kidney Epithelial Cells Determined by ATR-FTIR Spectroscopy and Chemometric Analysis. *Chem Res Toxicol,* 29**,** 924-32.

GORROCHATEGUI, E., PEREZ-ALBALADEJO, E., CASAS, J., LACORTE, S. & PORTE, C. 2014. Perfluorinated chemicals: differential toxicity, inhibition of aromatase activity and alteration of cellular lipids in human placental cells. *Toxicol Appl Pharmacol,* 277**,** 124-30.

GOVERNINI, L., GUERRANTI, C., DE LEO, V., BOSCHI, L., LUDDI, A., GORI, M., ORVIETO, R. & PIOMBONI, P. 2015. Chromosomal aneuploidies and DNA fragmentation of human spermatozoa from patients exposed to perfluorinated compounds. *Andrologia,* 47**,** 1012-9.

GRAY, W. A. & BILLOCK, V. A. 2017. Developmental neurotoxicity and autism: A potential link between indoor neuroactive pollutants and the curious birth order risk factor. *Int J Dev Neurosci,* 62**,** 32-36.

GREGORASZCZUK, E. L., RAK, A., KAWALEC, K. & ROPSTAD, E. 2008. Steroid secretion following exposure of ovarian follicular cells to single congeners and defined mixture of polybrominateddibenzoethers (PBDEs), p,p'-DDT and its metabolite p,p'-DDE. *Toxicol Lett,* 178**,** 103-9.

GUO, X., LI, Q., SHI, J., SHI, L., LI, B., XU, A., ZHAO, G. & WU, L. 2016. Perfluorooctane sulfonate exposure causes gonadal developmental toxicity in Caenorhabditis elegans through ROS-induced DNA damage. *Chemosphere,* 155**,** 115-126.

GURUGE, K. S., TANIYASU, S., YAMASHITA, N., WIJERATNA, S., MOHOTTI, K. M., SENEVIRATNE, H. R., KANNAN, K., YAMANAKA, N. & MIYAZAKI, S. 2005. Perfluorinated organic compounds in human blood serum and seminal plasma: a study of urban and rural tea worker populations in Sri Lanka. *J Environ Monit,* 7**,** 371-7.

HAN, X. B., YUEN, K. W. & WU, R. S. 2013. Polybrominated diphenyl ethers affect the reproduction and development, and alter the sex ratio of zebrafish (Danio rerio). *Environ Pollut,* 182**,** 120-6.

HARLEY, K. G., CHEVRIER, J., AGUILAR SCHALL, R., SJODIN, A., BRADMAN, A. & ESKENAZI, B. 2011. Association of prenatal exposure to polybrominated diphenyl ethers and infant birth weight. *Am J Epidemiol,* 174**,** 885-92.

HARLEY, K. G., MARKS, A. R., CHEVRIER, J., BRADMAN, A., SJODIN, A. & ESKENAZI, B. 2010. PBDE concentrations in women's serum and fecundability. *Environ Health Perspect,* 118**,** 699-704.

HARRISON, P. T., HOLMES, P. & HUMFREY, C. D. 1997. Reproductive health in humans and wildlife: are adverse trends associated with environmental chemical exposure? *Sci Total Environ,* 205**,** 97-106.

HE, L. Z., GUIDEZ, F., TRIBIOLI, C., PERUZZI, D., RUTHARDT, M., ZELENT, A. & PANDOLFI, P. P. 1998. Distinct interactions of PML-RARalpha and PLZF-RARalpha with co-repressors determine differential responses to RA in APL. *Nat Genet,* 18**,** 126-35.

HENRY, B. J., CARLIN, J. P., HAMMERSCHMIDT, J. A., BUCK, R. C., BUXTON, L. W., FIEDLER, H., SEED, J. & HERNANDEZ, O. 2018. A critical review of the application of polymer of low concern and regulatory criteria to fluoropolymers. *Integr Environ Assess Manag,* 14**,** 316-334.

HERBSTMAN, J. B., SJODIN, A., KURZON, M., LEDERMAN, S. A., JONES, R. S., RAUH, V., NEEDHAM, L. L., TANG, D., NIEDZWIECKI, M., WANG, R. Y. & PERERA, F. 2010. Prenatal exposure to PBDEs and neurodevelopment. *Environ Health Perspect,* 118**,** 712-9.

HERTZ-PICCIOTTO, I., BERGMAN, A., FANGSTROM, B., ROSE, M., KRAKOWIAK, P., PESSAH, I., HANSEN, R. & BENNETT, D. H. 2011. Polybrominated diphenyl ethers in relation to autism and developmental delay: a case-control study. *Environ Health,* 10**,** 1.

HILL, K. L., HAMERS, T., KAMSTRA, J. H., WILLMORE, W. G. & LETCHER, R. J. 2018a. Organophosphate triesters and selected metabolites enhance binding of thyroxine to human transthyretin in vitro. *Toxicol Lett,* 285**,** 87-93.

HILL, K. L., MORTENSEN, A. K., TECLECHIEL, D., WILLMORE, W. G., SYLTE, I., JENSSEN, B. M. & LETCHER, R. J. 2018b. In Vitro and in Silico Competitive Binding of Brominated Polyphenyl Ether Contaminants with Human and Gull Thyroid Hormone Transport Proteins. *Environ Sci Technol,* 52**,** 1533-1541.

HOBBS, R. M., SEANDEL, M., FALCIATORI, I., RAFII, S. & PANDOLFI, P. P. 2010. Plzf regulates germline progenitor self-renewal by opposing mTORC1. *Cell,* 142**,** 468-79.

HOFFMAN, K., STAPLETON, H. M., LORENZO, A., BUTT, C. M., ADAIR, L., HERRING, A. H. & DANIELS, J. L. 2018. Prenatal exposure to organophosphates and associations with birthweight and gestational length. *Environ Int,* 116**,** 248-254.

HOFMANN, J., GUARDADO, J., KEIFER, M. & WESSELING, C. 2006. Mortality among a cohort of banana plantation workers in Costa Rica. *Int J Occup Environ Health,* 12**,** 321-8.

HONG, S. H., DAVID, G., WONG, C. W., DEJEAN, A. & PRIVALSKY, M. L. 1997. SMRT corepressor interacts with PLZF and with the PML-retinoic acid receptor alpha (RARalpha) and PLZF-RARalpha oncoproteins associated with acute promyelocytic leukemia. *Proc Natl Acad Sci U S A,* 94**,** 9028-33.

HONKISZ, E. & WOJTOWICZ, A. K. 2015. Modulation of estradiol synthesis and aromatase activity in human choriocarcinoma JEG-3 cells exposed to tetrabromobisphenol A. *Toxicol In Vitro,* 29**,** 44-50.

HU, M., LI, J., ZHANG, B., CUI, Q., WEI, S. & YU, H. 2014. Regional distribution of halogenated organophosphate flame retardants in seawater samples from three coastal cities in China. *Mar Pollut Bull,* 86**,** 569-74.

HU, W., JONES, P. D., DECOEN, W., KING, L., FRAKER, P., NEWSTED, J. & GIESY, J. P. 2003. Alterations in cell membrane properties caused by perfluorinated compounds. *Comp Biochem Physiol C Toxicol Pharmacol,* 135**,** 77-88.

HU, X. C., ANDREWS, D. Q., LINDSTROM, A. B., BRUTON, T. A., SCHAIDER, L. A., GRANDJEAN, P., LOHMANN, R., CARIGNAN, C. C., BLUM, A., BALAN, S. A., HIGGINS, C. P. & SUNDERLAND, E. M. 2016. Detection of Poly- and Perfluoroalkyl Substances (PFASs) in U.S. Drinking Water Linked to Industrial Sites, Military Fire Training Areas, and Wastewater Treatment Plants. *Environ Sci Technol Lett,* 3**,** 344-350.

HUANG, S., CUI, Y., GUO, X., WANG, L., LI, S., LU, Y., BI, Y., HUANG, X., LIN, M., XIA, Y., WANG, S., WANG, X., ZHOU, Z. & SHA, J. 2015. 2,2',4,4'-Tetrabromodiphenyl ether disrupts spermatogenesis, impairs mitochondrial function and induces apoptosis of early leptotene spermatocytes in rats. *Reprod Toxicol,* 51**,** 114-24.

HUANG, X., CHEN, C., SHANG, Y., ZHONG, Y., REN, G., YU, Z. & AN, J. 2016. In vitro study on the biotransformation and cytotoxicity of three hexabromocyclododecane diastereoisomers in liver cells. *Chemosphere,* 161**,** 251-8.

HUDEC, T., THEAN, J., KUEHL, D. & DOUGHERTY, R. C. 1981. Tris(dichloropropyl)phosphate, a mutagenic flame retardant: frequent cocurrence in human seminal plasma. *Science,* 211**,** 951-2.

INGLE, M. E., MINGUEZ-ALARCON, L., CARIGNAN, C. C., BUTT, C. M., STAPLETON, H. M., WILLIAMS, P. L., FORD, J. B., HAUSER, R., MEEKER, J. D. & TEAM, E. S. 2018. The association between urinary concentrations of phosphorous-containing flame retardant metabolites and semen parameters among men from a fertility clinic. *Int J Hyg Environ Health,* 221**,** 809-815.

JAKOBSSON, K., THURESSON, K., RYLANDER, L., SJODIN, A., HAGMAR, L. & BERGMAN, A. 2002. Exposure to polybrominated diphenyl ethers and tetrabromobisphenol A among computer technicians. *Chemosphere,* 46**,** 709-16.

JAROSIEWICZ, M. & BUKOWSKA, B. 2017. [Tetrabromobisphenol A - Toxicity, environmental and occupational exposures]. *Med Pr,* 68**,** 121-134.

JOENSEN, U. N., VEYRAND, B., ANTIGNAC, J. P., BLOMBERG JENSEN, M., PETERSEN, J. H., MARCHAND, P., SKAKKEBAEK, N. E., ANDERSSON, A. M., LE BIZEC, B. & JORGENSEN, N. 2013. PFOS (perfluorooctanesulfonate) in serum is negatively associated with testosterone levels, but not with semen quality, in healthy men. *Hum Reprod,* 28**,** 599-608.

JOHNSON, P. I., STAPLETON, H. M., MUKHERJEE, B., HAUSER, R. & MEEKER, J. D. 2013. Associations between brominated flame retardants in house dust and hormone levels in men. *Sci Total Environ,* 445-446**,** 177-84.

JOSEPH, A. D., TERRELL, M. L., SMALL, C. M., CAMERON, L. L. & MARCUS, M. 2009. Assessing inter-generational transfer of a brominated flame retardant. *J Environ Monit,* 11**,** 802-7.

JULIANO, C., WANG, J. & LIN, H. 2011. Uniting germline and stem cells: the function of Piwi proteins and the piRNA pathway in diverse organisms. *Annu Rev Genet,* 45**,** 447-69.

JUREWICZ, J., HANKE, W., RADWAN, M. & BONDE, J. P. 2009. Environmental factors and semen quality. *Int J Occup Med Environ Health,* 22**,** 305-29.

JUREWICZ, J., POLANSKA, K. & HANKE, W. 2013. Exposure to widespread environmental toxicants and children's cognitive development and behavioral problems. *Int J Occup Med Environ Health,* 26**,** 185-204.

JUSKO, T. A., OKTAPODAS, M., PALKOVICOVA MURINOVA, L., BABINSKA, K., BABJAKOVA, J., VERNER, M. A., DEWITT, J. C., THEVENET-MORRISON, K., CONKA, K., DROBNA, B., CHOVANCOVA, J., THURSTON, S. W., LAWRENCE, B. P., DOZIER, A. M., JARVINEN, K. M., PATAYOVA, H., TRNOVEC, T., LEGLER, J., HERTZ-PICCIOTTO, I. & LAMOREE, M. H. 2016. Demographic, Reproductive, and Dietary Determinants of Perfluorooctane Sulfonic (PFOS) and Perfluorooctanoic Acid (PFOA) Concentrations in Human Colostrum. *Environ Sci Technol,* 50**,** 7152-62.

KALKBRENNER, A. E., SCHMIDT, R. J. & PENLESKY, A. C. 2014. Environmental chemical exposures and autism spectrum disorders: a review of the epidemiological evidence. *Curr Probl Pediatr Adolesc Health Care,* 44**,** 277-318.

KARPETA, A. & GREGORASZCZUK, E. 2010. Mixture of dominant PBDE congeners (BDE-47, -99, -100 and -209) at levels noted in human blood dramatically enhances progesterone secretion by ovarian follicles. *Endocr Regul,* 44**,** 49-55.

KATO, H., FUJII, S., TAKAHASHI, M., MATSUMOTO, M., HIRATA-KOIZUMI, M., ONO, A. & HIROSE, A. 2015. Repeated dose and reproductive/developmental toxicity of perfluorododecanoic acid in rats. *Environ Toxicol,* 30**,** 1244-63.

KATO, K., WONG, L. Y., JIA, L. T., KUKLENYIK, Z. & CALAFAT, A. M. 2011. Trends in exposure to polyfluoroalkyl chemicals in the U.S. Population: 1999-2008. *Environ Sci Technol,* 45**,** 8037-45.

KE, H. 2002. Tetrabromobisphenol A [79-94-7]: Review of Toxicological Literature

KHALIL, A., PARKER, M., BROWN, S. E., CEVIK, S. E., GUO, L. W., JENSEN, J., OLMSTED, A., PORTMAN, D., WU, H. & SUVOROV, A. 2017. Perinatal exposure to 2,2',4'4' -Tetrabromodiphenyl ether induces testicular toxicity in adult rats. *Toxicology,* 389**,** 21-30.

KHARLYNGDOH, J. B., PRADHAN, A., ASNAKE, S., WALSTAD, A., IVARSSON, P. & OLSSON, P. E. 2015. Identification of a group of brominated flame retardants as novel androgen receptor antagonists and potential neuronal and endocrine disrupters. *Environ Int,* 74**,** 60-70.

KHOSRORAD, T., DOLATIAN, M., RIAZI, H., MAHMOODI, Z., ALAVIMAJD, H., SHAHSAVARI, S. & BAKHTIARI, M. 2015. Comparison of lifestyle in fertile and infertile couples in Kermanshah during 2013. *Iran J Reprod Med,* 13**,** 549-56.

KIM, S. H., NAM, K. H., HWANG, K. A. & CHOI, K. C. 2016. Influence of hexabromocyclododecane and 4-nonylphenol on the regulation of cell growth, apoptosis and migration in prostatic cancer cells. *Toxicol In Vitro,* 32**,** 240-7.

KLOPCIC, I., SKLEDAR, D. G., MASIC, L. P. & DOLENC, M. S. 2016. Comparison of in vitro hormone activities of novel flame retardants TBB, TBPH and their metabolites TBBA and TBMEPH using reporter gene assays. *Chemosphere,* 160**,** 244-51.

KOLESNICHENKO, M. & VOGT, P. K. 2011. Understanding PLZF: two transcriptional targets, REDD1 and smooth muscle alpha-actin, define new questions in growth control, senescence, self-renewal and tumor suppression. *Cell Cycle,* 10**,** 771-5.

KOTAJA, N. & SASSONE-CORSI, P. 2004. Plzf pushes stem cells. *Nat Genet,* 36**,** 551-3.

KRAJEWSKA-KULAK, E. & SENGUPTA, P. 2013. Thyroid function in male infertility. *Front Endocrinol (Lausanne),* 4**,** 174.

KRIVOSHIEV, B. V., DARDENNE, F., COVACI, A., BLUST, R. & HUSSON, S. J. 2016. Assessing in-vitro estrogenic effects of currently-used flame retardants. *Toxicol In Vitro,* 33**,** 153-62.

KUMAR, S. 2004. Occupational exposure associated with reproductive dysfunction. *J Occup Health,* 46**,** 1-19.

KURIYAMA, S. N. & CHAHOUD, I. 2004. In utero exposure to low-dose 2,3',4,4',5-pentachlorobiphenyl (PCB 118) impairs male fertility and alters neurobehavior in rat offspring. *Toxicology,* 202**,** 185-97.

KURIYAMA, S. N., TALSNESS, C. E., GROTE, K. & CHAHOUD, I. 2005. Developmental exposure to low dose PBDE 99: effects on male fertility and neurobehavior in rat offspring. *Environ Health Perspect,* 113**,** 149-54.

KVIST, L., GIWERCMAN, Y. L., JONSSON, B. A., LINDH, C. H., BONDE, J. P., TOFT, G., STRUCINSKI, P., PEDERSEN, H. S., ZVYEZDAY, V. & GIWERCMAN, A. 2012. Serum levels of perfluorinated compounds and sperm Y:X chromosome ratio in two European populations and in Inuit from Greenland. *Reprod Toxicol,* 34**,** 644-50.

LABBAYE, C., QUARANTA, M. T., PAGLIUCA, A., MILITI, S., LICHT, J. D., TESTA, U. & PESCHLE, C. 2002. PLZF induces megakaryocytic development, activates Tpo receptor expression and interacts with GATA1 protein. *Oncogene,* 21**,** 6669-79.

LAM, J., LANPHEAR, B. P., BELLINGER, D., AXELRAD, D. A., MCPARTLAND, J., SUTTON, P., DAVIDSON, L., DANIELS, N., SEN, S. & WOODRUFF, T. J. 2017. Developmental PBDE Exposure and IQ/ADHD in Childhood: A Systematic Review and Meta-analysis. *Environ Health Perspect,* 125**,** 086001.

LEI, M., ZHANG, L., LEI, J., ZONG, L., LI, J., WU, Z. & WANG, Z. 2015. Overview of Emerging Contaminants and Associated Human Health Effects. *Biomed Res Int,* 2015**,** 404796.

LEONETTI, C., BUTT, C. M., HOFFMAN, K., HAMMEL, S. C., MIRANDA, M. L. & STAPLETON, H. M. 2016a. Brominated flame retardants in placental tissues: associations with infant sex and thyroid hormone endpoints. *Environ Health,* 15**,** 113.

LEONETTI, C., BUTT, C. M., HOFFMAN, K., MIRANDA, M. L. & STAPLETON, H. M. 2016b. Concentrations of polybrominated diphenyl ethers (PBDEs) and 2,4,6-tribromophenol in human placental tissues. *Environ Int,* 88**,** 23-29.

LEVINE, H. J., NIELS; MARTINO-ANDRADE, ANDERSON; MENDIOLA, JAIME; WEKSLER-DERRI, DAN; MINDLIS, IRINA; PINOTTI, RACHEL; AND SHANNA H. SWAN 2017. Temporal trends in sperm count: a systematic review and meta-regression analysis. *Human Reproduction Update*.

LI, L., ZHANG, T., QIN, X. S., GE, W., MA, H. G., SUN, L. L., HOU, Z. M., CHEN, H., CHEN, P., QIN, G. Q., SHEN, W. & ZHANG, X. F. 2014a. Exposure to diethylhexyl phthalate (DEHP) results in a heritable modification of imprint genes DNA methylation in mouse oocytes. *Mol Biol Rep,* 41**,** 1227-35.

LI, P., YANG, C. Q., JIN, J., WANG, Y., LIU, W. Z. & DING, W. W. 2014b. [Correlations between HBCD and thyroid hormone concentrations in human serum from production source area]. *Huan Jing Ke Xue,* 35**,** 3970-6.

LI, R., ZHOU, P., GUO, Y., LEE, J. S. & ZHOU, B. 2017a. Tris (1, 3-dichloro-2-propyl) phosphate induces apoptosis and autophagy in SH-SY5Y cells: Involvement of ROS-mediated AMPK/mTOR/ULK1 pathways. *Food Chem Toxicol,* 100**,** 183-196.

LI, Y., FLETCHER, T., MUCS, D., SCOTT, K., LINDH, C. H., TALLVING, P. & JAKOBSSON, K. 2017b. Half-lives of PFOS, PFHxS and PFOA after end of exposure to contaminated drinking water. *Occup Environ Med*.

LIANG, S., YIN, L., SHENGYANG YU, K., HOFMANN, M. C. & YU, X. 2017. High-Content Analysis Provides Mechanistic Insights into the Testicular Toxicity of Bisphenol A and Selected Analogues in Mouse Spermatogonial Cells. *Toxicol Sci,* 155**,** 43-60.

LINHARTOVA, P., GAZO, I., SHALIUTINA-KOLESOVA, A., HULAK, M. & KASPAR, V. 2015. Effects of tetrabrombisphenol A on DNA integrity, oxidative stress, and sterlet (Acipenser ruthenus) spermatozoa quality variables. *Environ Toxicol,* 30**,** 735-45.

LIPSHULTZ, L. I., ROSS, C. E., WHORTON, D., MILBY, T., SMITH, R. & JOYNER, R. E. 1980. Dibromochloropropane and its effect on testicular function in man. *J Urol,* 124**,** 464-8.

LIU, C., QIAN, P., YANG, L., ZHANG, L., CHEN, C., HE, M., LU, Y., FENG, W., LI, M., ZHANG, Y., ZHONG, M., YU, Z. & ZHOU, Z. 2016a. Pubertal exposure to di-(2-ethylhexyl)-phthalate inhibits G9a-mediated histone methylation during spermatogenesis in mice. *Arch Toxicol,* 90**,** 955-69.

LIU, L. Y., HE, K., HITES, R. A. & SALAMOVA, A. 2016b. Hair and Nails as Noninvasive Biomarkers of Human Exposure to Brominated and Organophosphate Flame Retardants. *Environ Sci Technol,* 50**,** 3065-73.

LIU, T. M., LEE, E. H., LIM, B. & SHYH-CHANG, N. 2016c. Concise Review: Balancing Stem Cell Self-Renewal and Differentiation with PLZF. *Stem Cells,* 34**,** 277-87.

LIU, W., YANG, B., WU, L., ZOU, W., PAN, X., ZOU, T., LIU, F., XIA, L., WANG, X. & ZHANG, D. 2015. Involvement of NRF2 in Perfluorooctanoic Acid-Induced Testicular Damage in Male Mice. *Biol Reprod,* 93**,** 41.

LIU, X., JI, K. & CHOI, K. 2012. Endocrine disruption potentials of organophosphate flame retardants and related mechanisms in H295R and MVLN cell lines and in zebrafish. *Aquat Toxicol,* 114-115**,** 173-81.

LIU, X., JI, K., JO, A., MOON, H. B. & CHOI, K. 2013. Effects of TDCPP or TPP on gene transcriptions and hormones of HPG axis, and their consequences on reproduction in adult zebrafish (Danio rerio). *Aquat Toxicol,* 134-135**,** 104-11.

LOUIS, E. J. & BORTS, R. H. 2003. Meiotic recombination: too much of a good thing? *Curr Biol,* 13**,** R953-5.

LOUIS, G. M., CHEN, Z., SCHISTERMAN, E. F., KIM, S., SWEENEY, A. M., SUNDARAM, R., LYNCH, C. D., GORE-LANGTON, R. E. & BARR, D. B. 2015. Perfluorochemicals and Human Semen Quality: The LIFE Study. *Environ Health Perspect,* 123**,** 57-63.

LU, Y., PAN, Y., SHENG, N., ZHAO, A. Z. & DAI, J. 2016. Perfluorooctanoic acid exposure alters polyunsaturated fatty acid composition, induces oxidative stress and activates the AKT/AMPK pathway in mouse epididymis. *Chemosphere,* 158**,** 143-53.

LYALL, K., CROEN, L. A., WEISS, L. A., KHARRAZI, M., TRAGLIA, M., DELORENZE, G. N. & WINDHAM, G. C. 2017. Prenatal Serum Concentrations of Brominated Flame Retardants and Autism Spectrum Disorder and Intellectual Disability in the Early Markers of Autism Study: A Population-Based Case-Control Study in California. *Environ Health Perspect,* 125**,** 087023.

MAIN, K. M., KIVIRANTA, H., VIRTANEN, H. E., SUNDQVIST, E., TUOMISTO, J. T., TUOMISTO, J., VARTIAINEN, T., SKAKKEBAEK, N. E. & TOPPARI, J. 2007. Flame retardants in placenta and breast milk and cryptorchidism in newborn boys. *Environ Health Perspect,* 115**,** 1519-26.

MAIORINO, M. & URSINI, F. 2002. Oxidative stress, spermatogenesis and fertility. *Biol Chem,* 383**,** 591-7.

MAKEY, C. M., MCCLEAN, M. D., BRAVERMAN, L. E., PEARCE, E. N., SJODIN, A., WEINBERG, J. & WEBSTER, T. F. 2016. Polybrominated diphenyl ether exposure and reproductive hormones in North American men. *Reprod Toxicol,* 62**,** 46-52.

MAKINEN, M. S., MAKINEN, M. R., KOISTINEN, J. T., PASANEN, A. L., PASANEN, P. O., KALLIOKOSKI, P. J. & KORPI, A. M. 2009. Respiratory and dermal exposure to organophosphorus flame retardants and tetrabromobisphenol A at five work environments. *Environ Sci Technol,* 43**,** 941-7.

MARSHALL, S., WHORTON, D., KRAUSS, R. M. & PALMER, W. S. 1978. Effect of pesticides on testicular function. *Urology,* 11**,** 257-9.

MCGEE, S. P., COOPER, E. M., STAPLETON, H. M. & VOLZ, D. C. 2012. Early zebrafish embryogenesis is susceptible to developmental TDCPP exposure. *Environ Health Perspect,* 120**,** 1585-91.

MEEKER, J. D., COOPER, E. M., STAPLETON, H. M. & HAUSER, R. 2013. Exploratory analysis of urinary metabolites of phosphorus-containing flame retardants in relation to markers of male reproductive health. *Endocr Disruptors (Austin),* 1**,** e26306.

MEEKER, J. D. & HAUSER, R. 2010. Exposure to polychlorinated biphenyls (PCBs) and male reproduction. *Syst Biol Reprod Med,* 56**,** 122-31.

MEEKER, J. D. & STAPLETON, H. M. 2010. House dust concentrations of organophosphate flame retardants in relation to hormone levels and semen quality parameters. *Environ Health Perspect,* 118**,** 318-23.

MEERTS, I. A., LETCHER, R. J., HOVING, S., MARSH, G., BERGMAN, A., LEMMEN, J. G., VAN DER BURG, B. & BROUWER, A. 2001. In vitro estrogenicity of polybrominated diphenyl ethers, hydroxylated PDBEs, and polybrominated bisphenol A compounds. *Environ Health Perspect,* 109**,** 399-407.

MIRANDA, A. & SOUSA, N. 2018. Maternal hormonal milieu influence on fetal brain development. *Brain Behav,* 8**,** e00920.

MULLER, M. H., POLDER, A., BRYNILDSRUD, O. B., LIE, E., LOKEN, K. B., MANYILIZU, W. B., MDEGELA, R. H., MOKITI, F., MURTADHA, M., NONGA, H. E., SKAARE, J. U. & LYCHE, J. L. 2016. Brominated flame retardants (BFRs) in breast milk and associated health risks to nursing infants in Northern Tanzania. *Environ Int,* 89-90**,** 38-47.

MUMFORD, S. L., KIM, S., CHEN, Z., GORE-LANGTON, R. E., BOYD BARR, D. & BUCK LOUIS, G. M. 2015. Persistent organic pollutants and semen quality: The LIFE Study. *Chemosphere,* 135**,** 427-35.

NAKAGAWA, Y., SUZUKI, T., ISHII, H. & OGATA, A. 2007. Biotransformation and cytotoxicity of a brominated flame retardant, tetrabromobisphenol A, and its analogues in rat hepatocytes. *Xenobiotica,* 37**,** 693-708.

NETO, F. T., BACH, P. V., NAJARI, B. B., LI, P. S. & GOLDSTEIN, M. 2016. Spermatogenesis in humans and its affecting factors. *Semin Cell Dev Biol,* 59**,** 10-26.

OGUNBAYO, O. A., LAI, P. F., CONNOLLY, T. J. & MICHELANGELI, F. 2008. Tetrabromobisphenol A (TBBPA), induces cell death in TM4 Sertoli cells by modulating Ca2+ transport proteins and causing dysregulation of Ca2+ homeostasis. *Toxicol In Vitro,* 22**,** 943-52.

OLSEN, G. W., ELLEFSON, M. E., MAIR, D. C., CHURCH, T. R., GOLDBERG, C. L., HERRON, R. M., MEDHDIZADEHKASHI, Z., NOBILETTI, J. B., RIOS, J. A., REAGEN, W. K. & ZOBEL, L. R. 2011. Analysis of a homologous series of perfluorocarboxylates from American Red Cross adult blood donors, 2000-2001 and 2006. *Environ Sci Technol,* 45**,** 8022-9.

OLSEN, J. 1994. Is human fecundity declining--and does occupational exposures play a role in such a decline if it exists? *Scand J Work Environ Health,* 20 Spec No**,** 72-7.

OSIMITZ, T. G., DROEGE, W. & HAYES, A. W. 2016. Subchronic toxicology of tetrabromobisphenol A in rats. *Hum Exp Toxicol*.

OTSUKA, S., ISHIHARA, A. & YAMAUCHI, K. 2014. Ioxynil and tetrabromobisphenol A suppress thyroid-hormone-induced activation of transcriptional elongation mediated by histone modifications and RNA polymerase II phosphorylation. *Toxicol Sci,* 138**,** 290-9.

OULHOTE, Y., CHEVRIER, J. & BOUCHARD, M. F. 2016. Exposure to Polybrominated Diphenyl Ethers (PBDEs) and Hypothyroidism in Canadian Women. *J Clin Endocrinol Metab,* 101**,** 590-8.

PEARSON, R., FLEETWOOD, J., EATON, S., CROSSLEY, M. & BAO, S. 2008. Kruppel-like transcription factors: a functional family. *Int J Biochem Cell Biol,* 40**,** 1996-2001.

PELTIER, M. R., KOO, H. C., GETAHUN, D. & MENON, R. 2015. Does exposure to flame retardants increase the risk for preterm birth? *J Reprod Immunol,* 107**,** 20-5.

PEVERLY, A. A., SALAMOVA, A. & HITES, R. A. 2014. Air is still contaminated 40 years after the Michigan Chemical plant disaster in St. Louis, Michigan. *Environ Sci Technol,* 48**,** 11154-60.

PHILLIPS, B. T., GASSEI, K. & ORWIG, K. E. 2010. Spermatogonial stem cell regulation and spermatogenesis. *Philos Trans R Soc Lond B Biol Sci,* 365**,** 1663-78.

POLLOCK, T., MANTELLA, L., REALI, V. & DECATANZARO, D. 2017. Influence of Tetrabromobisphenol A, with or without Concurrent Triclosan, upon Bisphenol A and Estradiol Concentrations in Mice. *Environ Health Perspect,* 125**,** 087014.

POOTHONG, S., THOMSEN, C., PADILLA-SANCHEZ, J. A., PAPADOPOULOU, E. & HAUG, L. S. 2017. Distribution of Novel and Well-Known Poly- and Perfluoroalkyl Substances (PFASs) in Human Serum, Plasma, and Whole Blood. *Environ Sci Technol,* 51**,** 13388-13396.

POTASHNIK, G., YANAI-INBAR, I., SACKS, M. I. & ISRAELI, R. 1979. Effect of dibromochloropropane on human testicular function. *Isr J Med Sci,* 15**,** 438-42.

PRADOS, J., STENZ, L., SOMM, E., STOUDER, C., DAYER, A. & PAOLONI-GIACOBINO, A. 2015. Prenatal Exposure to DEHP Affects Spermatogenesis and Sperm DNA Methylation in a Strain-Dependent Manner. *PLoS One,* 10**,** e0132136.

PREVENTION, C. F. D. C. A. 2017. Fourth National Report on Human Exposure to Environmental Chemicals, Updated Tables, January 2017, Volume One.

QIU, L., QIAN, Y., LIU, Z., WANG, C., QU, J., WANG, X. & WANG, S. 2016. Perfluorooctane sulfonate (PFOS) disrupts blood-testis barrier by down-regulating junction proteins via p38 MAPK/ATF2/MMP9 signaling pathway. *Toxicology,* 373**,** 1-12.

QU, J. H., LU, C. C., XU, C., CHEN, G., QIU, L. L., JIANG, J. K., BEN, S., WANG, Y. B., GU, A. H. & WANG, X. R. 2016. Perfluorooctane sulfonate-induced testicular toxicity and differential testicular expression of estrogen receptor in male mice. *Environ Toxicol Pharmacol,* 45**,** 150-7.

QUAAS, A. & DOKRAS, A. 2008. Diagnosis and treatment of unexplained infertility. *Rev Obstet Gynecol,* 1**,** 69-76.

RAWN, D. F., GAERTNER, D. W., WEBER, D., CURRAN, I. H., COOKE, G. M. & GOODYER, C. G. 2014a. Hexabromocyclododecane concentrations in Canadian human fetal liver and placental tissues. *Sci Total Environ,* 468-469**,** 622-9.

RAWN, D. F., RYAN, J. J., SADLER, A. R., SUN, W. F., WEBER, D., LAFFEY, P., HAINES, D., MACEY, K. & VAN OOSTDAM, J. 2014b. Brominated flame retardant concentrations in sera from the Canadian Health Measures Survey (CHMS) from 2007 to 2009. *Environ Int,* 63**,** 26-34.

RAYMER, J. H., MICHAEL, L. C., STUDABAKER, W. B., OLSEN, G. W., SLOAN, C. S., WILCOSKY, T. & WALMER, D. K. 2012. Concentrations of perfluorooctane sulfonate (PFOS) and perfluorooctanoate (PFOA) and their associations with human semen quality measurements. *Reprod Toxicol,* 33**,** 419-27.

REISTAD, T., MARIUSSEN, E., RING, A. & FONNUM, F. 2007. In vitro toxicity of tetrabromobisphenol-A on cerebellar granule cells: cell death, free radical formation, calcium influx and extracellular glutamate. *Toxicol Sci,* 96**,** 268-78.

REPPING, S., SKALETSKY, H., LANGE, J., SILBER, S., VAN DER VEEN, F., OATES, R. D., PAGE, D. C. & ROZEN, S. 2002. Recombination between palindromes P5 and P1 on the human Y chromosome causes massive deletions and spermatogenic failure. *Am J Hum Genet,* 71**,** 906-22.

RING, J. D., LWIN, A. A. & KOHLER, T. S. 2016. Current medical management of endocrine-related male infertility. *Asian J Androl,* 18**,** 357-63.

ROELOFS, M. J., VAN DEN BERG, M., BOVEE, T. F., PIERSMA, A. H. & VAN DUURSEN, M. B. 2015. Structural bisphenol analogues differentially target steroidogenesis in murine MA-10 Leydig cells as well as the glucocorticoid receptor. *Toxicology,* 329**,** 10-20.

ROY, J. R., CHAKRABORTY, S. & CHAKRABORTY, T. R. 2009. Estrogen-like endocrine disrupting chemicals affecting puberty in humans--a review. *Med Sci Monit,* 15**,** RA137-45.

ROZE, E., MEIJER, L., BAKKER, A., VAN BRAECKEL, K. N., SAUER, P. J. & BOS, A. F. 2009. Prenatal exposure to organohalogens, including brominated flame retardants, influences motor, cognitive, and behavioral performance at school age. *Environ Health Perspect,* 117**,** 1953-8.

RYTER, S. W., KIM, H. P., HOETZEL, A., PARK, J. W., NAKAHIRA, K., WANG, X. & CHOI, A. M. 2007. Mechanisms of cell death in oxidative stress. *Antioxid Redox Signal,* 9**,** 49-89.

SAGIV, S. K., KOGUT, K., GASPAR, F. W., GUNIER, R. B., HARLEY, K. G., PARRA, K., VILLASENOR, D., BRADMAN, A., HOLLAND, N. & ESKENAZI, B. 2015. Prenatal and childhood polybrominated diphenyl ether (PBDE) exposure and attention and executive function at 9-12 years of age. *Neurotoxicol Teratol,* 52**,** 151-61.

SALAMONE, M. F. & KATZ, M. 1981. Mutagenicity of Tris(2,3-dibromopropyl) phosphate in mammalian gonad and bone marrow tissue. *J Natl Cancer Inst,* 66**,** 691-5.

SARKAR, D., CHOWDHURY, J. P. & SINGH, S. K. 2016. Effect of polybrominated diphenyl ether (BDE-209) on testicular steroidogenesis and spermatogenesis through altered thyroid status in adult mice. *Gen Comp Endocrinol,* 239**,** 50-61.

SCHECTER, A., JOHNSON-WELCH, S., TUNG, K. C., HARRIS, T. R., PAPKE, O. & ROSEN, R. 2007. Polybrominated diphenyl ether (PBDE) levels in livers of U.S. human fetuses and newborns. *J Toxicol Environ Health A,* 70**,** 1-6.

SCHECTER, A., SZABO, D. T., MILLER, J., GENT, T. L., MALIK-BASS, N., PETERSEN, M., PAEPKE, O., COLACINO, J. A., HYNAN, L. S., HARRIS, T. R., MALLA, S. & BIRNBAUM, L. S. 2012. Hexabromocyclododecane (HBCD) stereoisomers in U.S. food from Dallas, Texas. *Environ Health Perspect,* 120**,** 1260-4.

SCHMIDT, C. W. 2010. Unraveling Environmental Effects on Mitochondria. *Environ Health Perspect,* 118**,** A292-A297.

SEGEV, O., KUSHMARO, A. & BRENNER, A. 2009. Environmental impact of flame retardants (persistence and biodegradability). *Int J Environ Res Public Health,* 6**,** 478-91.

SHAW, S. D., BERGER, M. L., HARRIS, J. H., YUN, S. H., WU, Q., LIAO, C., BLUM, A., STEFANI, A. & KANNAN, K. 2013. Persistent organic pollutants including polychlorinated and polybrominated dibenzo-p-dioxins and dibenzofurans in firefighters from Northern California. *Chemosphere,* 91**,** 1386-94.

SHEINER, E. K., SHEINER, E., HAMMEL, R. D., POTASHNIK, G. & CAREL, R. 2003. Effect of occupational exposures on male fertility: literature review. *Ind Health,* 41**,** 55-62.

SHI, H., QIAN, L., GUO, S., ZHANG, X., LIU, J. & CAO, Q. 2010. Teratogenic effects of tetrabromobisphenol A on Xenopus tropicalis embryos. *Comp Biochem Physiol C Toxicol Pharmacol,* 152**,** 62-8.

SMALL, C. M., DECARO, J. J., TERRELL, M. L., DOMINGUEZ, C., CAMERON, L. L., WIRTH, J. & MARCUS, M. 2009. Maternal exposure to a brominated flame retardant and genitourinary conditions in male offspring. *Environ Health Perspect,* 117**,** 1175-9.

SMALL, C. M., MURRAY, D., TERRELL, M. L. & MARCUS, M. 2011. Reproductive outcomes among women exposed to a brominated flame retardant in utero. *Arch Environ Occup Health,* 66**,** 201-8.

SODERLUND, E. J., BRUNBORG, G., DYBING, E., TRYGG, B., NELSON, S. D. & HOLME, J. A. 1992. Organ-specific DNA damage of tris(2,3-dibromopropyl)-phosphate and its diester metabolite in the rat. *Chem Biol Interact,* 82**,** 195-207.

SOUBRY, A., HOYO, C., BUTT, C. M., FIEUWS, S., PRICE, T. M., MURPHY, S. K. & STAPLETON, H. M. 2017. Human exposure to flame-retardants is associated with aberrant DNA methylation at imprinted genes in sperm. *Environ Epigenet,* 3**,** dvx003.

SPECHT, I. O., HOUGAARD, K. S., SPANO, M., BIZZARO, D., MANICARDI, G. C., LINDH, C. H., TOFT, G., JONSSON, B. A., GIWERCMAN, A. & BONDE, J. P. 2012. Sperm DNA integrity in relation to exposure to environmental perfluoroalkyl substances - a study of spouses of pregnant women in three geographical regions. *Reprod Toxicol,* 33**,** 577-83.

STAPLETON, H. M., ALLEN, J. G., KELLY, S. M., KONSTANTINOV, A., KLOSTERHAUS, S., WATKINS, D., MCCLEAN, M. D. & WEBSTER, T. F. 2008. Alternate and new brominated flame retardants detected in U.S. house dust. *Environ Sci Technol,* 42**,** 6910-6.

STAPLETON, H. M., DODDER, N. G., OFFENBERG, J. H., SCHANTZ, M. M. & WISE, S. A. 2005. Polybrominated diphenyl ethers in house dust and clothes dryer lint. *Environ Sci Technol,* 39**,** 925-31.

STAPLETON, H. M., KLOSTERHAUS, S., KELLER, A., FERGUSON, P. L., VAN BERGEN, S., COOPER, E., WEBSTER, T. F. & BLUM, A. 2011. Identification of flame retardants in polyurethane foam collected from baby products. *Environ Sci Technol,* 45**,** 5323-31.

STEENLAND, K., TINKER, S., FRISBEE, S., DUCATMAN, A. & VACCARINO, V. 2009. Association of perfluorooctanoic acid and perfluorooctane sulfonate with serum lipids among adults living near a chemical plant. *Am J Epidemiol,* 170**,** 1268-78.

STEENLAND, K. & WOSKIE, S. 2012. Cohort mortality study of workers exposed to perfluorooctanoic acid. *Am J Epidemiol,* 176**,** 909-17.

STEVES, A. N., BRADNER, J. M., FOWLER, K. L., CLARKSON-TOWNSEND, D., GILL, B. J., TURRY, A. C., CAUDLE, W. M., MILLER, G. W., CHAN, A. W. S. & EASLEY, C. A. T. 2018a. Ubiquitous Flame-Retardant Toxicants Impair Spermatogenesis in a Human Stem Cell Model. *iScience,* 3**,** 161-176.

STEVES, A. N., TURRY, A., GILL, B., CLARKSON-TOWNSEND, D., BRADNER, J. M., BACHLI, I., CAUDLE, W. M., MILLER, G. W., CHAN, A. W. S. & EASLEY, C. A. T. 2018b. Per- and polyfluoroalkyl substances impact human spermatogenesis in a stem-cell-derived model. *Syst Biol Reprod Med,* 64**,** 225-239.

STROHEKER, T., REGNIER, J. F., LASSURGUERE, J. & CHAGNON, M. C. 2006. Effect of in utero exposure to di-(2-ethylhexyl)phthalate: distribution in the rat fetus and testosterone production by rat fetal testis in culture. *Food Chem Toxicol,* 44**,** 2064-9.

SUH, K. S., CHOI, E. M., RHEE, S. Y., OH, S., KIM, S. W., PAK, Y. K., CHOE, W., HA, J. & CHON, S. 2017. Tetrabromobisphenol A induces cellular damages in pancreatic beta-cells in vitro. *J Environ Sci Health A Tox Hazard Subst Environ Eng,* 52**,** 624-631.

TA, N., LI, C., FANG, Y., LIU, H., LIN, B., JIN, H., TIAN, L., ZHANG, H., ZHANG, W. & XI, Z. 2014. Toxicity of TDCPP and TCEP on PC12 cell: changes in CAMKII, GAP43, tubulin and NF-H gene and protein levels. *Toxicol Lett,* 227**,** 164-71.

TERRELL, M. L., BERZEN, A. K., SMALL, C. M., CAMERON, L. L., WIRTH, J. J. & MARCUS, M. 2009. A cohort study of the association between secondary sex ratio and parental exposure to polybrominated biphenyl (PBB) and polychlorinated biphenyl (PCB). *Environ Health,* 8**,** 35.

TERRELL, M. L., HARTNETT, K. P., LIM, H., WIRTH, J. & MARCUS, M. 2015. Maternal exposure to brominated flame retardants and infant Apgar scores. *Chemosphere,* 118**,** 178-86.

THOMSEN, C., LEKNES, H., LUNDANES, E. & BECHER, G. 2002a. A new method for determination of halogenated flame retardants in human milk using solid-phase extraction. *J Anal Toxicol,* 26**,** 129-37.

THOMSEN, C., LUNDANES, E. & BECHER, G. 2001. Brominated flame retardants in plasma samples from three different occupational groups in Norway. *J Environ Monit,* 3**,** 366-70.

THOMSEN, C., LUNDANES, E. & BECHER, G. 2002b. Brominated flame retardants in archived serum samples from Norway: a study on temporal trends and the role of age. *Environ Sci Technol,* 36**,** 1414-8.

THOMSEN, C., MOLANDER, P., DAAE, H. L., JANAK, K., FROSHAUG, M., LIANE, V. H., THORUD, S., BECHER, G. & DYBING, E. 2007. Occupational exposure to hexabromocyclododecane at an industrial plant. *Environ Sci Technol,* 41**,** 5210-6.

THOMSON, J. A., ITSKOVITZ-ELDOR, J., SHAPIRO, S. S., WAKNITZ, M. A., SWIERGIEL, J. J., MARSHALL, V. S. & JONES, J. M. 1998. Embryonic stem cell lines derived from human blastocysts. *Science,* 282**,** 1145-7.

TOFT, G., JONSSON, B. A., LINDH, C. H., GIWERCMAN, A., SPANO, M., HEEDERIK, D., LENTERS, V., VERMEULEN, R., RYLANDER, L., PEDERSEN, H. S., LUDWICKI, J. K., ZVIEZDAI, V. & BONDE, J. P. 2012. Exposure to perfluorinated compounds and human semen quality in Arctic and European populations. *Hum Reprod,* 27**,** 2532-40.

TREINEN, K. A., CHAPIN, R. E., GULATI, D. K., MOUNCE, R., MORRIS, L. Z. & LAMB, J. C. T. 1989. Reproductive toxicity of 2,2-bis(bromomethyl)-1,3-propanediol in a continuous breeding protocol in Swiss (CD-1) mice. *Fundam Appl Toxicol,* 13**,** 245-55.

TSENG, L. H., HSU, P. C., LEE, C. W., TSAI, S. S., PAN, M. H. & LI, M. H. 2013. Developmental exposure to decabrominated diphenyl ether (BDE-209): effects on sperm oxidative stress and chromatin DNA damage in mouse offspring. *Environ Toxicol,* 28**,** 380-9.

TSENG, L. H., LEE, C. W., PAN, M. H., TSAI, S. S., LI, M. H., CHEN, J. R., LAY, J. J. & HSU, P. C. 2006. Postnatal exposure of the male mouse to 2,2',3,3',4,4',5,5',6,6'-decabrominated diphenyl ether: decreased epididymal sperm functions without alterations in DNA content and histology in testis. *Toxicology,* 224**,** 33-43.

UNITED NATIONS ENVIRONMENT PROGRAMME, I. L. O., WORLD HEALTH ORGANIZATION 2004. FLAME RETARDANTS: TRIS(CHLOROPROPYL) PHOSPHATE AND TRIS(2-CHLOROETHYL) PHOSPHATE.

VALLI, H., SUKHWANI, M., DOVEY, S. L., PETERS, K. A., DONOHUE, J., CASTRO, C. A., CHU, T., MARSHALL, G. R. & ORWIG, K. E. 2014. Fluorescence- and magnetic-activated cell sorting strategies to isolate and enrich human spermatogonial stem cells. *Fertil Steril,* 102**,** 566-580 e7.

VAN BEERENDONK, G. J., NELSON, S. D. & MEERMAN, J. H. 1994. Metabolism and genotoxicity of the halogenated alkyl compound tris(2,3-dibromopropyl)phosphate. *Hum Exp Toxicol,* 13**,** 861-5.

VAN DER VEEN, I. & DE BOER, J. 2012. Phosphorus flame retardants: properties, production, environmental occurrence, toxicity and analysis. *Chemosphere,* 88**,** 1119-53.

VESTED, A., RAMLAU-HANSEN, C. H., OLSEN, S. F., BONDE, J. P., KRISTENSEN, S. L., HALLDORSSON, T. I., BECHER, G., HAUG, L. S., ERNST, E. H. & TOFT, G. 2013. Associations of in utero exposure to perfluorinated alkyl acids with human semen quality and reproductive hormones in adult men. *Environ Health Perspect,* 121**,** 453-8.

VOLZ, D. C., LEET, J. K., CHEN, A., STAPLETON, H. M., KATIYAR, N., KAUNDAL, R., YU, Y. & WANG, Y. 2016. Tris(1,3-dichloro-2-propyl)phosphate Induces Genome-Wide Hypomethylation within Early Zebrafish Embryos. *Environ Sci Technol,* 50**,** 10255-63.

WAN, H. T., MRUK, D. D., WONG, C. K. & CHENG, C. Y. 2014. Perfluorooctanesulfonate (PFOS) perturbs male rat Sertoli cell blood-testis barrier function by affecting F-actin organization via p-FAK-Tyr(407): an in vitro study. *Endocrinology,* 155**,** 249-62.

WAN, H. T., ZHAO, Y. G., WONG, M. H., LEE, K. F., YEUNG, W. S., GIESY, J. P. & WONG, C. K. 2011. Testicular signaling is the potential target of perfluorooctanesulfonate-mediated subfertility in male mice. *Biol Reprod,* 84**,** 1016-23.

WANG, K. L., HSIA, S. M., MAO, I. F., CHEN, M. L., WANG, S. W. & WANG, P. S. 2011a. Effects of polybrominated diphenyl ethers on steroidogenesis in rat Leydig cells. *Hum Reprod,* 26**,** 2209-17.

WANG, Q., LAM, J. C., HAN, J., WANG, X., GUO, Y., LAM, P. K. & ZHOU, B. 2015a. Developmental exposure to the organophosphorus flame retardant tris(1,3-dichloro-2-propyl) phosphate: estrogenic activity, endocrine disruption and reproductive effects on zebrafish. *Aquat Toxicol,* 160**,** 163-71.

WANG, W., ABUALNAJA, K. O., ASIMAKOPOULOS, A. G., COVACI, A., GEVAO, B., JOHNSON-RESTREPO, B., KUMOSANI, T. A., MALARVANNAN, G., MINH, T. B., MOON, H. B., NAKATA, H., SINHA, R. K. & KANNAN, K. 2015b. A comparative assessment of human exposure to tetrabromobisphenol A and eight bisphenols including bisphenol A via indoor dust ingestion in twelve countries. *Environ Int,* 83**,** 183-91.

WANG, Z. X., DUAN, H. Y., WANG, L. & CHEN, D. J. 2011b. [Mouse sperm DNA damage induced by exogenous BDE-209]. *Nan Fang Yi Ke Da Xue Xue Bao,* 31**,** 108-12.

WATANABE, I. & SAKAI, S. 2003. Environmental release and behavior of brominated flame retardants. *Environ Int,* 29**,** 665-82.

WEISSMAN, T. A. & PAN, Y. A. 2015. Brainbow: new resources and emerging biological applications for multicolor genetic labeling and analysis. *Genetics,* 199**,** 293-306.

WHORTON, D., KRAUSS, R. M., MARSHALL, S. & MILBY, T. H. 1977. Infertility in male pesticide workers. *Lancet,* 2**,** 1259-61.

WHORTON, D., MILBY, T. H., KRAUSS, R. M. & STUBBS, H. A. 1979. Testicular function in DBCP exposed pesticide workers. *J Occup Med,* 21**,** 161-6.

WIELSOE, M., LONG, M., GHISARI, M. & BONEFELD-JORGENSEN, E. C. 2015. Perfluoroalkylated substances (PFAS) affect oxidative stress biomarkers in vitro. *Chemosphere,* 129**,** 239-45.

WILDING BC, C. K., WELKER-HOOD K 2013. Hazardous Chemicals in Healthcare: A Snapshot of Chemicals in Doctors and Nurses.

WONG, E. W. & CHENG, C. Y. 2011. Impacts of environmental toxicants on male reproductive dysfunction. *Trends Pharmacol Sci,* 32**,** 290-9.

WONG, O., BROCKER, W., DAVIS, H. V. & NAGLE, G. S. 1984. Mortality of workers potentially exposed to organic and inorganic brominated chemicals, DBCP, TRIS, PBB, and DDT. *Br J Ind Med,* 41**,** 15-24.

WORLEY, R. R., MOORE, S. M., TIERNEY, B. C., YE, X., CALAFAT, A. M., CAMPBELL, S., WOUDNEH, M. B. & FISHER, J. 2017. Per- and polyfluoroalkyl substances in human serum and urine samples from a residentially exposed community. *Environ Int,* 106**,** 135-143.

WU, M., ZUO, Z., LI, B., HUANG, L., CHEN, M. & WANG, C. 2013. Effects of low-level hexabromocyclododecane (HBCD) exposure on cardiac development in zebrafish embryos. *Ecotoxicology,* 22**,** 1200-7.

WU, X. M., BENNETT, D. H., CALAFAT, A. M., KATO, K., STRYNAR, M., ANDERSEN, E., MORAN, R. E., TANCREDI, D. J., TULVE, N. S. & HERTZ-PICCIOTTO, I. 2015. Serum concentrations of perfluorinated compounds (PFC) among selected populations of children and adults in California. *Environ Res,* 136**,** 264-73.

YAN, W. & MCCARREY, J. R. 2009. Sex chromosome inactivation in the male. *Epigenetics,* 4**,** 452-6.

YARD, E. E., TERRELL, M. L., HUNT, D. R., CAMERON, L. L., SMALL, C. M., MCGEEHIN, M. A. & MARCUS, M. 2011. Incidence of thyroid disease following exposure to polybrominated biphenyls and polychlorinated biphenyls, Michigan, 1974-2006. *Chemosphere,* 84**,** 863-8.

YI, S., LIU, J. G., JIN, J. & ZHU, J. 2016a. Assessment of the occupational and environmental risks of hexabromocyclododecane (HBCD) in China. *Chemosphere,* 150**,** 431-437.

YI, S., LIU, J. G., JIN, J. & ZHU, J. 2016b. Assessment of the occupational and environmental risks of hexabromocyclododecane (HBCD) in China. *Chemosphere,* 150**,** 431-7.

ZATECKA, E., CASTILLO, J., ELZEINOVA, F., KUBATOVA, A., DED, L., PEKNICOVA, J. & OLIVA, R. 2014. The effect of tetrabromobisphenol A on protamine content and DNA integrity in mouse spermatozoa. *Andrology,* 2**,** 910-7.

ZATECKA, E., DED, L., ELZEINOVA, F., KUBATOVA, A., DOROSH, A., MARGARYAN, H., DOSTALOVA, P. & PEKNICOVA, J. 2013. Effect of tetrabrombisphenol A on induction of apoptosis in the testes and changes in expression of selected testicular genes in CD1 mice. *Reprod Toxicol,* 35**,** 32-9.

ZHANG, D. Y., XU, X. L., SHEN, X. Y., RUAN, Q. & HU, W. L. 2015. Analysis of apoptosis induced by perfluorooctane sulfonates (PFOS) in mouse Leydig cells in vitro. *Toxicol Mech Methods,* 25**,** 21-5.

ZHANG, H., LU, Y., LUO, B., YAN, S., GUO, X. & DAI, J. 2014. Proteomic analysis of mouse testis reveals perfluorooctanoic acid-induced reproductive dysfunction via direct disturbance of testicular steroidogenic machinery. *J Proteome Res,* 13**,** 3370-85.

ZHANG, J., WILLIAMS, T. D., CHIPMAN, J. K. & VIANT, M. R. 2016a. Defensive and adverse energy-related molecular responses precede tris (1, 3-dichloro-2-propyl) phosphate cytotoxicity. *J Appl Toxicol,* 36**,** 649-58.

ZHANG, Q., JI, C., YIN, X., YAN, L., LU, M. & ZHAO, M. 2016b. Thyroid hormone-disrupting activity and ecological risk assessment of phosphorus-containing flame retardants by in vitro, in vivo and in silico approaches. *Environ Pollut,* 210**,** 27-33.

ZHANG, X., YANG, F., ZHANG, X., XU, Y., LIAO, T., SONG, S. & WANG, J. 2008. Induction of hepatic enzymes and oxidative stress in Chinese rare minnow (Gobiocypris rarus) exposed to waterborne hexabromocyclododecane (HBCDD). *Aquat Toxicol,* 86**,** 4-11.

ZHAO, Y., AO, H., CHEN, L., SOTTAS, C. M., GE, R. S. & ZHANG, Y. 2011. Effect of brominated flame retardant BDE-47 on androgen production of adult rat Leydig cells. *Toxicol Lett,* 205**,** 209-14.

ZHOU, W., SHAO, H., ZHANG, D., DONG, J., CHENG, W., WANG, L., TENG, Y. & YU, Z. 2015. PTEN signaling is required for the maintenance of spermatogonial stem cells in mouse, by regulating the expressions of PLZF and UTF1. *Cell Biosci,* 5**,** 42.

ZHOU, X., GUO, J., ZHANG, W., ZHOU, P., DENG, J. & LIN, K. 2014. Tetrabromobisphenol A contamination and emission in printed circuit board production and implications for human exposure. *J Hazard Mater,* 273**,** 27-35.

ZHU, Y., MA, X., SU, G., YU, L., LETCHER, R. J., HOU, J., YU, H., GIESY, J. P. & LIU, C. 2015. Environmentally Relevant Concentrations of the Flame Retardant Tris(1,3-dichloro-2-propyl) Phosphate Inhibit Growth of Female Zebrafish and Decrease Fecundity. *Environ Sci Technol,* 49**,** 14579-87.

ZOTA, A. R., PARK, J. S., WANG, Y., PETREAS, M., ZOELLER, R. T. & WOODRUFF, T. J. 2011. Polybrominated diphenyl ethers, hydroxylated polybrominated diphenyl ethers, and measures of thyroid function in second trimester pregnant women in California. *Environ Sci Technol,* 45**,** 7896-905.